

# UNCLASSIFIED

AD NUMBER
AD860089
NEW LIMITATION CHANGE
TO Approved for public release, distribution unlimited
FROM Distribution authorized to U.S. Gov't. agencies only; Administrative/Operational Use; 20 May 1969. Other requests shall be referred to Naval Ordnance Laboratory, White Oak, MD.
AUTHORITY
USNOL ltr, 29 Aug 1974

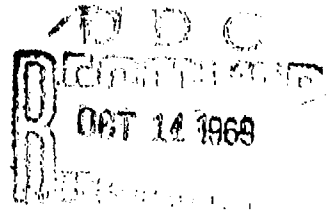
THIS PAGE IS UNCLASSIFIED

AD 860089

NOLTR 69-100

STATIC-STABILITY INDEX AND AERODYNAMIC  
COEFFICIENTS FOR THE 0.125-SCALE MODEL  
MARK 82 LOW-DRAG BOMB WITH STANDARD  
AND EMTEX SNAKEYE I FINS WITH SIX  
RETARDATION ANGLES AT SUBSONIC SPEEDS

By  
V. L. Schermerhorn



NOL

20 MAY 1969

UNITED STATES NAVAL ORDNANCE LABORATORY, WHITE OAK, MARYLAND

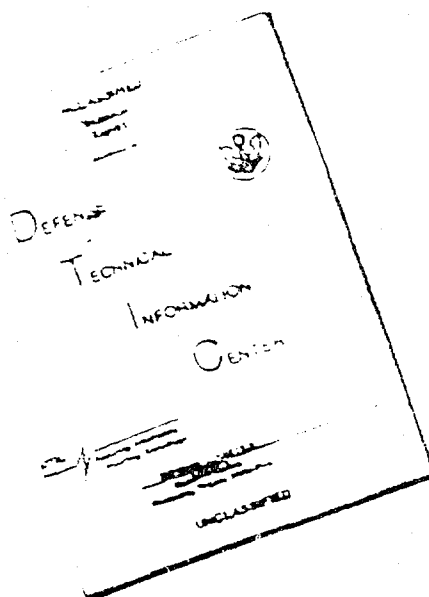
NOLTR 69-100

ATTENTION

Each transmittal of this document outside the agencies of the U. S. Government must have prior approval of NOL



# DISCLAIMER NOTICE



THIS DOCUMENT IS BEST  
QUALITY AVAILABLE. THE COPY  
FURNISHED TO DTIC CONTAINED  
A SIGNIFICANT NUMBER OF  
PAGES WHICH DO NOT  
REPRODUCE LEGIBLY.

REPRODUCED FROM  
BEST AVAILABLE COPY

STATIC-STABILITY INDEX AND AERODYNAMIC COEFFICIENTS FOR THE  
0.125-SCALE MODEL MARK 82 LOW-DRAG BOMB WITH STANDARD AND  
EMTEX SNAKEYE I FINS WITH SIX RETARDATION ANGLES AT SUBSONIC SPEEDS

Prepared by:  
V. L. Schermerhorn

ABSTRACT: The static-stability index, force and moment coefficients are presented as functions of angle of attack for the Mk 82 Low-Drag Bomb with Standard and Emtex Snakeye I Fins. For these tests the fin-opening angles were 60, 70, 80, 90, 100 and 110 degrees; the models' angle of attack ranged from -10 to +20 degrees; the free-stream Mach number was varied from 0.25 to 0.95, and roll angles were at 0, 22.5 and 45 degrees.

U. S. NAVAL ORDNANCE LABORATORY  
WHITE OAK, MARYLAND

NOLTR 69-100

20 May 1969

STATIC-STABILITY INDEX AND AERODYNAMIC COEFFICIENTS FOR THE 0.125-  
SCALE MODEL MARK 82 LOW-DRAG BOMB WITH STANDARD AND EMTX SNAKEYE I  
FINS WITH SIX RETARDATION ANGLES AT SUBSONIC SPEEDS

The purpose of this test program was to determine whether or not the Emtex fin, designed to minimize the opening shock at launch, would be sufficiently stable to warrant changing the configuration from that employing the Standard Snakeye I fins. These tests were conducted at the request of the Naval Weapons Center under Task No. NOL-483/NWC.

E. F. SCHREITER  
Captain, USN  
Commander

*L. H. Schindel*  
L. H. SCHINDEL  
By direction

## CONTENTS

	Page
INTRODUCTION .....	1
SYMBOLS .....	1
MODELS, DATA ACQUISITION AND DATA REDUCTION .....	2
RESULTS .....	4
CONCLUSIONS .....	5
REFERENCES .....	6

## TABLES

Table	Title
1	Nominal Wind-Tunnel Test Conditions

## ILLUSTRATIONS

Figure	Title
1	Mk 82 Low-Drag Bomb - 0.125-Scale Model with Standard and Emtrex Snakeye I Tail Assemblies
2	Mk 82 Low-Drag Bomb with Standard Snakeye I Tail Assembly
3	Mk 82 Low-Drag Bomb with Emtrex Snakeye I Tail Assembly
4-93	Normal-Force and Pitching-Moment Coefficients, $C_N$ and $C_m$ , vs Angle of Attack, $\alpha$ , for the 0.125-Scale Model Mk 82 Snakeye Bomb with Fins Open ( <u>Standard Tail</u> : $\beta_a = 60^\circ, 70^\circ, 80^\circ, 90^\circ, 100^\circ$ and $110^\circ$ ; $\phi = 0^\circ, 22.5^\circ$ and $45^\circ$ ; $M = 0.25, 0.50, 0.80, 0.90$ and $0.95$ )
94-183	Side-Force, Yawing-Moment, Rolling-Moment and Axial-Force Coefficients, $C_y, C_n, C_l$ and $C_{A_f}$ vs Angle of Attack, $\alpha$ , for the 0.125-Scale Model Mk 82 Snakeye Bomb with Fins Open ( <u>Standard Tail</u> : $\beta_a = 60^\circ, 70^\circ, 80^\circ, 90^\circ, 100^\circ$ and $110^\circ$ ; $\phi = 0^\circ, 22.5^\circ$ and $45^\circ$ ; $M = 0.25, 0.50, 0.80, 0.90$ and $0.95$ )
184-273	Normal-Force and Pitching-Moment Coefficients, $C_N$ and $C_m$ , vs Angle of Attack, $\alpha$ , for the 0.125-Scale Model Mk 82 Snakeye Bomb with Fins Open ( <u>Emtex Tail</u> : $\beta_f = 60^\circ, 70^\circ, 80^\circ, 90^\circ, 100^\circ$ and $110^\circ$ ; $\phi = 0^\circ, 22.5^\circ$ and $45^\circ$ ; $M = 0.25, 0.50, 0.80, 0.90$ and $0.95$ )
274-363	Side-Force, Yawing-Moment, Rolling-Moment and Axial-Force Coefficients, $C_y, C_n, C_l$ and $C_{A_f}$ , vs Angle of Attack, $\alpha$ , for the 0.125-Scale Model Mk 82 Snakeye Bomb with Fins Open ( <u>Emtex Tail</u> : $\beta_f = 60^\circ, 70^\circ, 80^\circ, 90^\circ, 100^\circ$ and $110^\circ$ ; $\phi = 0^\circ, 22.5^\circ$ and $45^\circ$ ; $M = 0.25, 0.50, 0.80, 0.90$ and $0.95$ )

ILLUSTRATIONS (Cont'd)

- 364 Center-of-Pressure Location, in Calibers, from the Moment Reference Center,  $C_{m\alpha} / C_{N\alpha}$ , vs Mach Number for the 0.125-Scale Model Mk 82 Low-Drag Bomb with Standard and Emtex Snakeye I Tails ( $\beta = 60^\circ, 70^\circ, 80^\circ, 90^\circ, 100^\circ$  and  $110^\circ$ )
- 365 Center-of-Pressure Location, in Calibers, from the Moment Reference Center,  $C_{m\alpha} / C_{N\alpha}$ , vs Fin-Opening Angle for the 0.125-Scale Model Mk 82 Low-Drag Bomb with Standard and Emtex Snakeye I Tails ( $M = 0.25, 0.50, 0.80, 0.90$  and  $0.95$ )
- 366-367 Axial-Force Coefficient at Zero Angle of Attack,  $C_{A_{f_0}}$ , vs Fin-Opening Angle for the 0.125-Scale Model Mk 82 Low-Drag Bomb with Standard and Emtex Snakeye I Tails
- 368-369 Axial-Force Coefficient at Zero Angle of Attack,  $C_{A_{f_0}}$ , vs Mach Number for the 0.125-Scale Model Mk 82 Low-Drag Bomb with Standard and Emtex Snakeye I Tails ( $\beta = 60^\circ, 70^\circ, 80^\circ, 90^\circ, 100^\circ$  and  $110^\circ$ )
- 370 Average Location of the Center of Pressure vs Fin-Opening Angle for the 0.125-Scale Model Mk 82 Low-Drag Bomb with Standard and Emtex Snakeye I Fins.
- 371 Average Axial-Force Coefficient, and Average Nondimensional Center-of-Pressure Location vs Fin-Opening Angle for the 0.125-Scale Model Mk 82 Low-Drag Bomb with Standard and Emtex Snakeye I Tails
- 372 Base-Pressure Ratio,  $P_b/P_o$ , vs Mach Number for the 0.125-Scale Model Mk 82 Low-Drag Bomb with Emtex Tail ( $\beta = 60^\circ$  and  $110^\circ$ )
- 373 Drag-Chamber-Pressure Ratio,  $P_c/P_o$ , vs Mach Number for the 0.125-Scale Model Mk 82 Low-Drag Bomb with Standard and Emtex Snakeye I Tails ( $\beta = 60^\circ$  and  $110^\circ$ )
- 374-375 Base-Pressure Ratio,  $P_b/P_o$ , vs Angle of Attack for the 0.125-Scale Model Mk 82 Low-Drag Bomb with Emtex Tail ( $\beta = 60^\circ$  and  $110^\circ$ ;  $M = 0.26, 0.38, 0.50, 0.65, 0.80, 0.85, 0.90, 0.93, 0.95$  and  $0.98$ )
- 376-377 Drag-Chamber-Pressure Ratio,  $P_c/P_o$ , vs Angle of Attack for the 0.125-Scale Model Mk 82 Low-Drag Bomb with Emtex Tail ( $\beta = 60^\circ$  and  $110^\circ$ ;  $M = 0.26, 0.38, 0.50, 0.65, 0.80, 0.85, 0.90, 0.93, 0.95$  and  $0.98$ )

## INTRODUCTION

Standard Snakeye I fins and Emtex fins were fitted to an 0.125-scale model Navy Mk 82 low-drag bomb. Since the opening shock loads are known to damage the standard fins, the Emtex fins have been designed to minimize these loads.

## SYMBOLS

$A$	body cross-sectional area reference, $\pi d^2/4$ (1.424 in. <sup>2</sup> )
$C_A$	axial-force coefficient, $F_A/q_A$
$C_{A_f}$	corrected axial-force coefficient
$C_{A_{f_0}}$	axial-force coefficient at zero angle of attack
$C_r$	rolling-moment coefficient, $M_x/qAd$
$C_m$	pitching-moment coefficient $M_y/qAd$
$C_{m_\alpha}$	pitching-moment derivative
$C_N$	normal-force coefficient, $F_N/qA$
$C_{N_\alpha}$	normal-force coefficient derivative
$C_n$	yawing-moment coefficient, $M_z/qAd$
$C_y$	side-force coefficient, $F_y/qA$
c.g.	moment reference center
$d$	maximum body diameter (1.347 in.)
$F_A$	axial force
$F_N$	normal force
$F_y$	side force
$L$	axial distance from c.g. to fin-tip plane (calibers)
$M$	Mach number
$M_x$	rolling moment

$M_y$	pitching moment
$M_z$	yawing moment
$P_b$	base pressure
$P_c$	drag-chamber pressure
$P_s$	free-stream static pressure
$P_o$	stagnation pressure,
$q$	dynamic pressure, $\rho V^2/2$
$Re$	Reynolds number per foot
$V$	wind-tunnel free-stream speed
$x, y, z$	body axes
$\alpha$	angle of attack
$\beta_a$	fin-opening angle (standard fin)
$\beta_f$	fin-opening angle (Emtex fin)
$\rho$	free-stream density
$\phi$	roll angle

## MODELS, DATA ACQUISITION AND DATA REDUCTION

### MODELS

The Mk 82 low-drag bomb, with two Snakeye I tail configurations, was tested (Fig. 1). The standard Snakeye I fins are shown in the sketch on Figure 2; while the Emtex fins are shown in the sketch on Figure 3. Figure 1 is a photograph of the 0.125-scale models as tested in the wind tunnel. Both models have the same fin panels; these differ only in hinge location. The standard tail is mounted on fixed hinges at the base with the struts hinge mounted on a movable ring over the center shaft (Fig. 2). The Emtex fins are hinge mounted, at the rear, to a movable ring; and, the struts are mounted to fixed hinges at the root of the tail assembly (Fig. 3). Both assemblies have the same external shape when closed ( $R = 0^\circ$ ).

The models tested were 11.248 inches long, and had a maximum diameter of 1.347 inches.

BALANCES

The NOL 5-39 balance with the 1-35 external drag link was used to obtain the data shown herein. These data were acquired and stored in digital form on magnetic tape.

TEST CONDITIONS

Both models were tested at fin-opening angles of 60, 70, 80, 90, 100 and 110 degrees; at roll angles of 0, 22.5 and 45 degrees; at angles of attack ranging from -10 to +20 degrees; and, at nominal free-stream Mach numbers of 0.25, 0.50, 0.80, 0.90 and 0.95. The tests were conducted in the NOL Supersonic Tunnel No. 1 fitted with the subsonic nozzle blocks. The nominal wind-tunnel test conditions, which may vary slightly from day to day due to atmospheric pressure and temperature changes, are noted in Table 1.

DATA REDUCTION

These data have been reduced to aerodynamic coefficient form, and are referred to a c.g. located 6.234 inches ahead of the base of the model. Corrections have been made to the angle of attack to account for elastic deflection of the sting balance due to aerodynamic loading.

Since an external drag link was used for these tests, the axial-force data have been corrected by means of the following expression:

$$C_{A_f} = C_A + [(P_b - P_s) (A_b - A_s + A_s (P_c - P_s))] / qA$$

In this expression values for the pressures,  $P_b$  and  $P_c$ , have been determined from the data obtained at the 110 degrees fin-opening angle and at zero angle of attack. For the models tested the value of  $A_b$  and  $A_s$  were as follows:

<u>Configuration</u>	<u><math>A_s</math></u>	<u><math>A_b</math></u>
Standard	0.159 in. <sup>2</sup>	0.4255 (fixed hexagonal base ring)
Extex	0.103 in. <sup>2</sup>	0.3525 (shaft area)

Base and drag-chamber pressures as a function of angle of attack, and for 60 and 110 degrees fin-opening angle, were obtained for the



model fitted with the Emtex tail. A check on these data, made at a 60-degree fin-open angle, using the base- and drag-chamber pressures as determined for both 60 and 110 degrees fin angles, indicates that the maximum error (of 0.3 percent of the total axial force) was introduced when one uses the values determined from tests with 110-degree fin angle only. That is, the maximum increment in  $C_{A_{f_0}}$  was noted to be:

$$\Delta C_{A_{f_0}} = 0.054 \text{ at } M = 0.95$$

### RESULTS

The experimentally determined normal-force and pitching-moment coefficients are presented, as functions of angle of attack, on Figures 4 through 93, for the model fitted with the standard tail. The corresponding side-force, yawing-moment, rolling-moment and axial-force coefficients - versus angle of attack - are presented on Figures 94 through 183. Similar plots for the Emtex tail configuration are found on Figures 184 through 273, and figures 274 through 363, respectively.

During the tests on the model fitted with the standard tail, the pitch-plane fins were noted to undergo stressing and subsequent relaxing as the fins were moved out of, or into, the leeward side of the model, as the angle of attack was changed. The fins were noted to have a tendency to roll in a negative direction at the onset of the wind-tunnel test blow. At the end of the blow, however, the fins relaxed and resumed their original setting. The Emtex fins, which were attached more rigidly to the model, did not appear to have as much fin movement; however, the induced rolling moment was greater and (generally) of opposite sign. In general, most of the discontinuities which appear in the plotted data can be attributed to fin movement occurring during a given run.

Figures 364 and 365 are composite plots showing the location of the center of pressure, in calibers, as measured from the center of gravity. These locations are plotted versus Mach number and fin-opening angle, respectively, for both model configurations. Axial-force coefficients, measured at zero angle of attack, and plotted as a function of fin-opening angle, with Mach number as the parameter, are presented on Figures 366 and 367 for the standard and Emtex tail configurations, respectively. Figures 368 and 369 are cross plots of these data with the fin angle used as a parameter. The average center-of-pressure location, for all Mach numbers, versus fin-opening

angle, is shown on Figure 370. Figure 371 depicts the average axial-force coefficient, for both tail configurations, as a function of fin-opening angle. Also shown is the average center-of-pressure location, nondimensionalized by the distance from the c.g. to the fin-tip plane, for each configuration plotted as a function of the fin-opening angle. Figures 372 through 377 are plots of the base and drag-chamber pressures versus free-stream Mach number, and angle of attack, for tests with 0, 60 and 110 degrees fin-opening angles.

### CONCLUSIONS

Both of the configurations tested were statically stable; very little change in stability with Mach number was noted (see Fig. 364). A small increase in static stability did occur as the fin-opening angle was increased (see Fig. 365). In general, the center of pressure is located approximately one caliber further aft on the model when the standard tail was used (see Fig. 370). The center-of-pressure location, nondimensionalized by the distance to the fin-tip plane from the c.g., was noted to have identical curves for both configurations (see Fig. 371). This indicates that accounting for the large fin span the static margin is almost entirely dependent on fin-tip location alone.

The maximum-drag coefficient (at  $\alpha = 0$ ) for both configurations occurs at approximately a 90-degree fin-opening angle (see Figs. 366 to 369). Since the Emtex tail (with fins open) does not extend as far from the main body as the standard tail, it has less fin surface exposed to the free stream and has a smaller drag compared to the standard tail (which extends more into the wake from the body (see Fig. 371)).

Only a small change in base pressure was noted to occur with changes in fin-opening angle (see Fig. 372). The dip in base-pressure measurements, versus angle of attack (see Figs. 374, 375) between  $\alpha = -8^\circ$  and  $\alpha = +8^\circ$ , seems to coincide with the greatest fin movement noted to occur during the test; this was the test range when the fins underwent a bending and a relaxing as they moved out of or into the lee of the model.

The side-force, yawing-moment and induced rolling-moment coefficients were smaller for the standard tail. However, this configuration rotated slightly at onset of blowing; more so than the Emtex tail, which had a more rigid construction. This action would seem to indicate that, if the fins were allowed to rotate more freely, some compensation for fin misalignment could be obtained. Thus, it

## NOLTR 69-100

would seem likely that some of the stressing, which tends to break off the fins at launch, would be alleviated if the fins were allowed to rotate more freely.

### REFERENCES

- (a) V. L. Schermerhorn, "Static-Stability Index and Aerodynamic Coefficients for the 0.125-Scale Model Mark 82 Low-Drag Bomb with Closed Snakeye I Fins at Subsonic and Transonic Speeds," NOLTR (in preparation)

Table 1

NOMINAL WIND-TUNNEL TEST CONDITIONS

Average Supply Temperature = 22 Degrees Centigrade

Average Mach No.	Average Supply Pressure mm Hg.	Reynolds Number (Re/ft)10 <sup>-6</sup>
0.26	760	1.80
0.50	748	2.90
0.60	745	3.80
0.70	742	3.90
0.80	740	4.15
0.90	738	4.35
0.95	738	4.40
0.99	738	4.45

**BLANK PAGE**

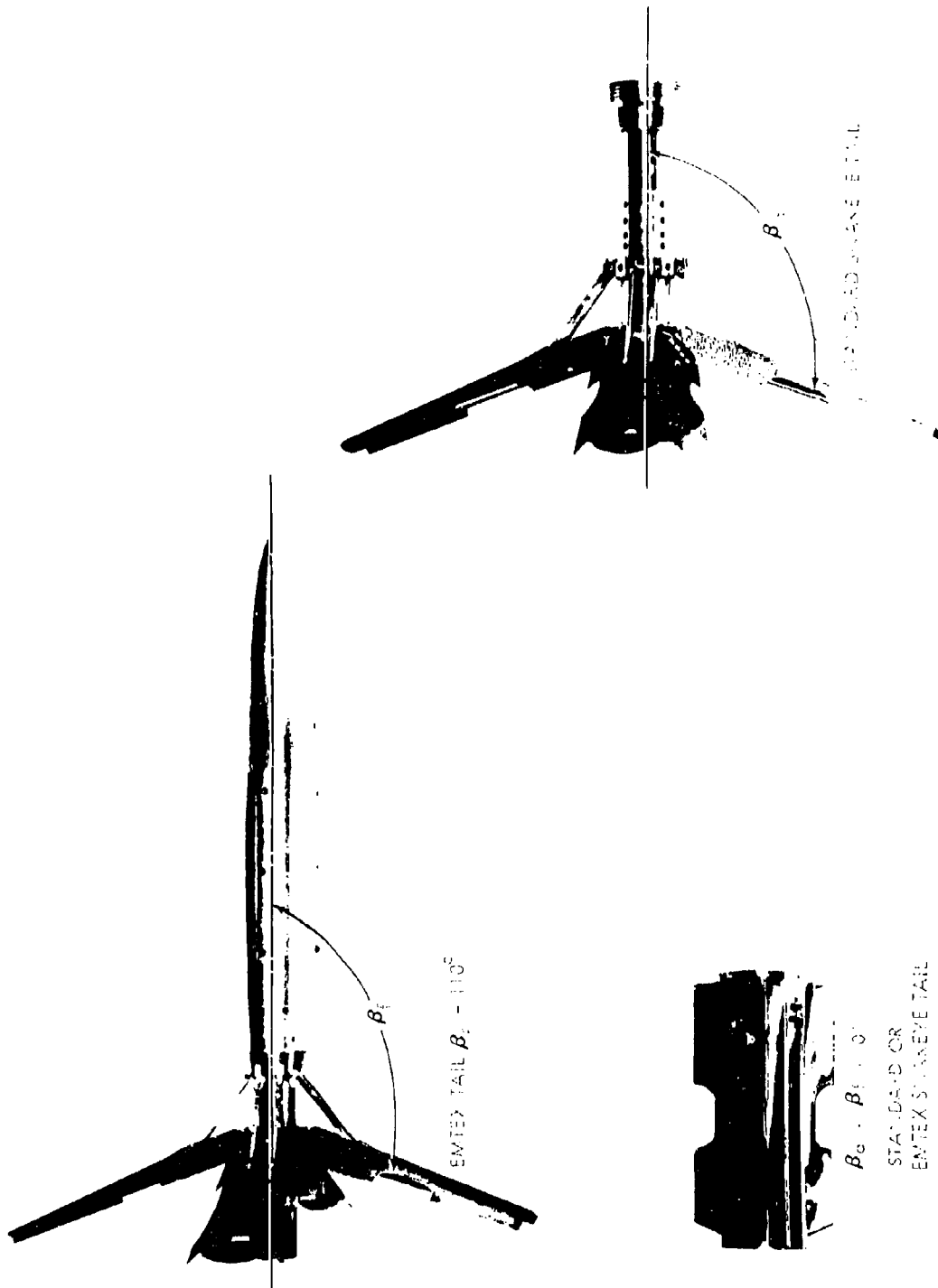


FIG 1 MK82 LOW DRAG BOMB 0.125 SCALE MODEL WITH STANDARD AND EMTX SNAKEYE 1 TAIL ASSEMBLIES

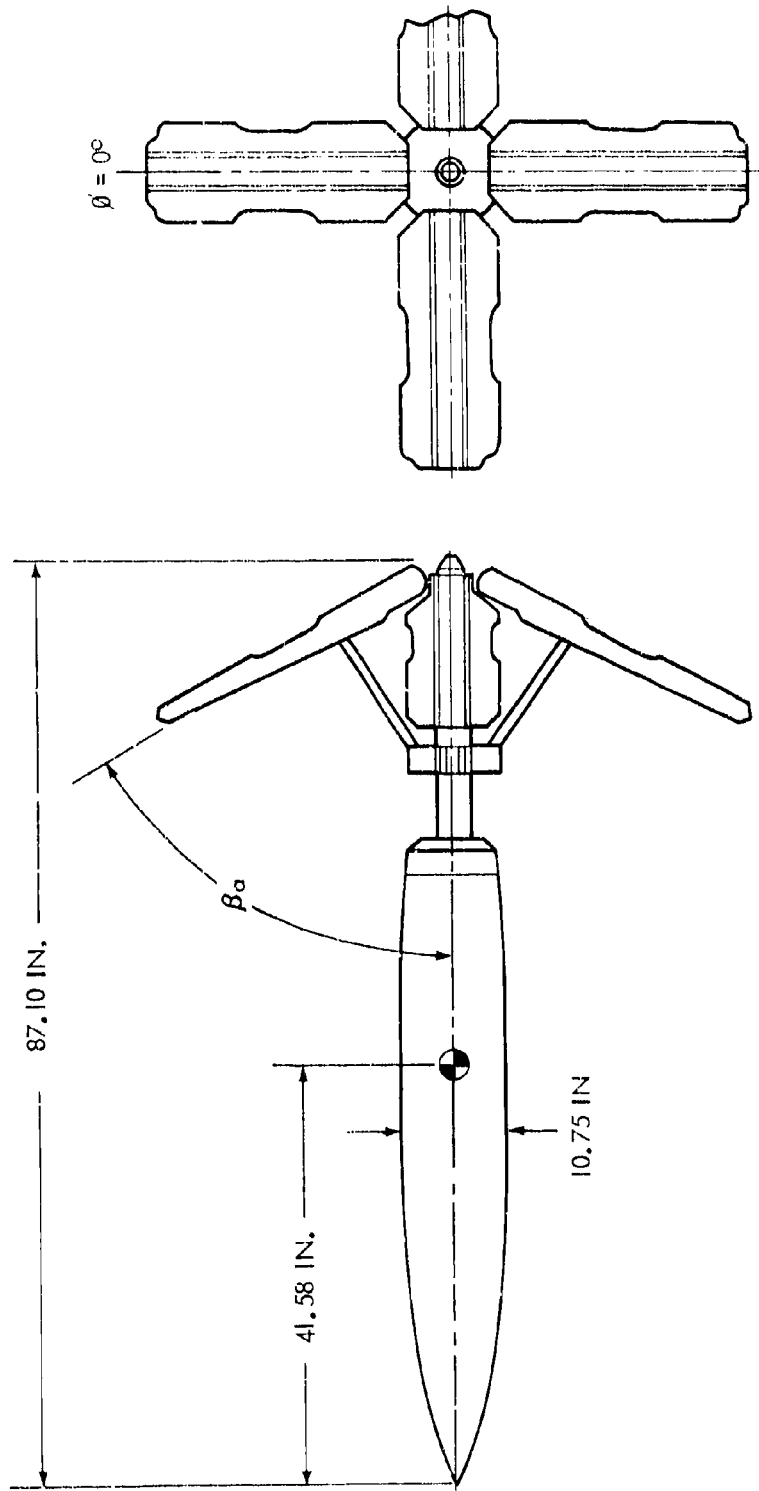


FIG. 2 MK82 LOW DRAG BOMB WITH STANDARD SNAKEYE I FINS

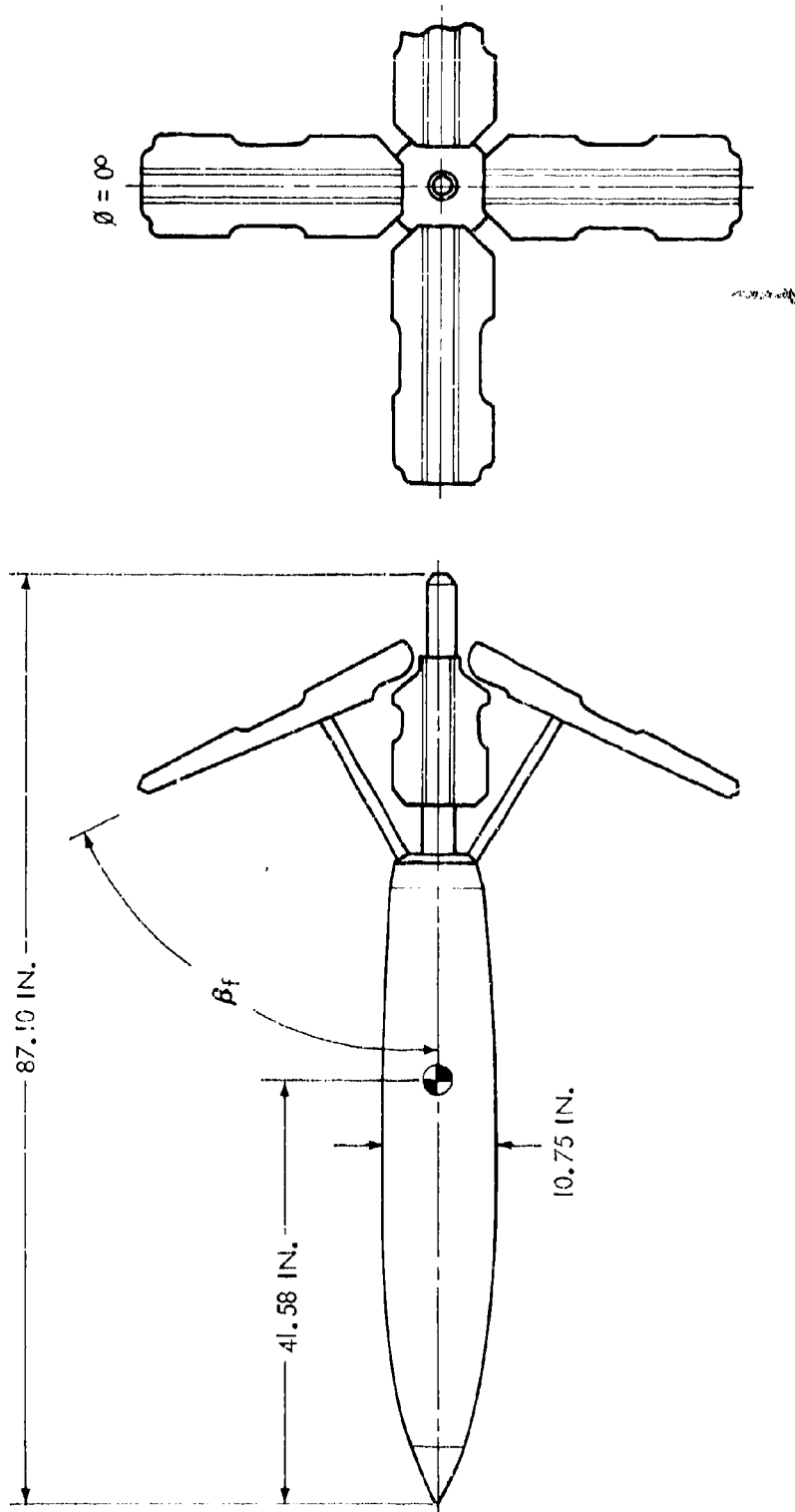
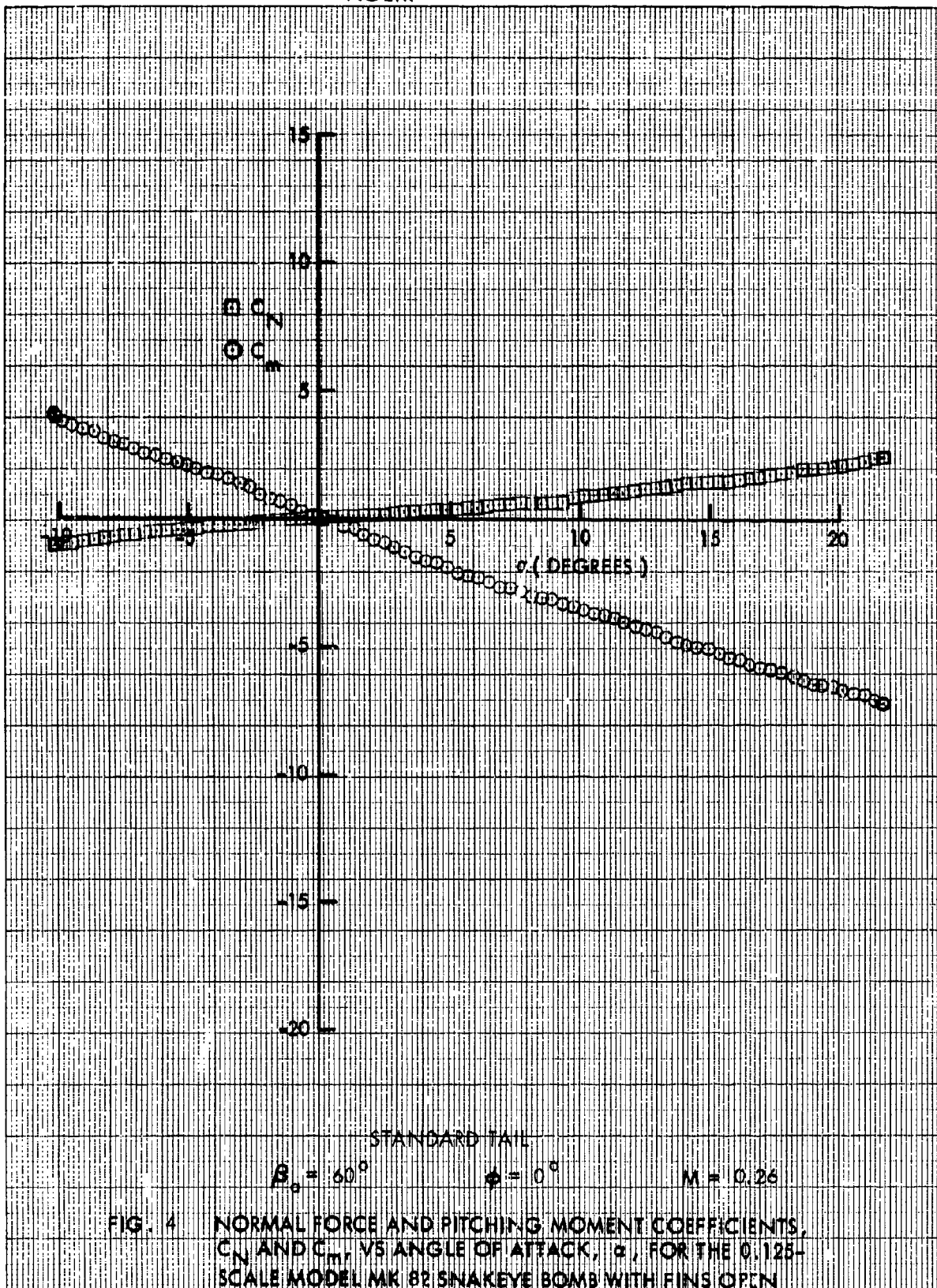
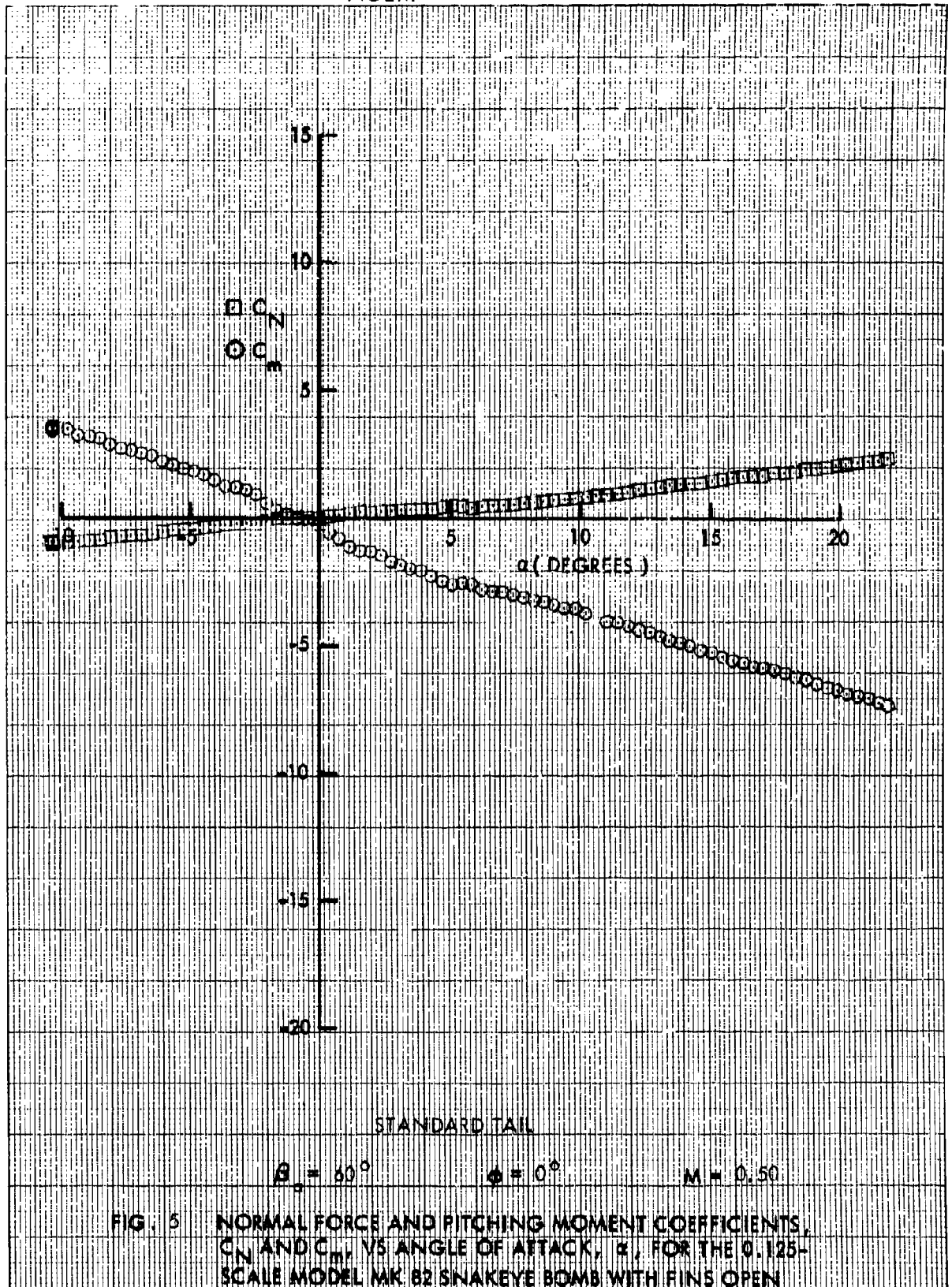
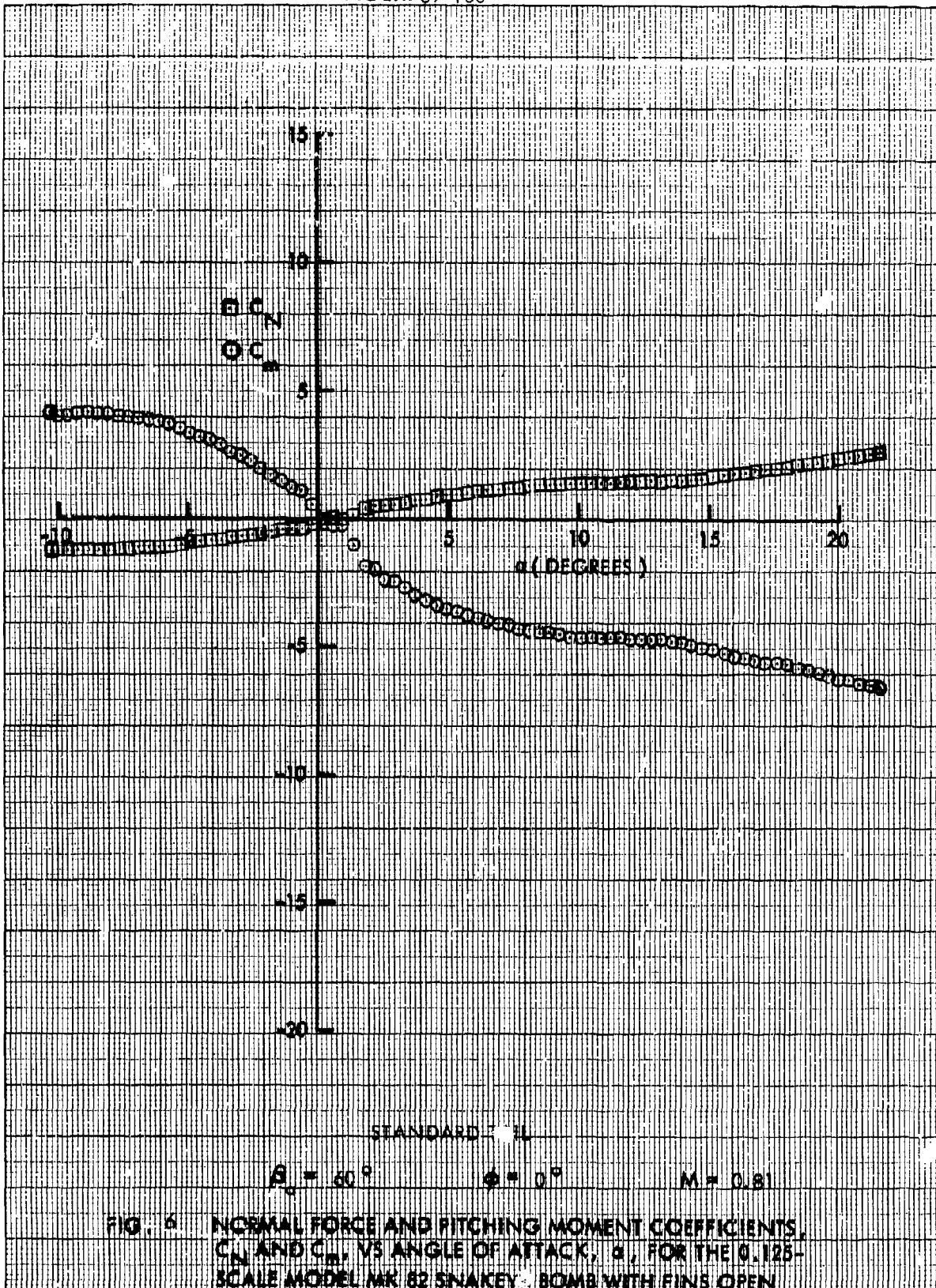


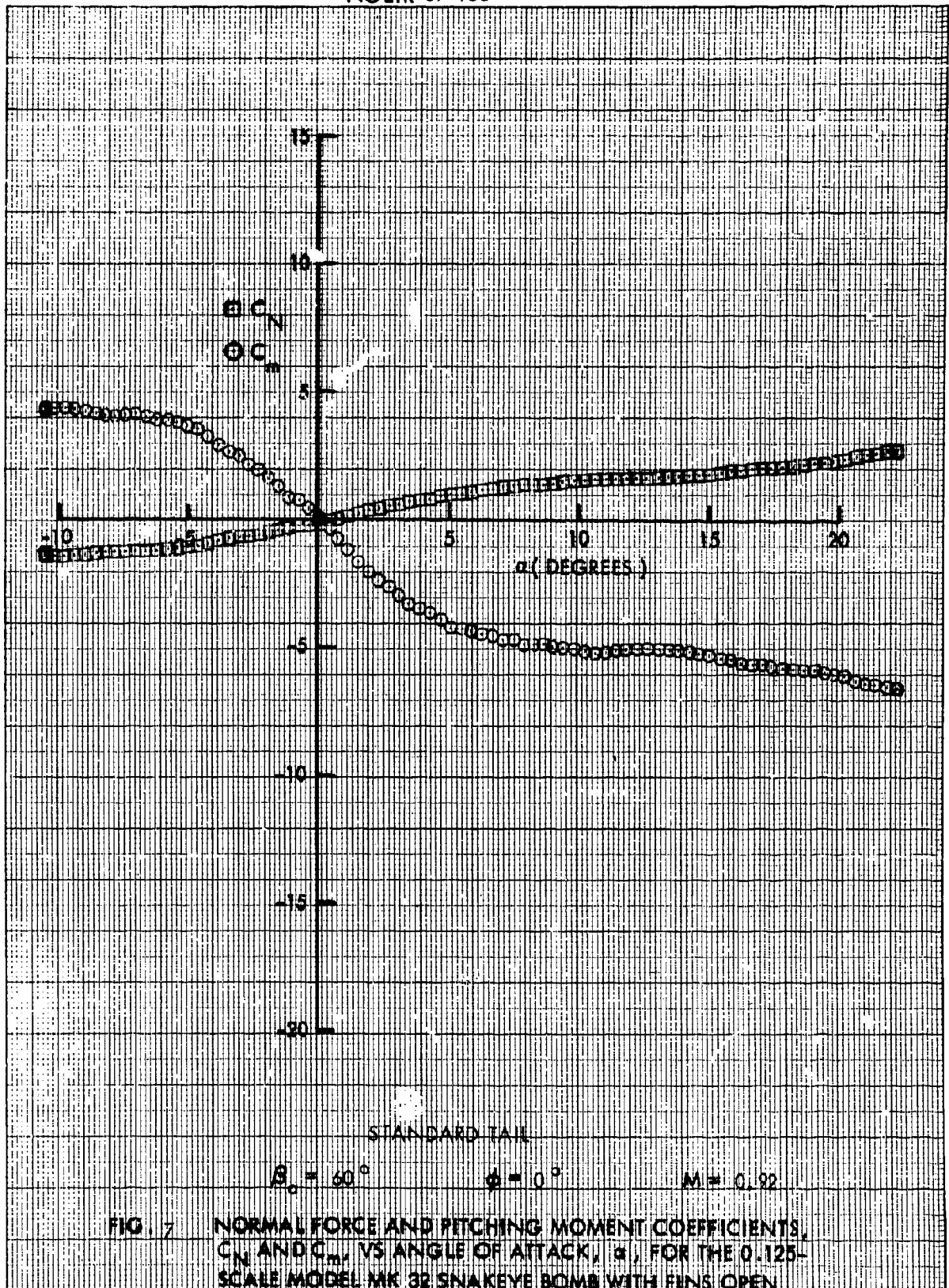
FIG 3 MARK 82 LOW DRAG BOMB WITH EMTEx SNAKEYE I FINS

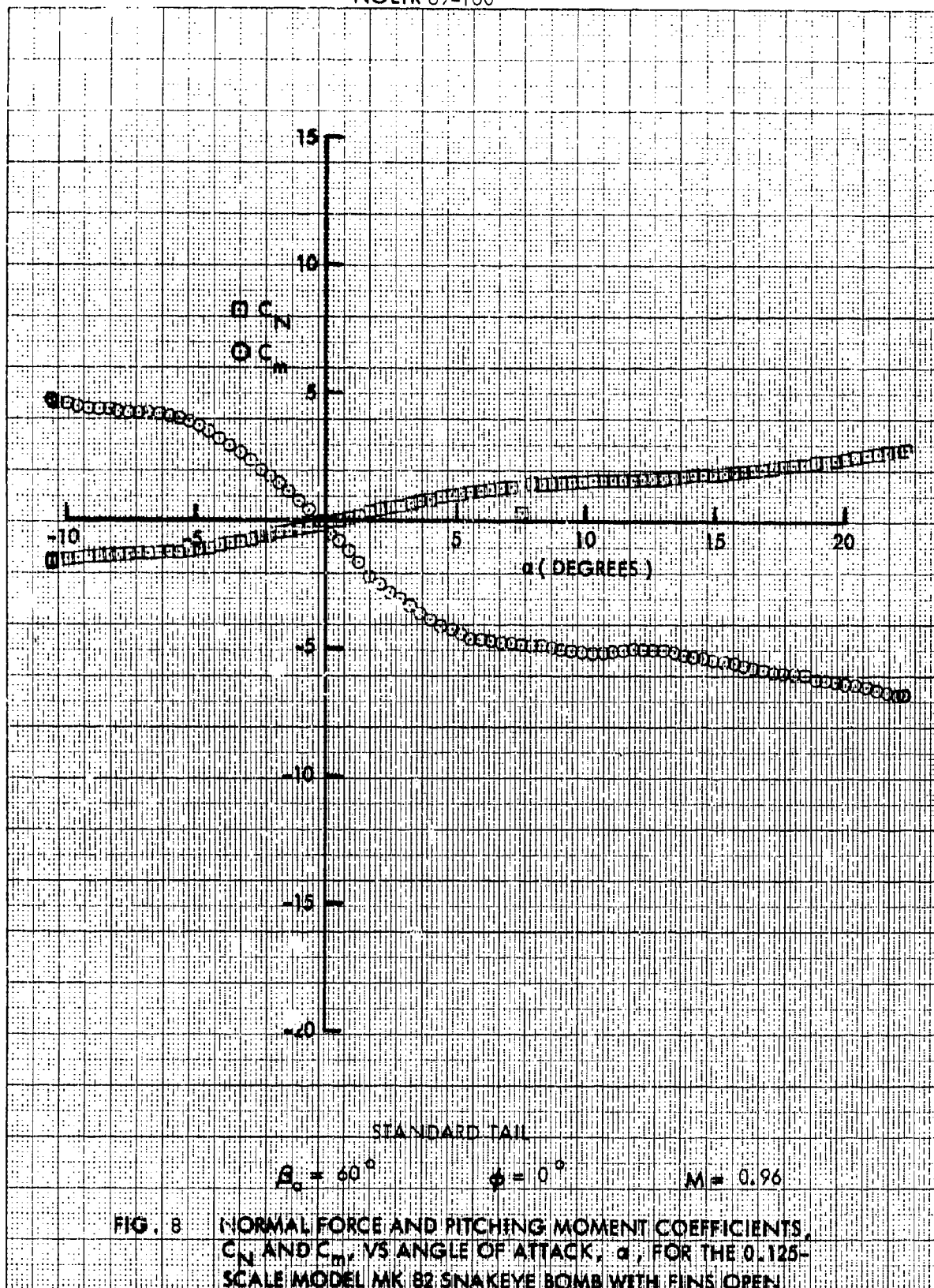




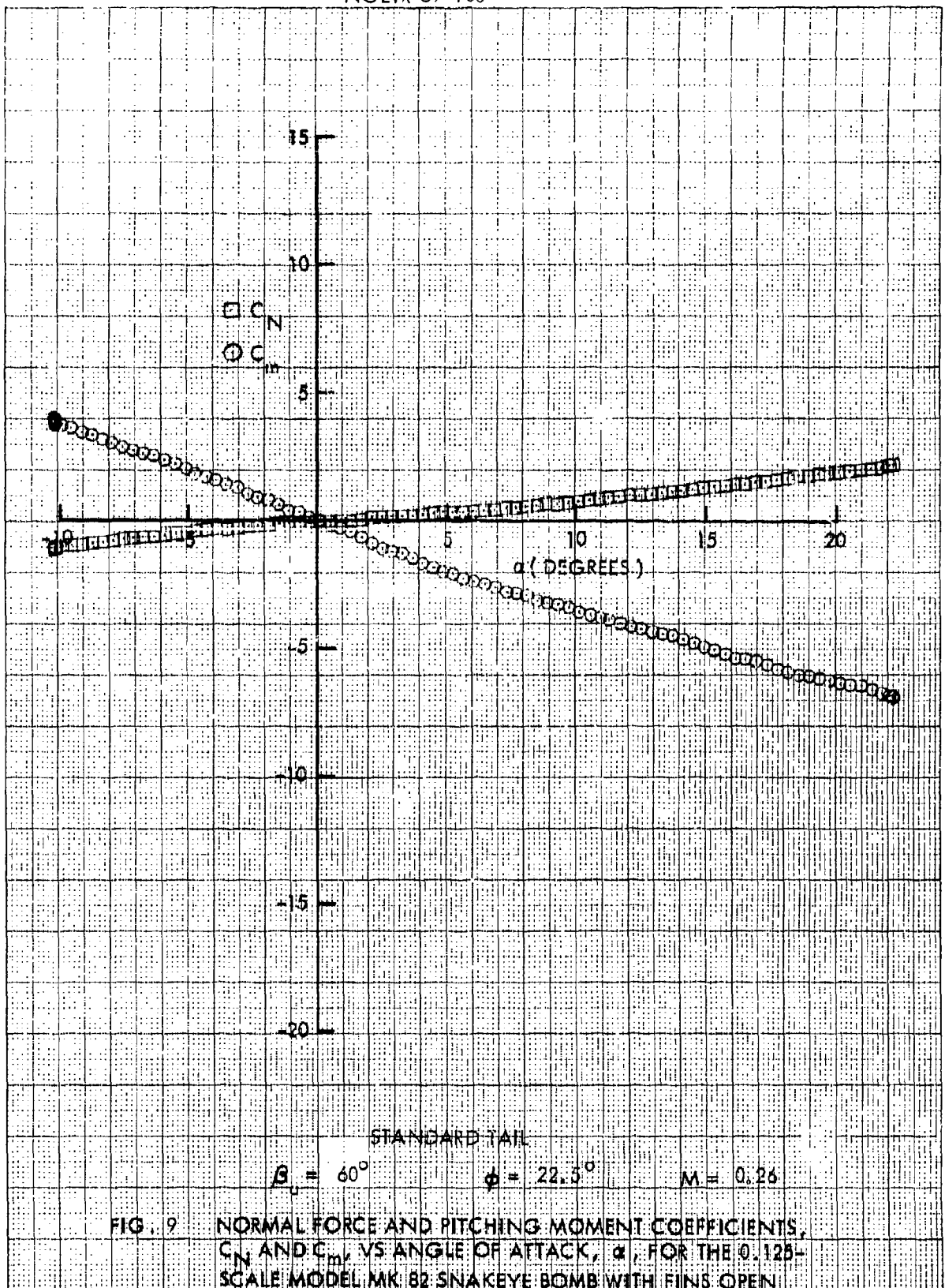


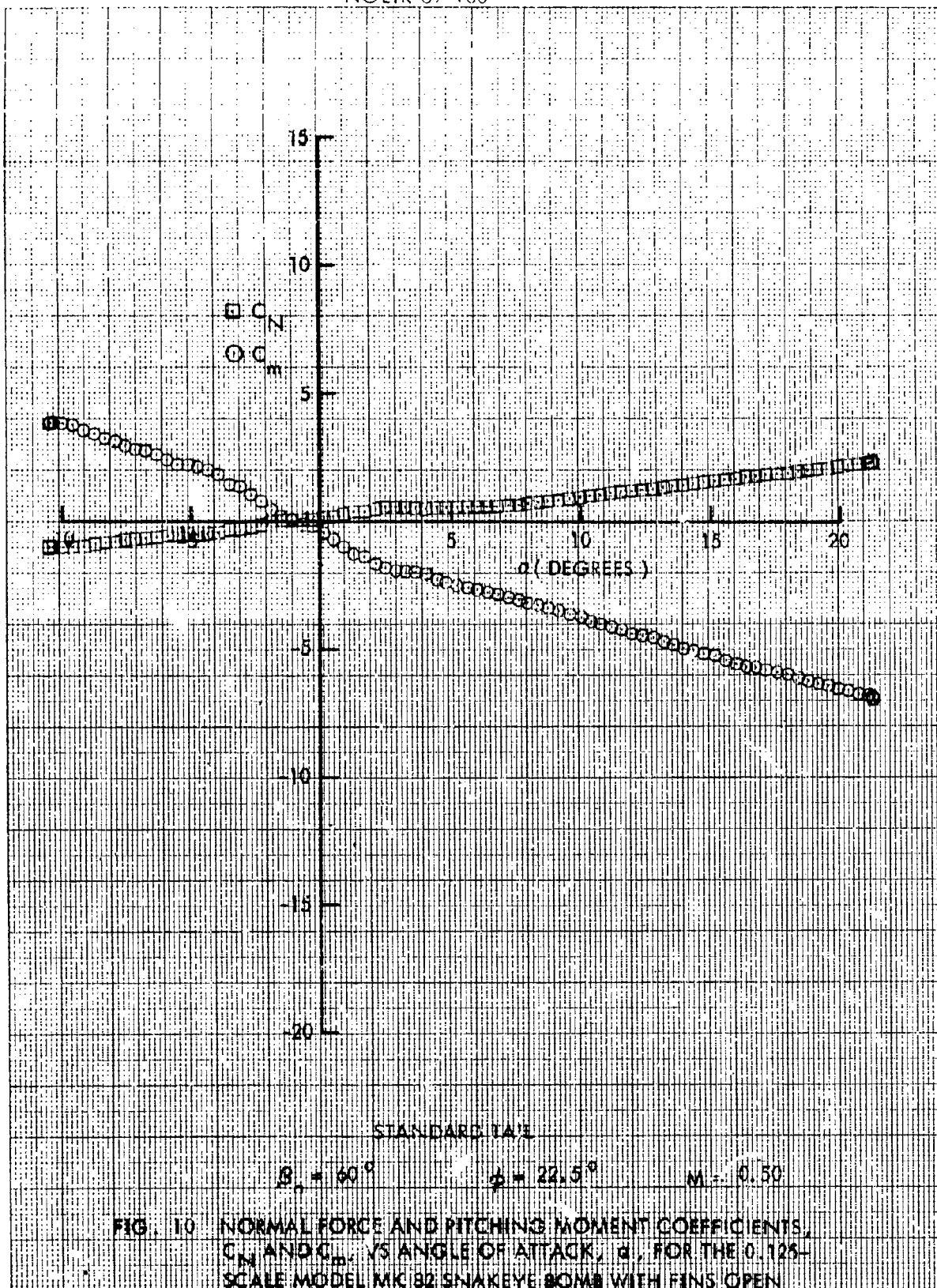












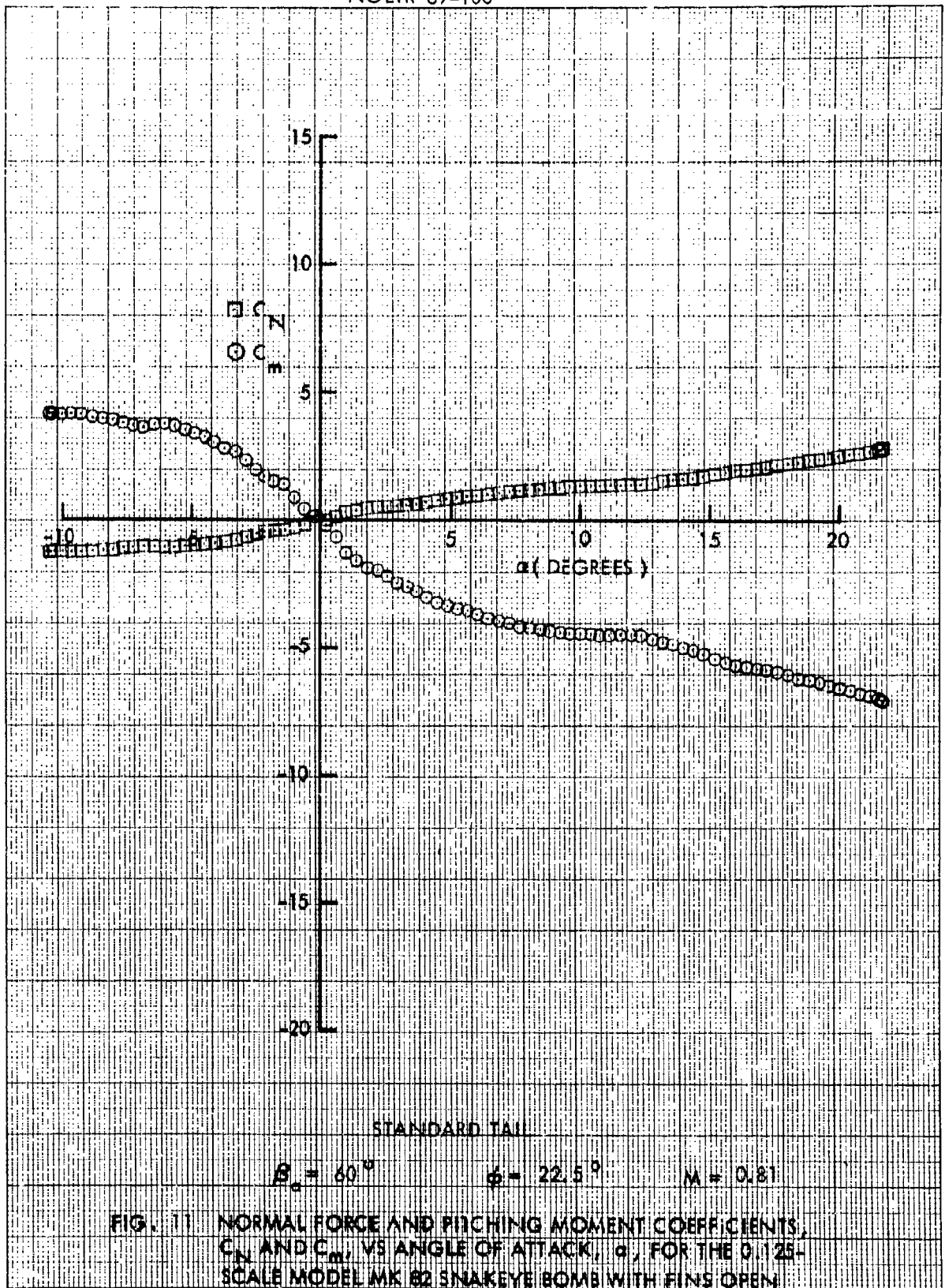
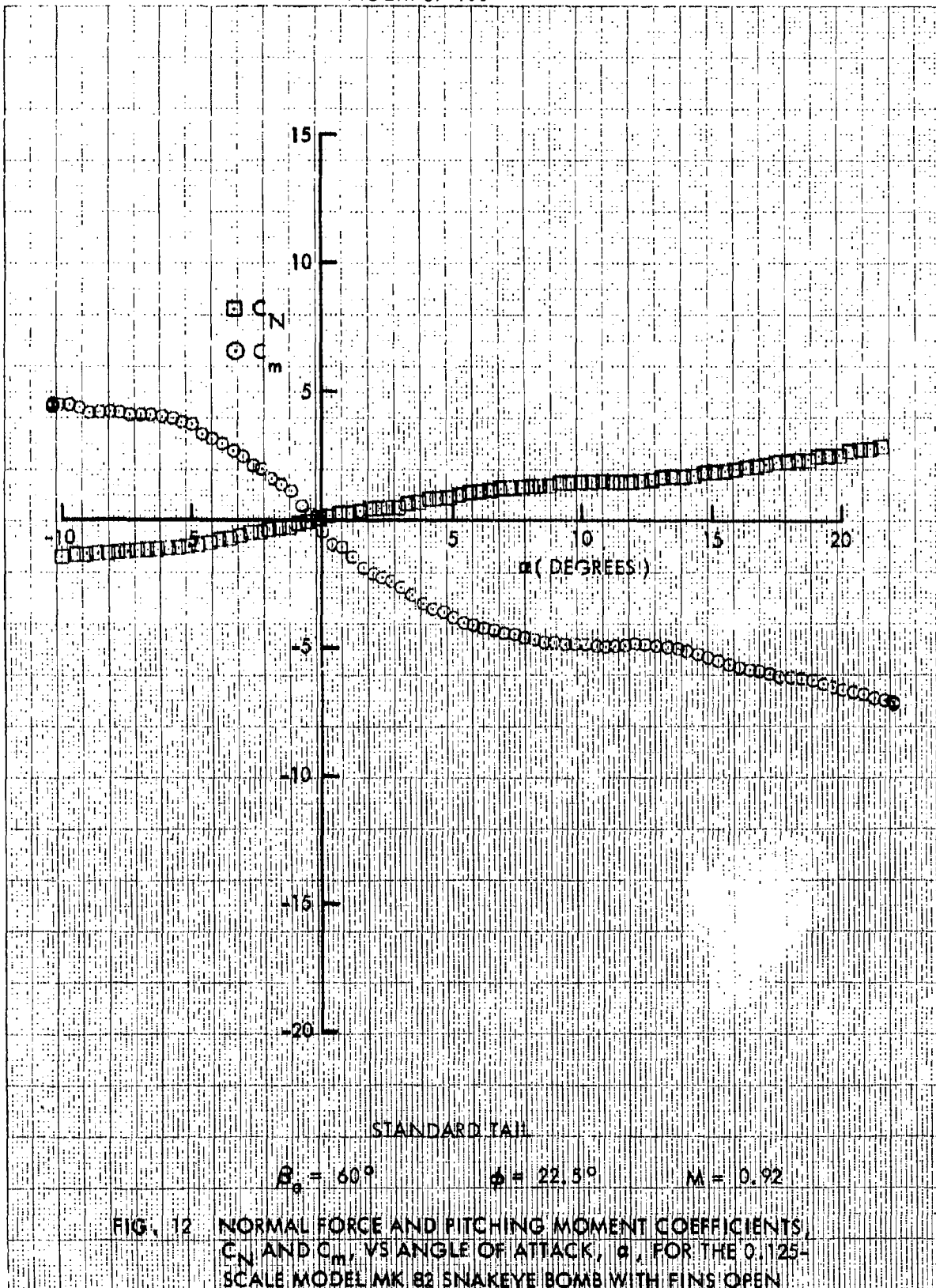
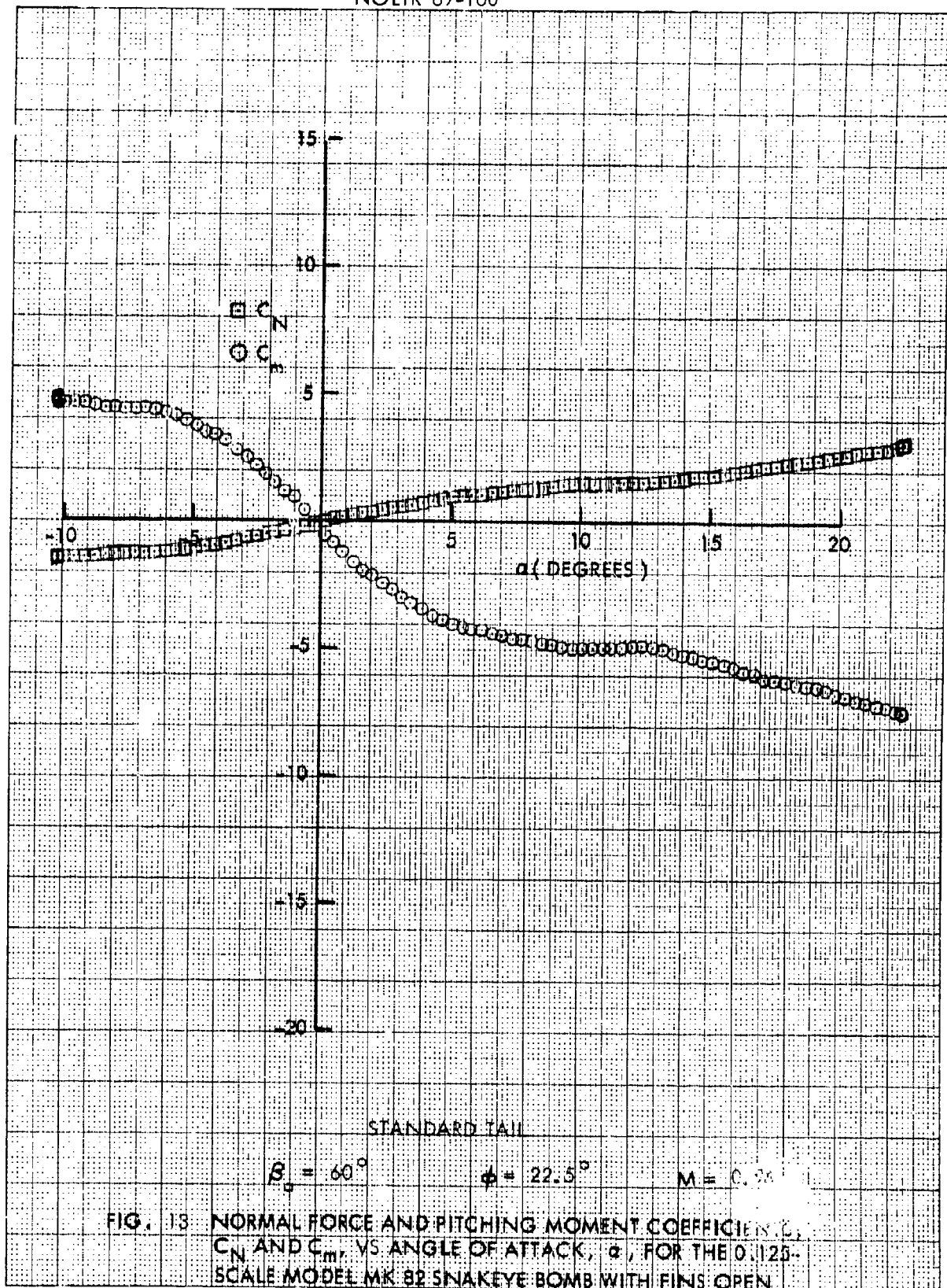
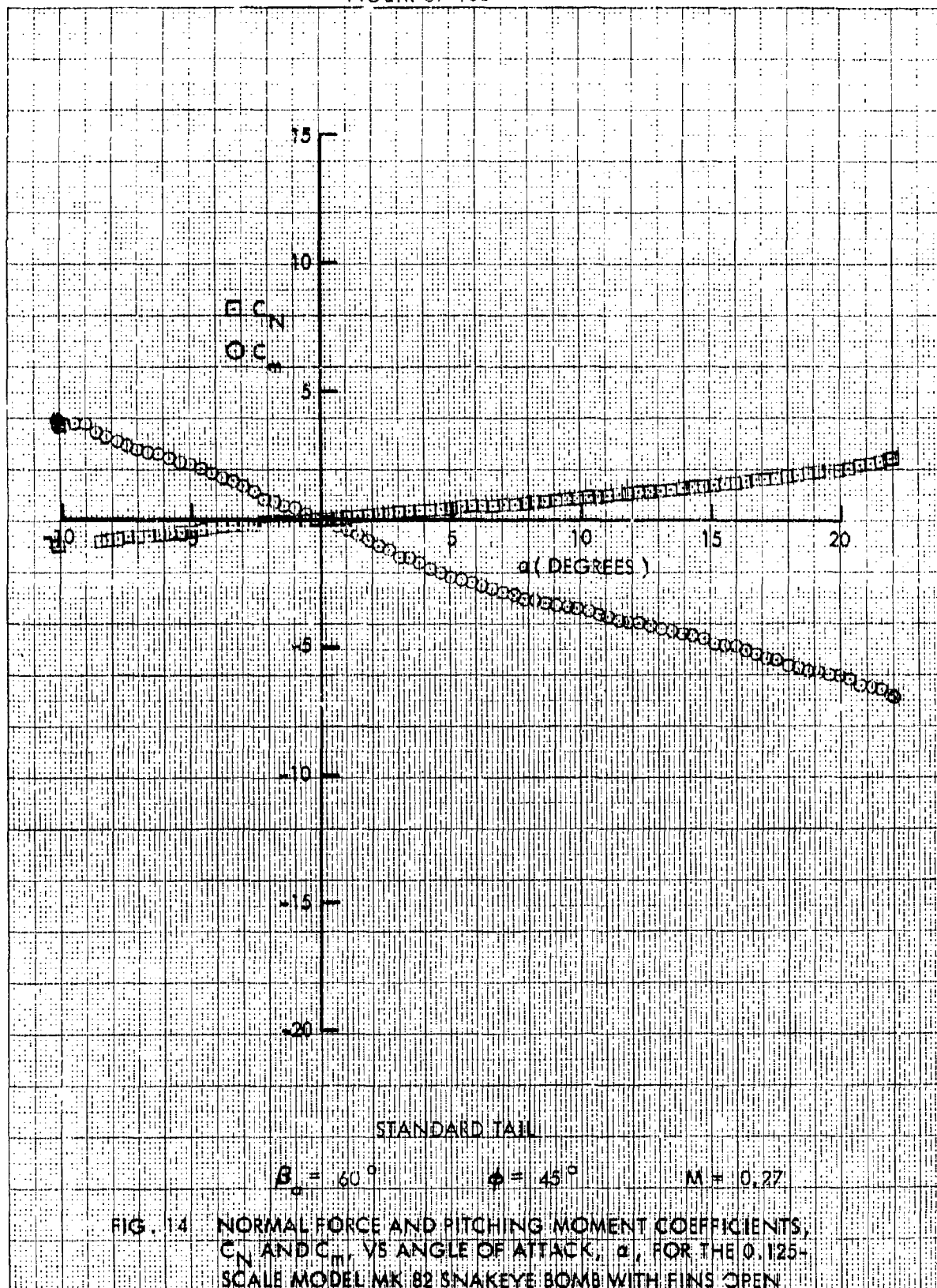


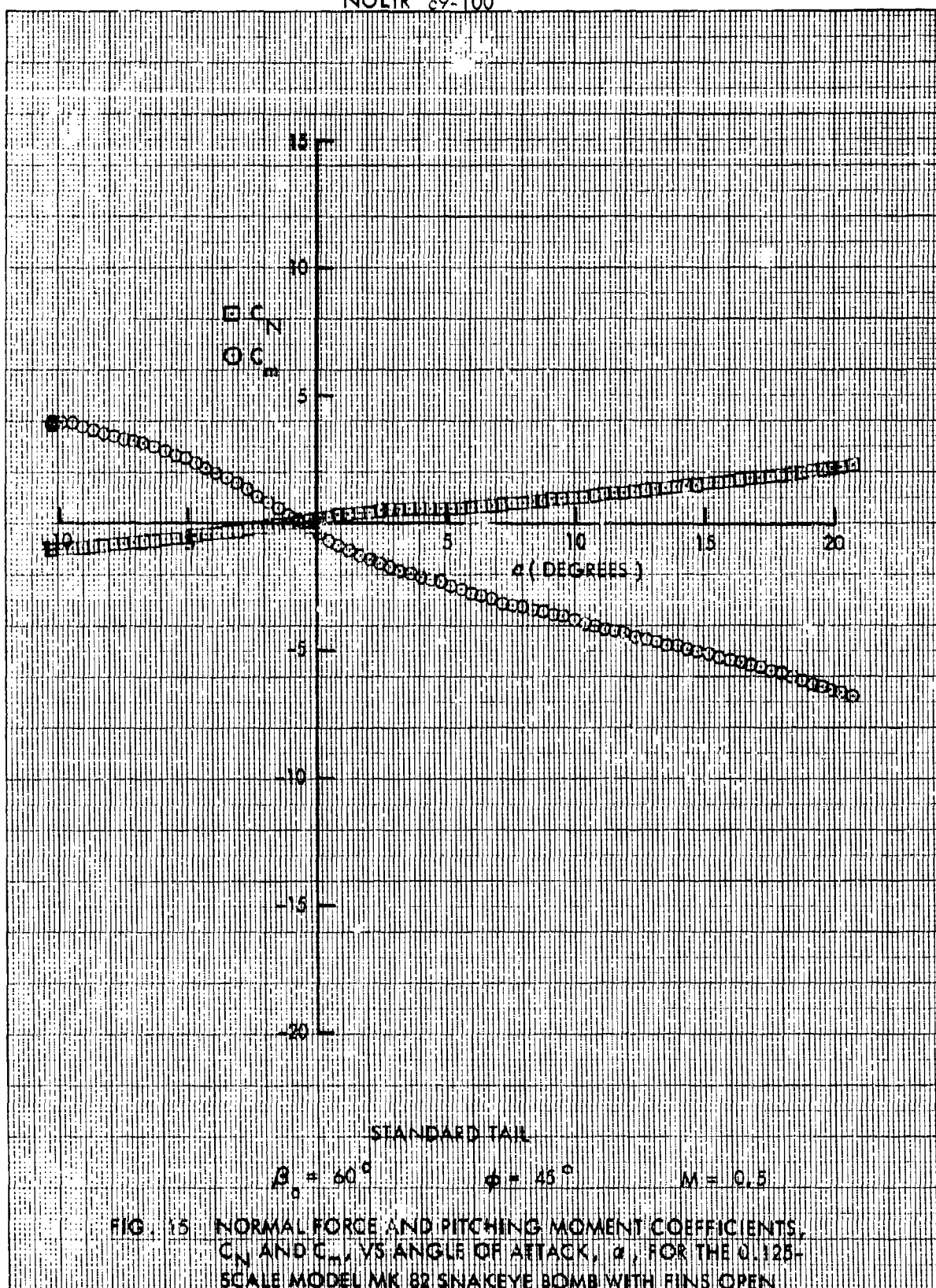
FIG. 11 NORMAL FORCE AND PITCHING MOMENT COEFFICIENTS,  $C_N$  AND  $C_m$ , VS ANGLE OF ATTACK,  $\alpha$ , FOR THE 0.125-SCALE MODEL MK 82 SNAKEYE BOMB WITH FINS OPEN

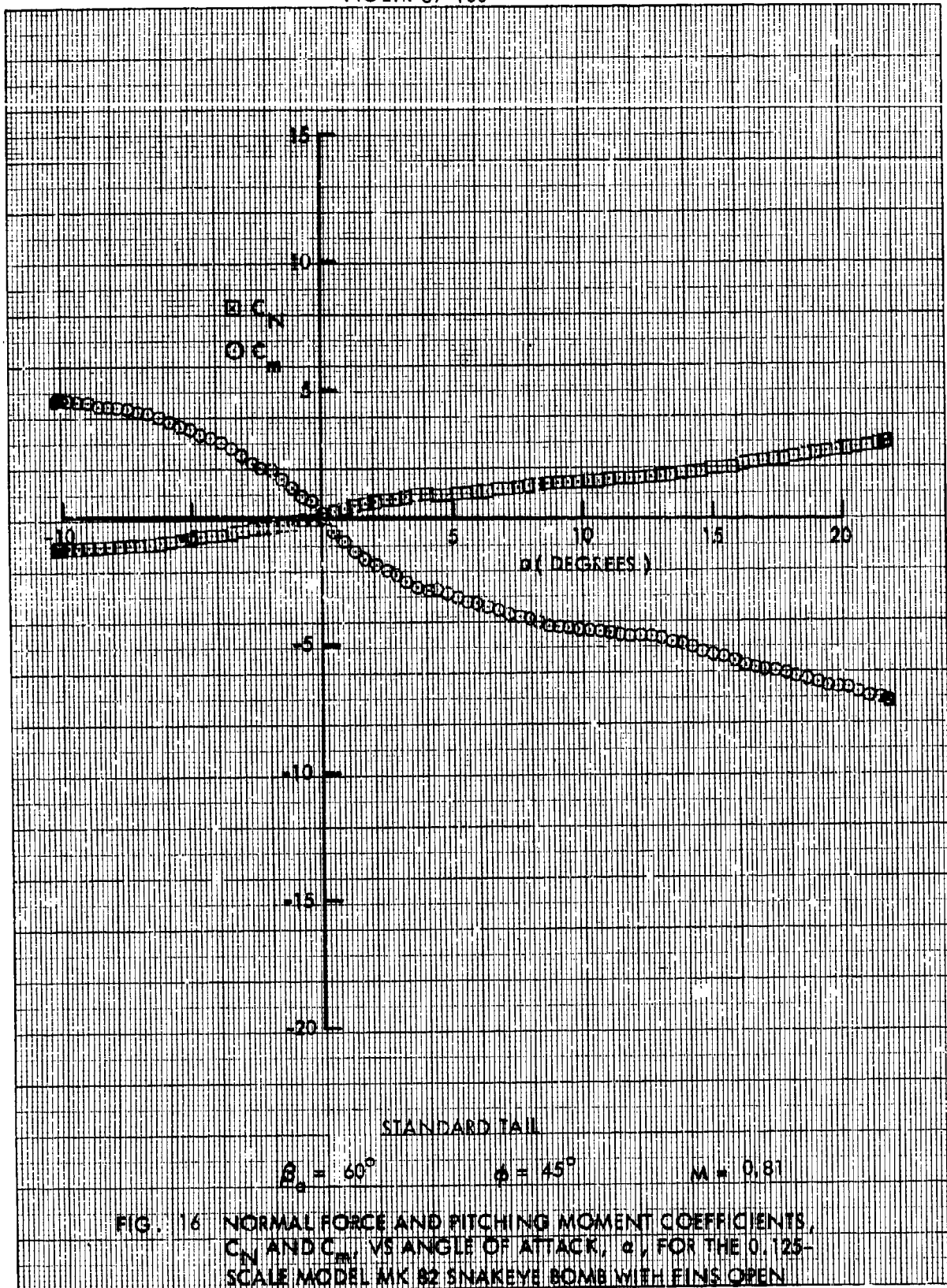


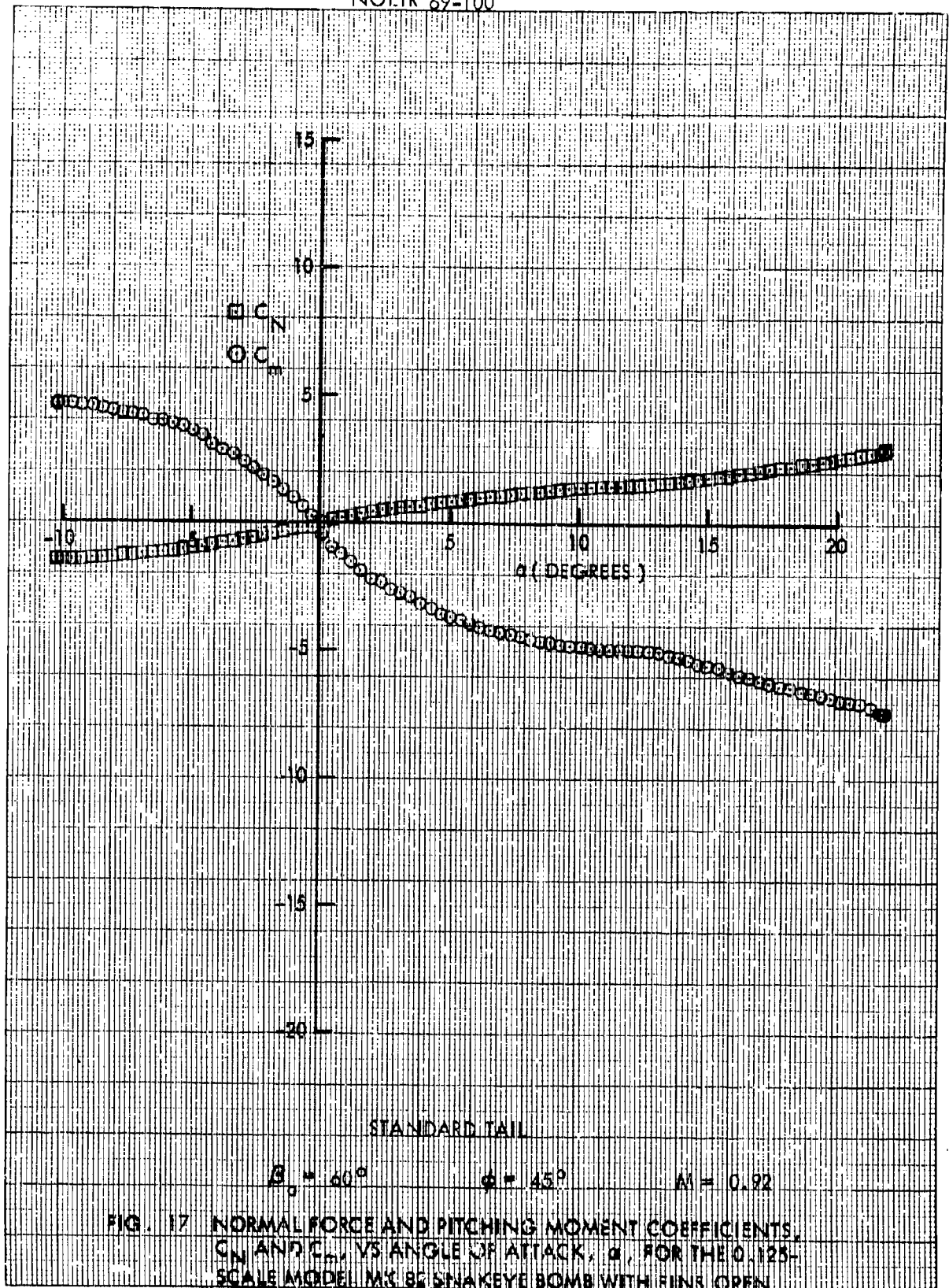




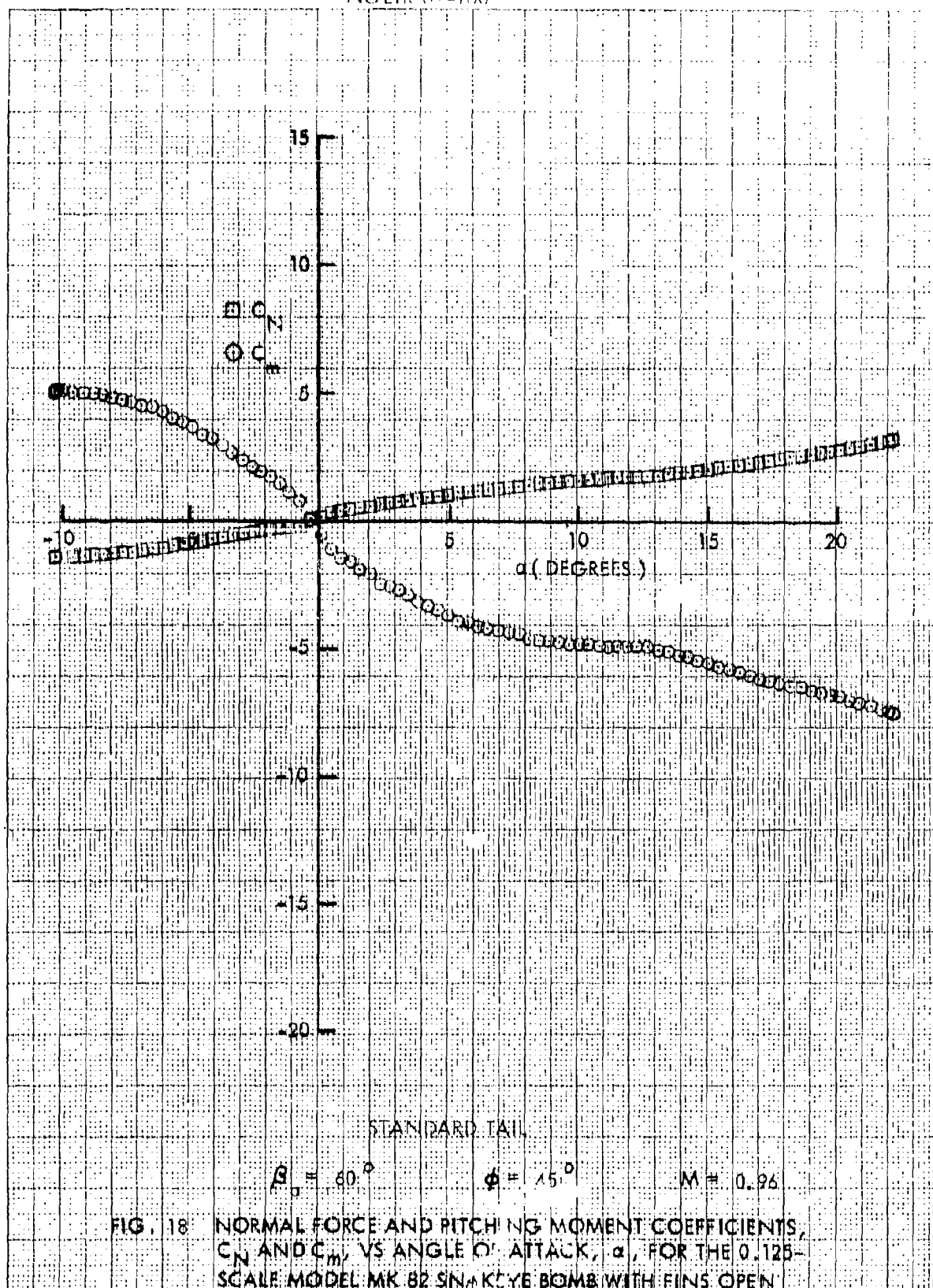


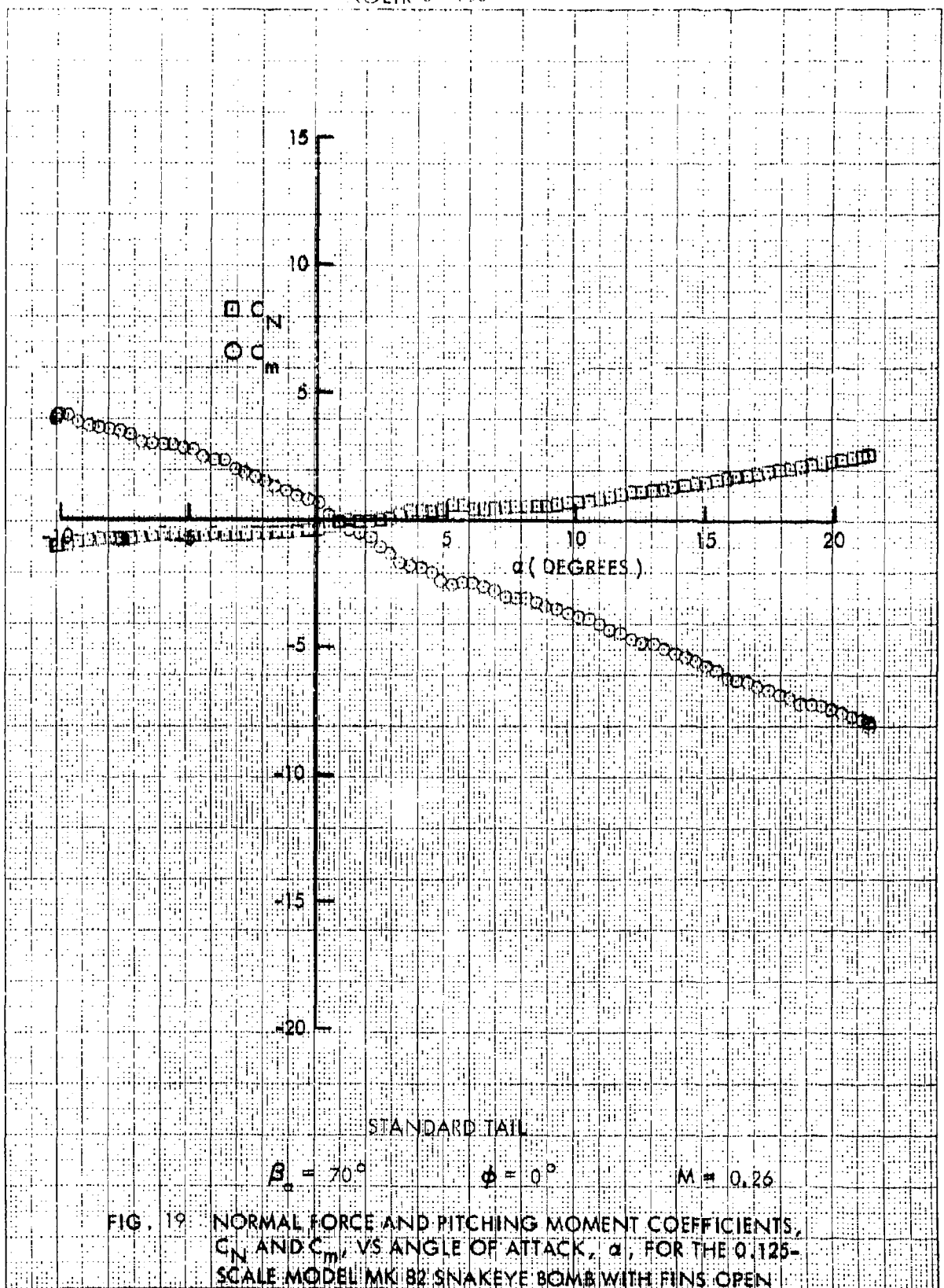




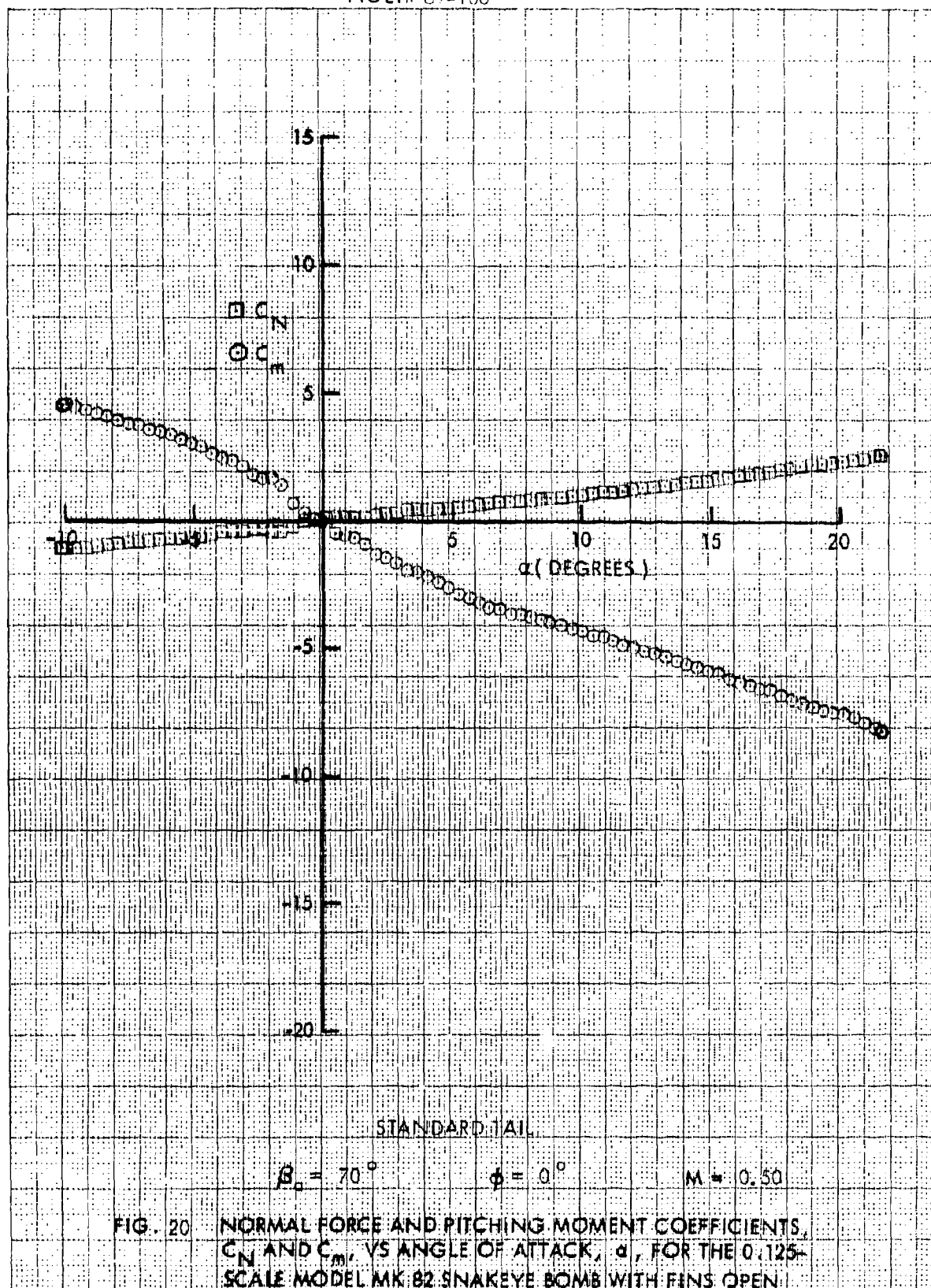


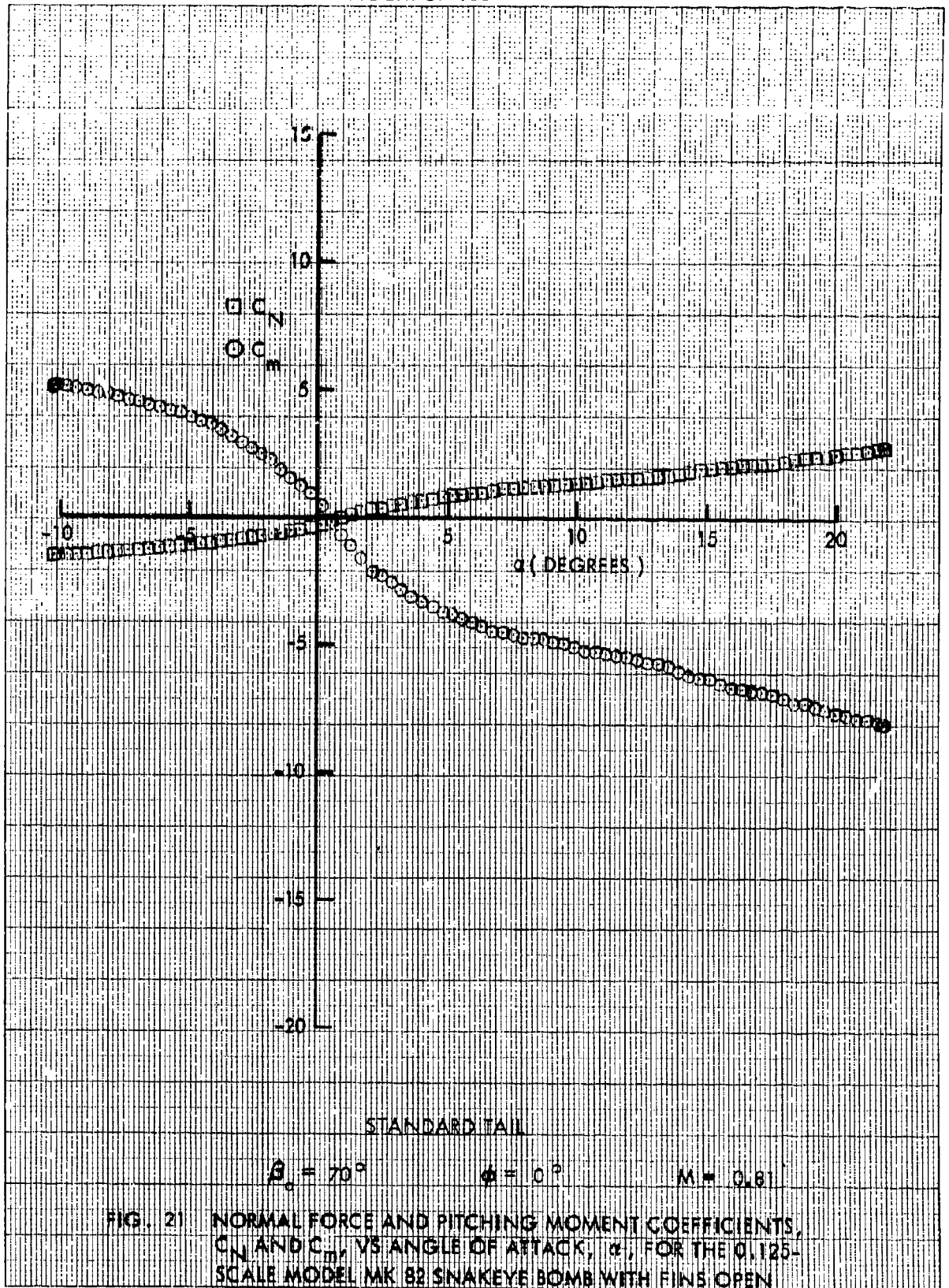


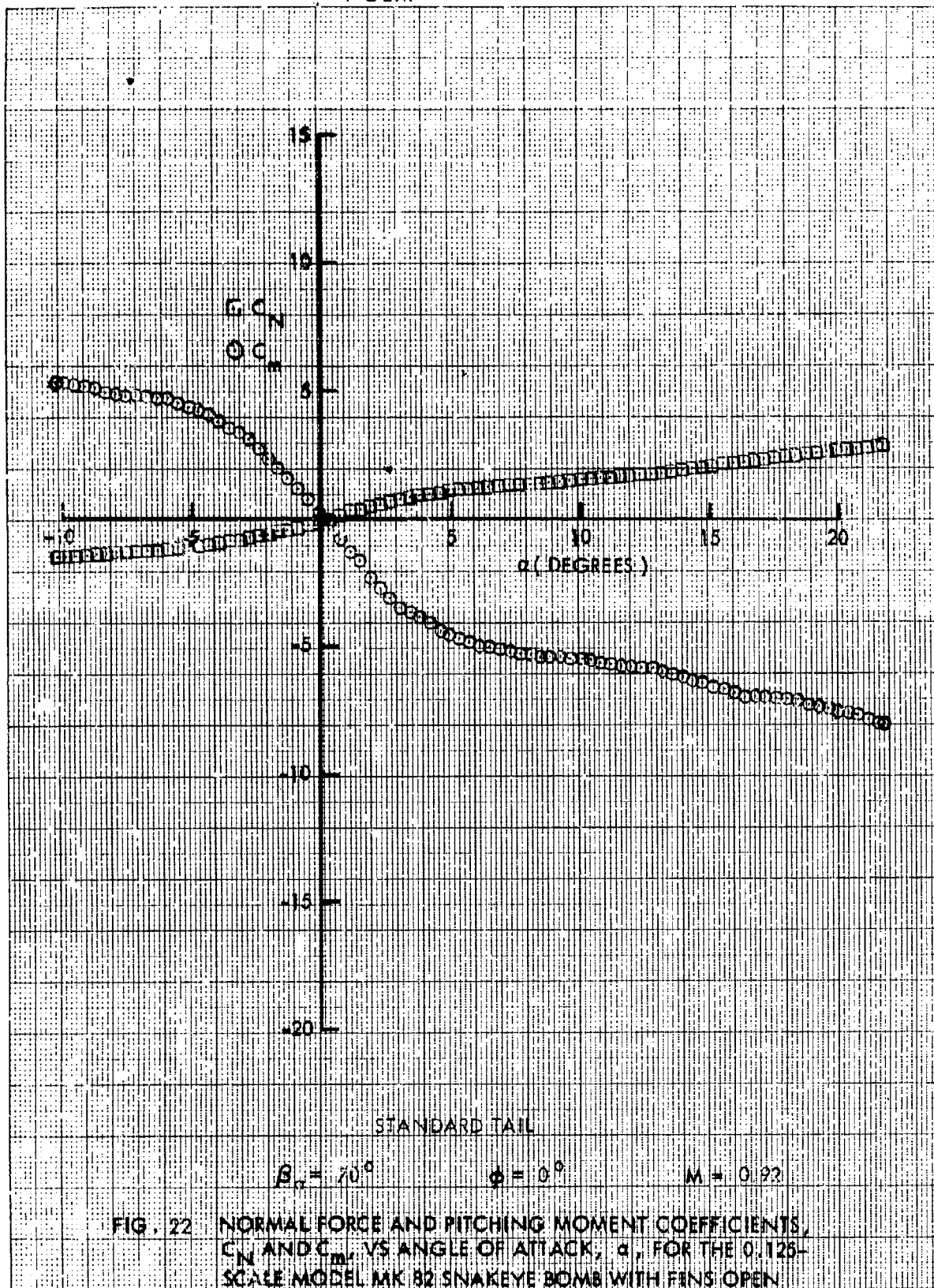


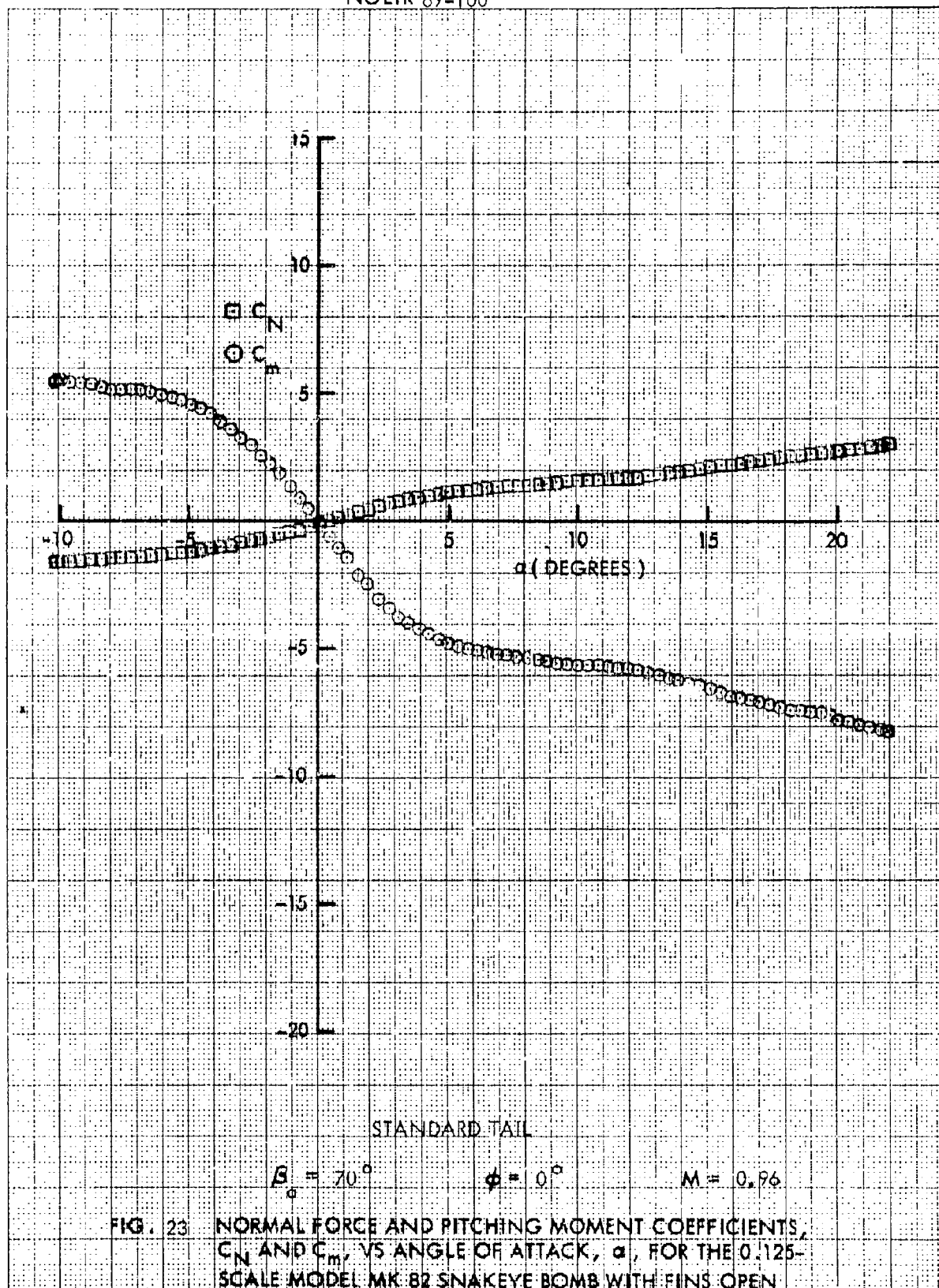


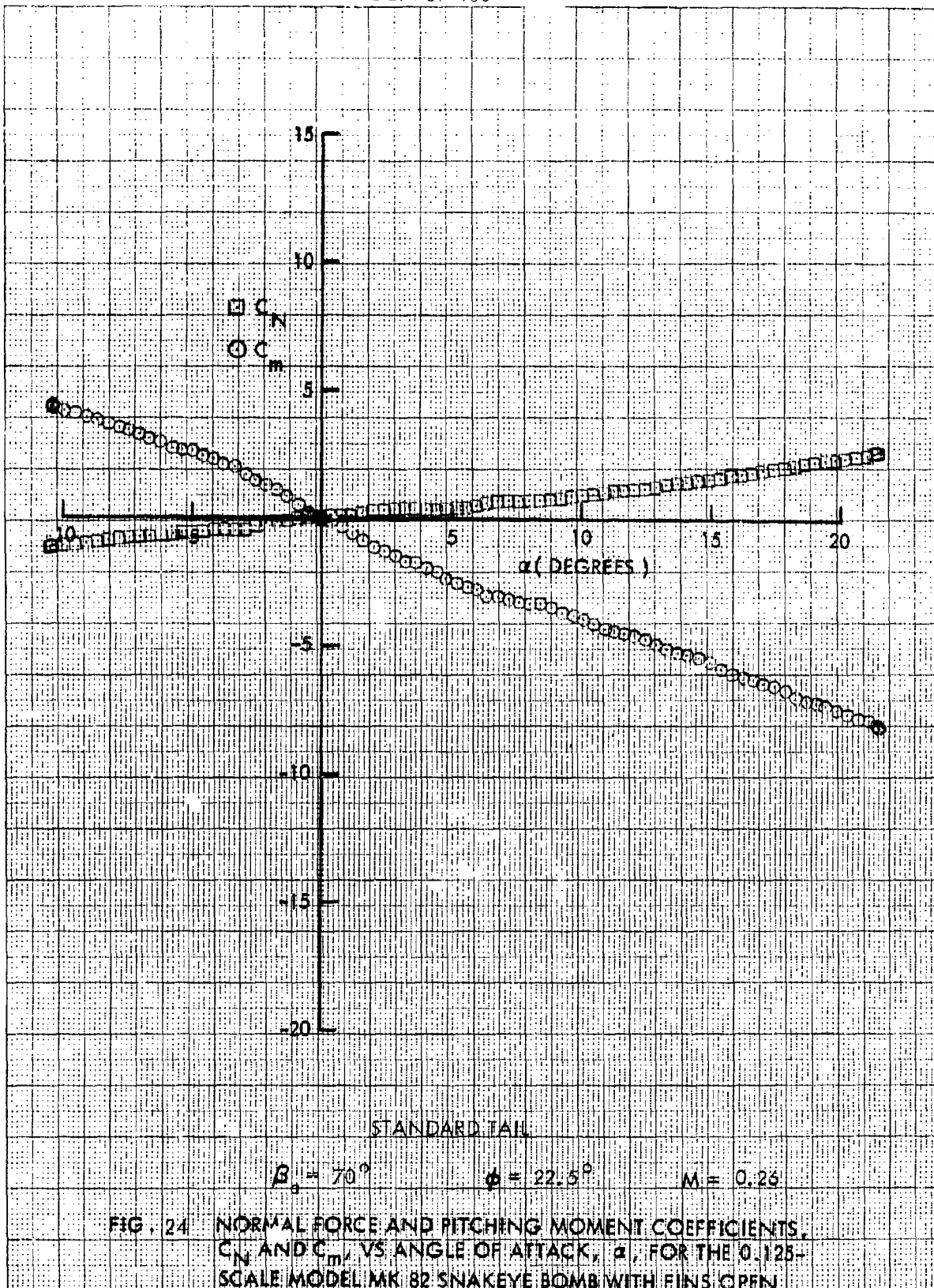


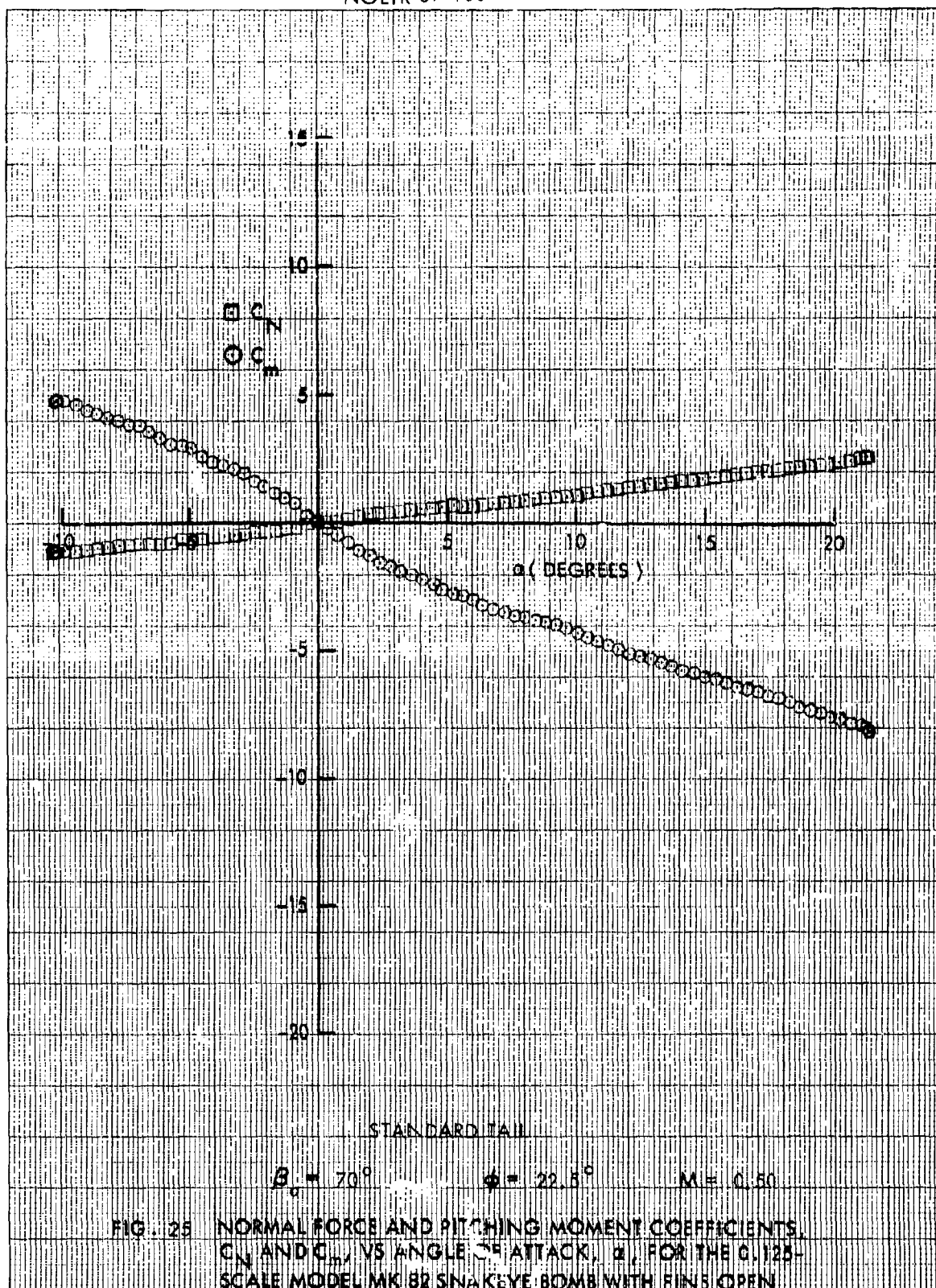




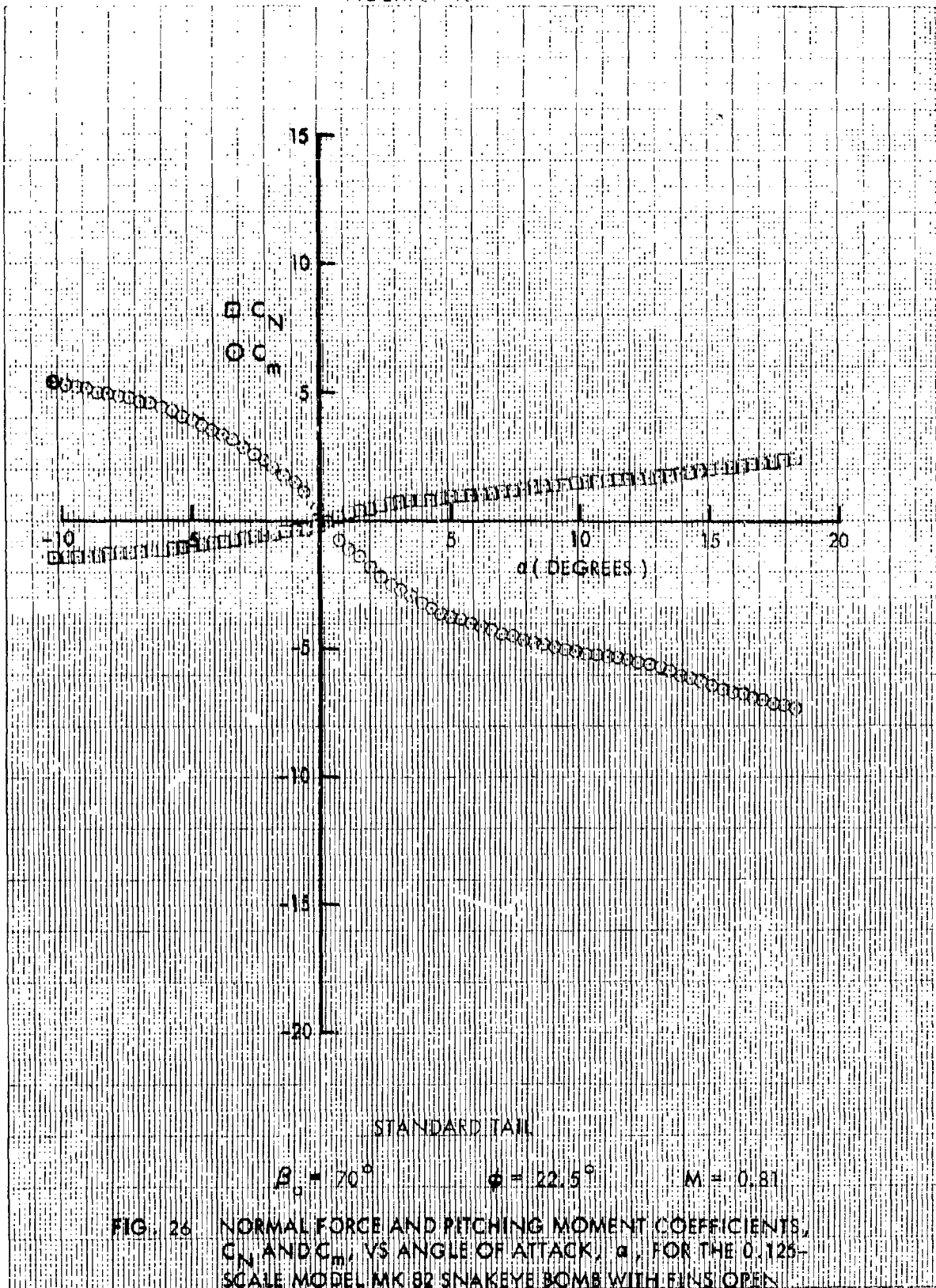


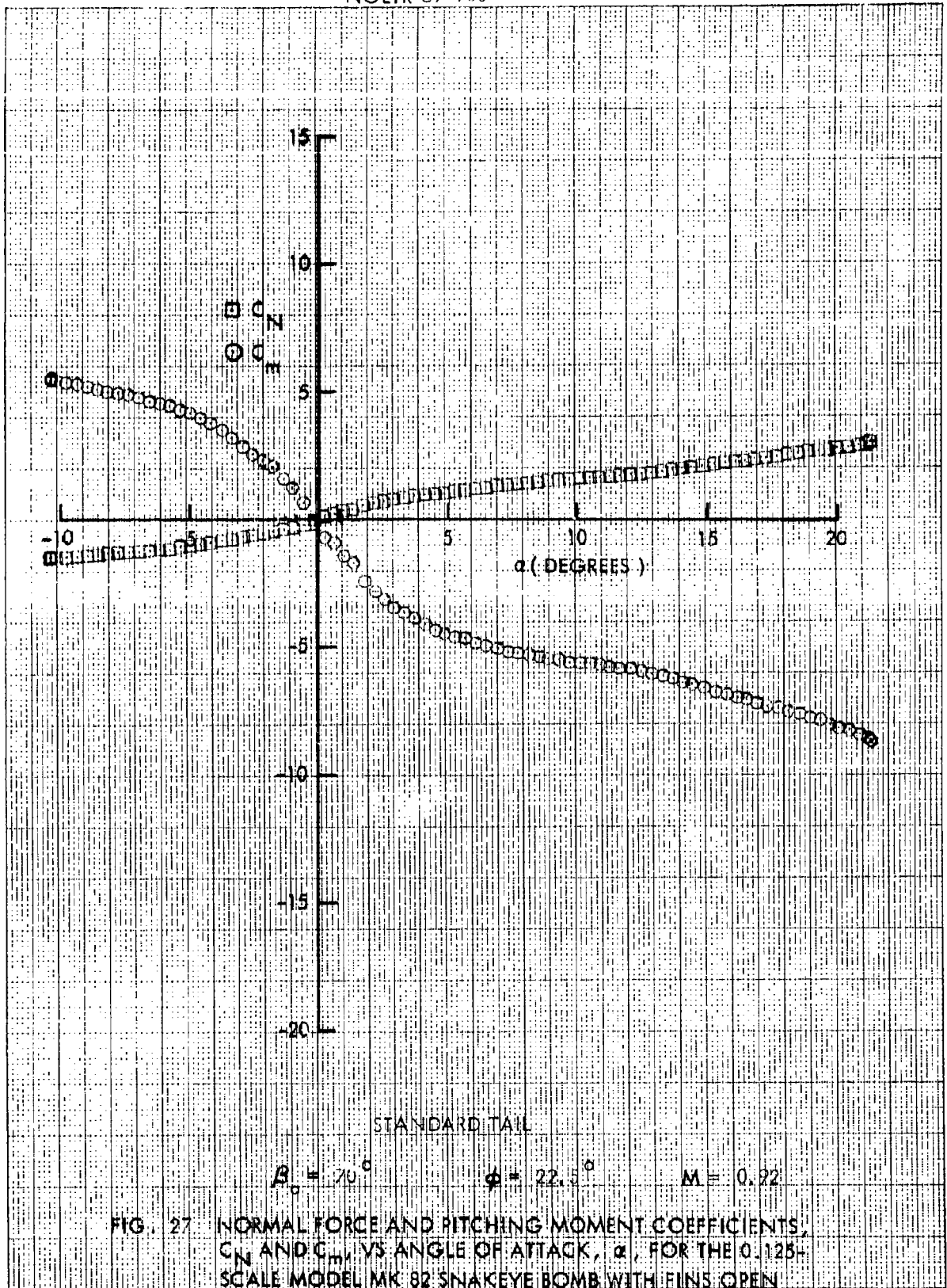




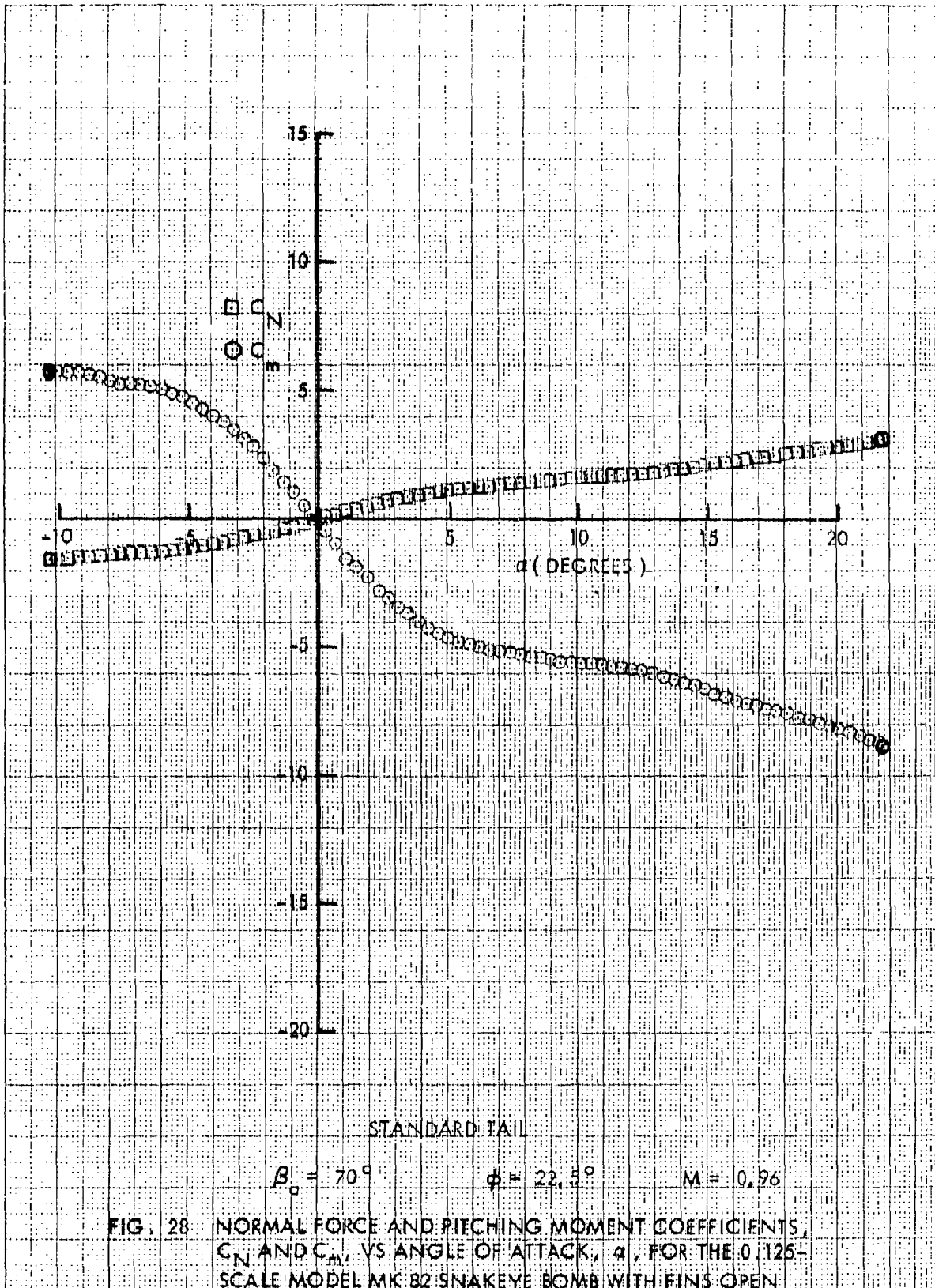


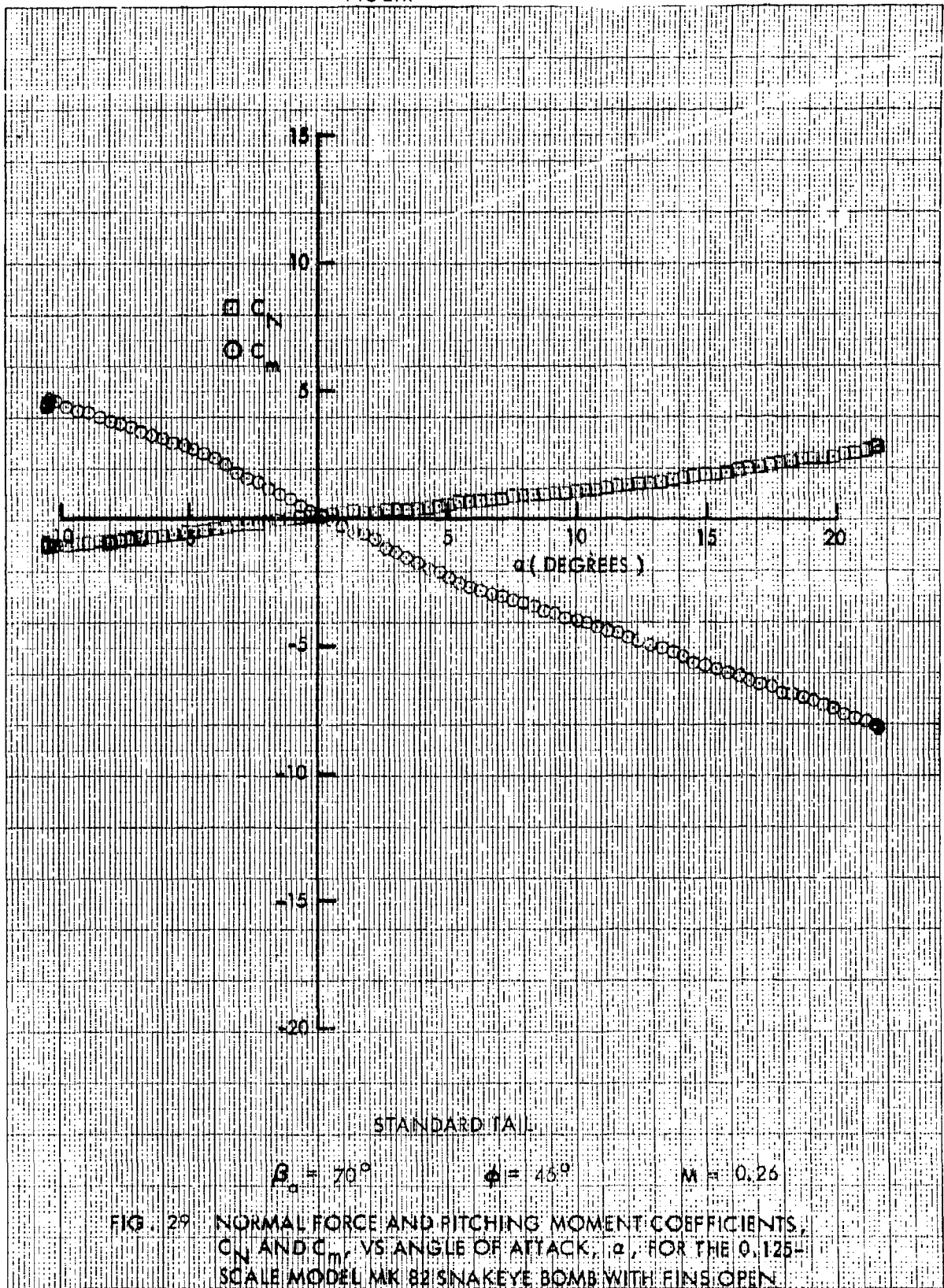


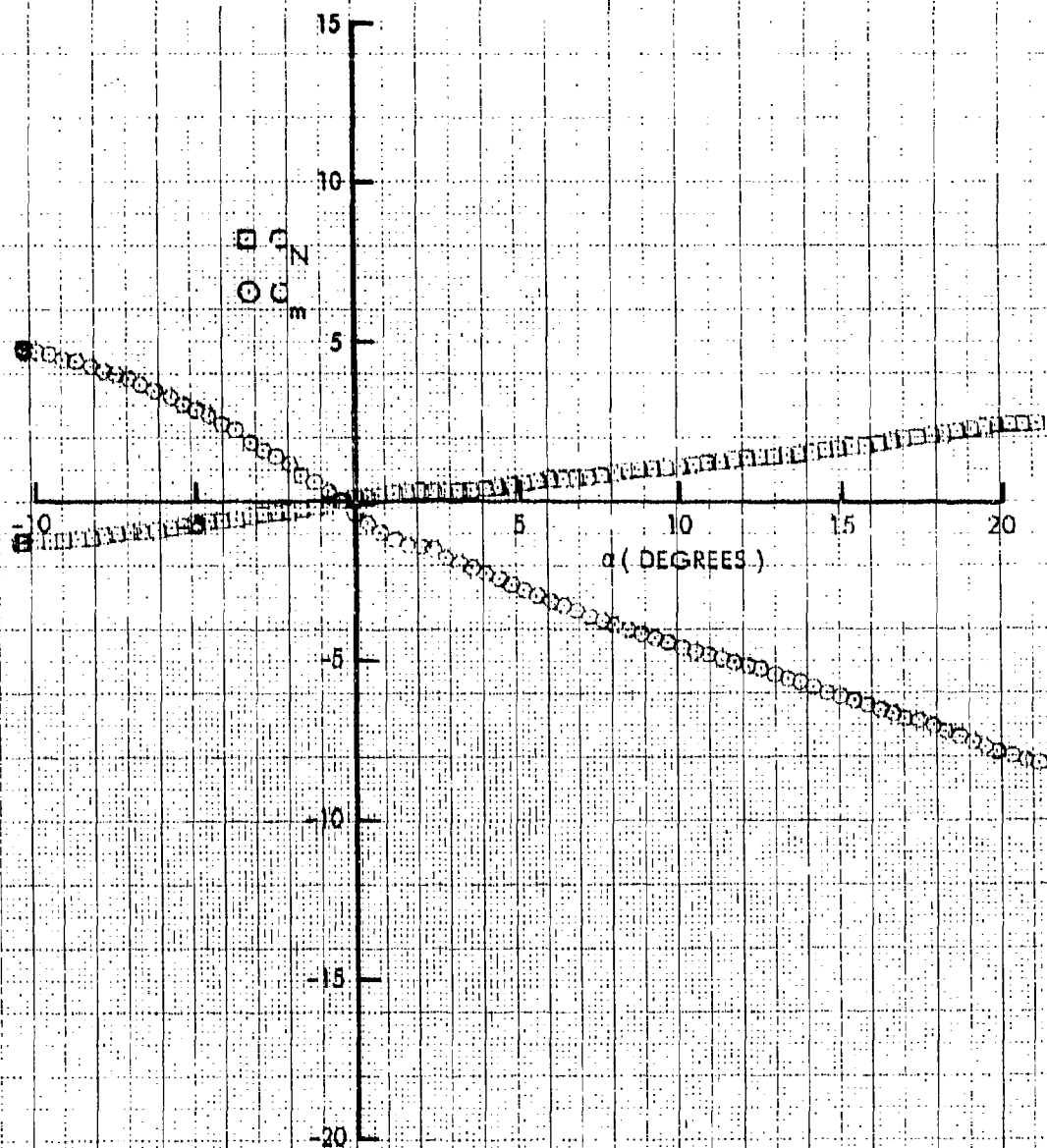












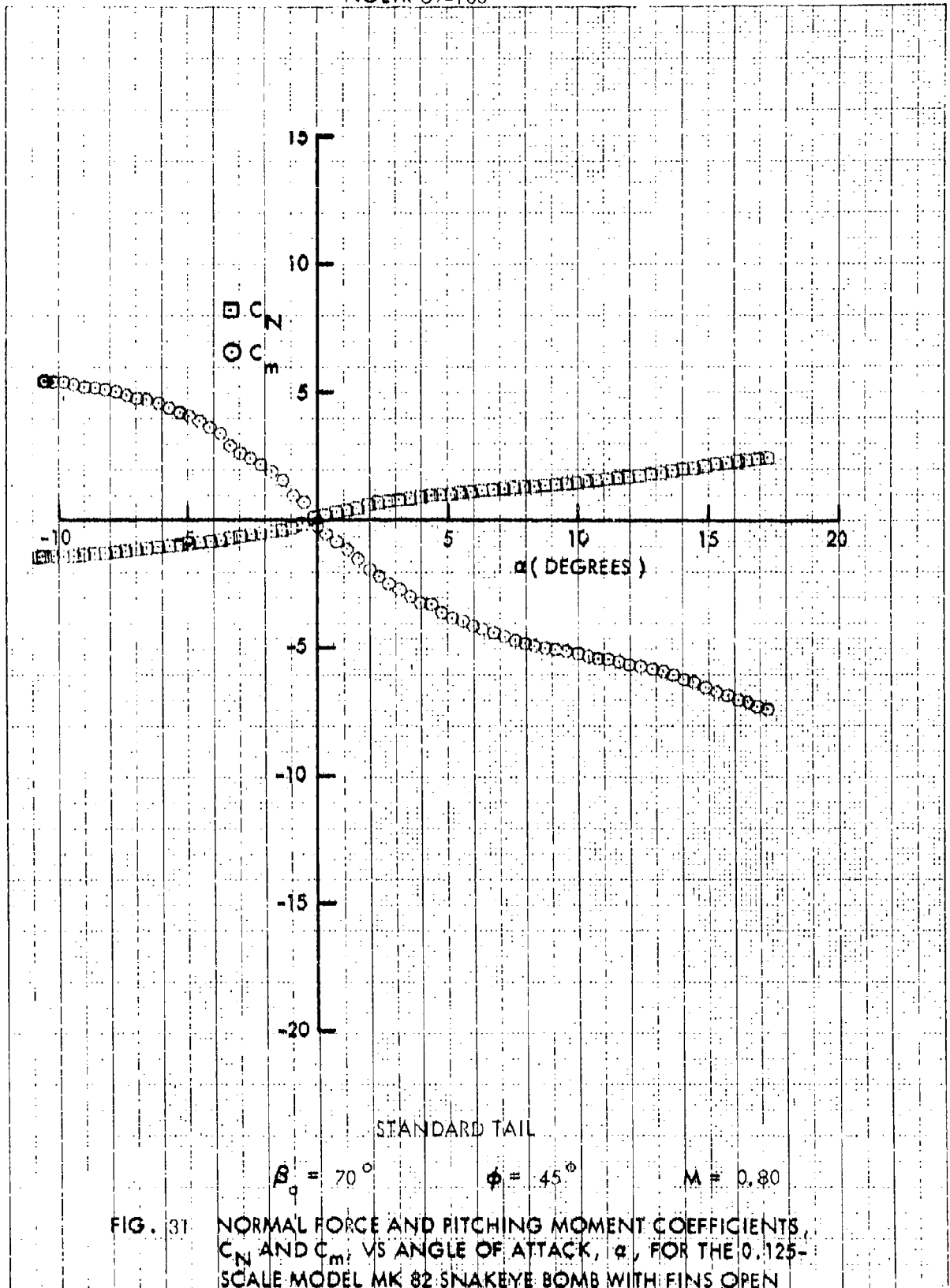
STANDARD TAIL

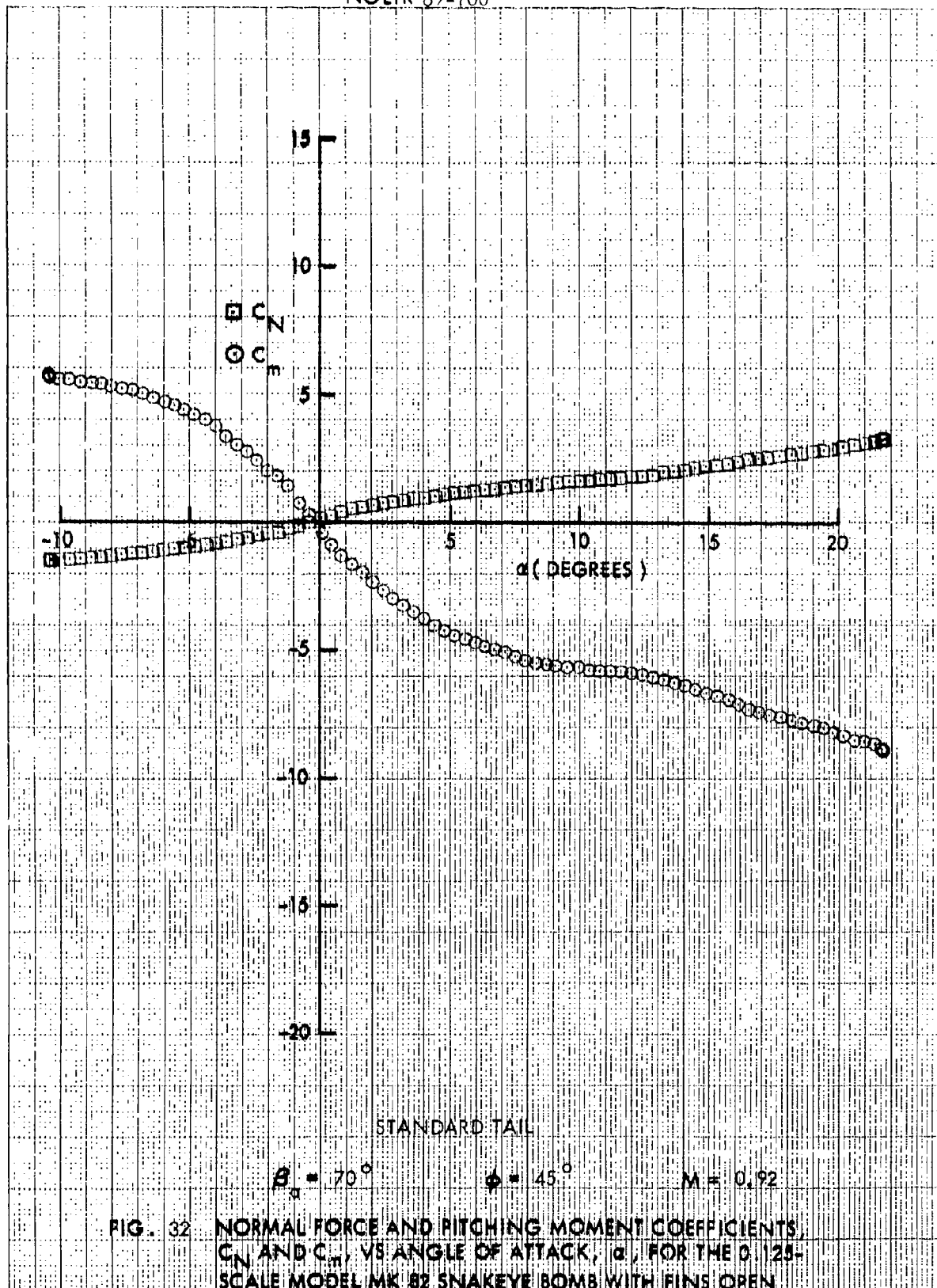
$$\beta_a = 70^\circ$$

$$\phi = 45^\circ$$

$$M = 0.50$$

FIG. 30 NORMAL FORCE AND PITCHING MOMENT COEFFICIENTS,  $C_N$  AND  $C_m$ , VS ANGLE OF ATTACK,  $\alpha$ , FOR THE 0.125-SCALE MODEL MK 82 SNAKEYE BOMB WITH FINS OPEN.





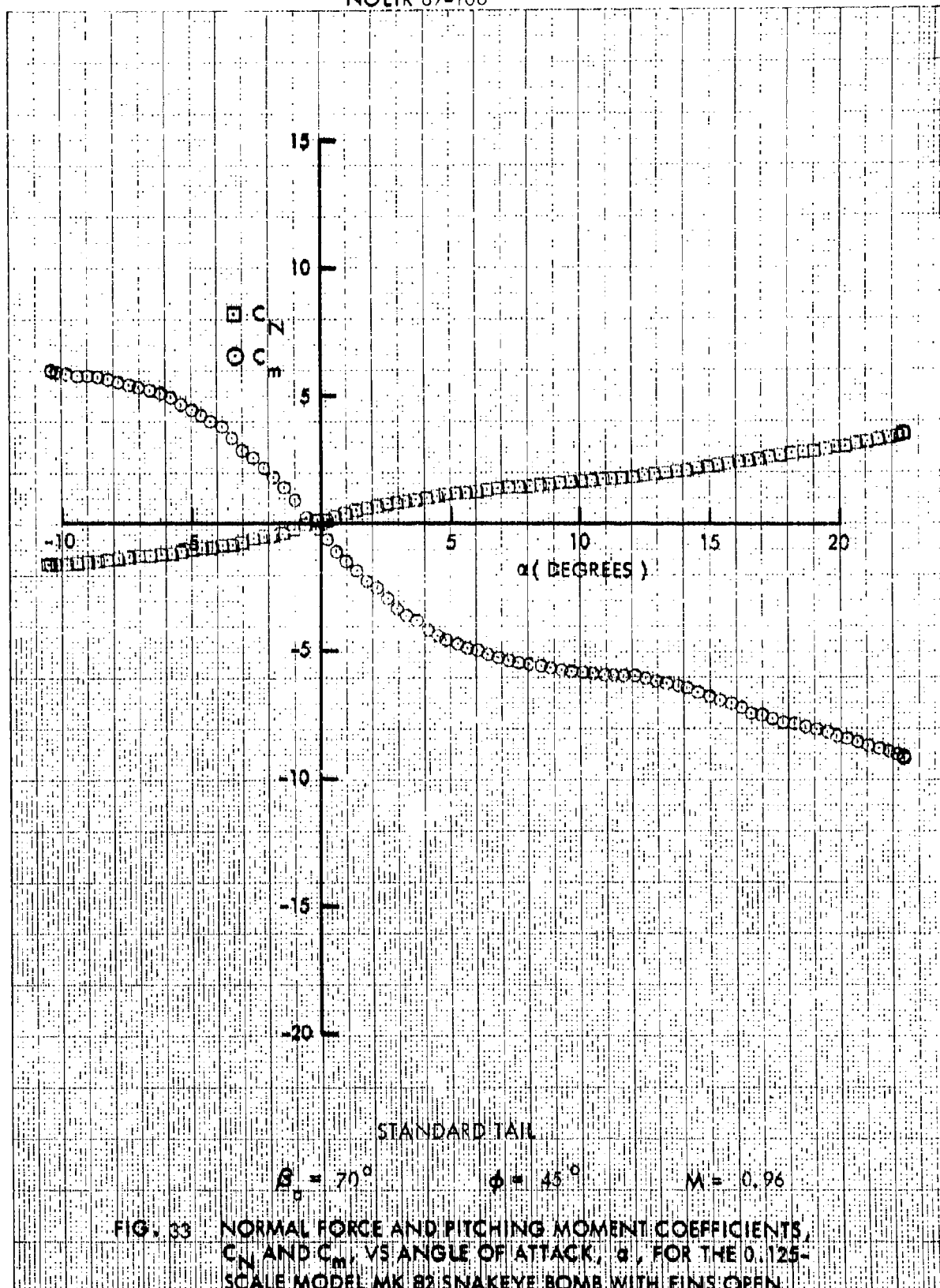
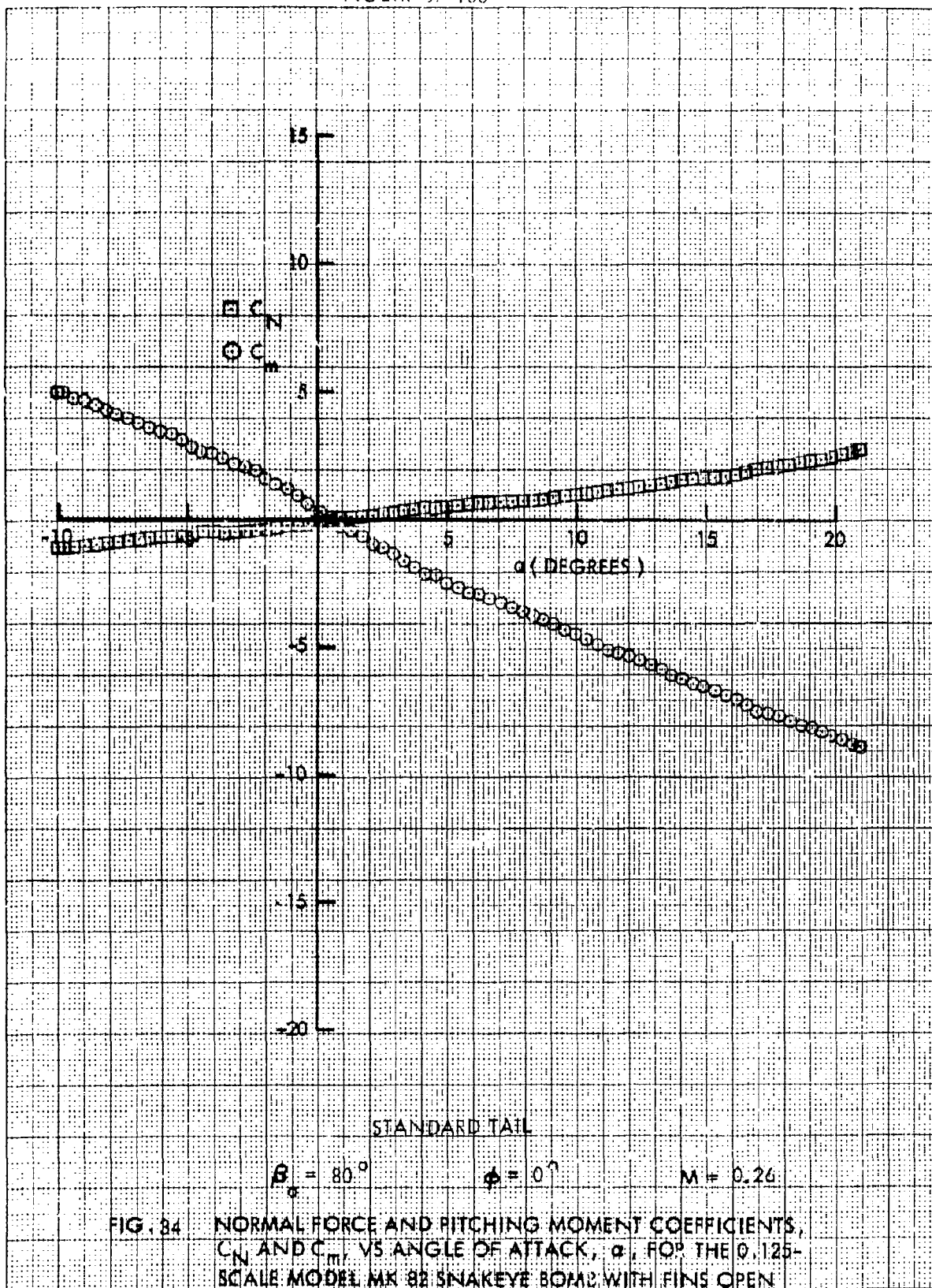
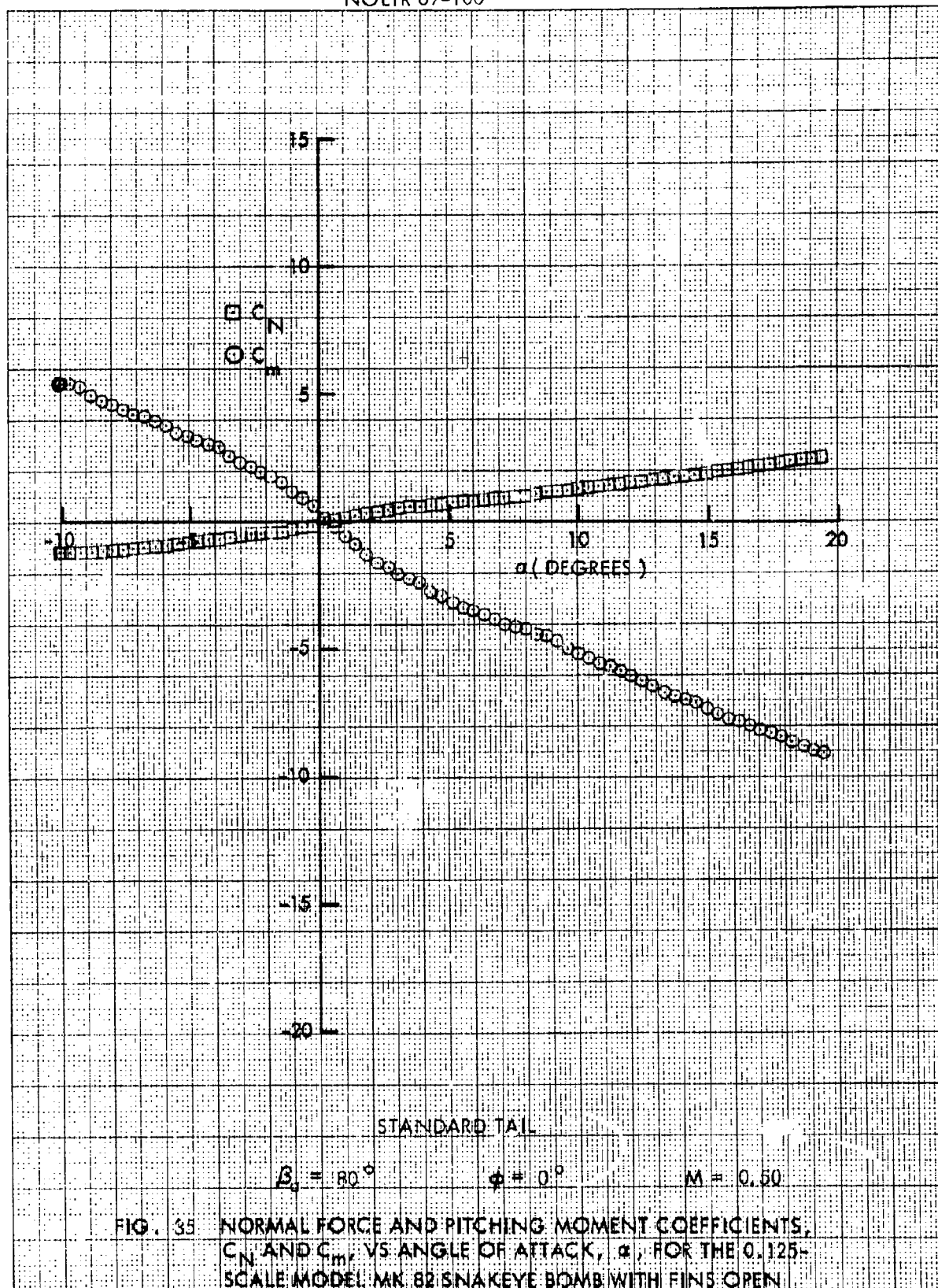


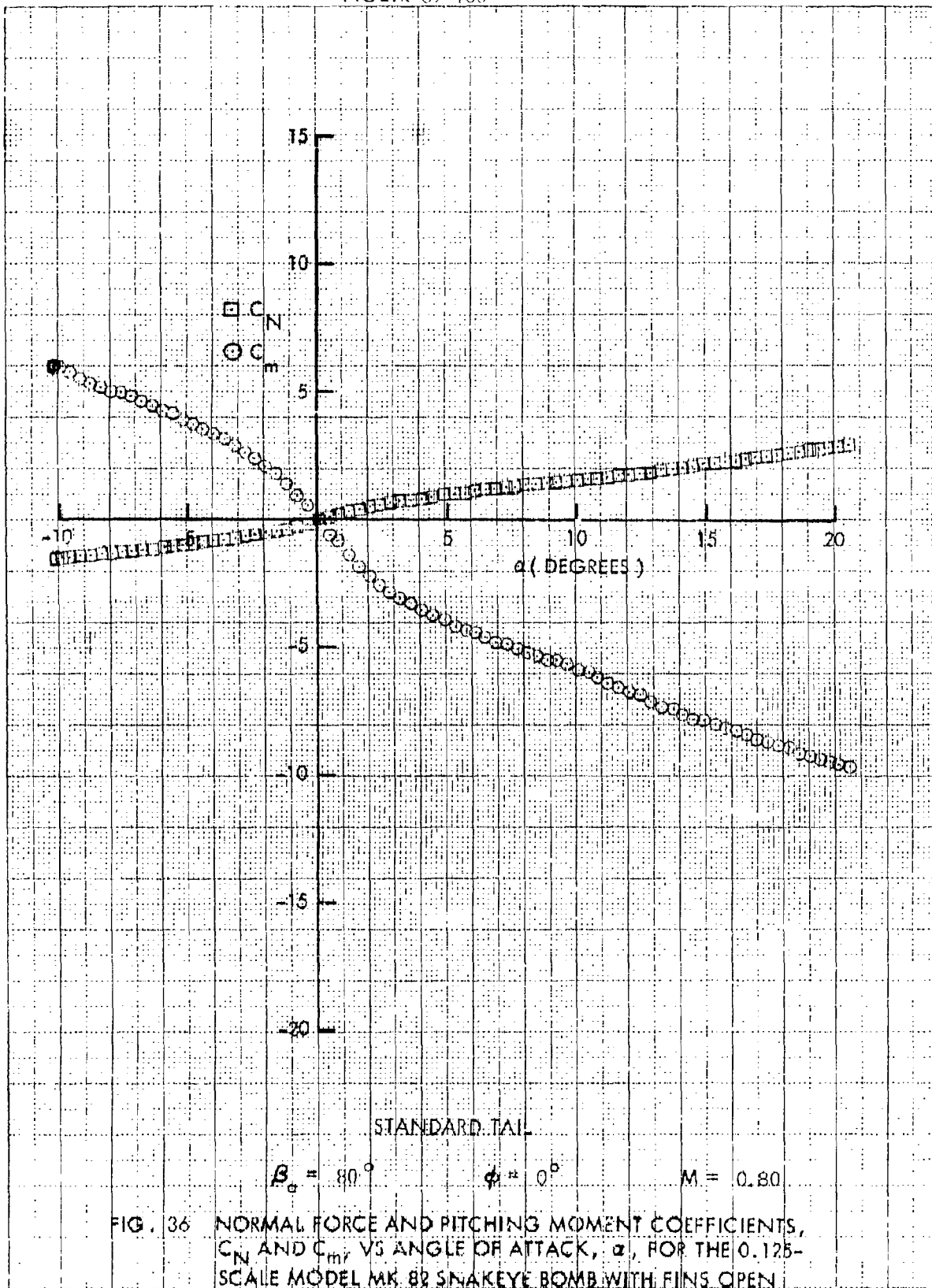
FIG. 33 NORMAL FORCE AND PITCHING MOMENT COEFFICIENTS,  $C_N$  AND  $C_m$ , VS ANGLE OF ATTACK,  $\alpha$ , FOR THE 0.125-SCALE MODEL MK 82 SNAKEYE BOMB WITH FINS OPEN

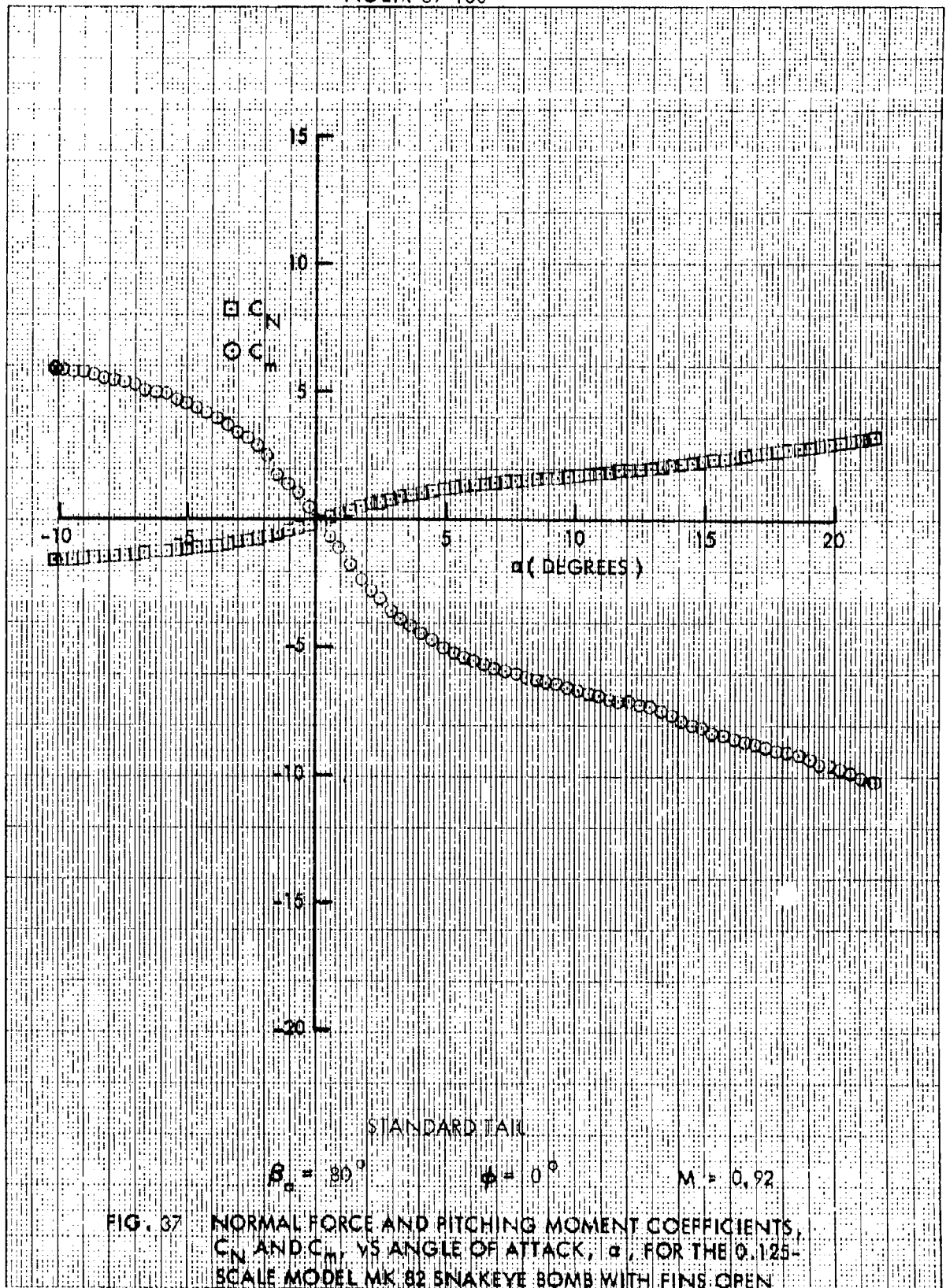


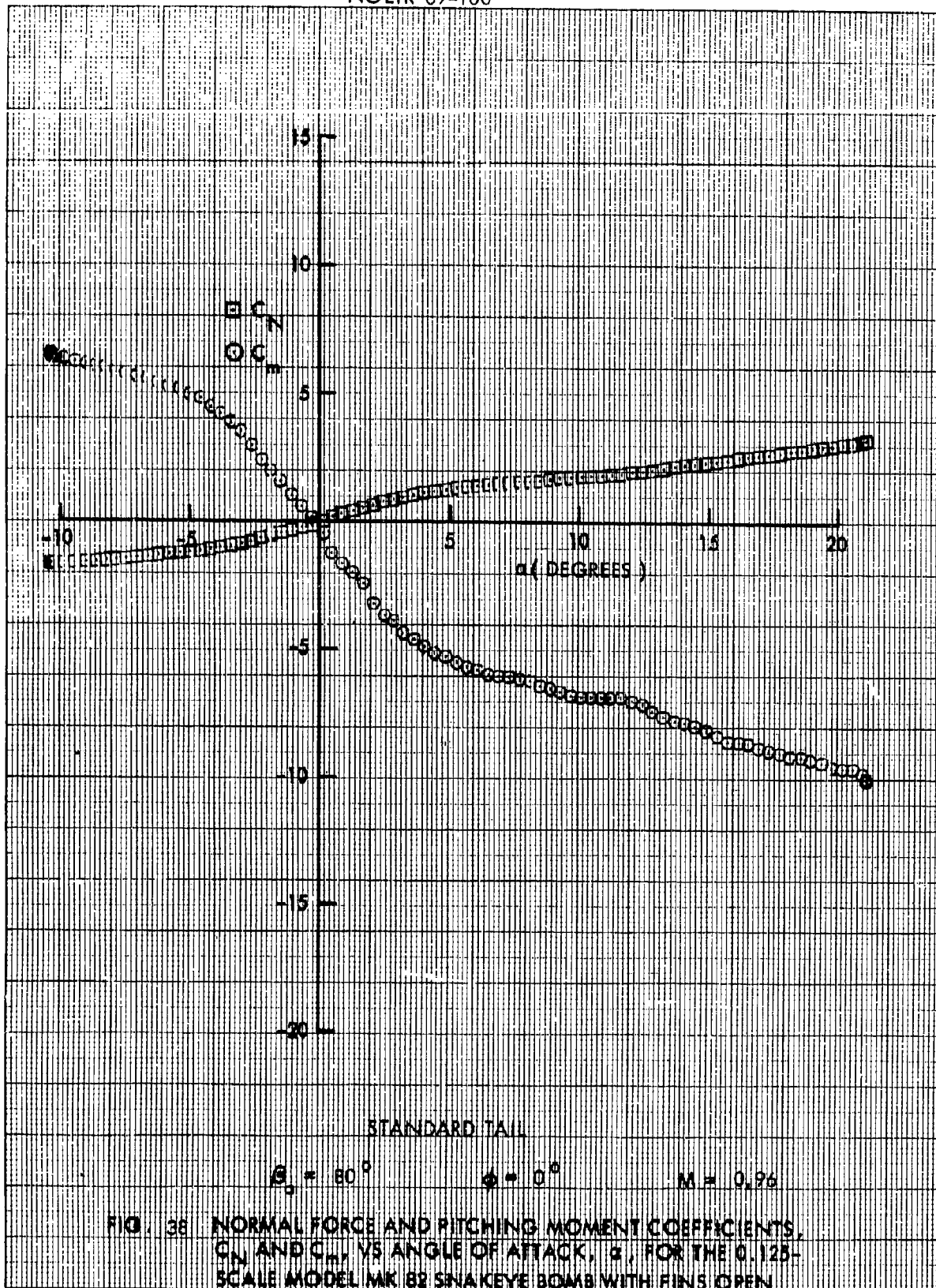


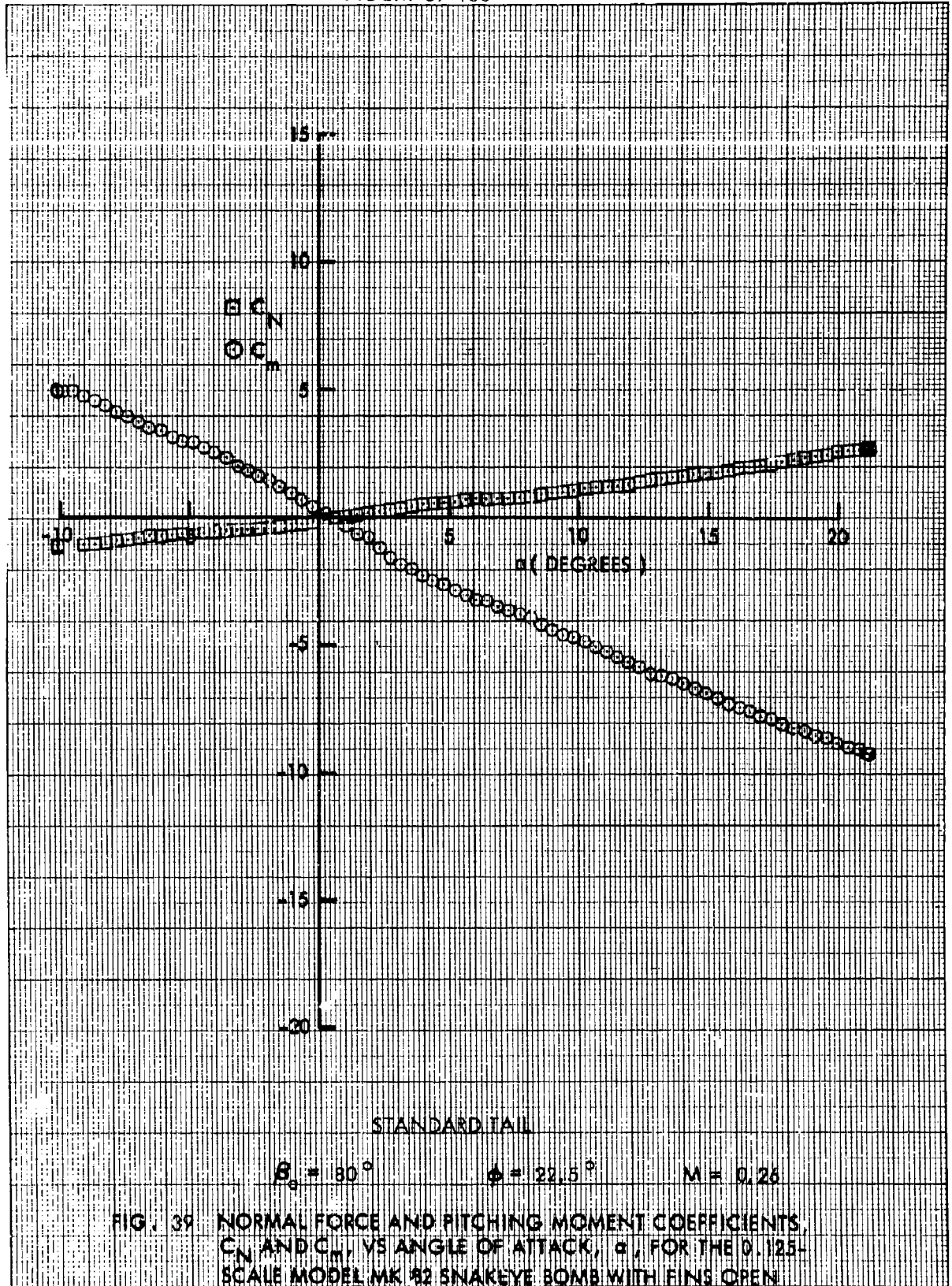


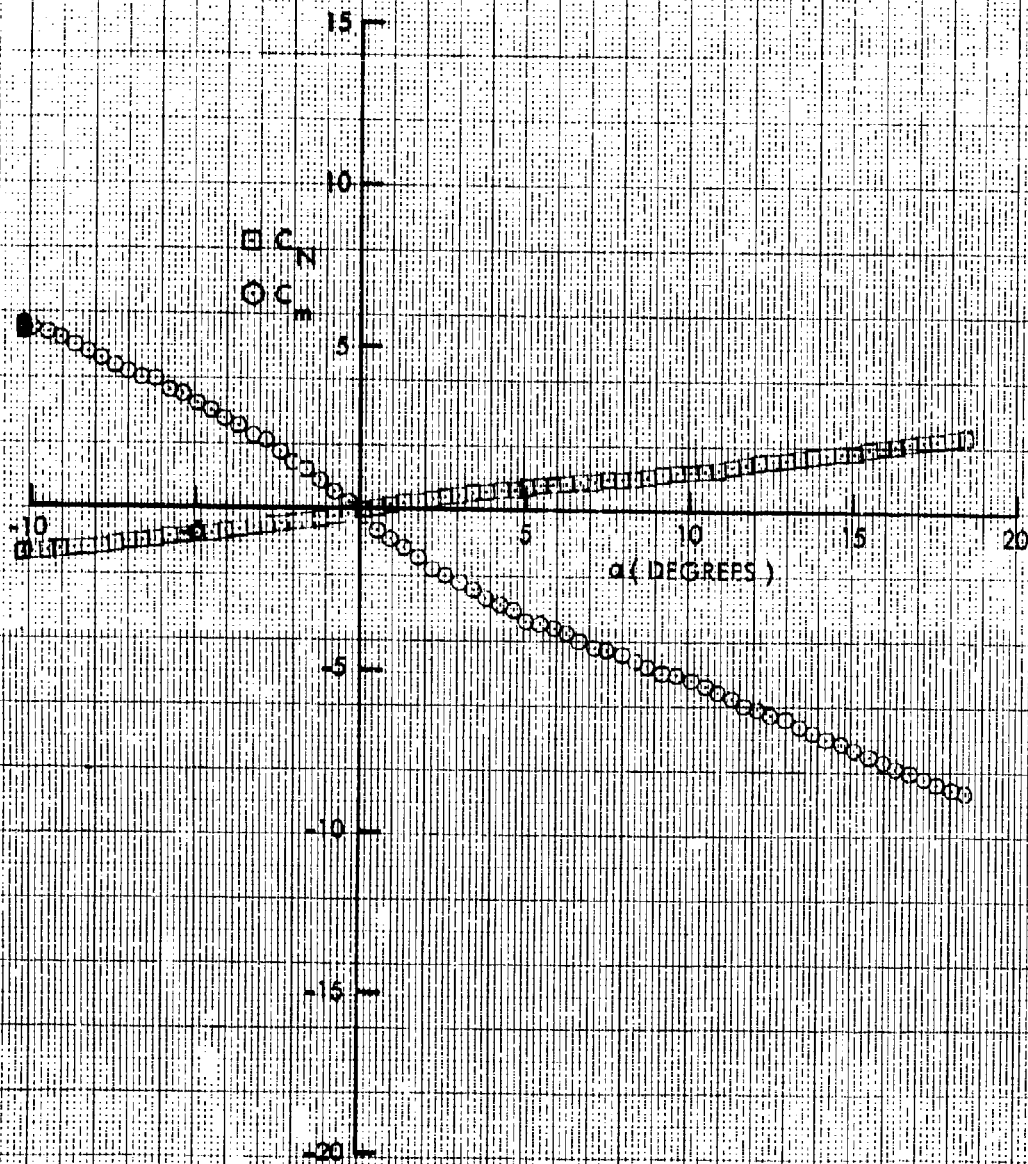








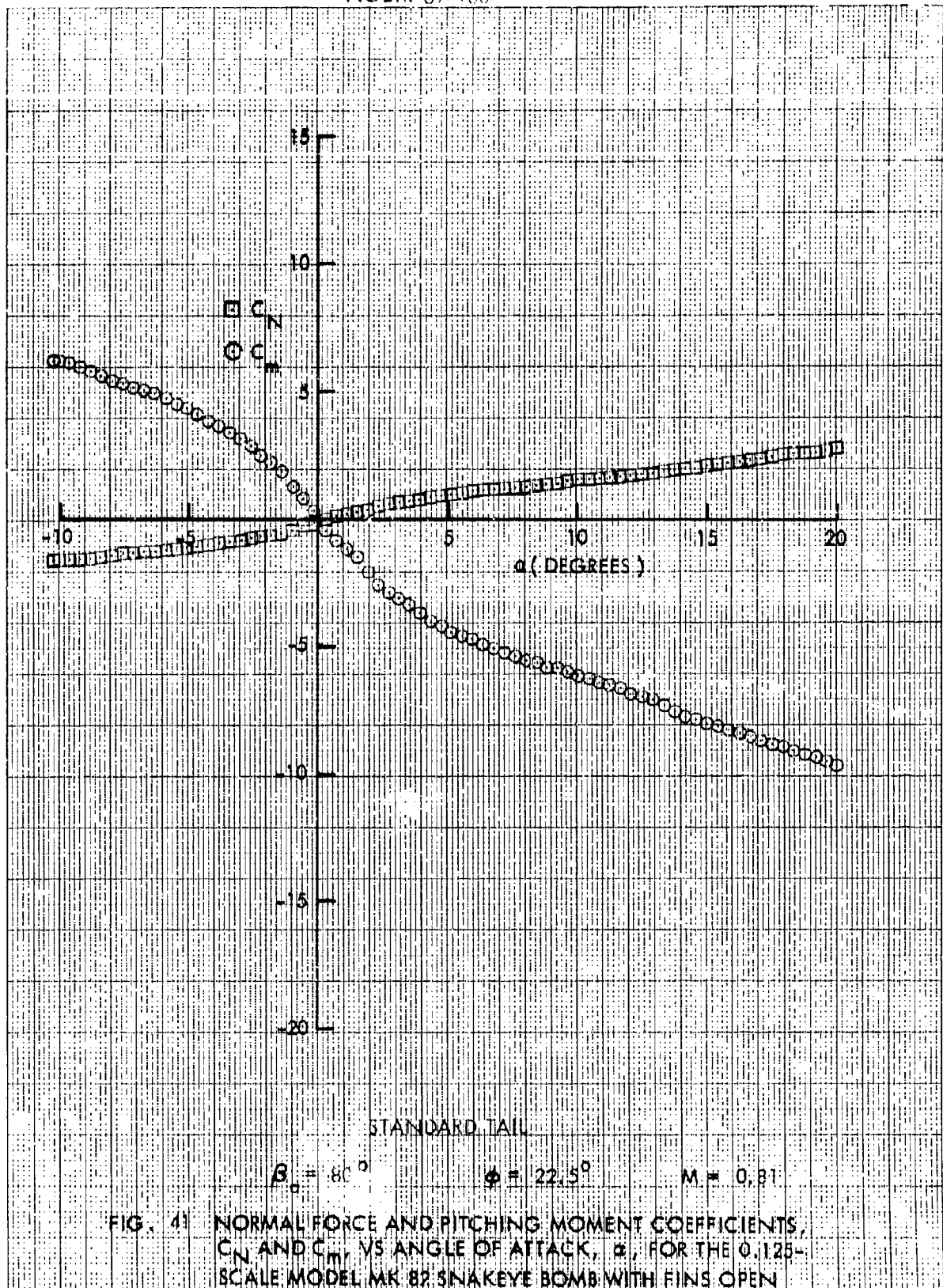




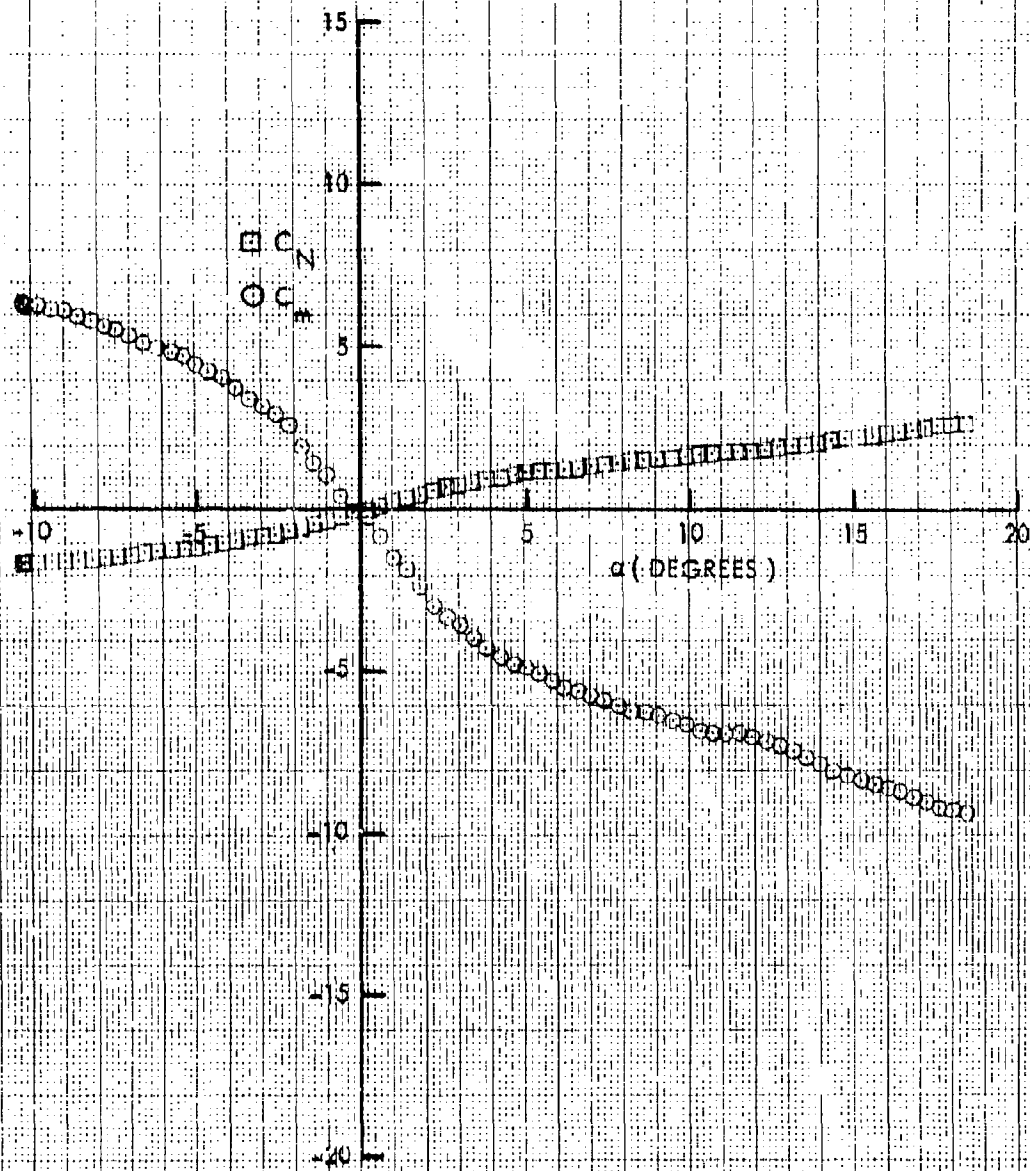
STANDARD TAIL

$\beta_0 = 80^\circ$        $\phi = 22.5^\circ$        $M = 0.50$

FIG. 40 NORMAL FORCE AND PITCHING MOMENT COEFFICIENTS,  $C_N$  AND  $C_m$ , VS ANGLE OF ATTACK,  $\alpha$ , FOR THE 0.125-SCALE MODEL MK 82 SNAKEEYE BOMB WITH FINS OPEN







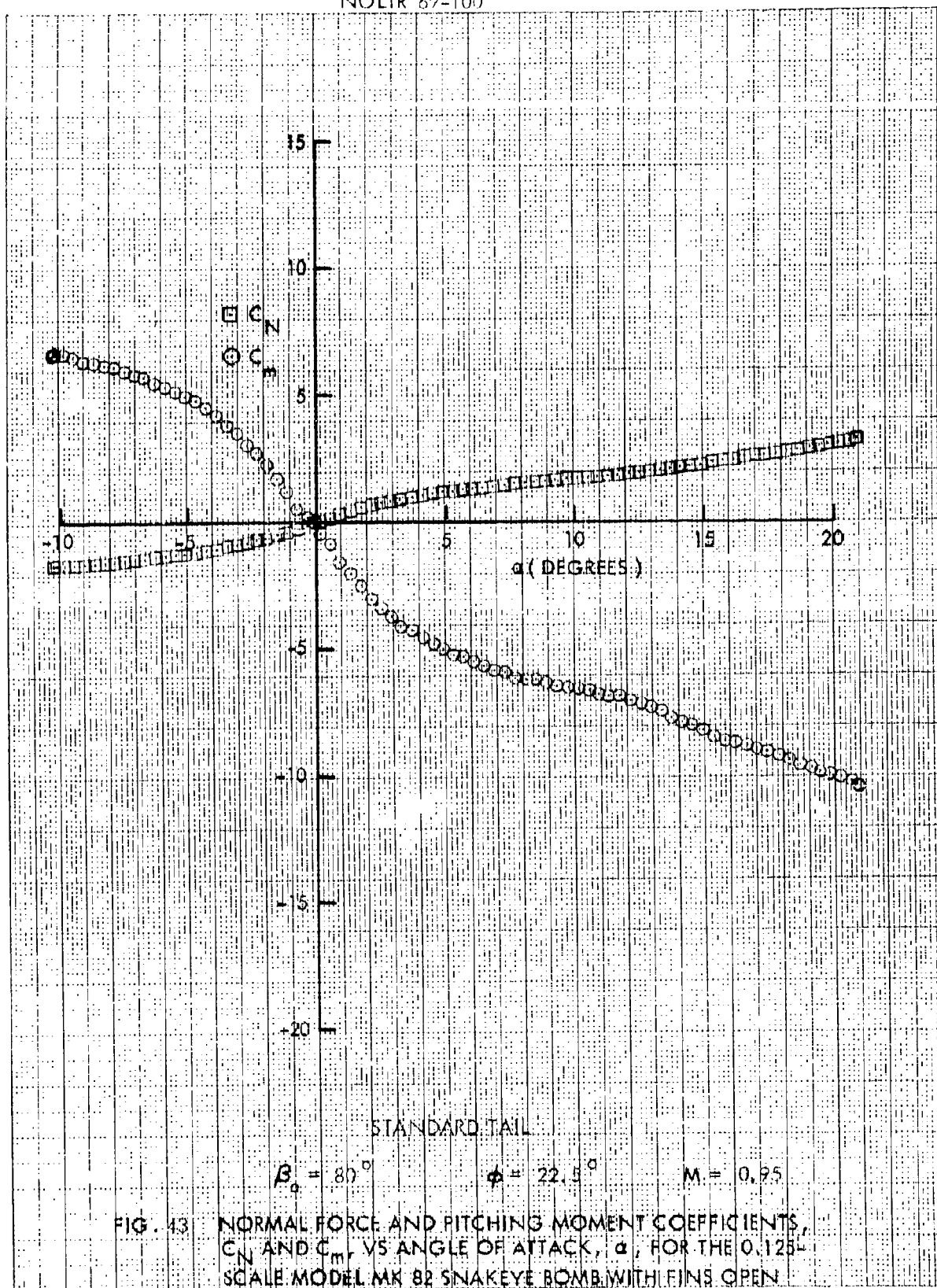
STANDARD TAIL

$$\beta_{\phi} = 80^{\circ}$$

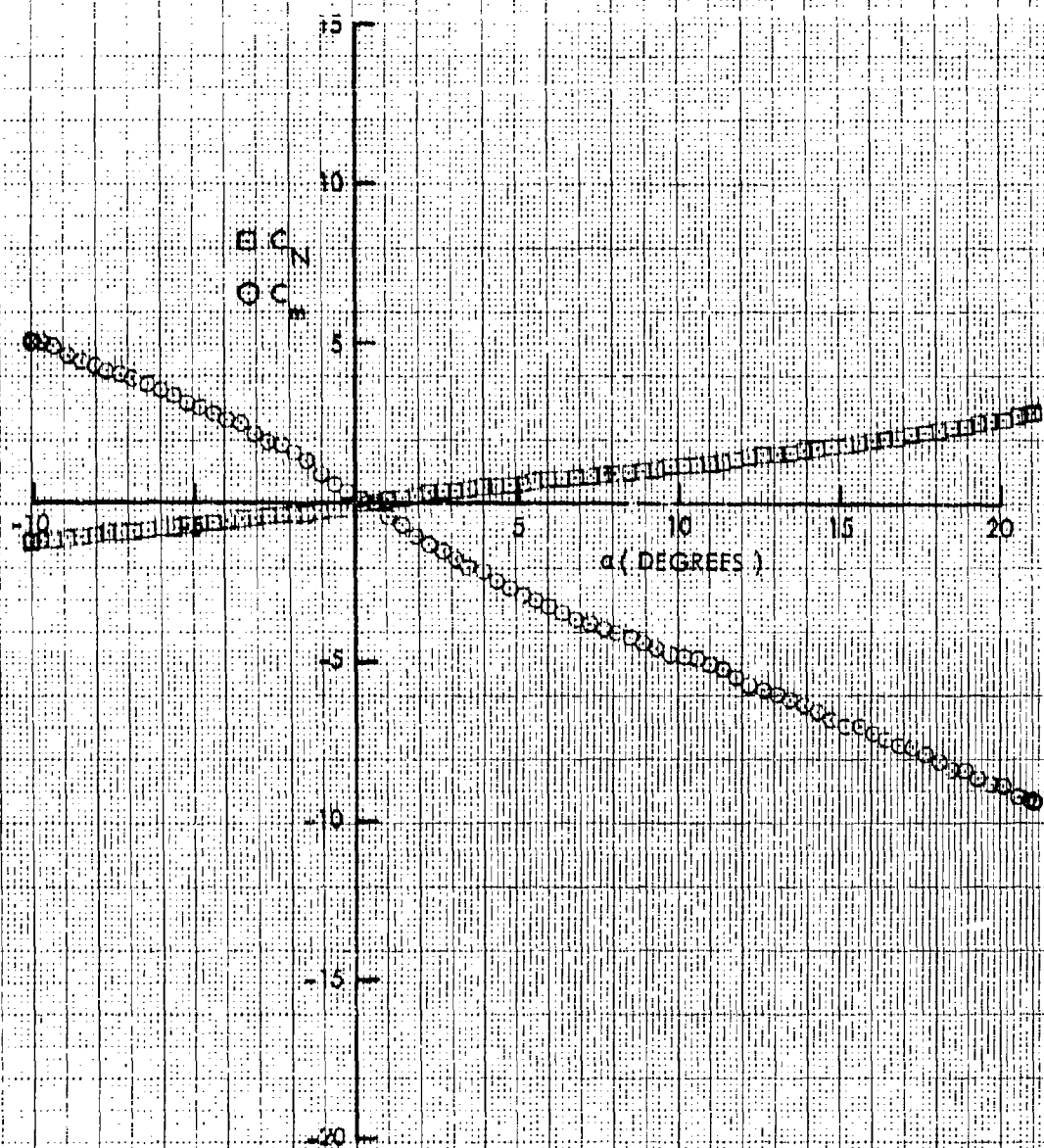
$$\phi = 22.5^{\circ}$$

$$M = 0.92$$

FIG. 42 NORMAL FORCE AND PITCHING MOMENT COEFFICIENTS,  $C_N$  AND  $C_m$ , VS ANGLE OF ATTACK,  $\alpha$ , FOR THE 0.125-SCALE MODEL MK 82 SNAKEYE BOMB WITH FINS OPEN







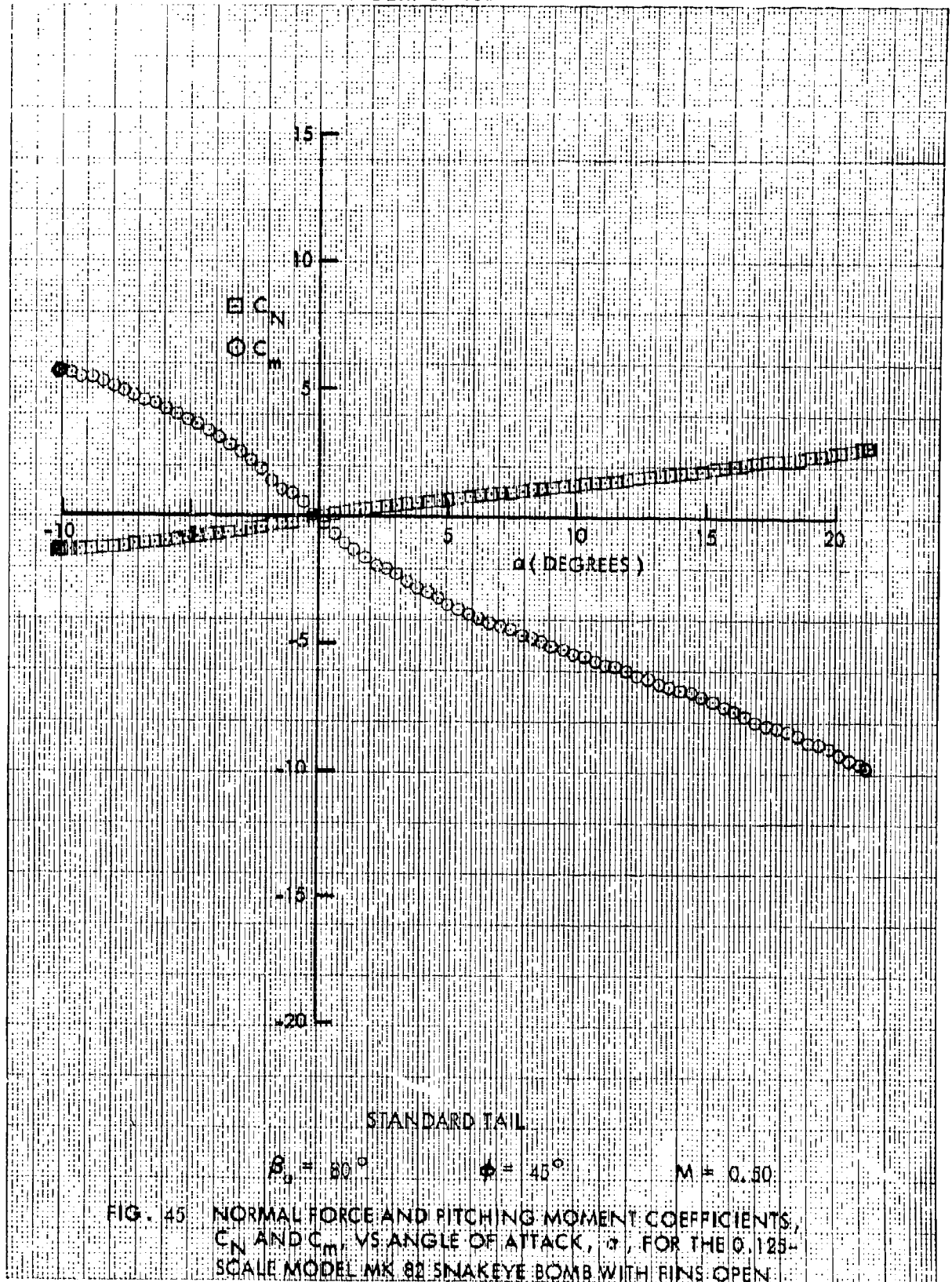
STANDARD TAIL

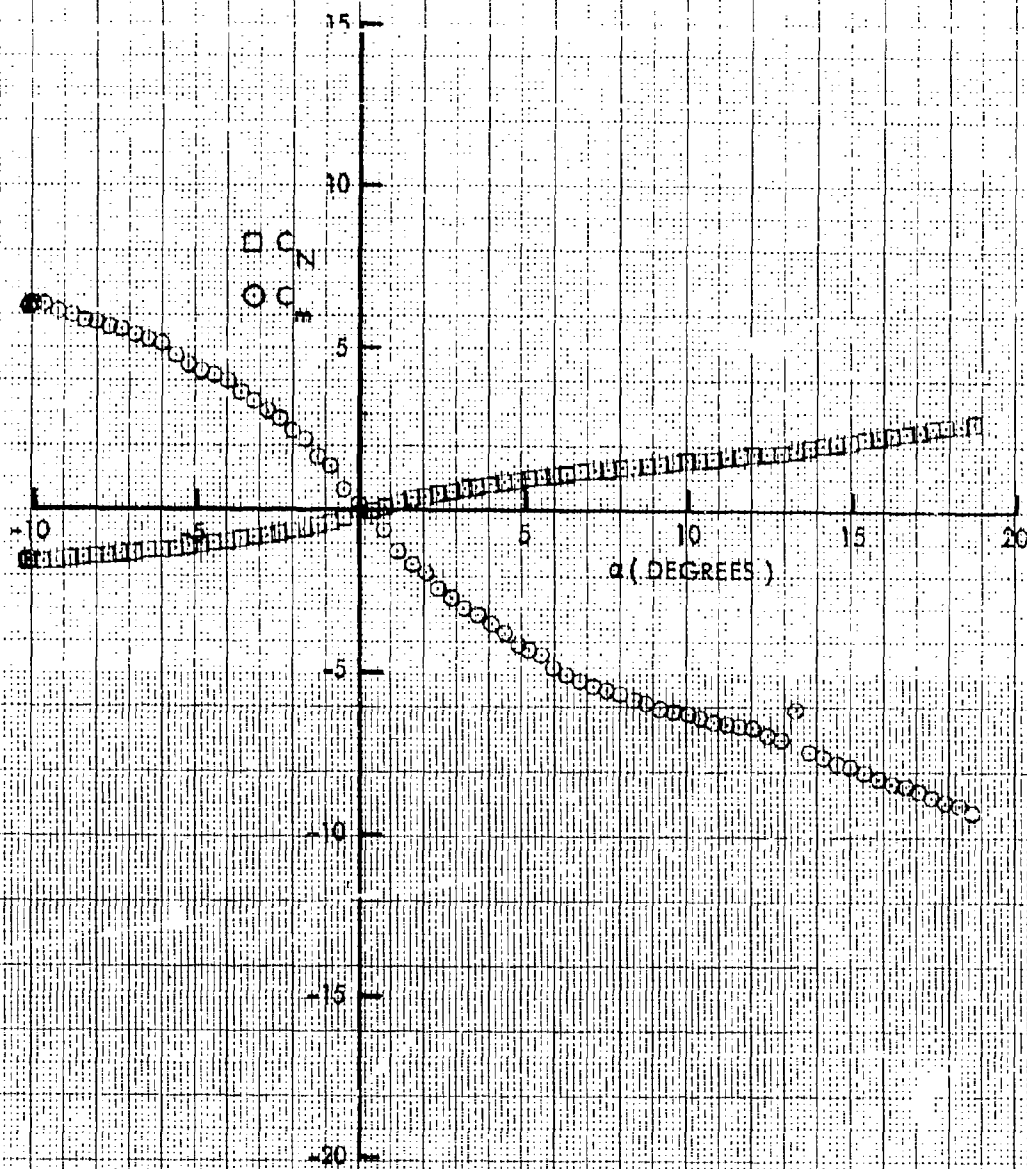
$$\beta_0 = 80^\circ$$

$$\phi = 45^\circ$$

$$M = 0.26$$

FIG. 44 NORMAL FORCE AND PITCHING MOMENT COEFFICIENTS,  $C_N$  AND  $C_m$ , VS ANGLE OF ATTACK,  $\alpha$ , FOR THE 0.125-SCALE MODEL MK 82 SNAKEYE BOMB WITH FINS OPEN





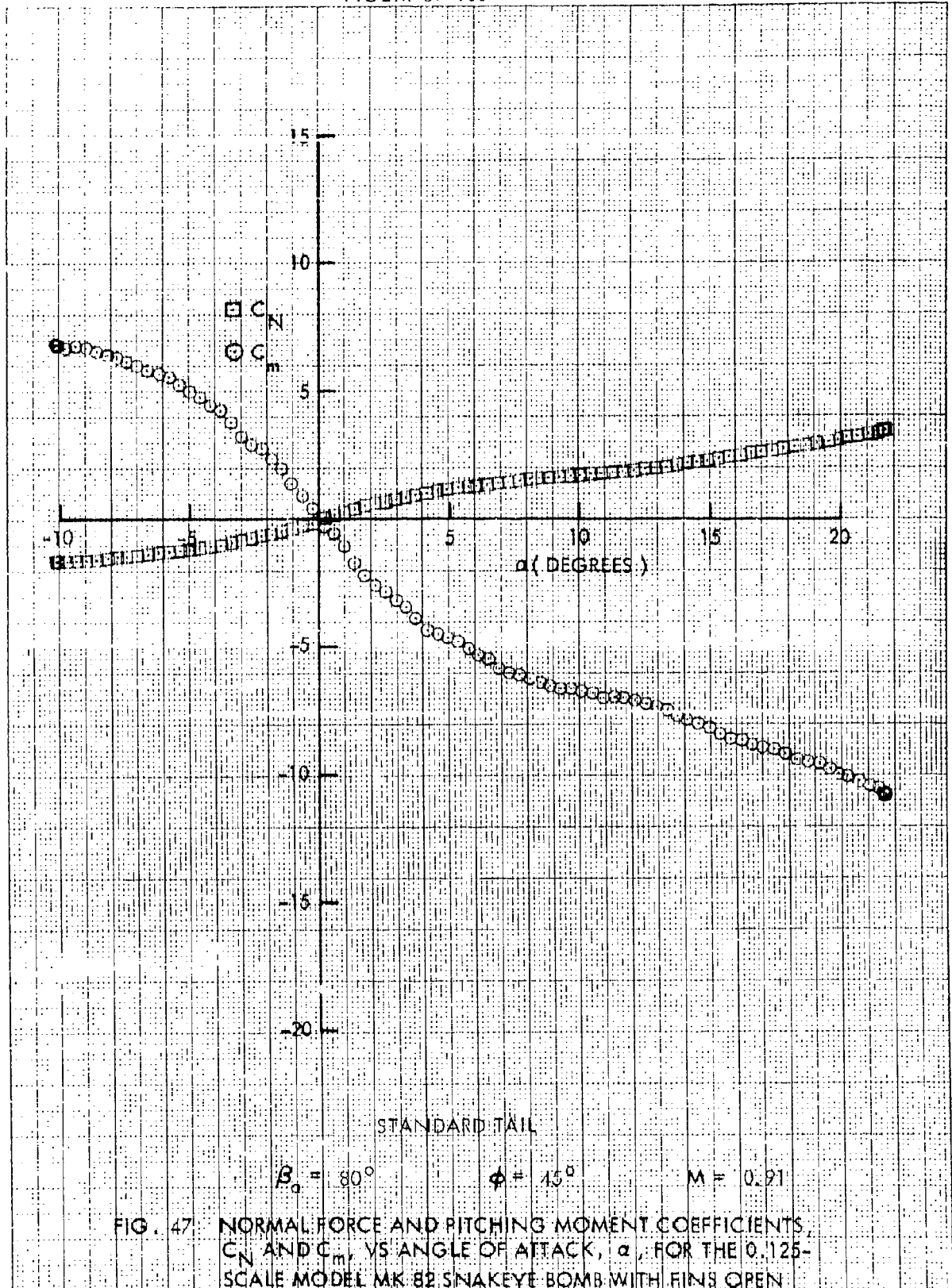
STANDARD TAIL

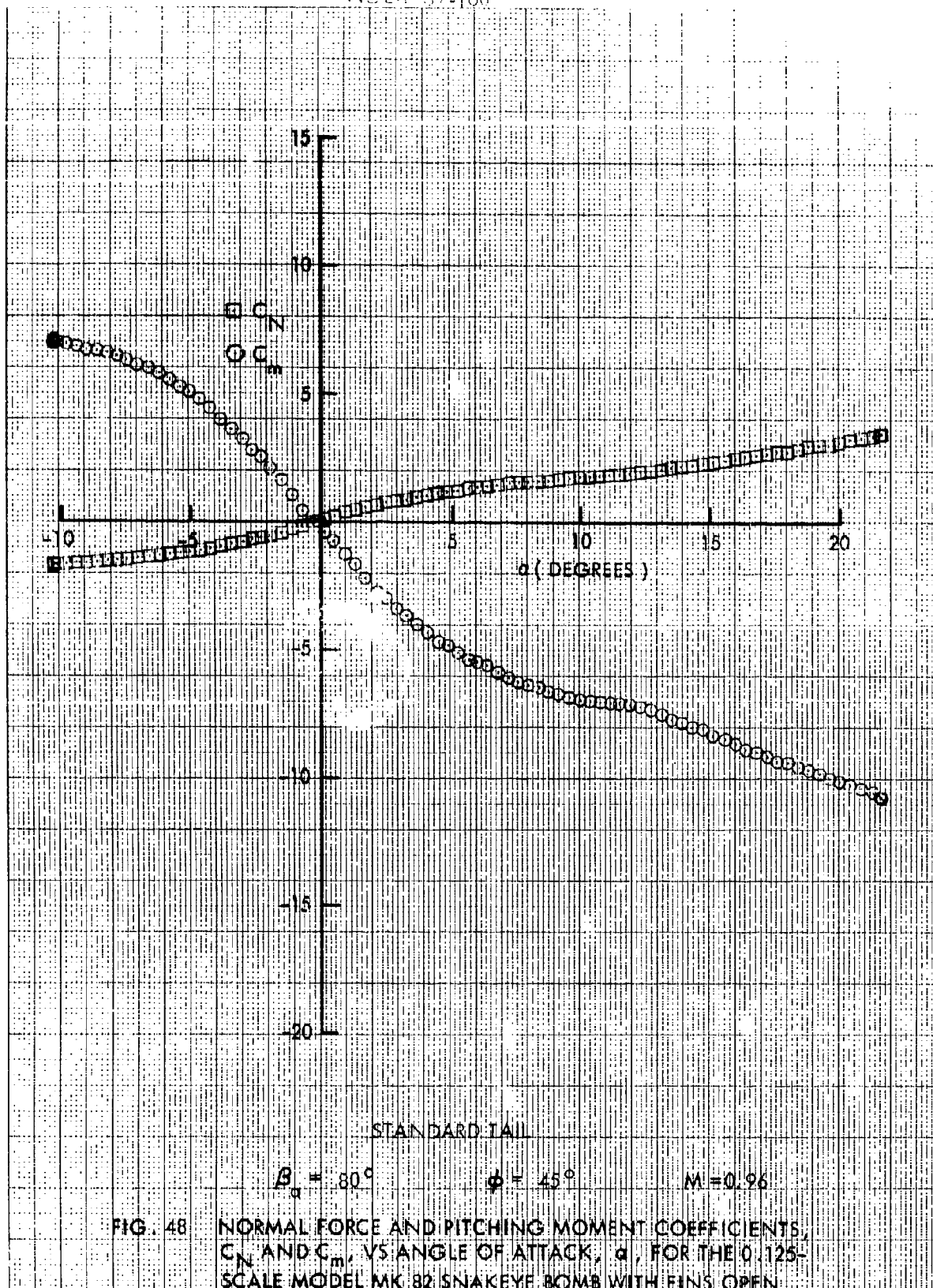
$\beta = 80^\circ$

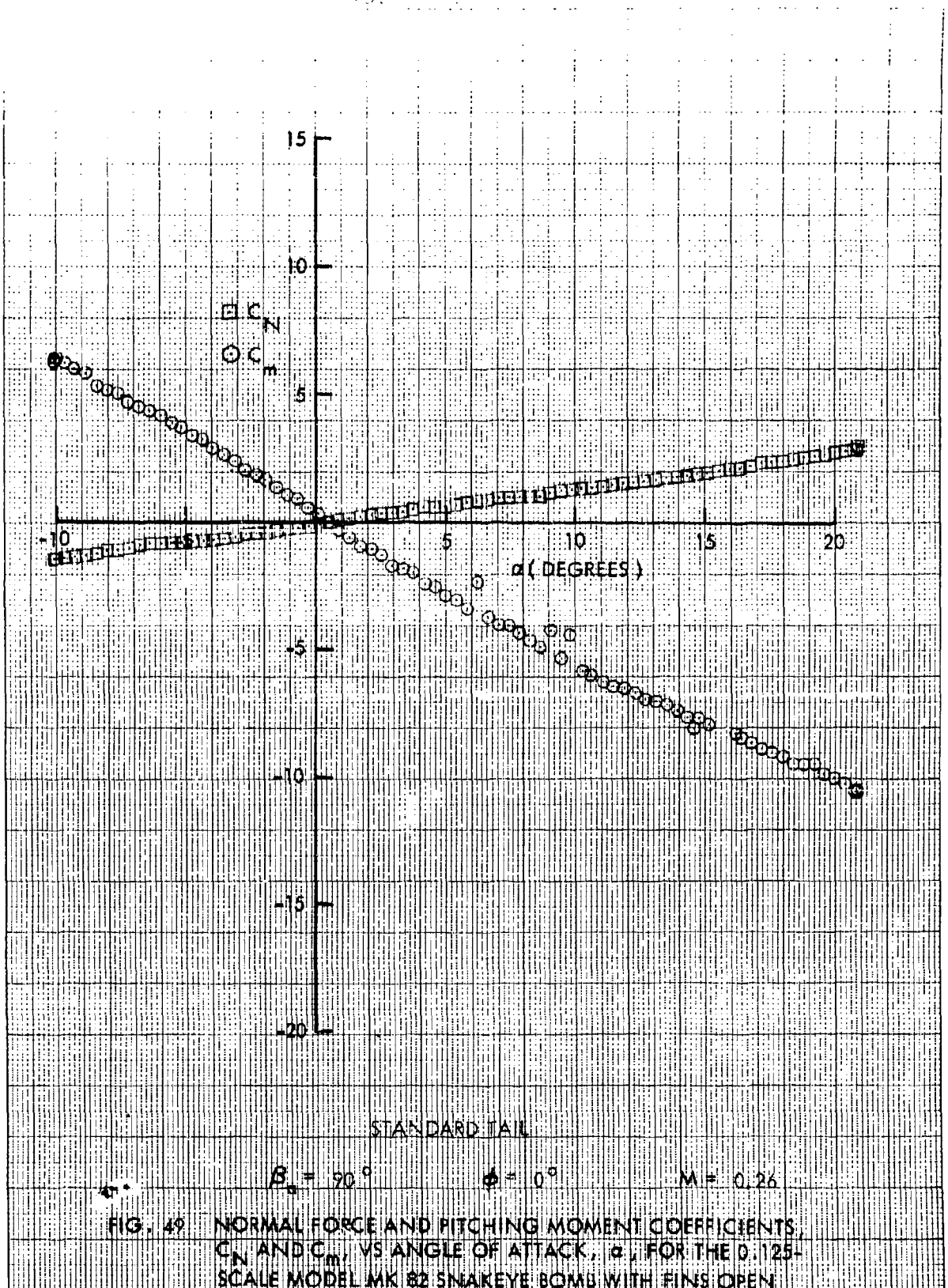
$\phi = 45^\circ$

$M = 0.81$

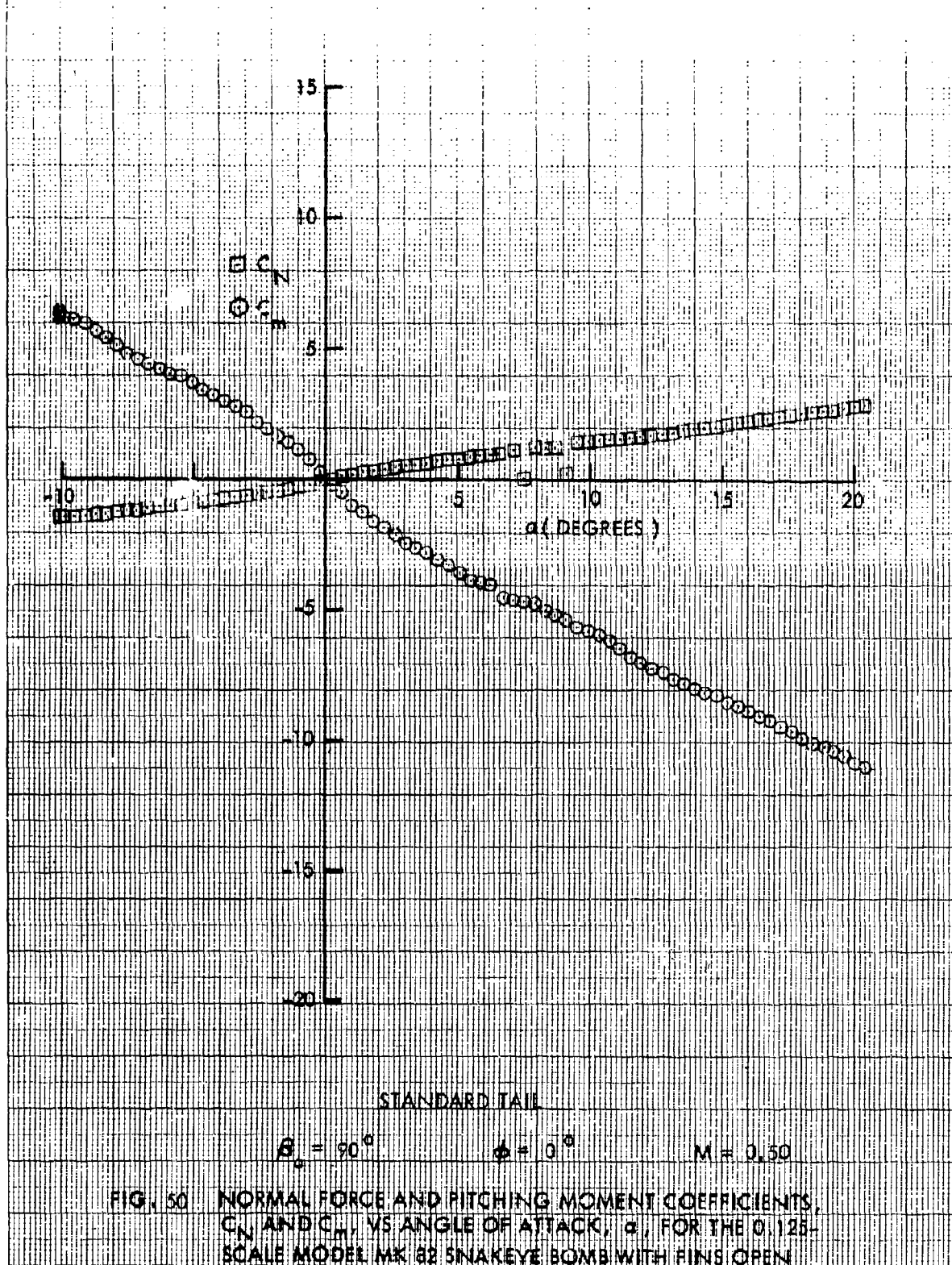
FIG. 46 NORMAL FORCE AND PITCHING MOMENT COEFFICIENTS,  $C_N$  AND  $C_m$ , VS ANGLE OF ATTACK,  $\alpha$ , FOR THE 0.125-SCALE MODEL MK 82 SNAKEYE BOMB WITH FINS OPEN

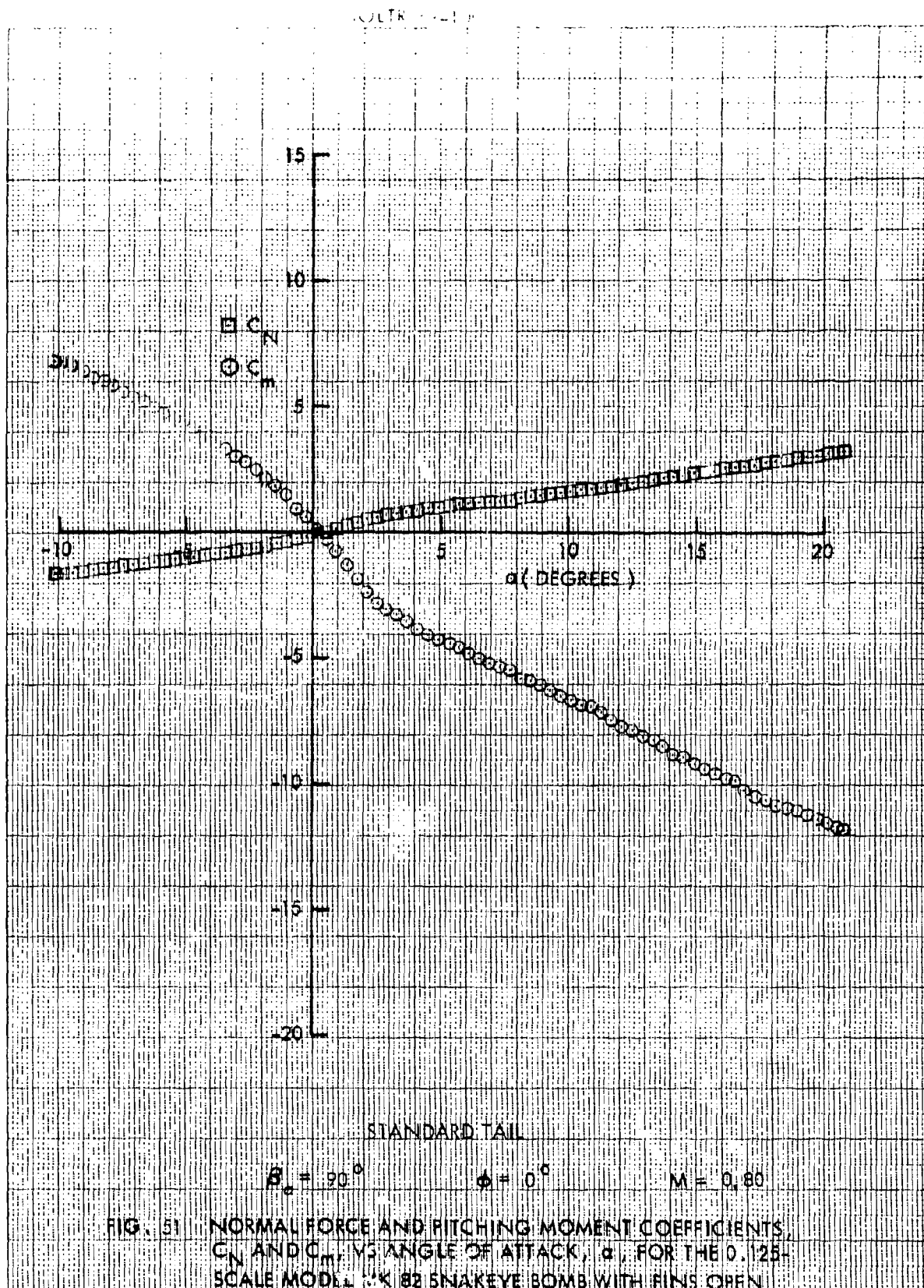




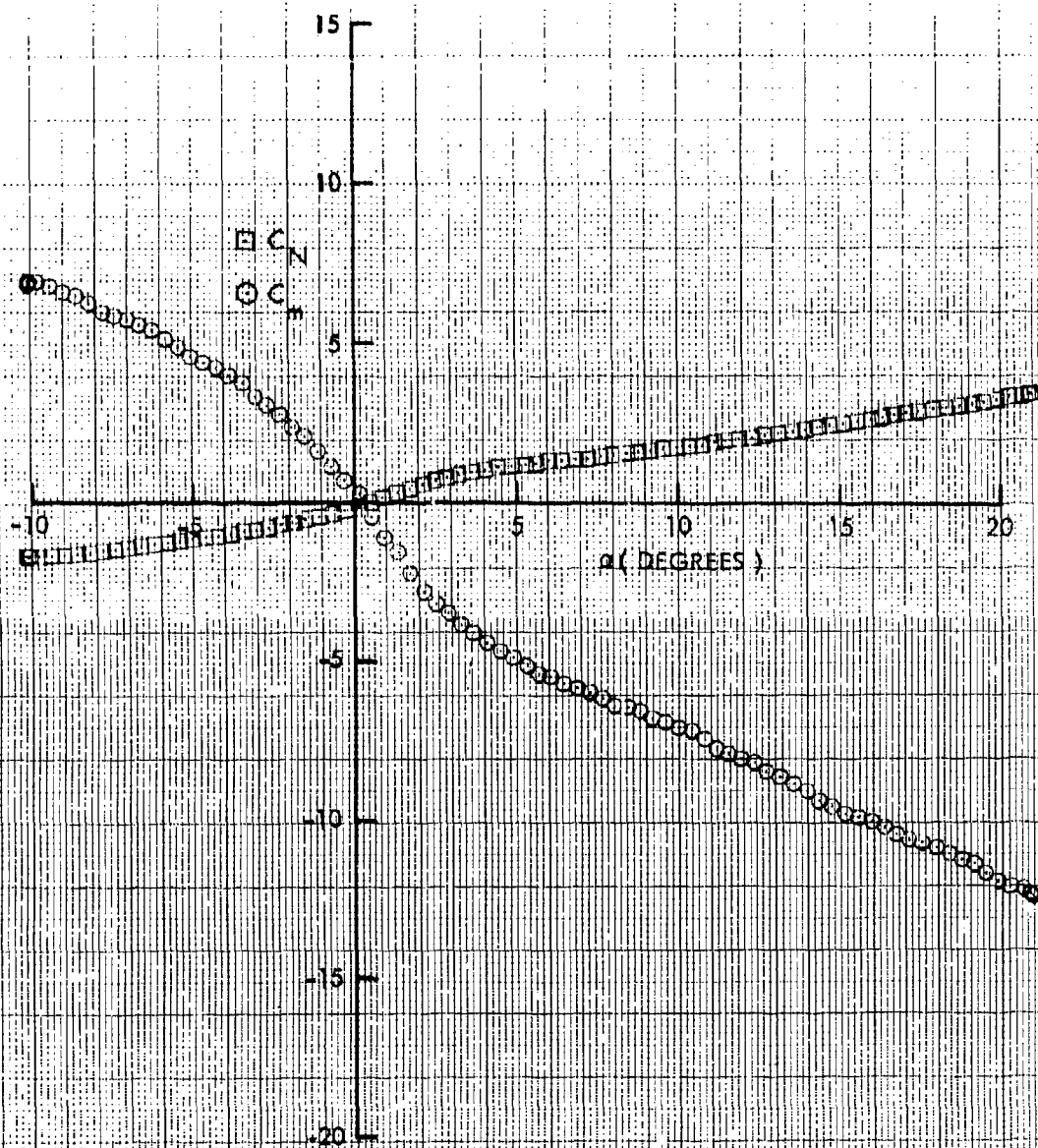












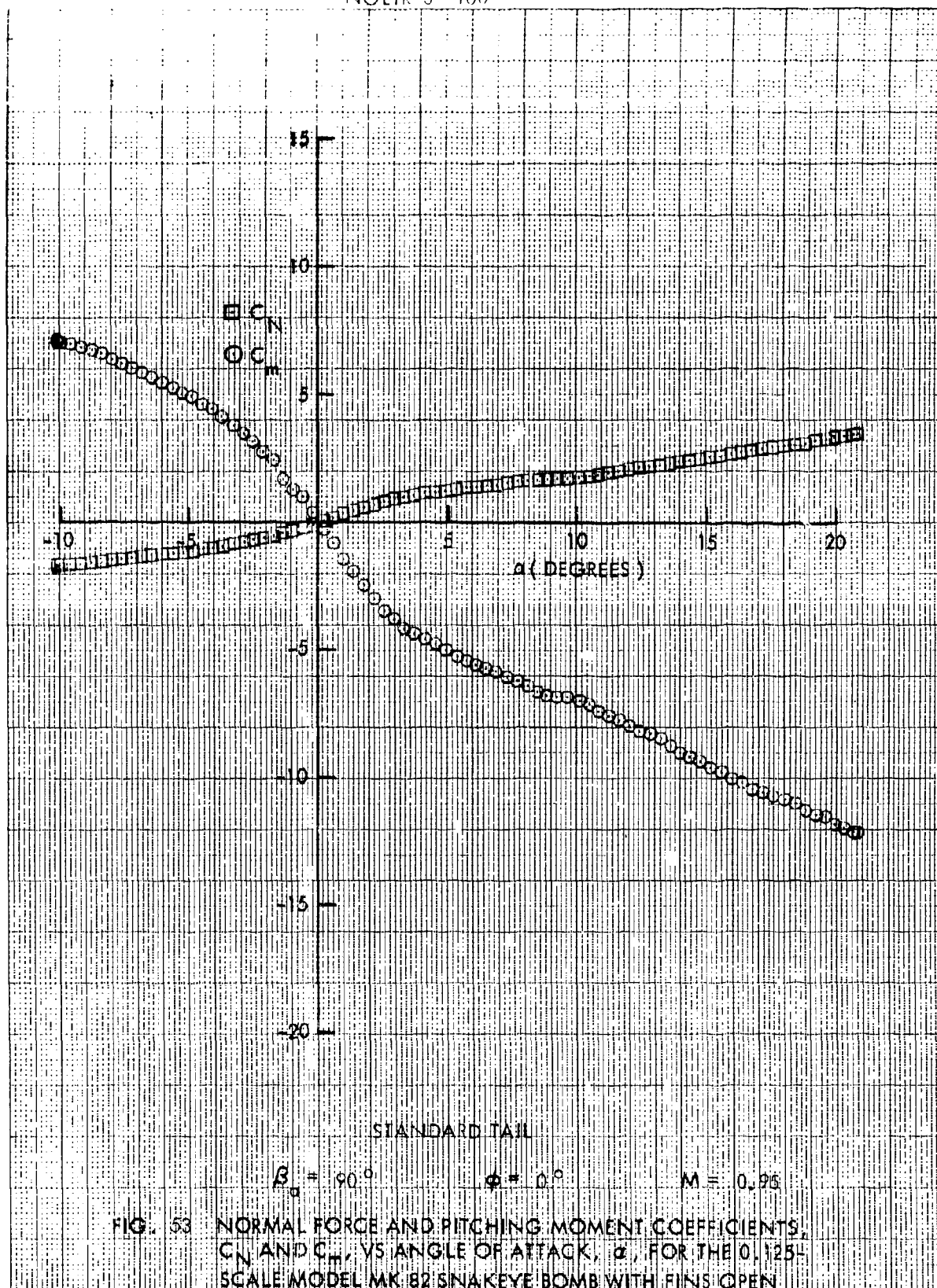
STANDARD TAIL

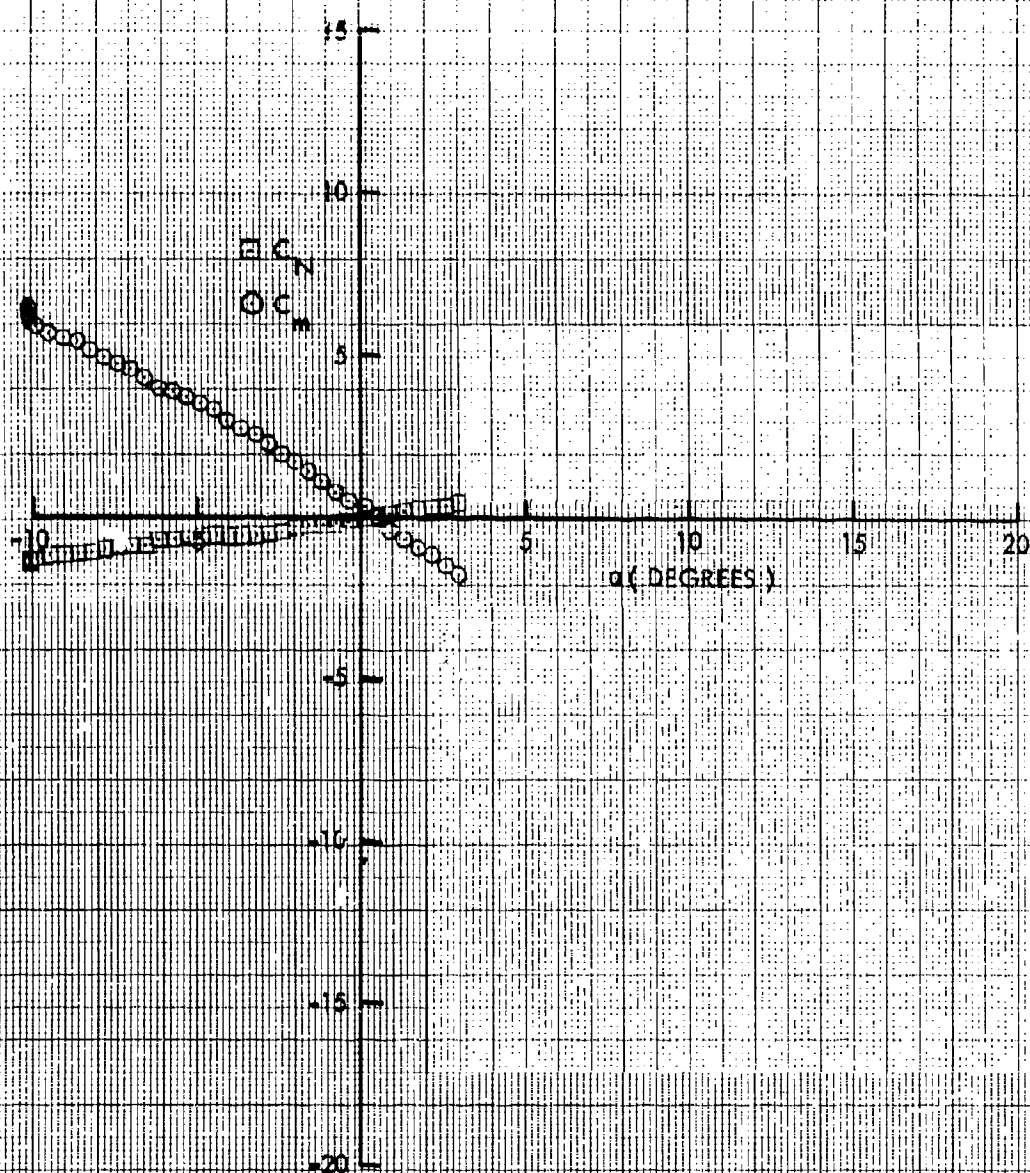
$$\beta_0 = 90^\circ$$

$$\phi = 0^\circ$$

$$M = 0.91$$

FIG. 52 NORMAL FORCE AND PITCHING MOMENT COEFFICIENTS,  $C_N$  AND  $C_m$ , VS ANGLE OF ATTACK,  $\alpha$ , FOR THE 0.125-SCALE MODEL MK 82 SNAKEYE BOMB WITH FINS OPEN





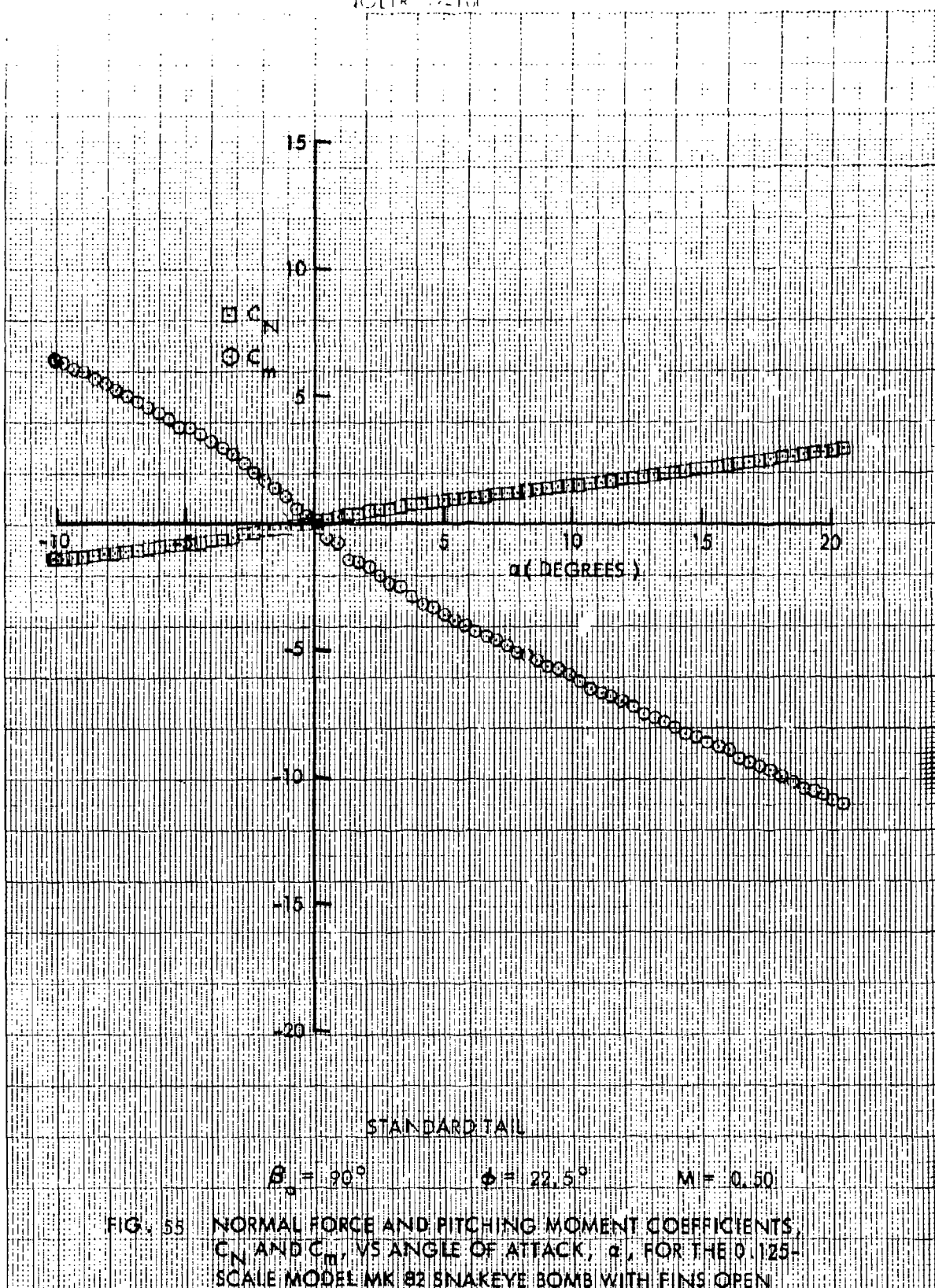
STANDARD TAIL

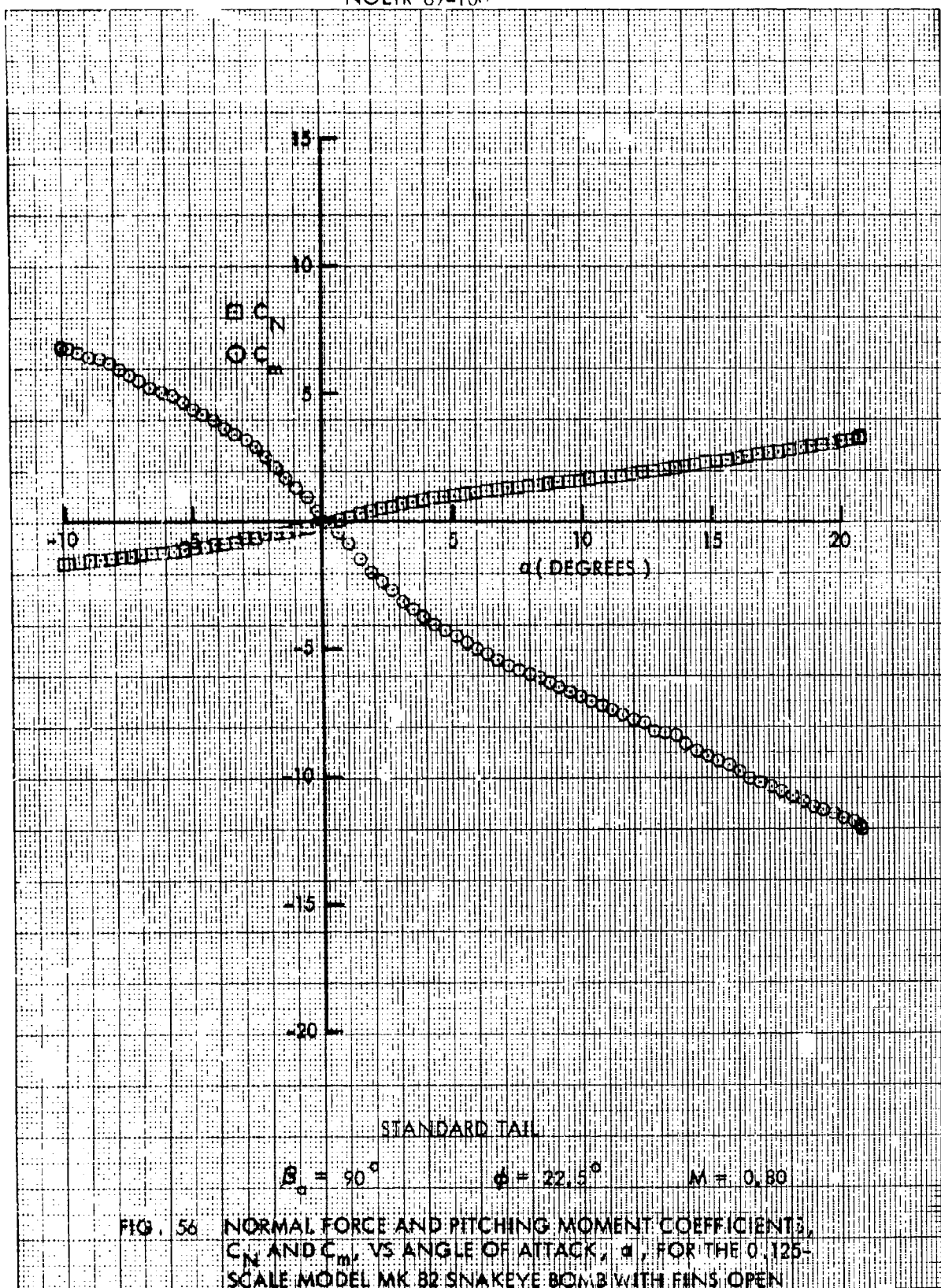
$$\beta_0 = 90^\circ$$

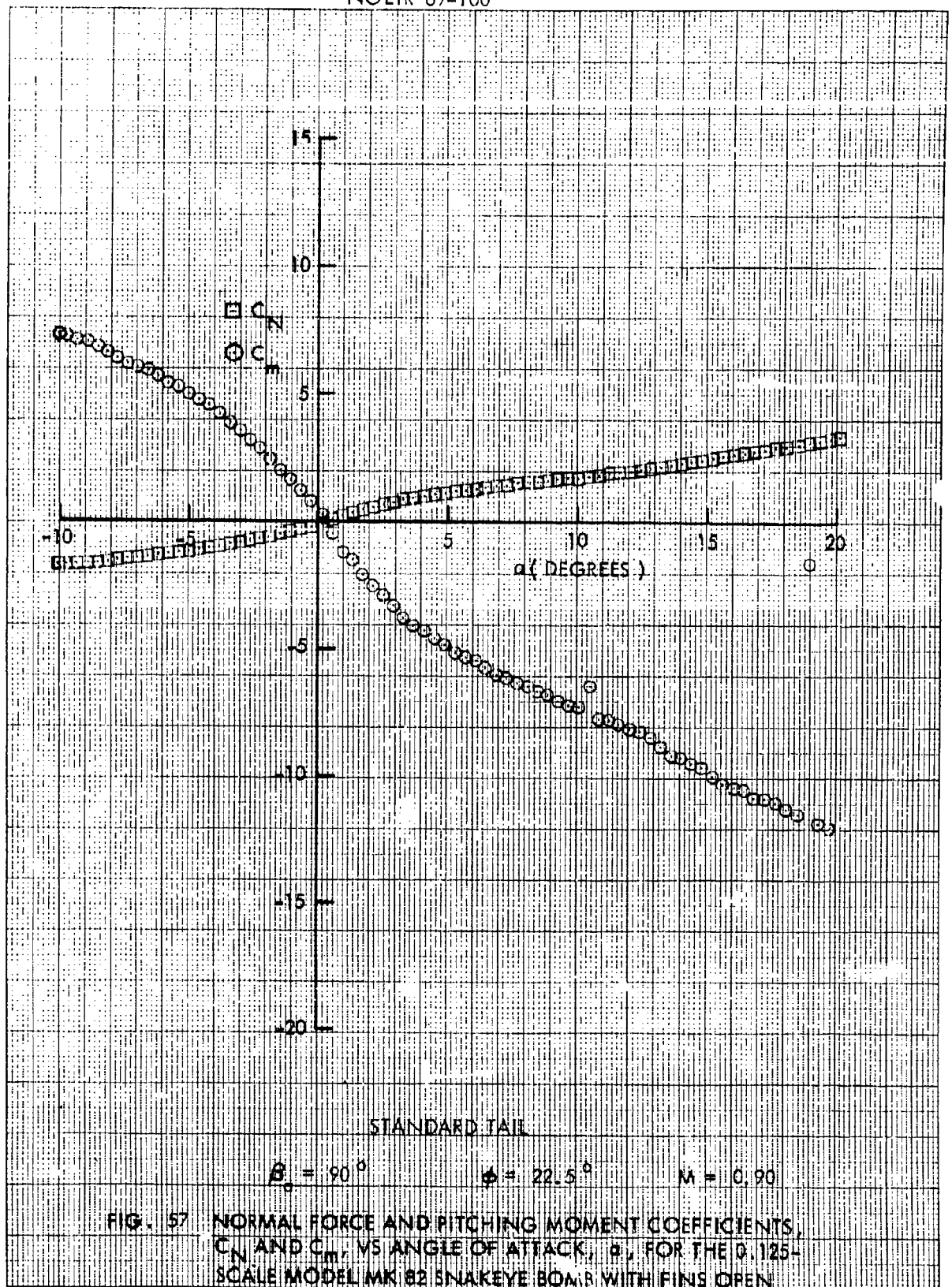
$$\phi = 22.5^\circ$$

$$M = 0.26$$

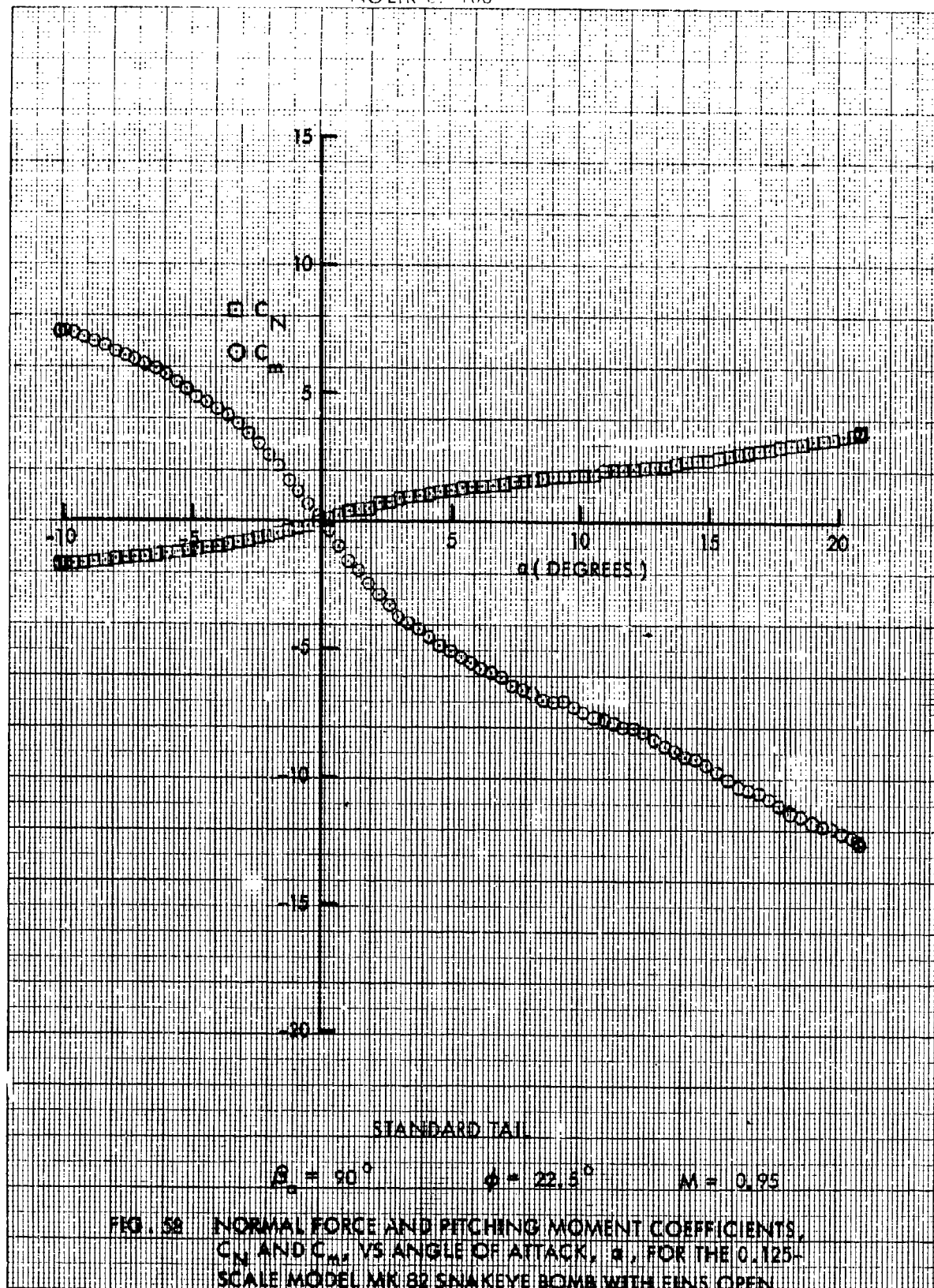
FIG. 54 NORMAL FORCE AND PITCHING MOMENT COEFFICIENTS,  $C_N$  AND  $C_m$ , VS ANGLE OF ATTACK,  $\alpha$ , FOR THE 0.125-SCALE MODEL MK 82 SNAKEYE BOMB WITH FINS OPEN











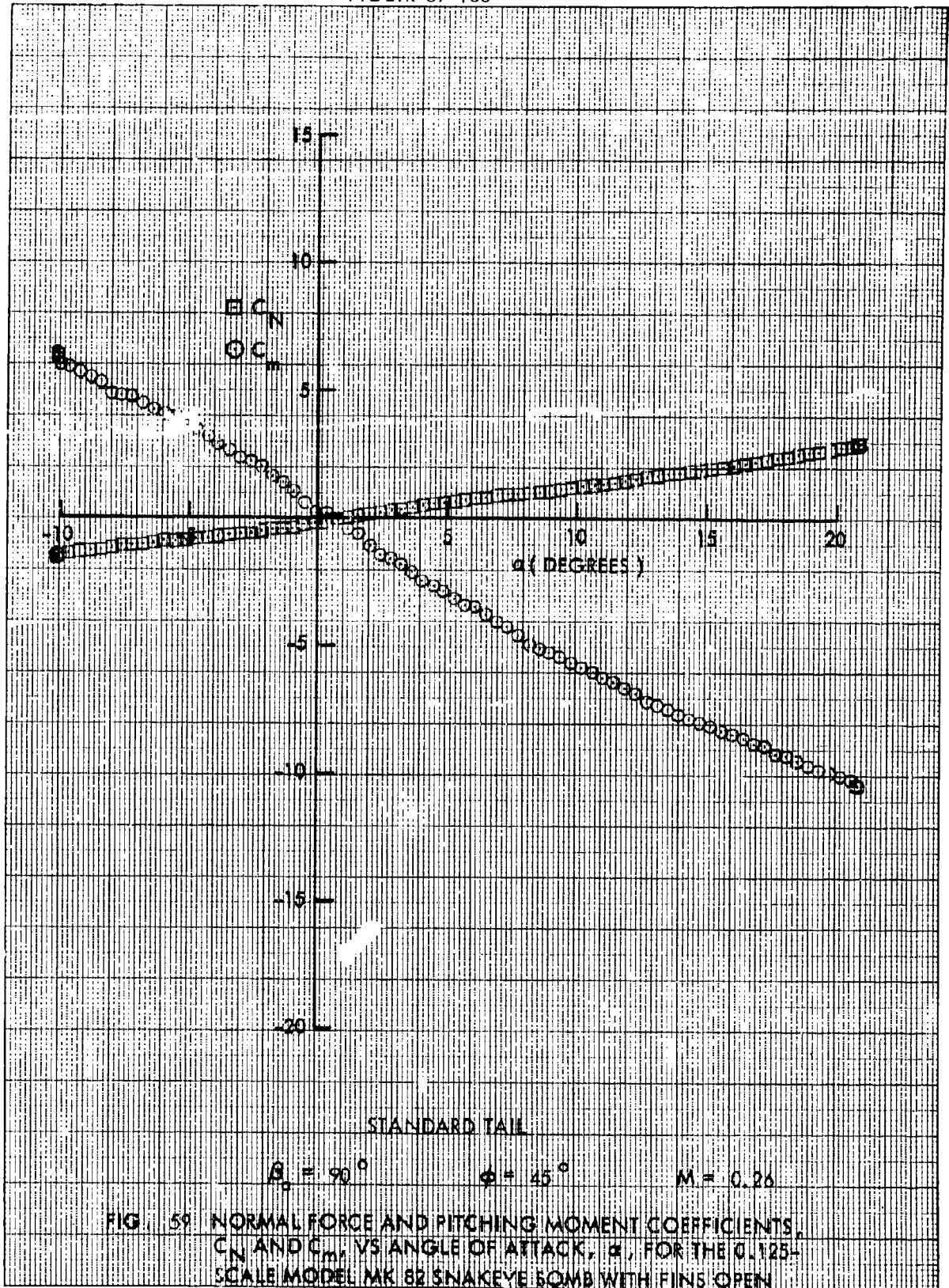
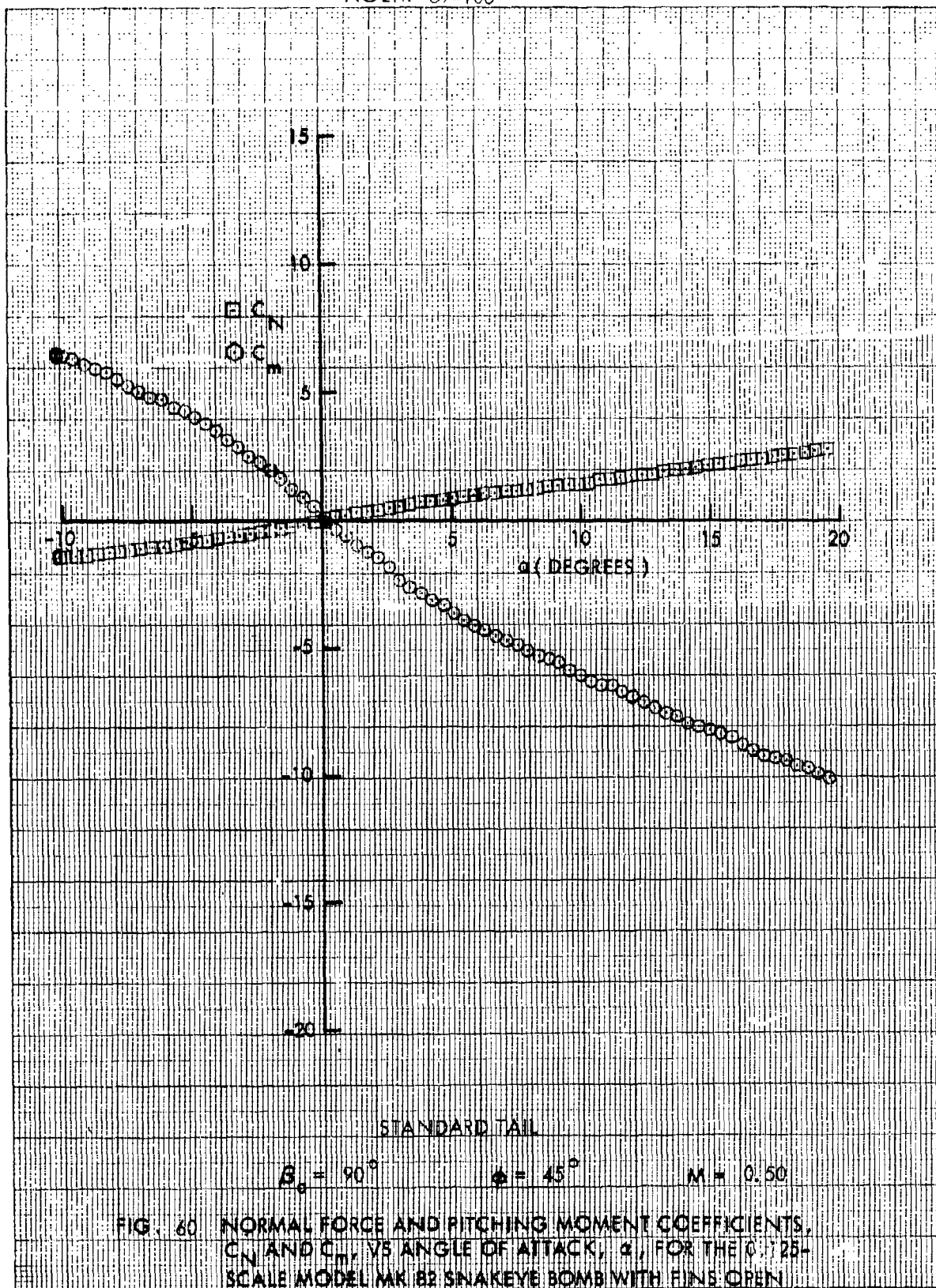
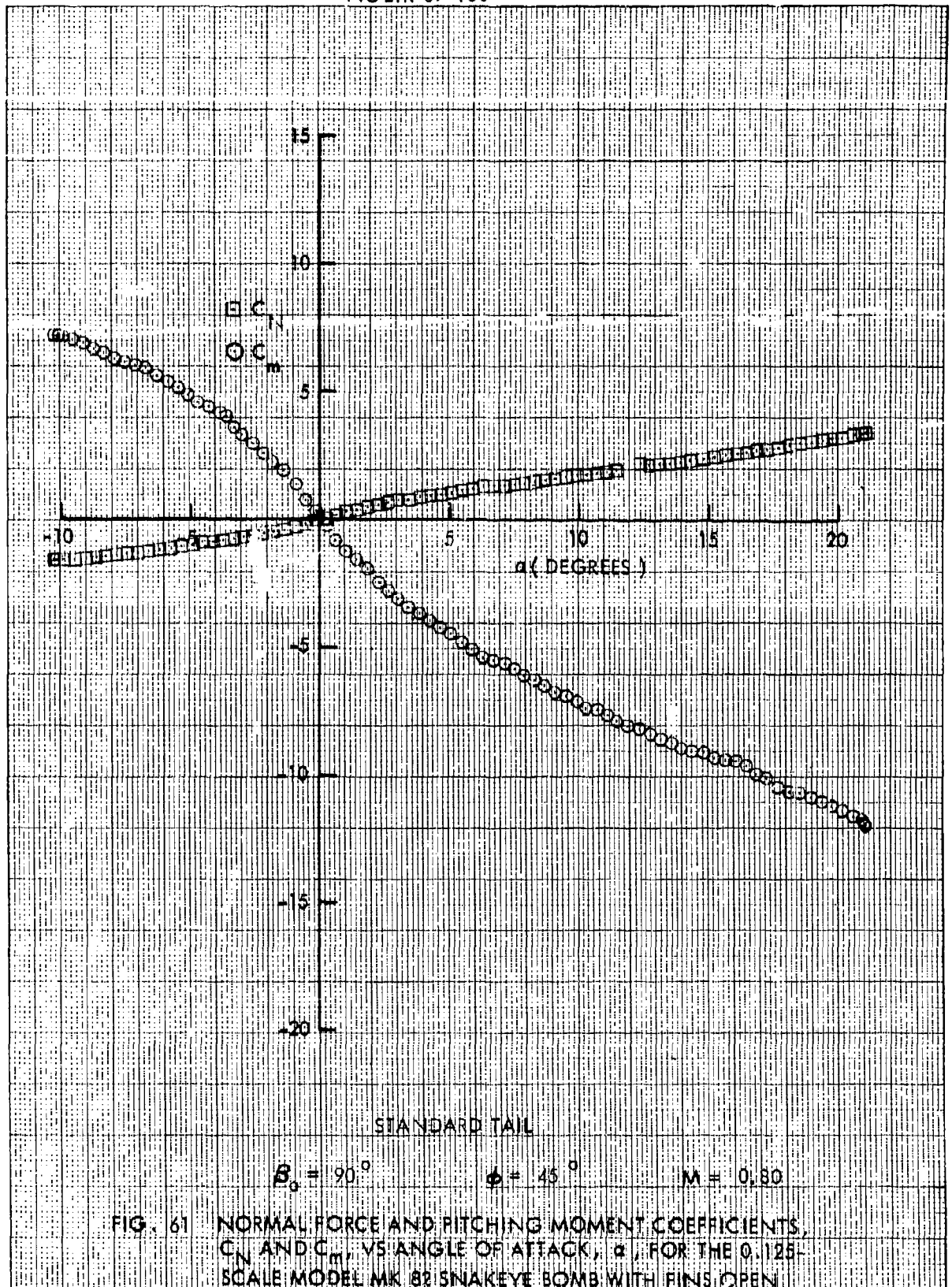
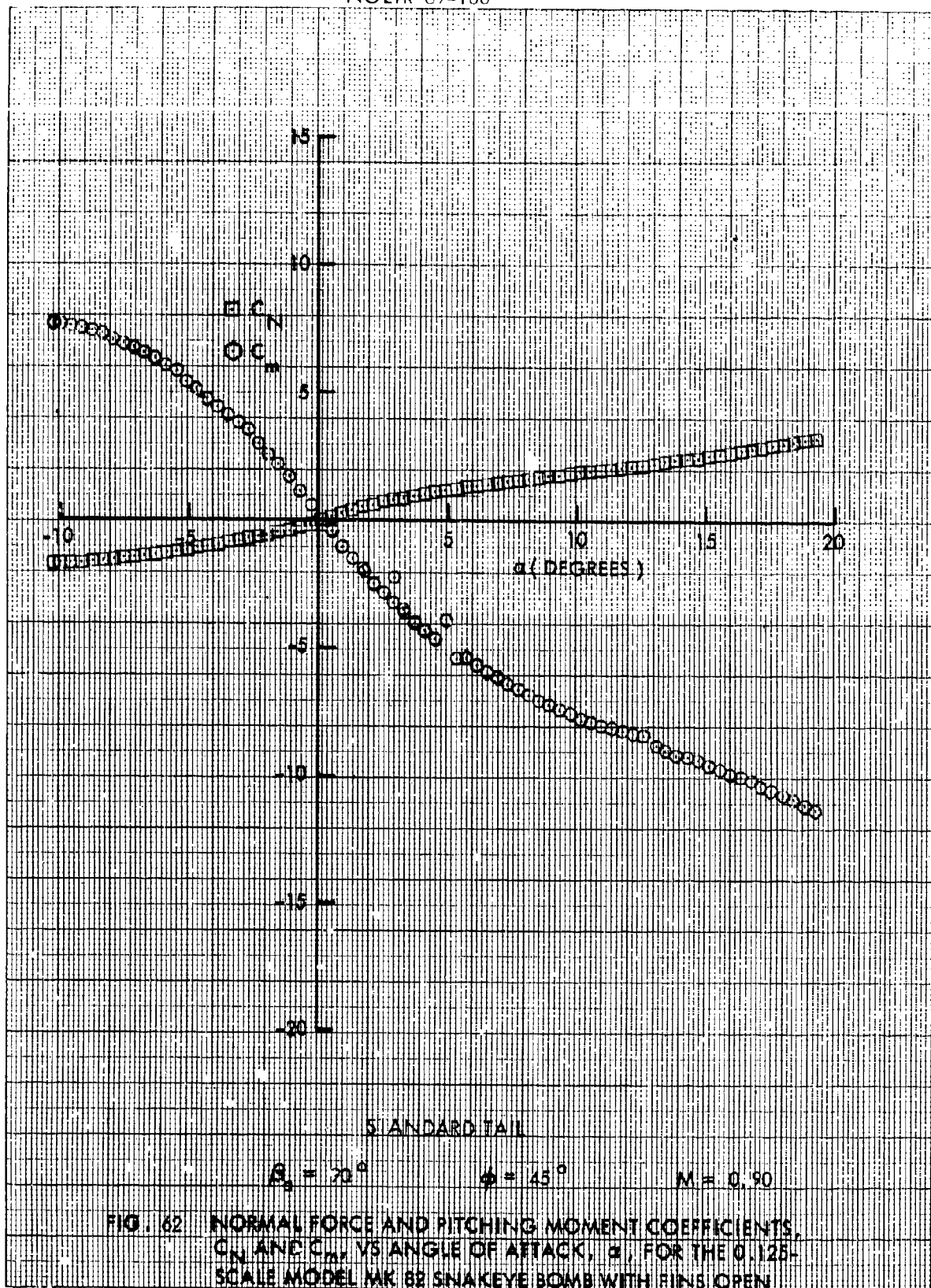


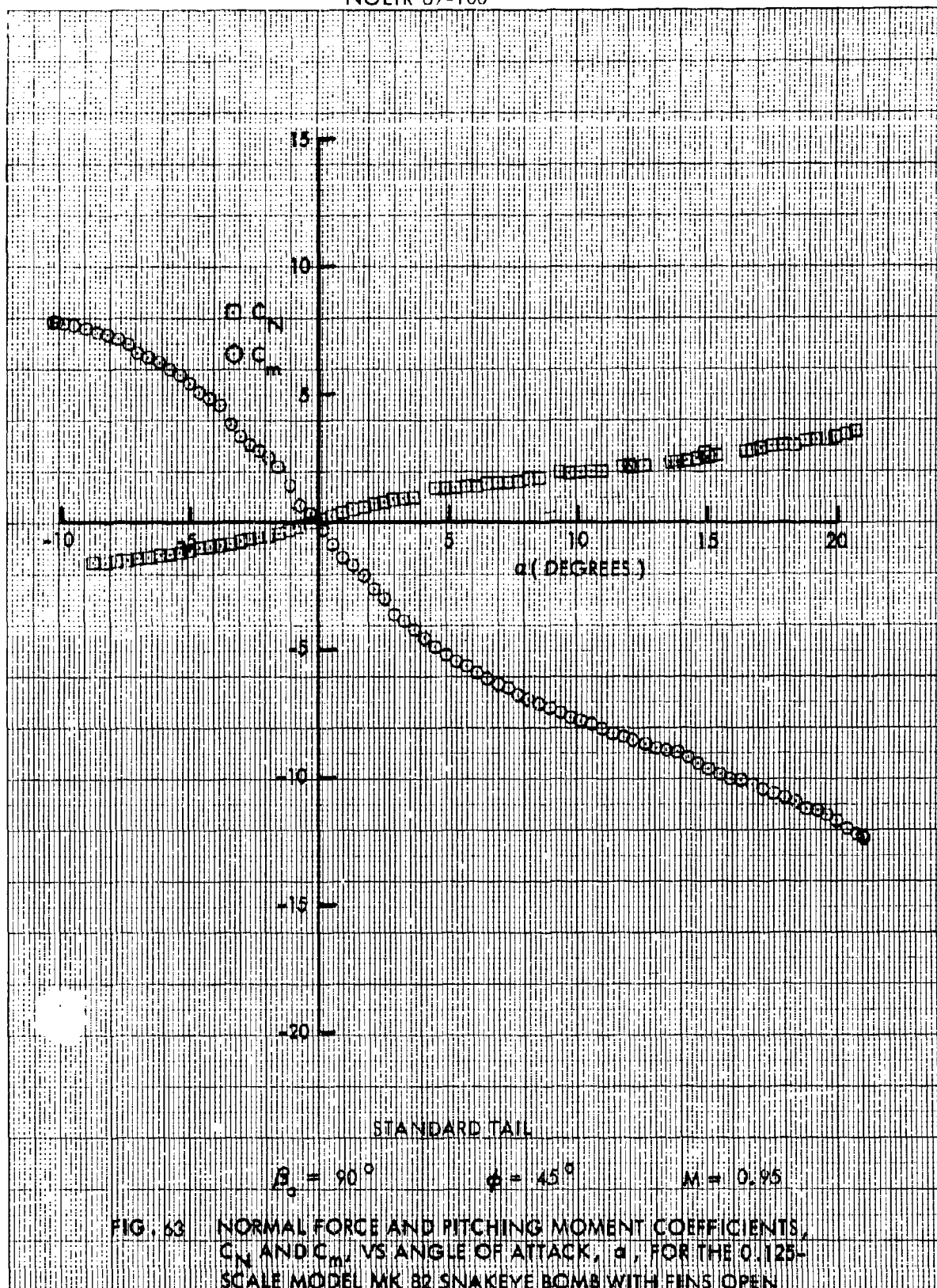
FIG. 59 NORMAL FORCE AND PITCHING MOMENT COEFFICIENTS,  $C_N$  AND  $C_m$ , VS ANGLE OF ATTACK,  $\alpha$ , FOR THE 0.125-SCALE MODEL MK 82 SNAKEYE BOMB WITH FINS OPEN

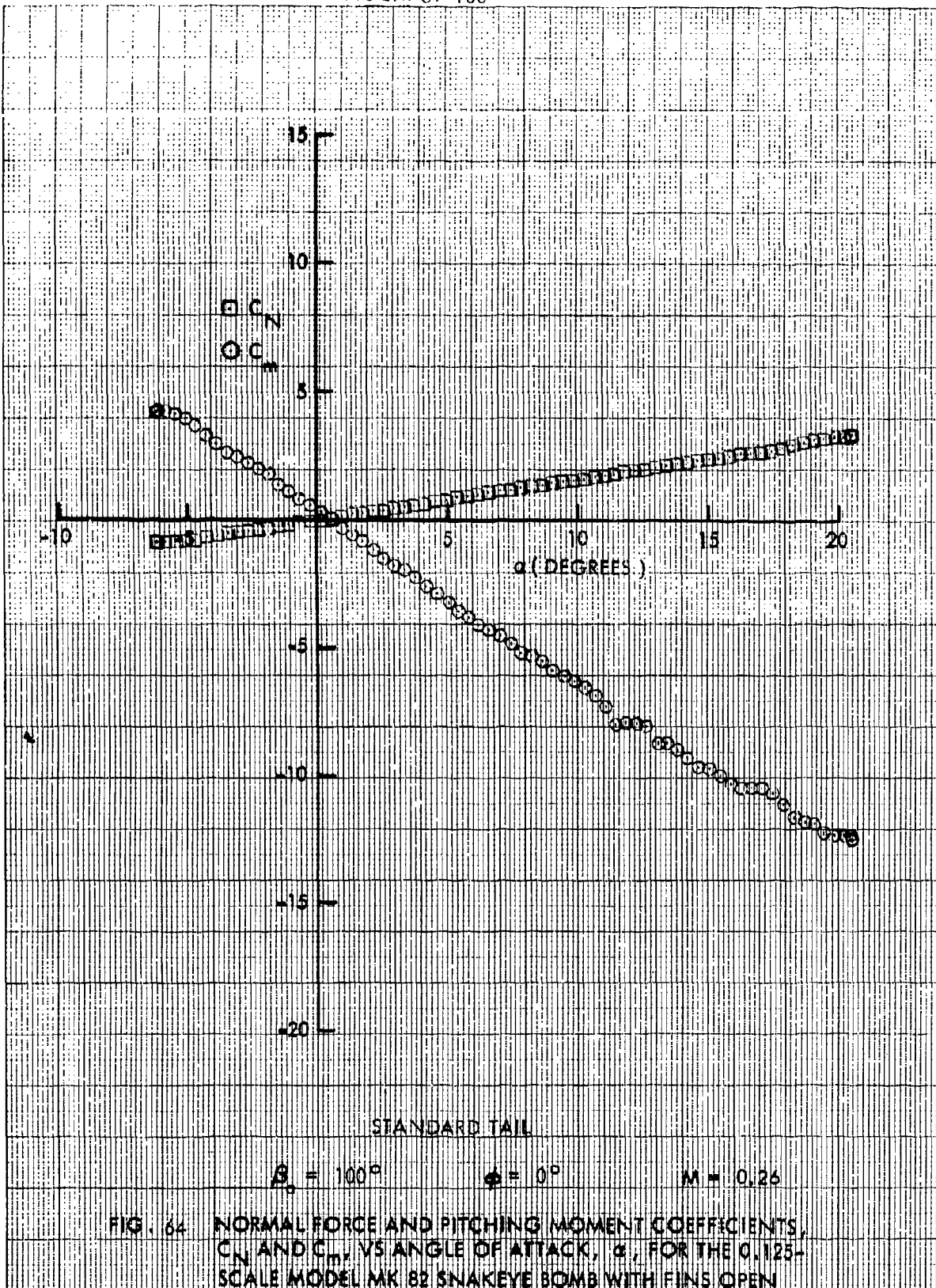




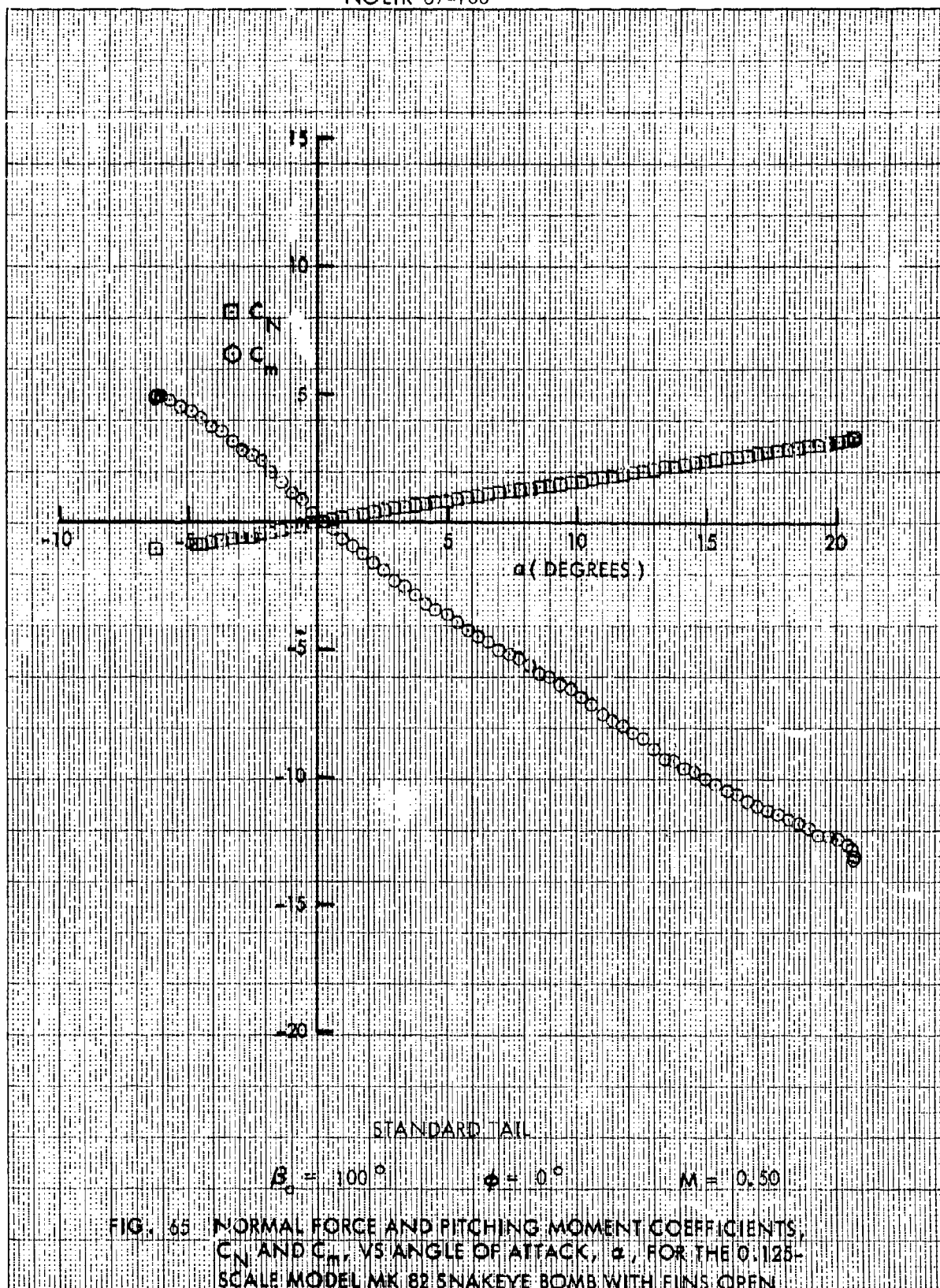


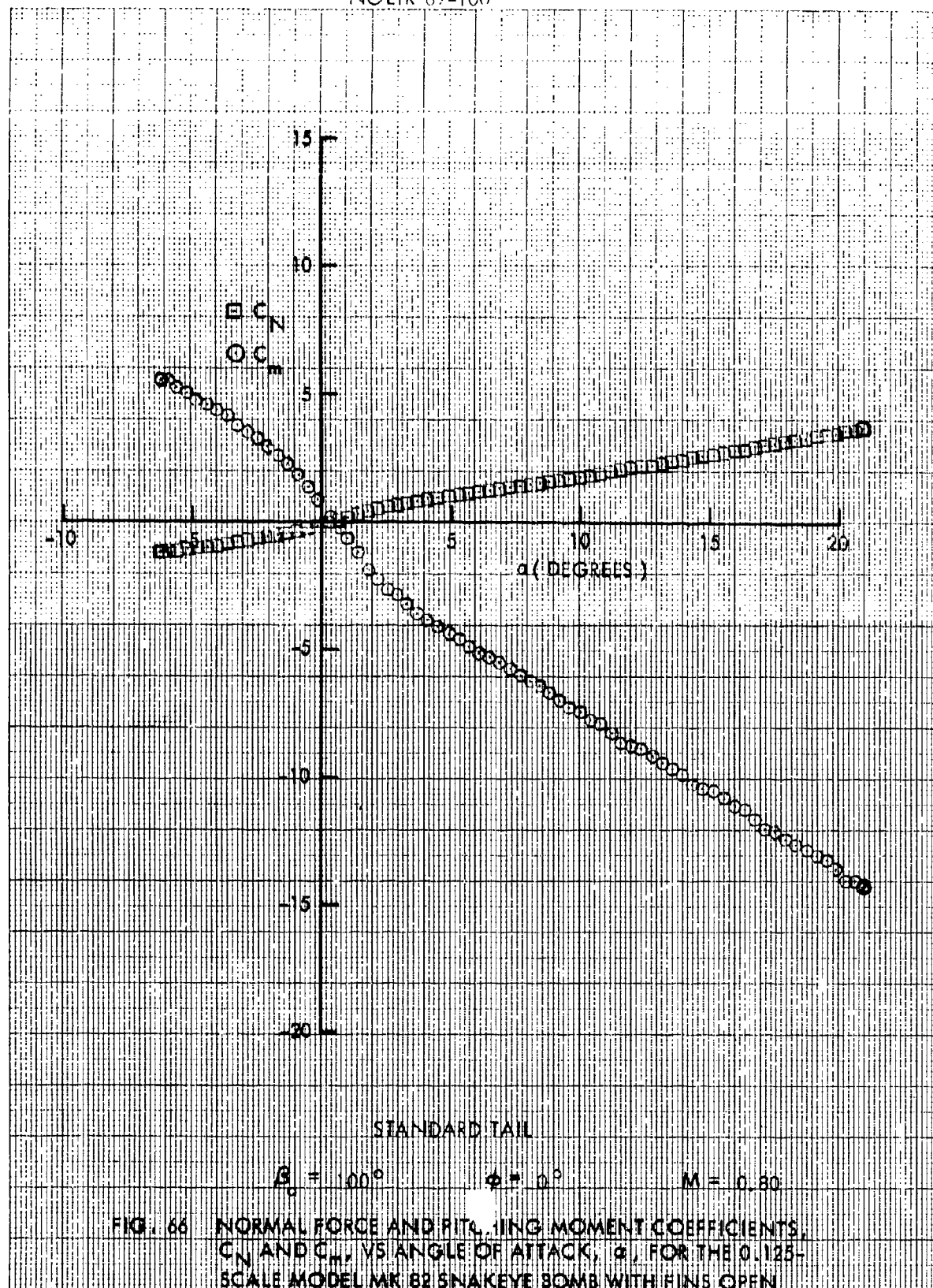


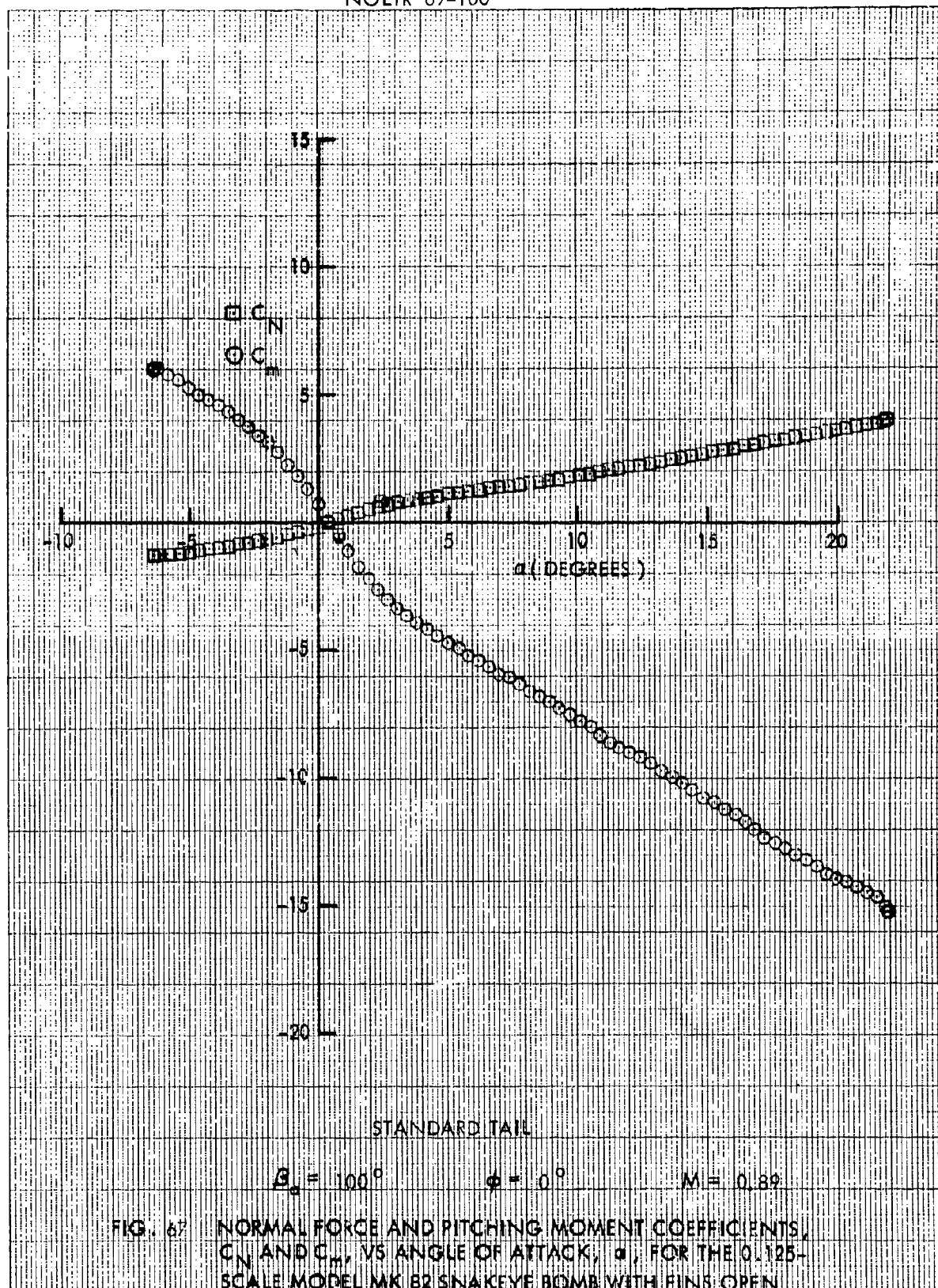




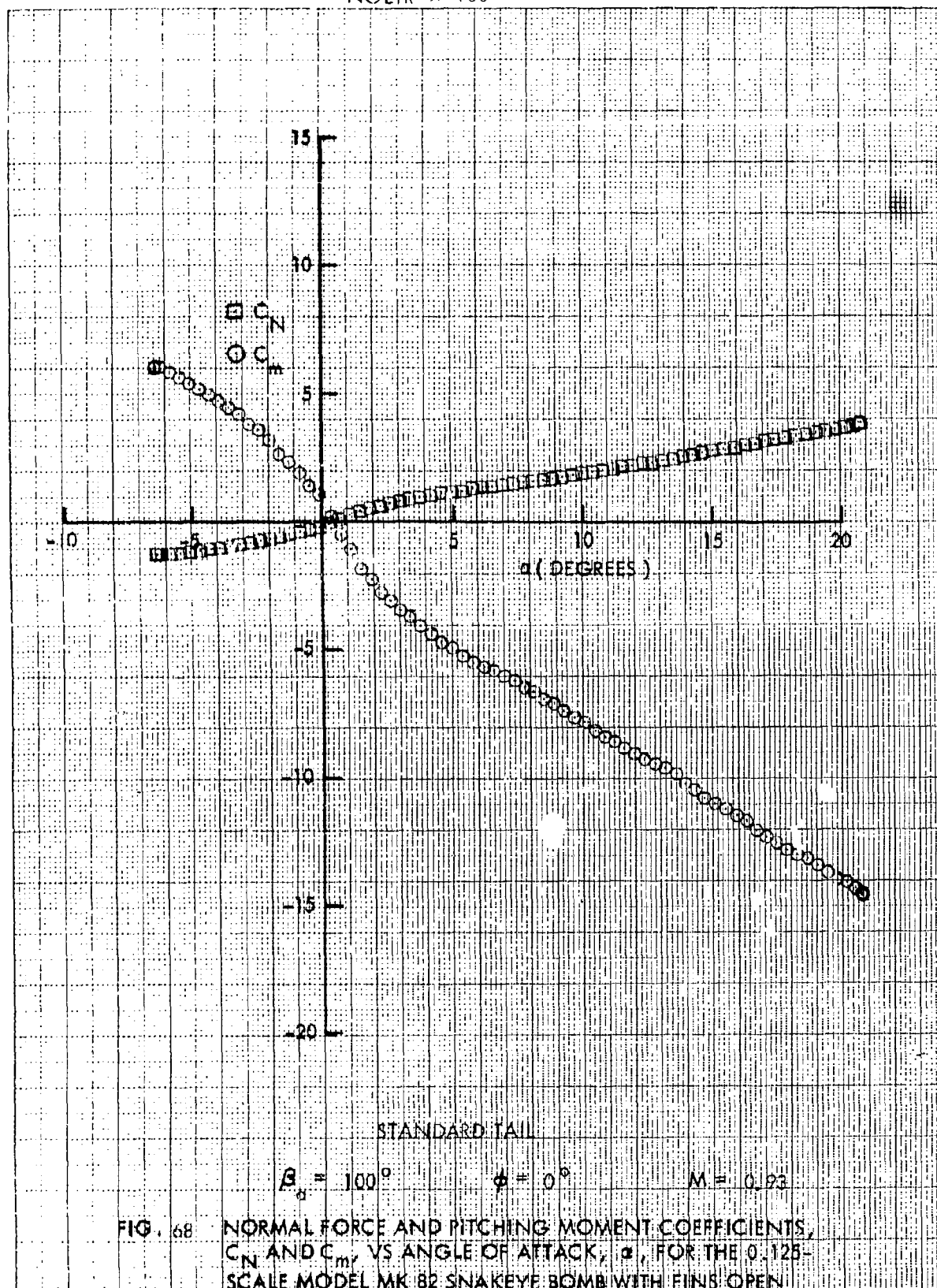


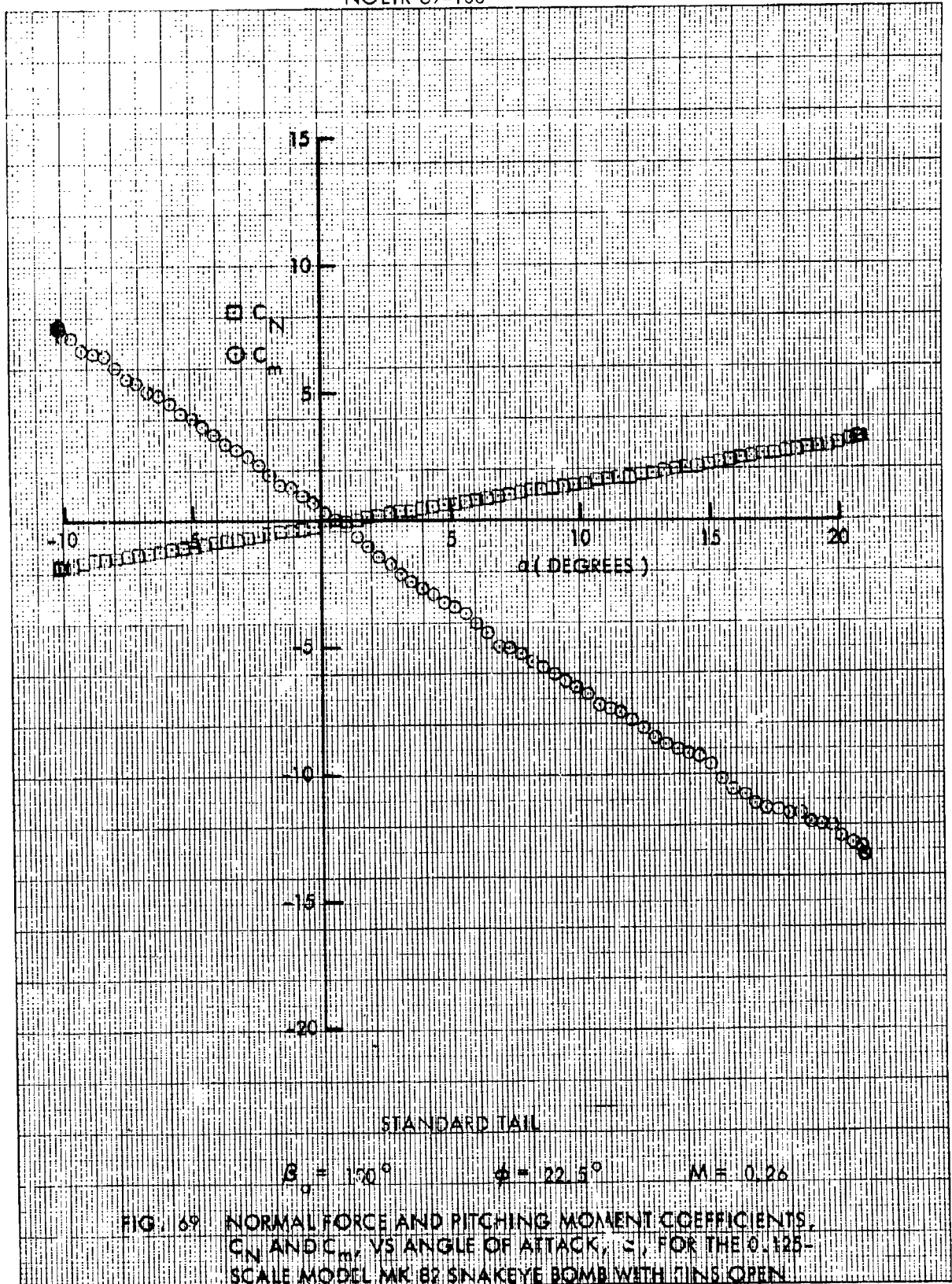


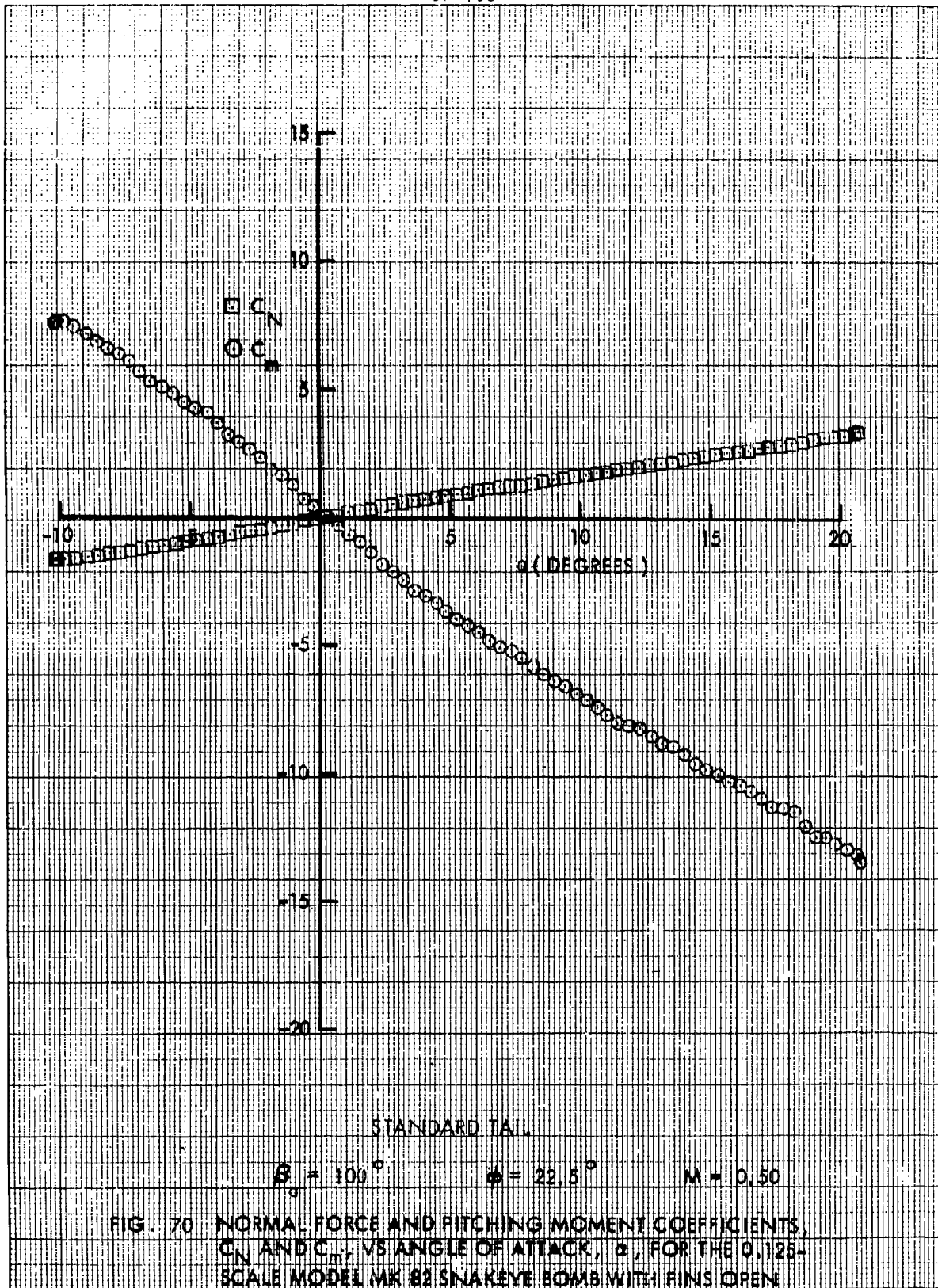


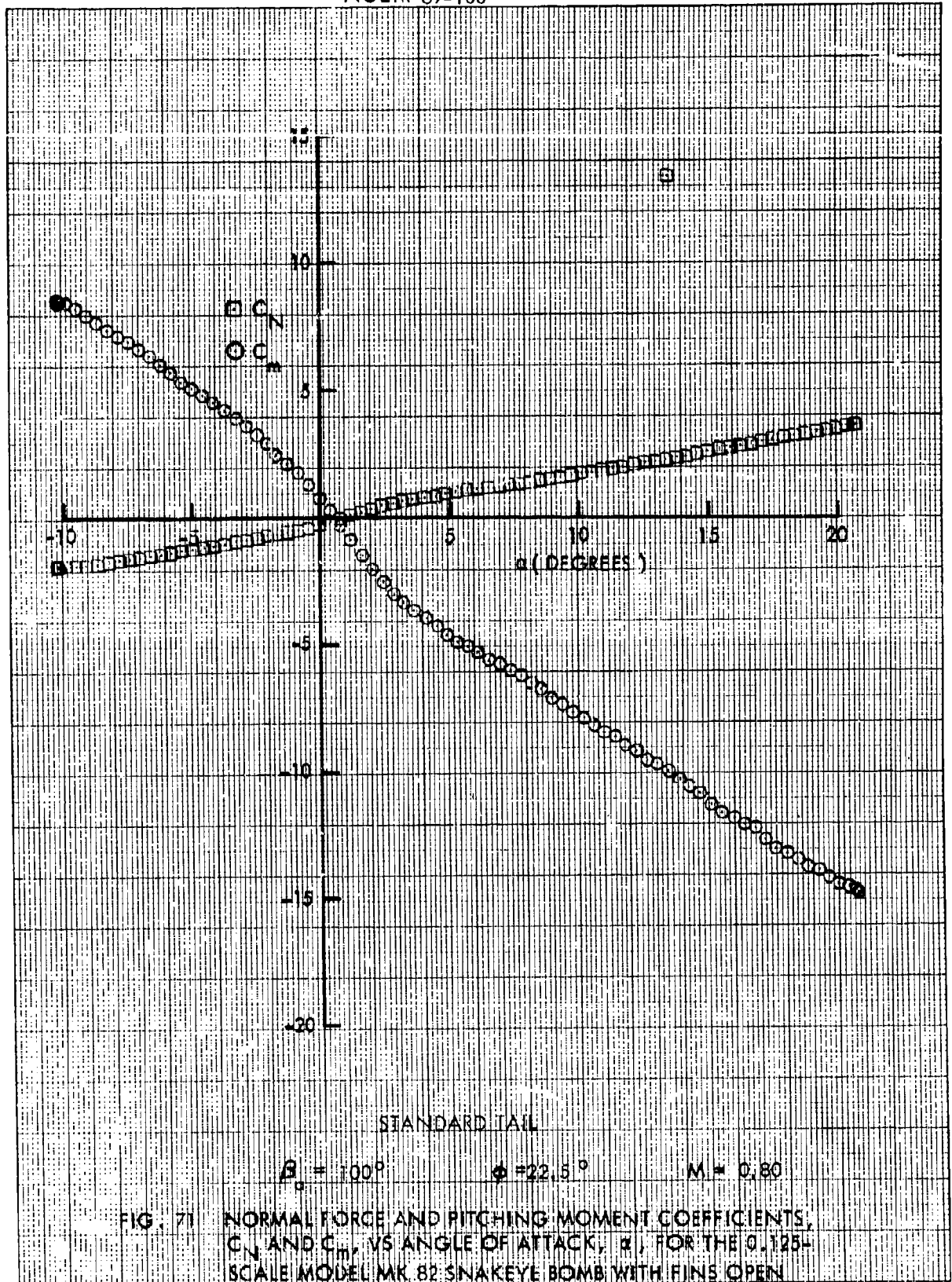


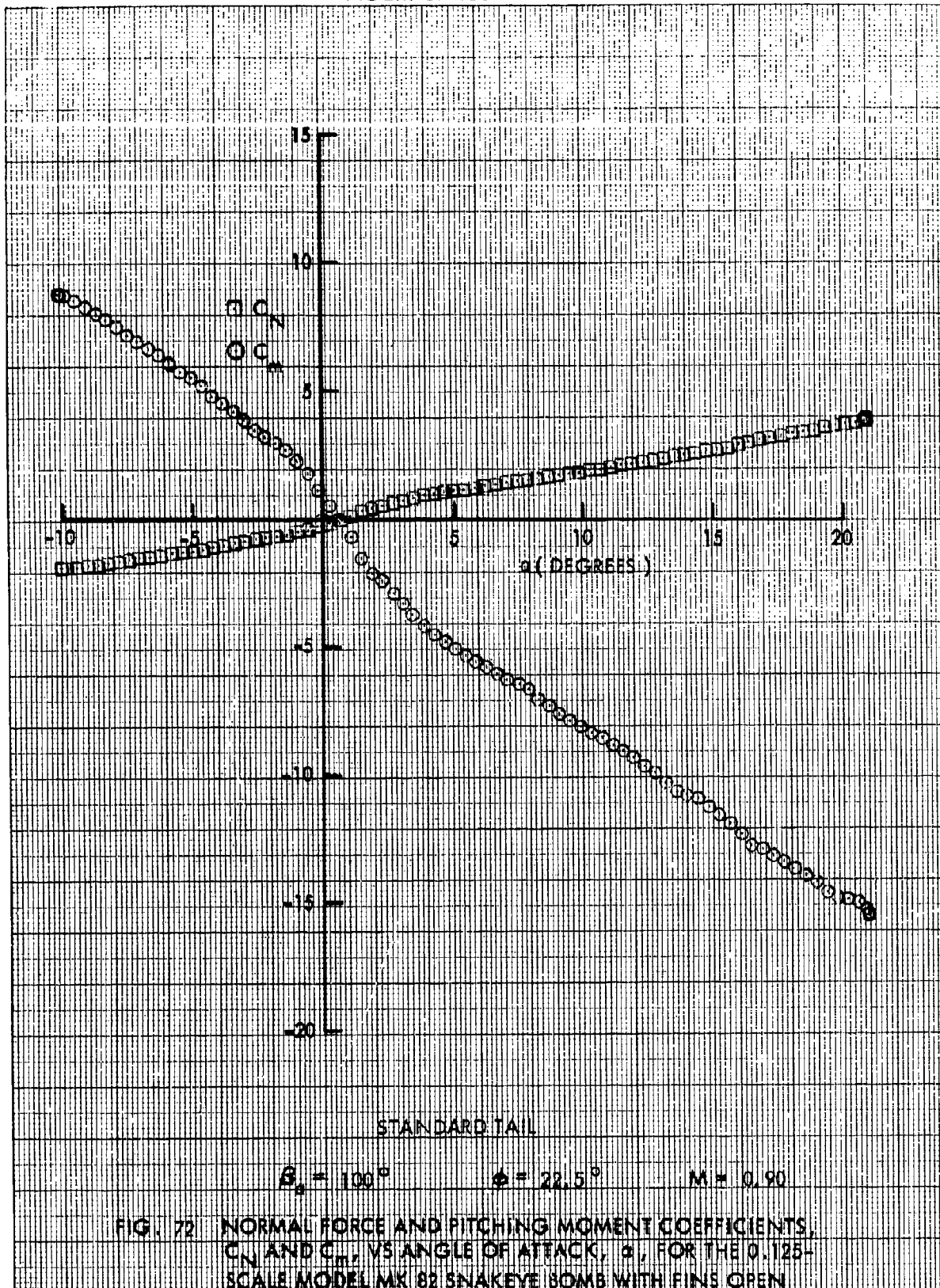




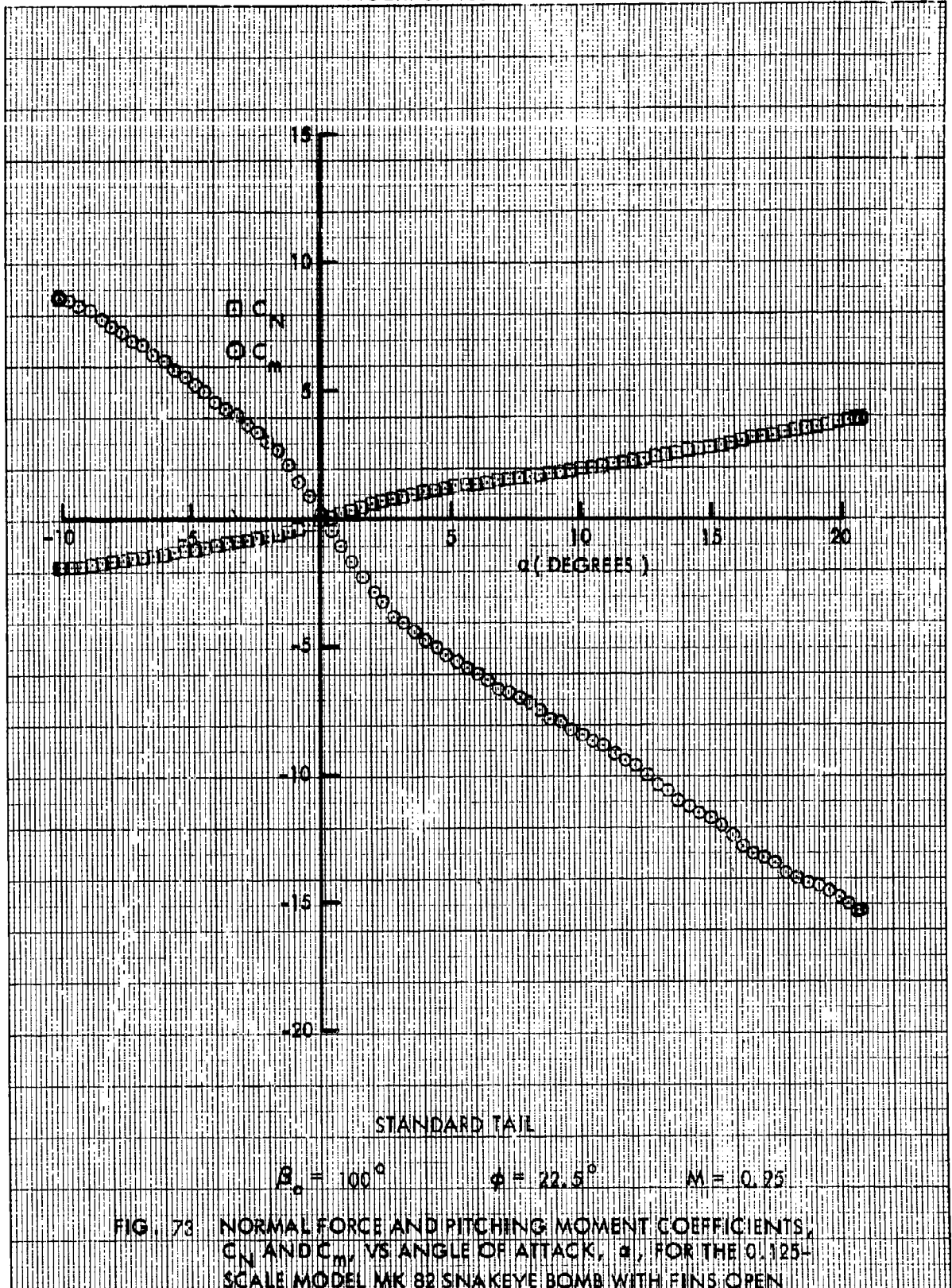


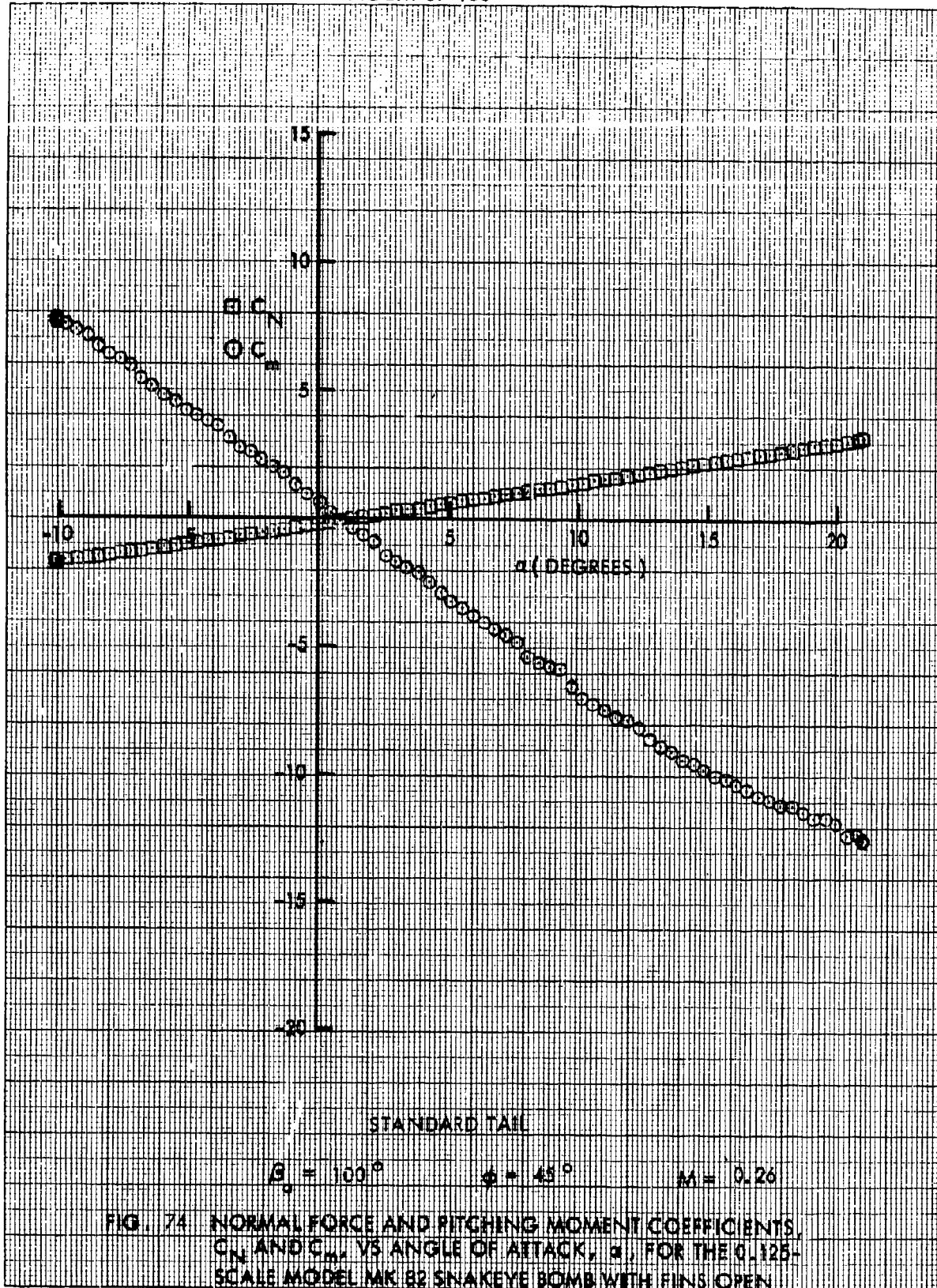


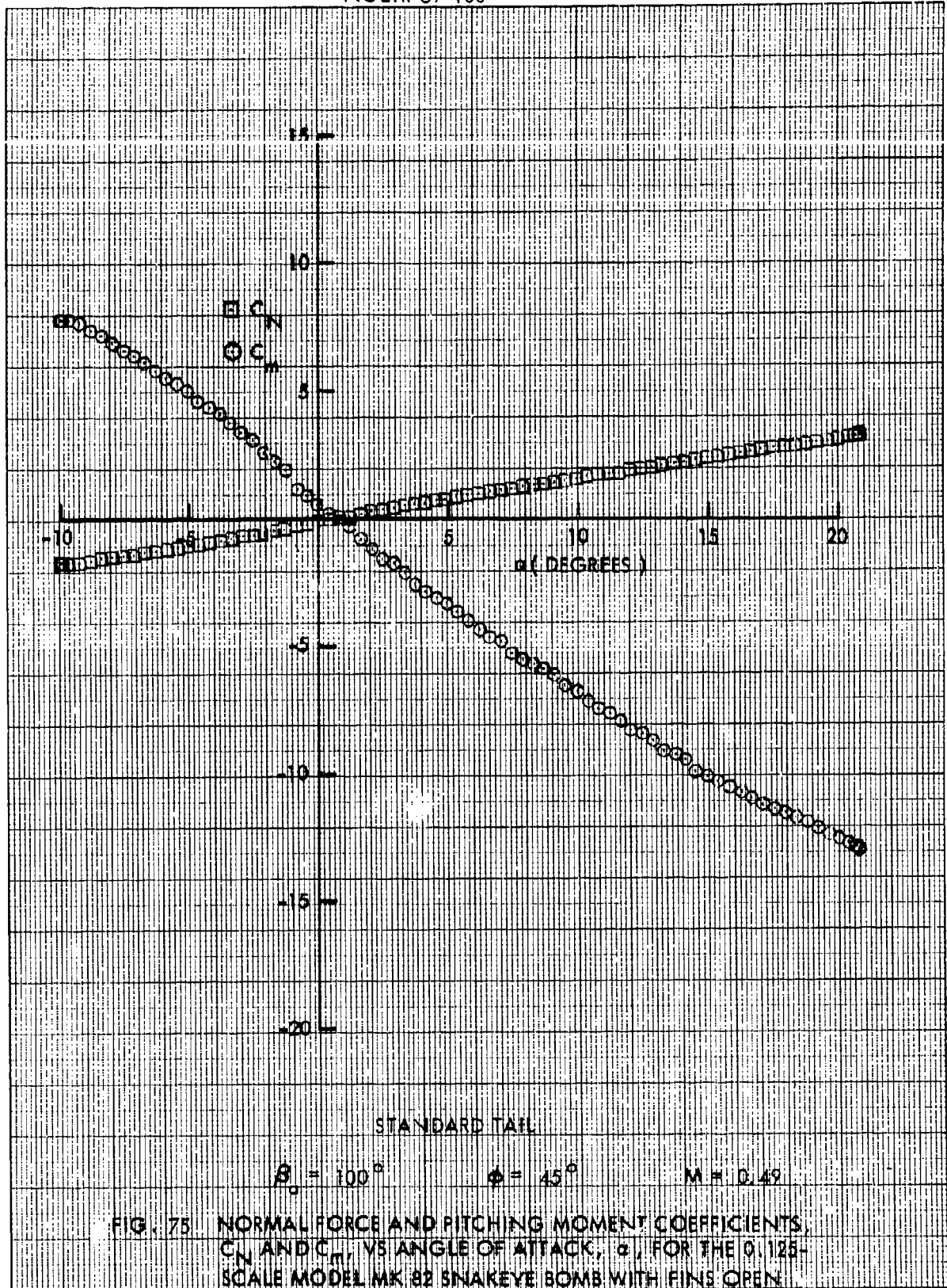




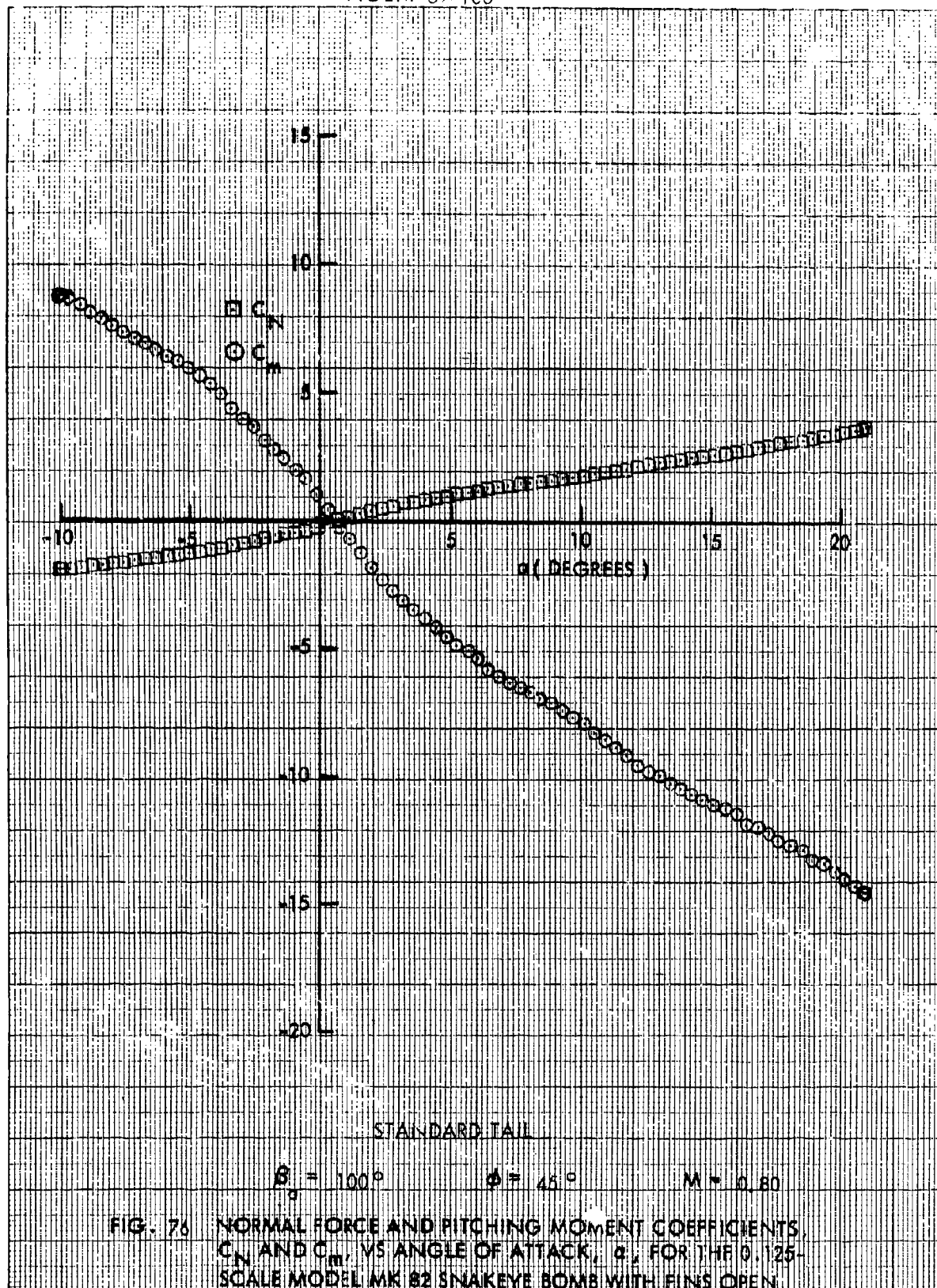


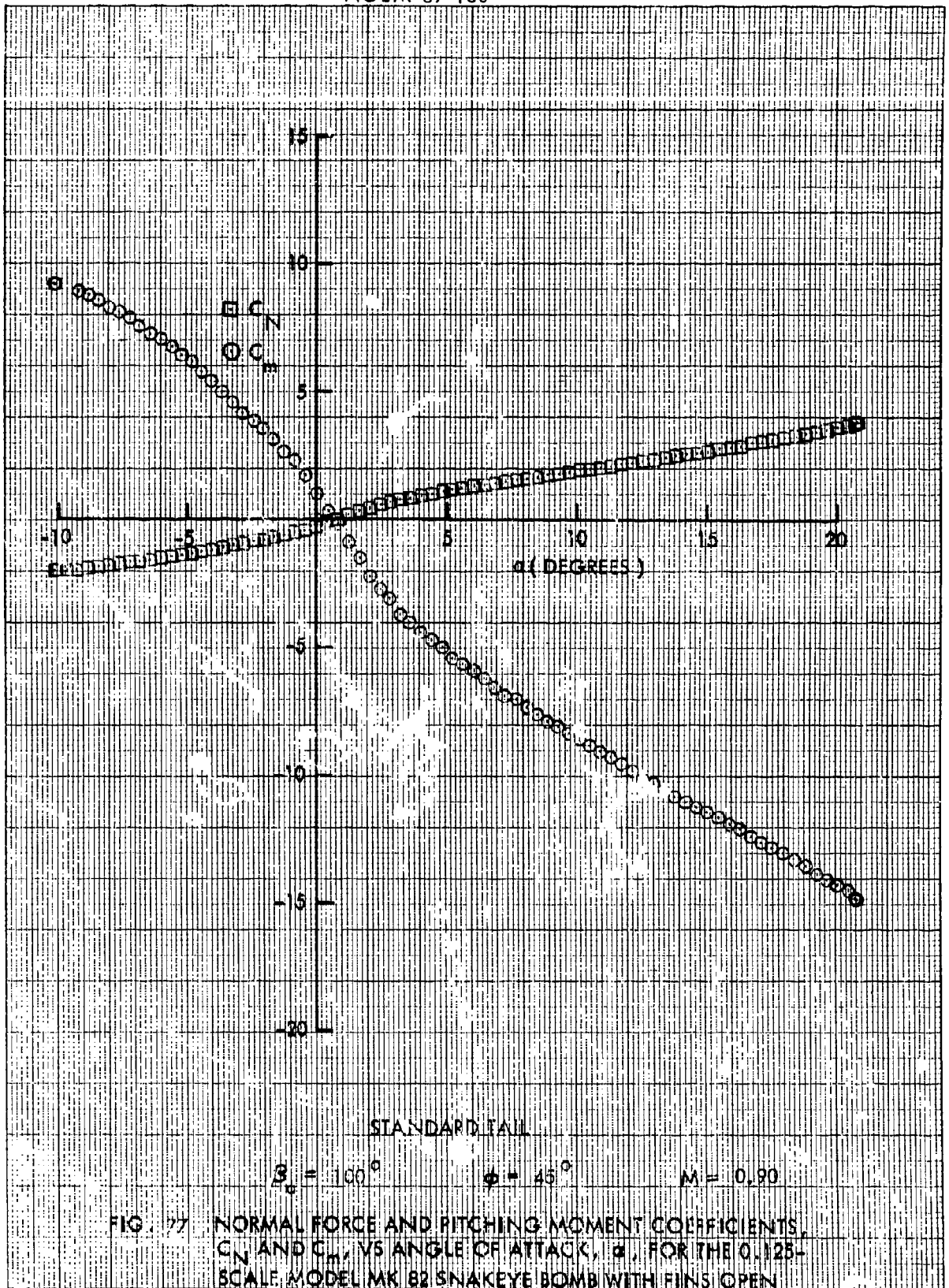


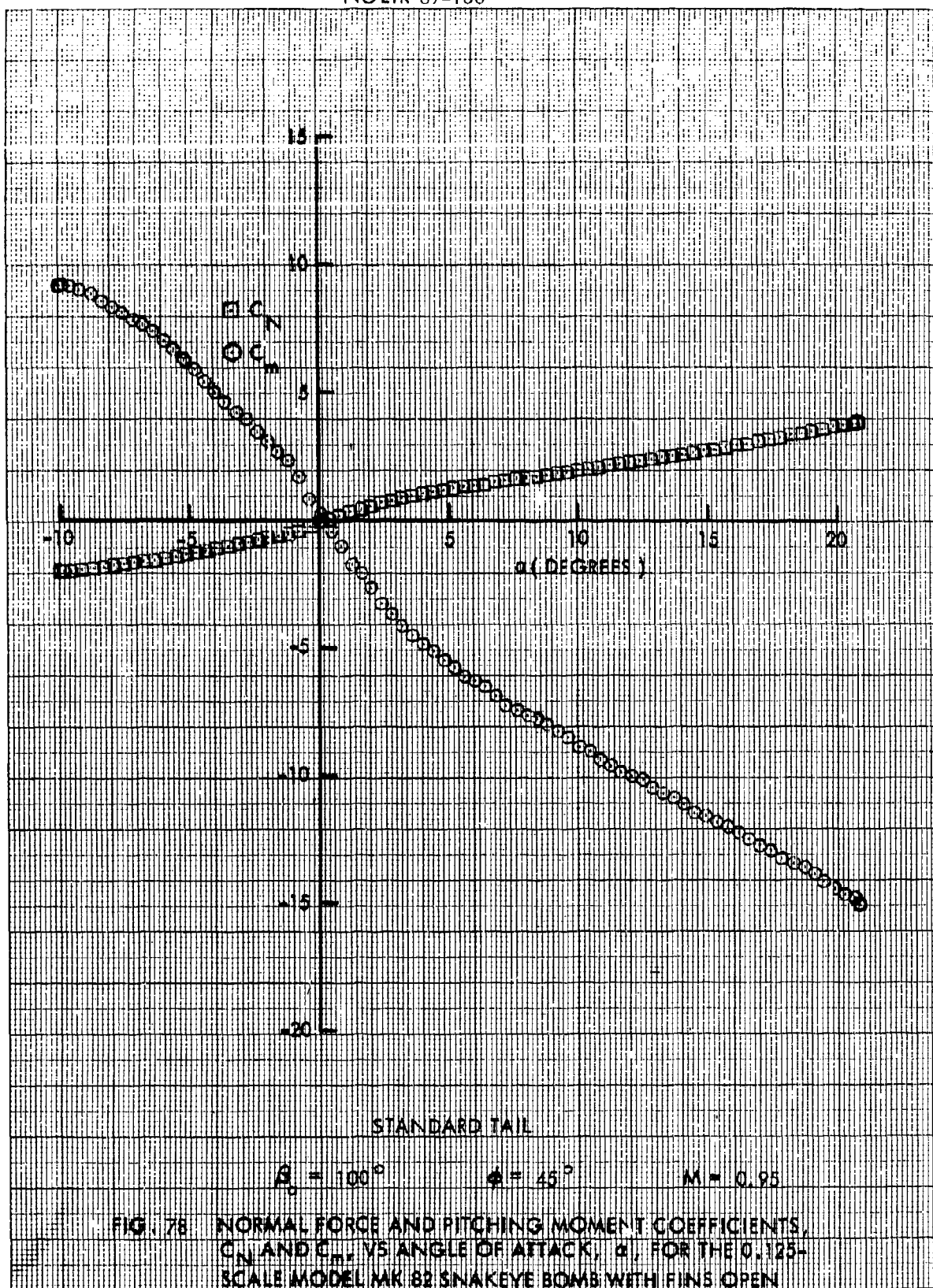


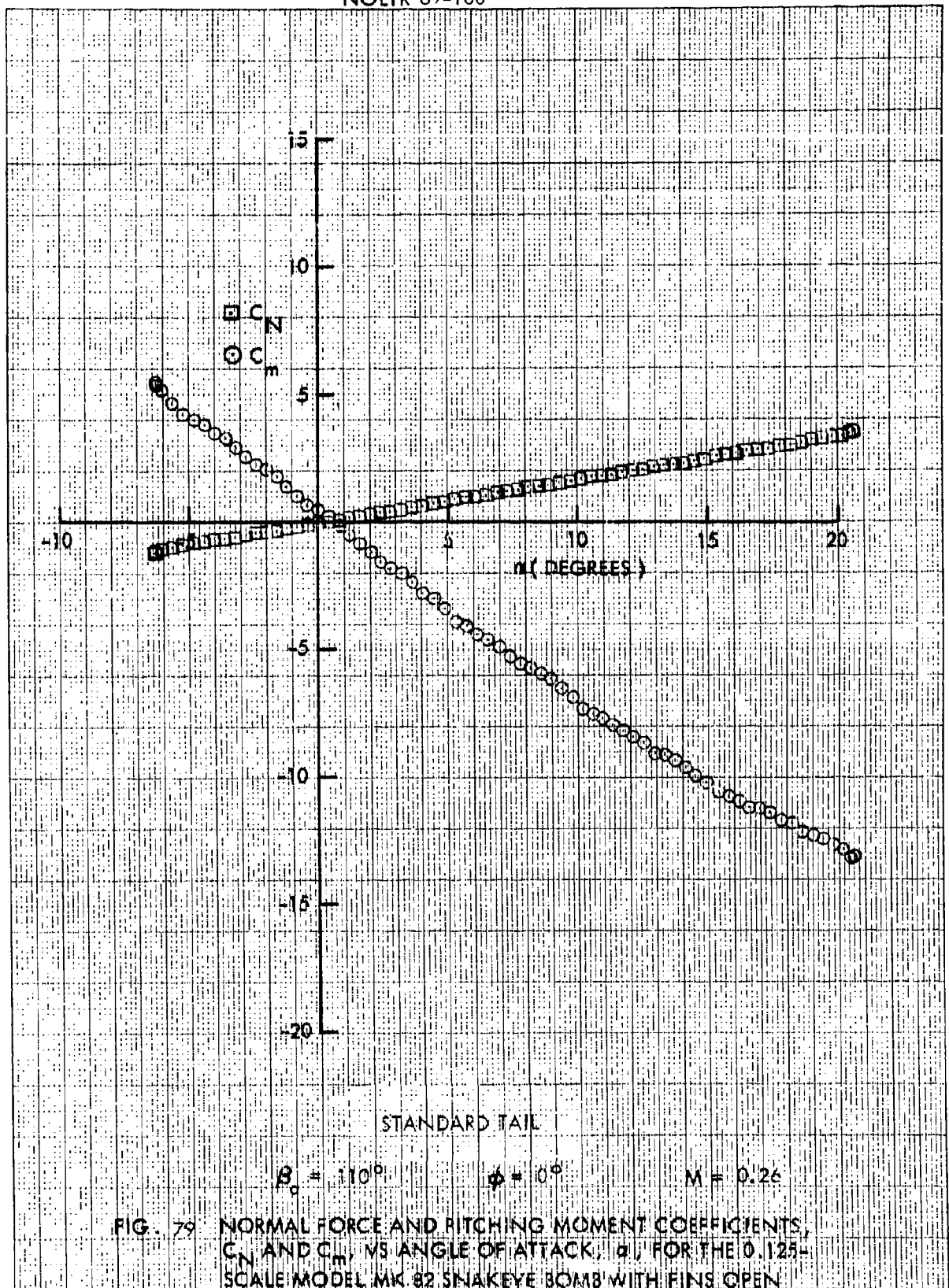


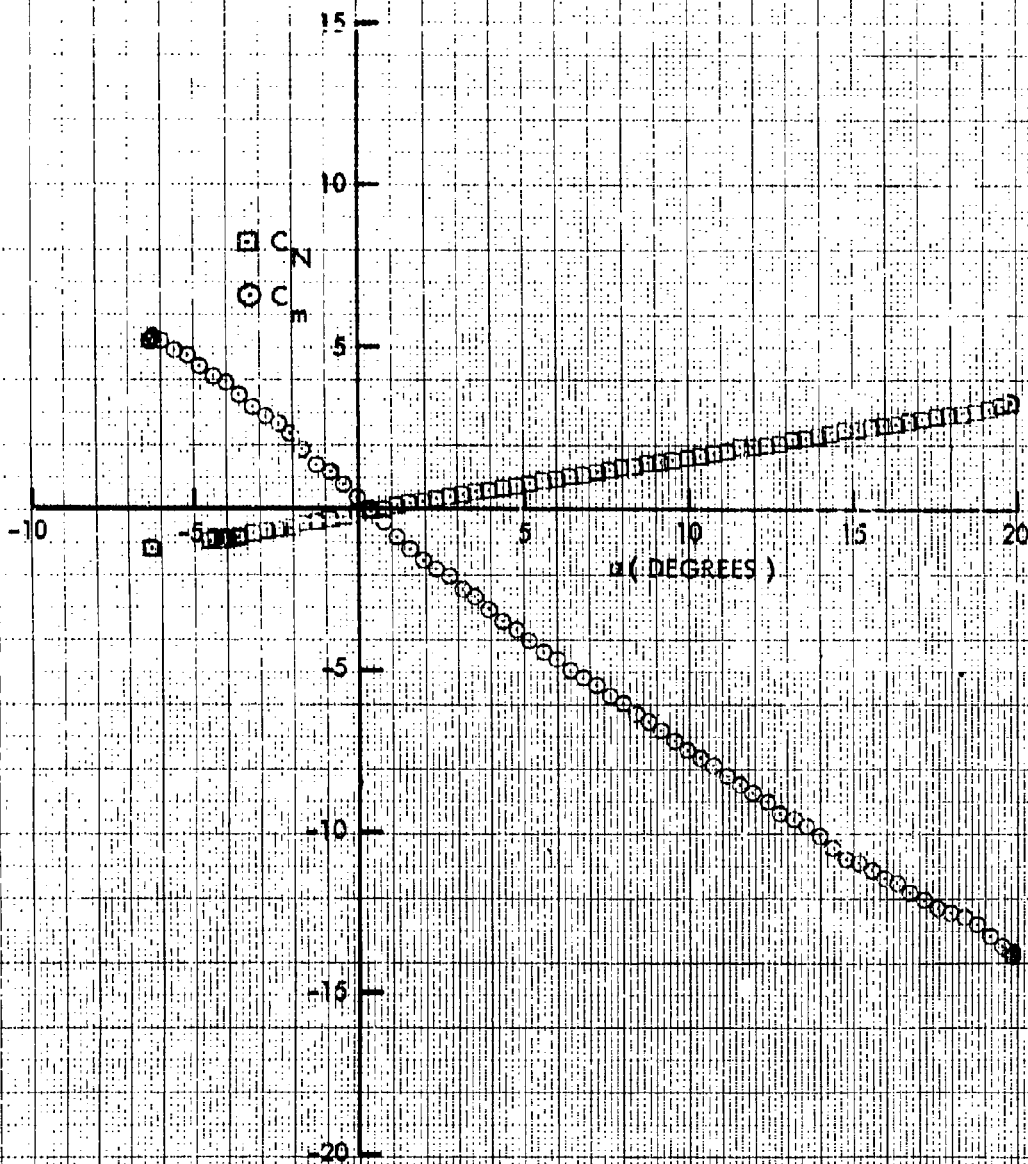












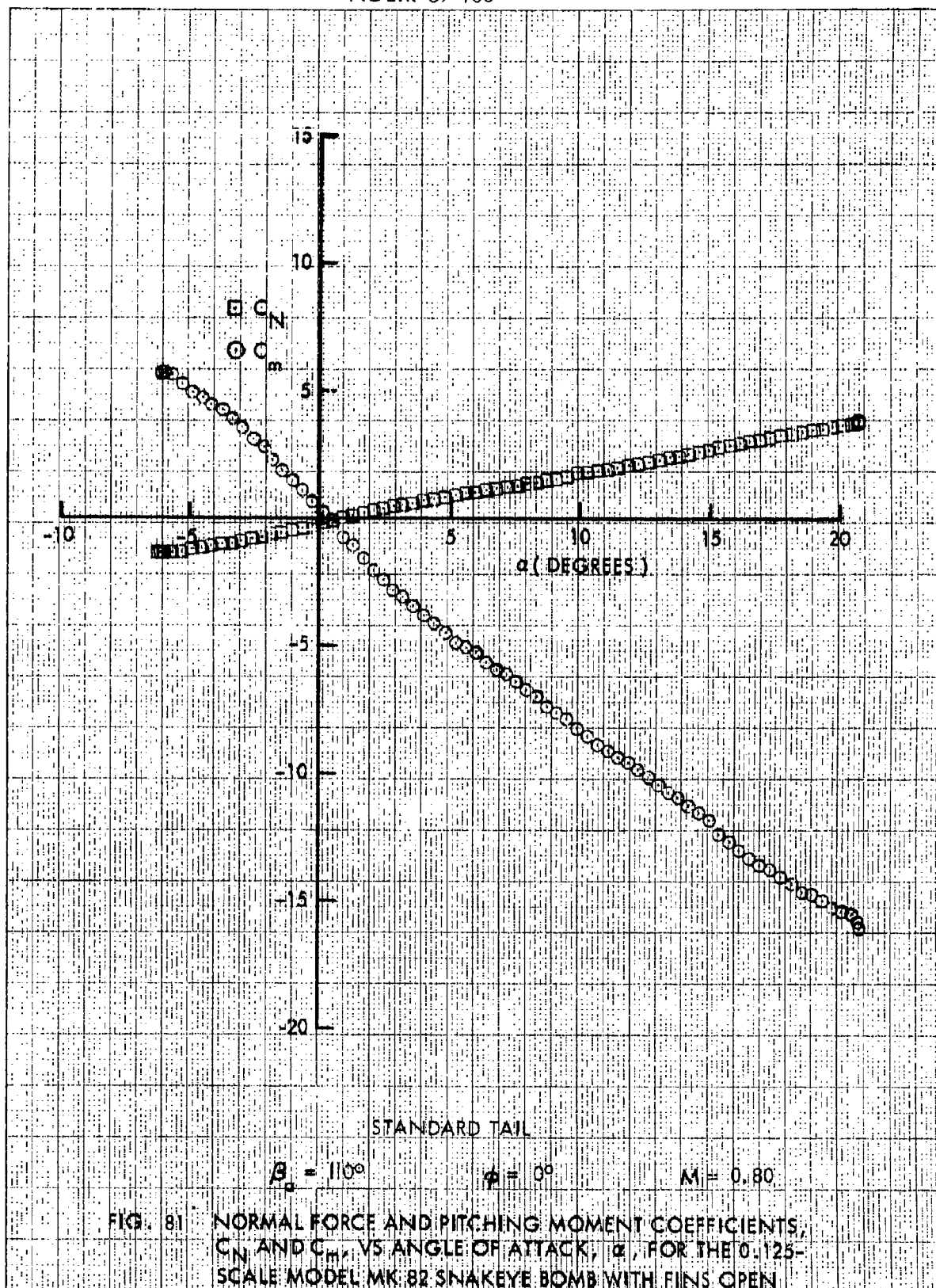
STANDARD TAIL

$$\beta_0 = 110^\circ$$

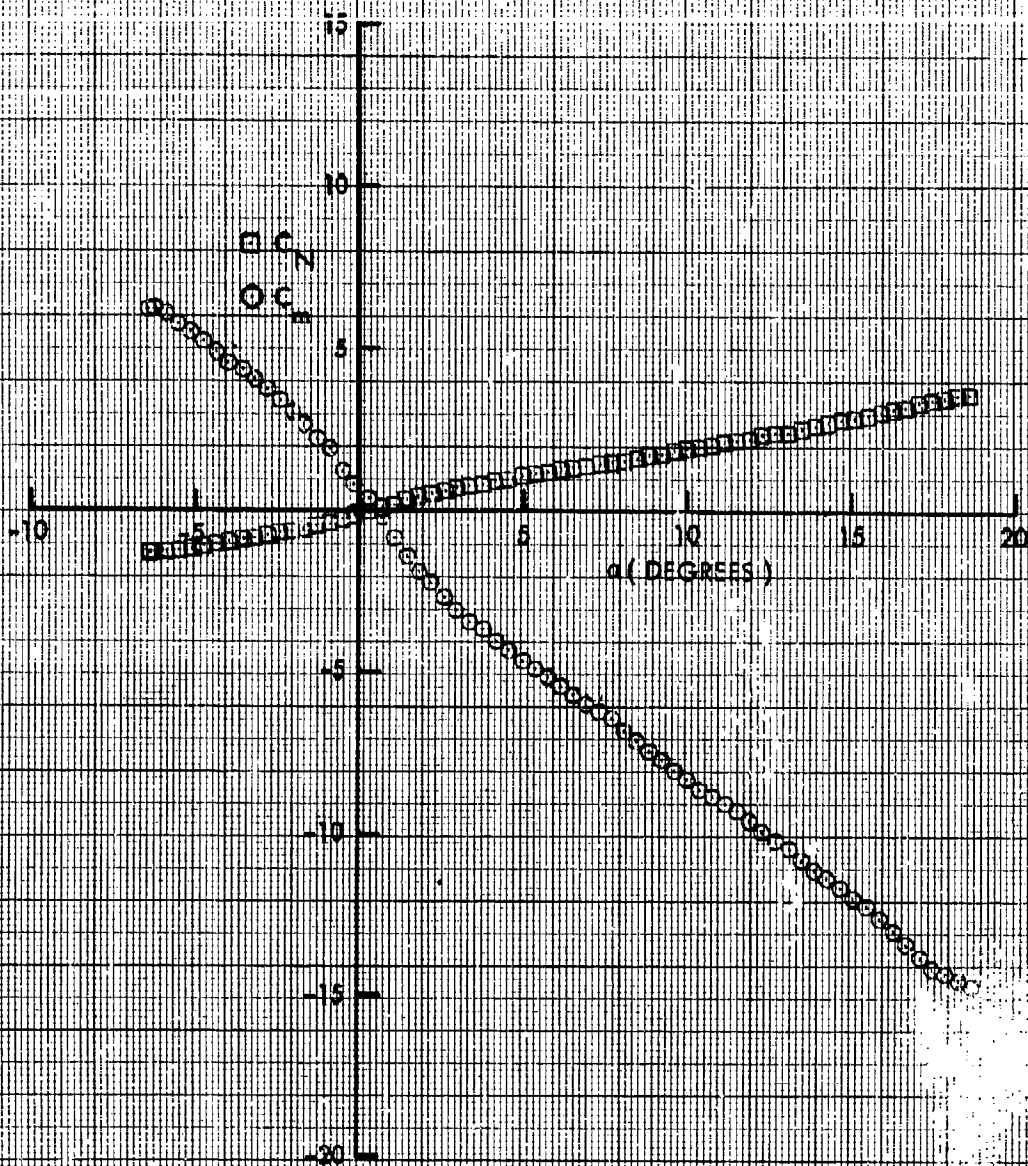
$$\phi = 0^\circ$$

$$M = 0.50$$

FIG. 80 NORMAL FORCE AND PITCHING MOMENT COEFFICIENTS,  $C_N$  AND  $C_m$ , VS ANGLE OF ATTACK,  $\alpha$ , FOR THE 0.125-SCALE MODEL MK 82 SNAKEYE BOMB WITH FINS OPEN







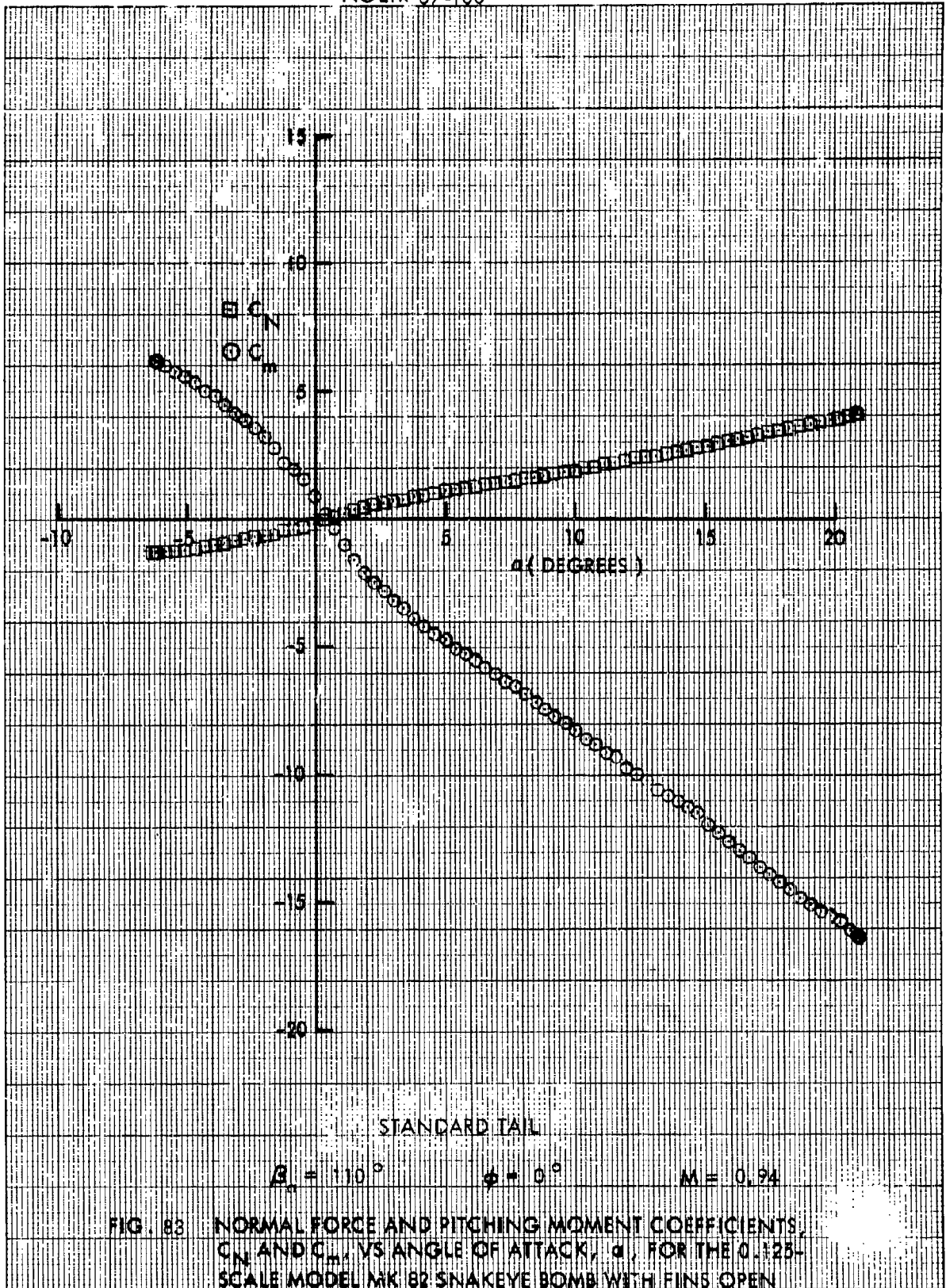
STANDARD TAIL

$$\delta_a = 110^\circ$$

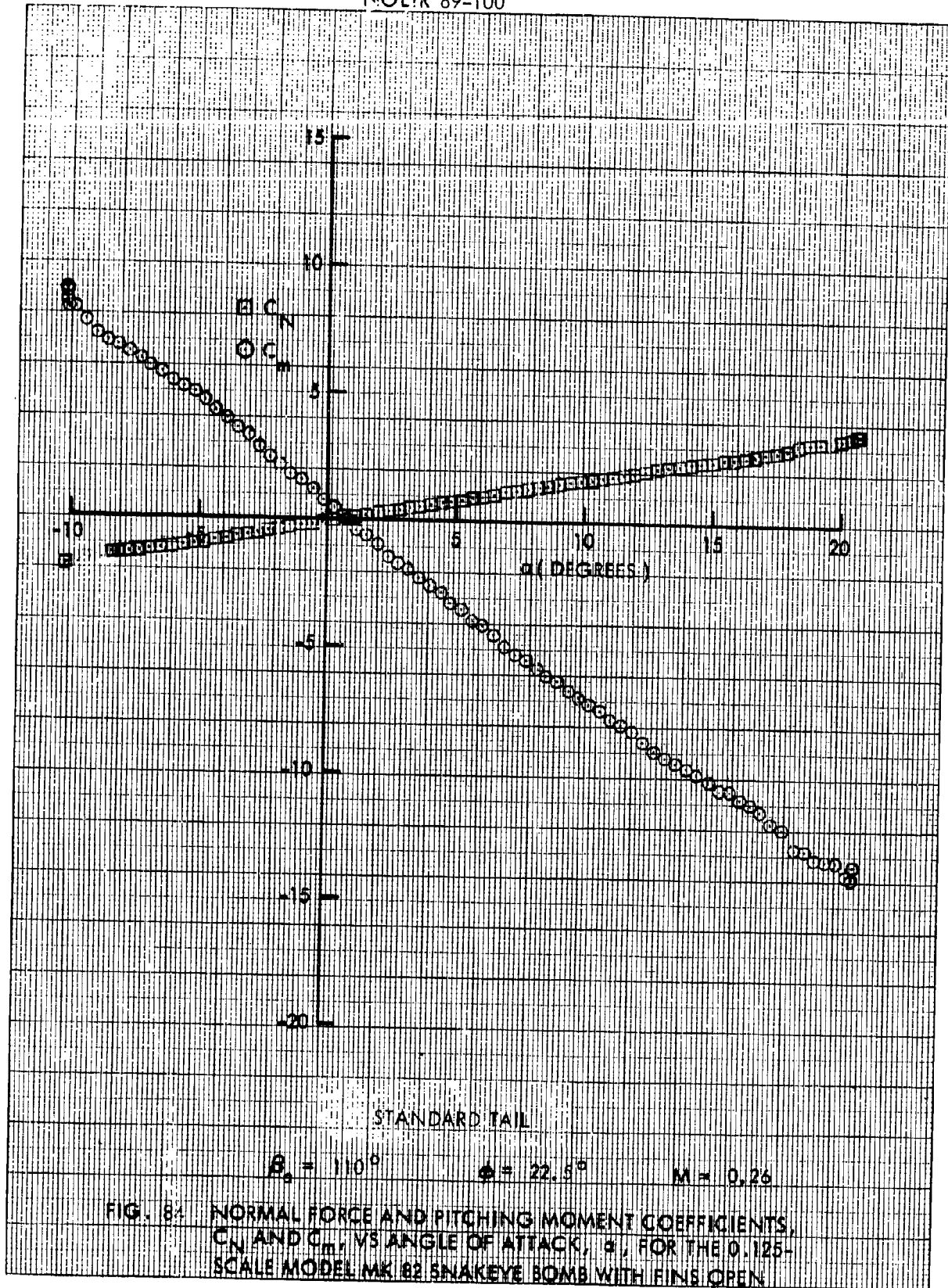
$$\phi = 0^\circ$$

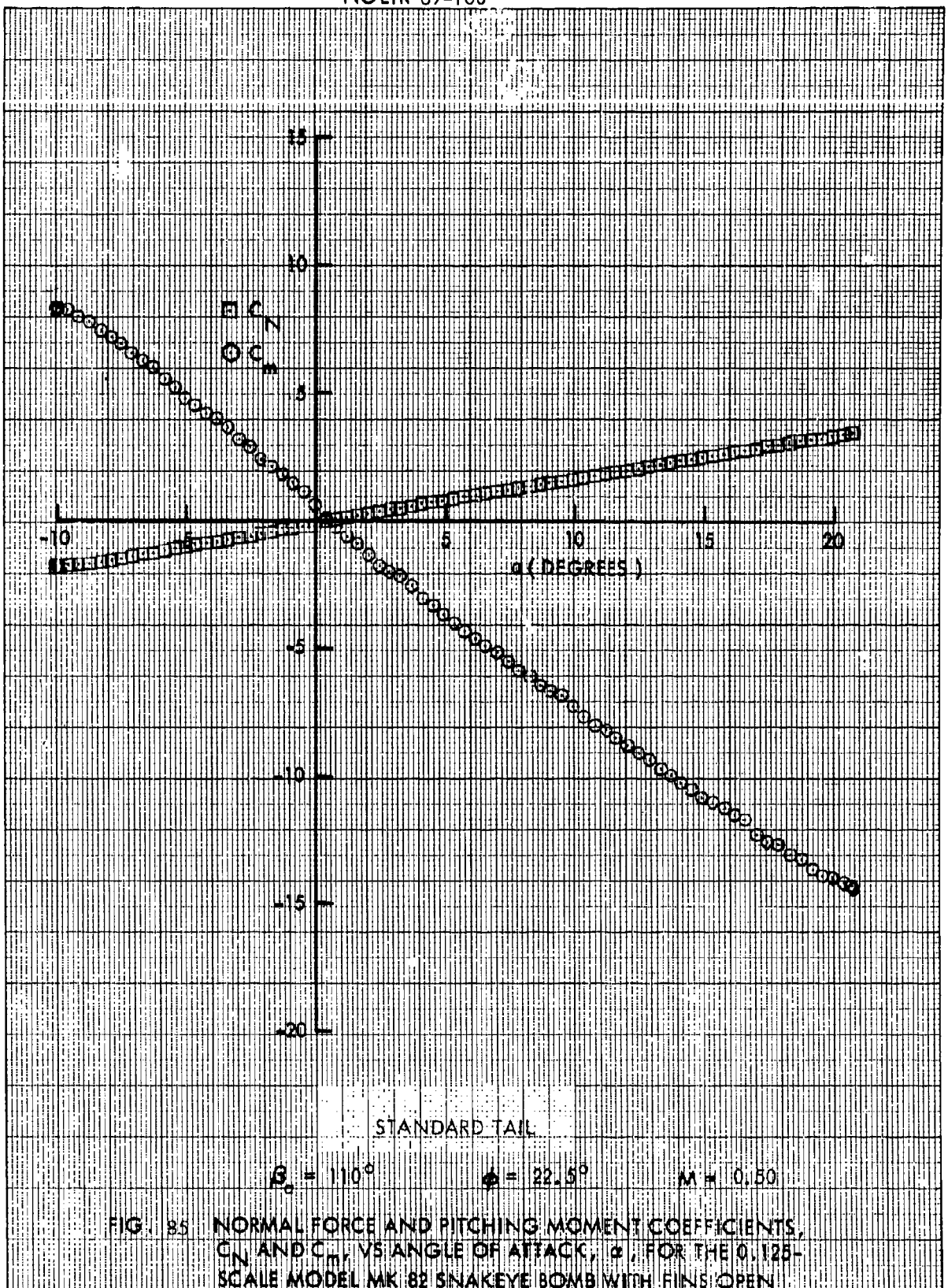
$$M = 0.90$$

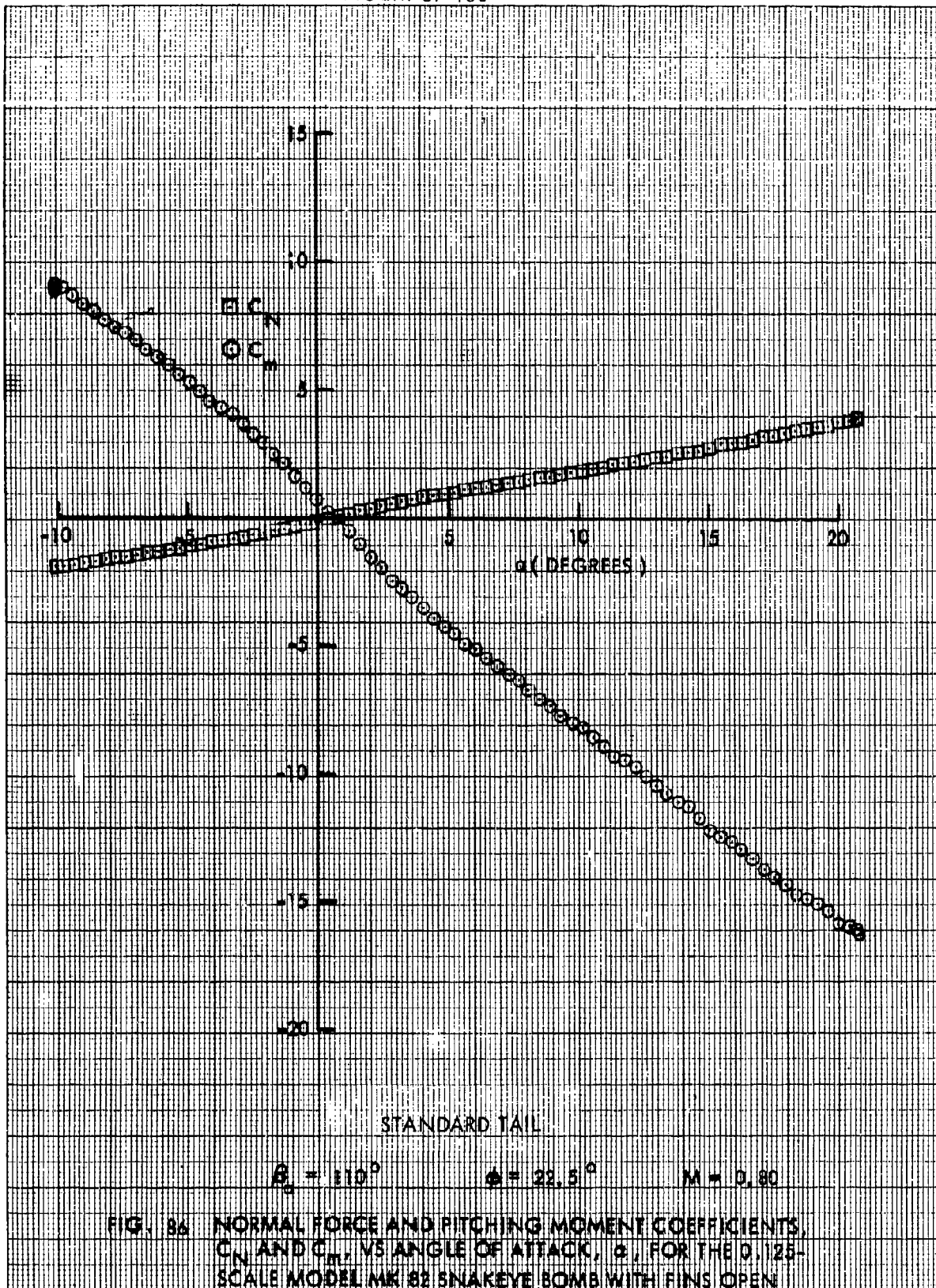
FIG. 82 NORMAL FORCE AND PITCHING MOMENT COEFFICIENTS,  $C_N$  AND  $C_M$ , VS ANGLE OF ATTACK,  $\alpha$ , FOR THE 0.125-SCALE MODEL MK 82 SNAKEYE BOMB WITH FINS OPEN

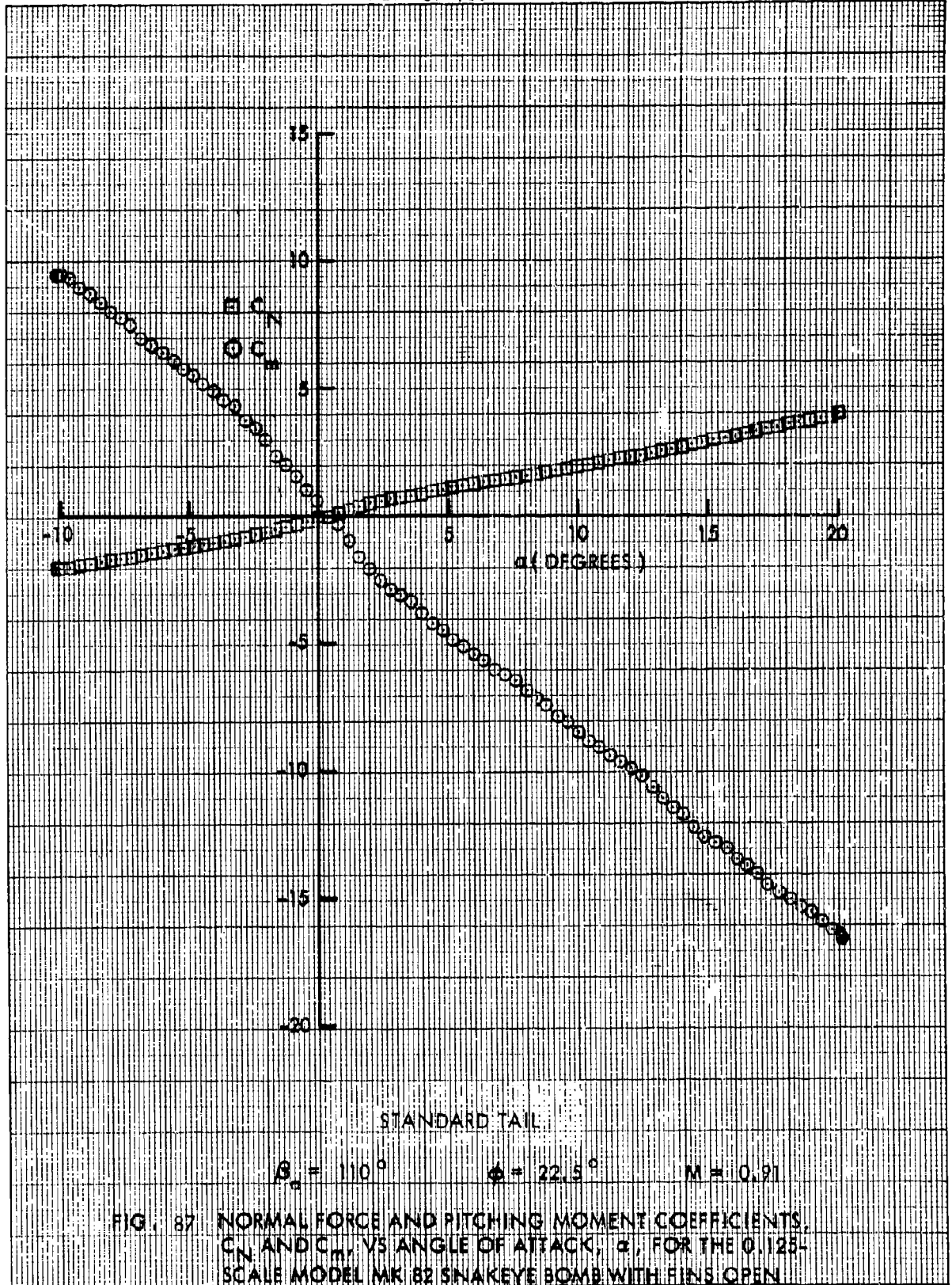


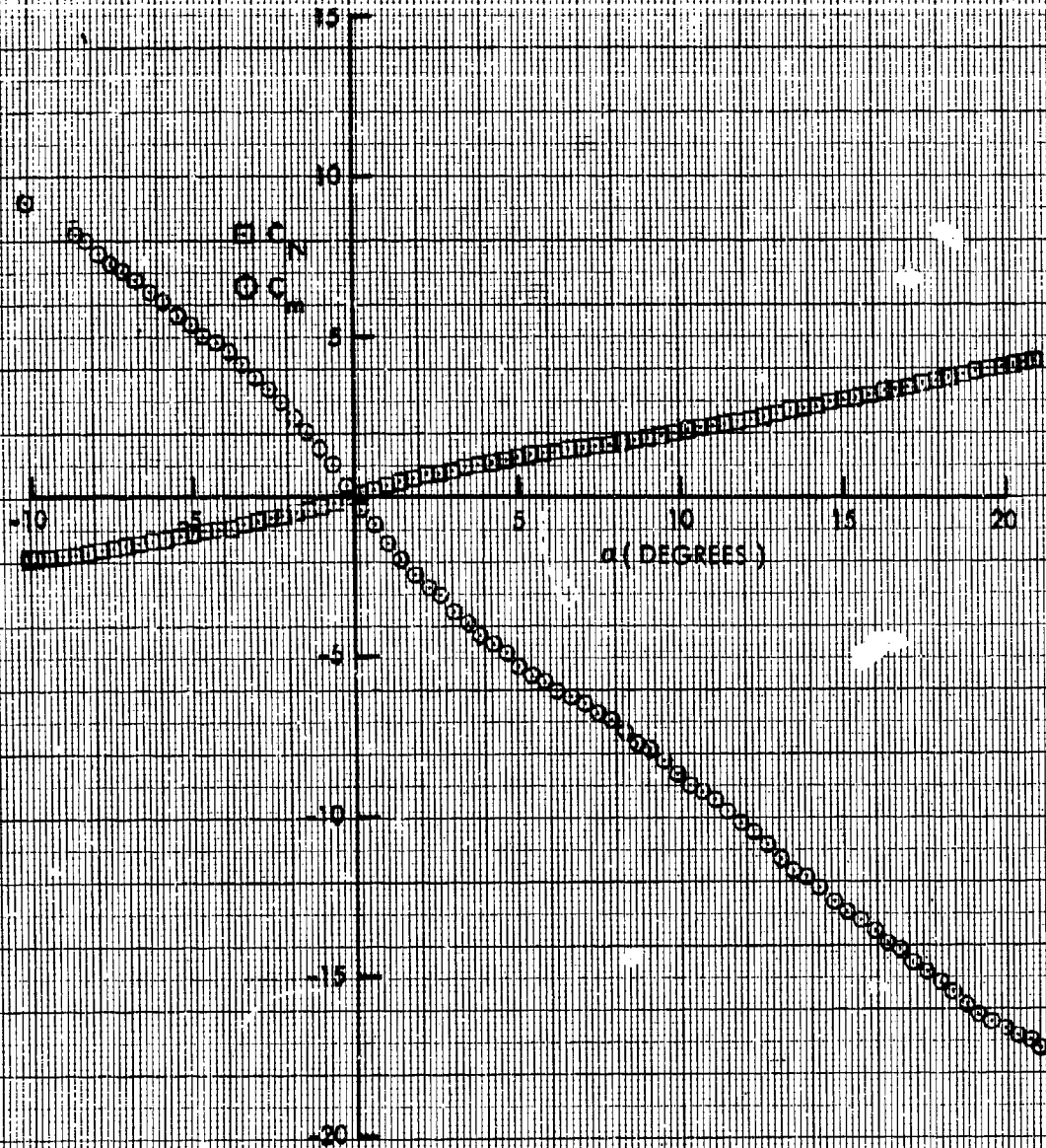












STANDARD TAIL

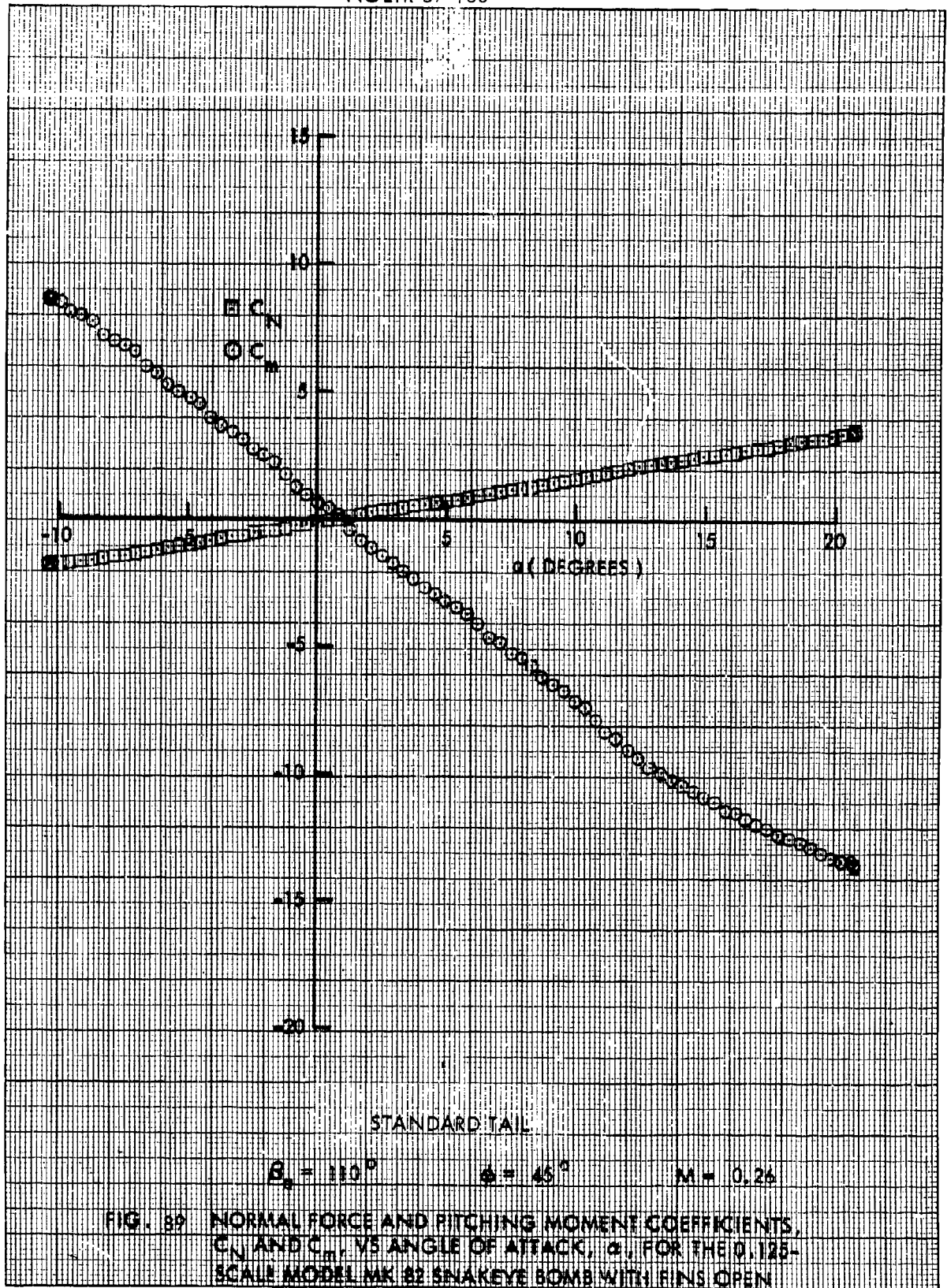
$$\beta_0 = 110^\circ$$

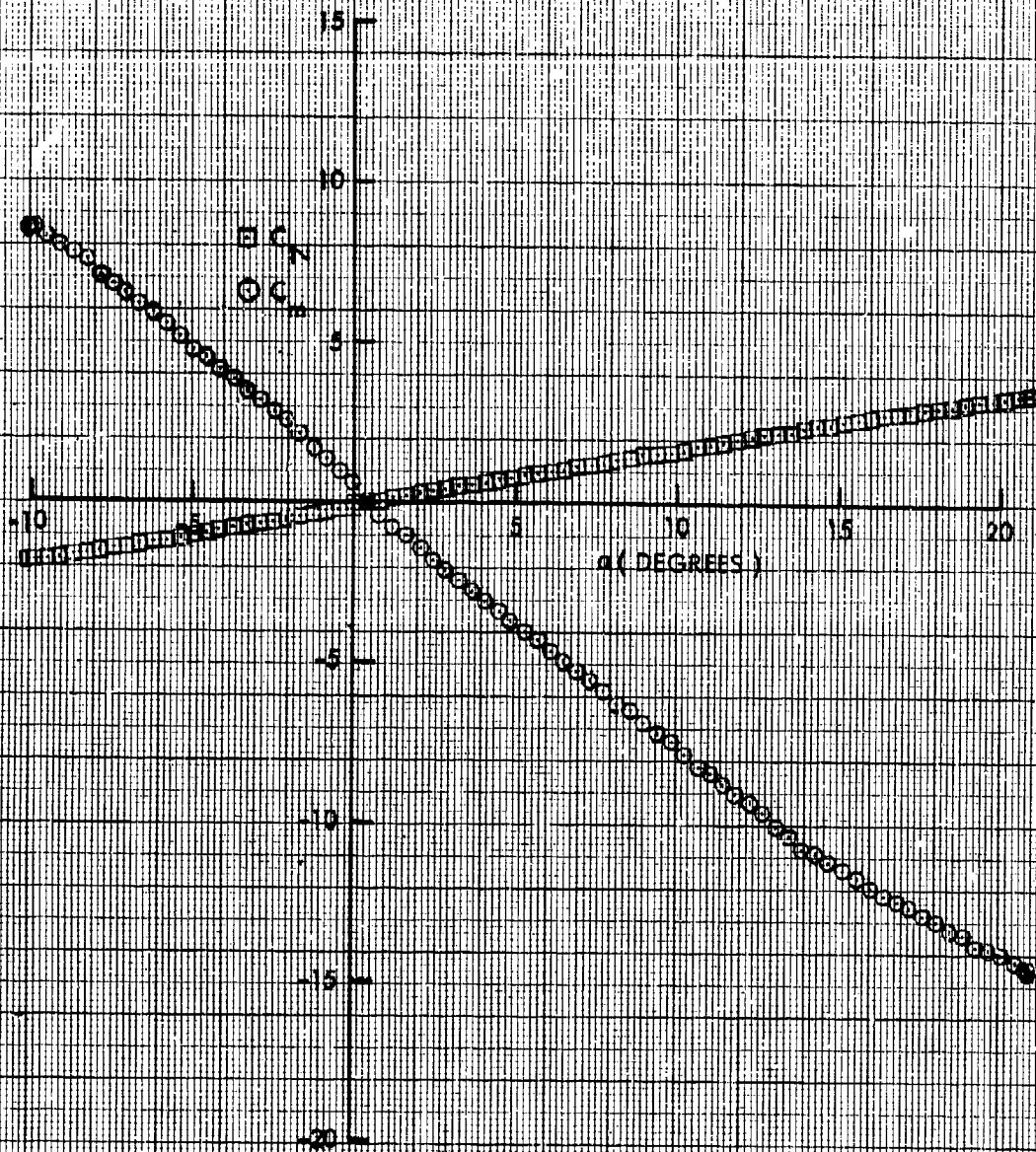
$$\phi = 22.5^\circ$$

$$M = 0.97$$

FIG. 88 NORMAL FORCE AND PITCHING MOMENT COEFFICIENTS,  $C_N$  AND  $C_m$ , VS ANGLE OF ATTACK,  $\alpha$ , FOR THE 0.125-SCALE MODEL MK 82 SNAKEEYE BOMB WITH FINS OPEN







STANDARD TAIL

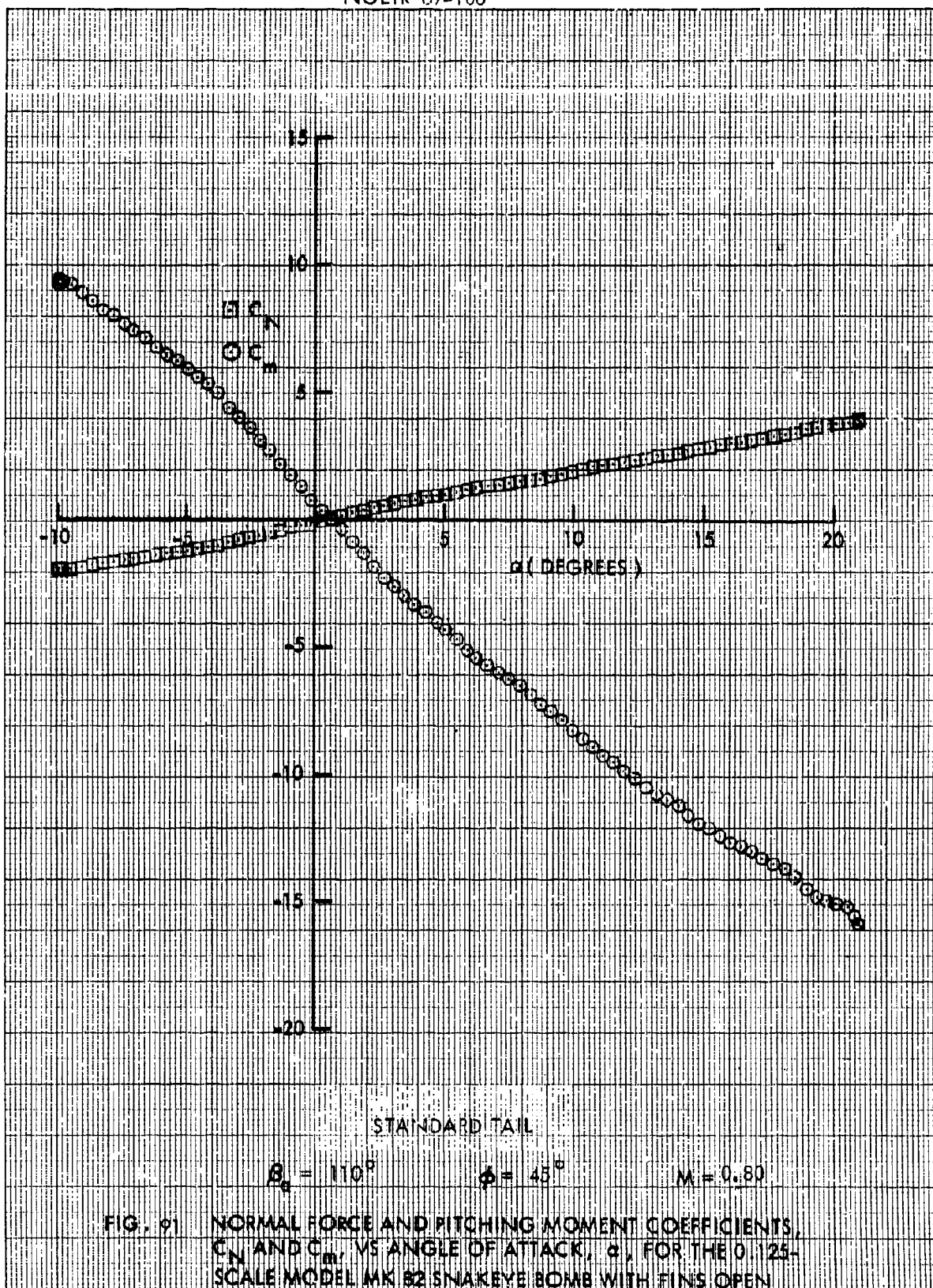
$$\theta_0 = 11.6^\circ$$

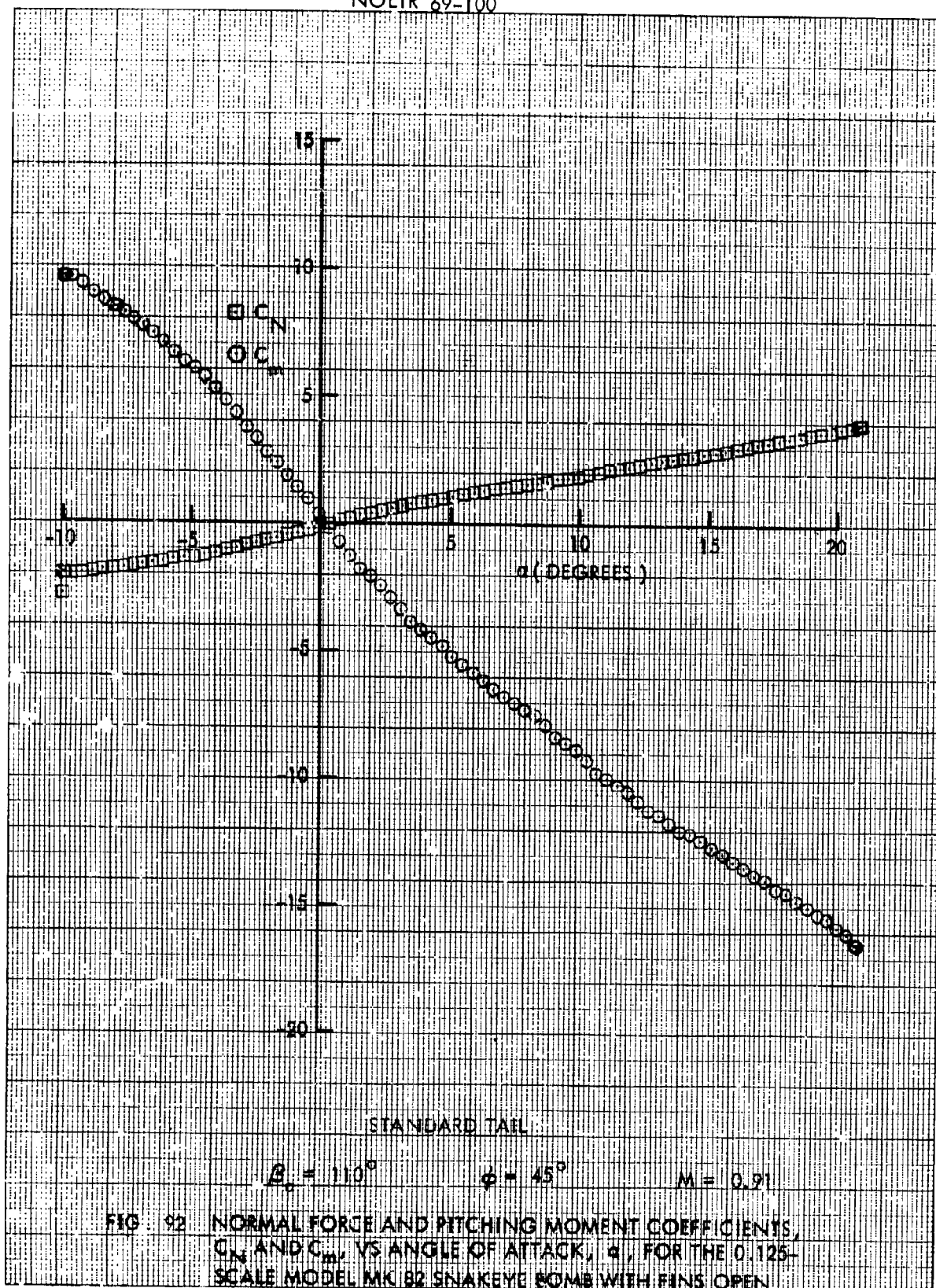
$$\theta = 45^\circ$$

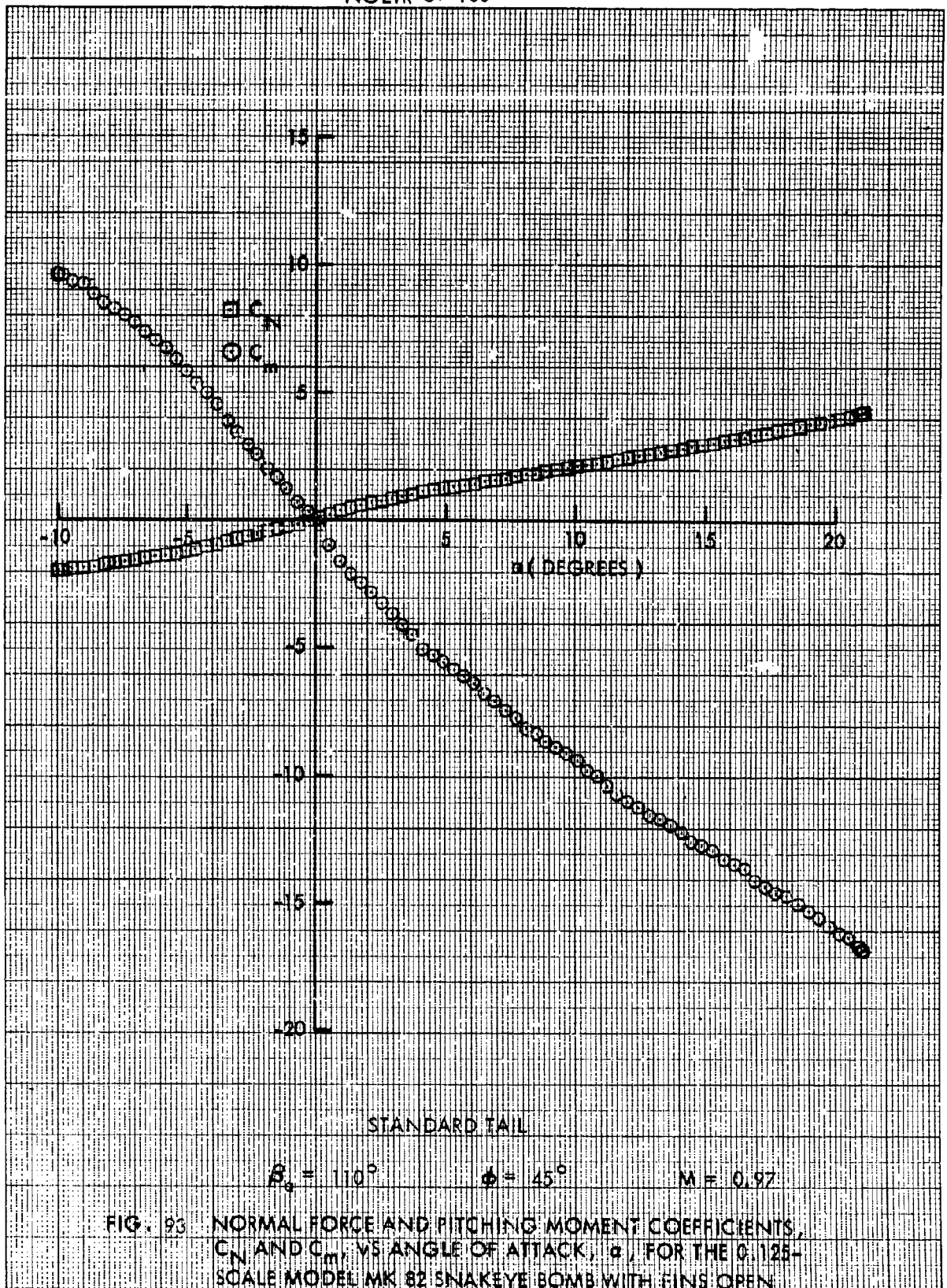
$$M = 0.50$$

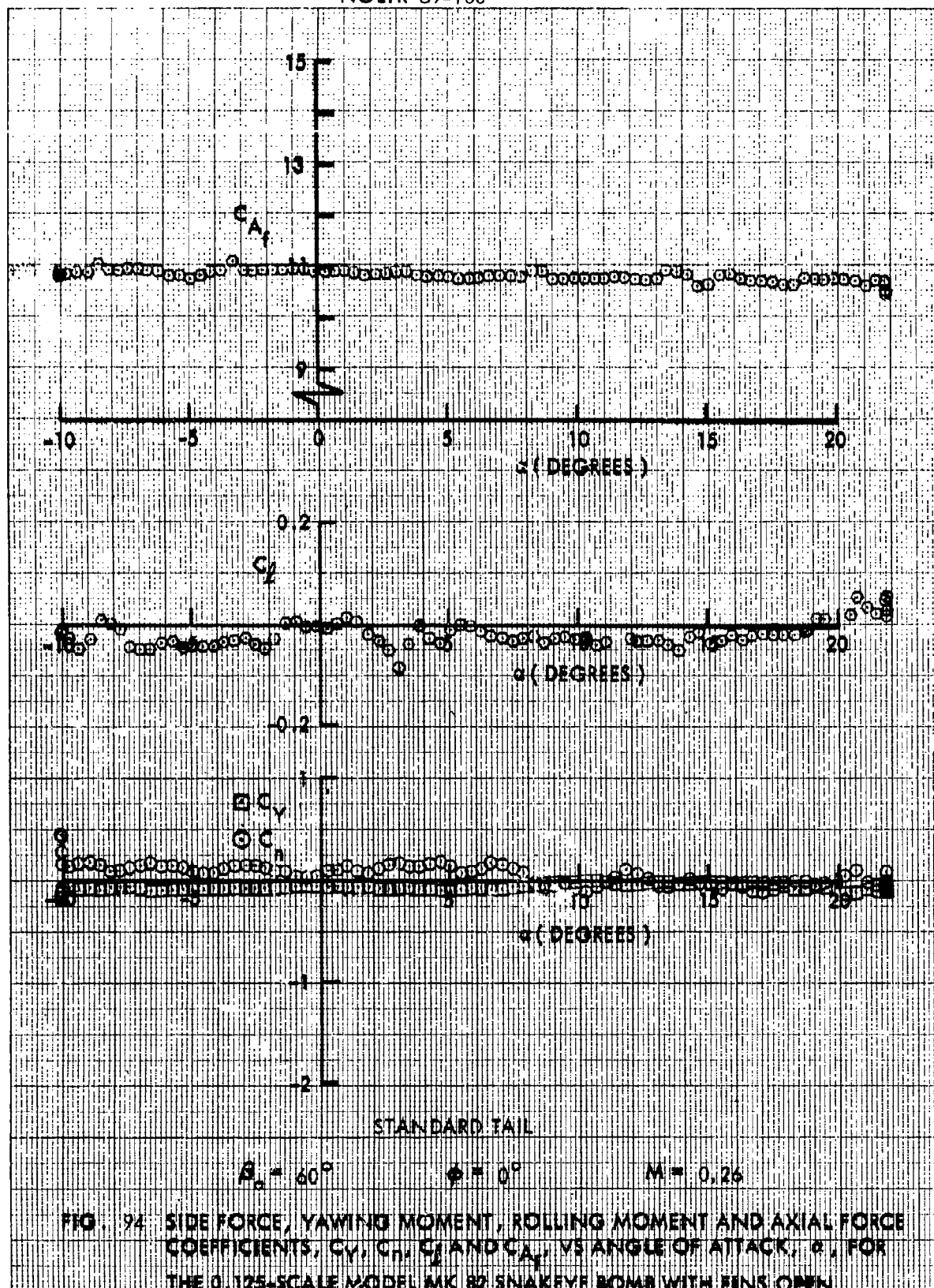
FIG. 90 NORMAL FORCE AND PITCHING MOMENT COEFFICIENTS,  $C_N$  AND  $C_m$ , VS ANGLE OF ATTACK,  $\alpha$ , FOR THE 0.125-SCALE MODEL MK 62 SNAKEYE BOMB WITH FINS OPEN

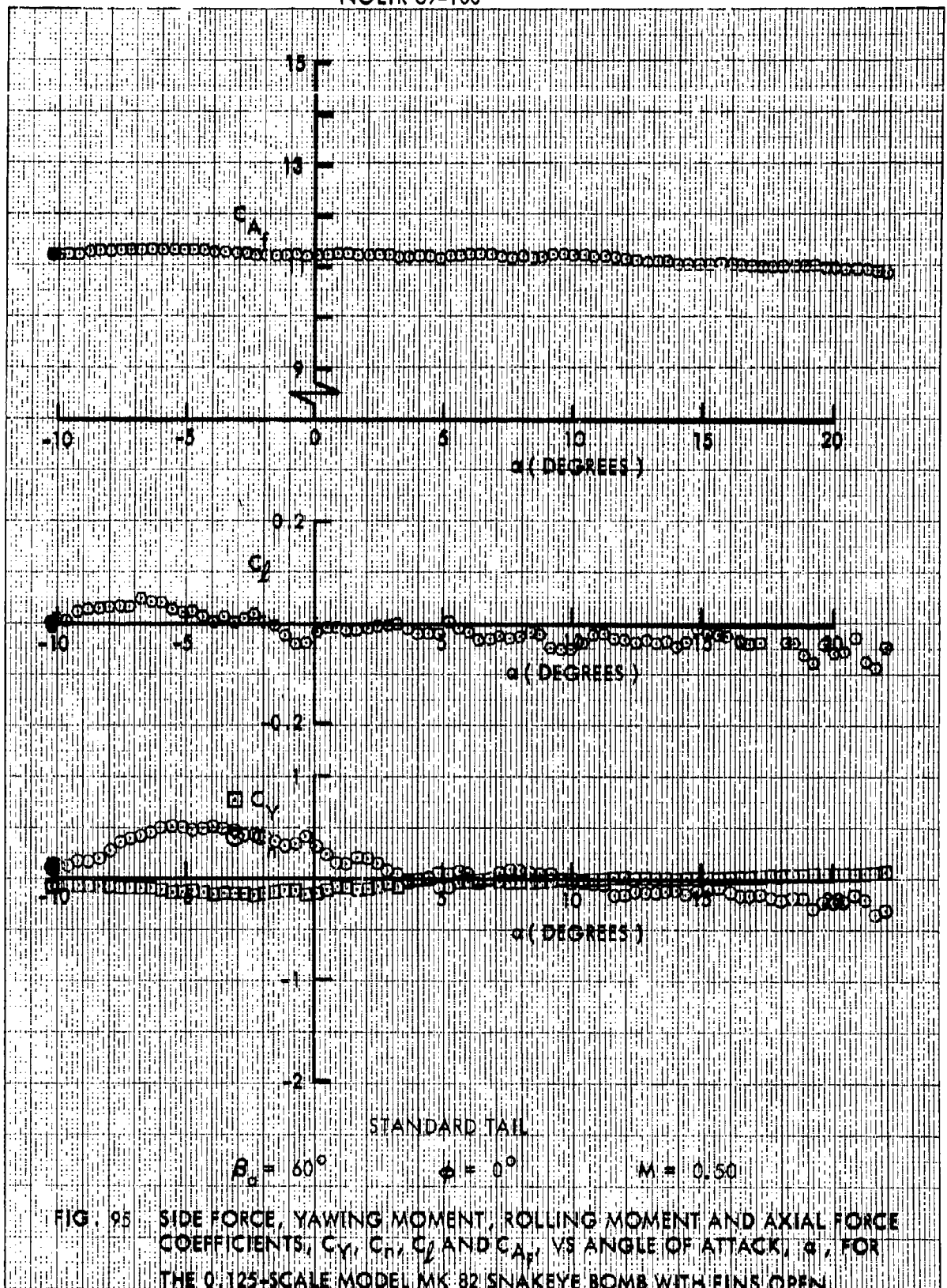




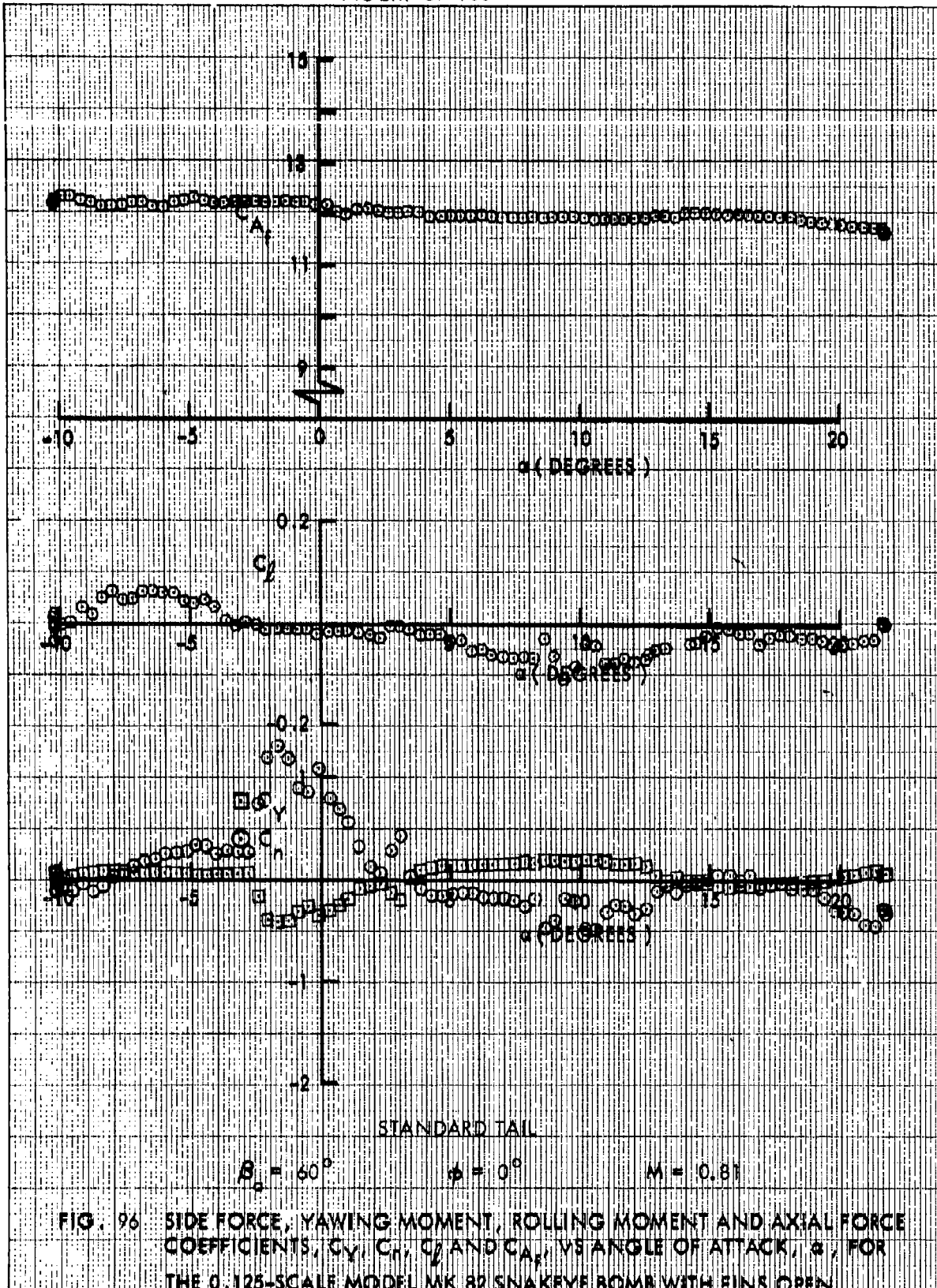


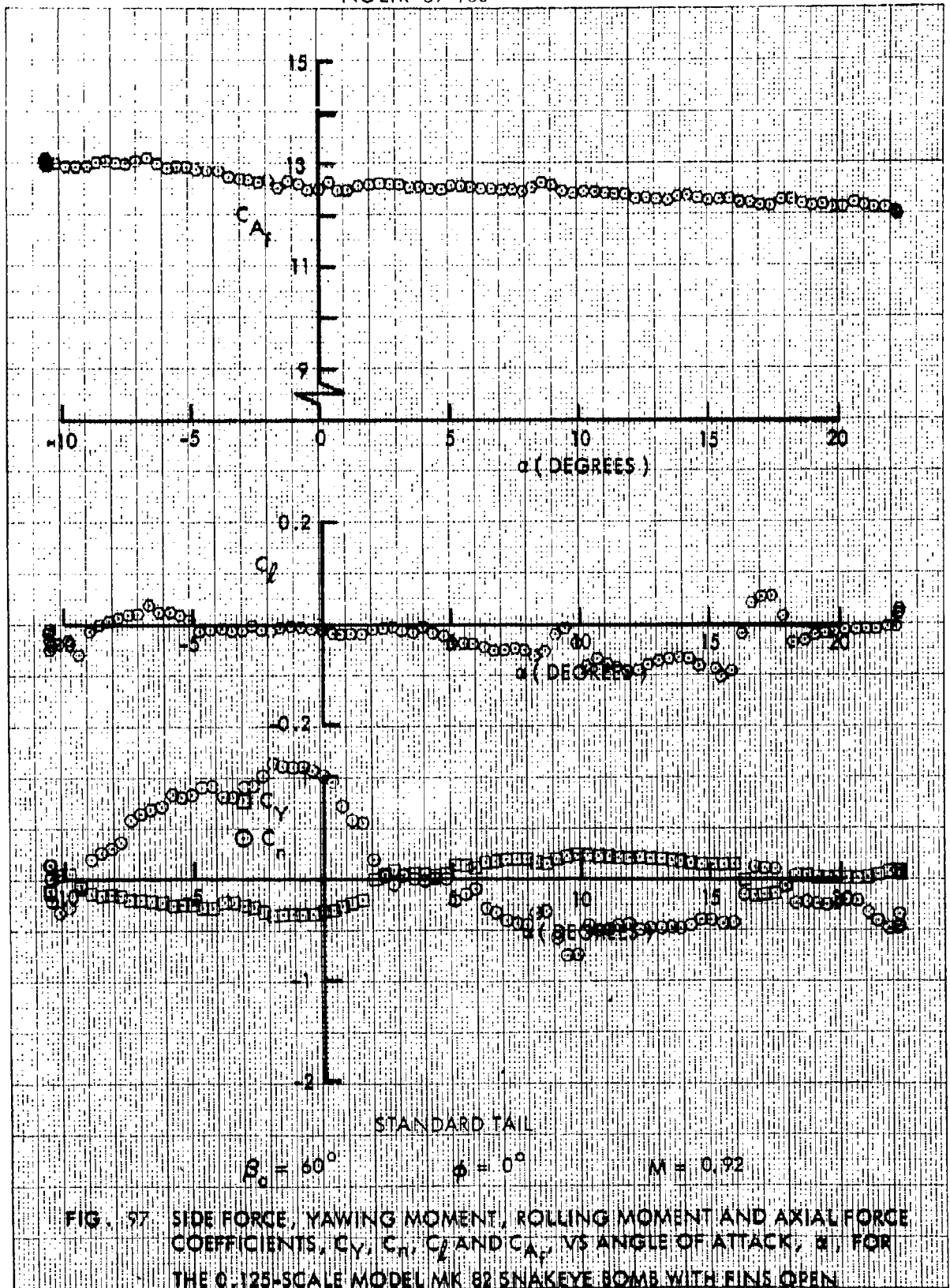




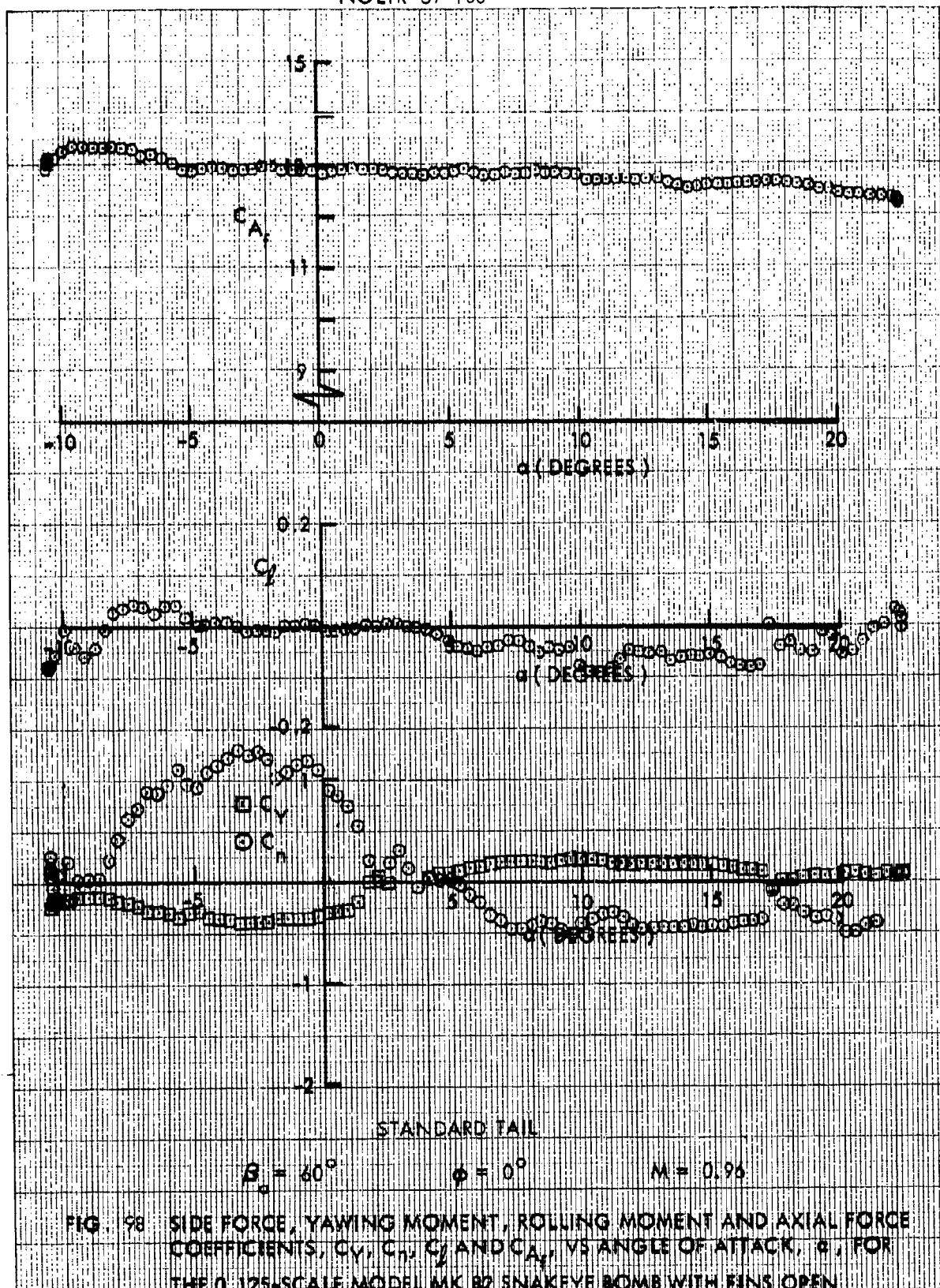


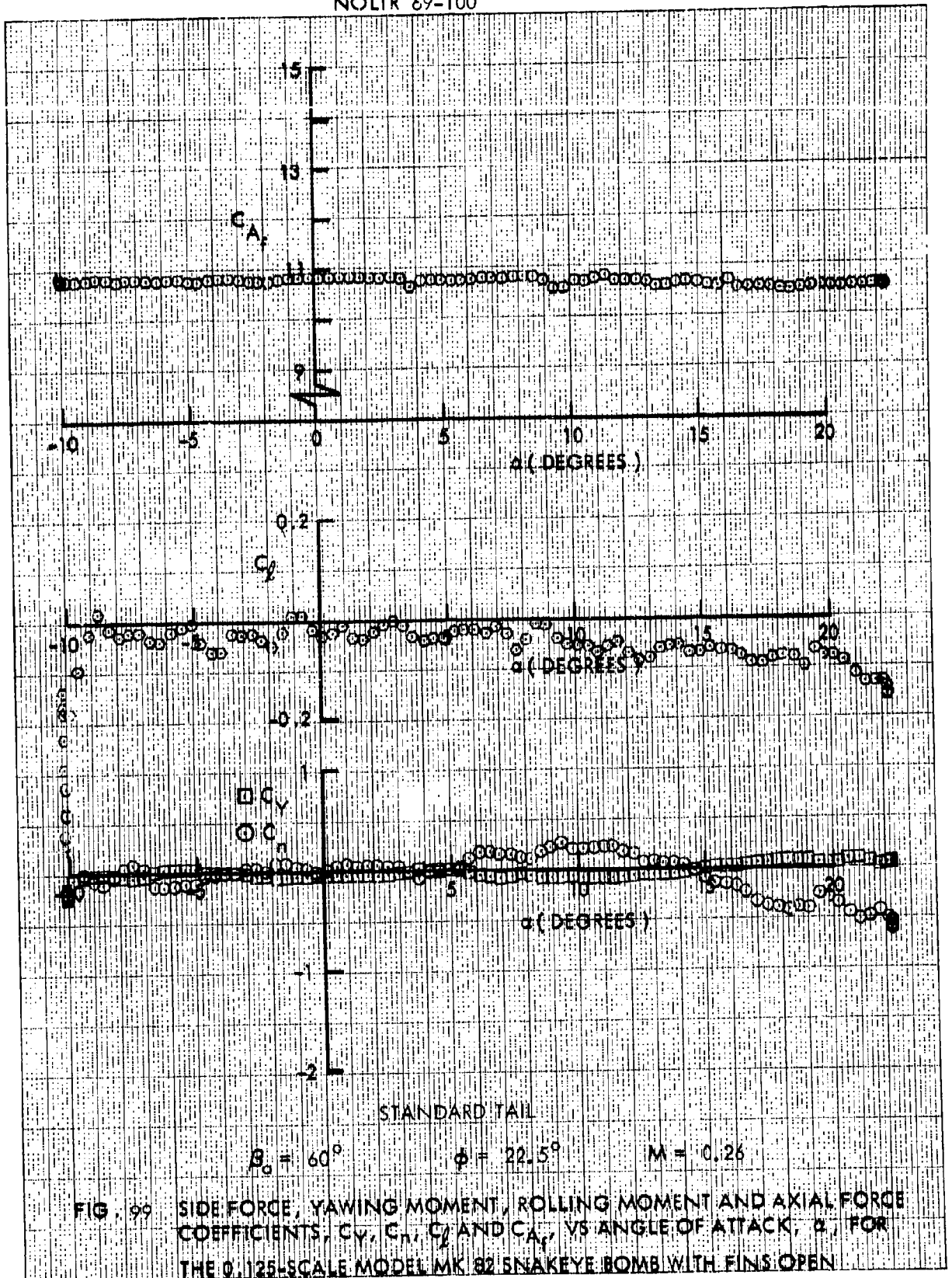


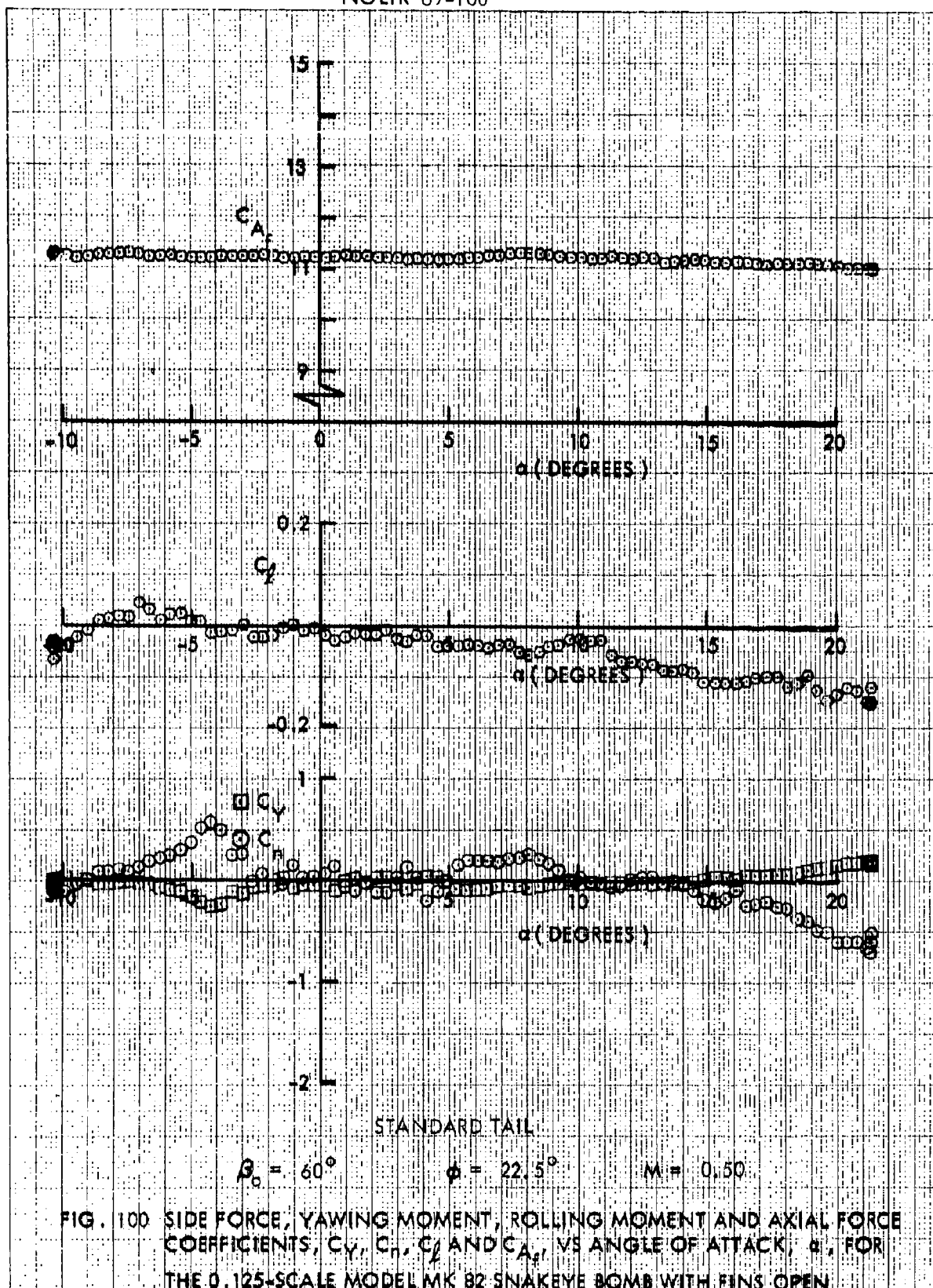


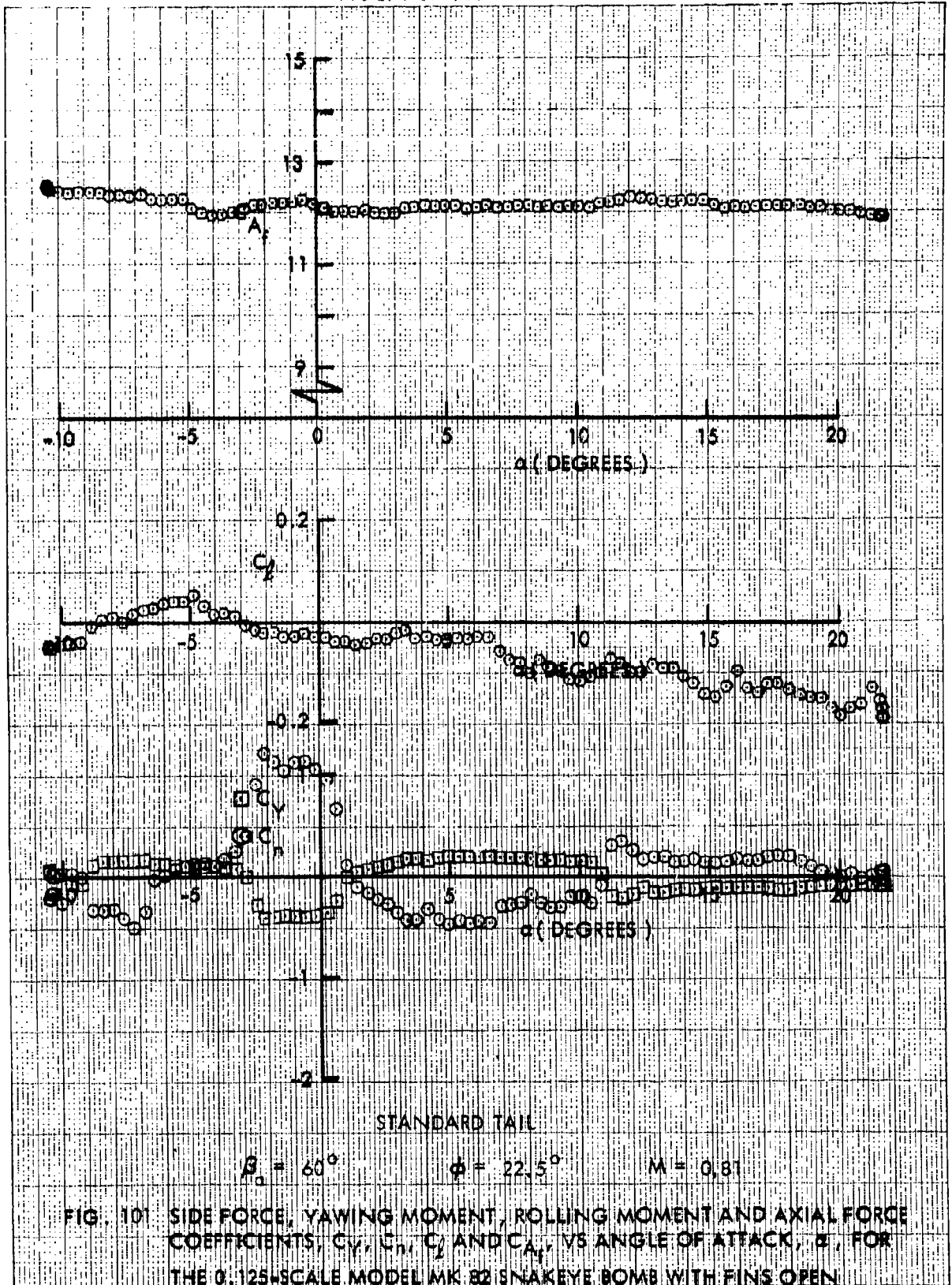


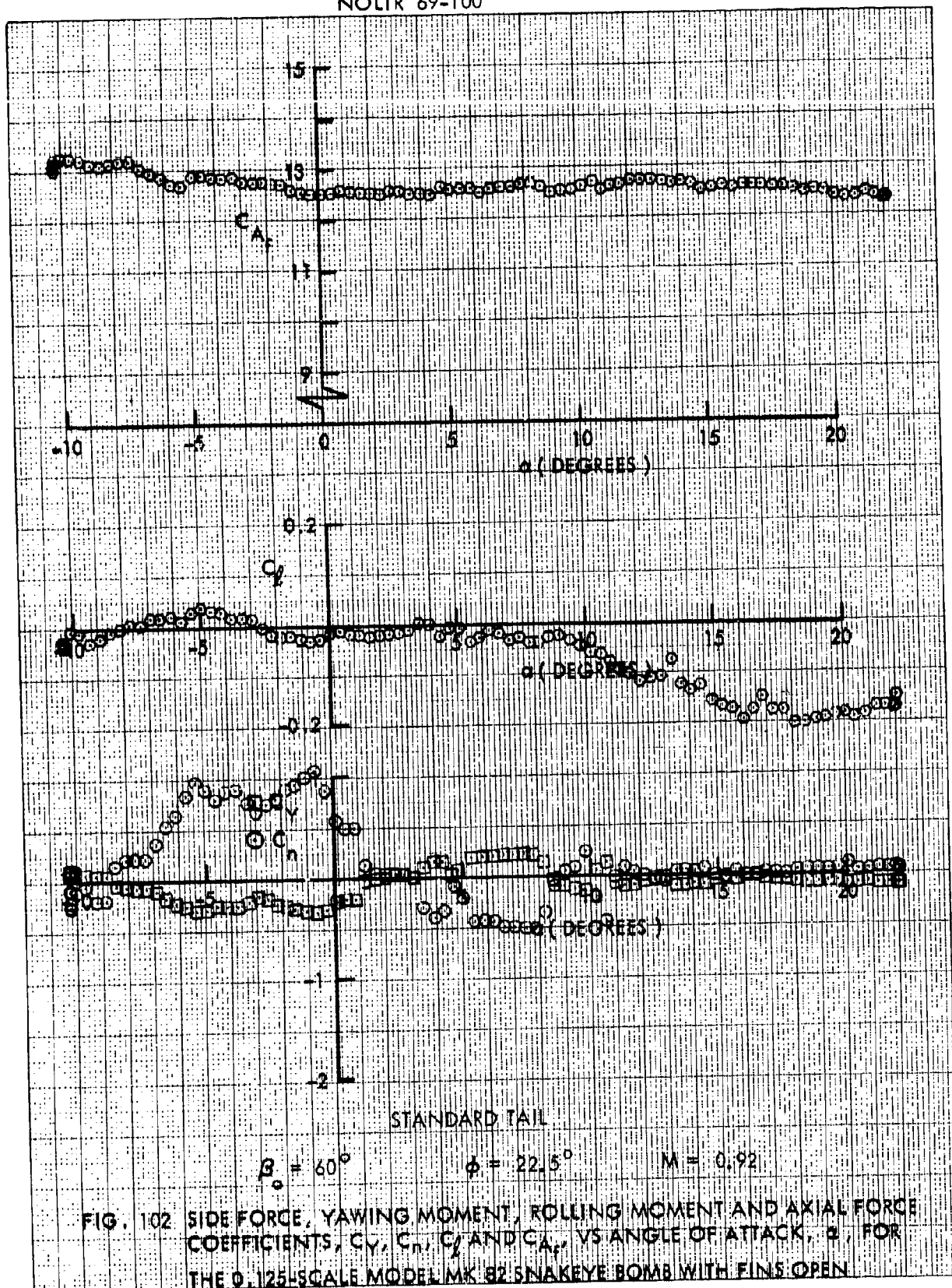


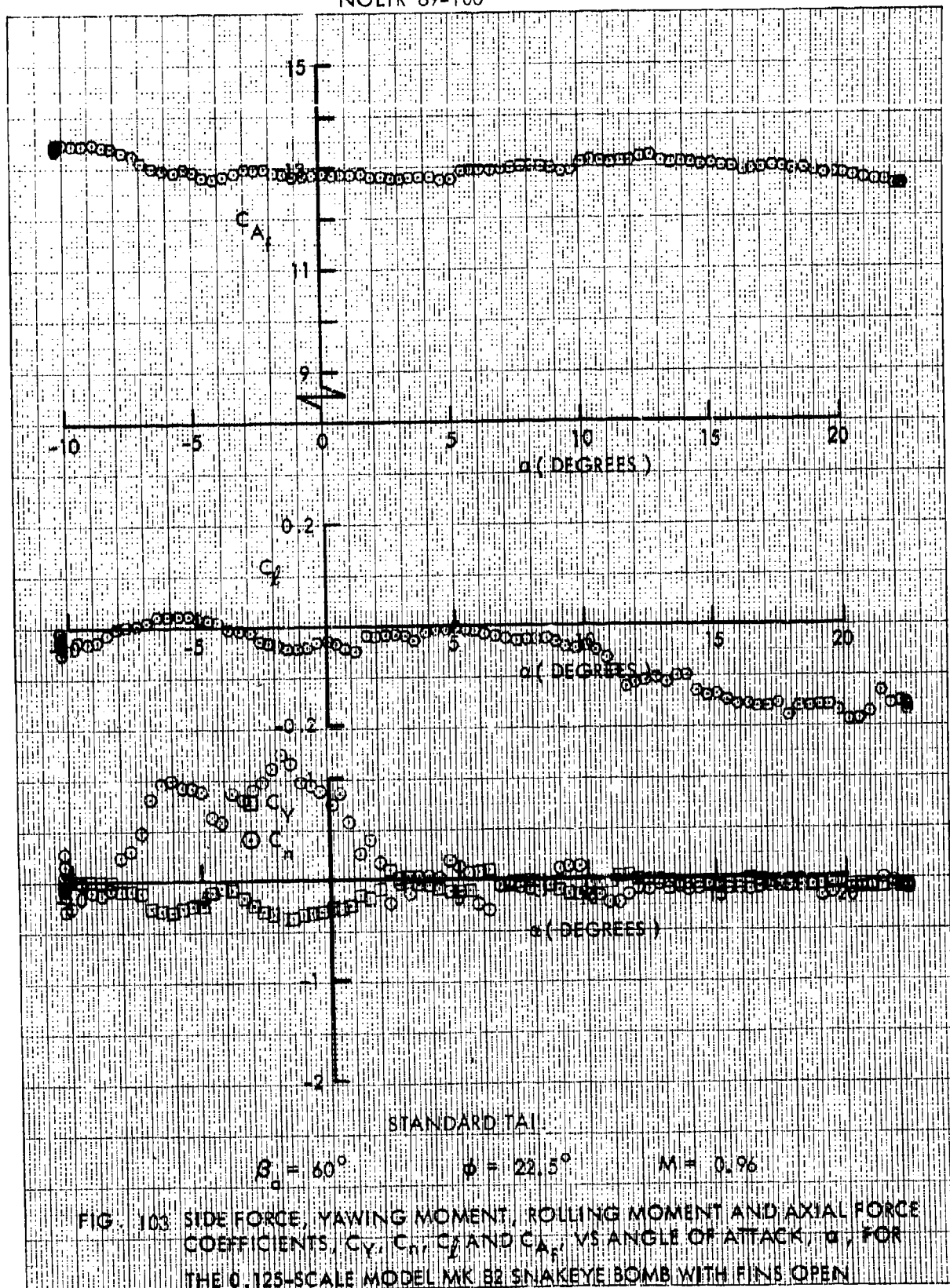




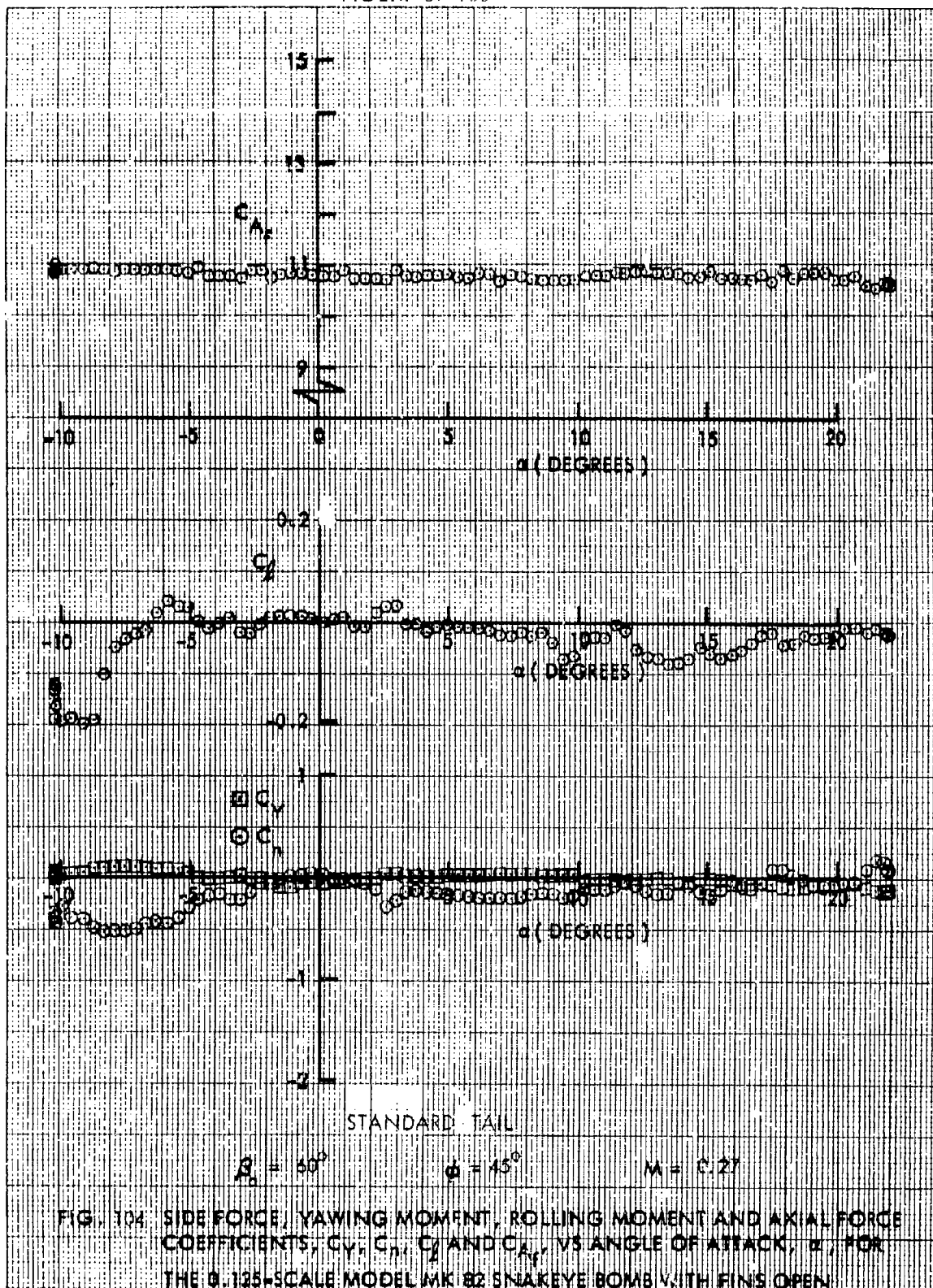




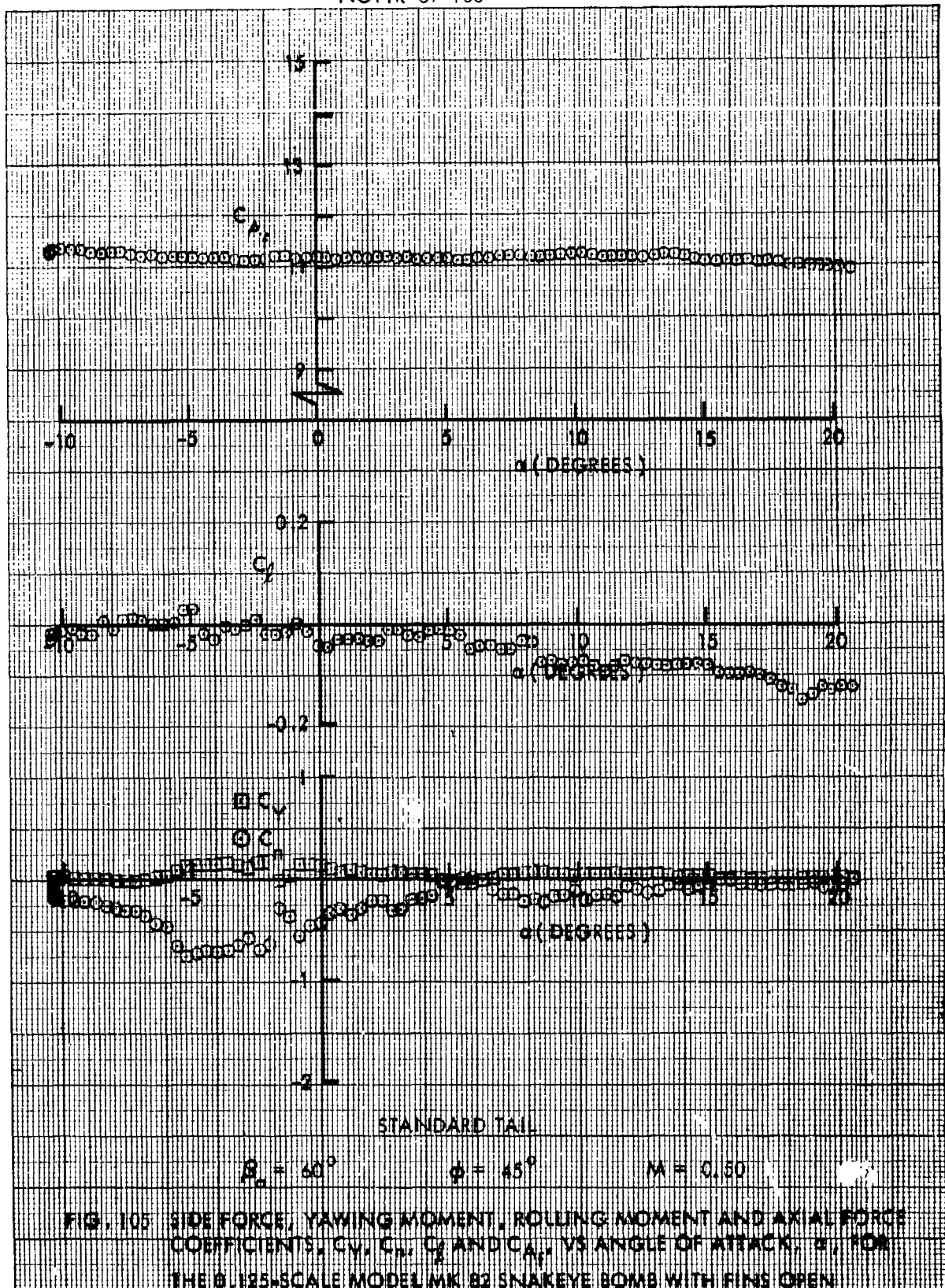


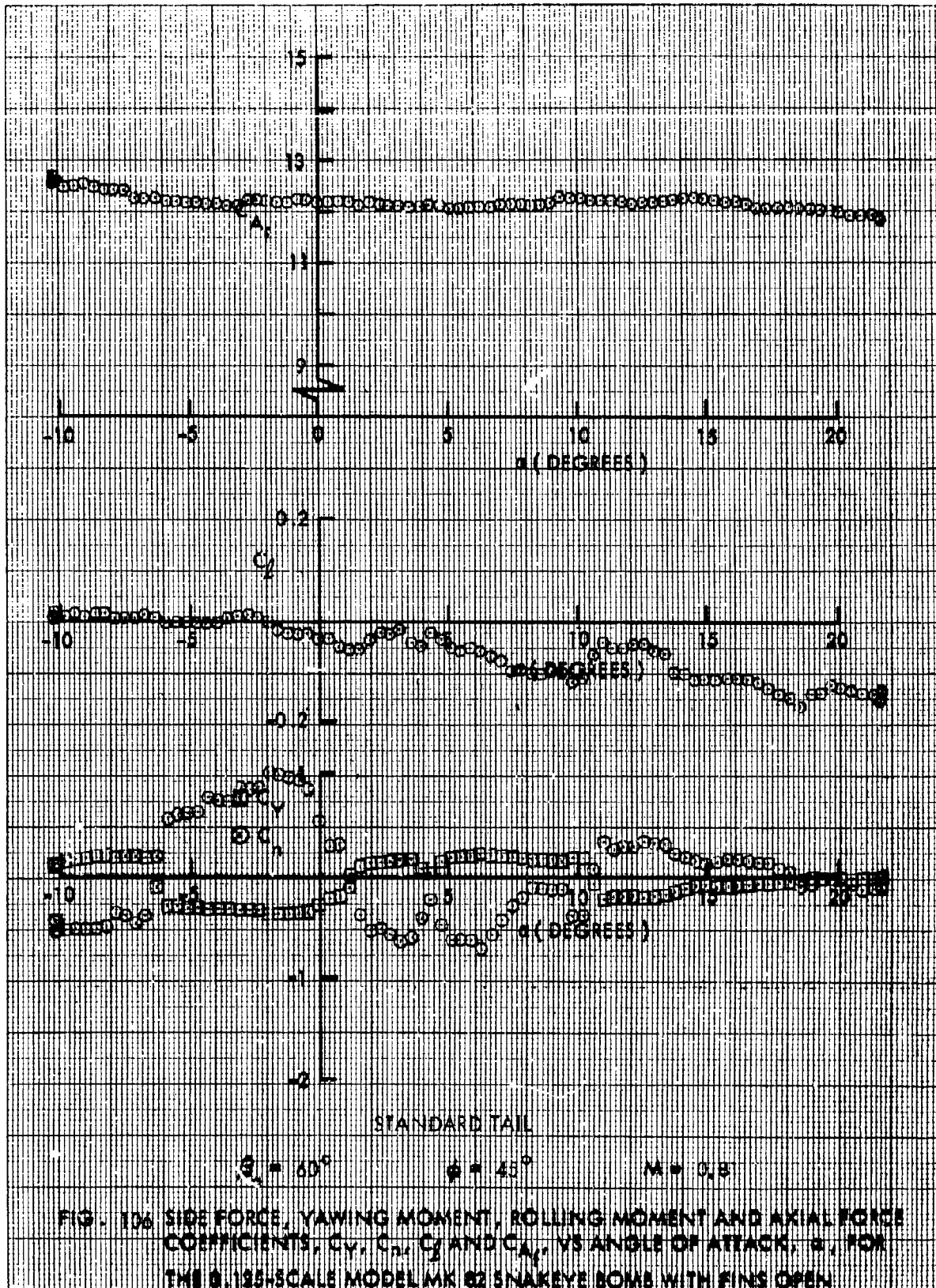


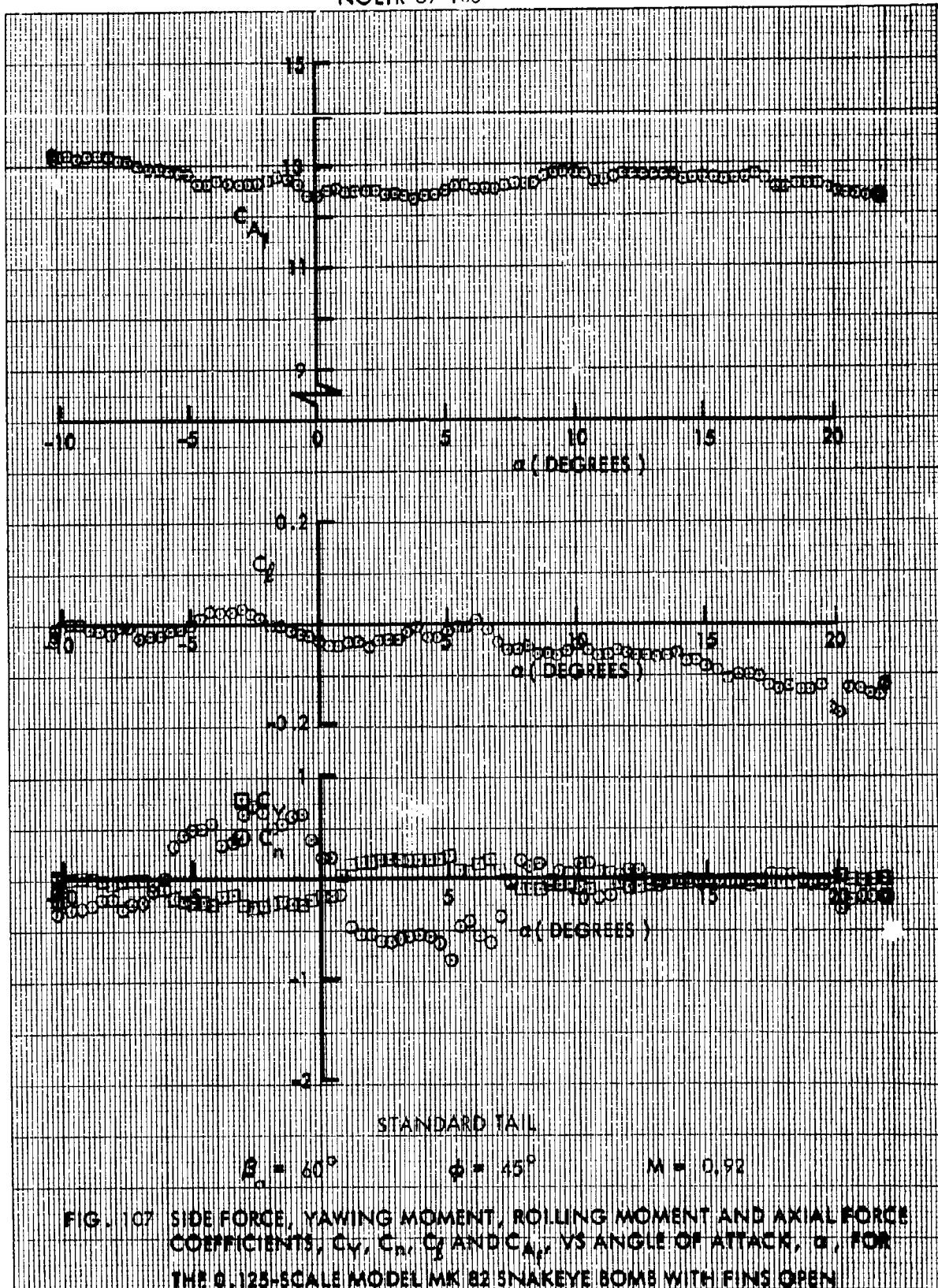


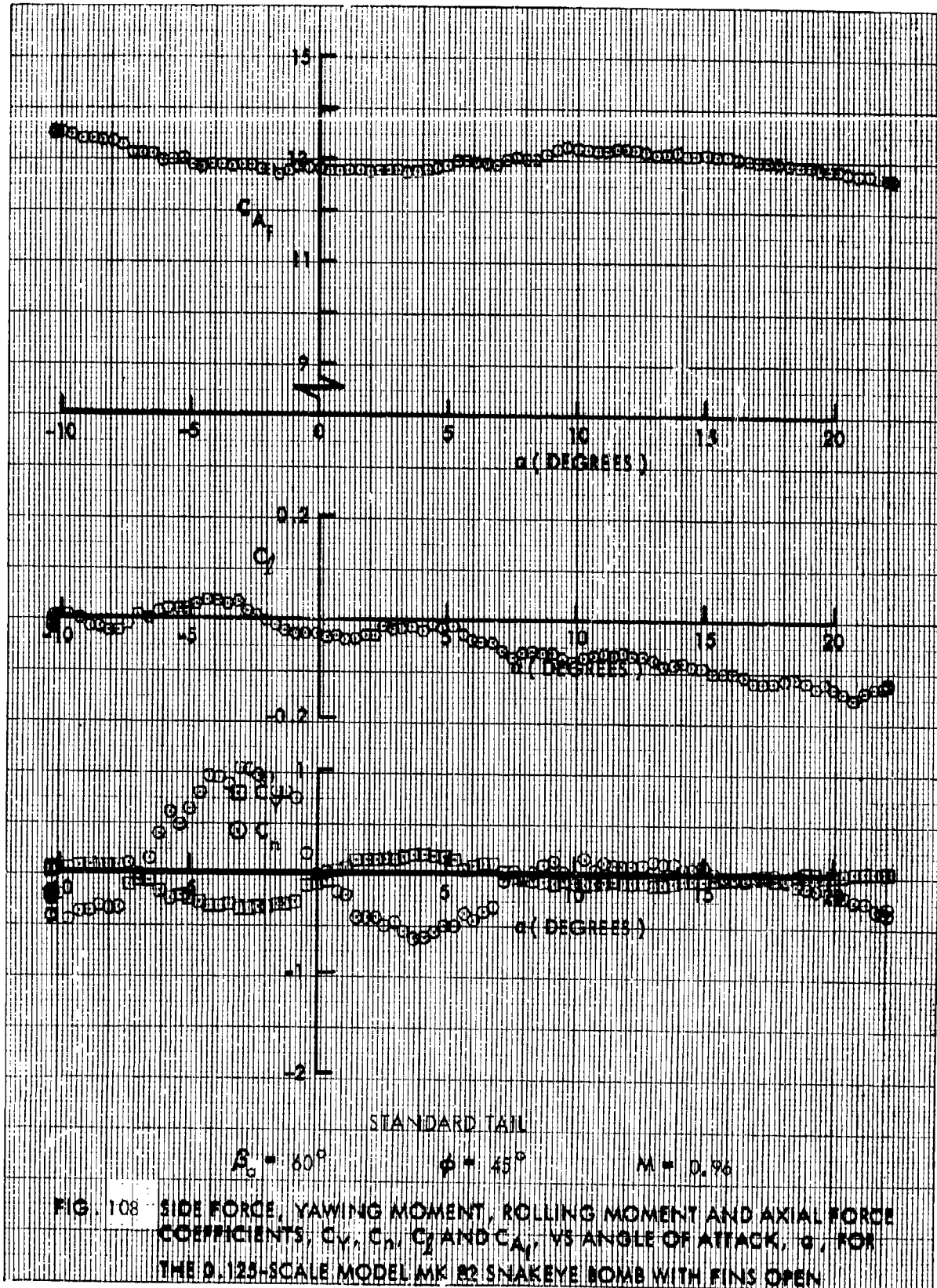












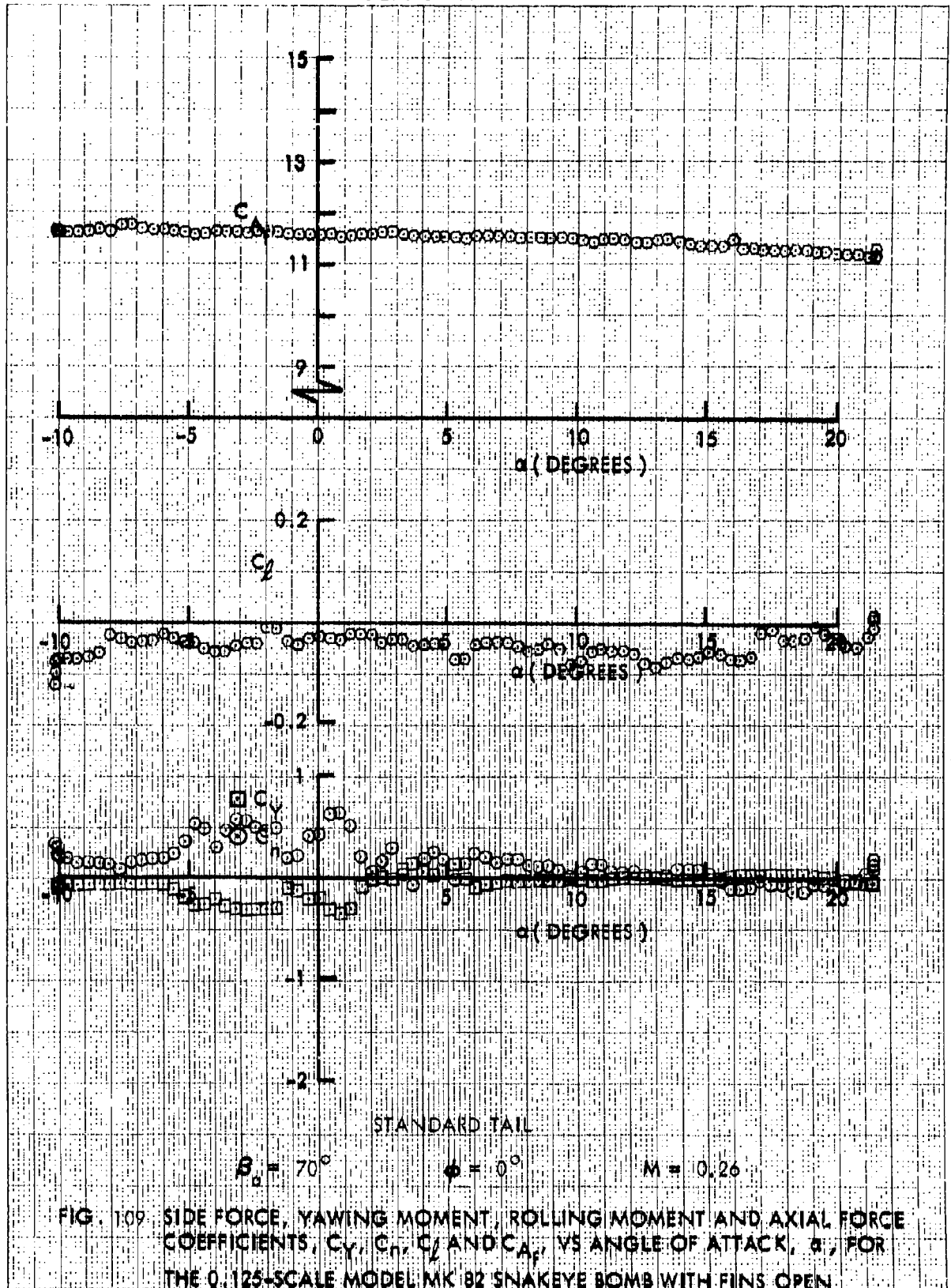
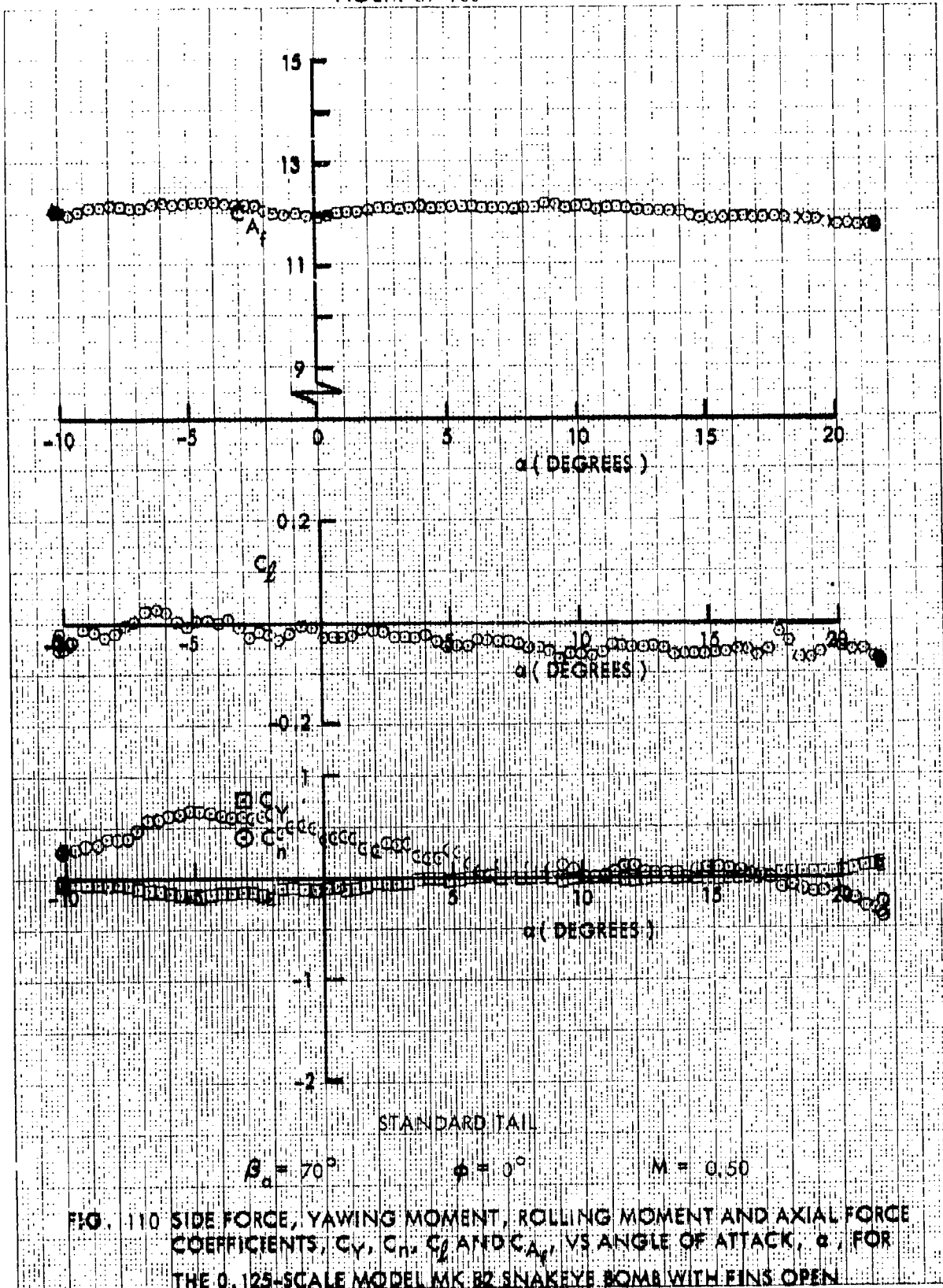
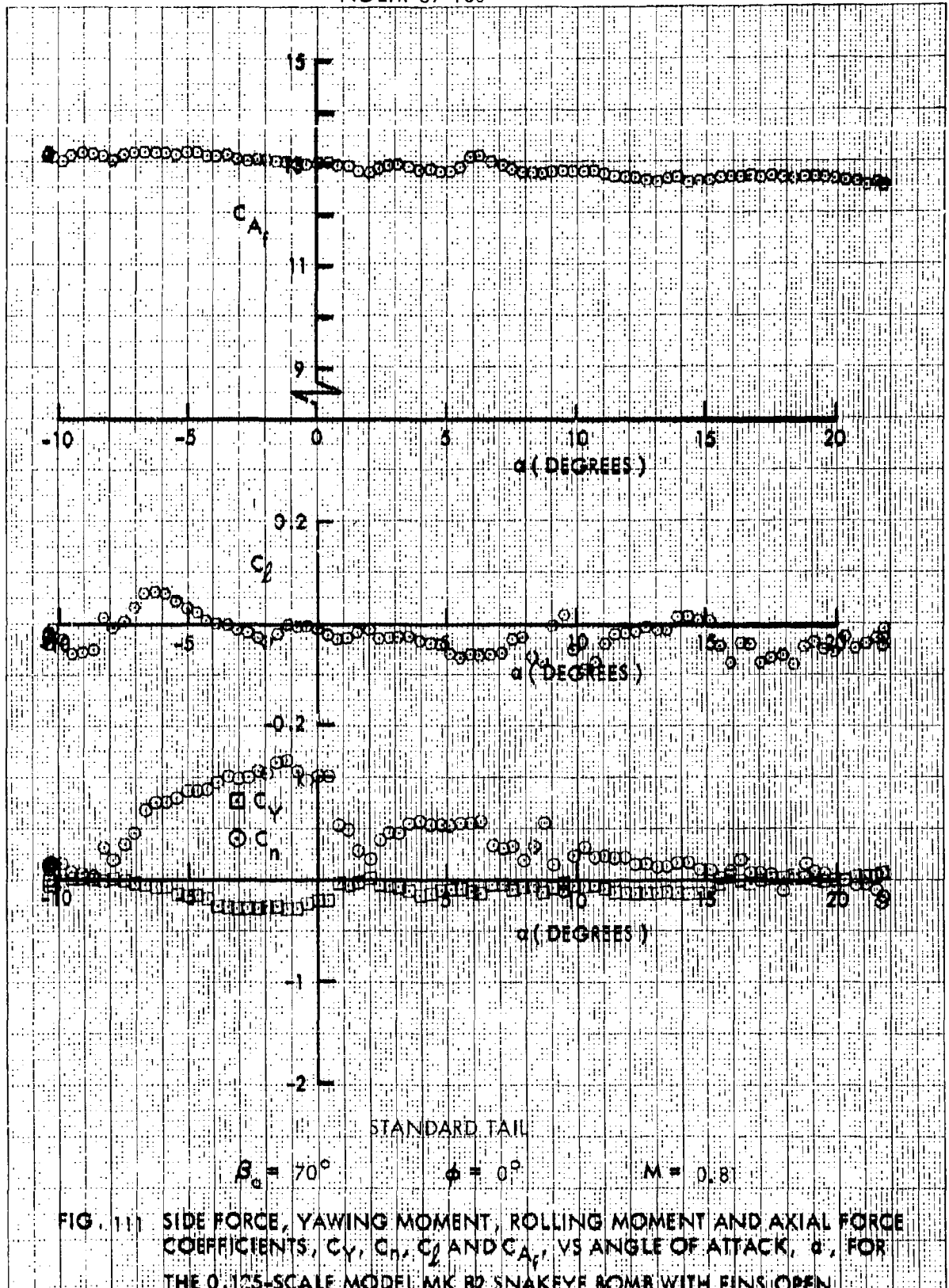


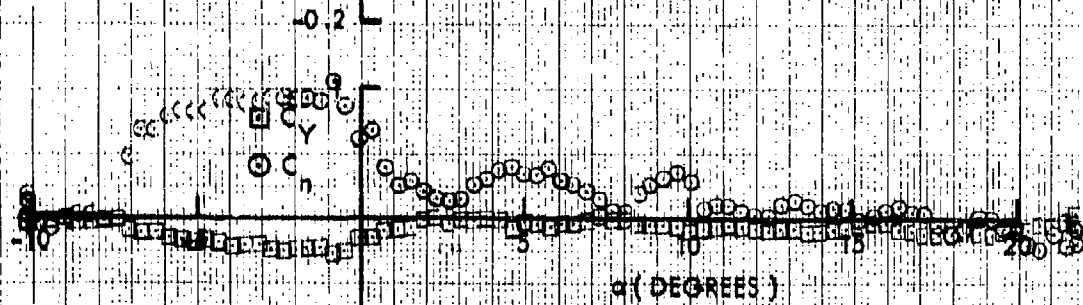
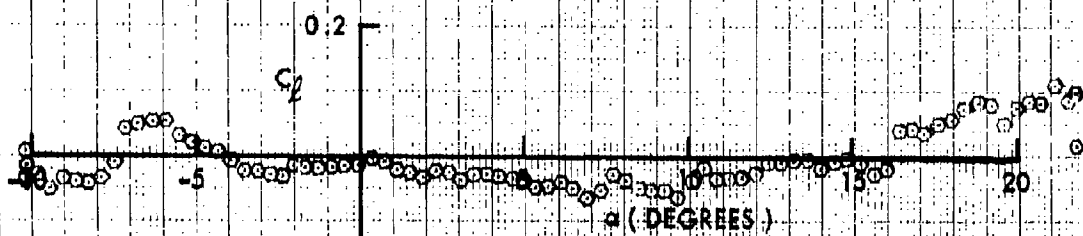
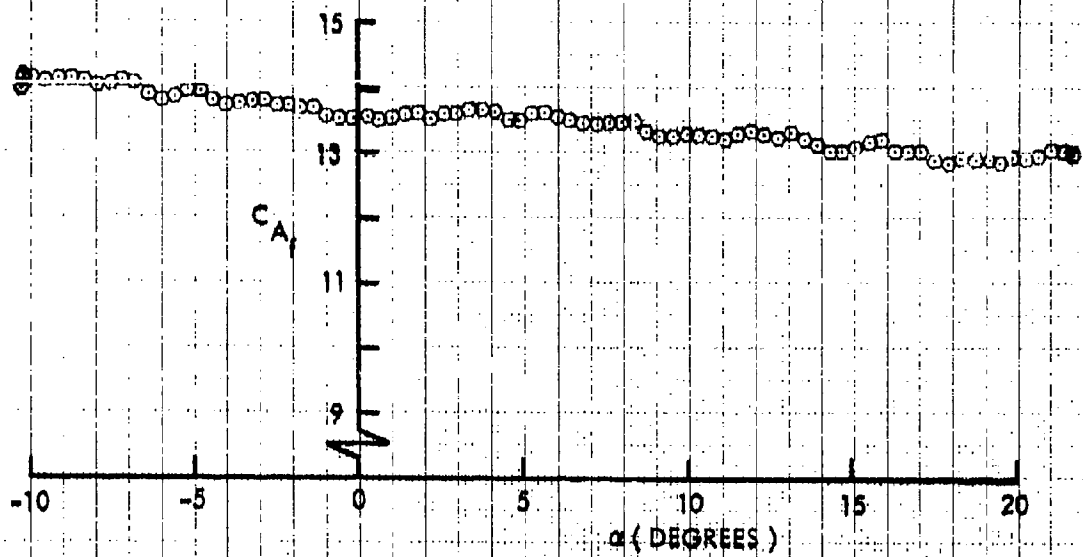
FIG. 109 SIDE FORCE, YAWING MOMENT, ROLLING MOMENT AND AXIAL FORCE COEFFICIENTS,  $C_Y$ ,  $C_n$ ,  $C_l$  AND  $C_A$ , VS ANGLE OF ATTACK,  $\alpha$ , FOR THE 0.125-SCALE MODEL MK 82 SNAKEYE BOMB WITH FINS OPEN











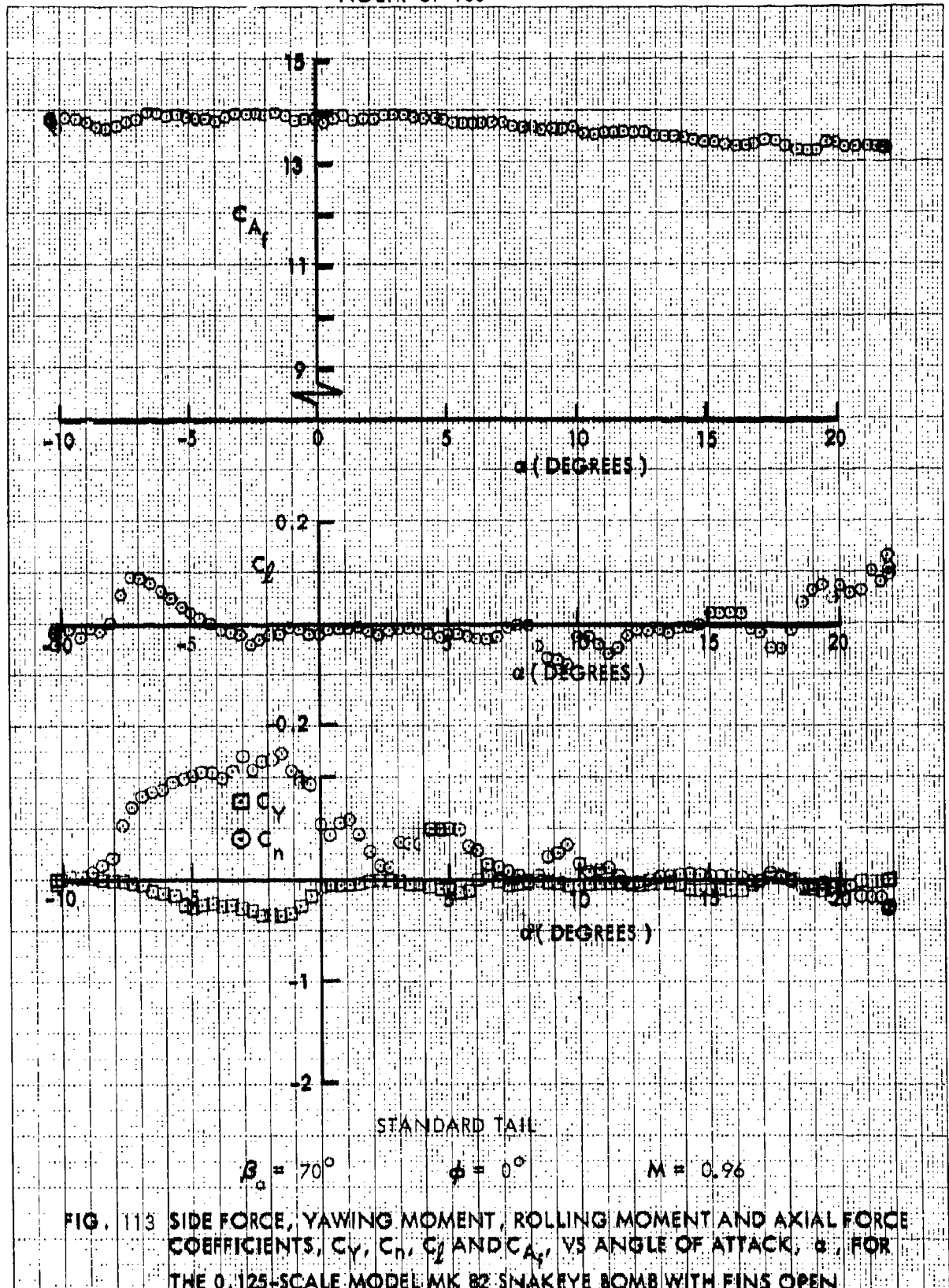
STANDARD TAIL

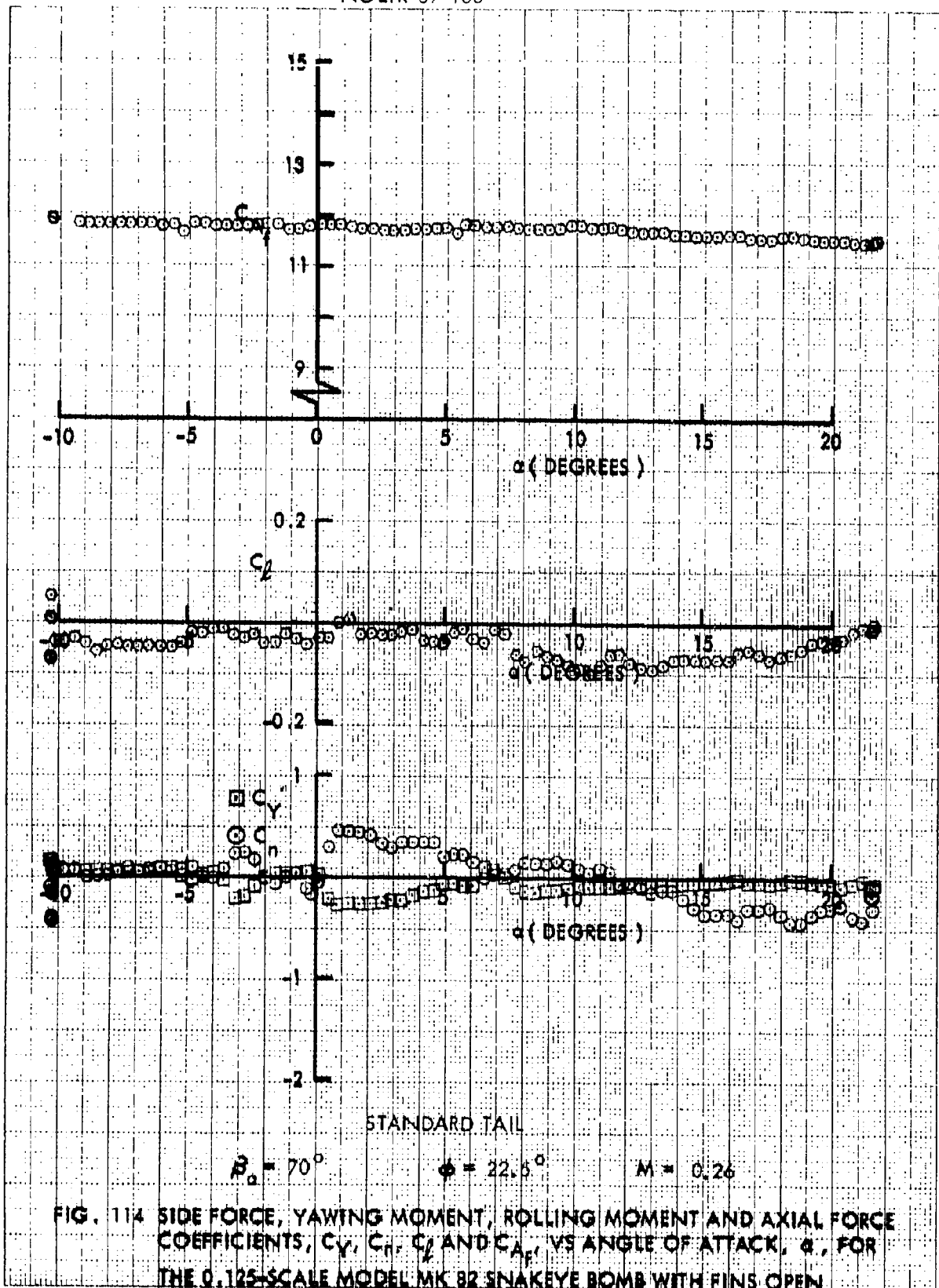
$$\beta_0 = 70^\circ$$

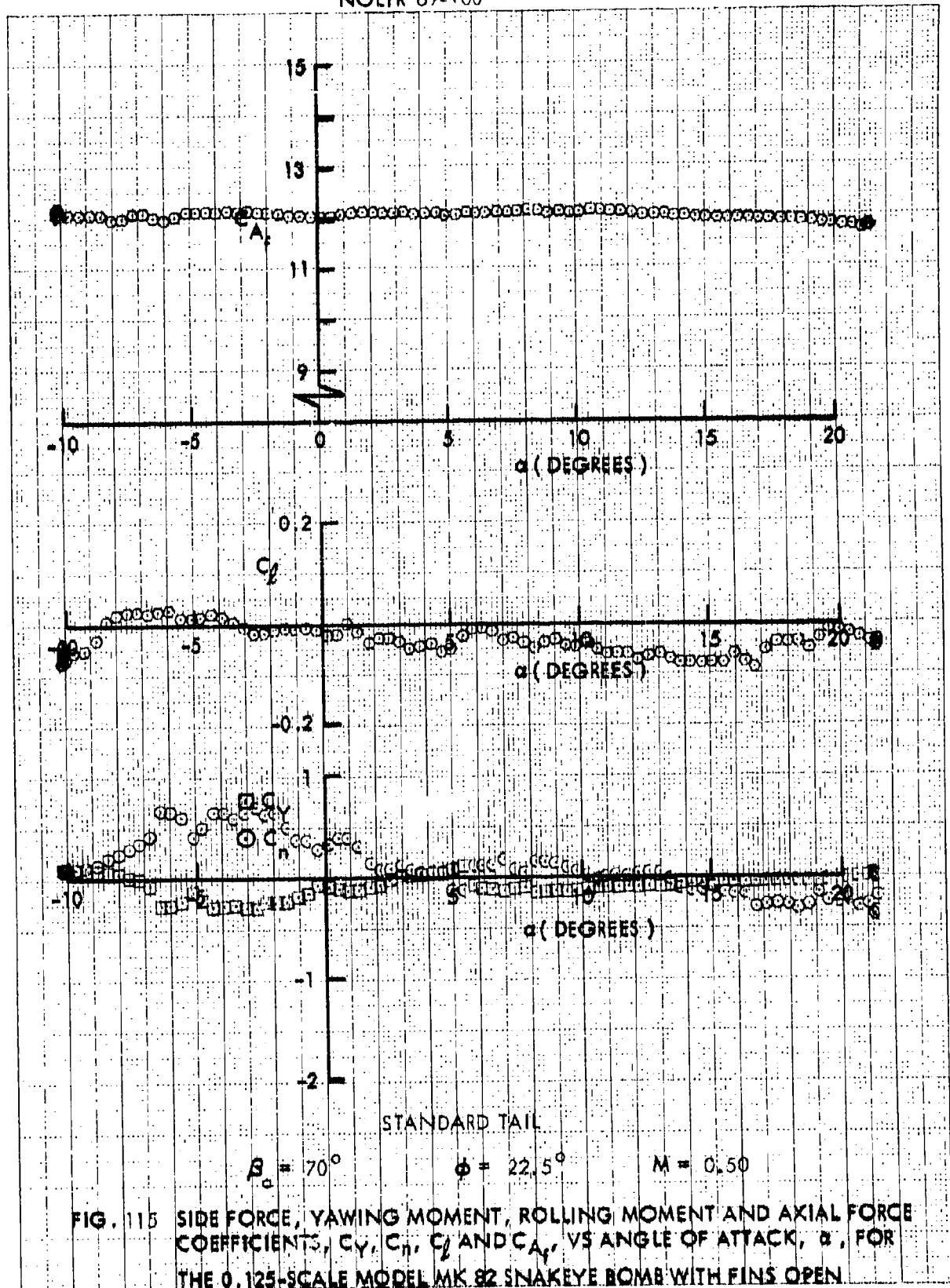
$$\phi = 0^\circ$$

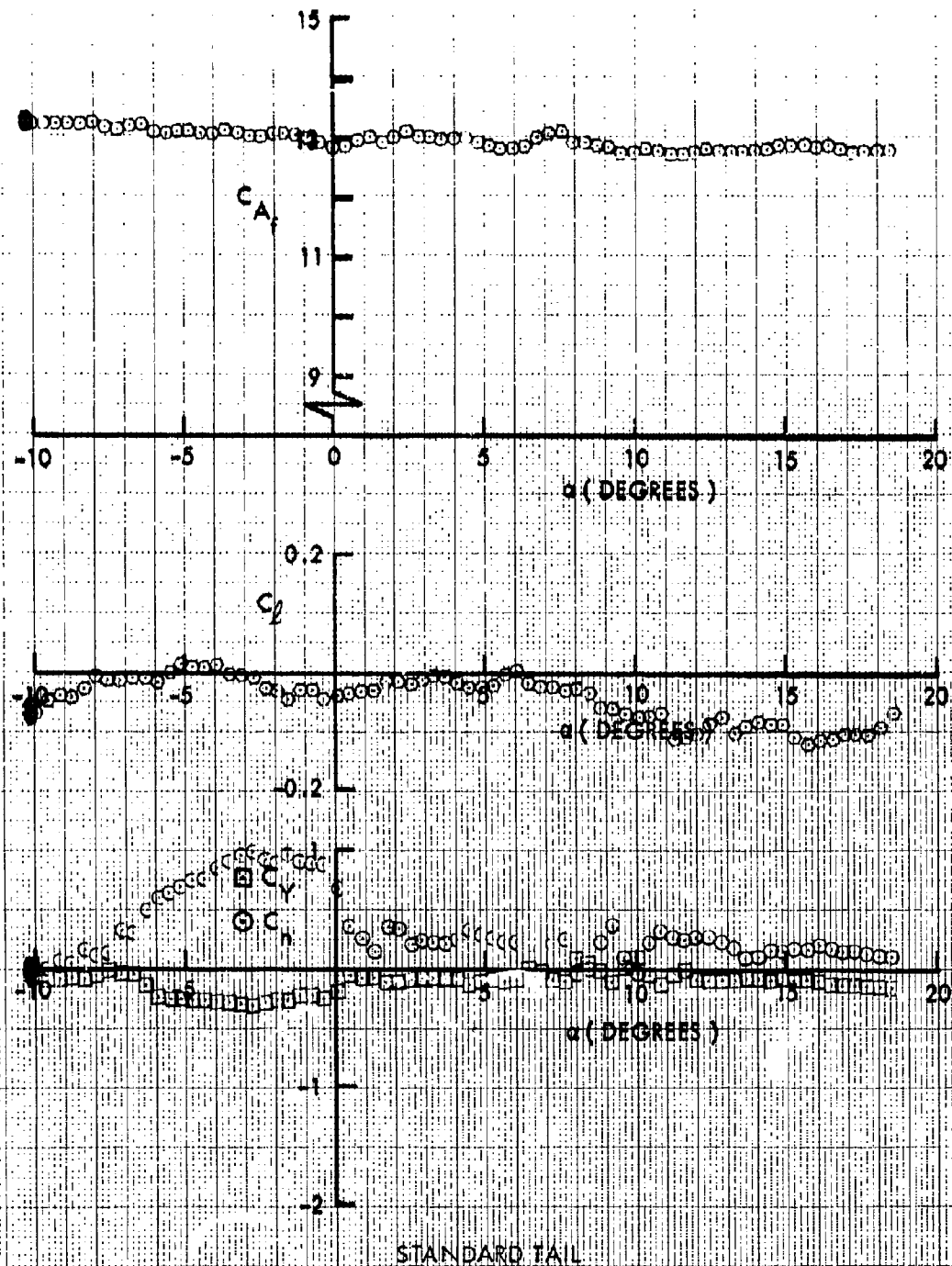
$$M = 0.92$$

FIG. 112 SIDE FORCE, YAWING MOMENT, ROLLING MOMENT AND AXIAL FORCE COEFFICIENTS,  $C_Y$ ,  $C_L$ ,  $C_R$  AND  $C_A$ , VS ANGLE OF ATTACK,  $\alpha$ , FOR THE 0.125-SCALE MODEL MK B2 SNAKEYE BOMB WITH FINS OPEN.









$$\beta_a = 70^\circ$$

$$\phi = 22.5^\circ$$

$$M = 0.81$$

FIG. 116 SIDE FORCE, YAWING MOMENT, ROLLING MOMENT AND AXIAL FORCE COEFFICIENTS,  $C_Y$ ,  $C_R$ ,  $C_Y$  AND  $C_A$ , VS ANGLE OF ATTACK,  $\alpha$ , FOR THE 0.125-SCALE MODEL MK 82 SNAKEYE BOMB WITH FINIS OPEN

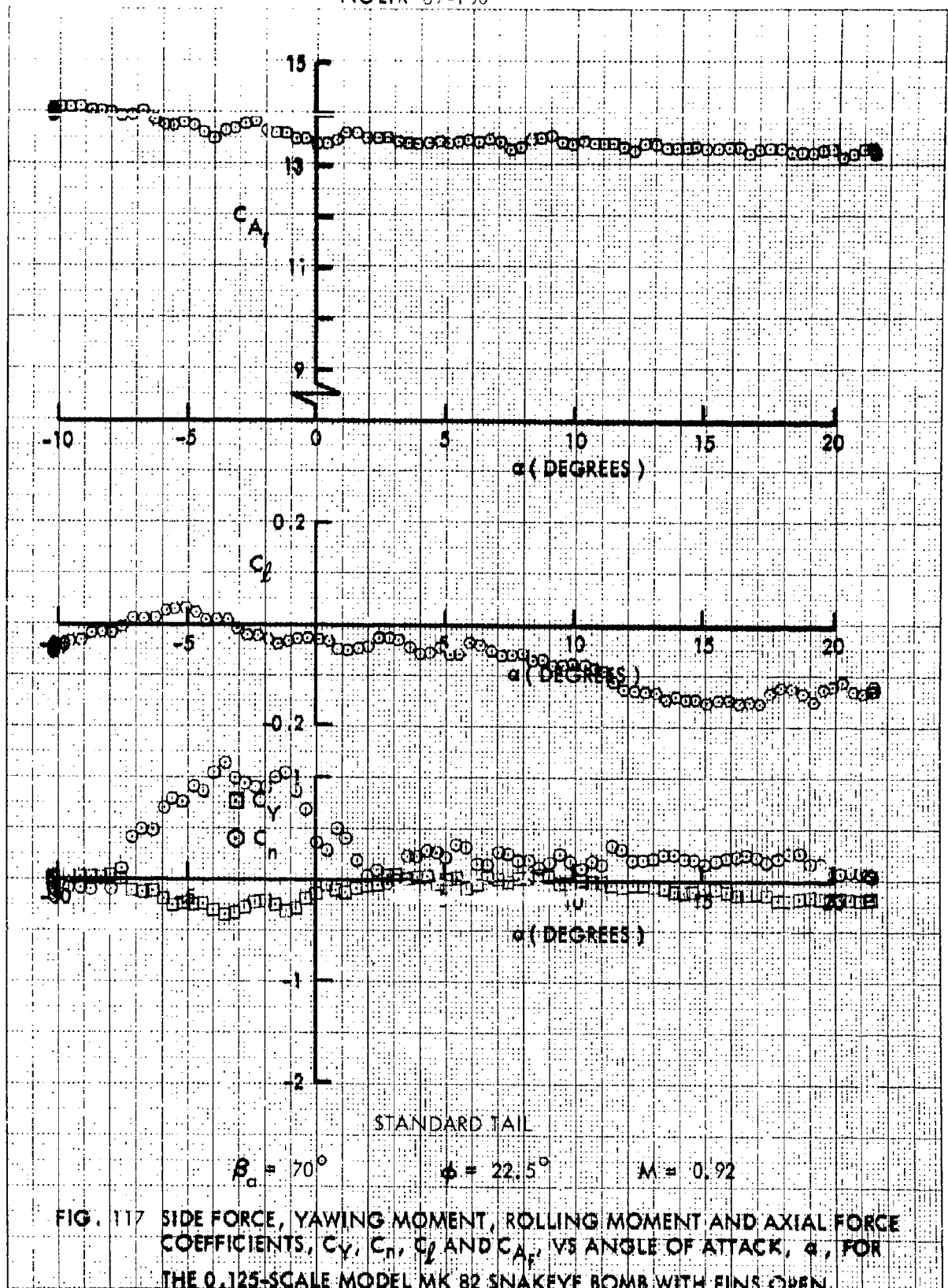
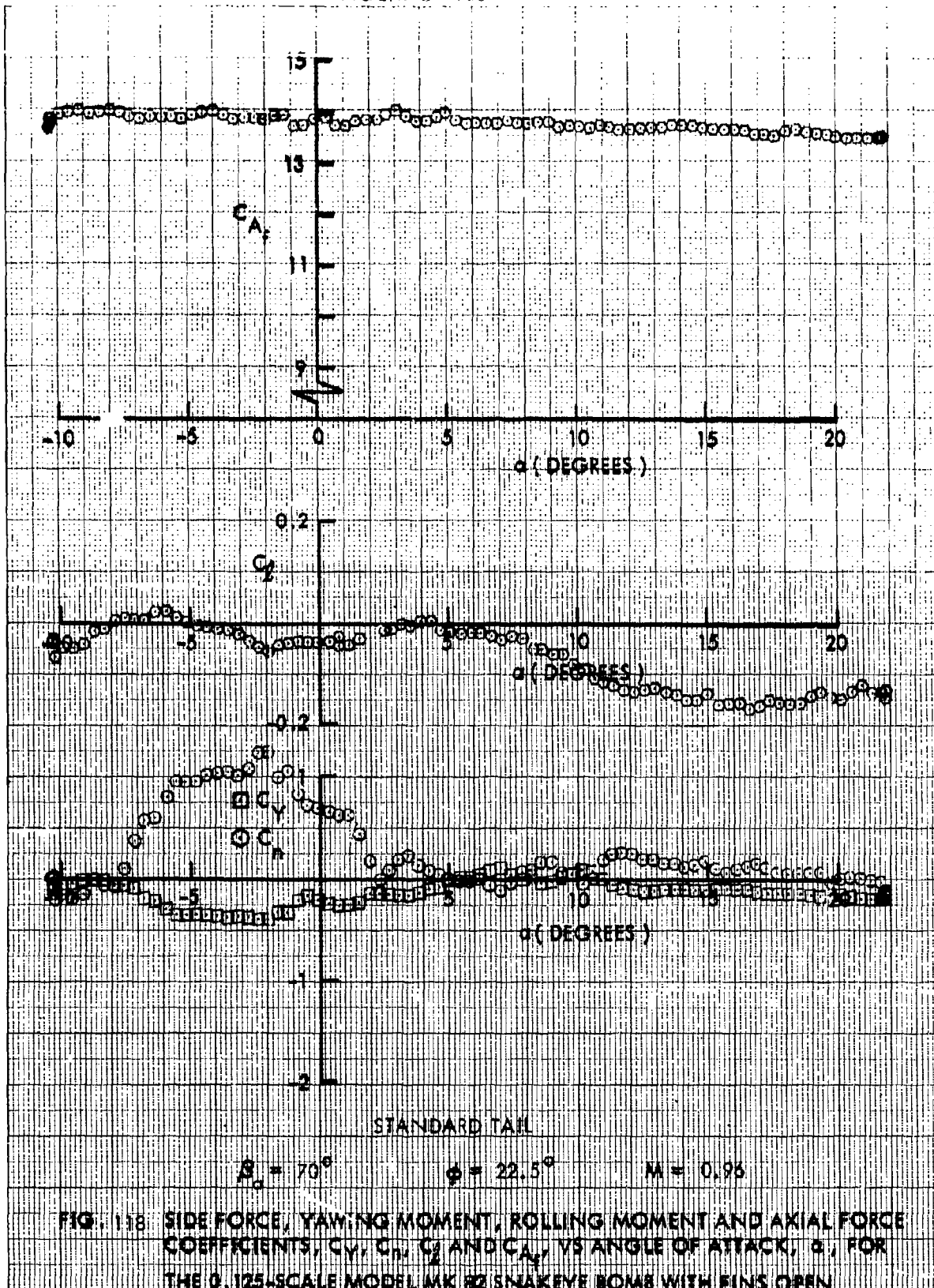
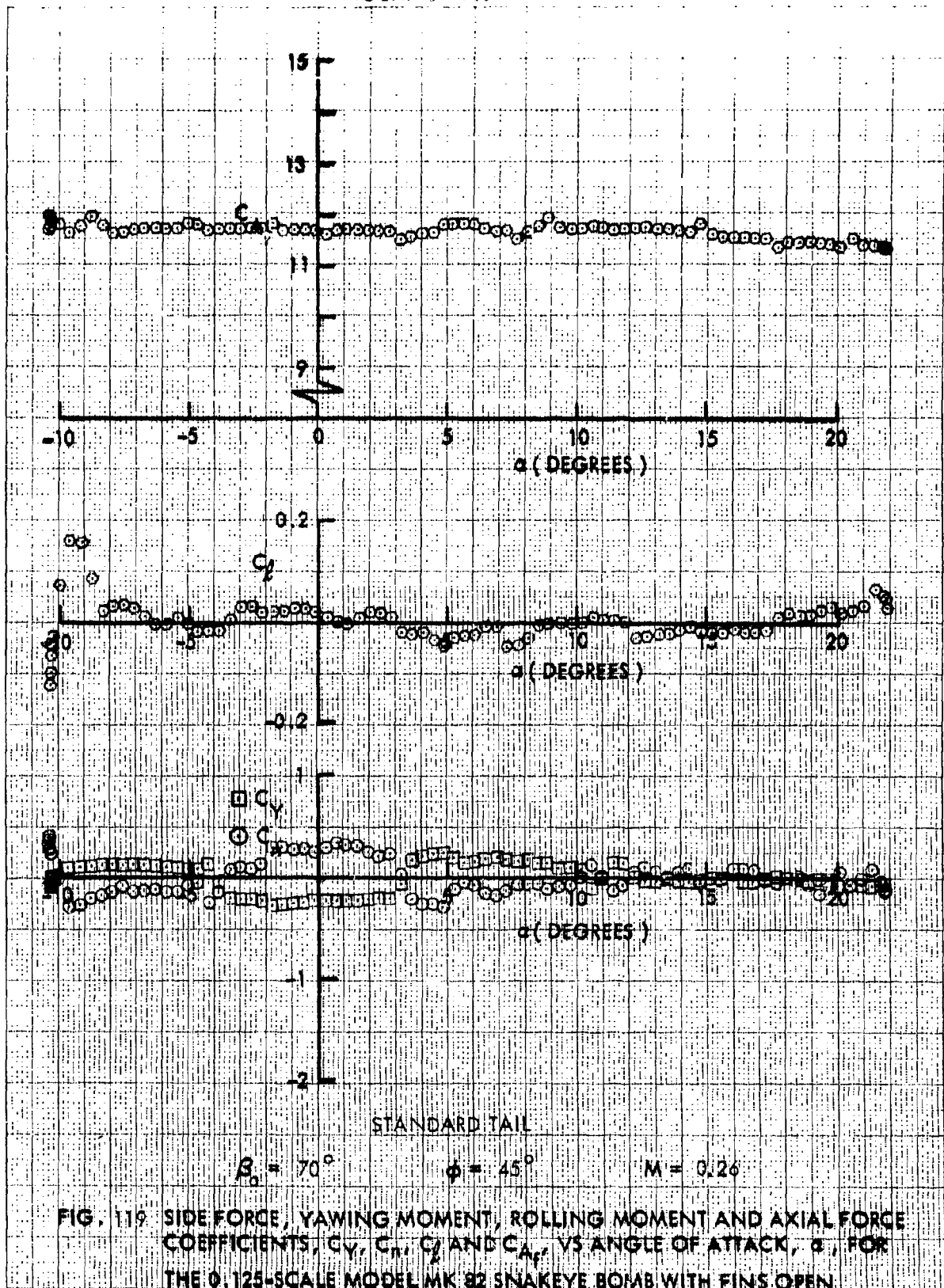
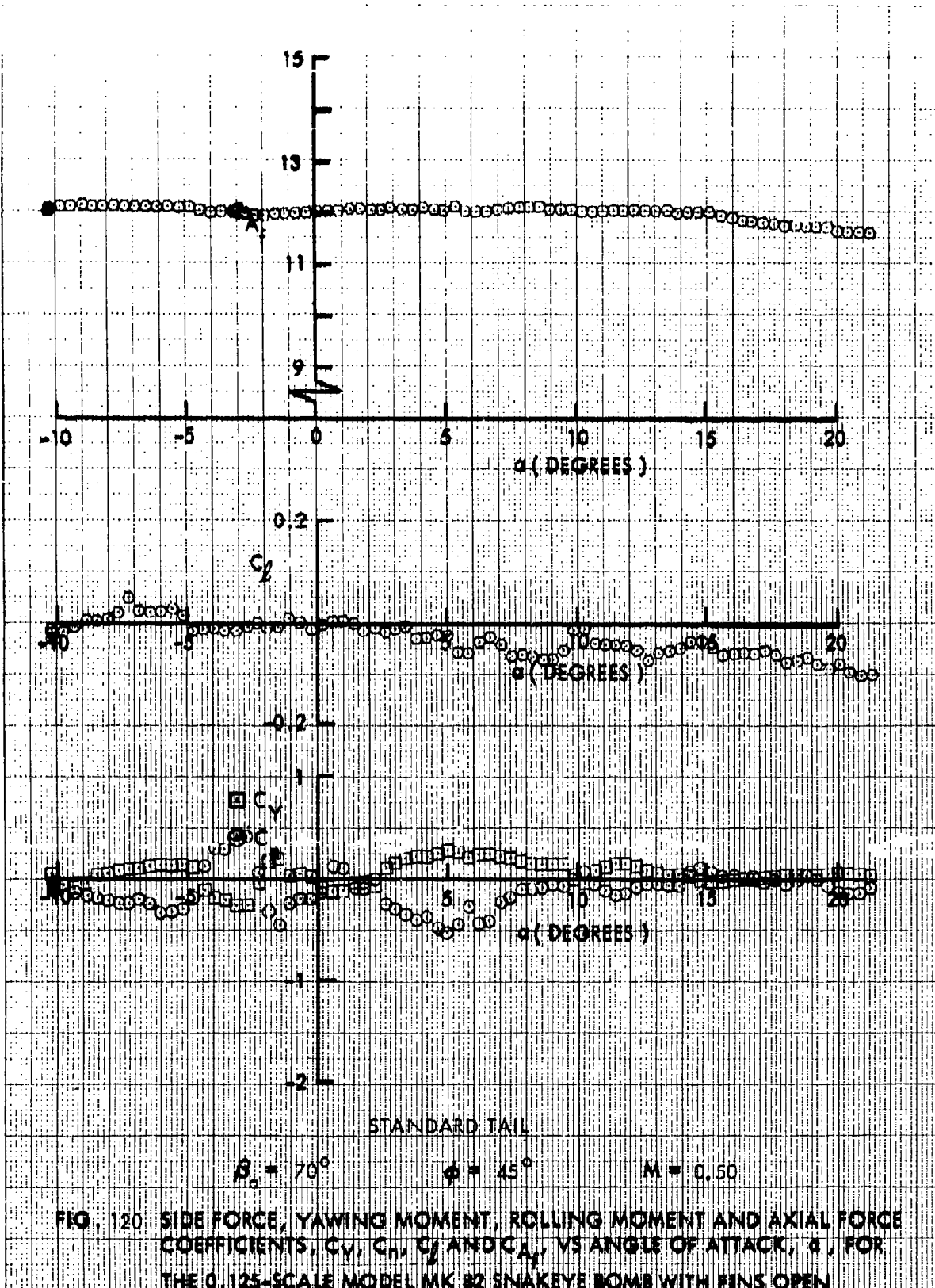


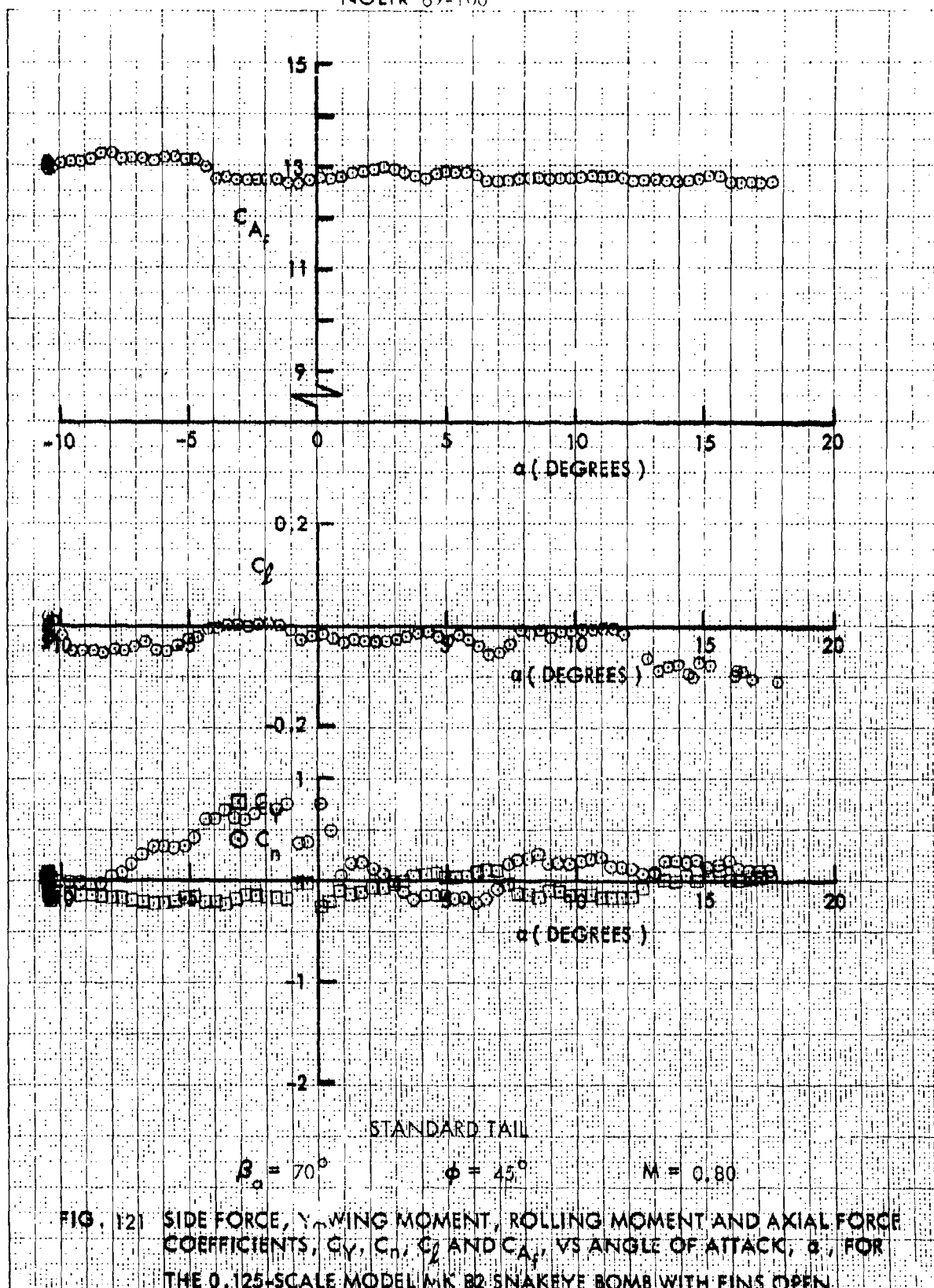
FIG. 117 SIDE FORCE, YAWING MOMENT, ROLLING MOMENT AND AXIAL FORCE COEFFICIENTS,  $C_Y$ ,  $C_n$ ,  $C_L$  AND  $C_A$ , VS ANGLE OF ATTACK,  $\alpha$ , FOR THE 0.125-SCALE MODEL MK 82 SNAKEYE BOMB WITH FINS OPEN

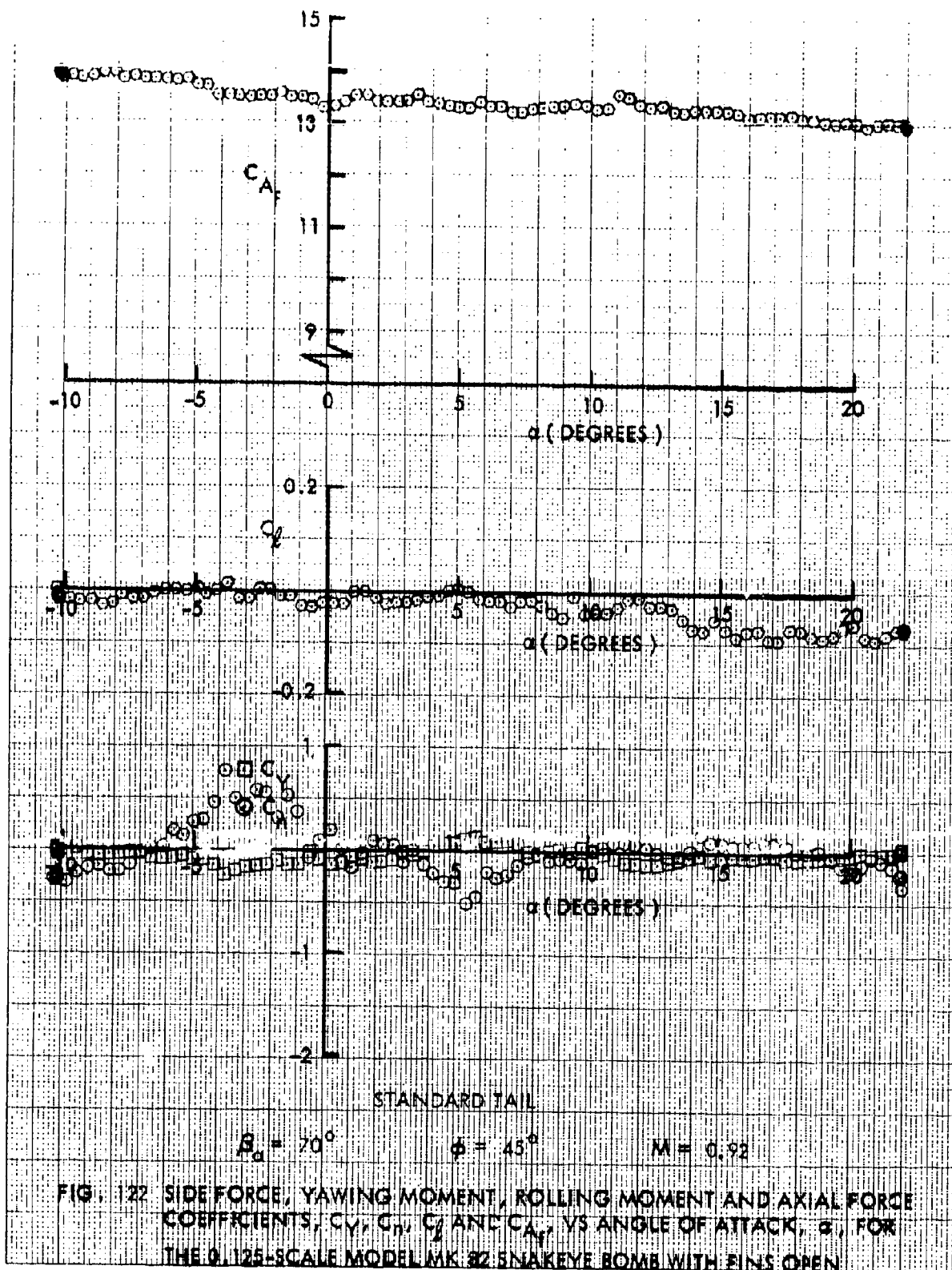


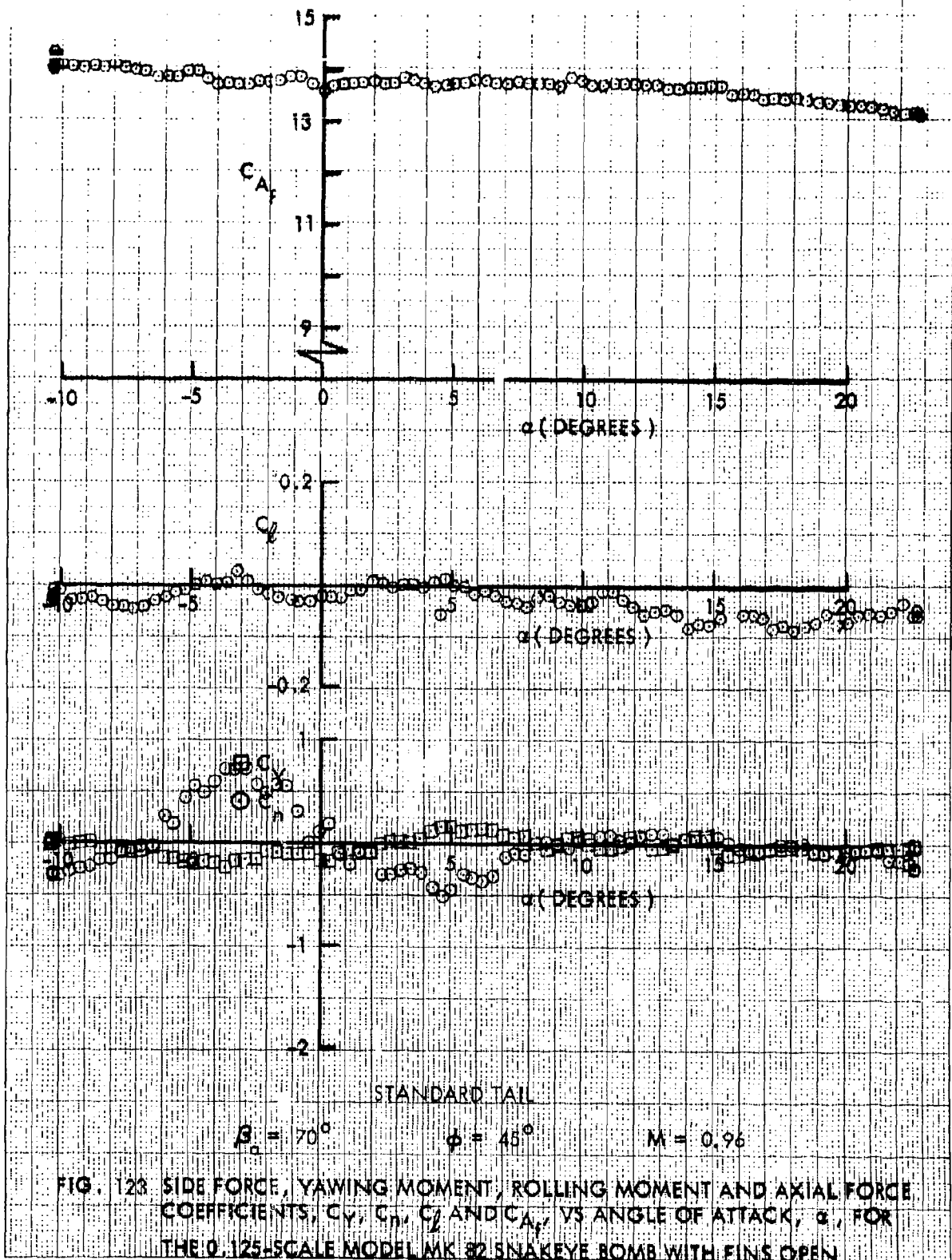




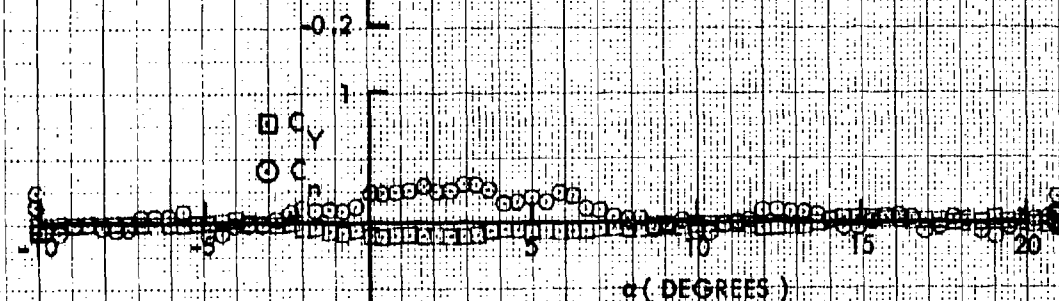
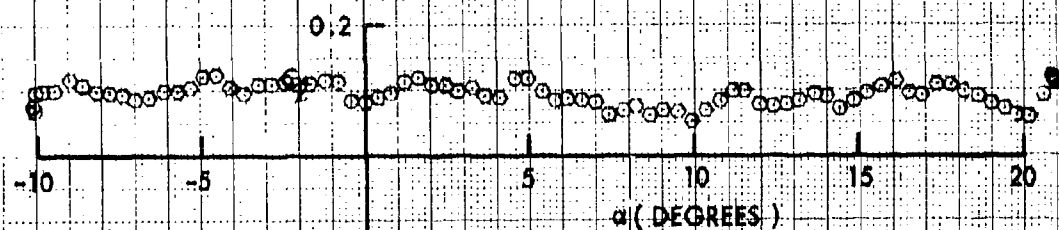
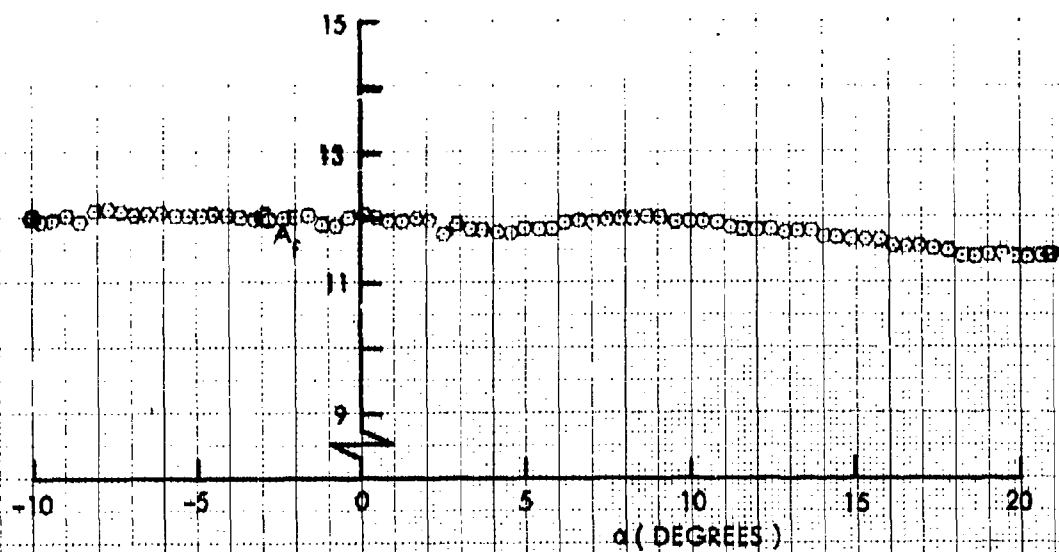












STANDARD TAIL

$\beta_a = 80^\circ$

$\phi = 0^\circ$

$M = 0.26$

FIG. 124 SIDE FORCE, YAWING MOMENT, ROLLING MOMENT AND AXIAL FORCE COEFFICIENTS,  $C_Y$ ,  $C_n$ ,  $C_l$  AND  $C_A$ , VS ANGLE OF ATTACK,  $\alpha$ , FOR THE 0.125-SCALE MODEL MK 82 SNAKEYE BOMB WITH FINS OPEN

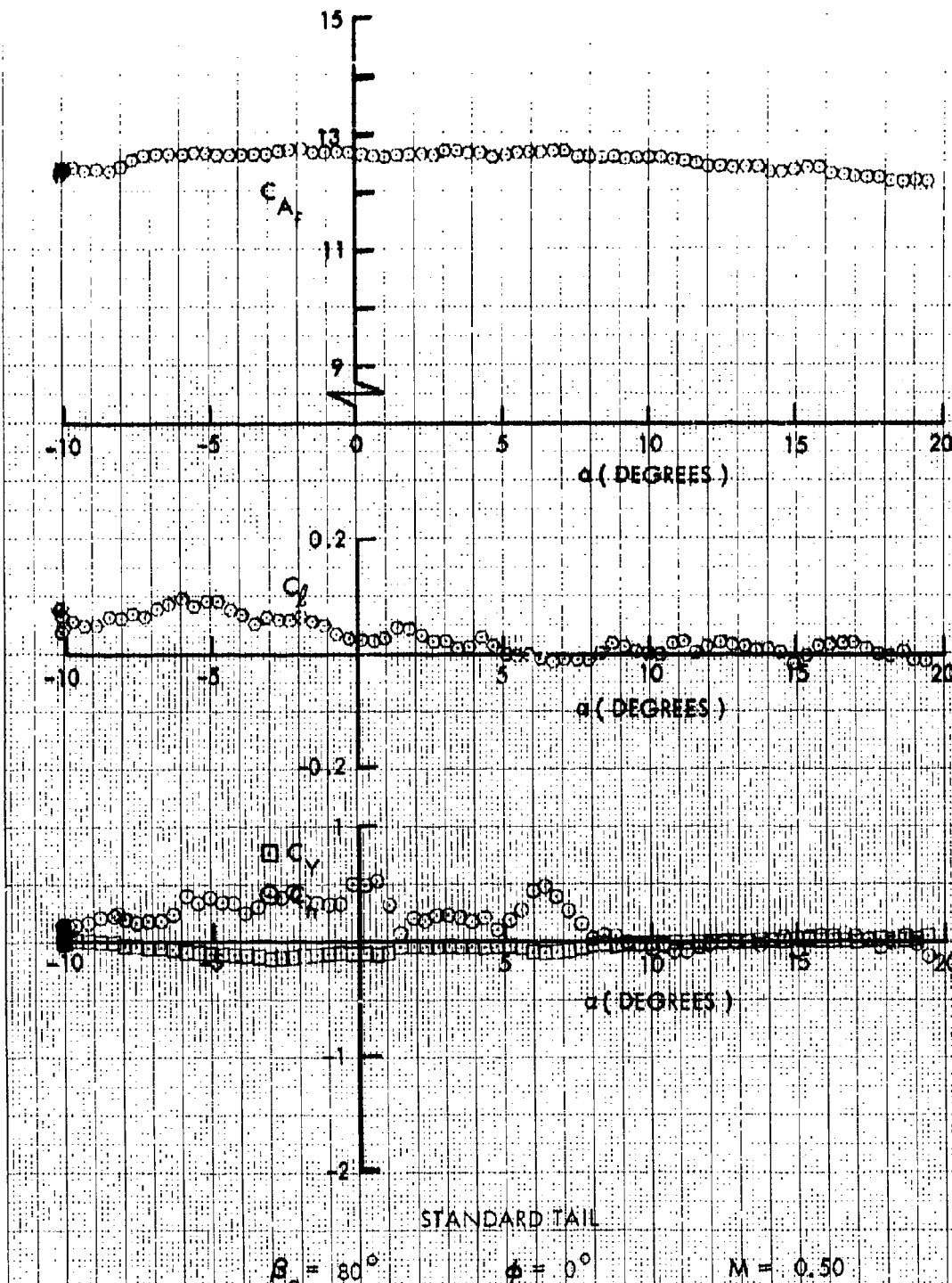
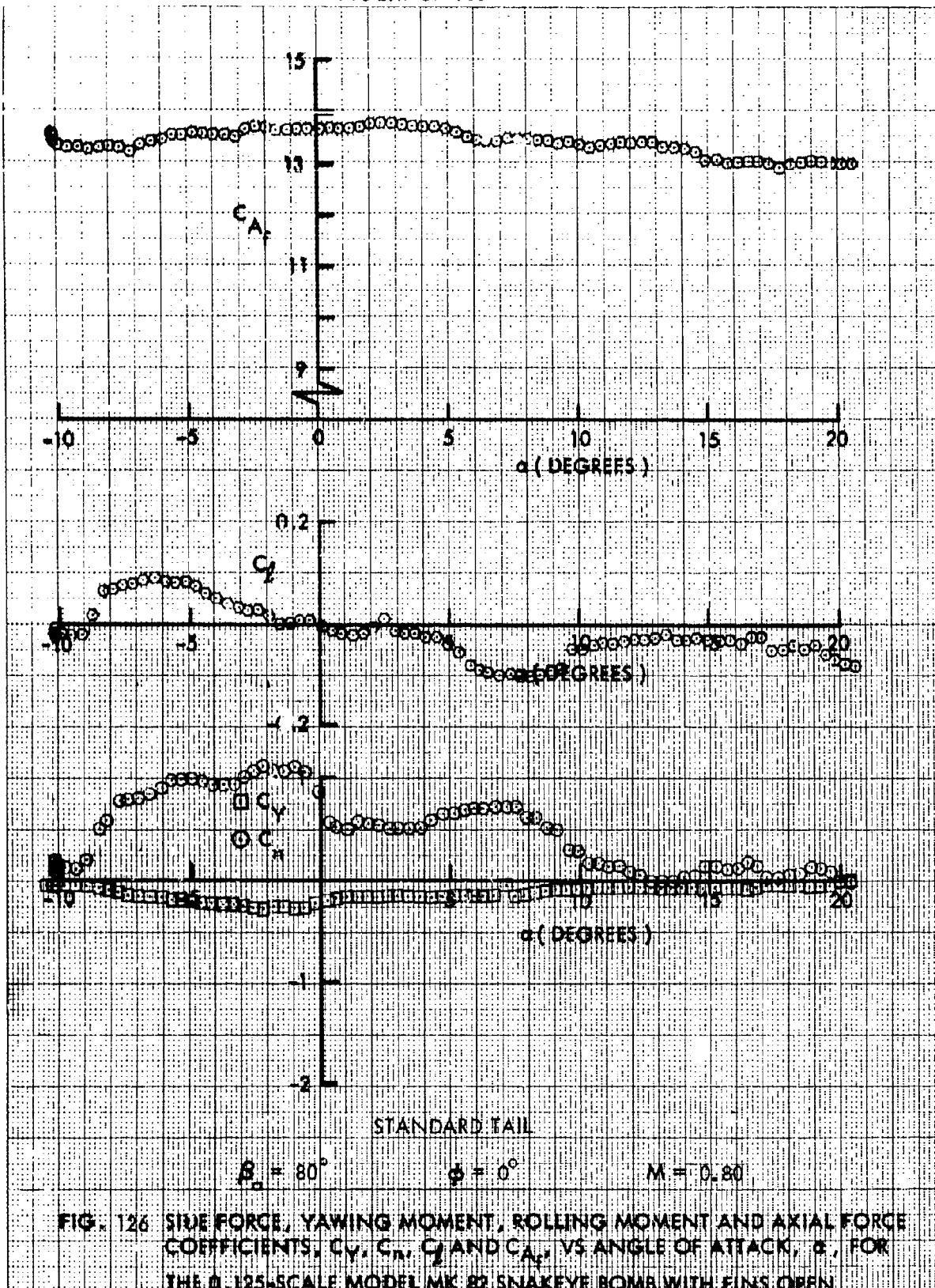
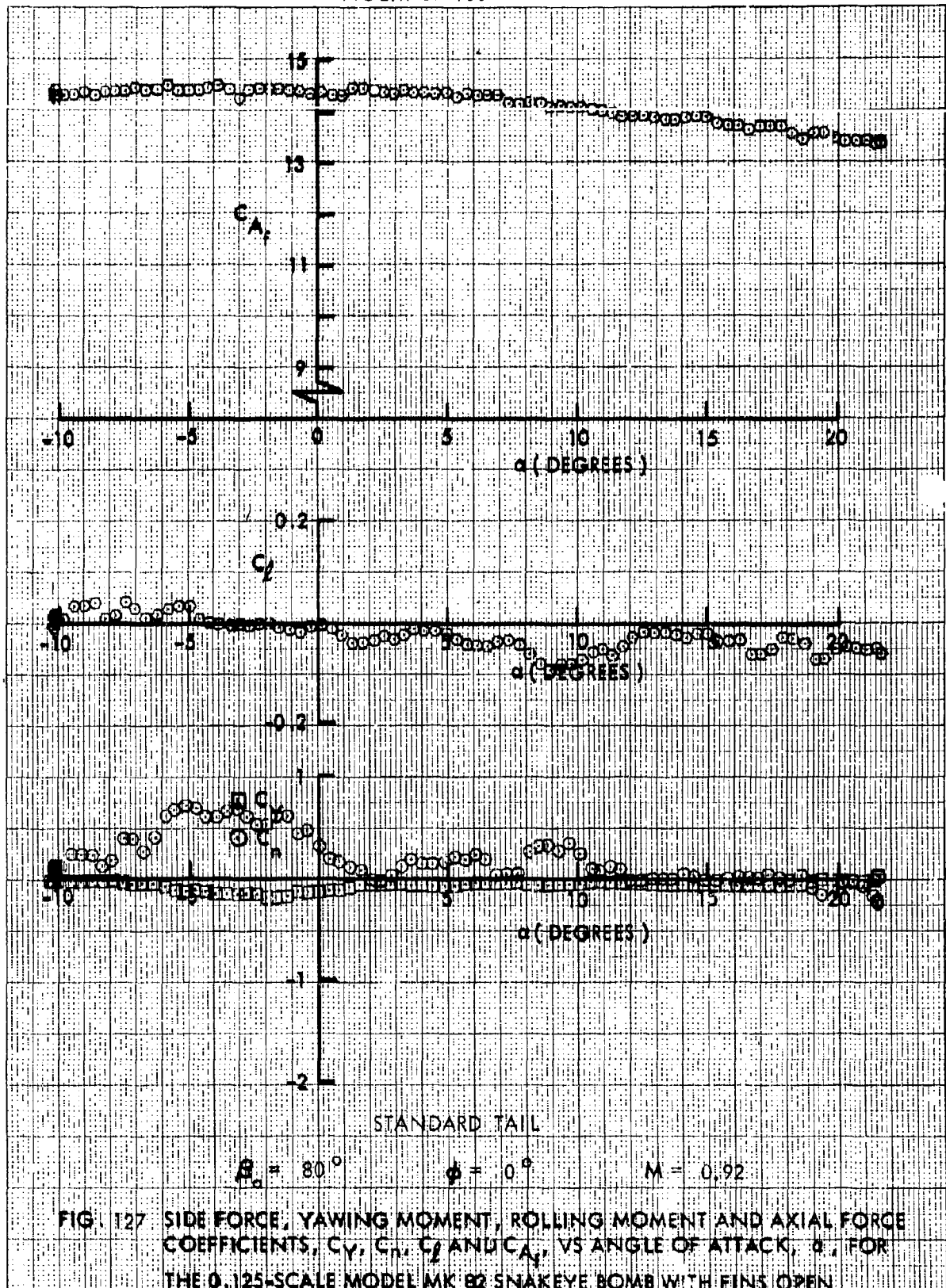
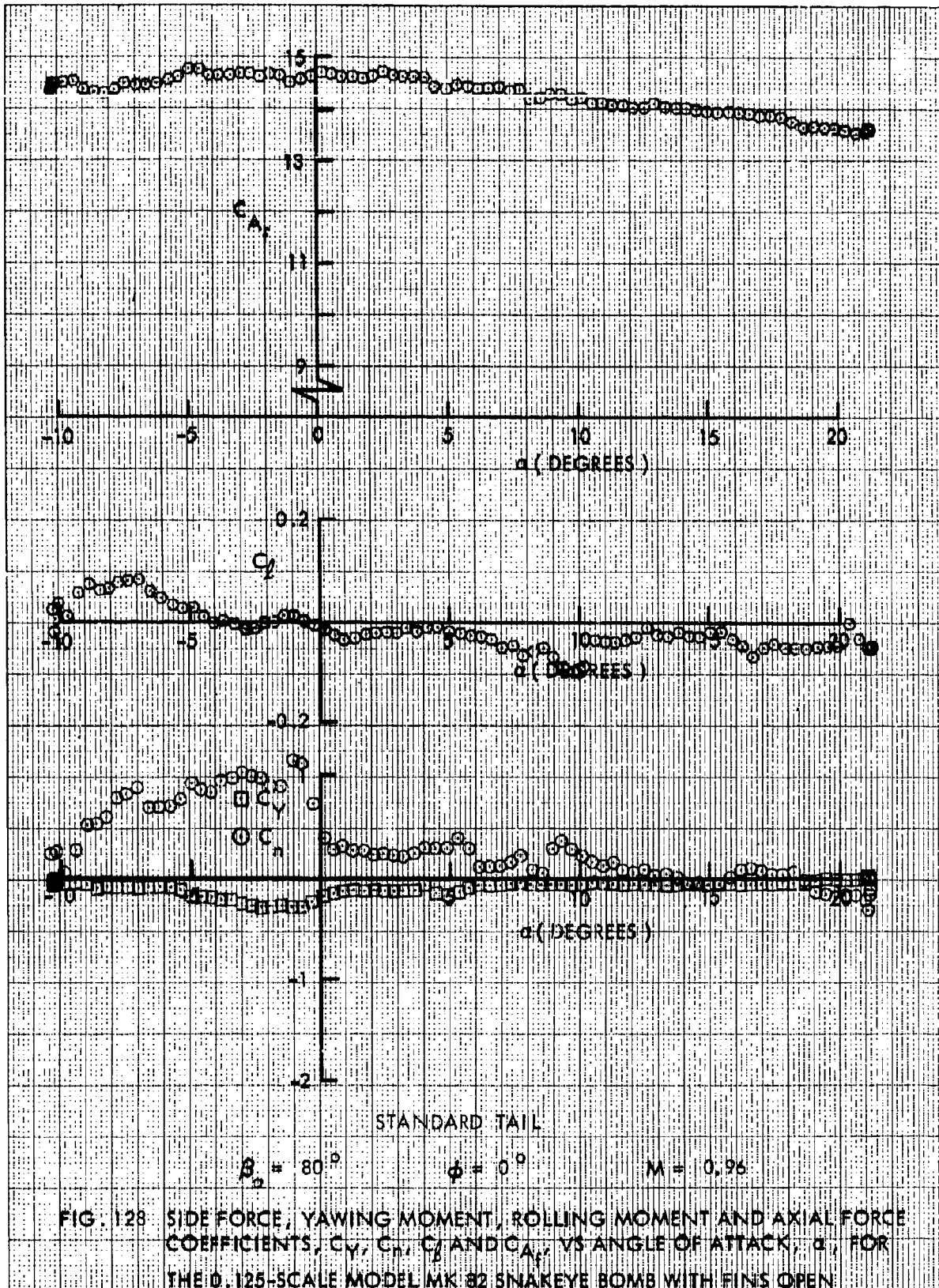
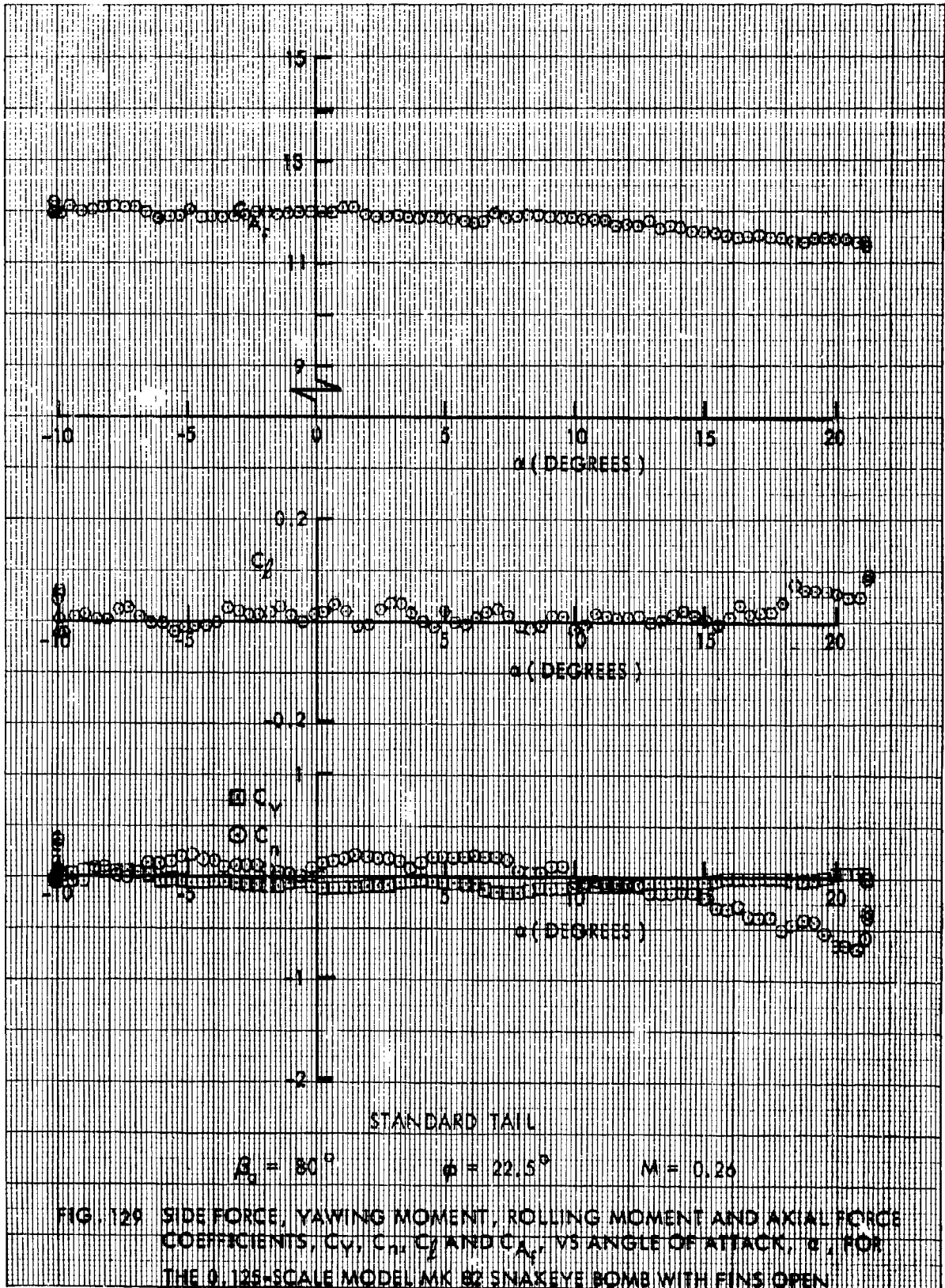


FIG. 125 SIDE FORCE, YAWING MOMENT, ROLLING MOMENT AND AXIAL FORCE COEFFICIENTS,  $C_y$ ,  $C_n$ ,  $C_l$  AND  $C_A$ , VS ANGLE OF ATTACK,  $\alpha$ , FOR THE 0.125-SCALE MODEL MK 82 SNAKEYE BOMB WITH FINS OPEN

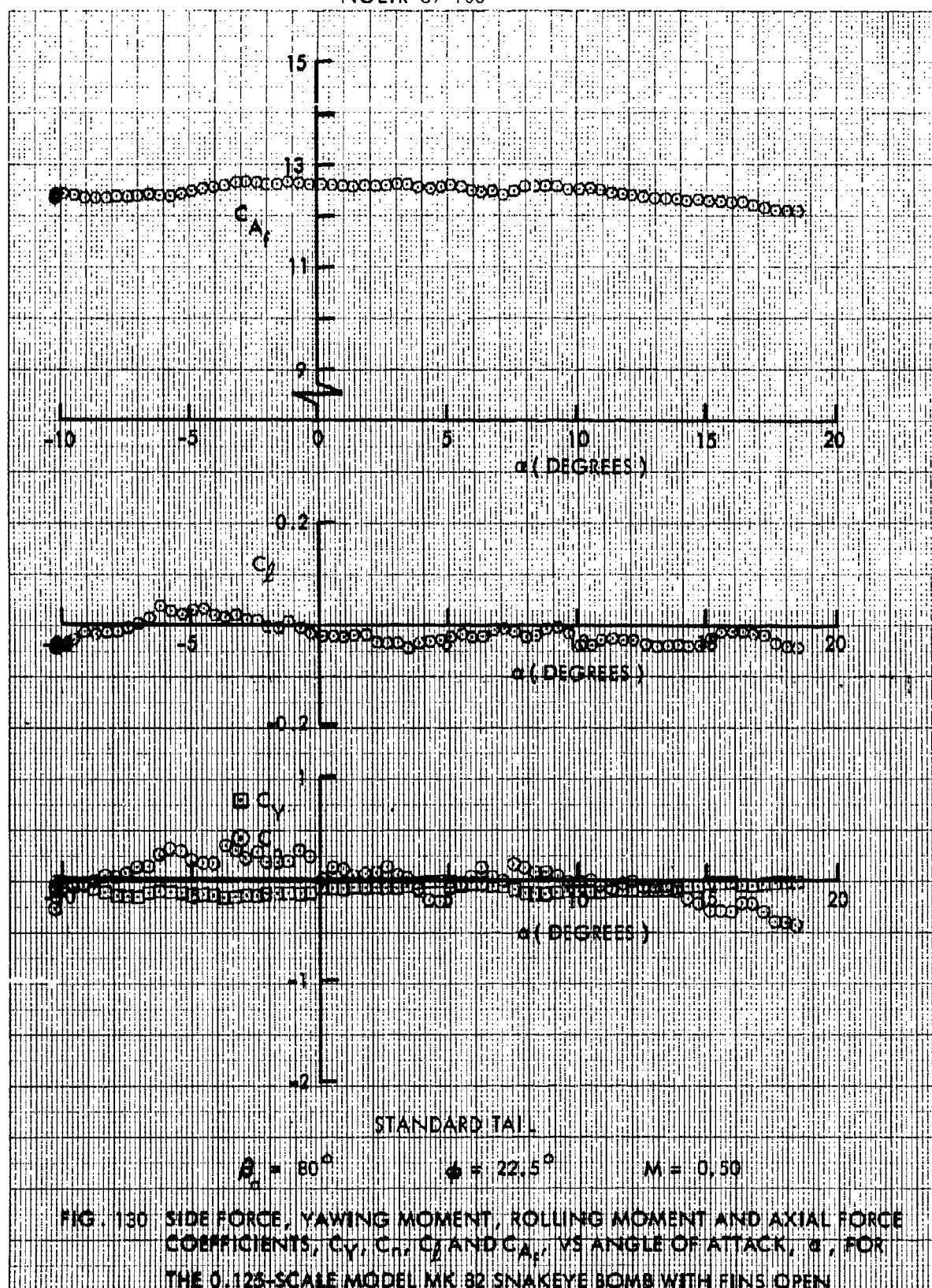


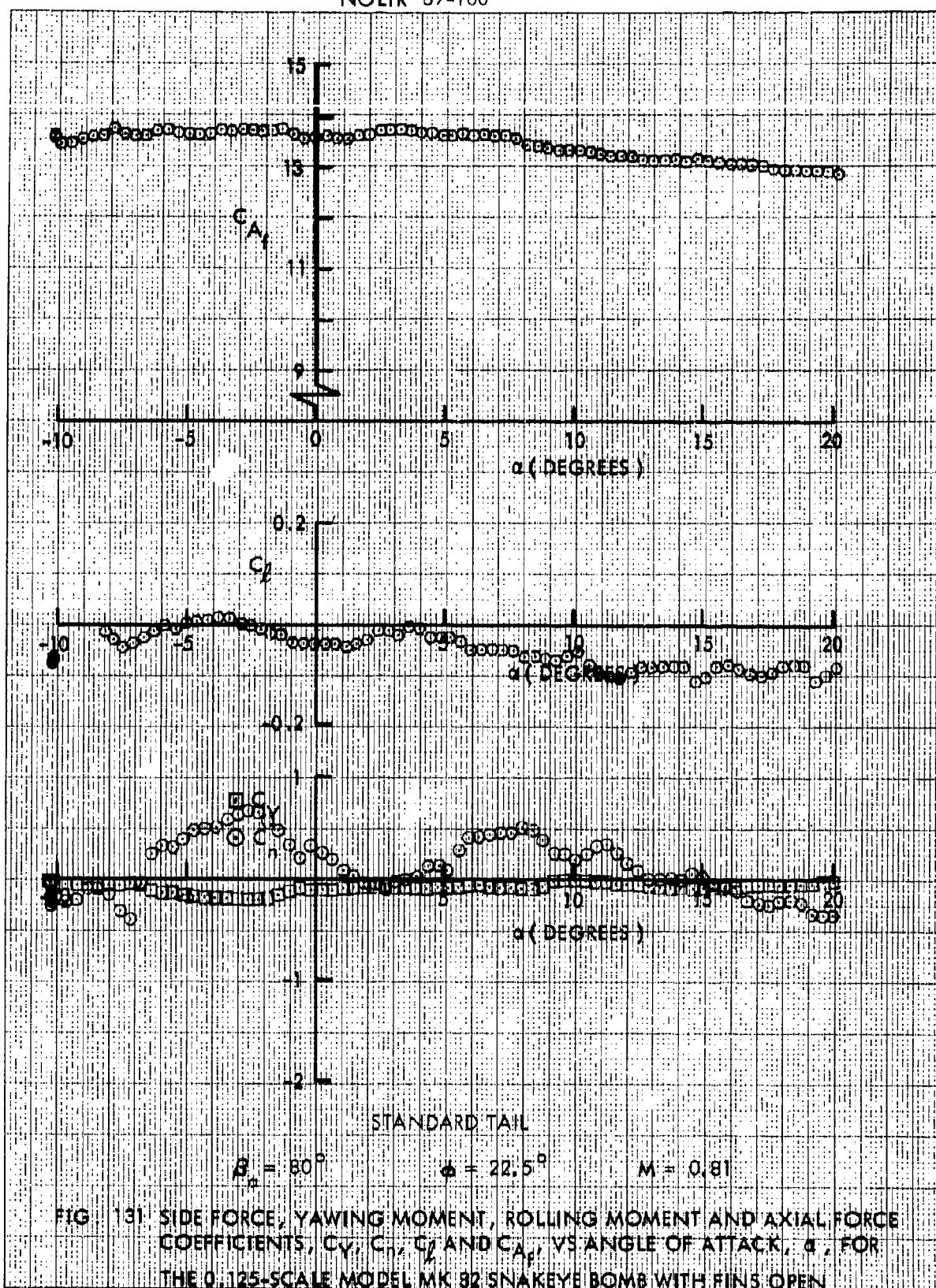


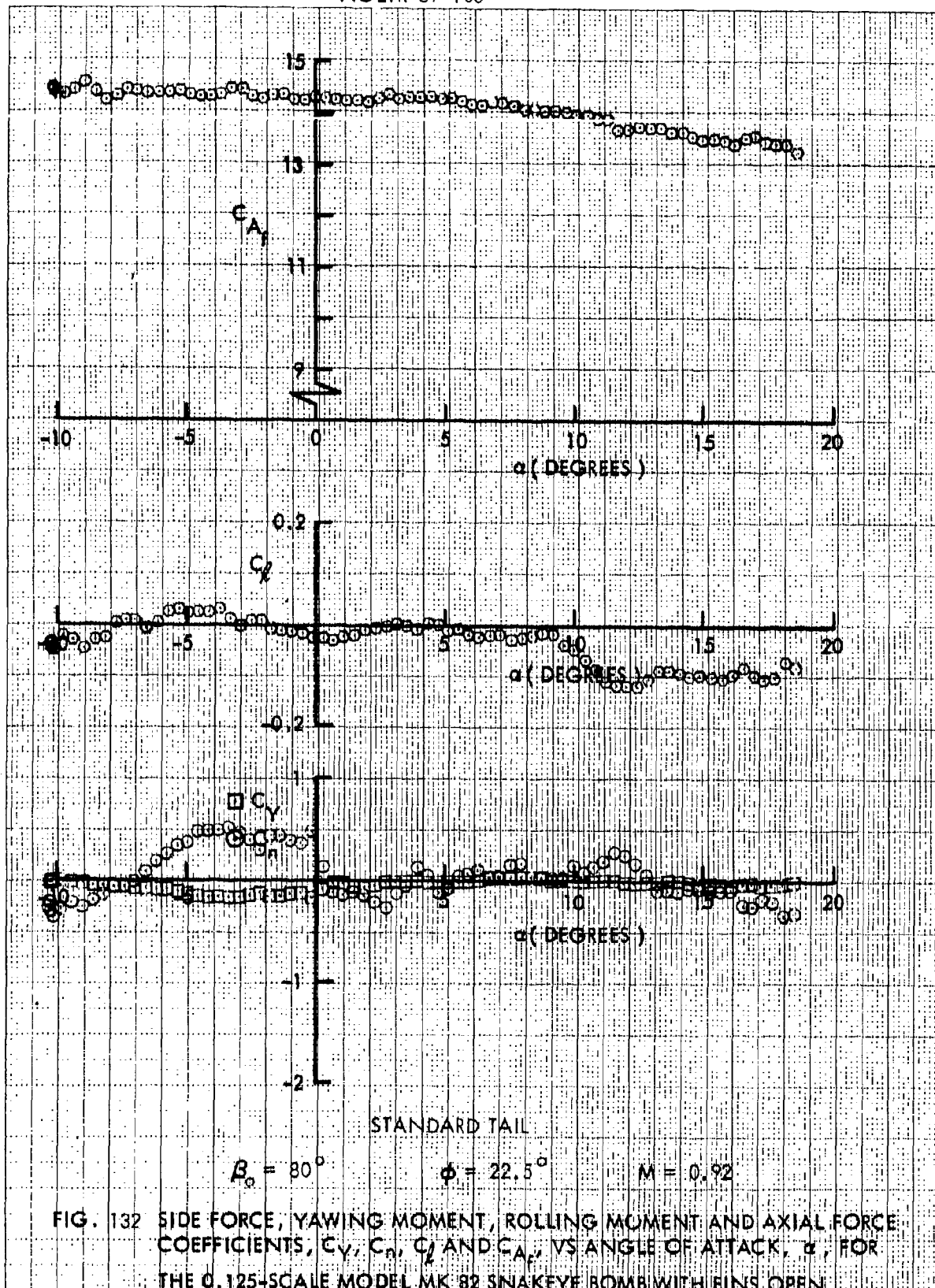


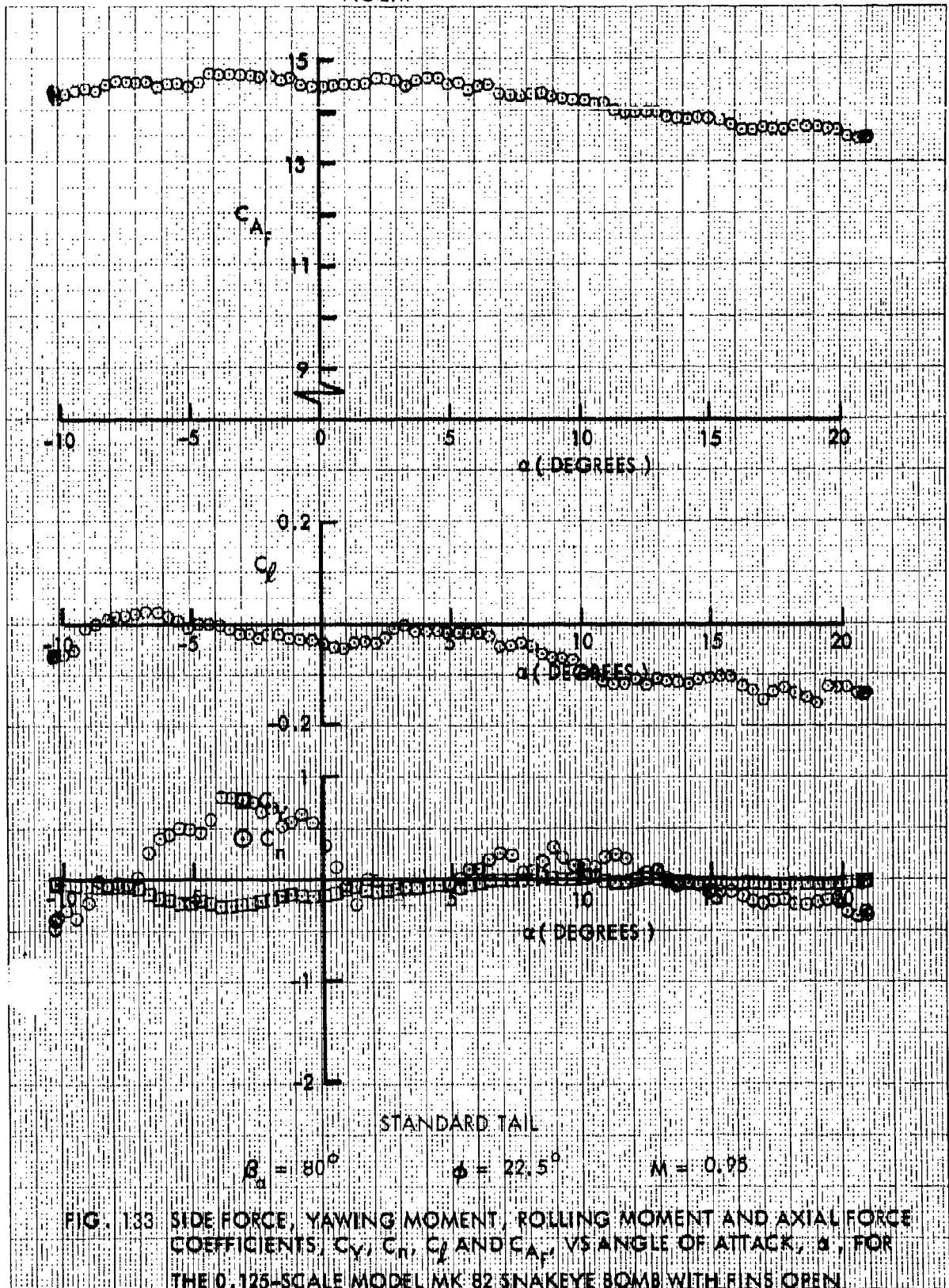


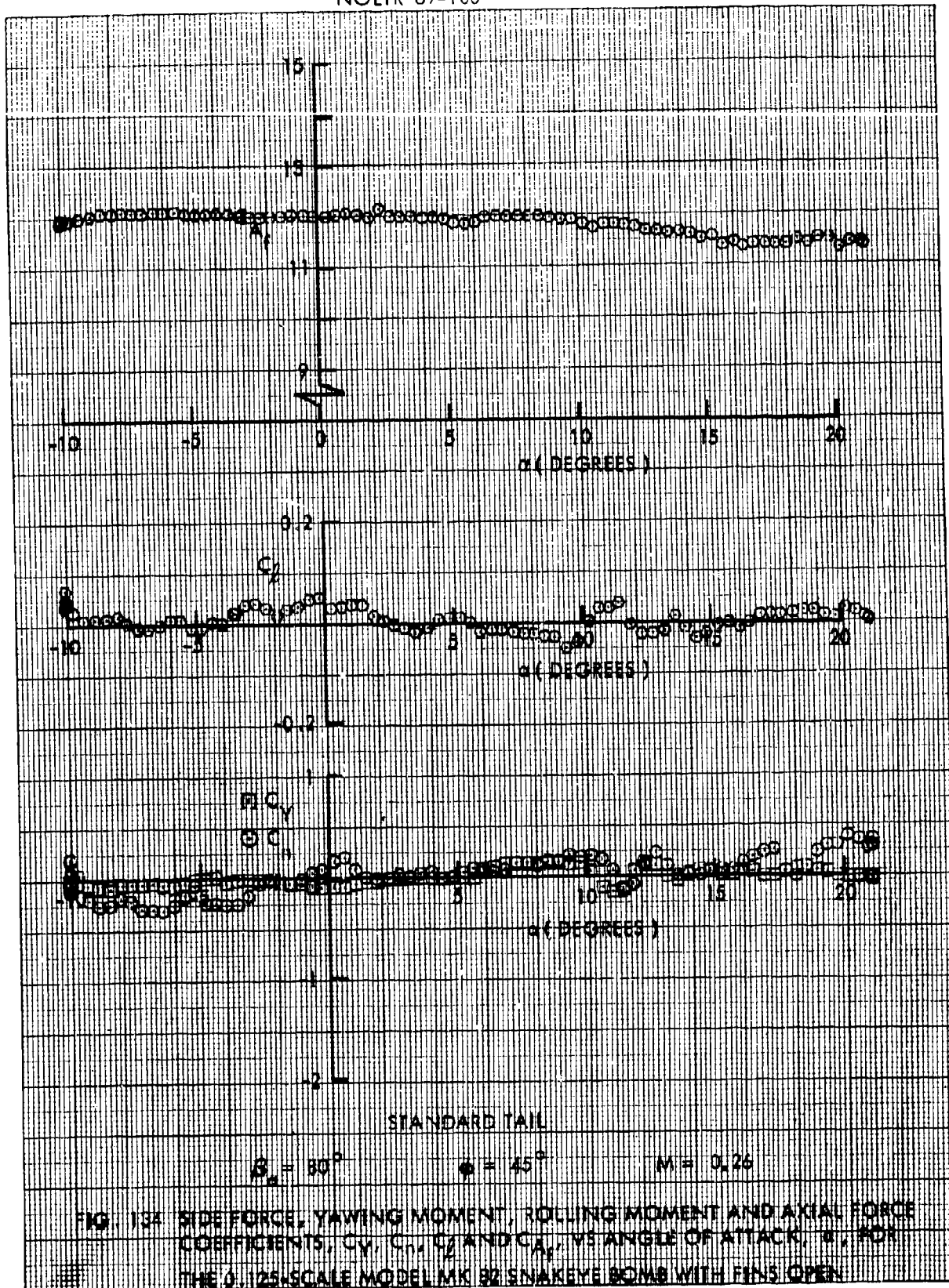


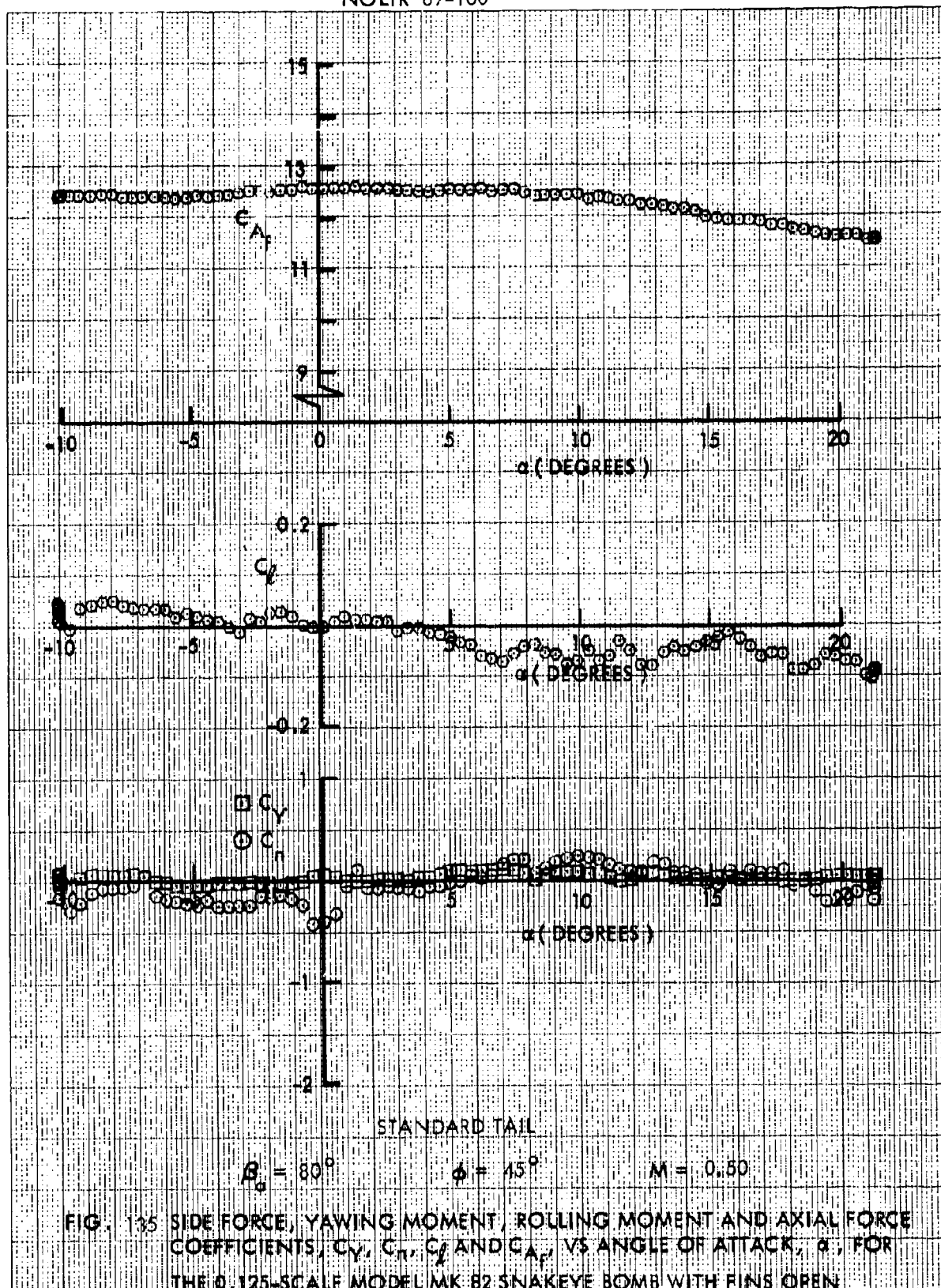




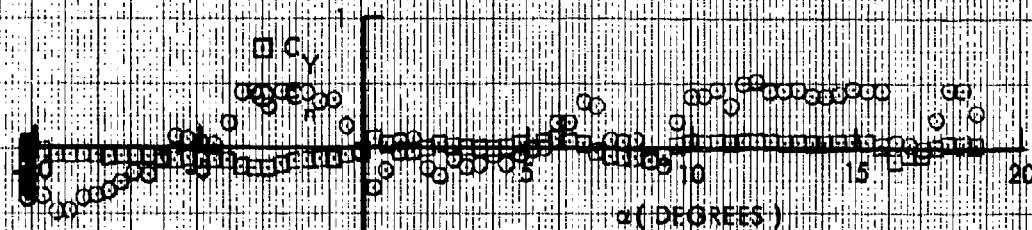
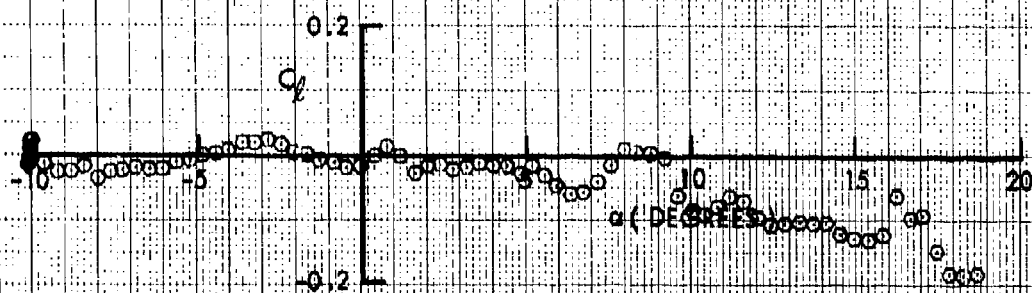
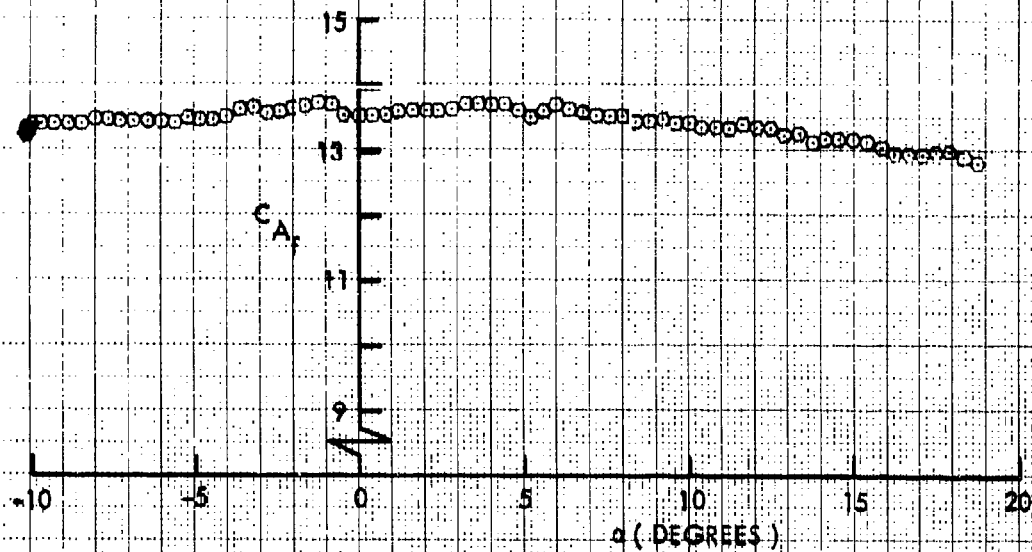












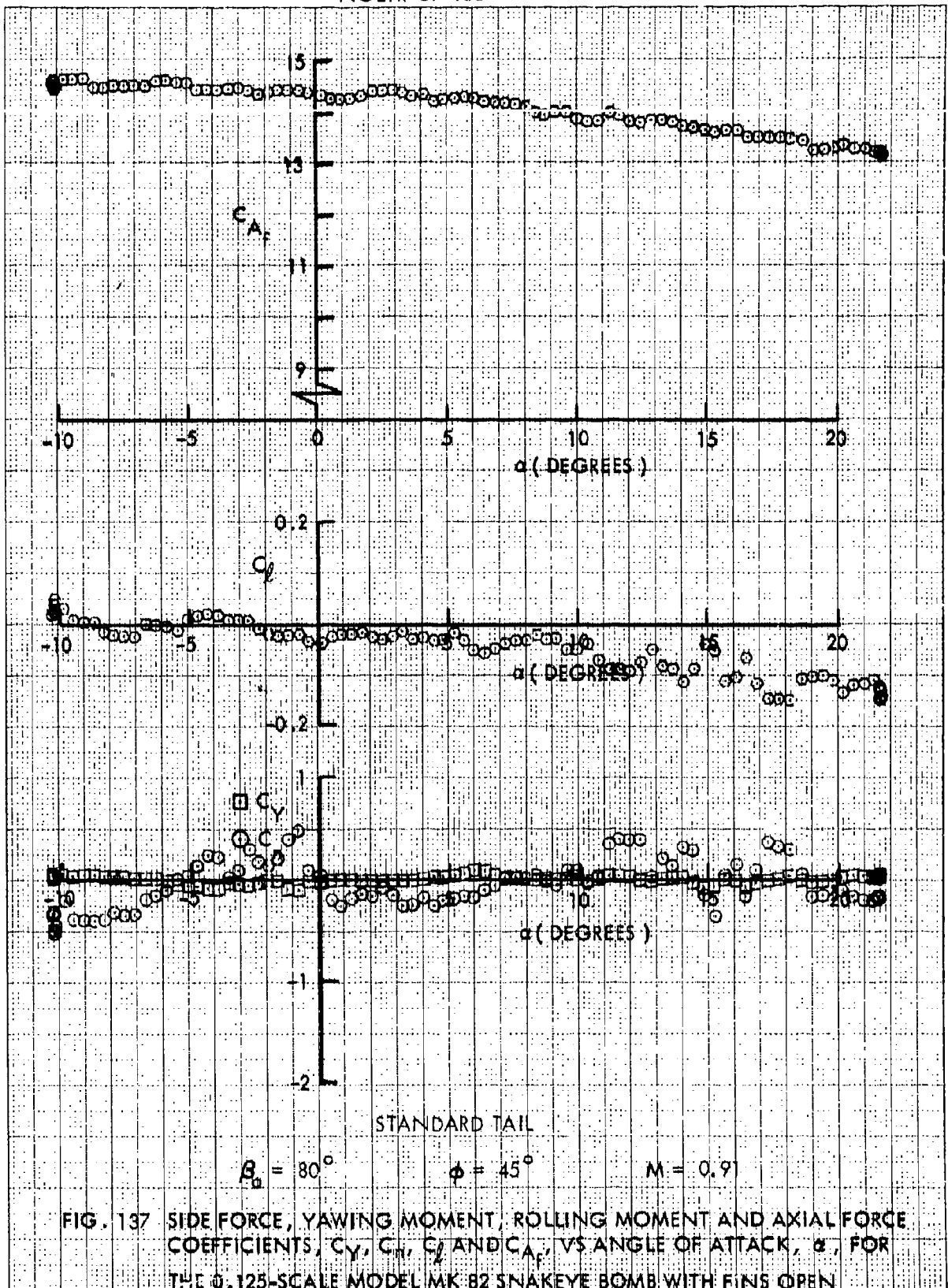
STANDARD TAIL

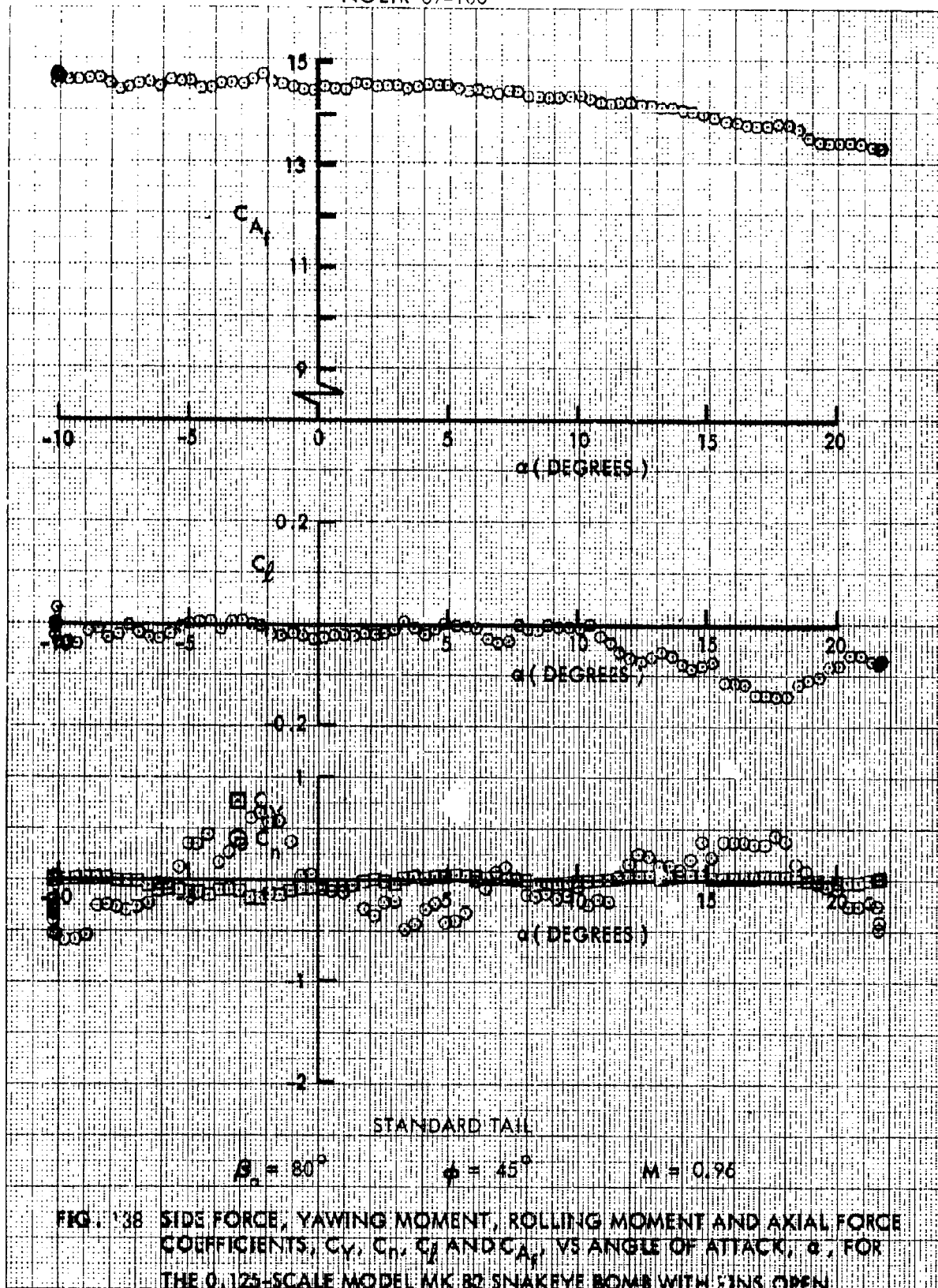
$$\beta_a = 80^\circ$$

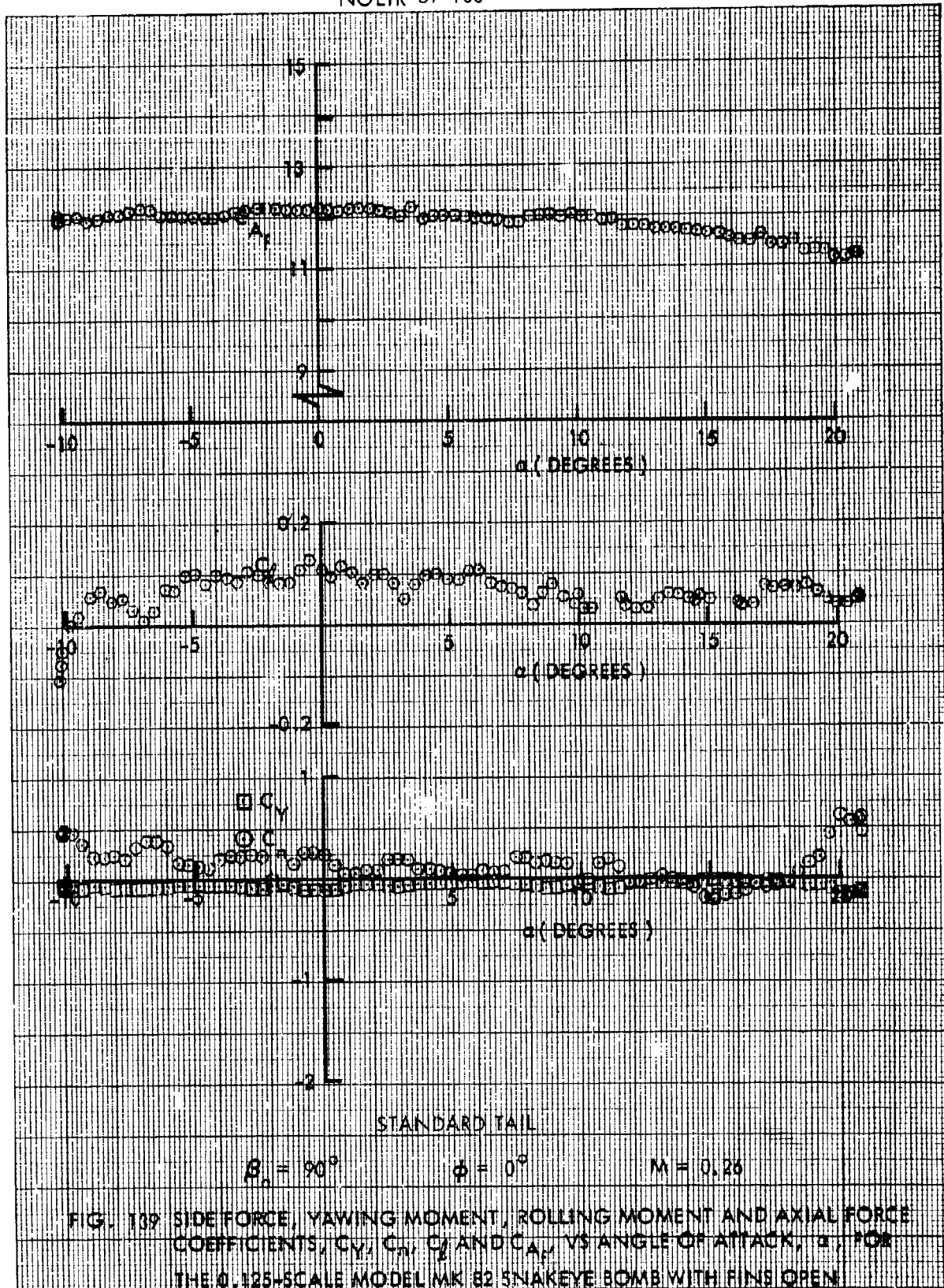
$$\phi = 45^\circ$$

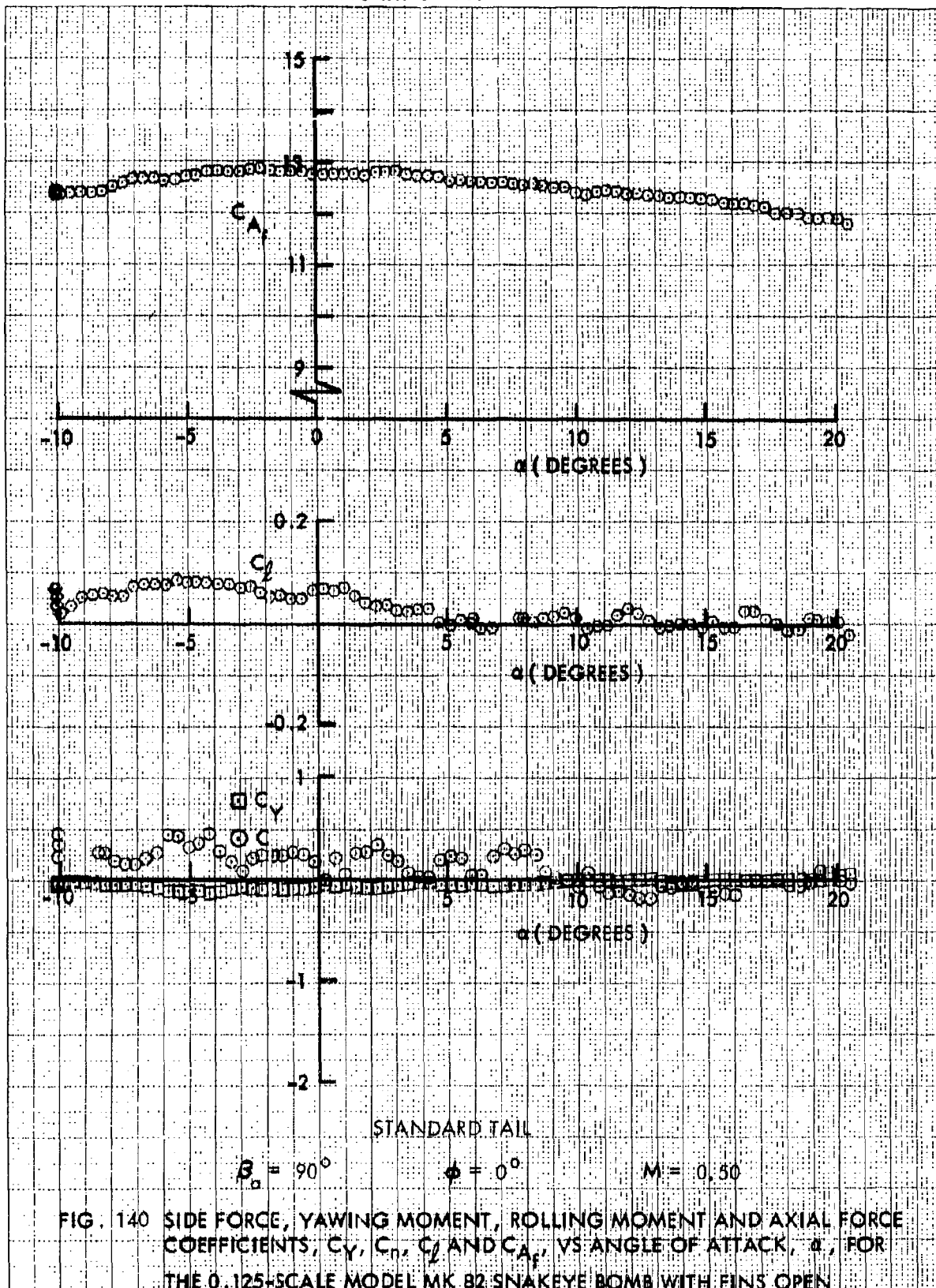
$$M = 0.81$$

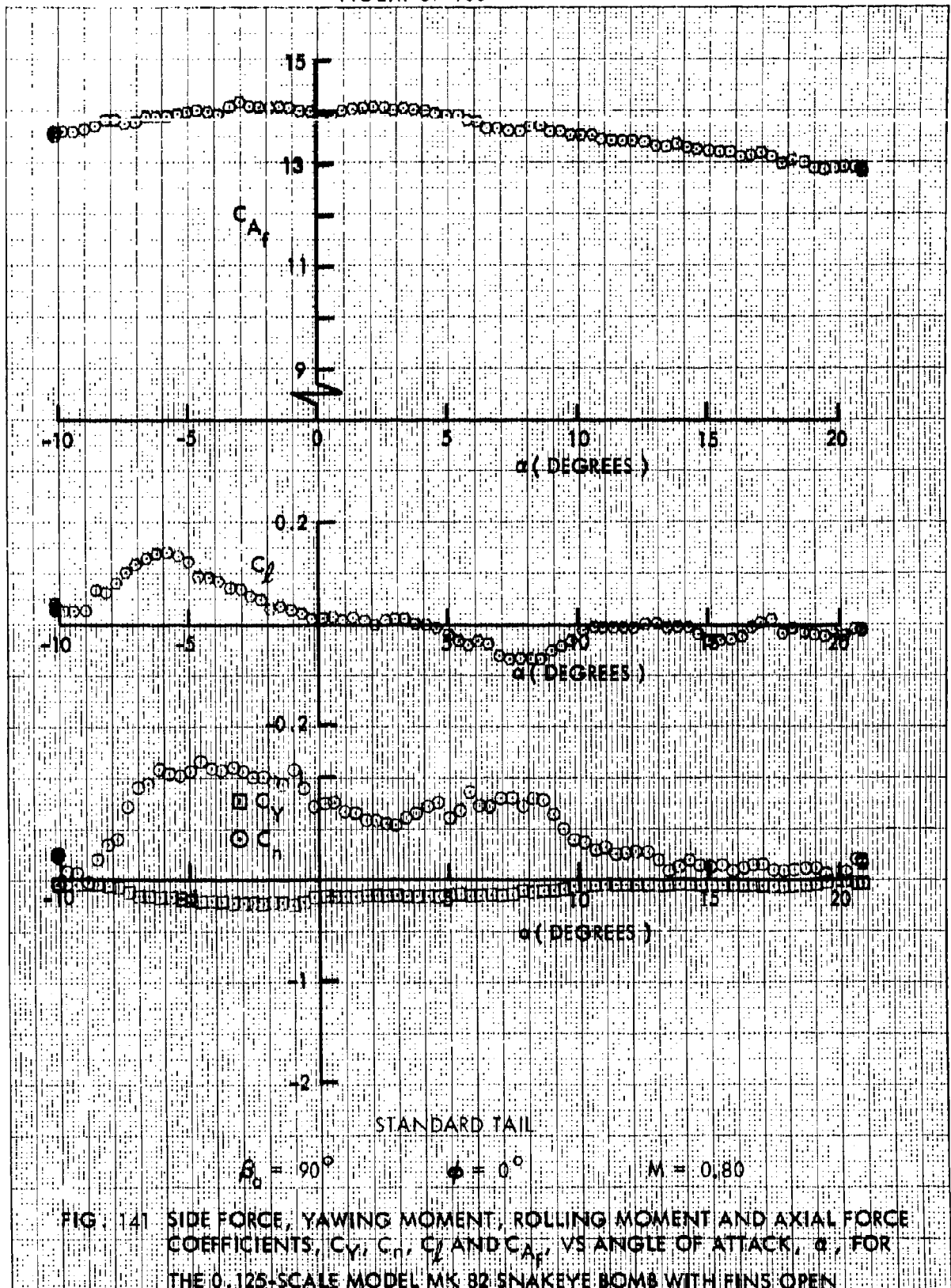
FIG. 136 SIDE FORCE, YAWING MOMENT, ROLLING MOMENT AND AXIAL FORCE COEFFICIENTS,  $C_Y$ ,  $C_N$ ,  $C_l$  AND  $C_A$ , VS ANGLE OF ATTACK,  $\alpha$ , FOR THE 0.125-SCALE MODEL MK 82 SNAKEYE BOMB WITH FINS OPEN



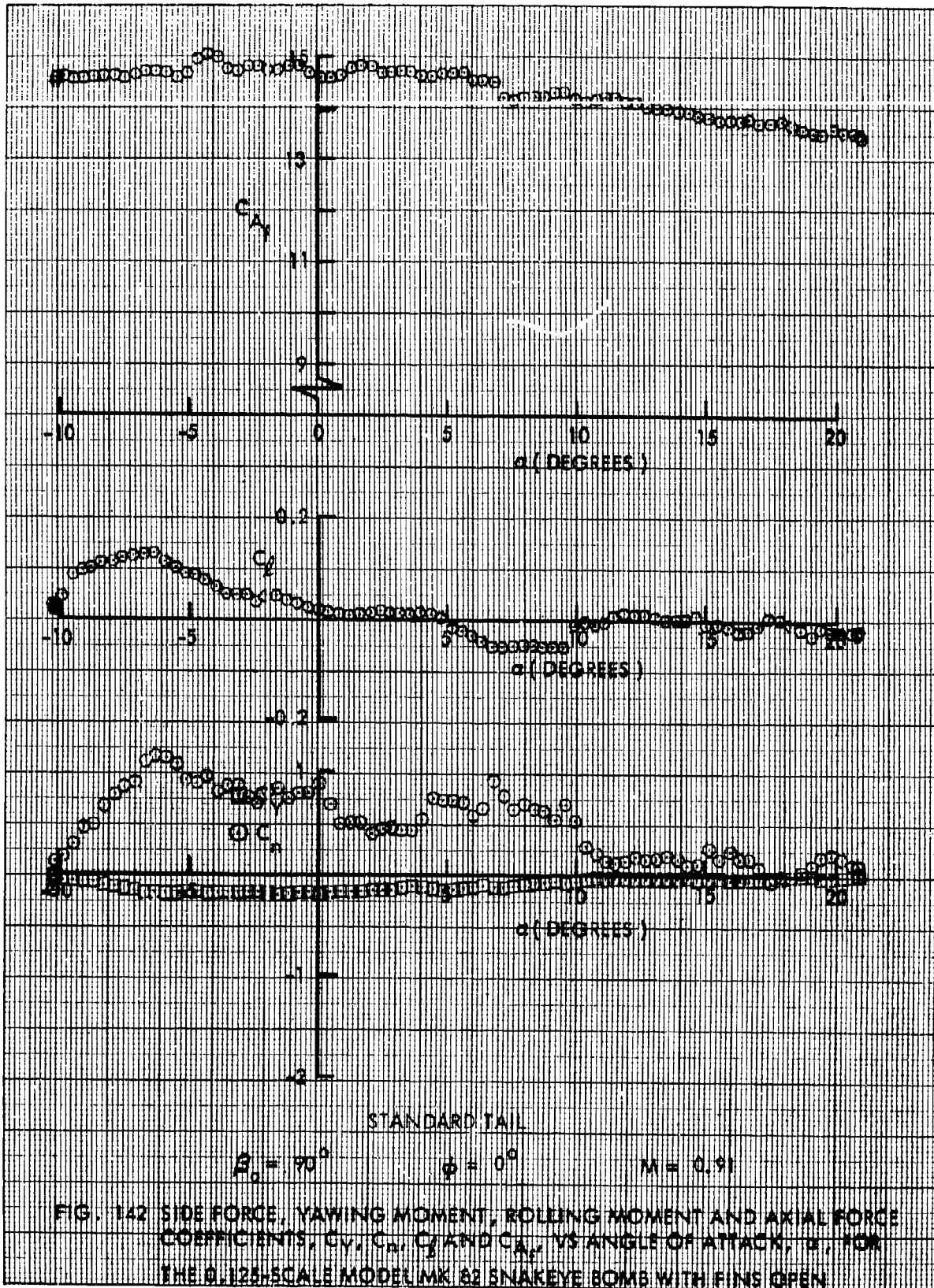


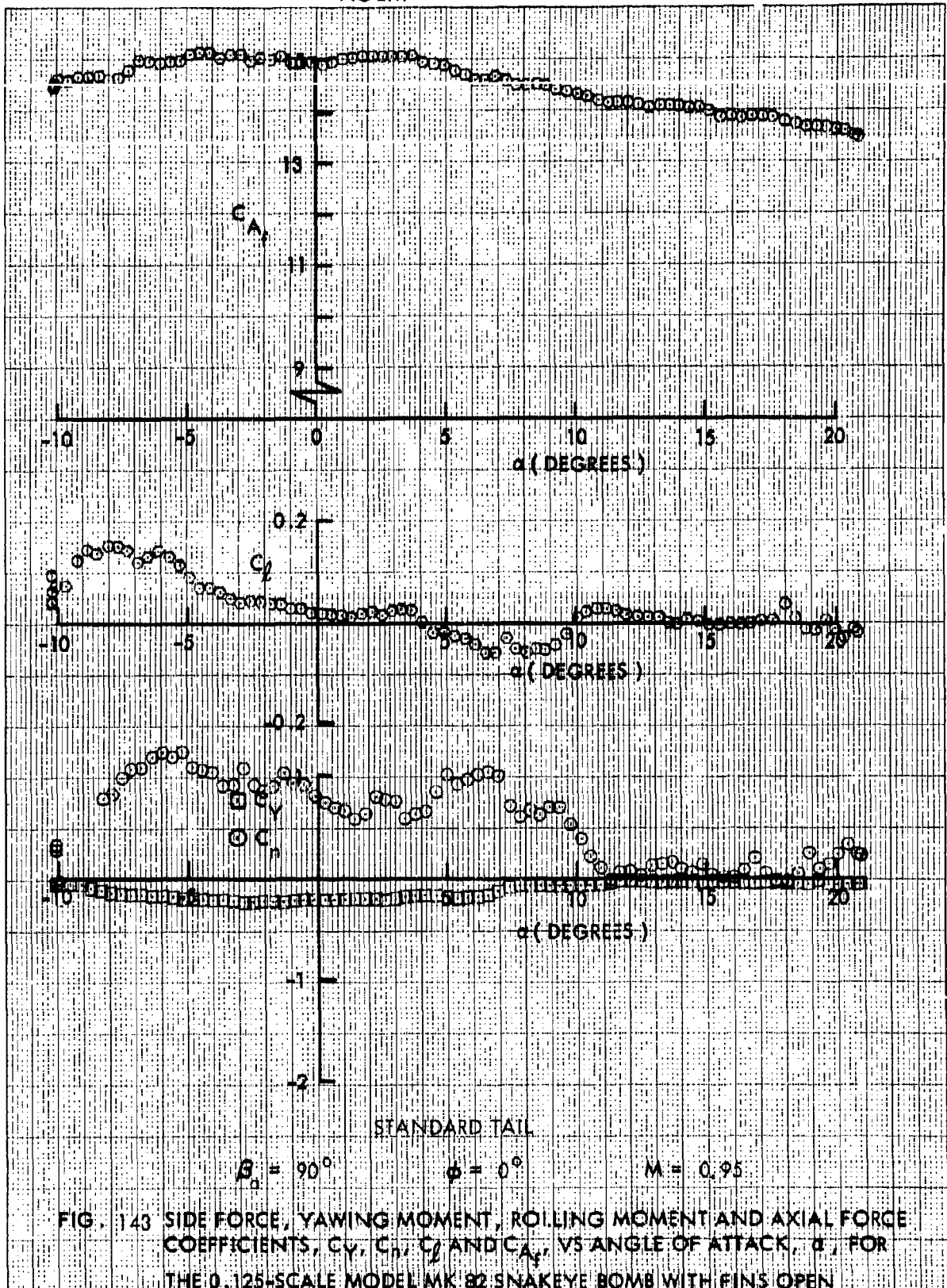


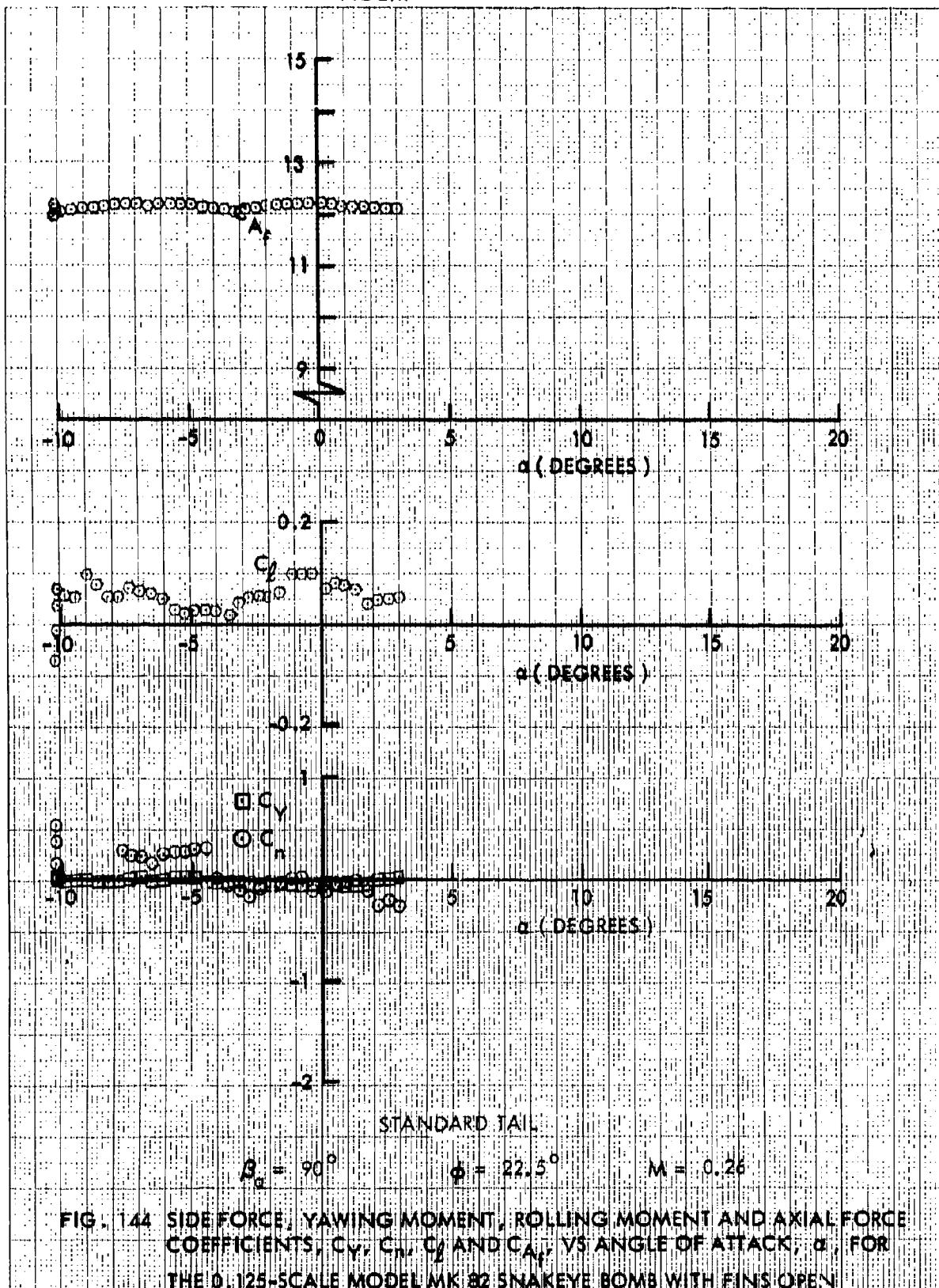


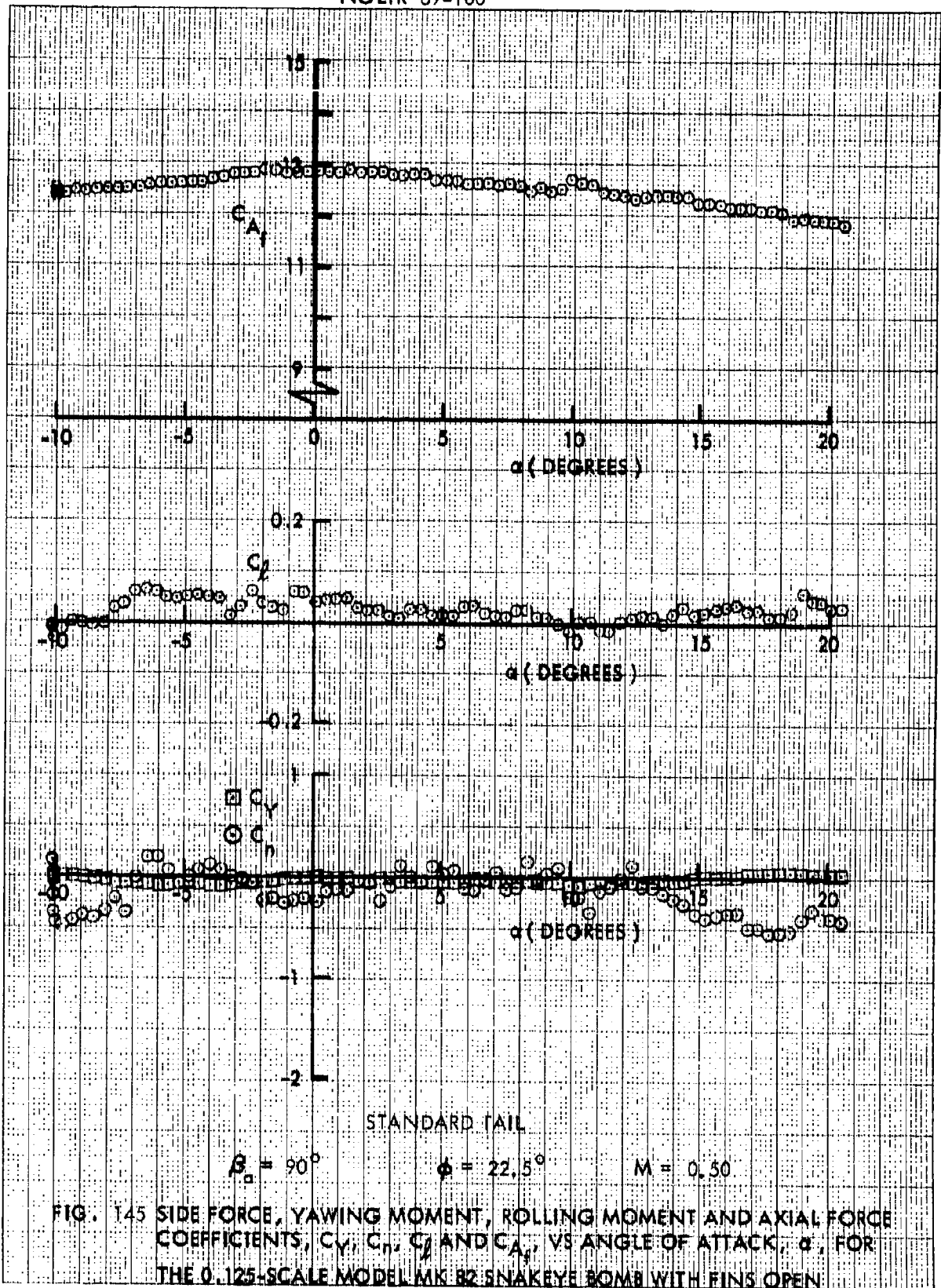


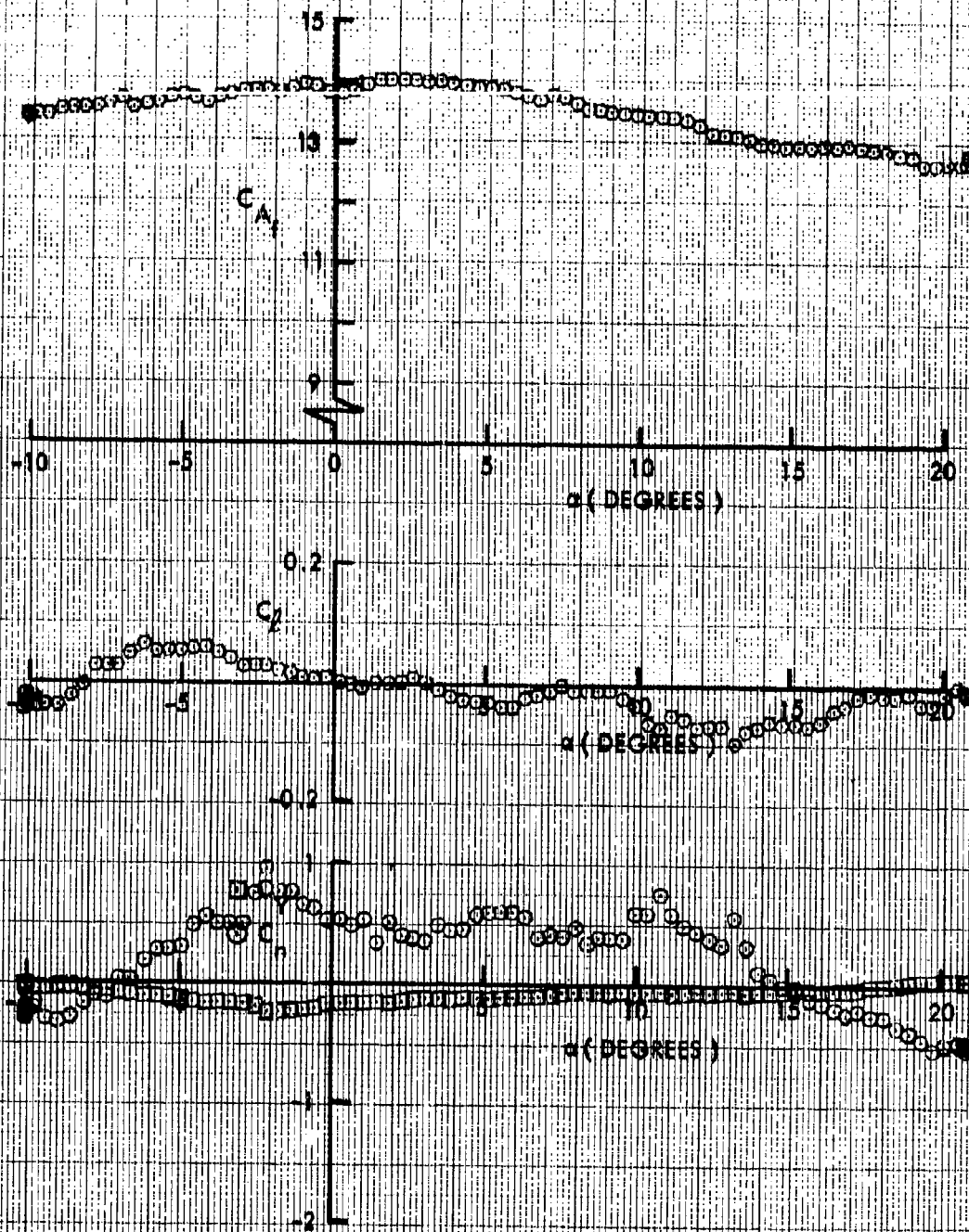












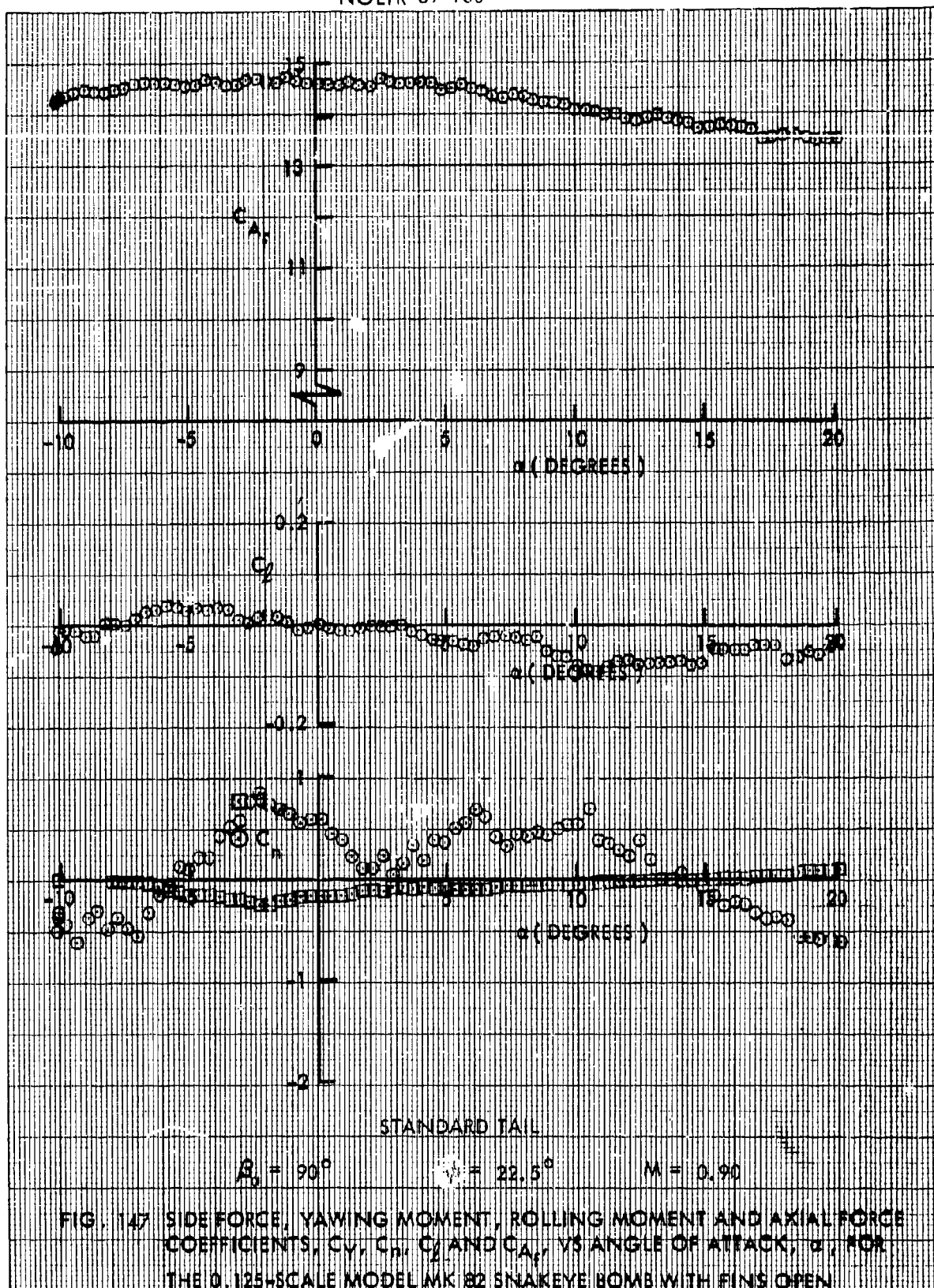
STANDARD TAIL

$$\beta_0 = 90^\circ$$

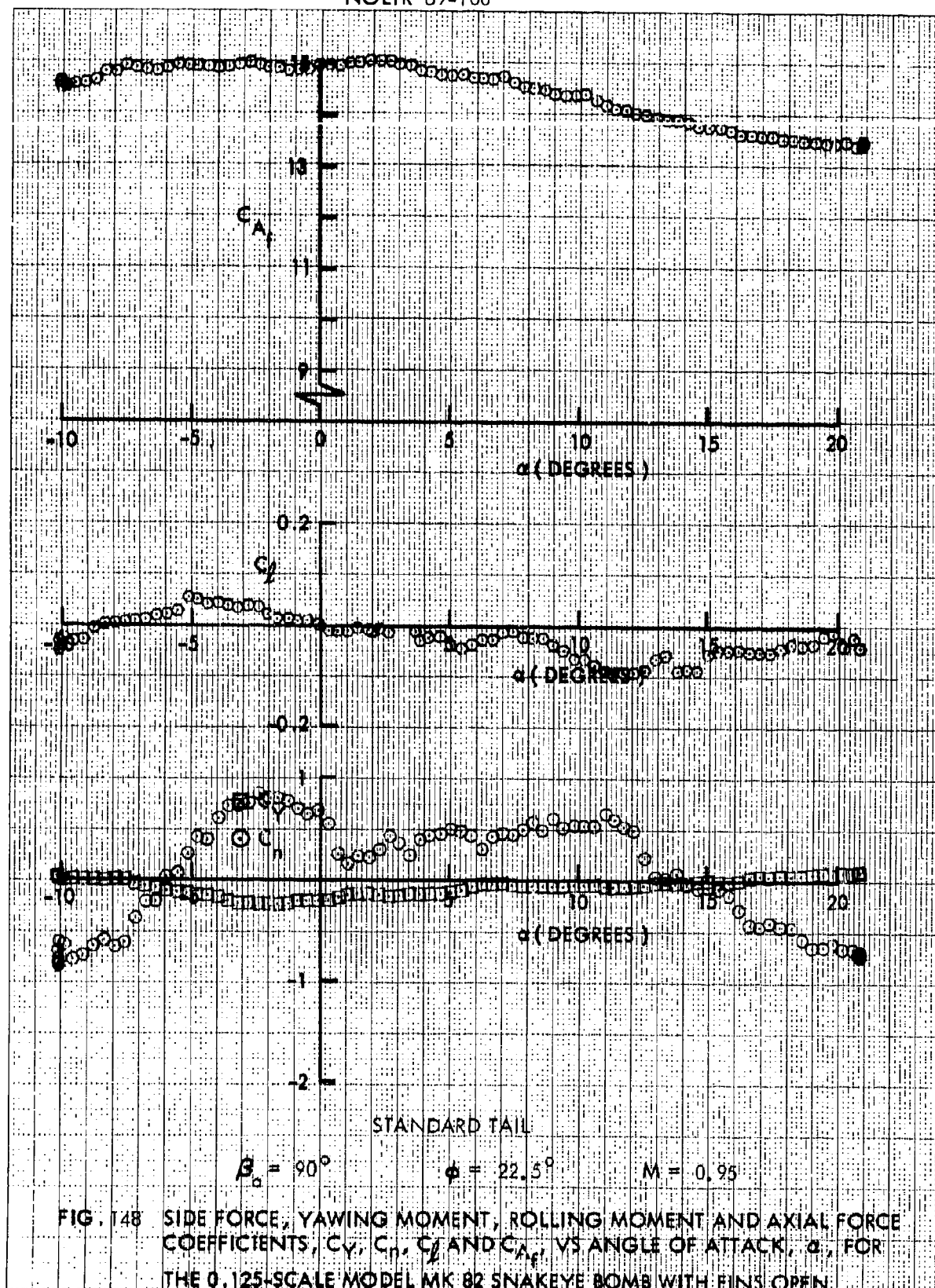
$$\phi = 22.5^\circ$$

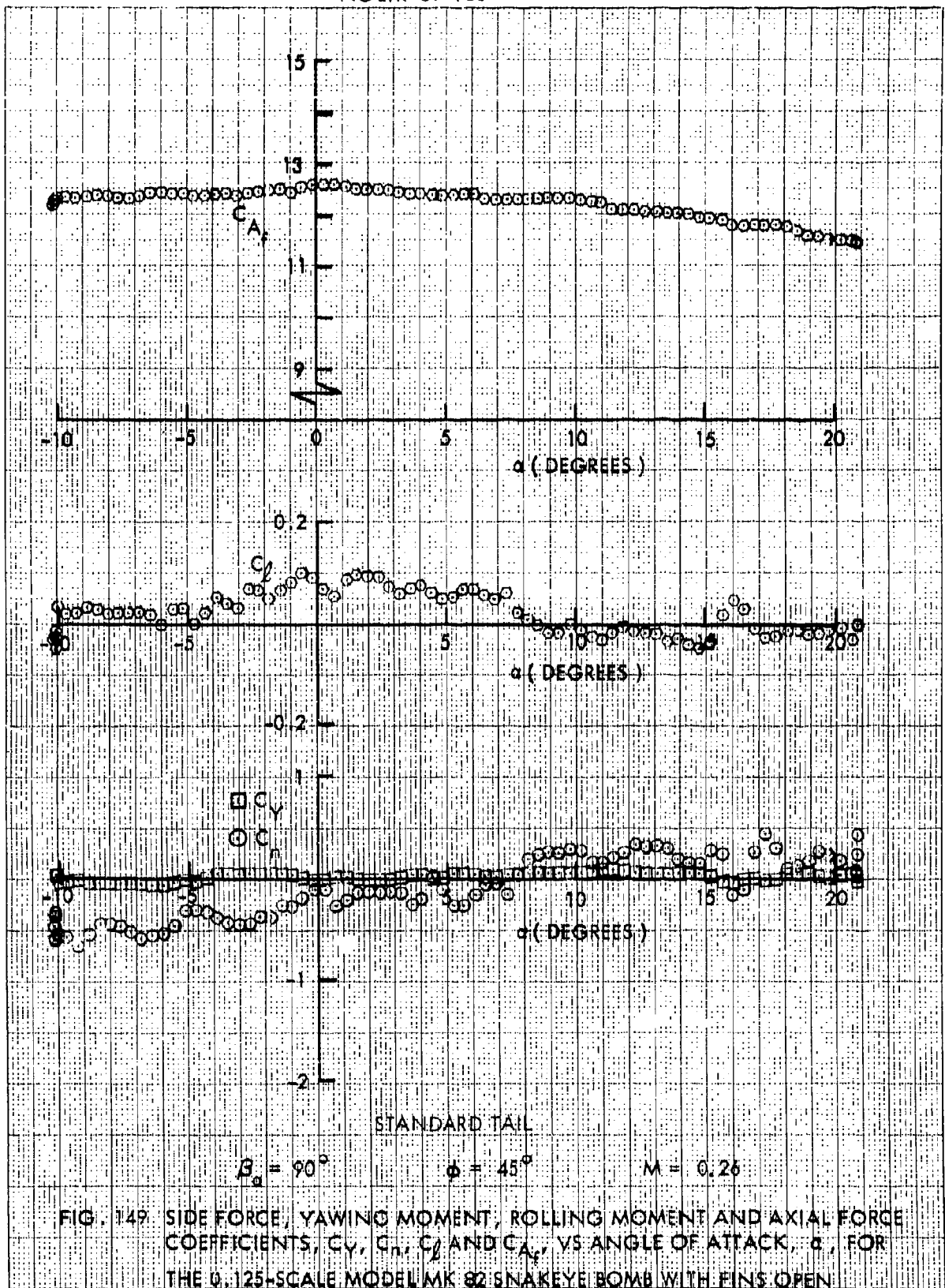
$$M = 0.80$$

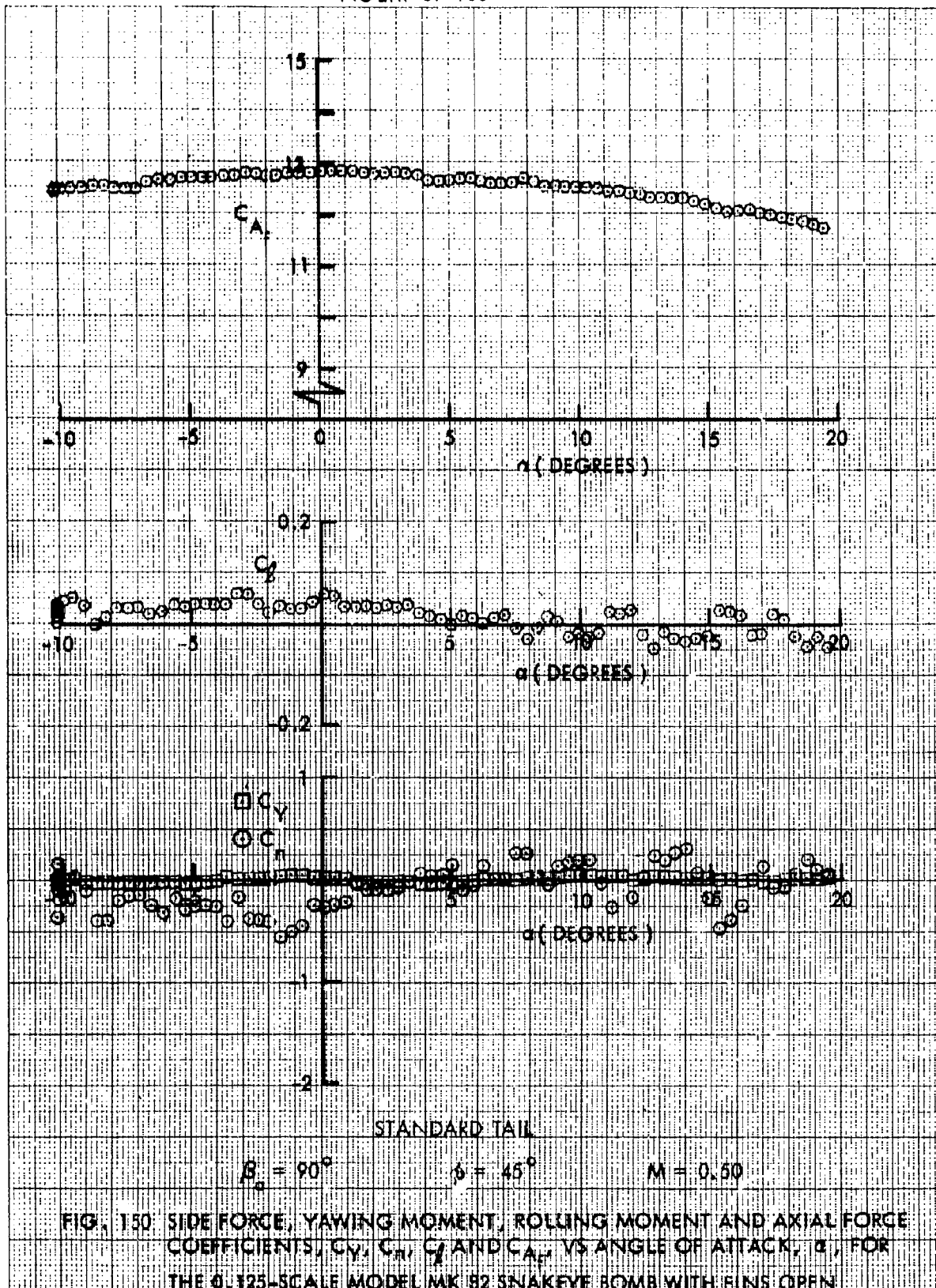
FIG. 146 SIDE FORCE, YAWING MOMENT, ROLLING MOMENT AND AXIAL FORCE COEFFICIENTS,  $C_Y$ ,  $C_r$ ,  $C_l$  AND  $C_{A_f}$ , VS ANGLE OF ATTACK,  $\alpha$ , FOR THE 0.125-SCALE MODEL MK 82 SNAKEYE BOMB WITH FINS OPEN.

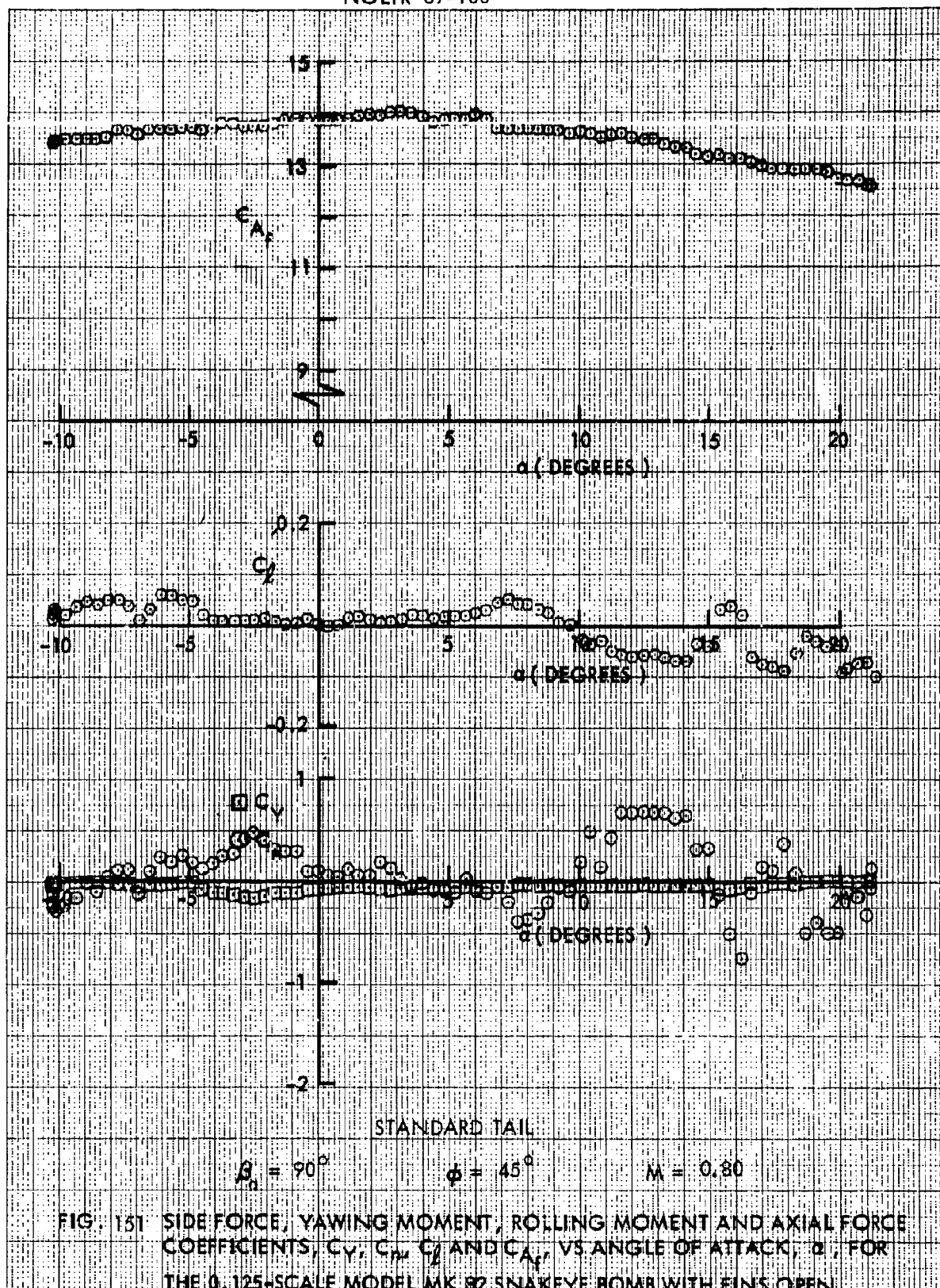


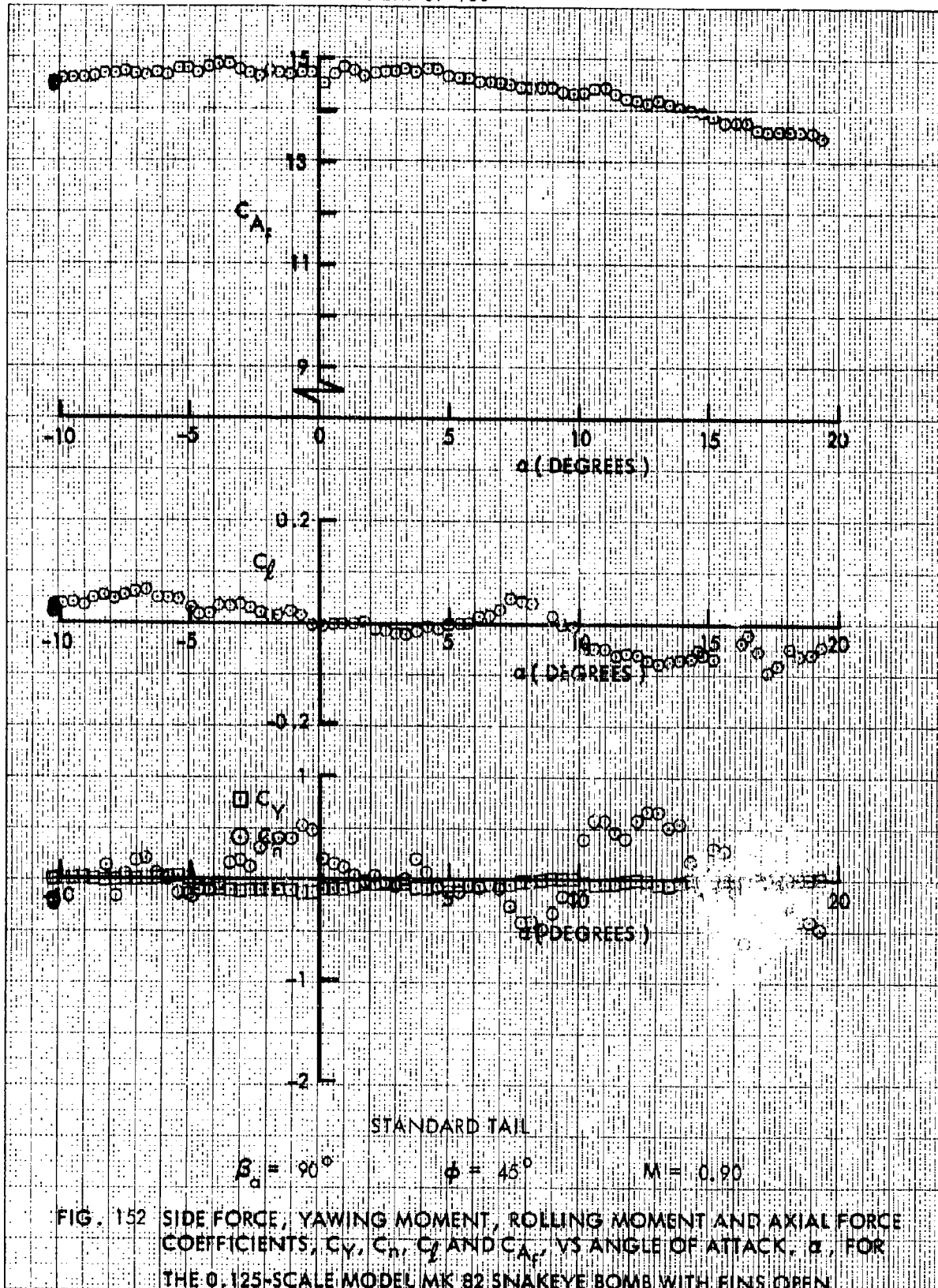


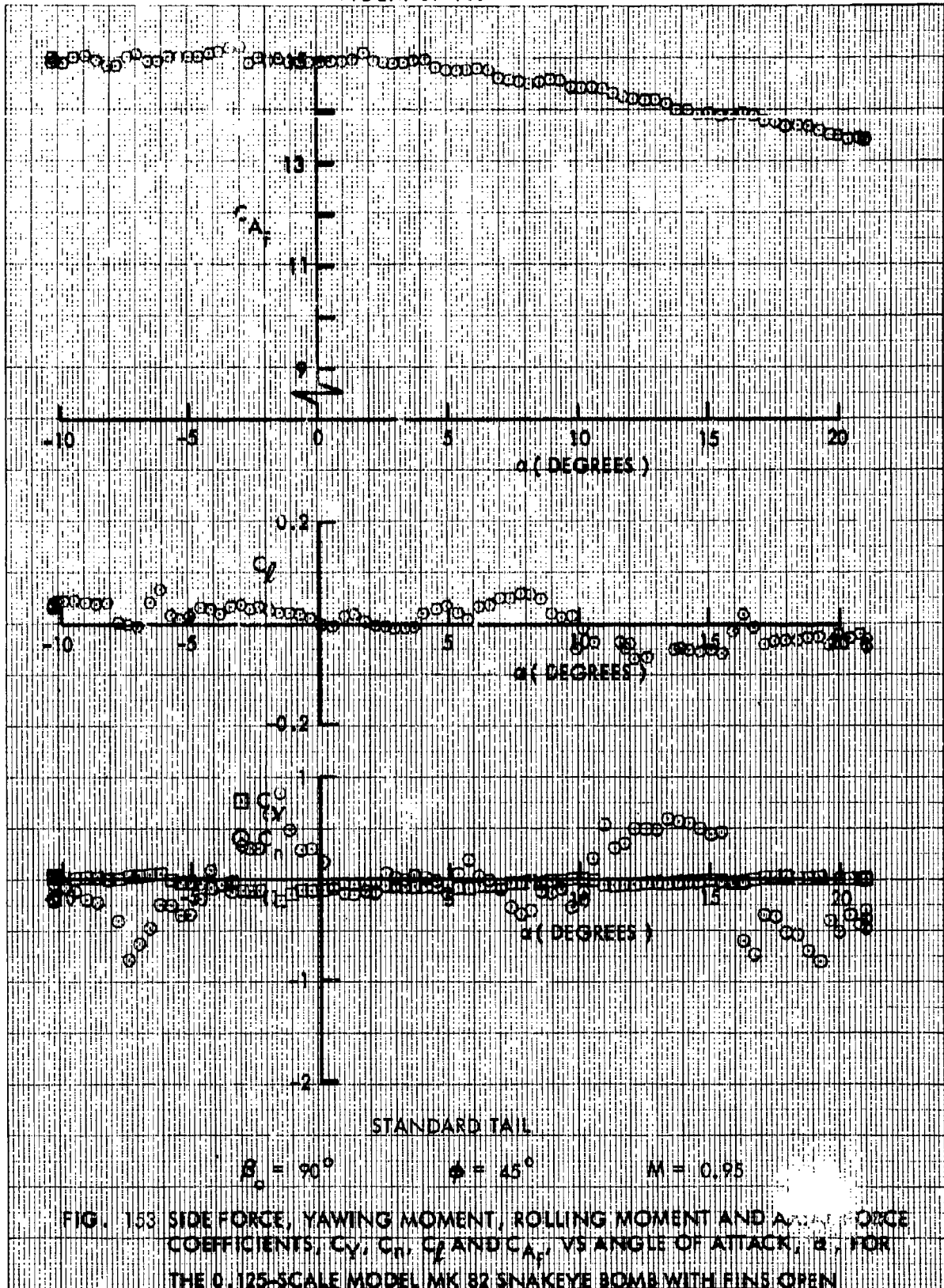




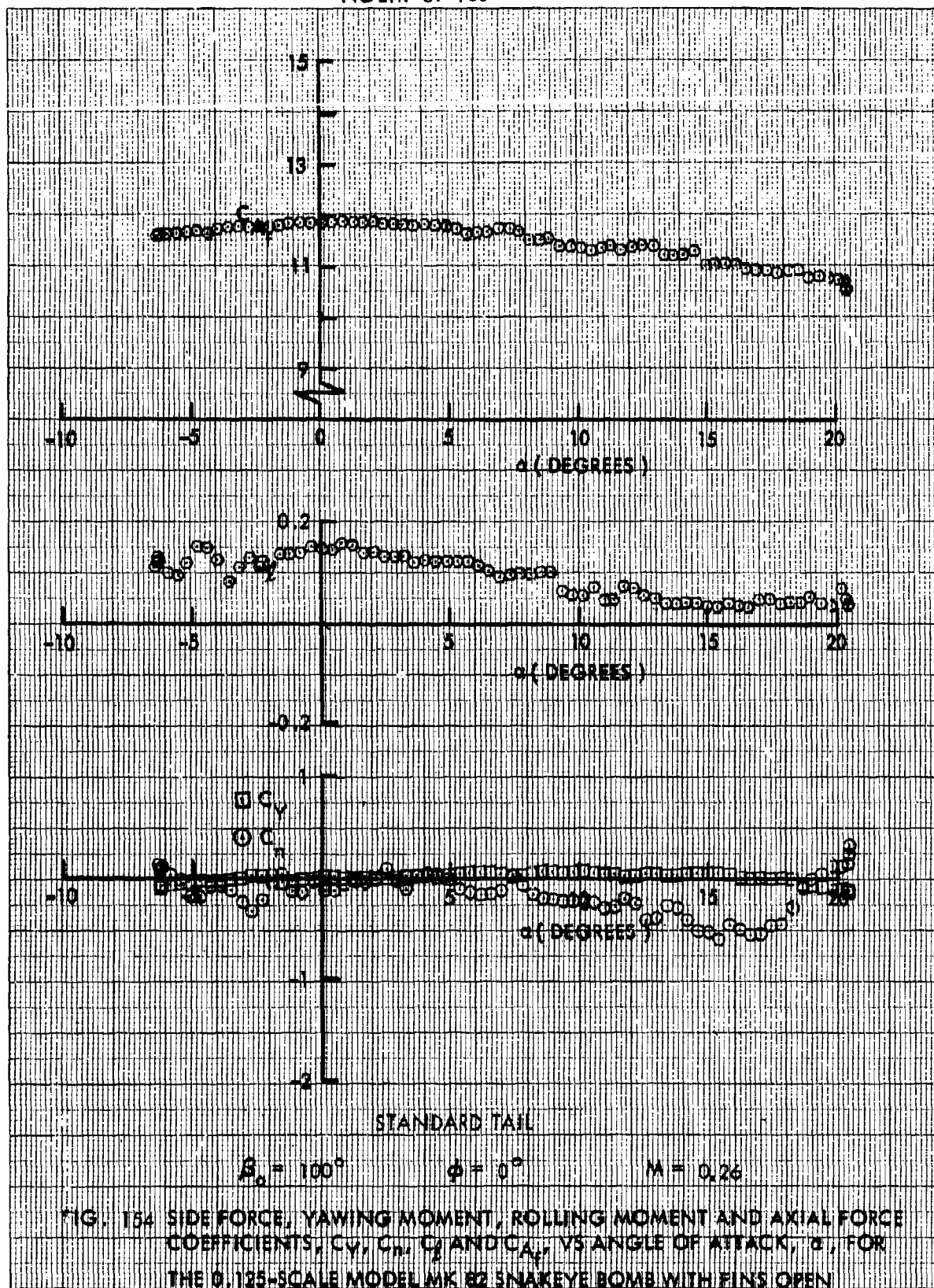


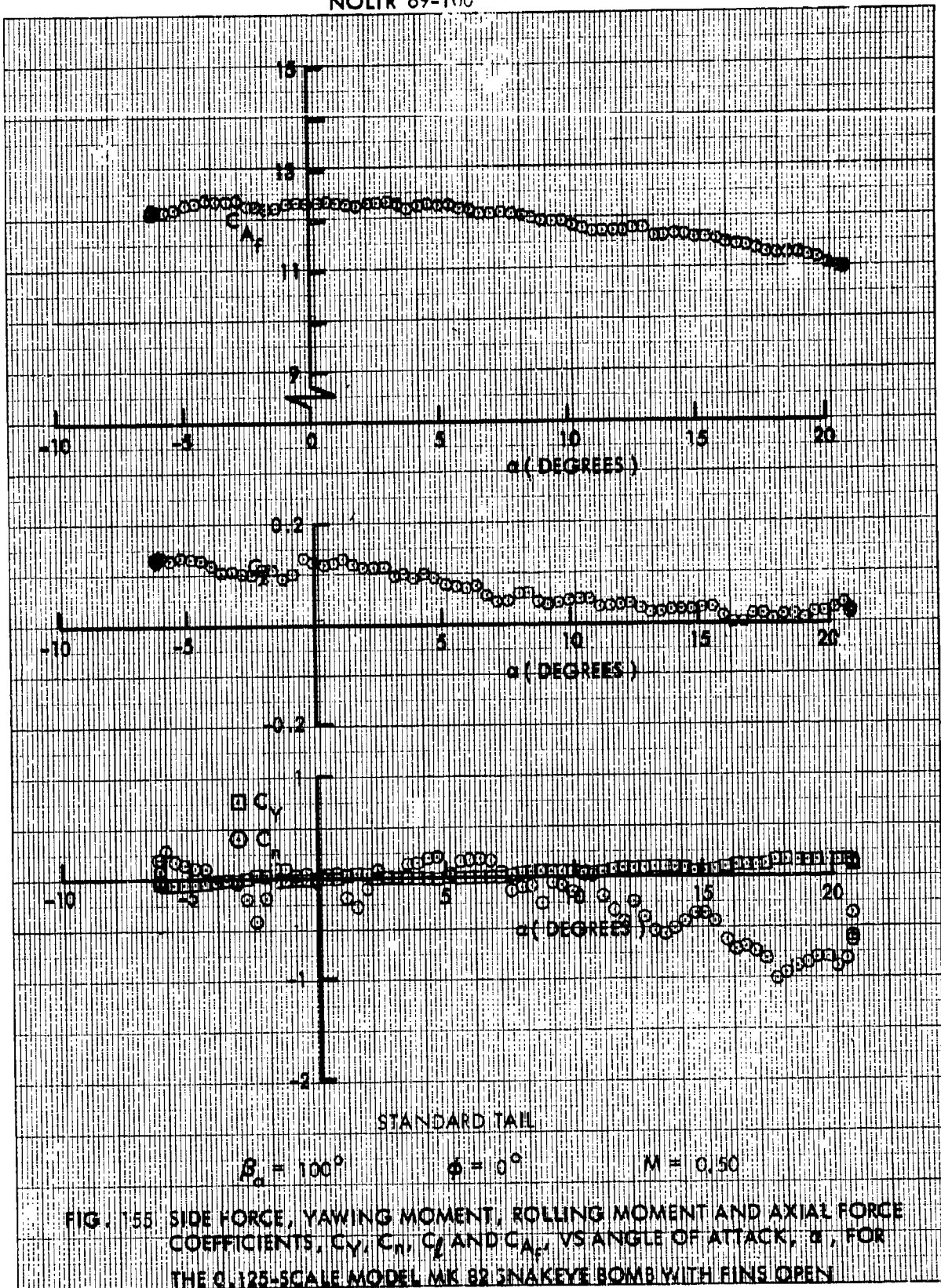


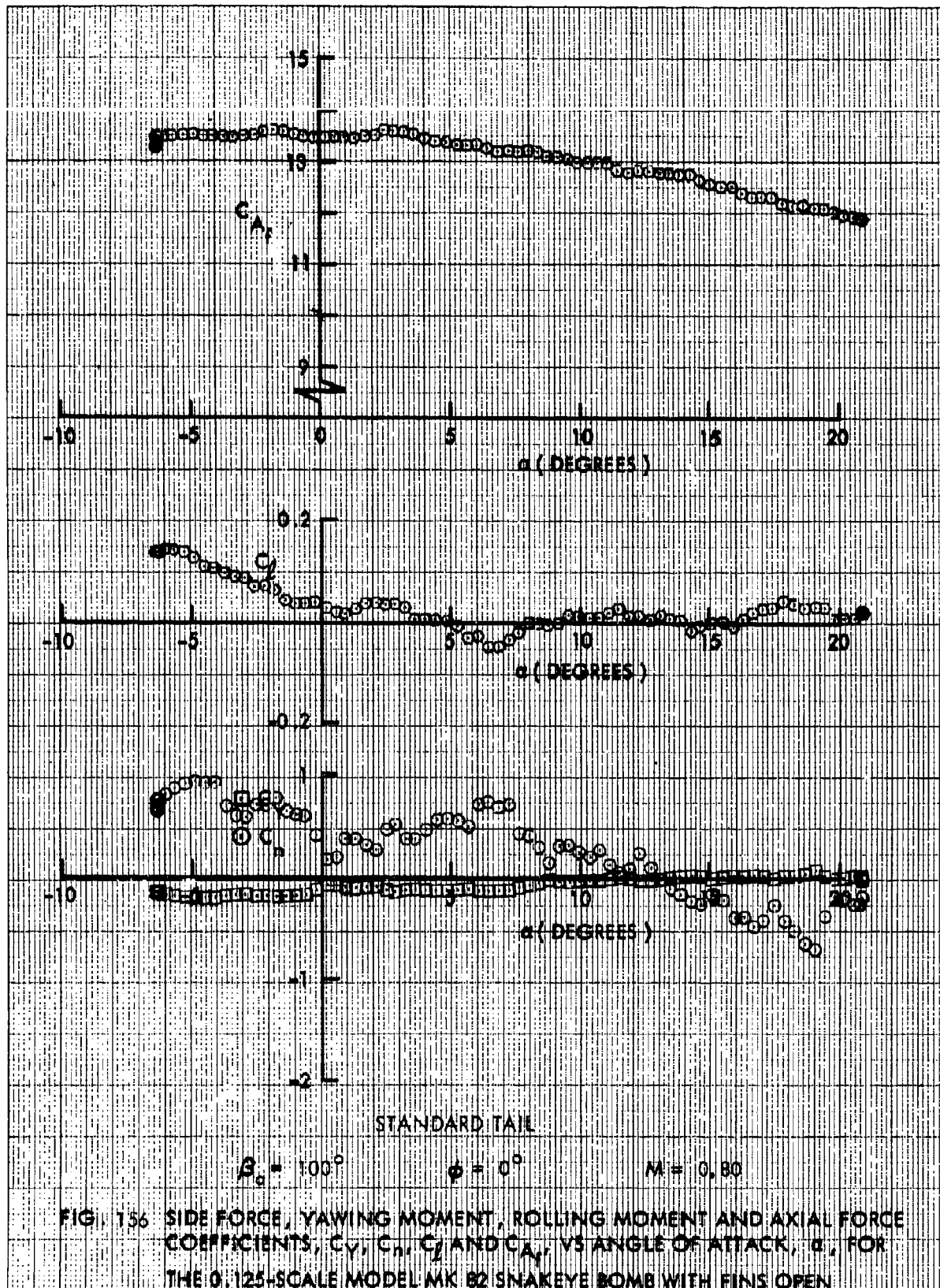


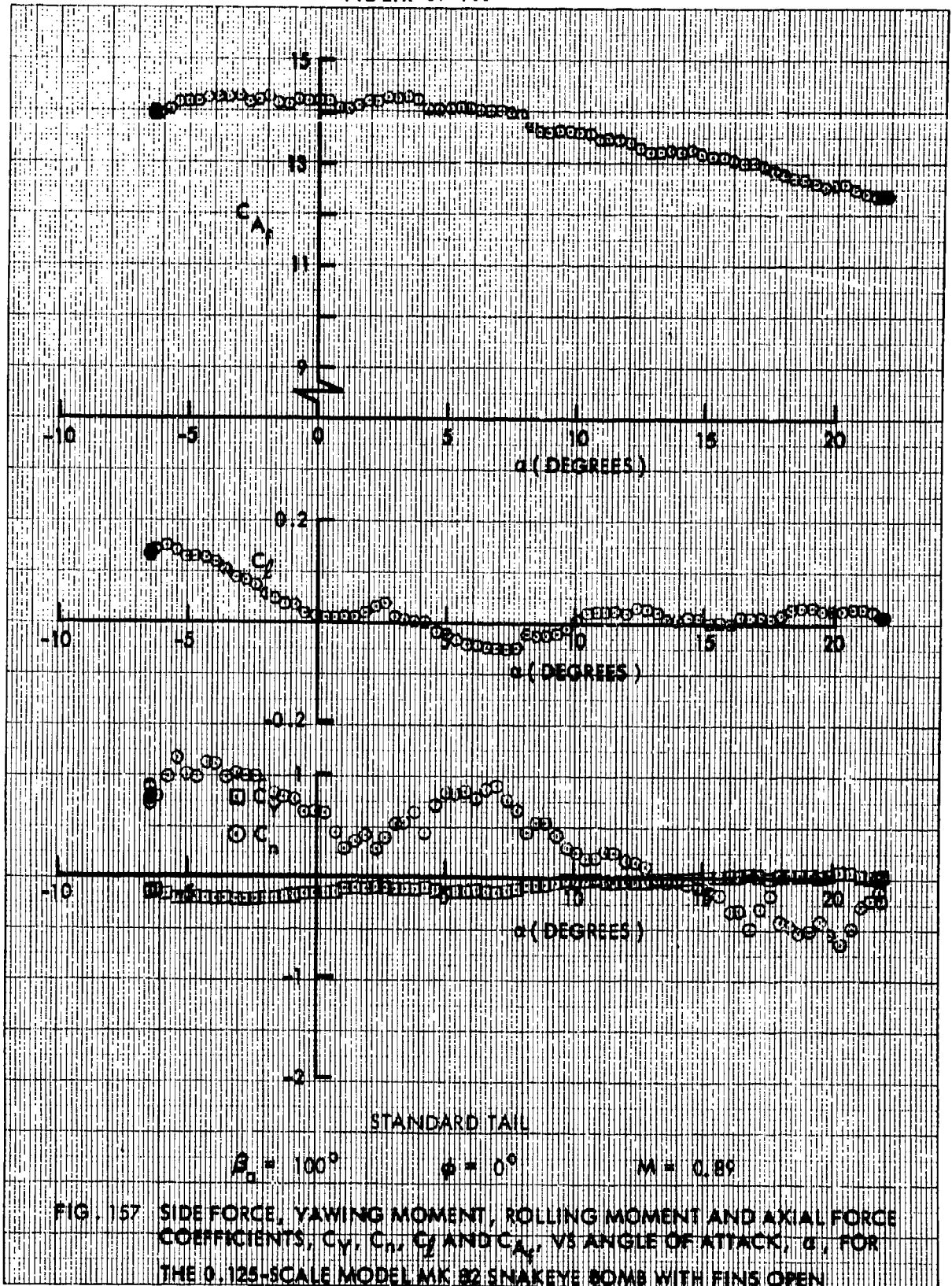


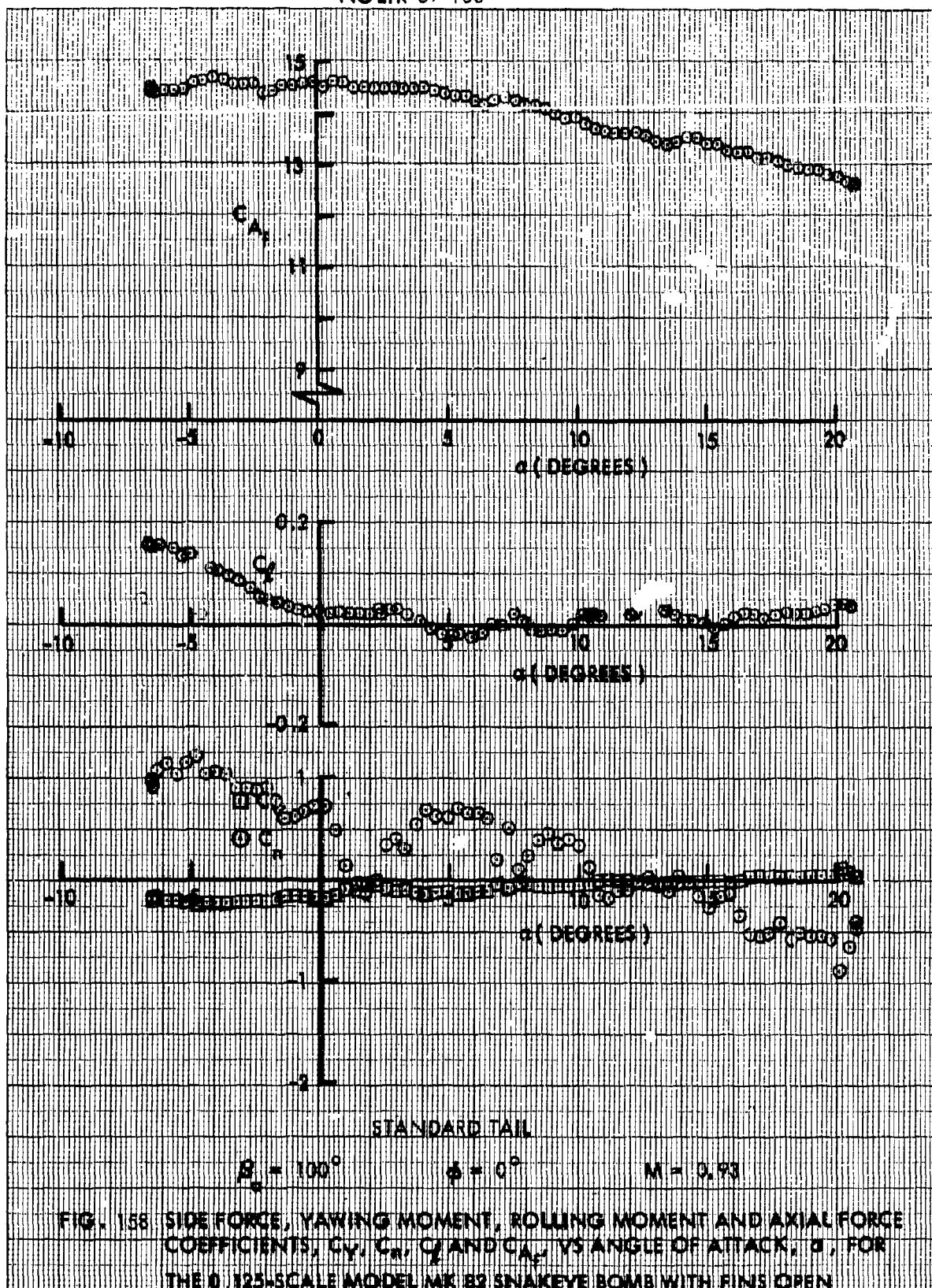




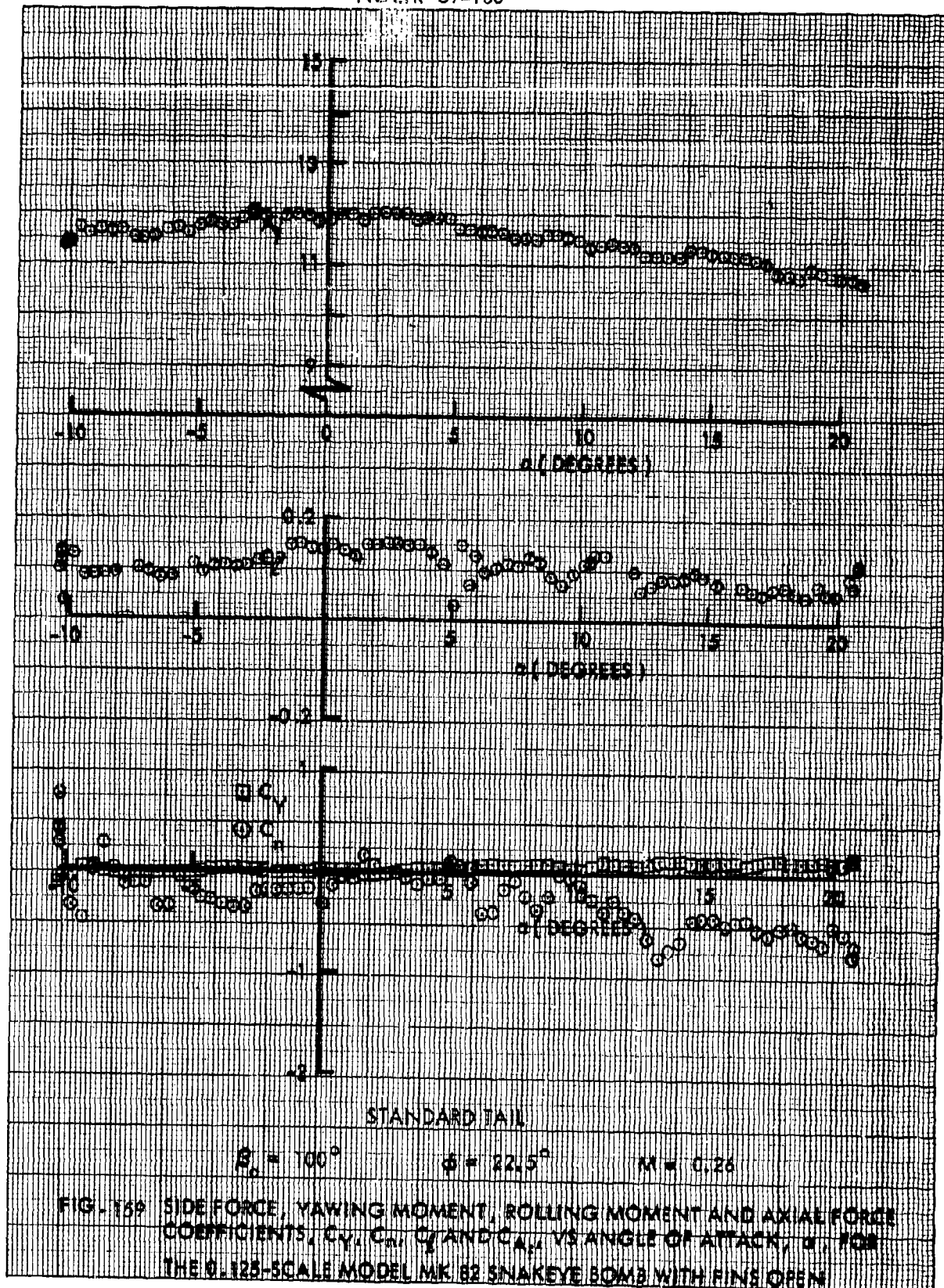














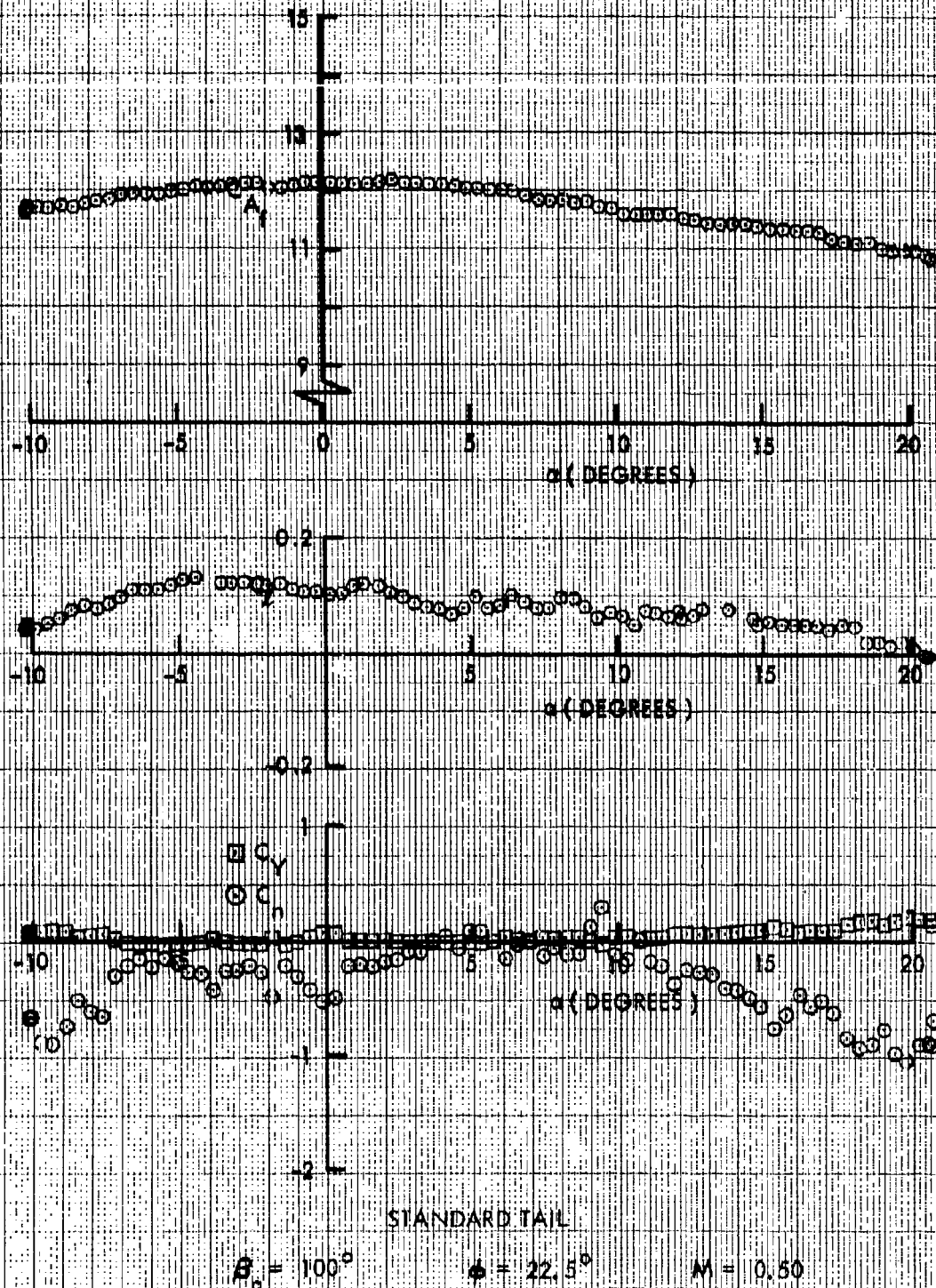
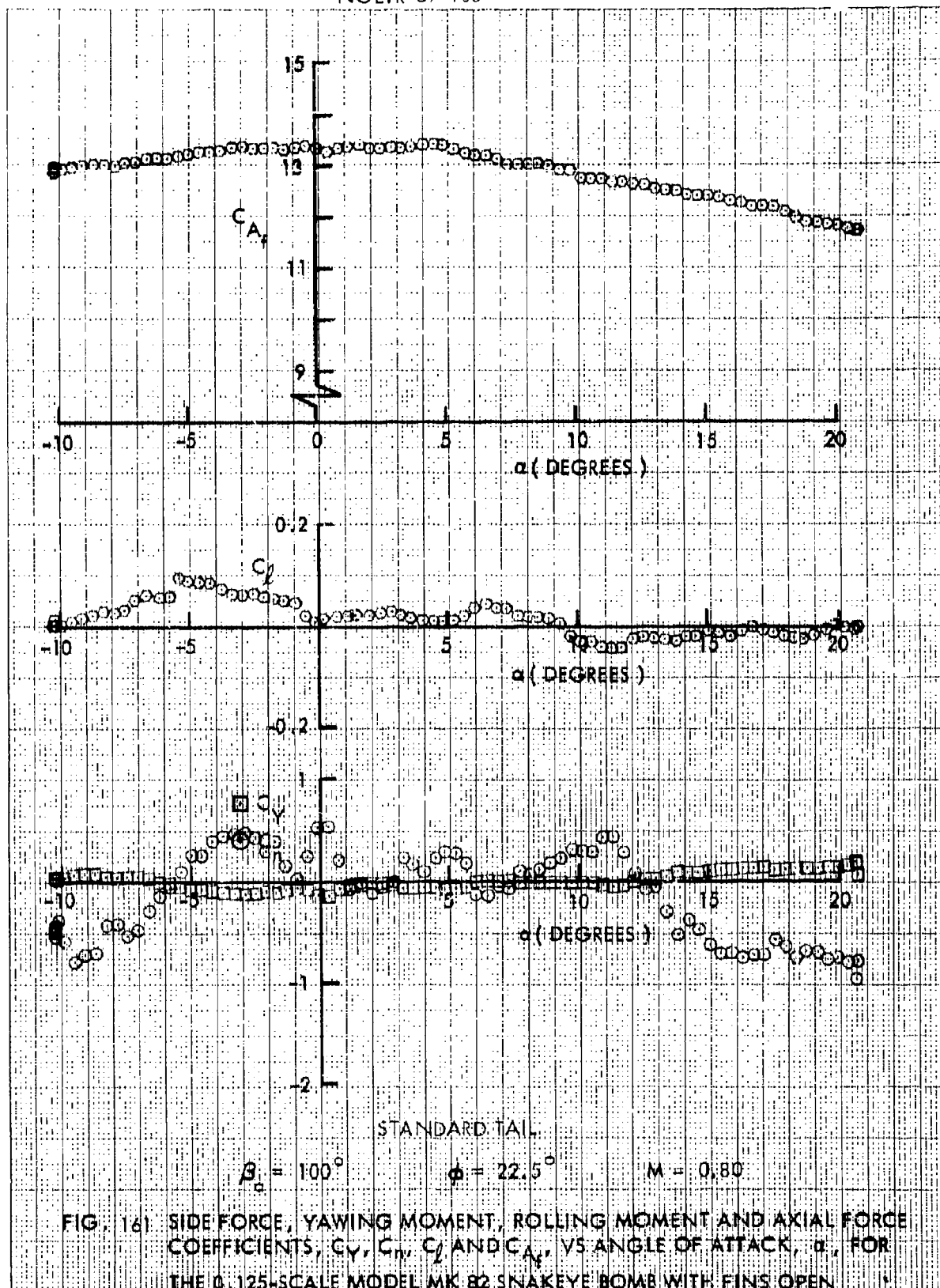


FIG. 160 SIDE FORCE, YAWING MOMENT, ROLLING MOMENT AND AXIAL FORCE COEFFICIENTS,  $C_Y$ ,  $C_n$ ,  $C_L$  AND  $C_A$ , VS ANGLE OF ATTACK,  $\alpha$ , FOR THE 0.125-SCALE MODEL MK BR SNAKEYE BOMB WITH FINS OPEN



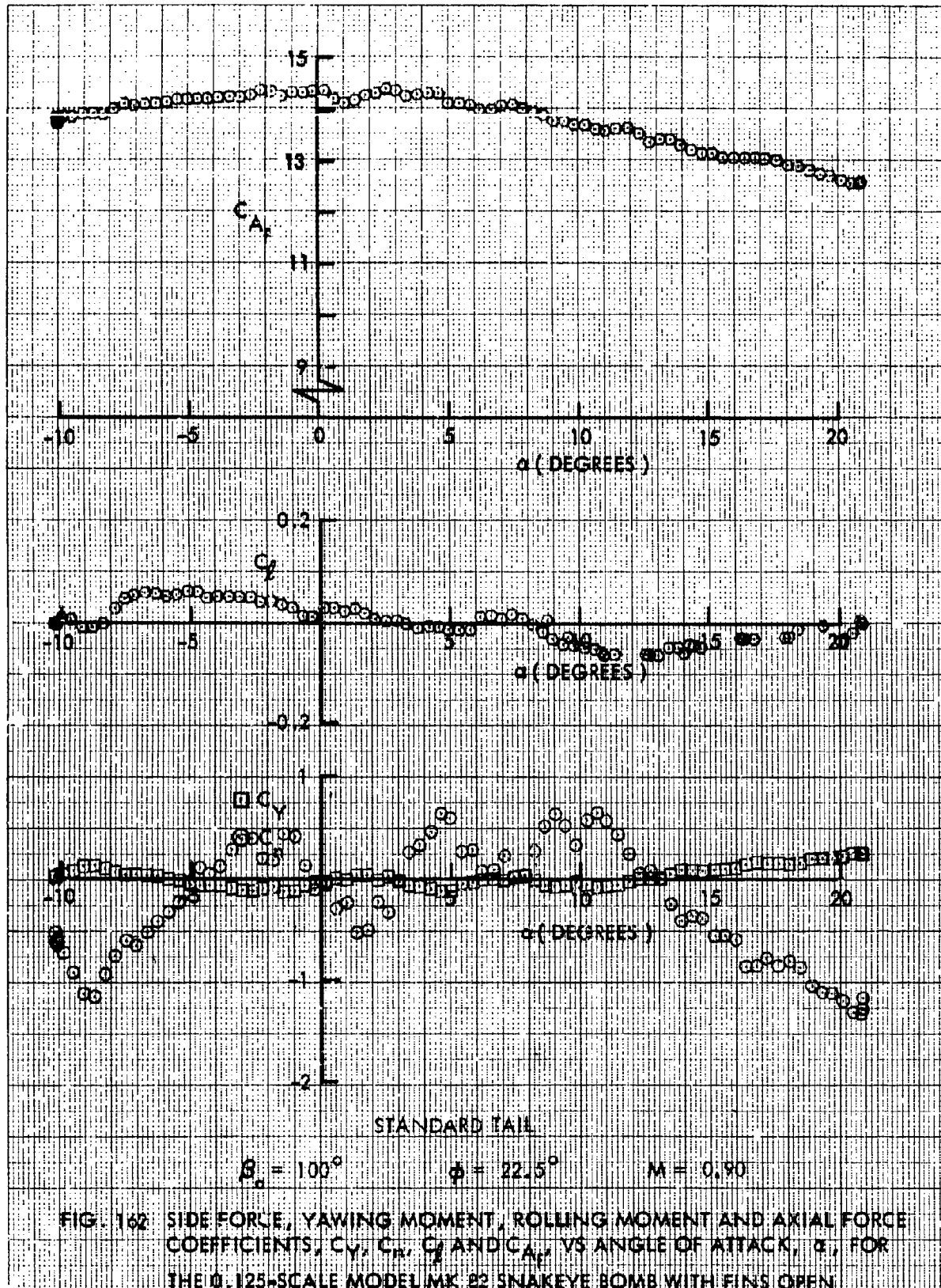
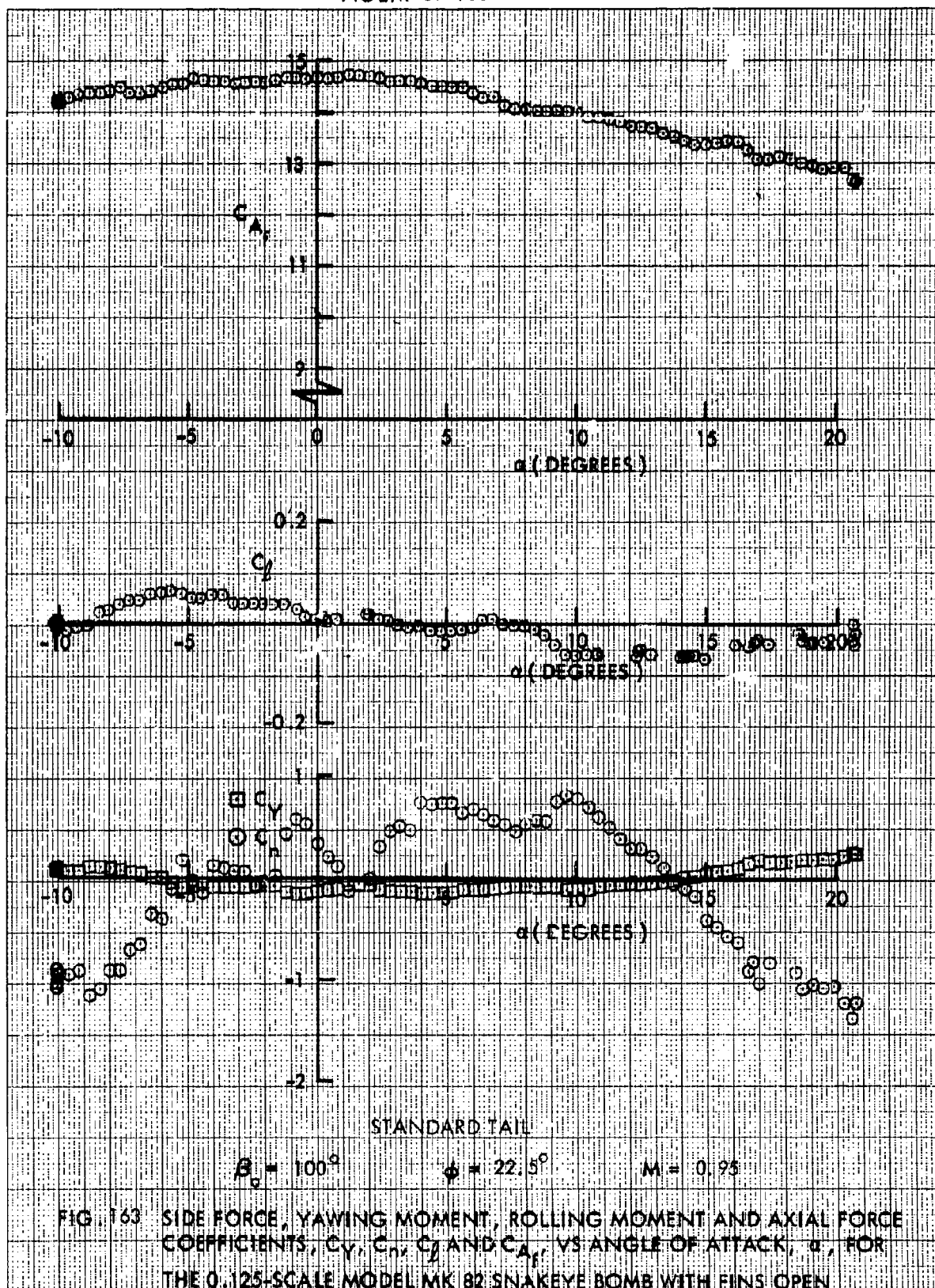
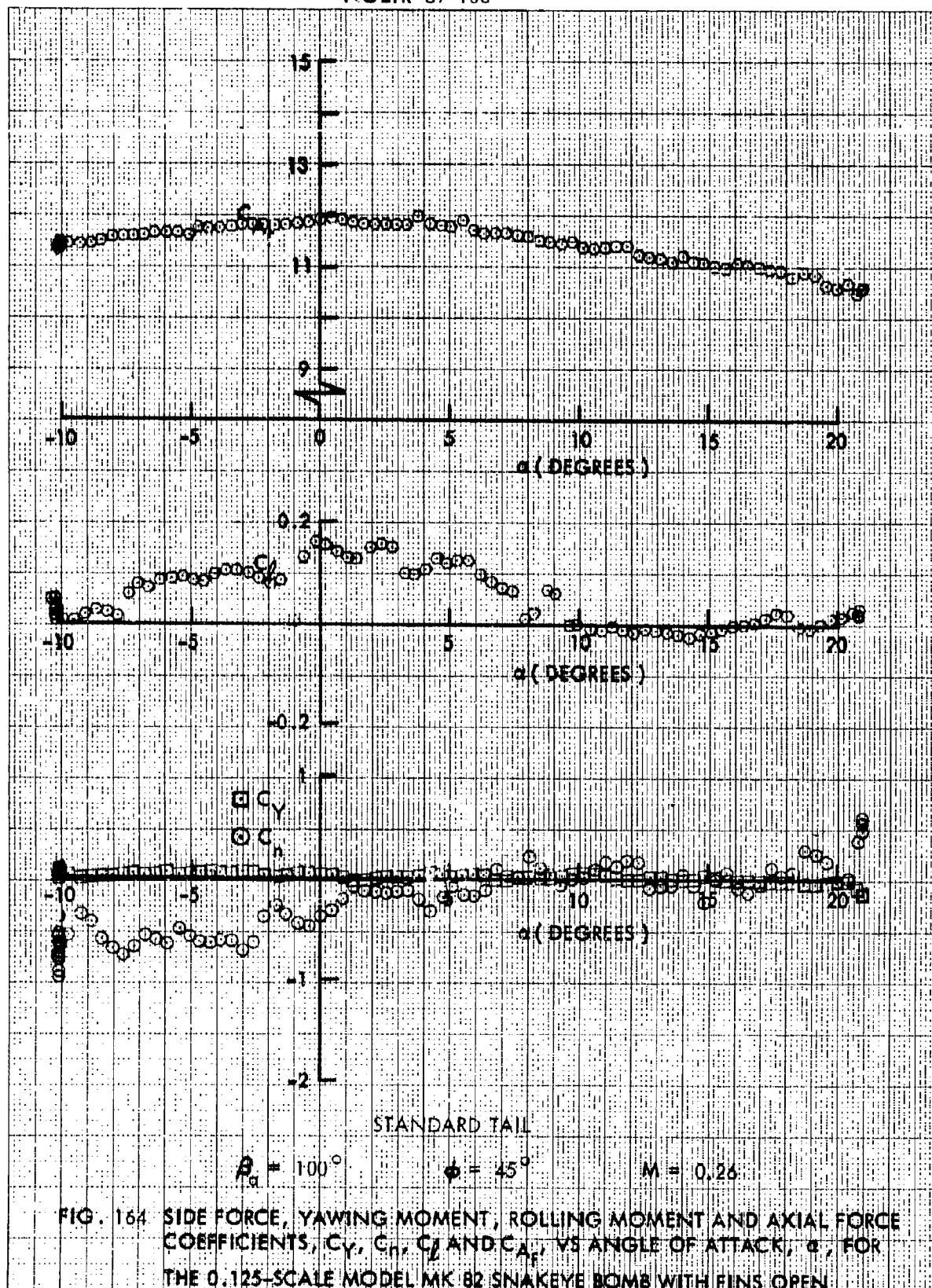
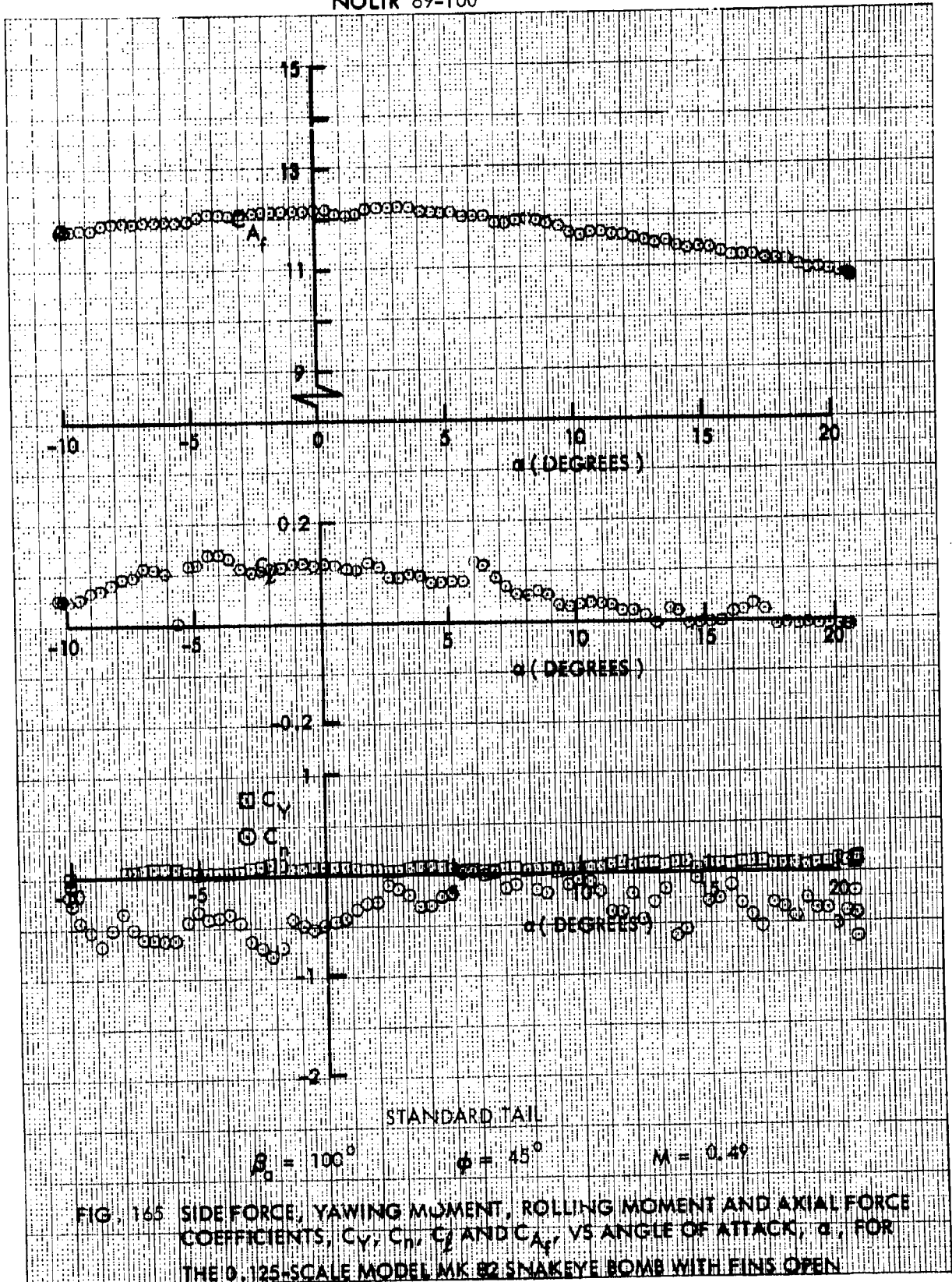


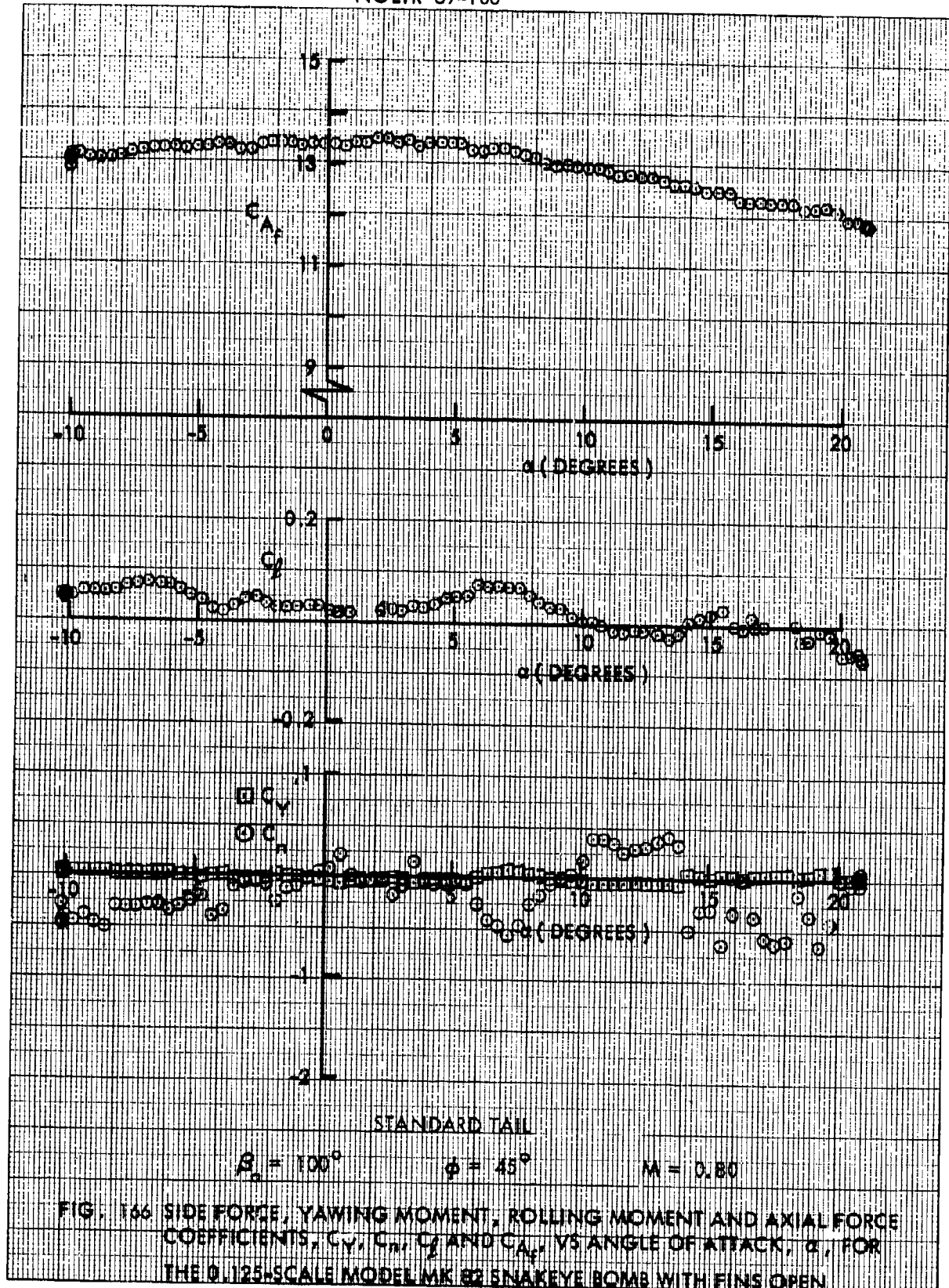
FIG. 162 SIDE FORCE, YAWING MOMENT, ROLLING MOMENT AND AXIAL FORCE COEFFICIENTS,  $C_Y$ ,  $C_N$ ,  $C_l$  AND  $C_A$ , VS ANGLE OF ATTACK,  $\alpha$ , FOR THE 0.125-SCALE MODEL MK 82 SNAKEYE BOMB WITH FINS OPEN

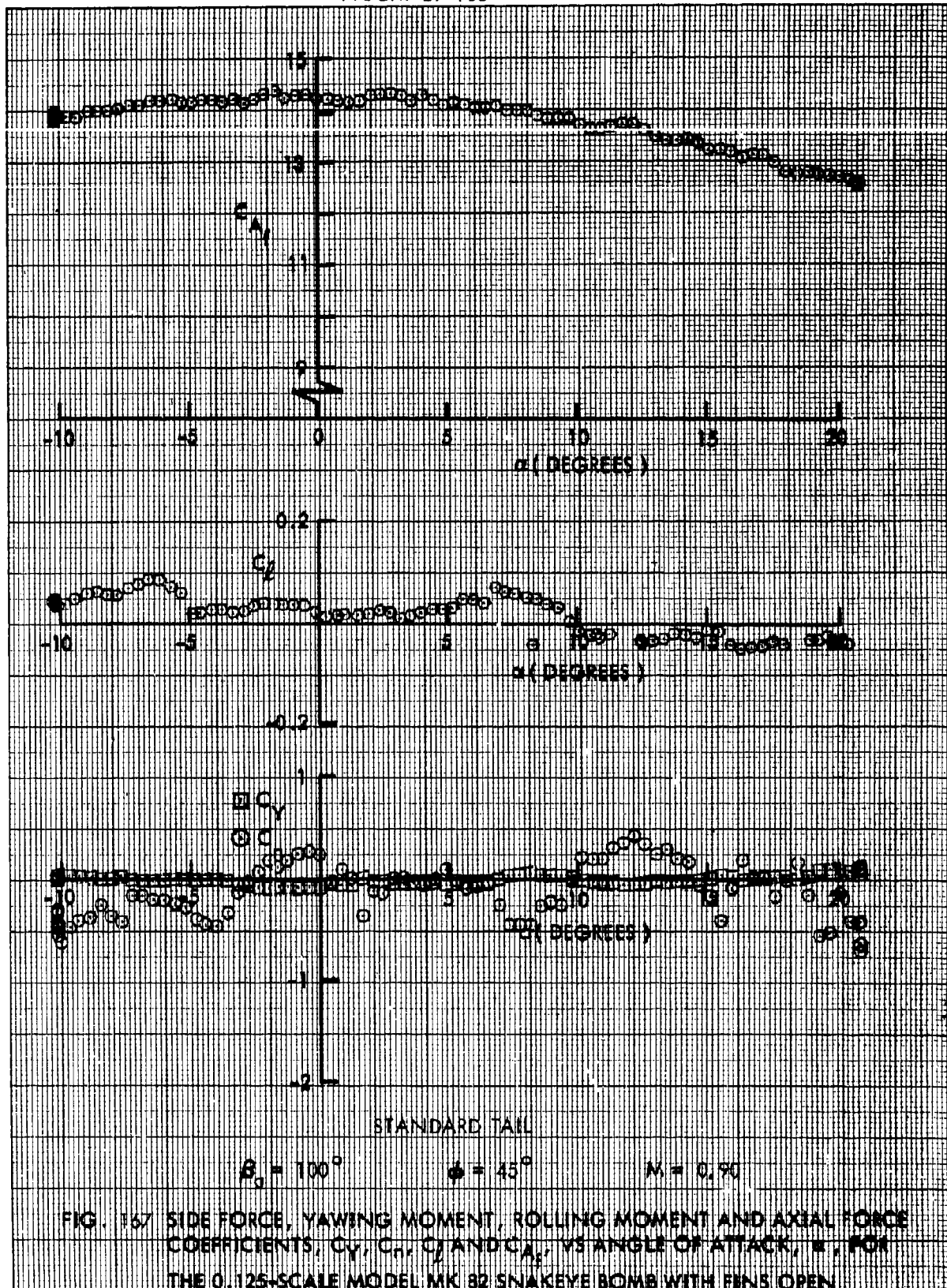


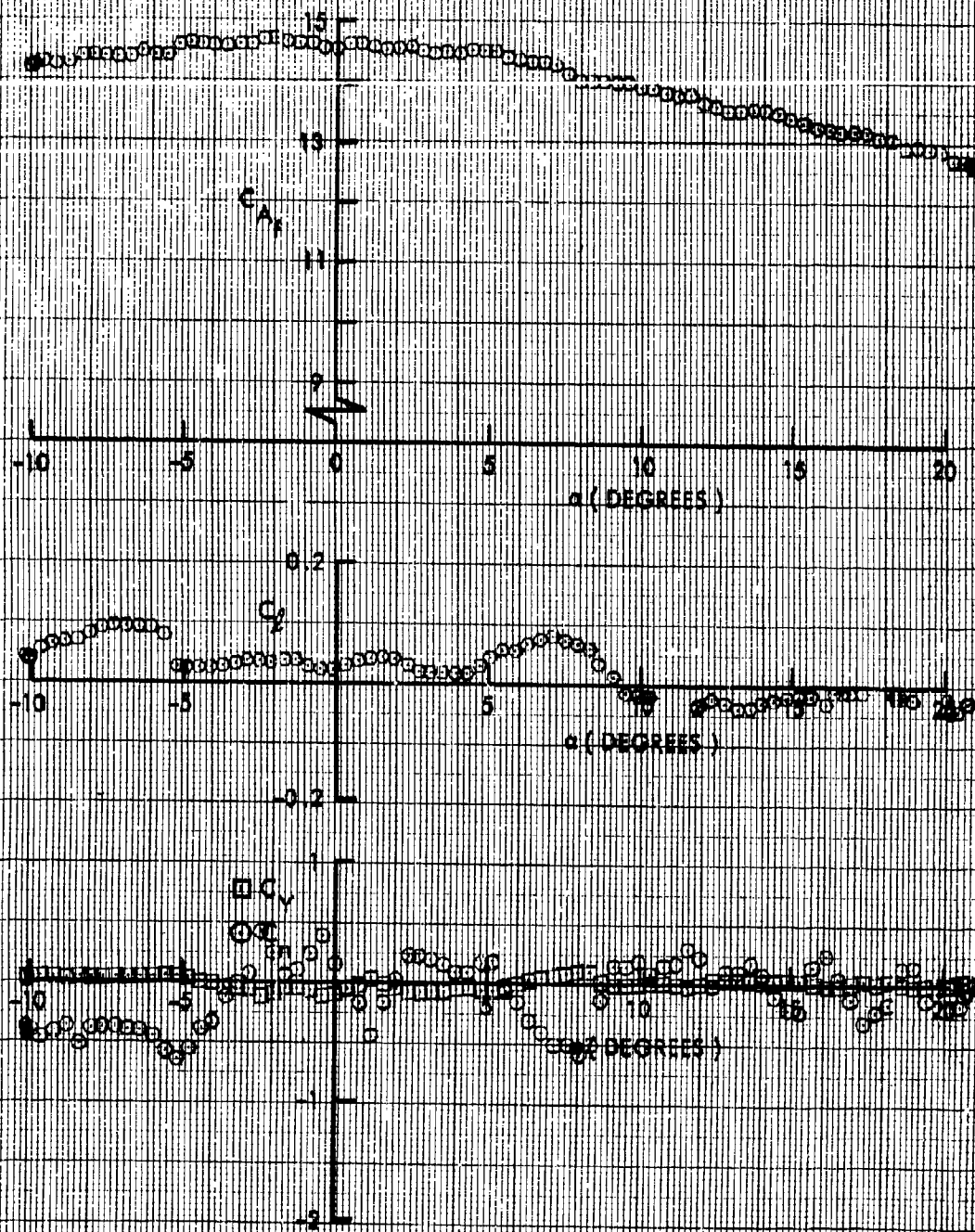












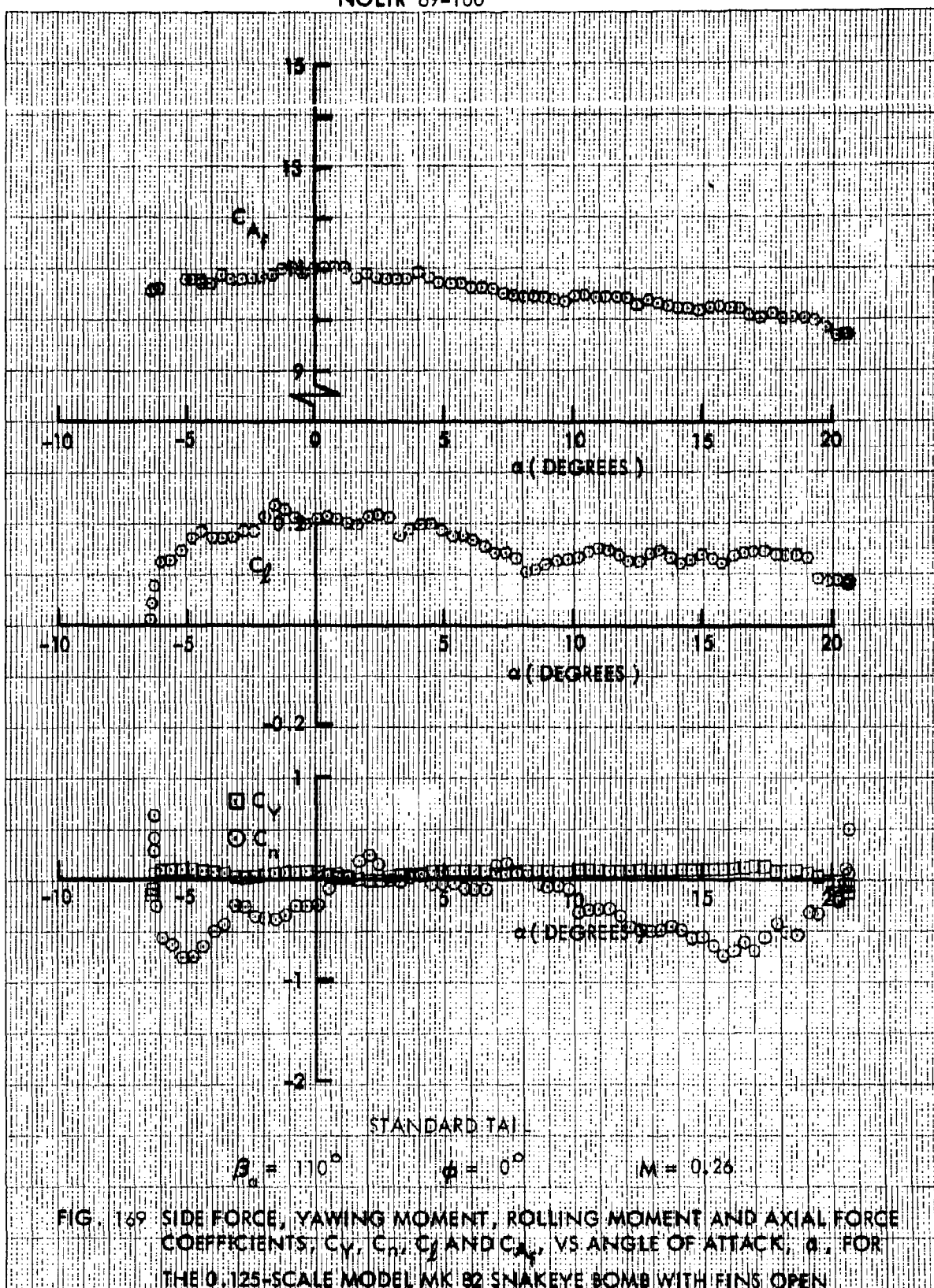
STANDARD TAIL

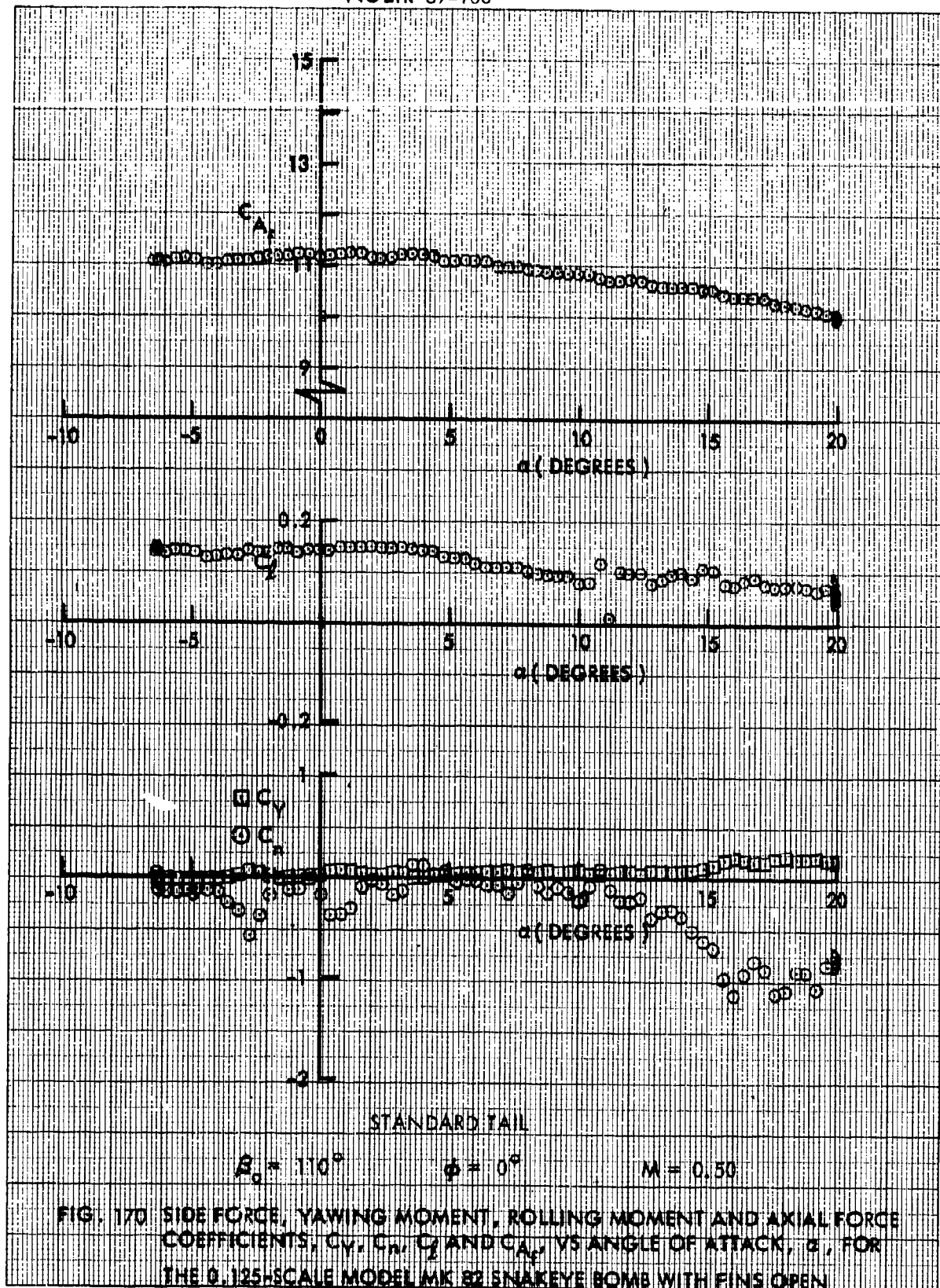
$$\beta_0 = 100^\circ$$

$$\phi = 45^\circ$$

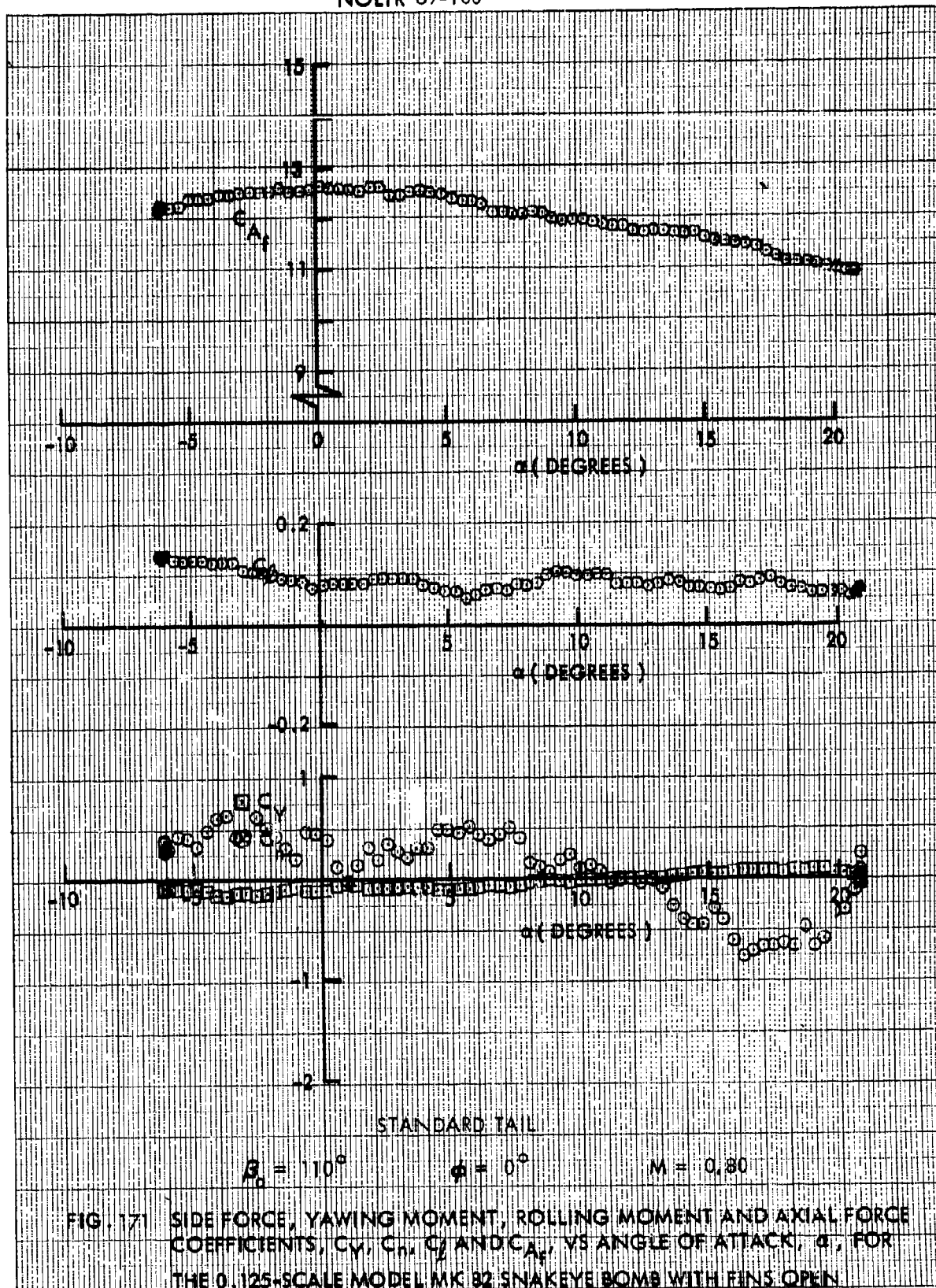
$$M = 0.95$$

FIG. 168 SIDE FORCE, YAWING MOMENT, ROLLING MOMENT AND AXIAL FORCE COEFFICIENTS,  $C_y$ ,  $C_n$ ,  $C_l$  AND  $C_{A_x}$ , VS ANGLE OF ATTACK,  $\alpha$ , FOR THE 0.325-SCALE MODEL MK 62 SNAKEYE BOMB WITH FINS OPEN











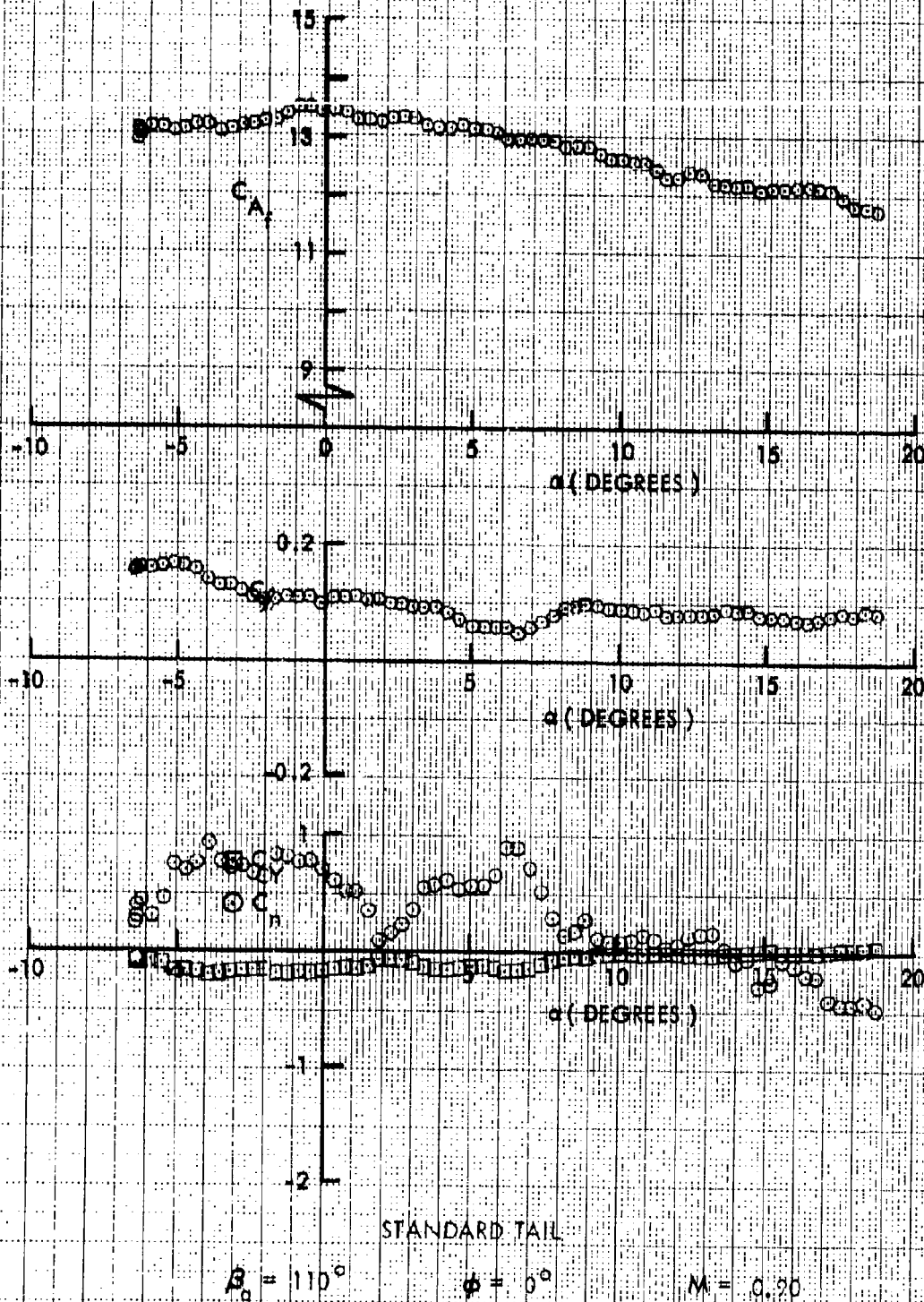
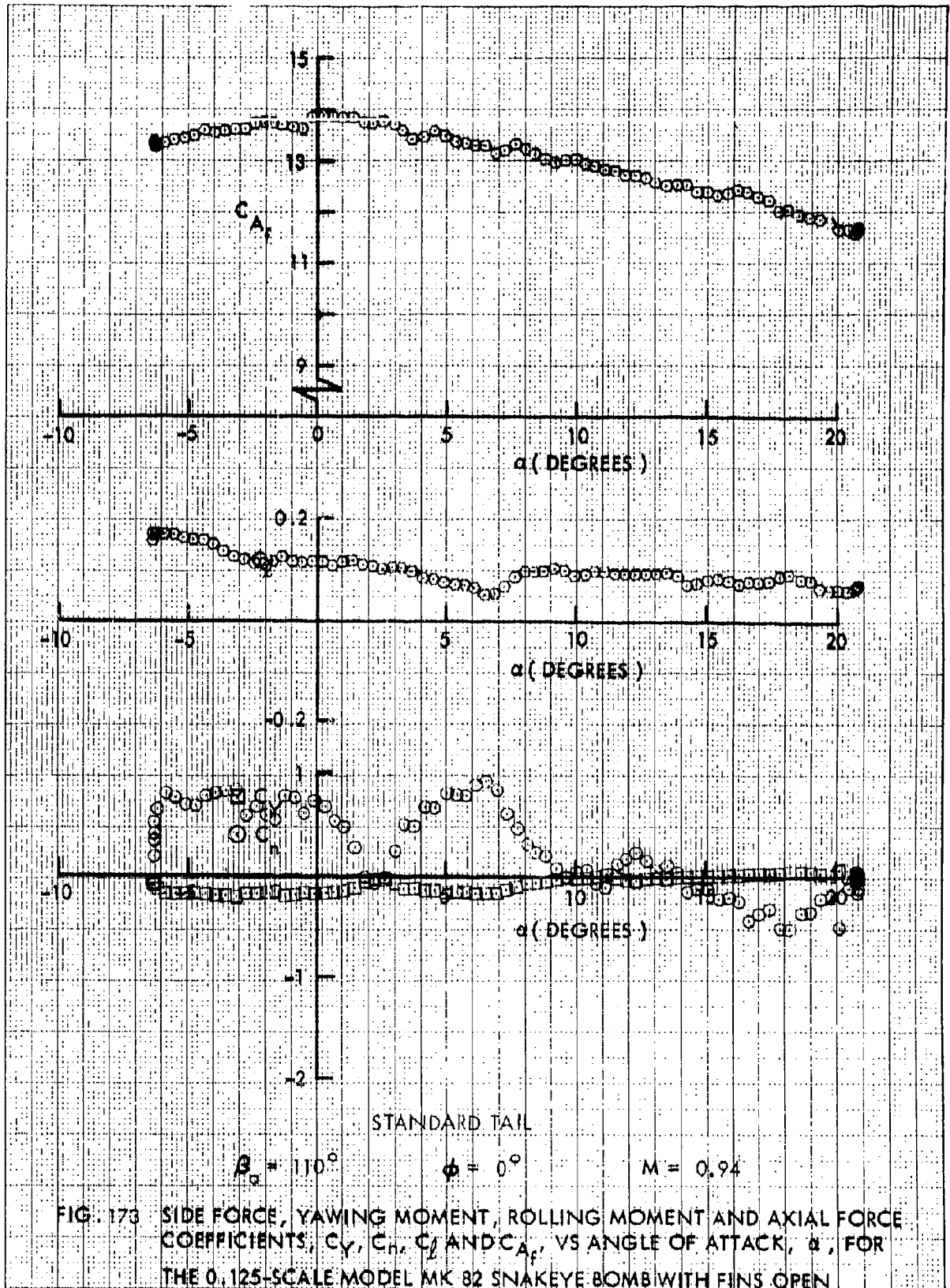
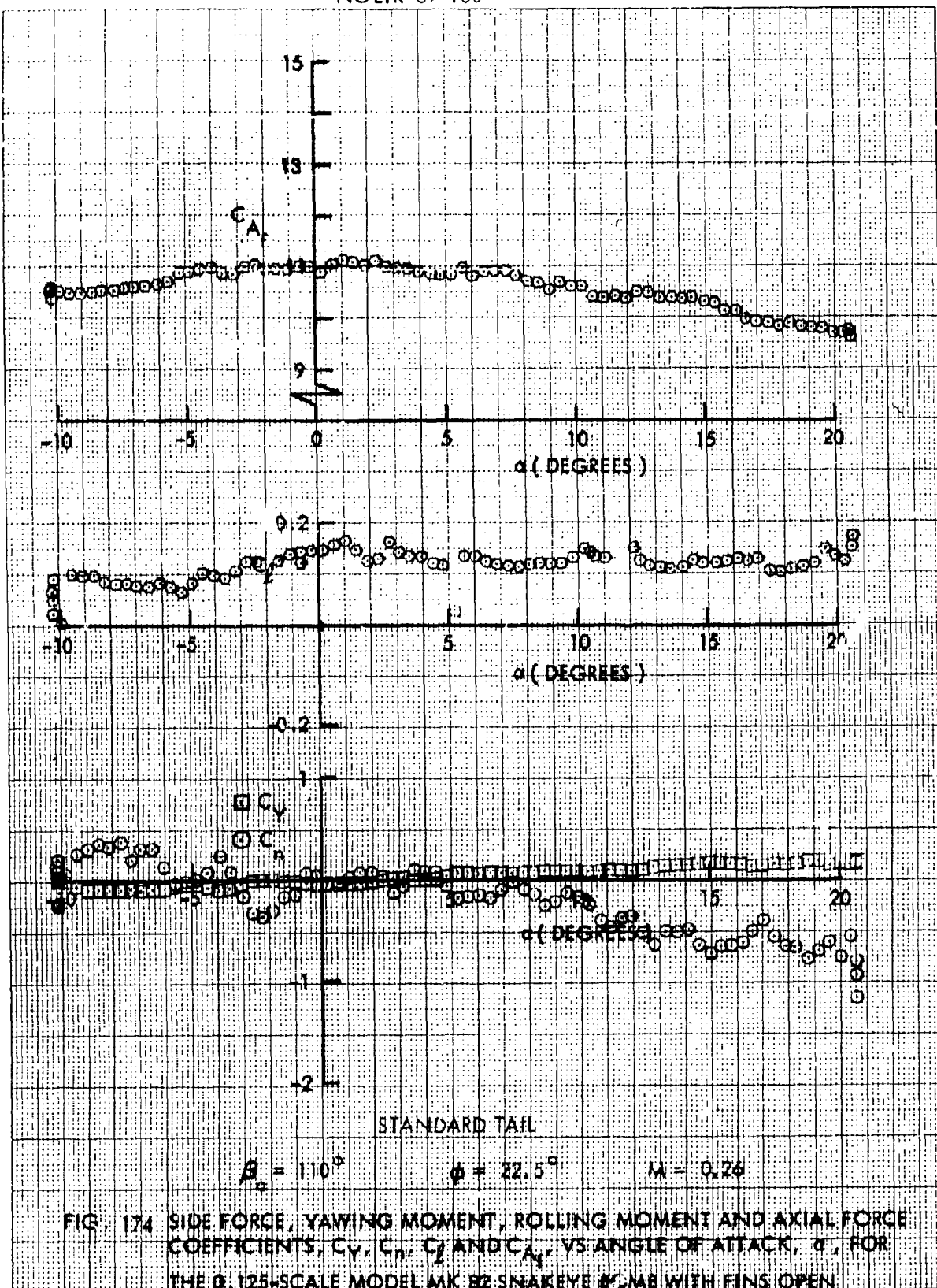
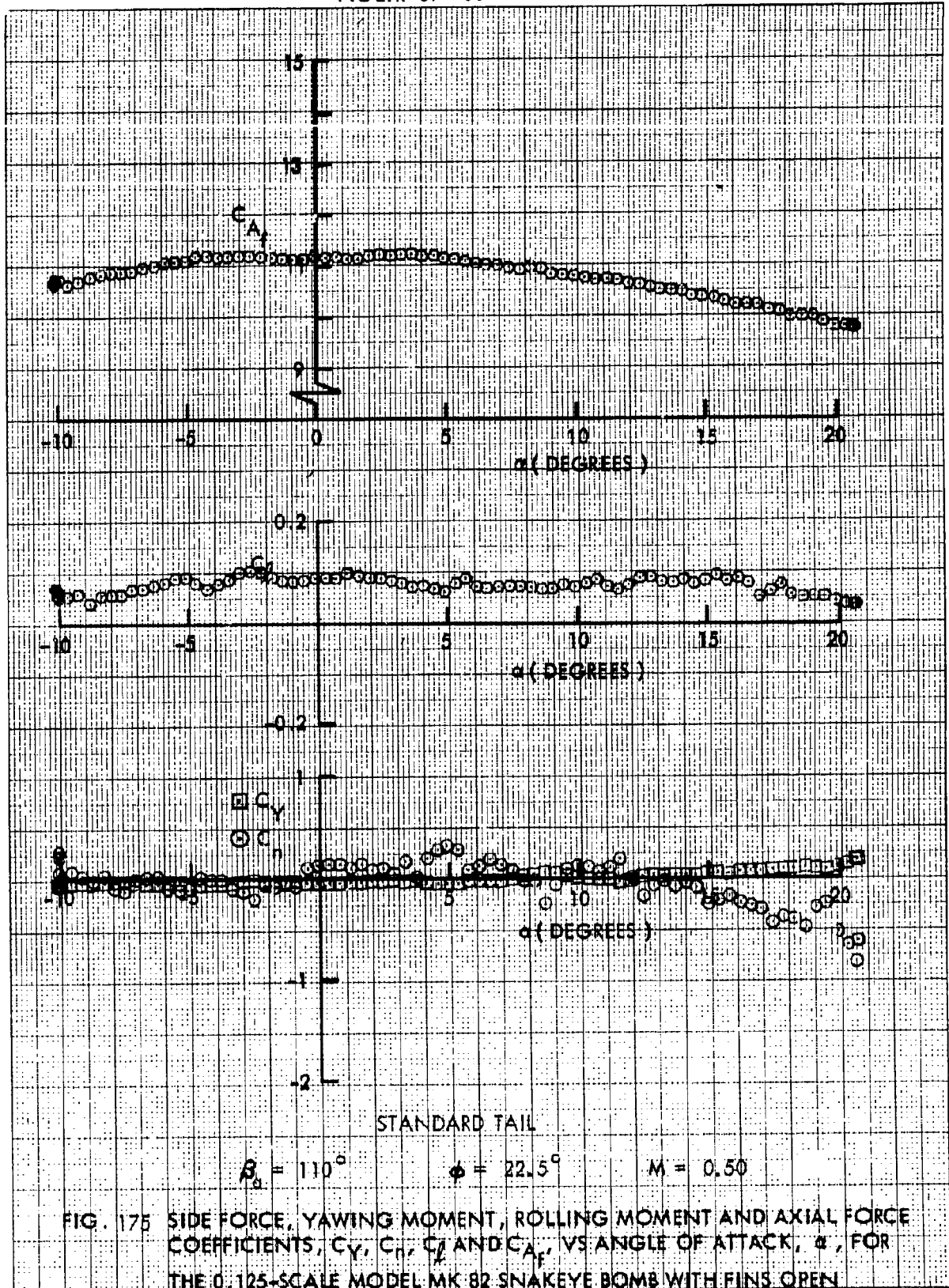
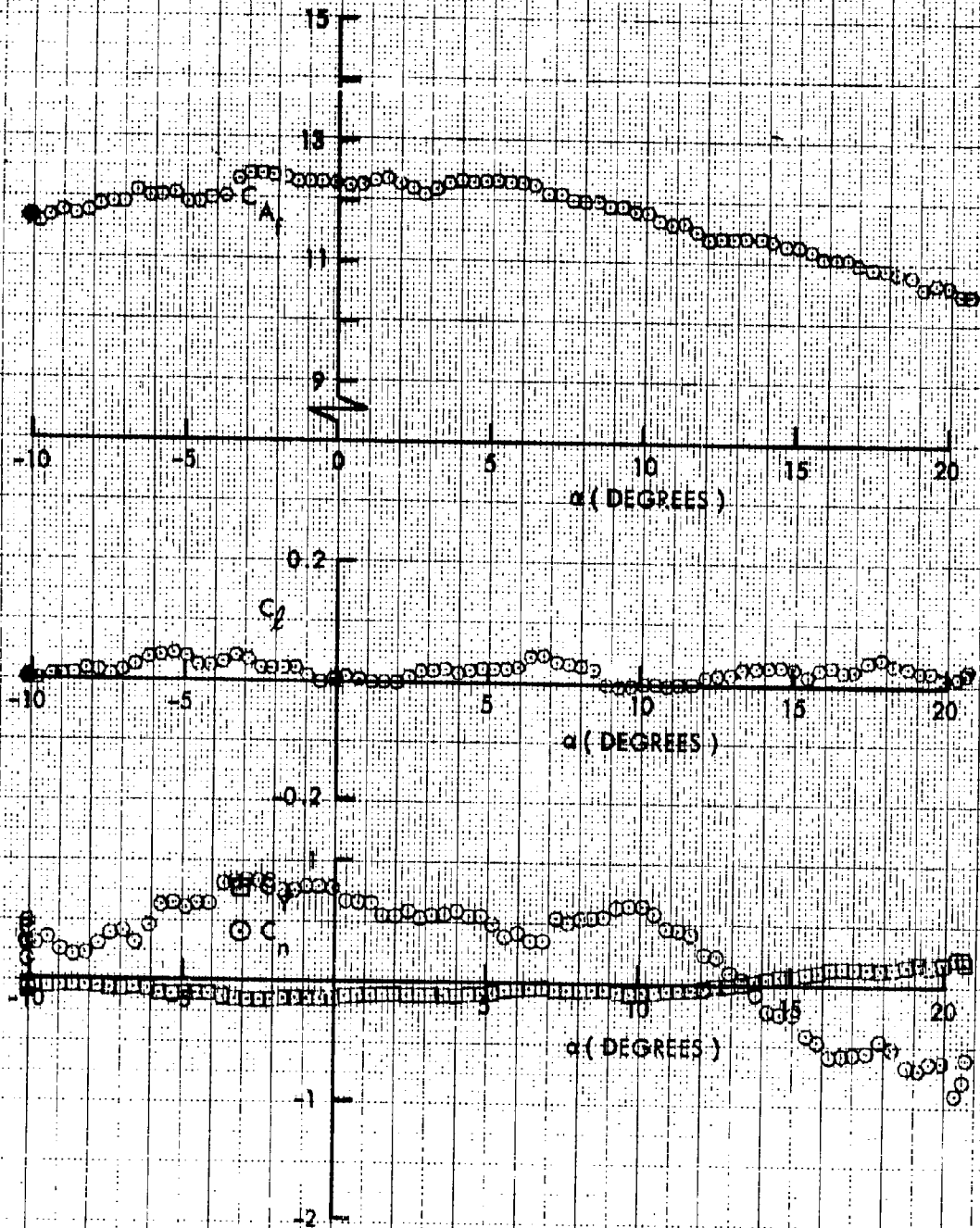


FIG. 172 SIDE FORCE, YAWING MOMENT, ROLLING MOMENT AND AXIAL FORCE COEFFICIENTS,  $C_Y$ ,  $C_n$ ,  $C_l$  AND  $C_A$ , VS ANGLE OF ATTACK,  $\alpha$ , FOR THE 0.125-SCALE MODEL MK 82 SNAKEYE BOMB WITH FINS OPEN









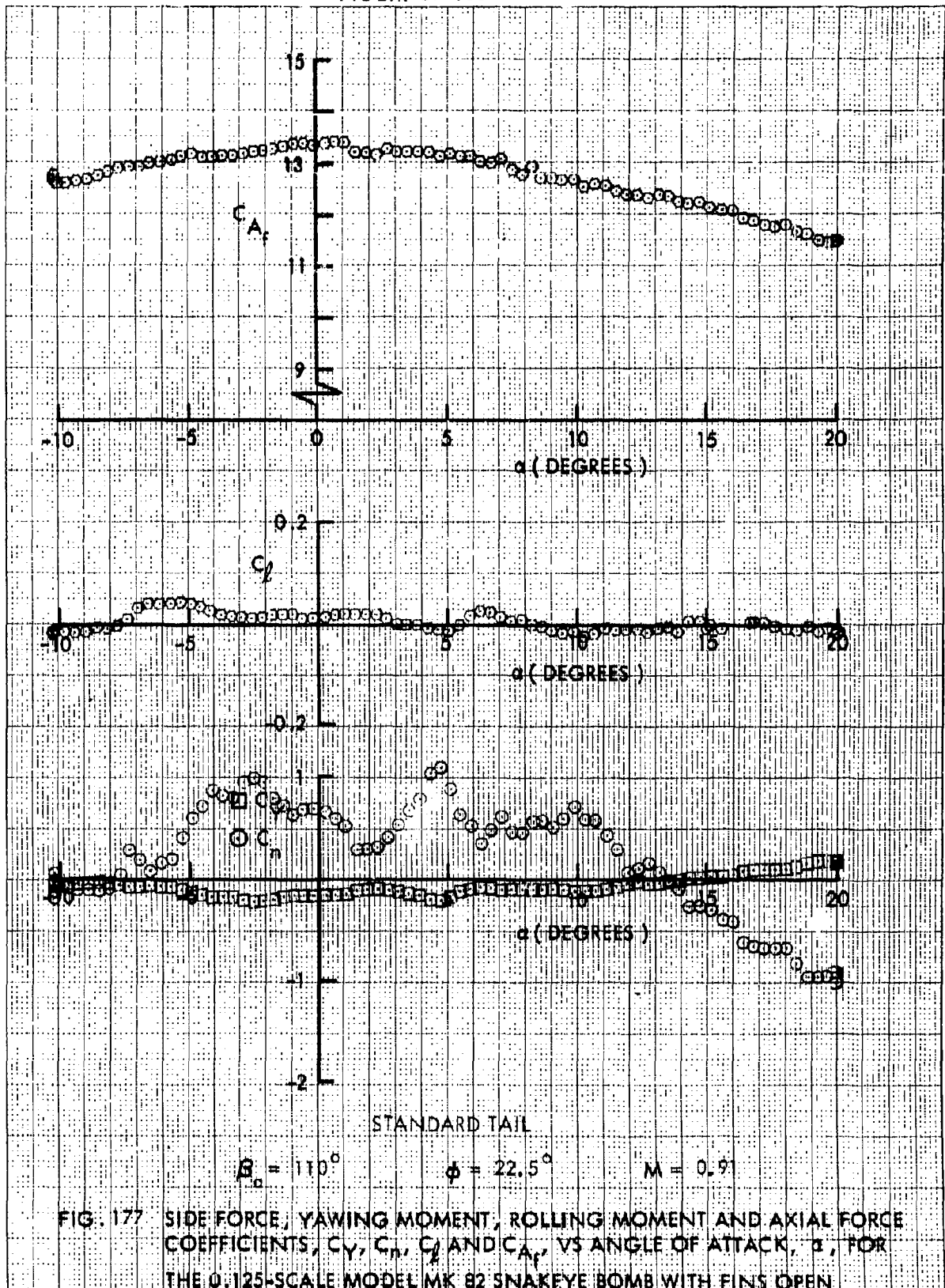
STANDARD TAIL

$$\beta_0 = 110^\circ$$

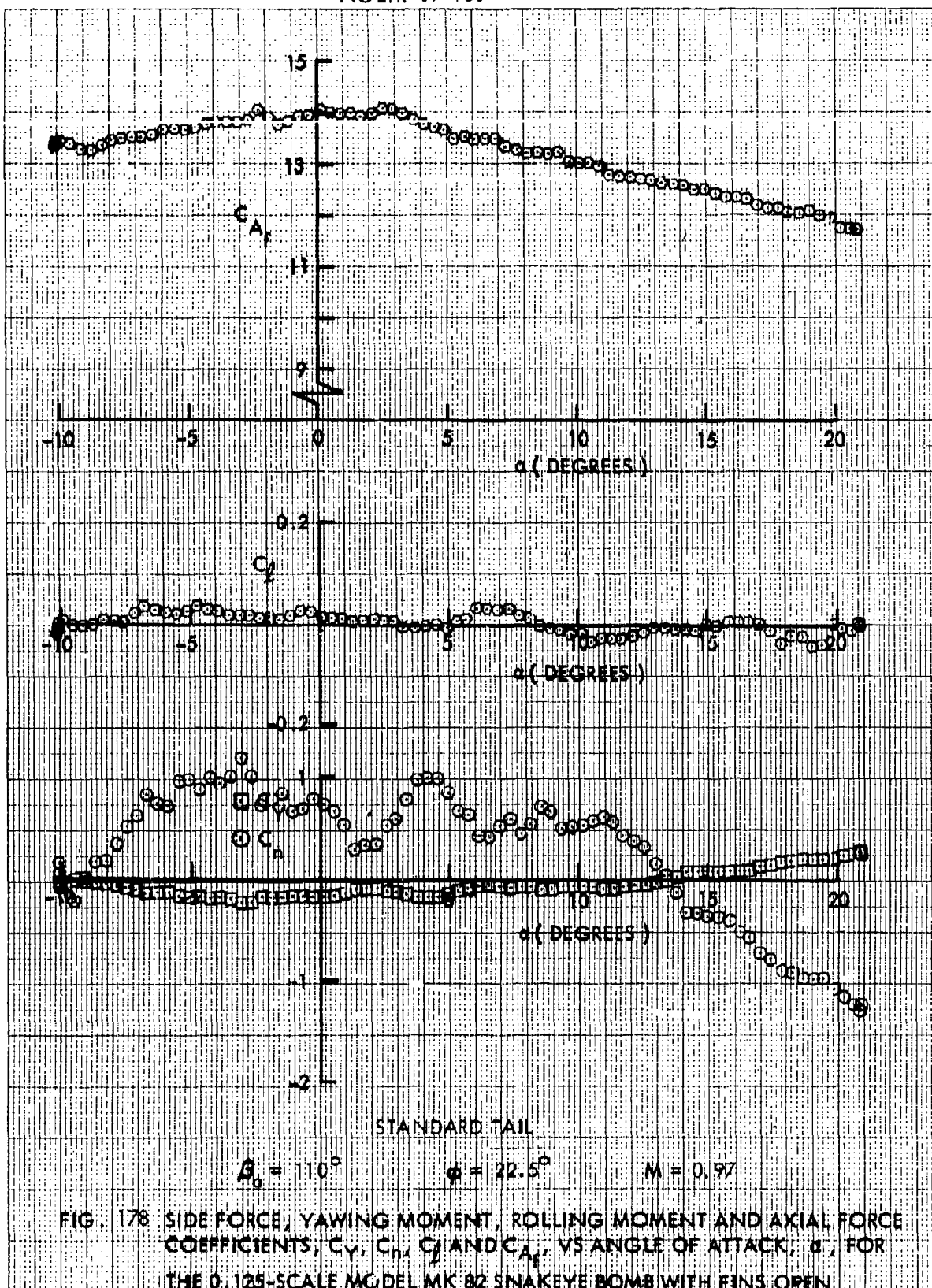
$$\phi = 22.5^\circ$$

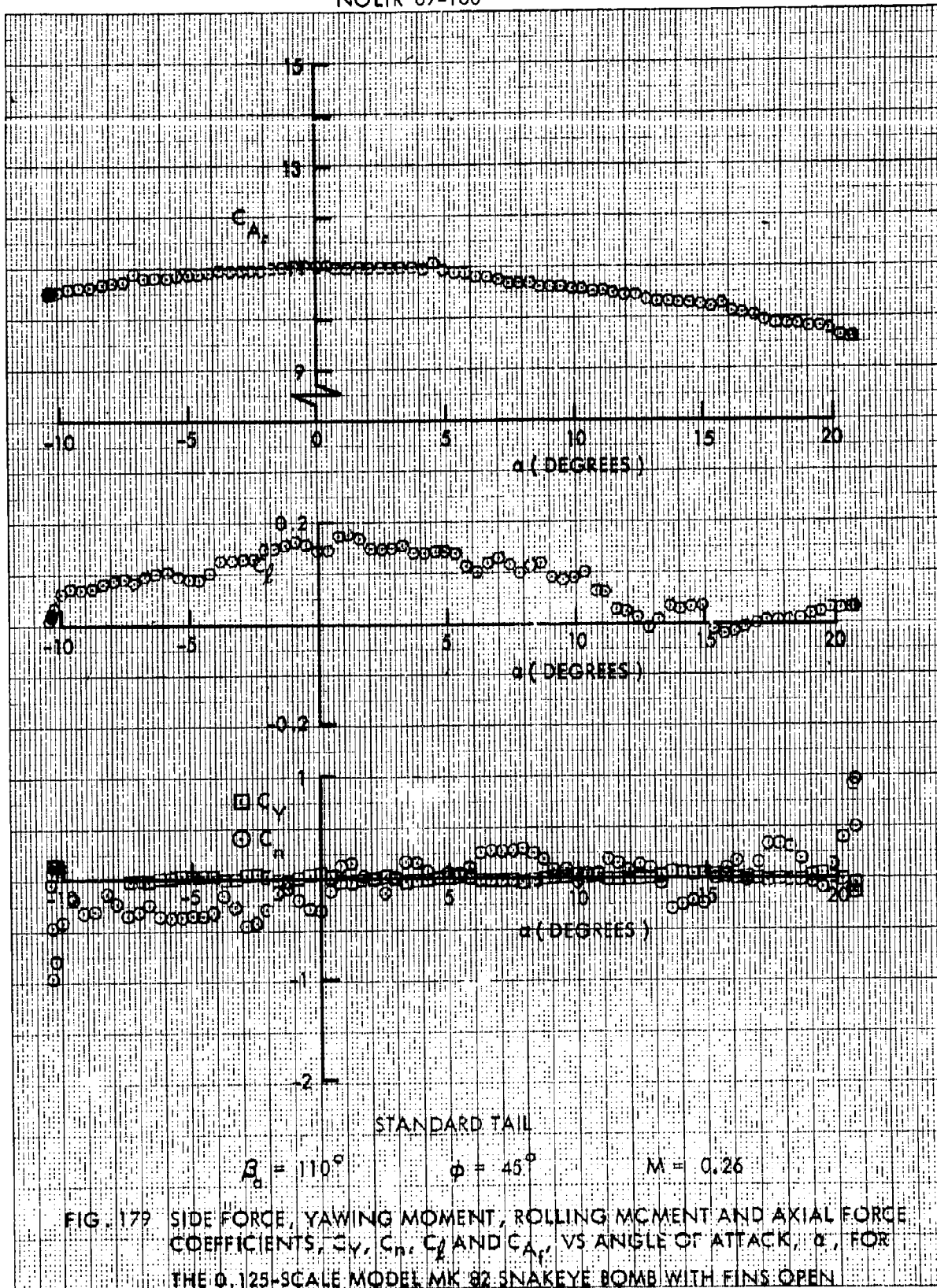
$$M = 0.80$$

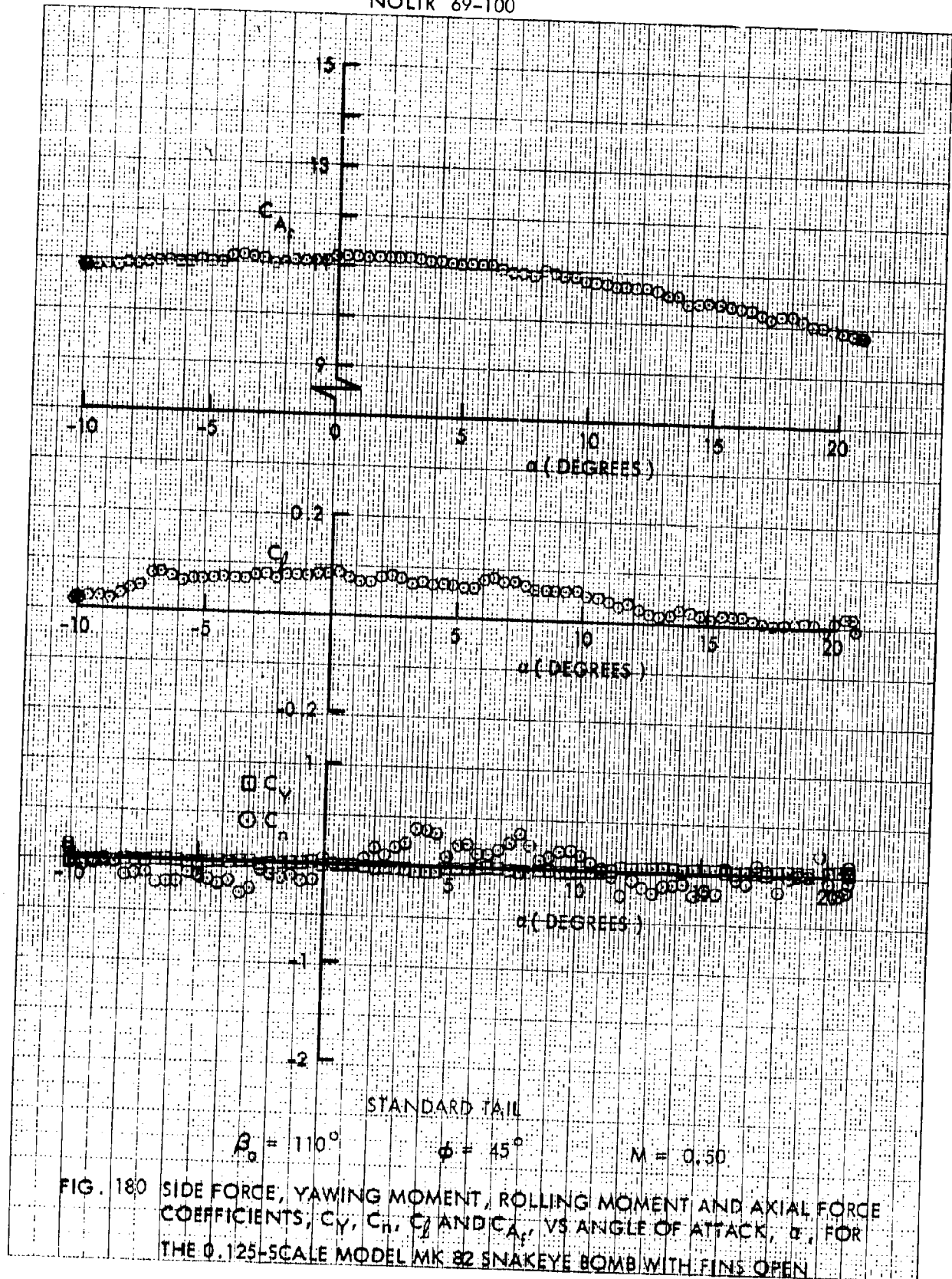
FIG. 176 SIDE FORCE, YAWING MOMENT, ROLLING MOMENT AND AXIAL FORCE COEFFICIENTS,  $C_Y$ ,  $C_n$ ,  $C_l$  AND  $C_{A_f}$ , VS ANGLE OF ATTACK,  $\alpha$ , FOR THE 0.125-SCALE MODEL MK 82 SNAKEYE BOMB WITH FINS OPEN

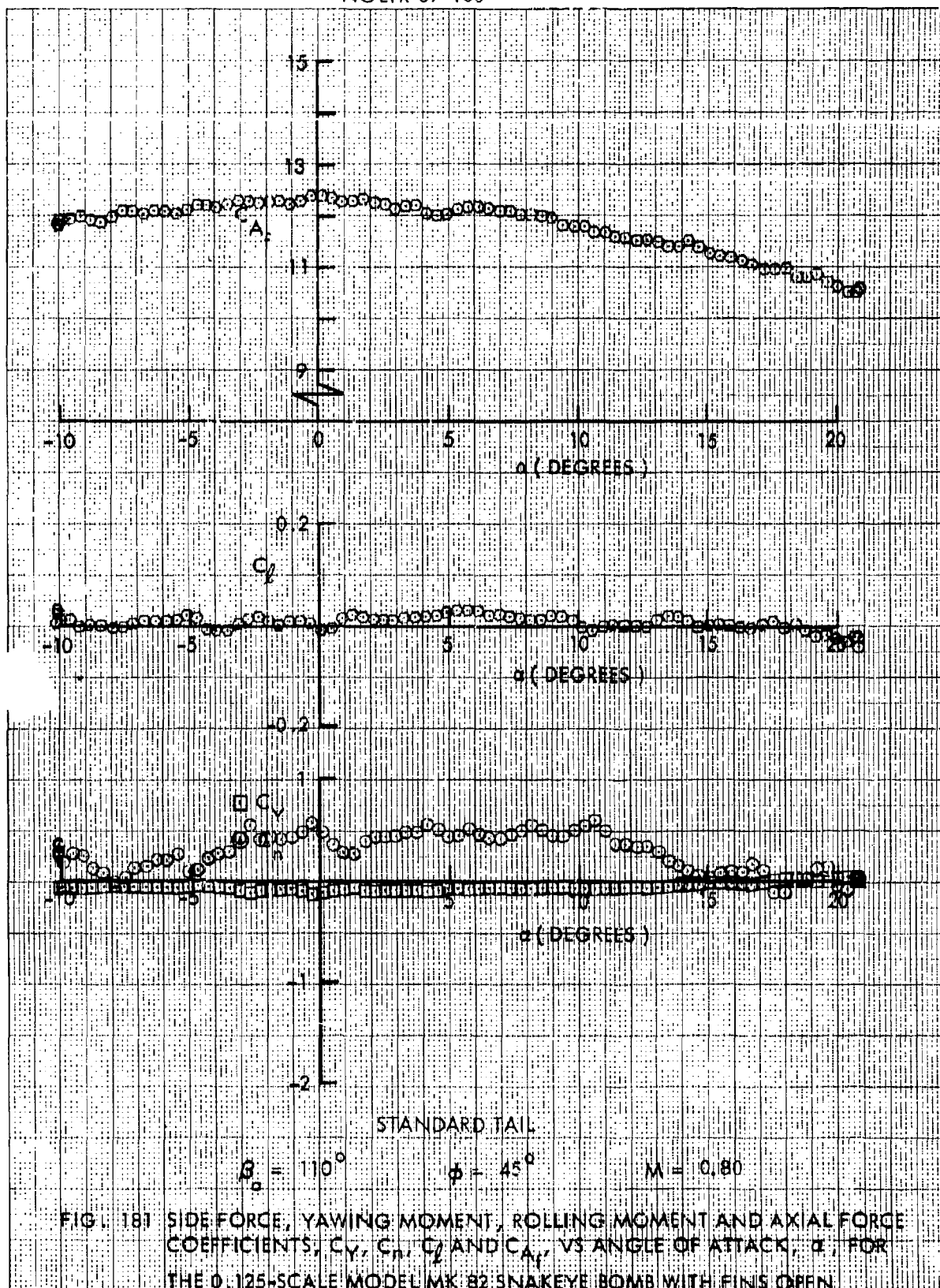


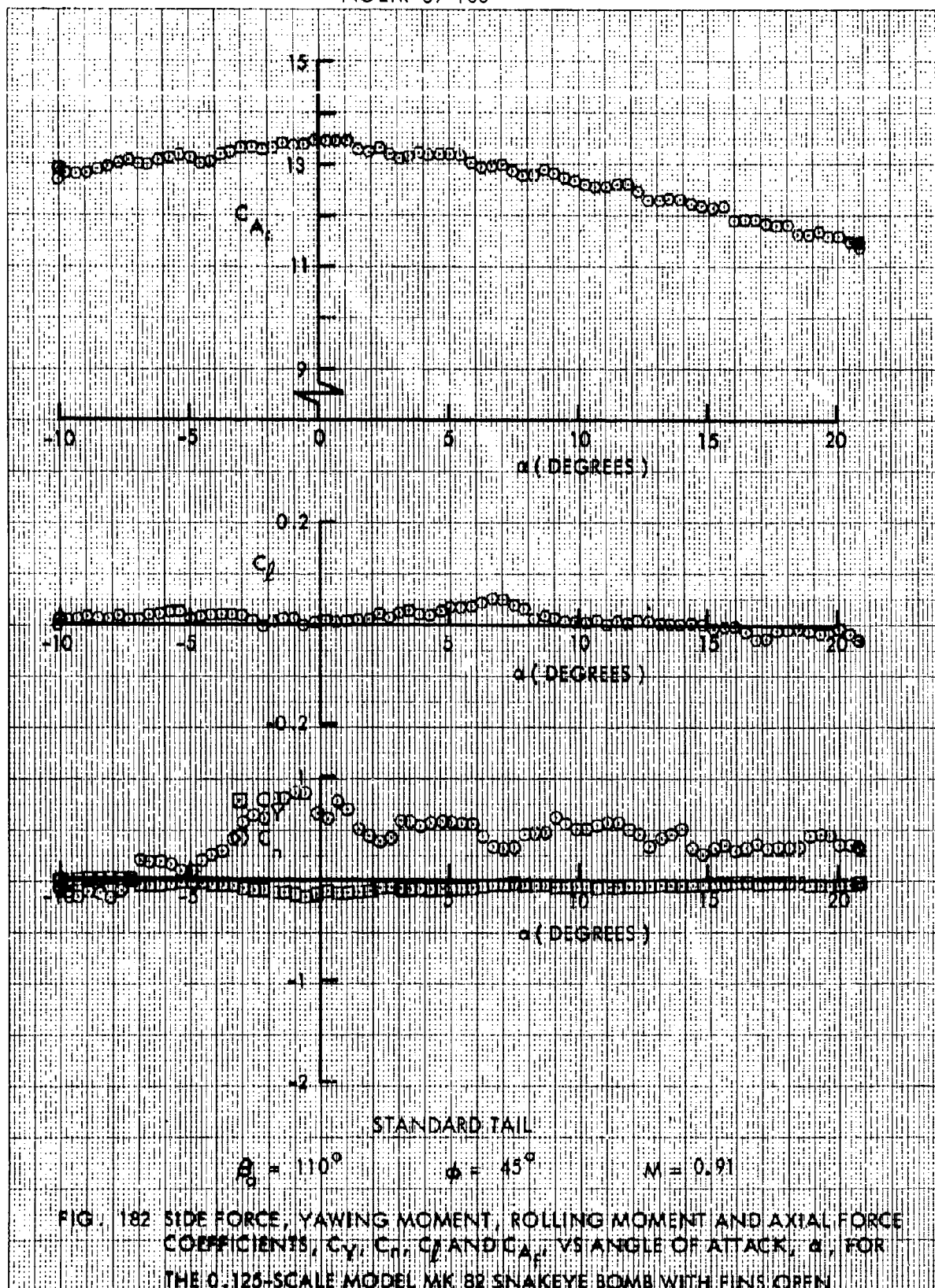




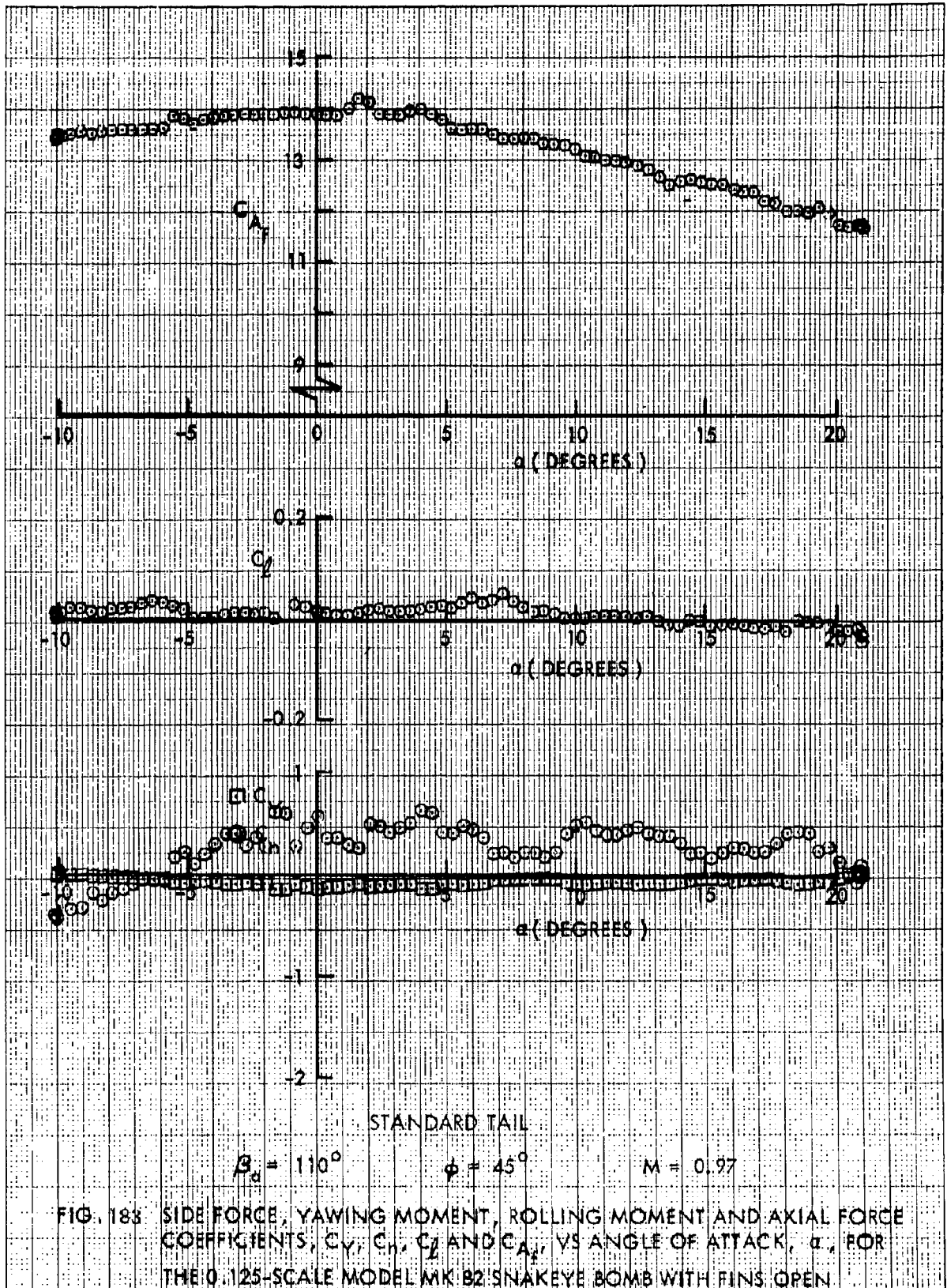




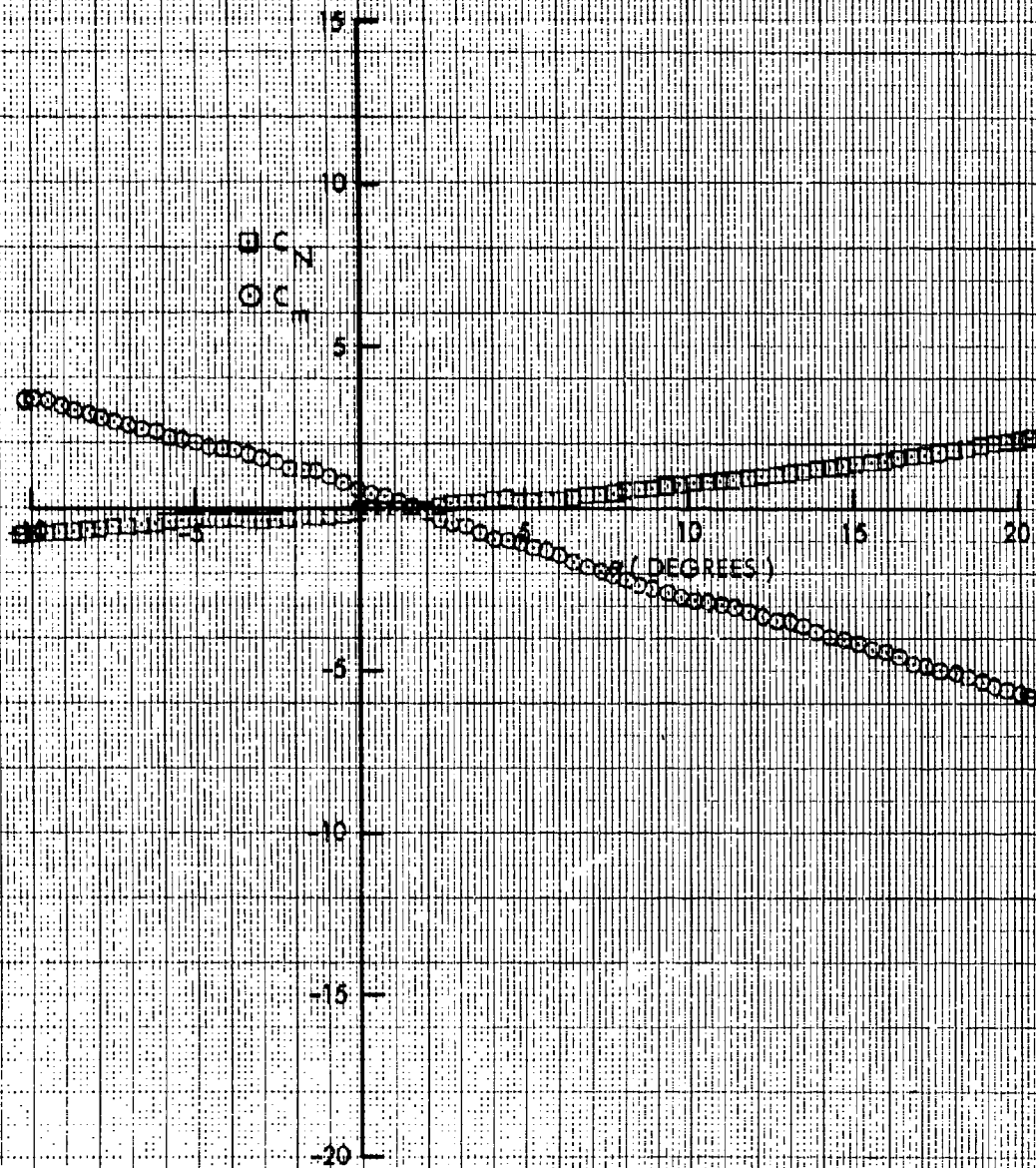












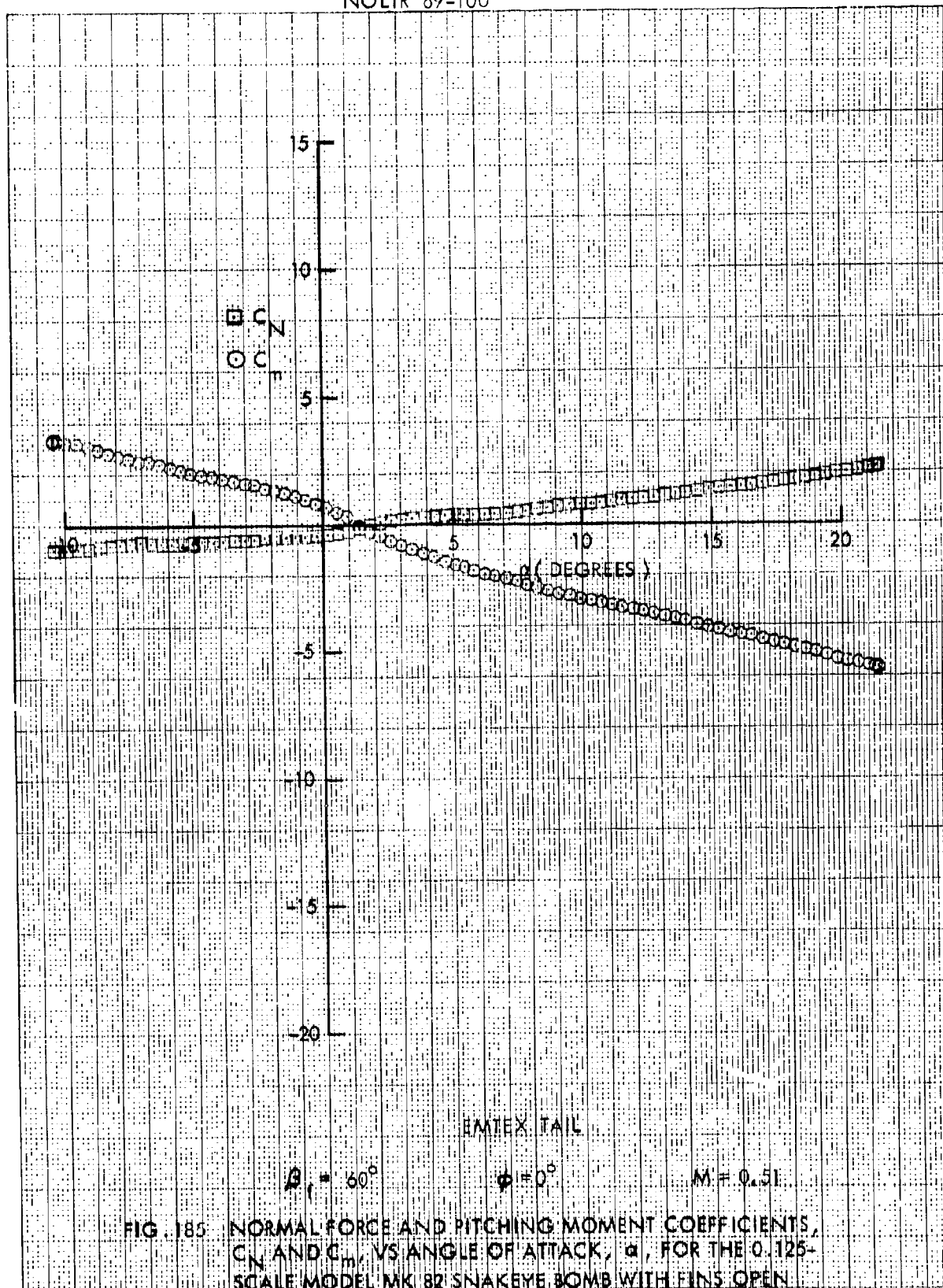
EMTEX TAIL

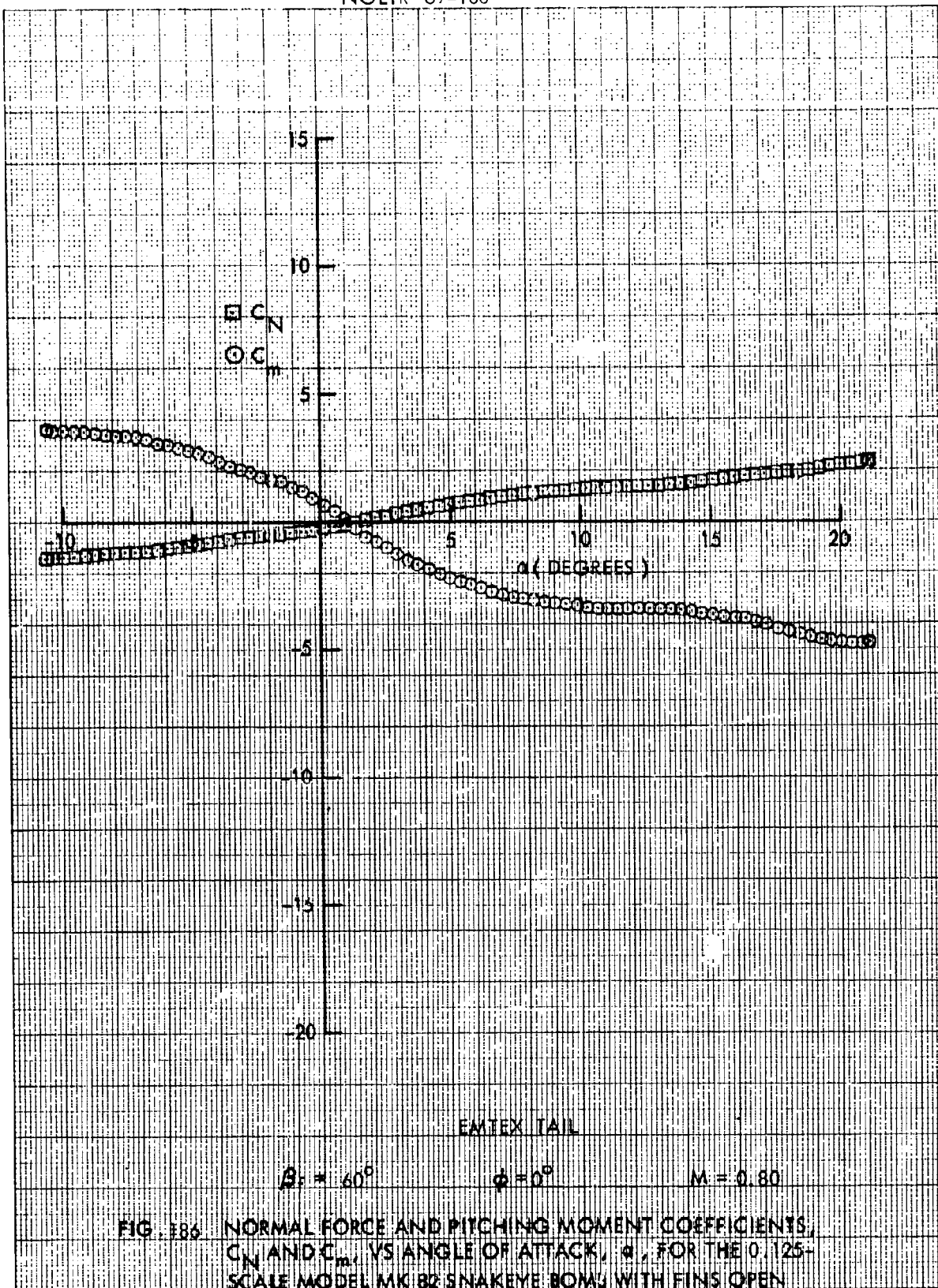
$\beta_f = 60^\circ$

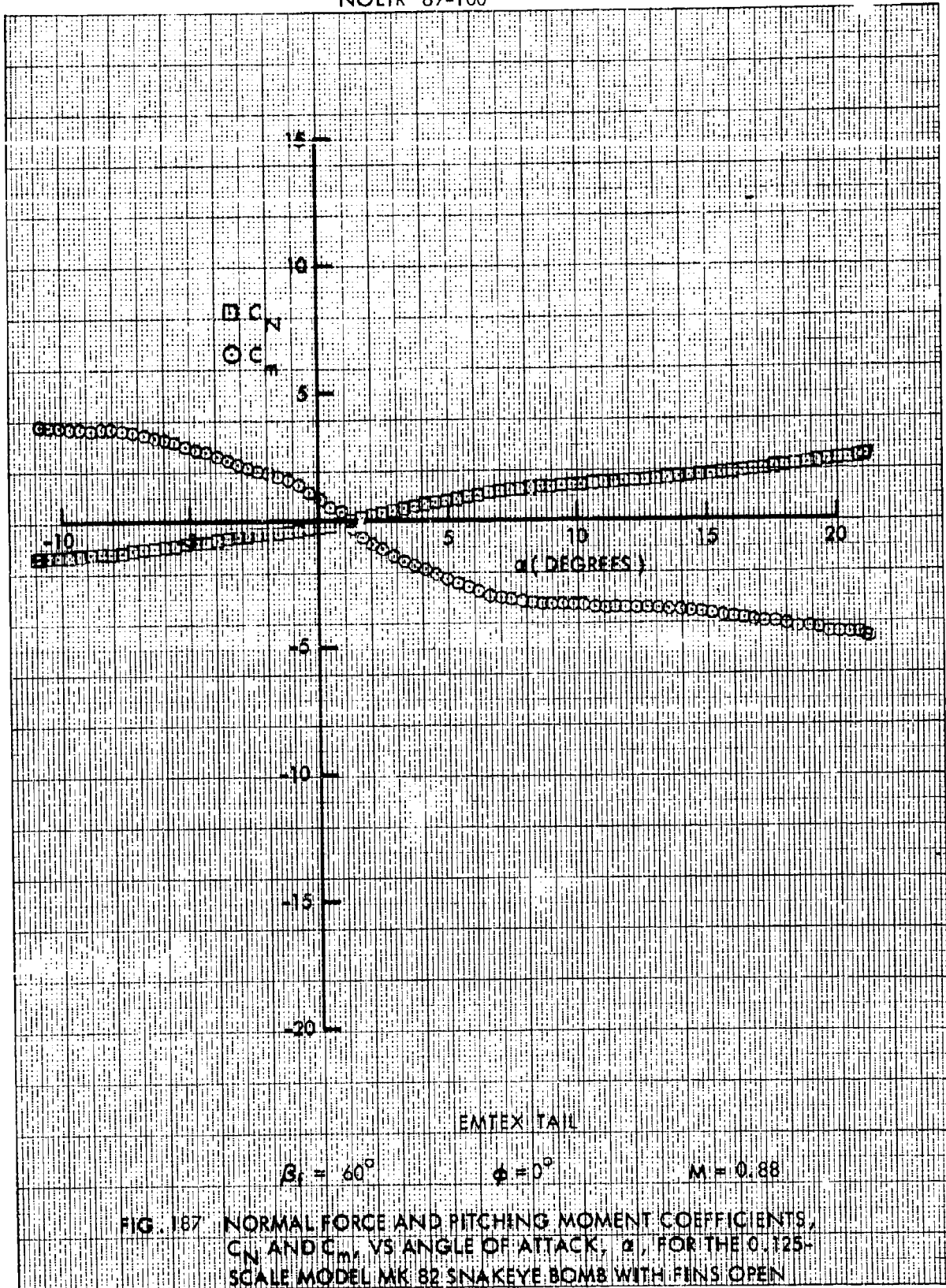
$\phi = 0^\circ$

$M = 0.26$

FIG. 184 NORMAL FORCE AND PITCHING MOMENT COEFFICIENTS,  $C_N$  AND  $C_m$ , VS ANGLE OF ATTACK,  $\alpha$ , FOR THE 0.125-SCALE MODEL MK 82 SNAKEYE BOMB WITH FINS OPEN







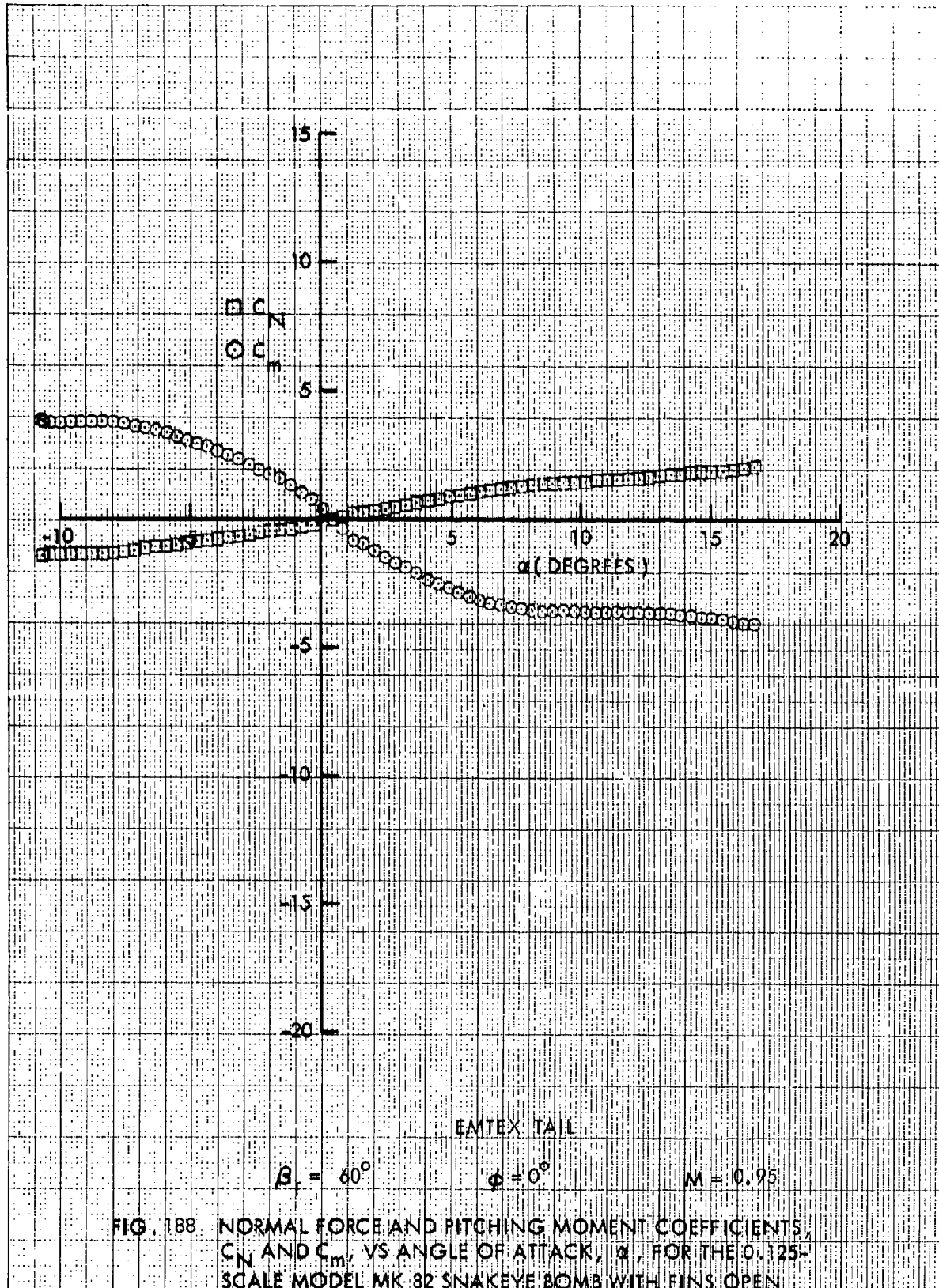


FIG. 1B8. NORMAL FORCE AND PITCHING MOMENT COEFFICIENTS,  $C_N$  AND  $C_m$ , VS ANGLE OF ATTACK,  $\alpha$ , FOR THE 0.125-SCALE MODEL MK 82 SNAKEYE BOMB WITH FINS OPEN

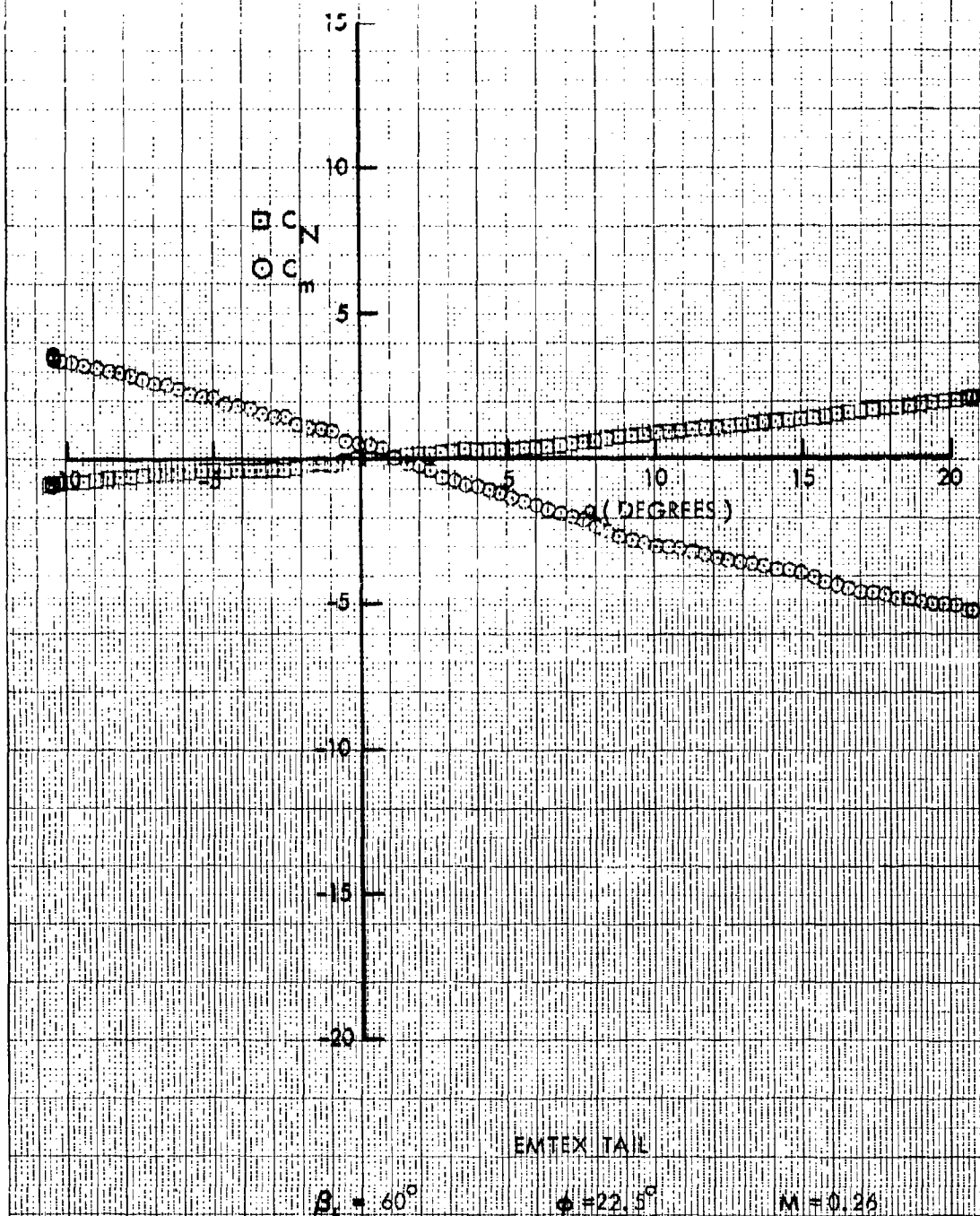
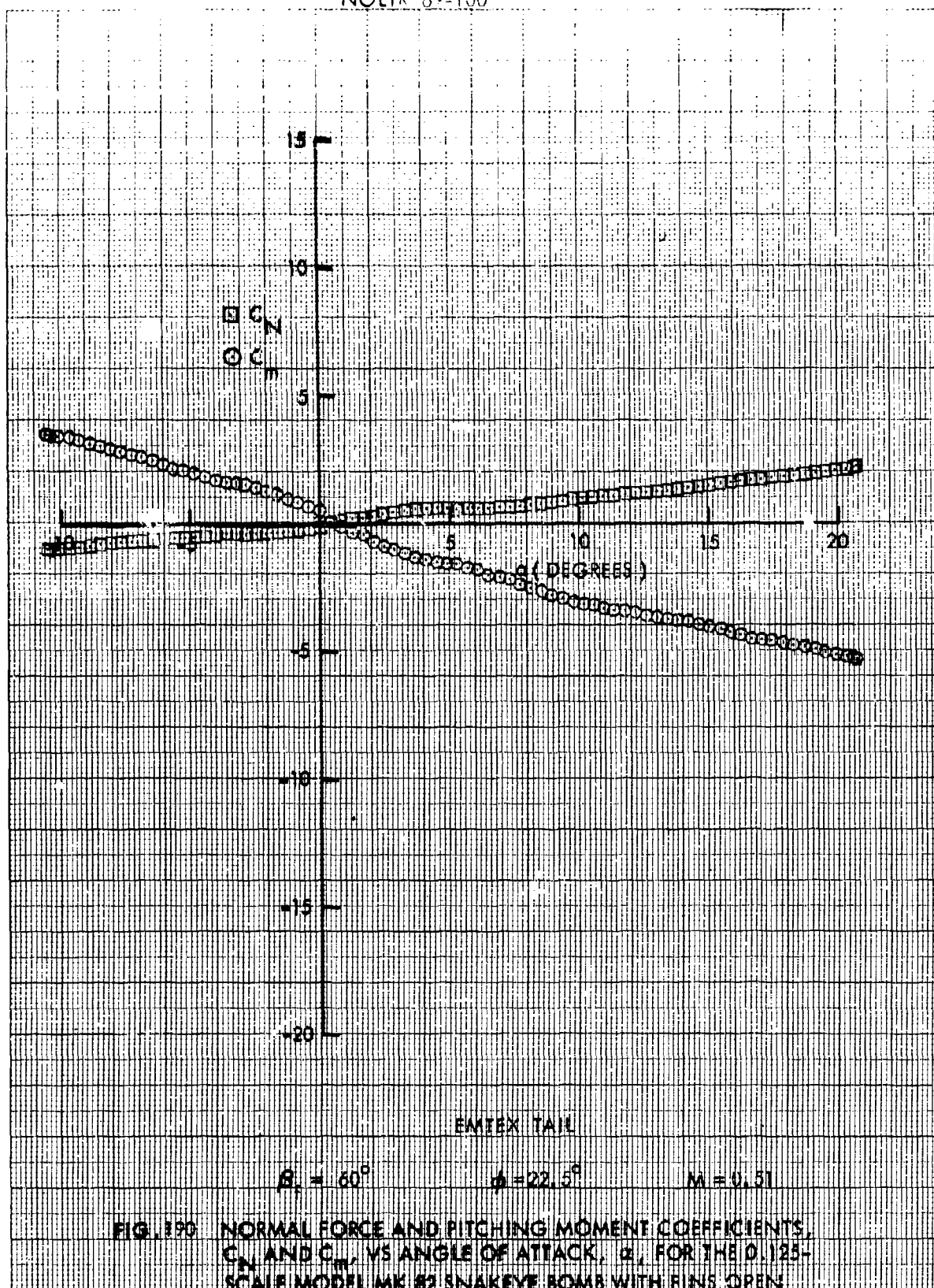
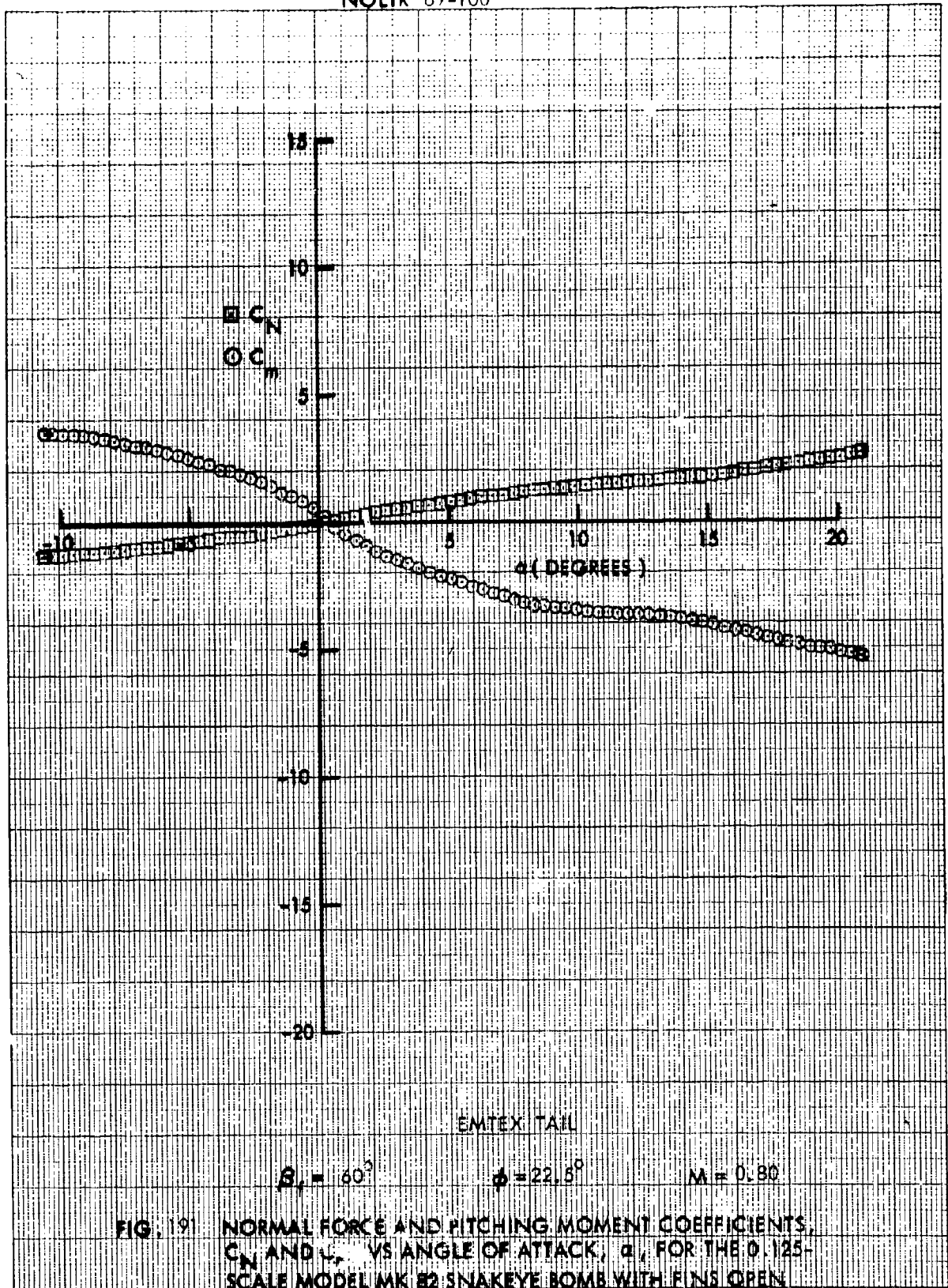
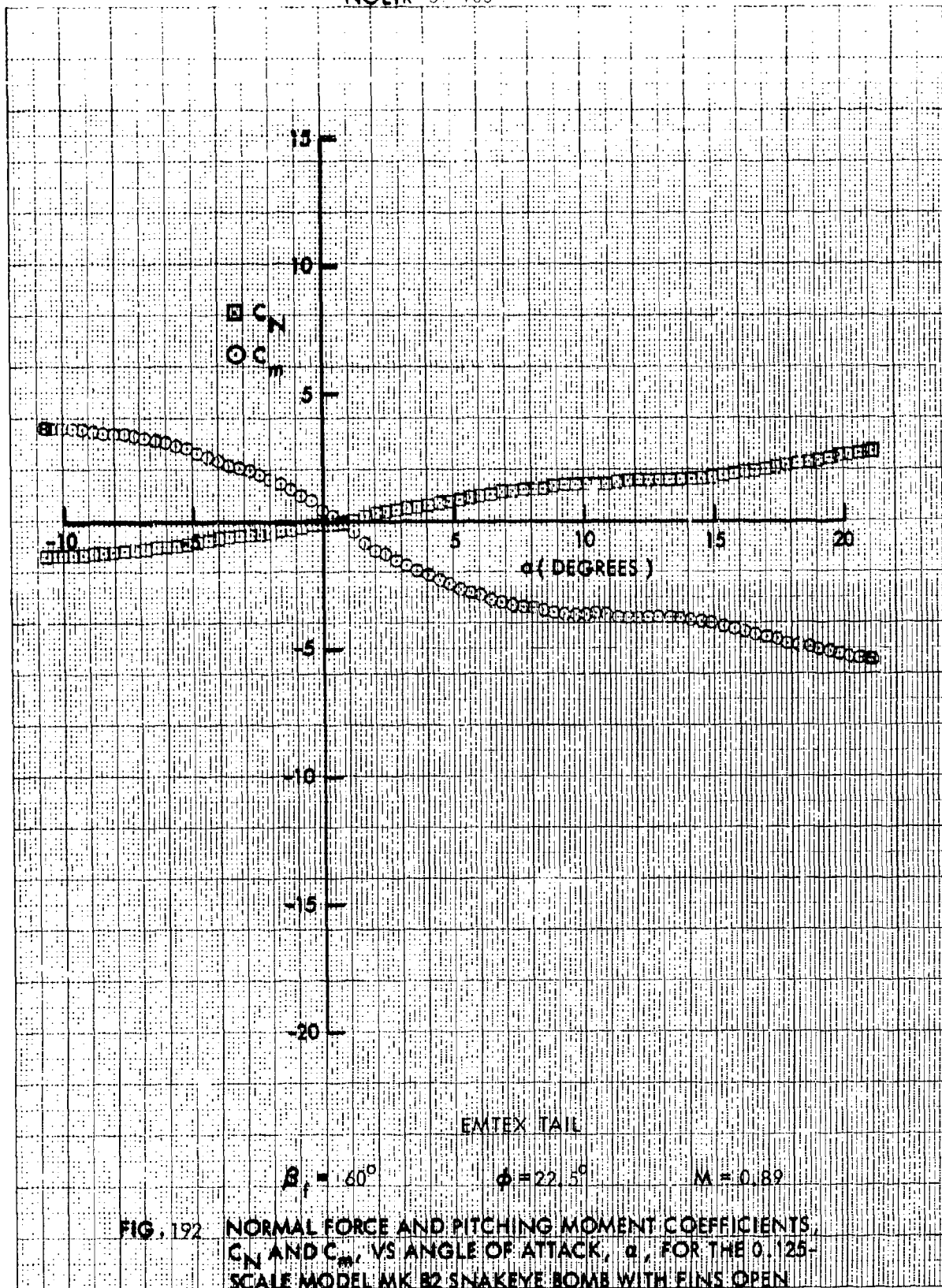


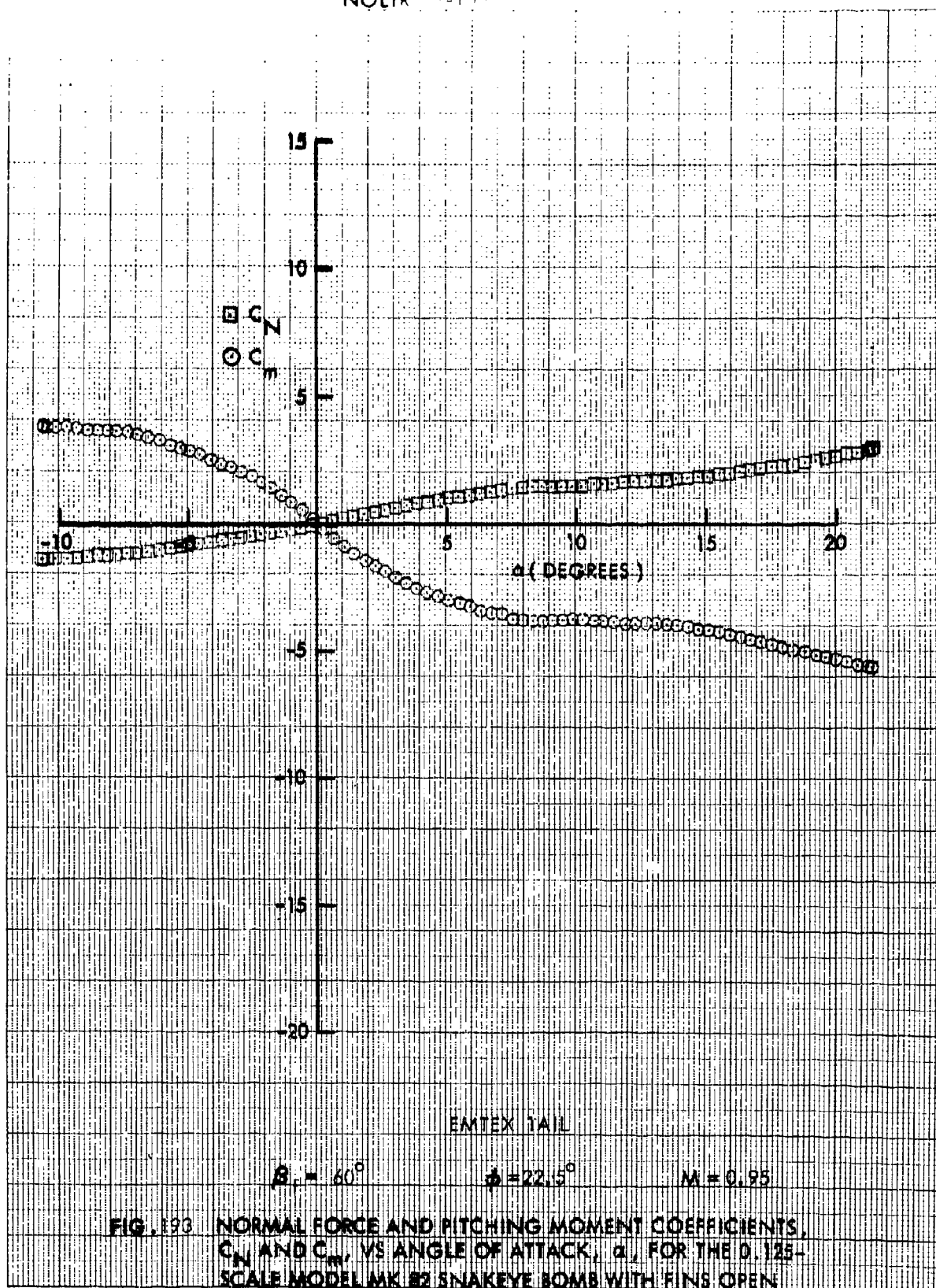
FIG. 189 NORMAL FORCE AND PITCHING MOMENT COEFFICIENTS,  $C_N$  AND  $C_m$ , VS ANGLE OF ATTACK,  $\alpha$ , FOR THE 0.125-SCALE MODEL MK 82 SNAKEYE BOMB WITH FINS OPEN

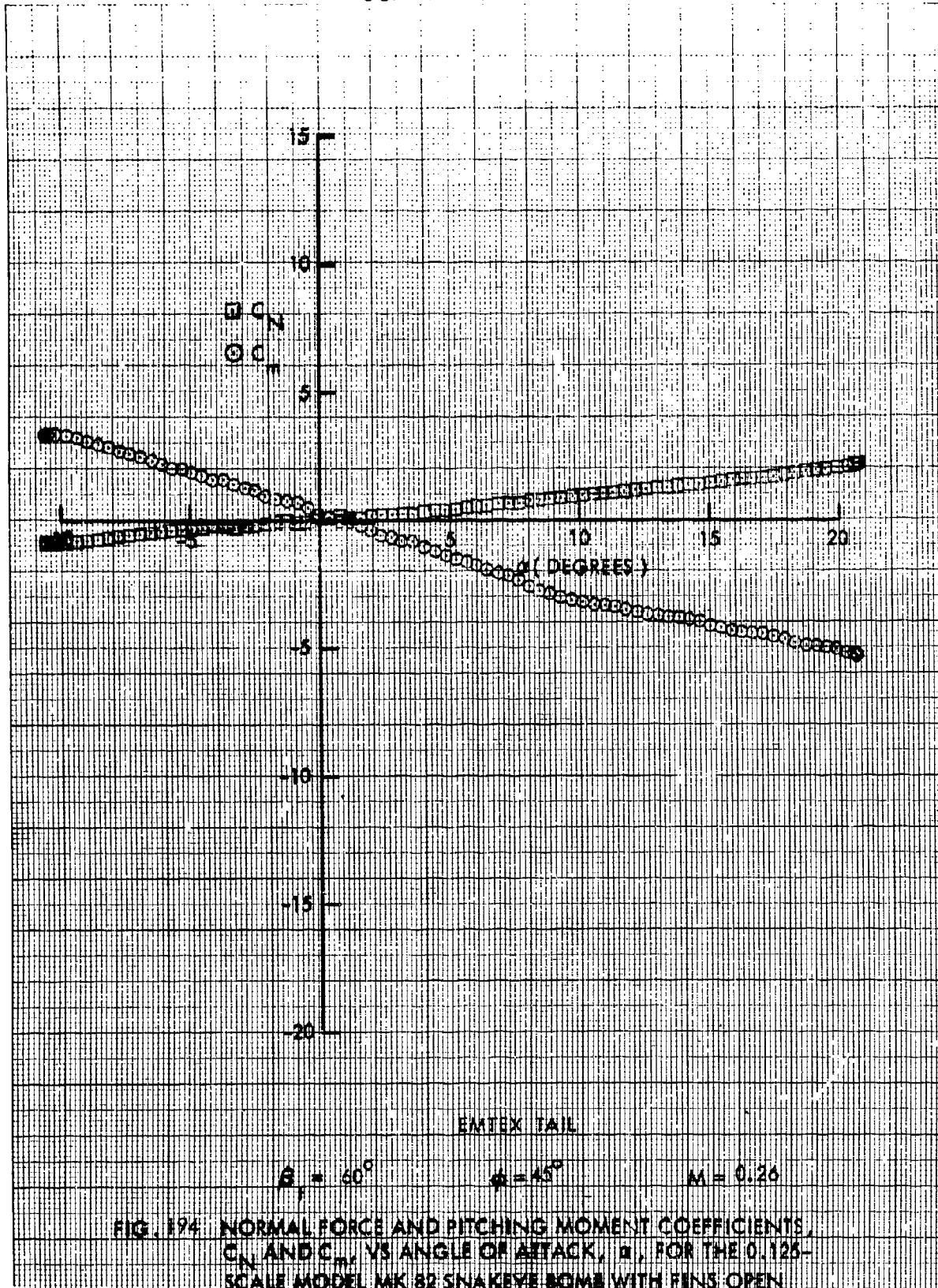




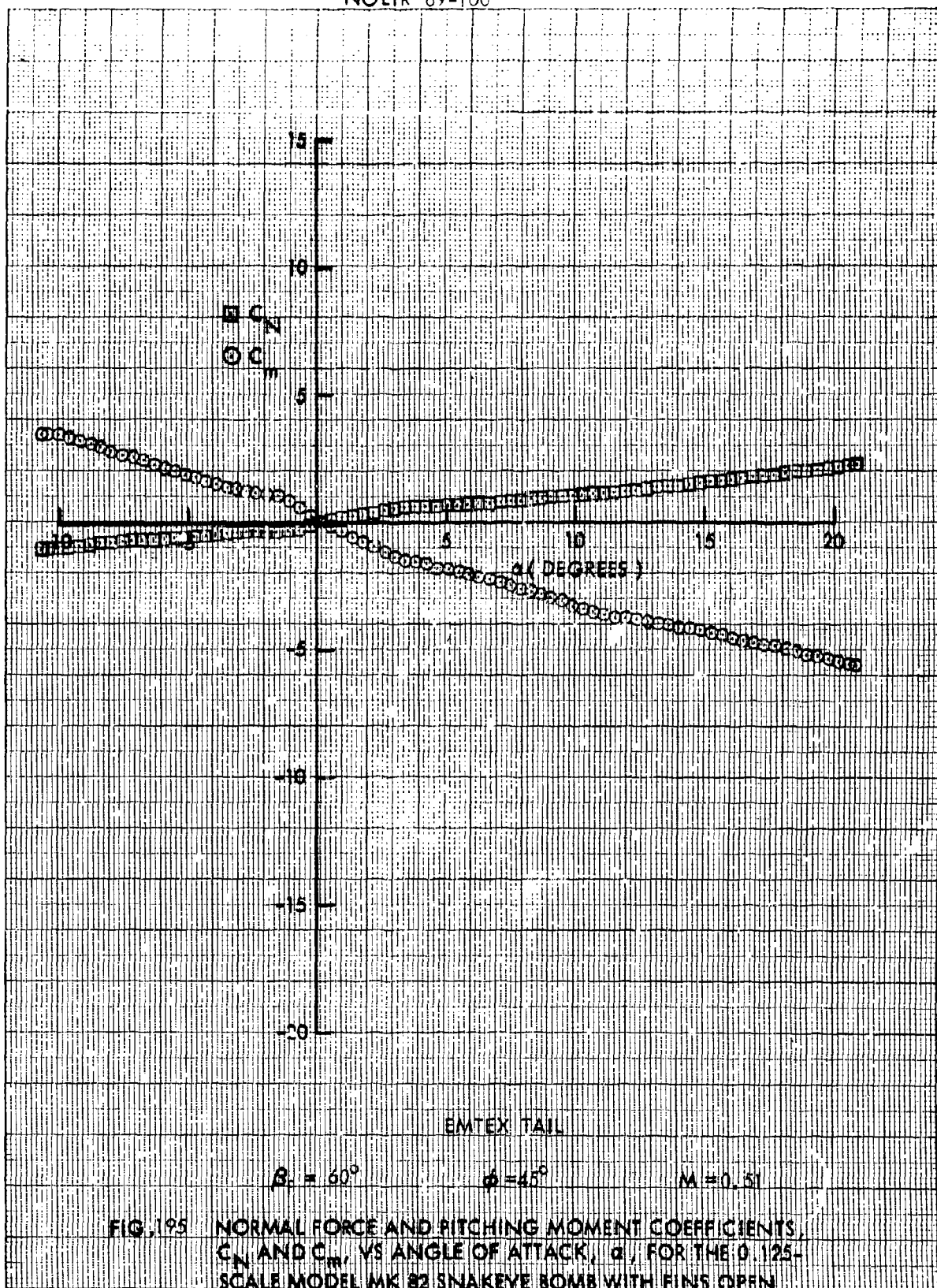




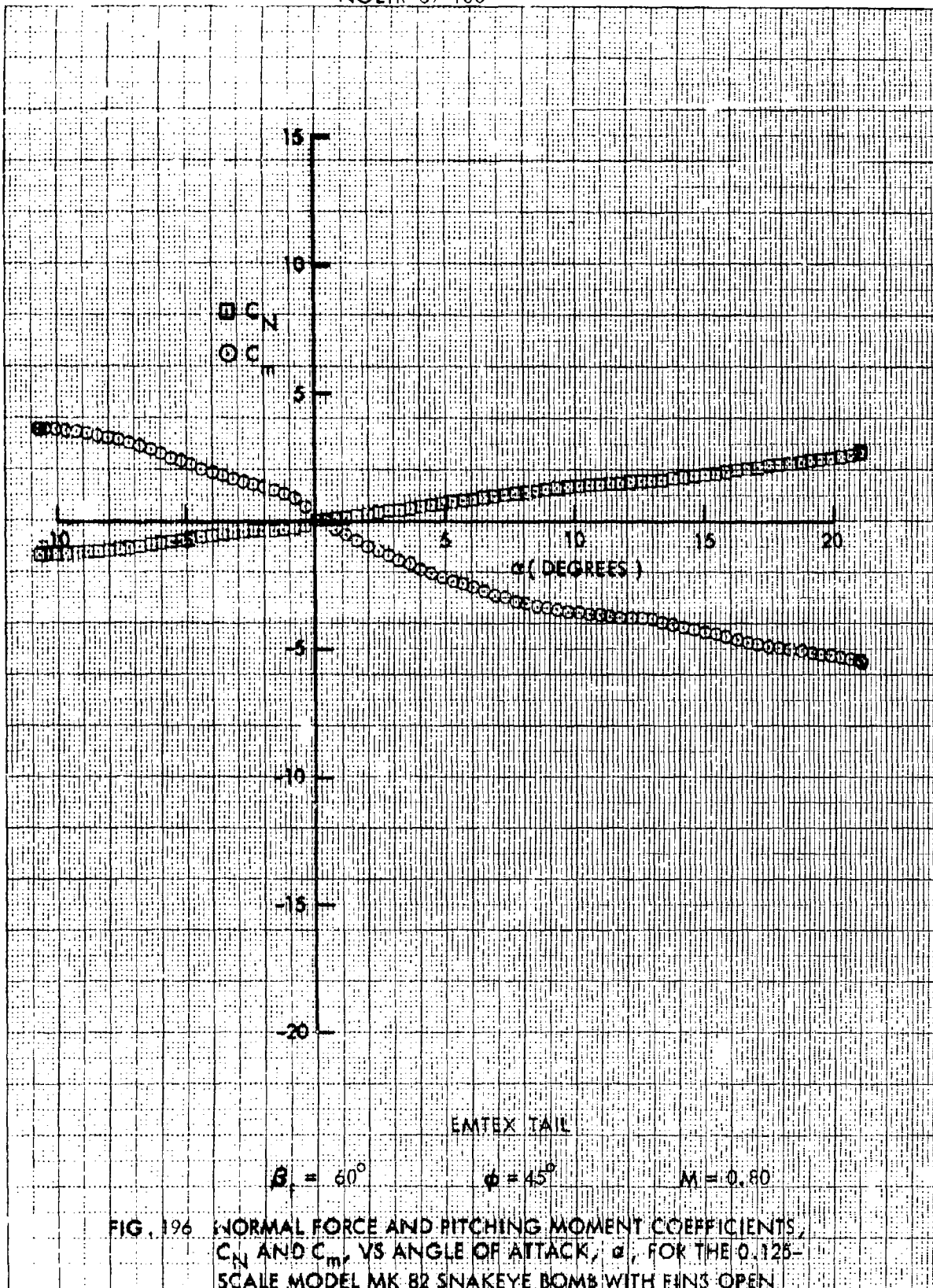


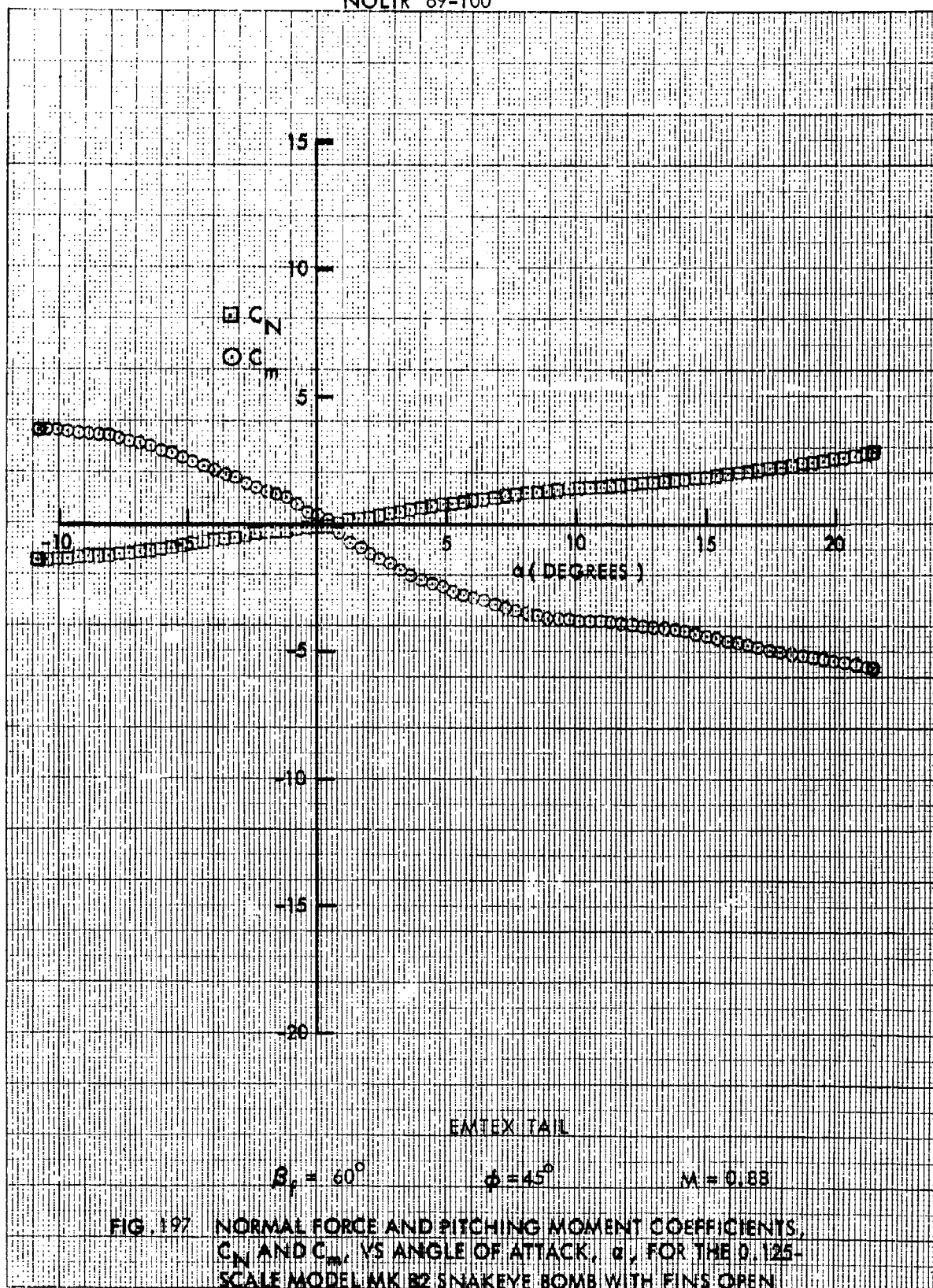


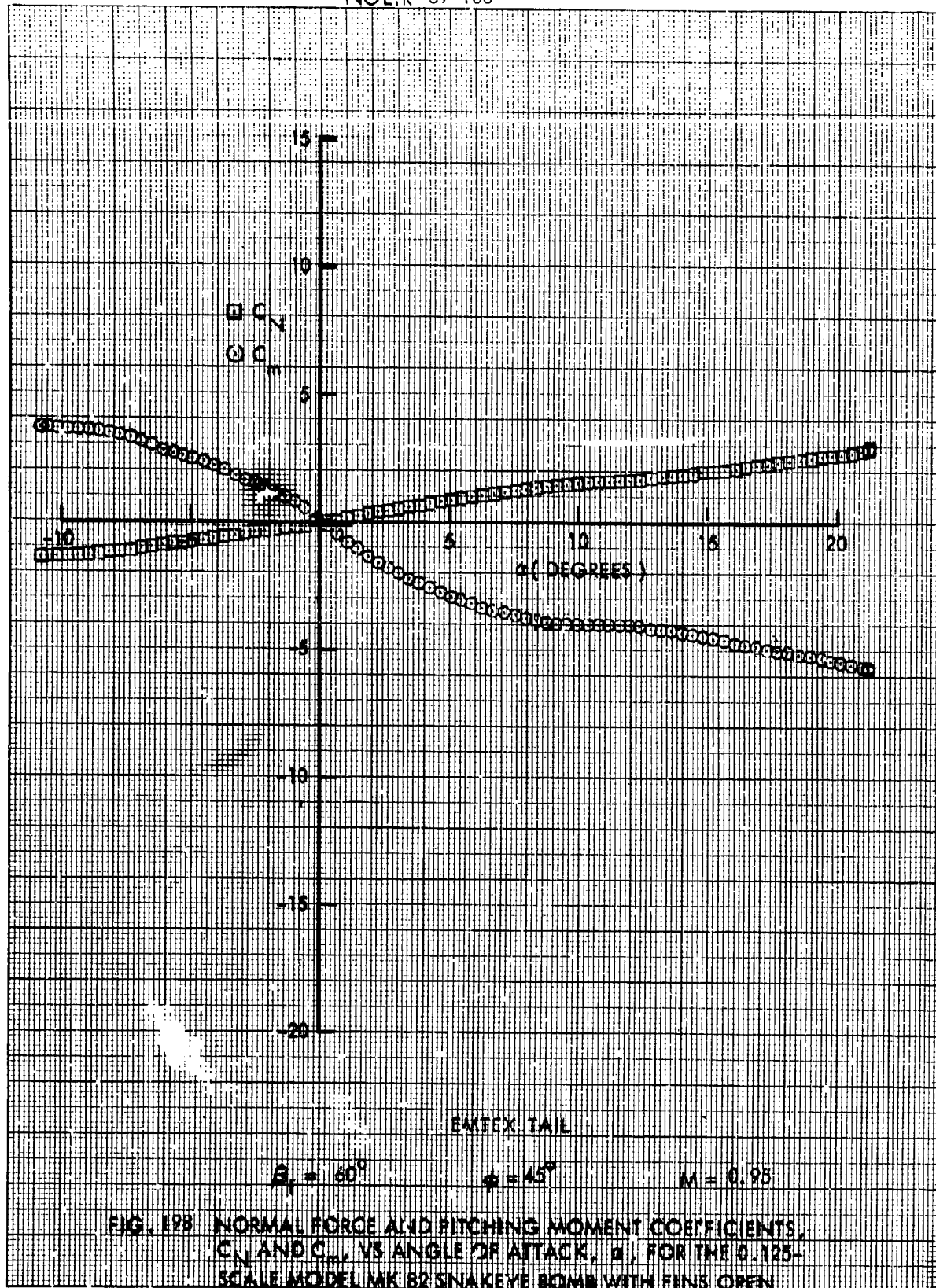


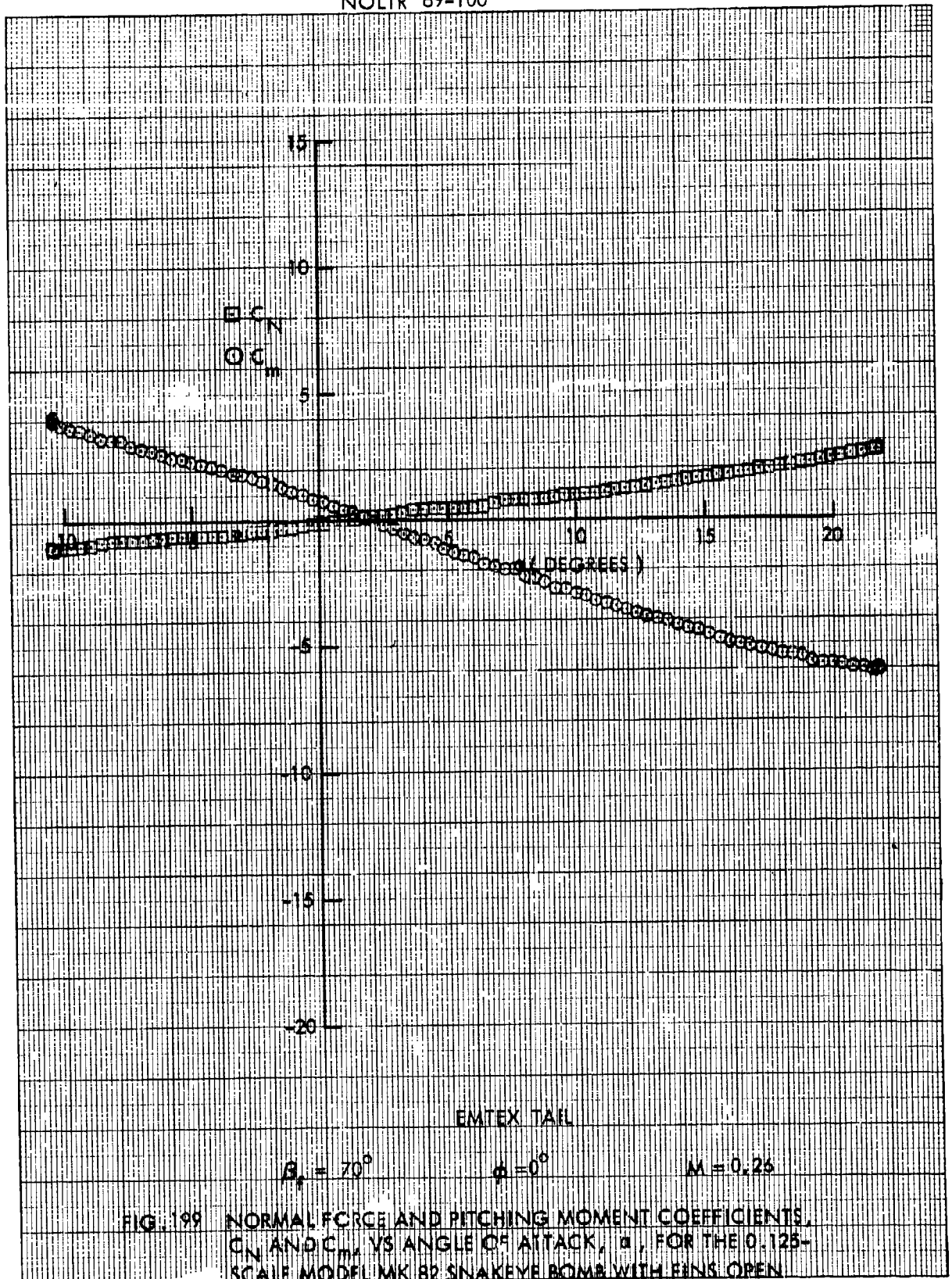


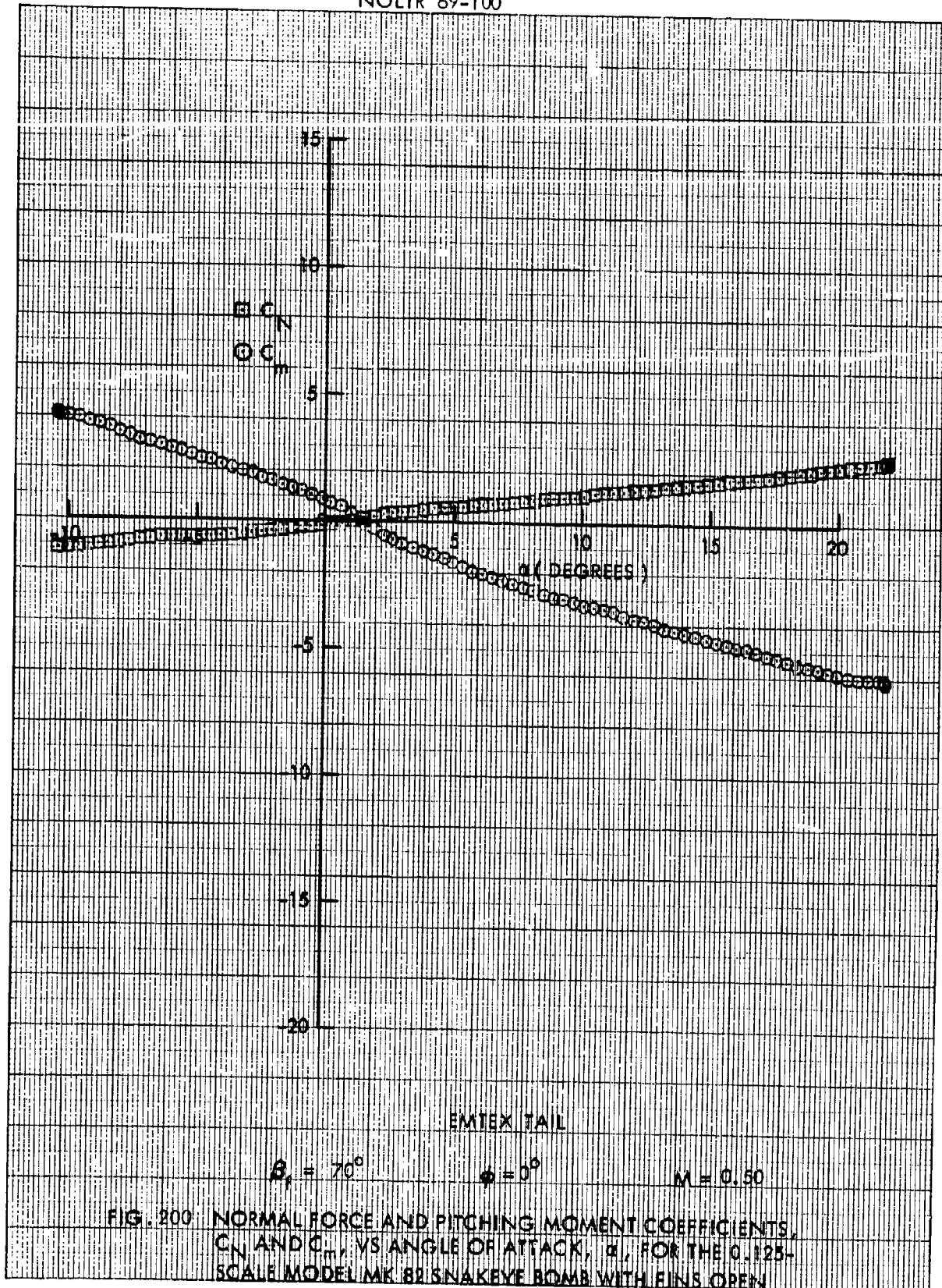




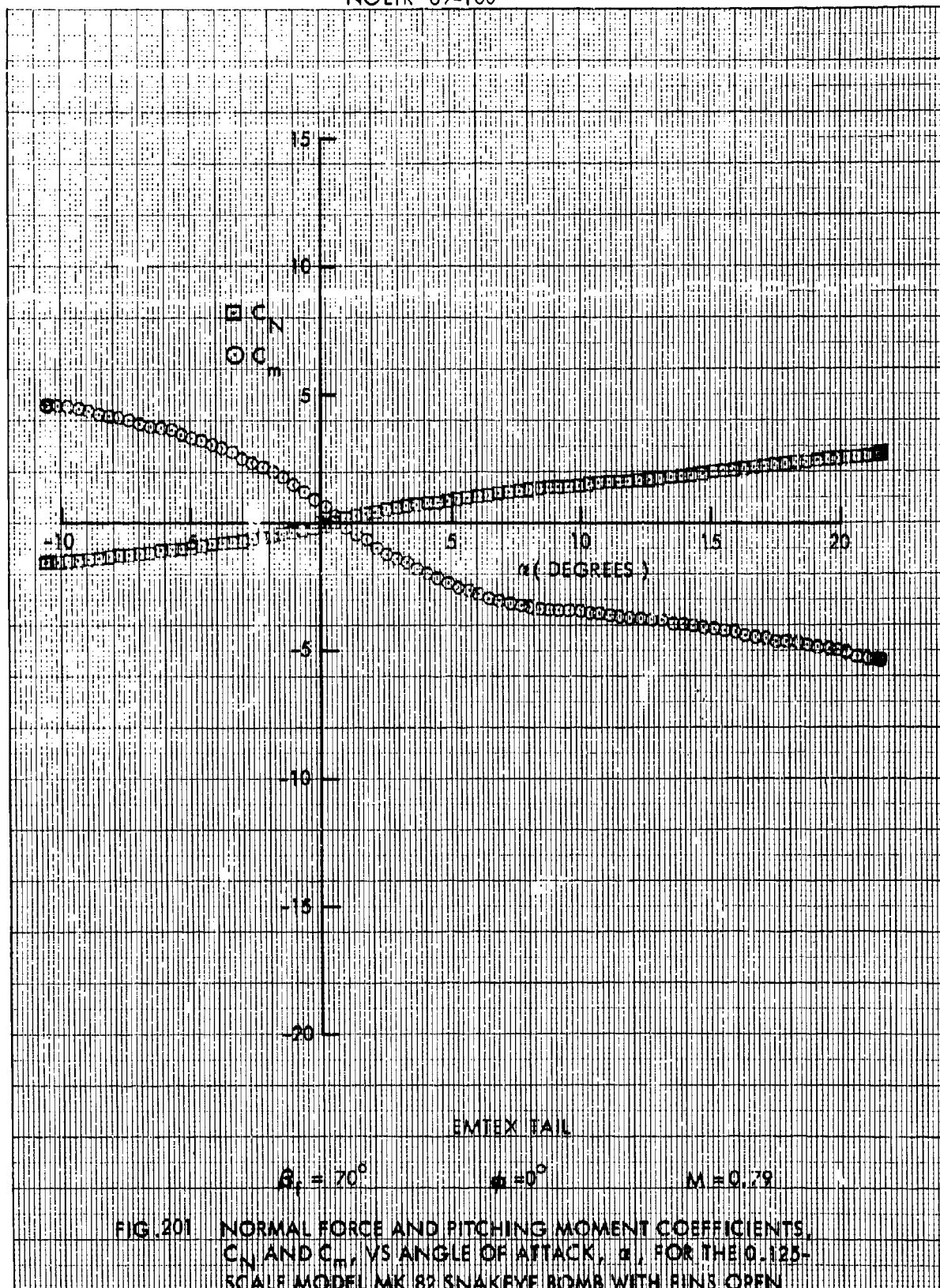




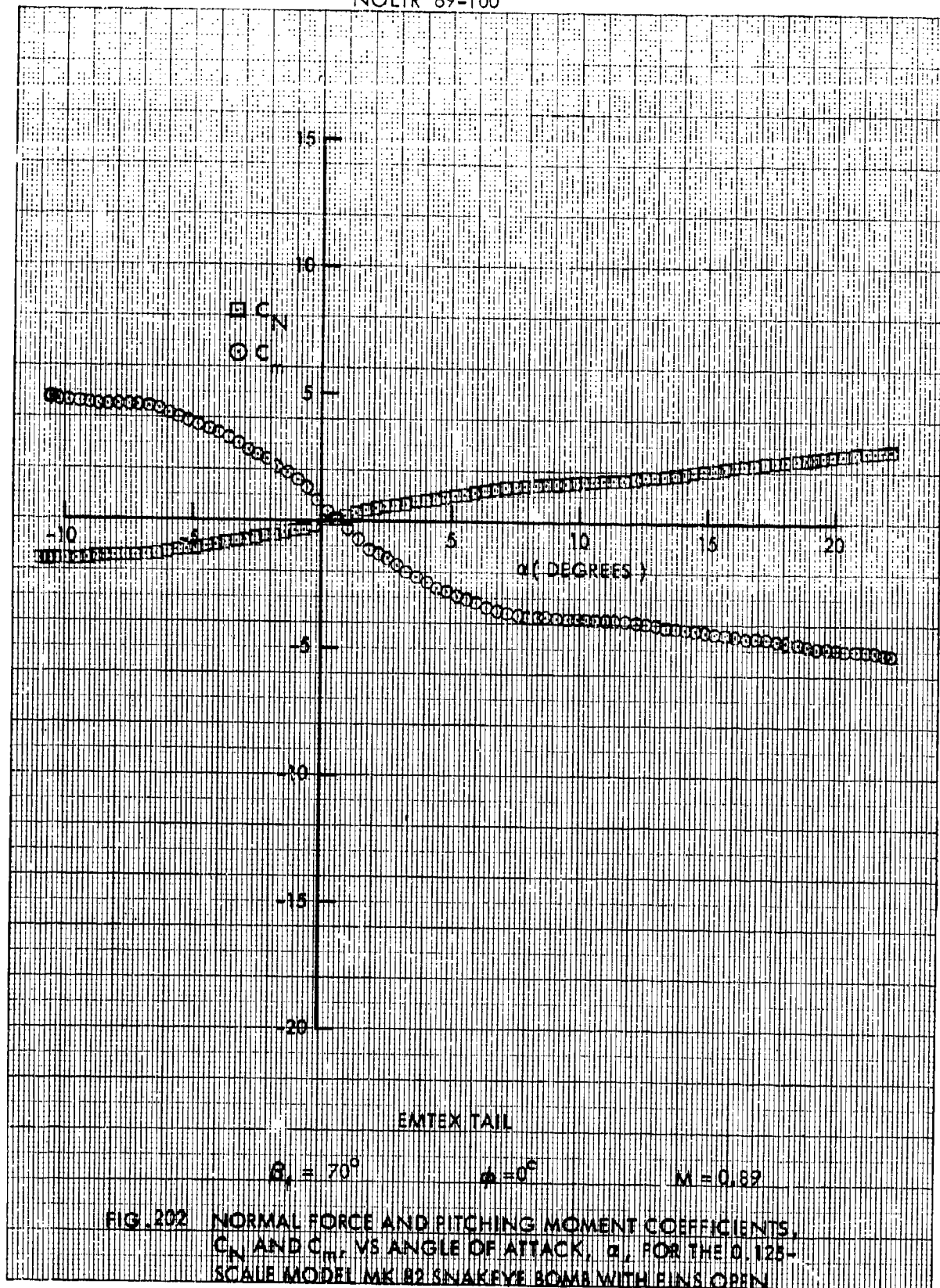


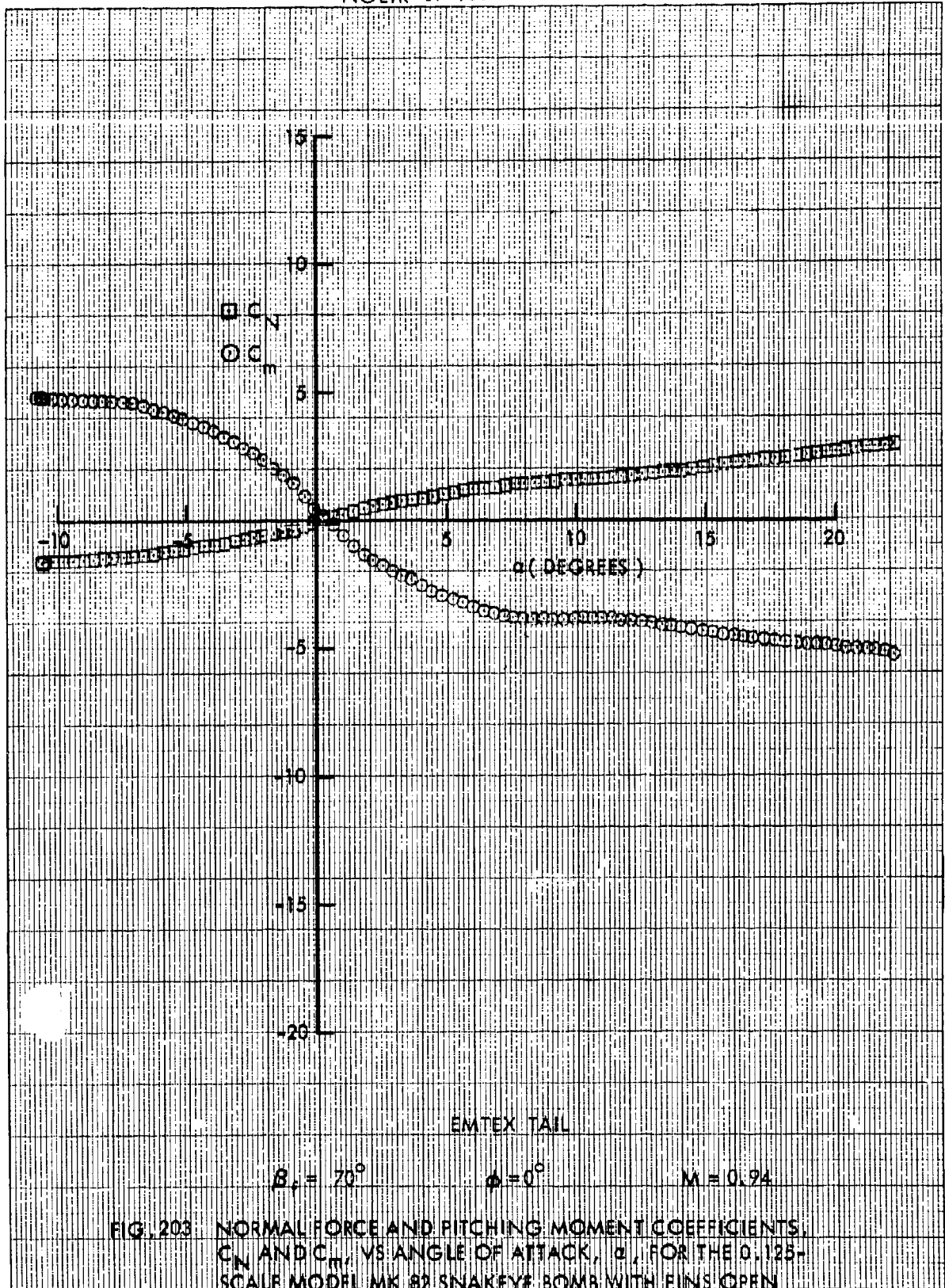


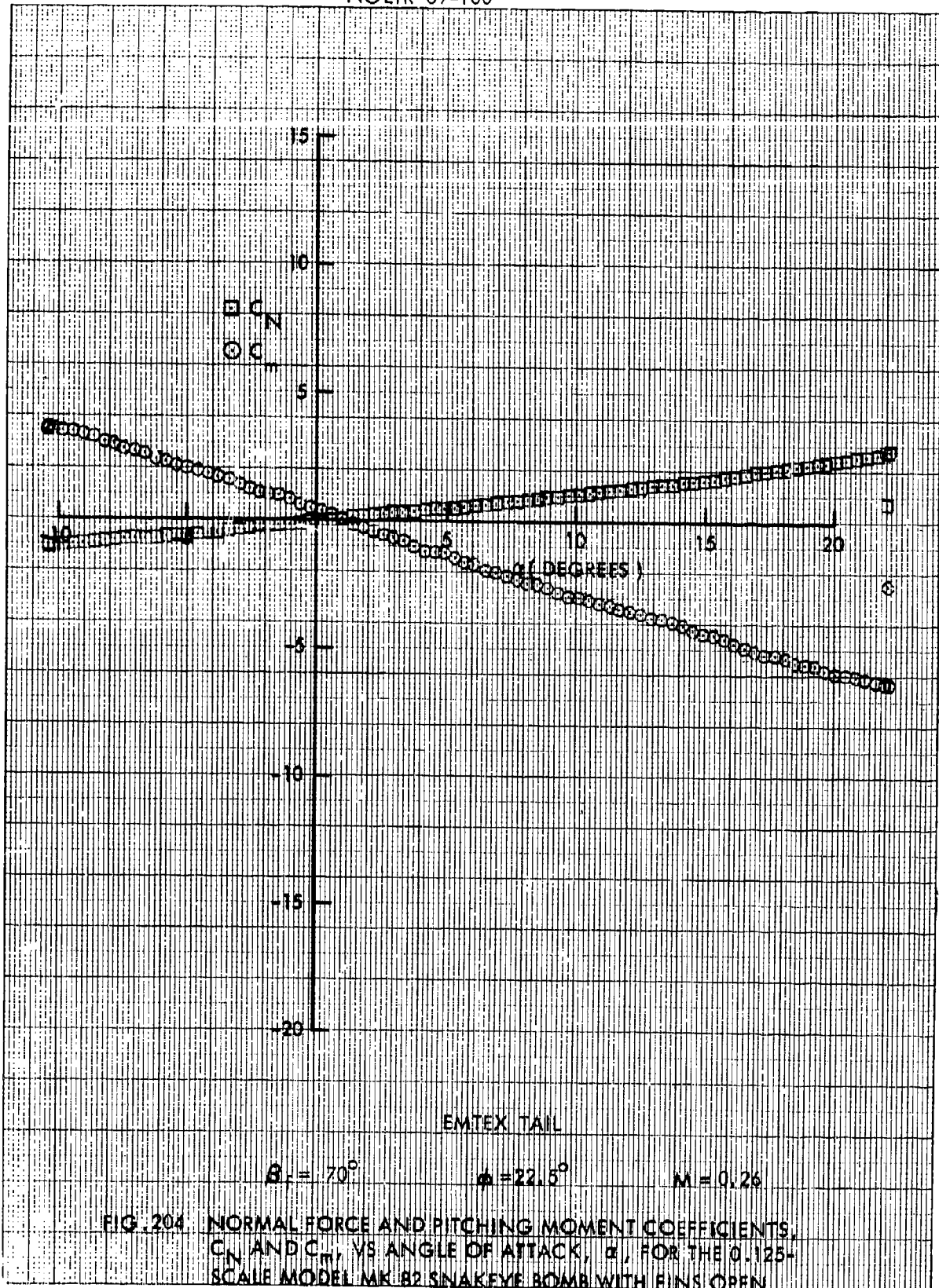


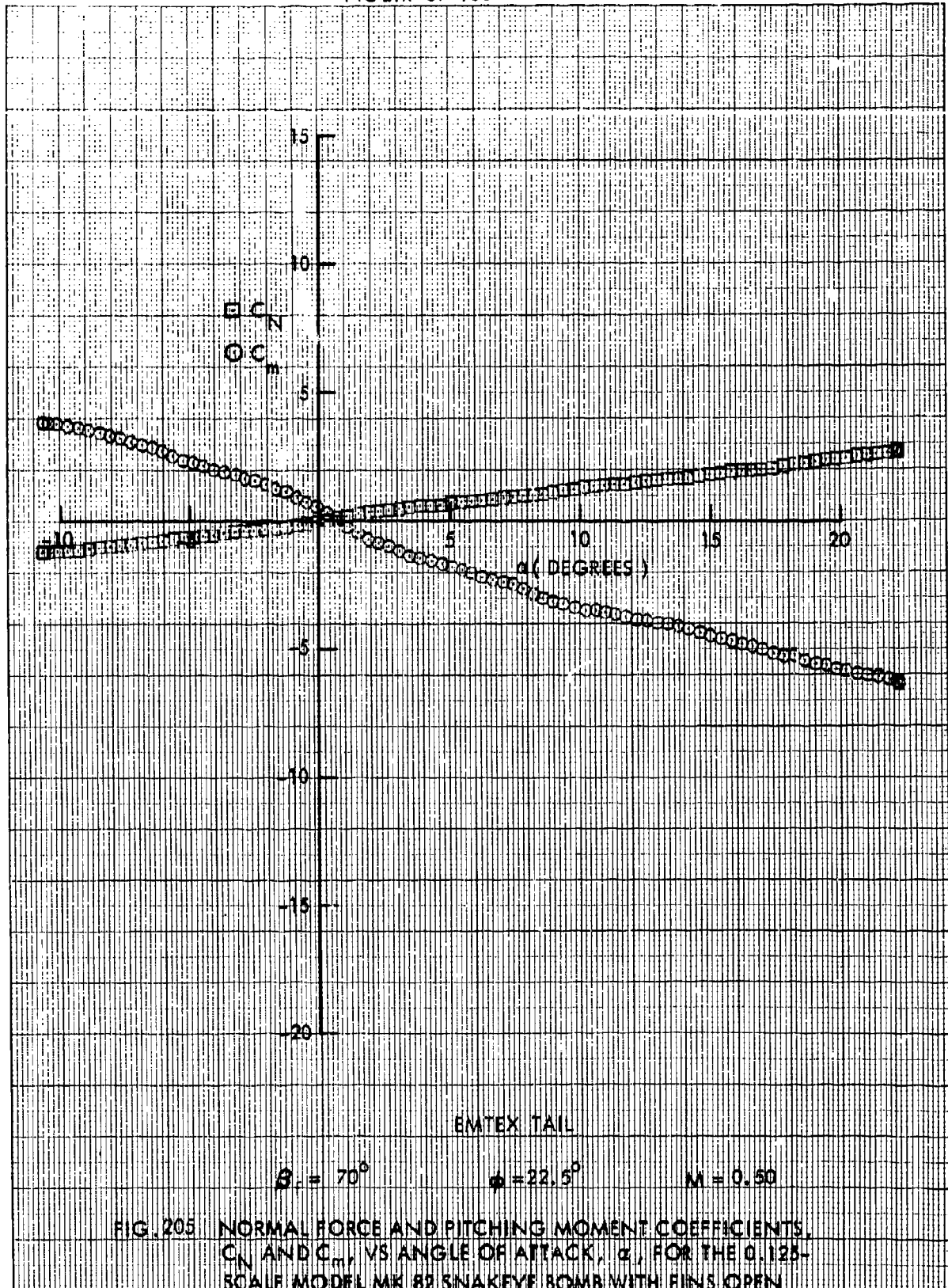


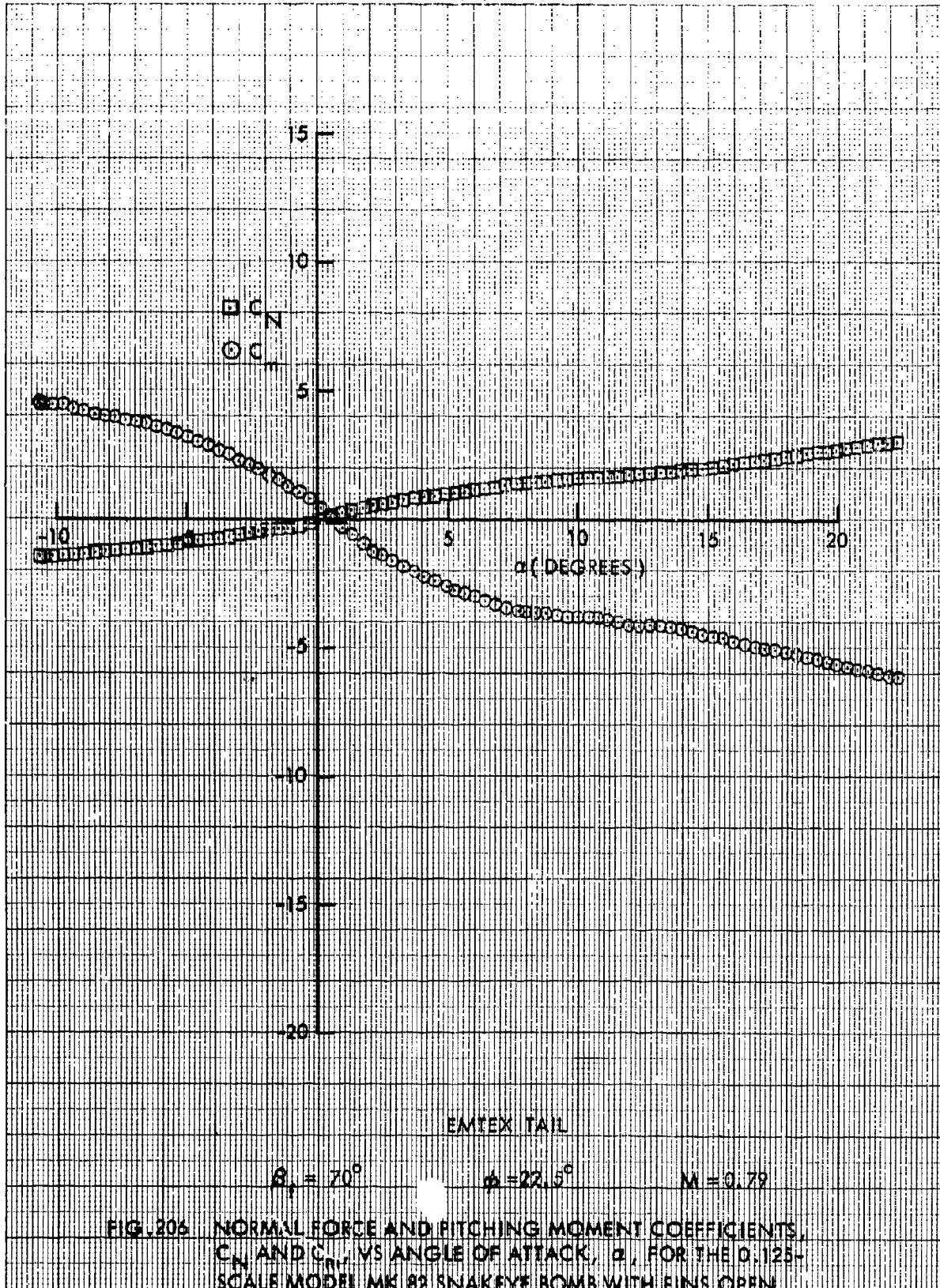




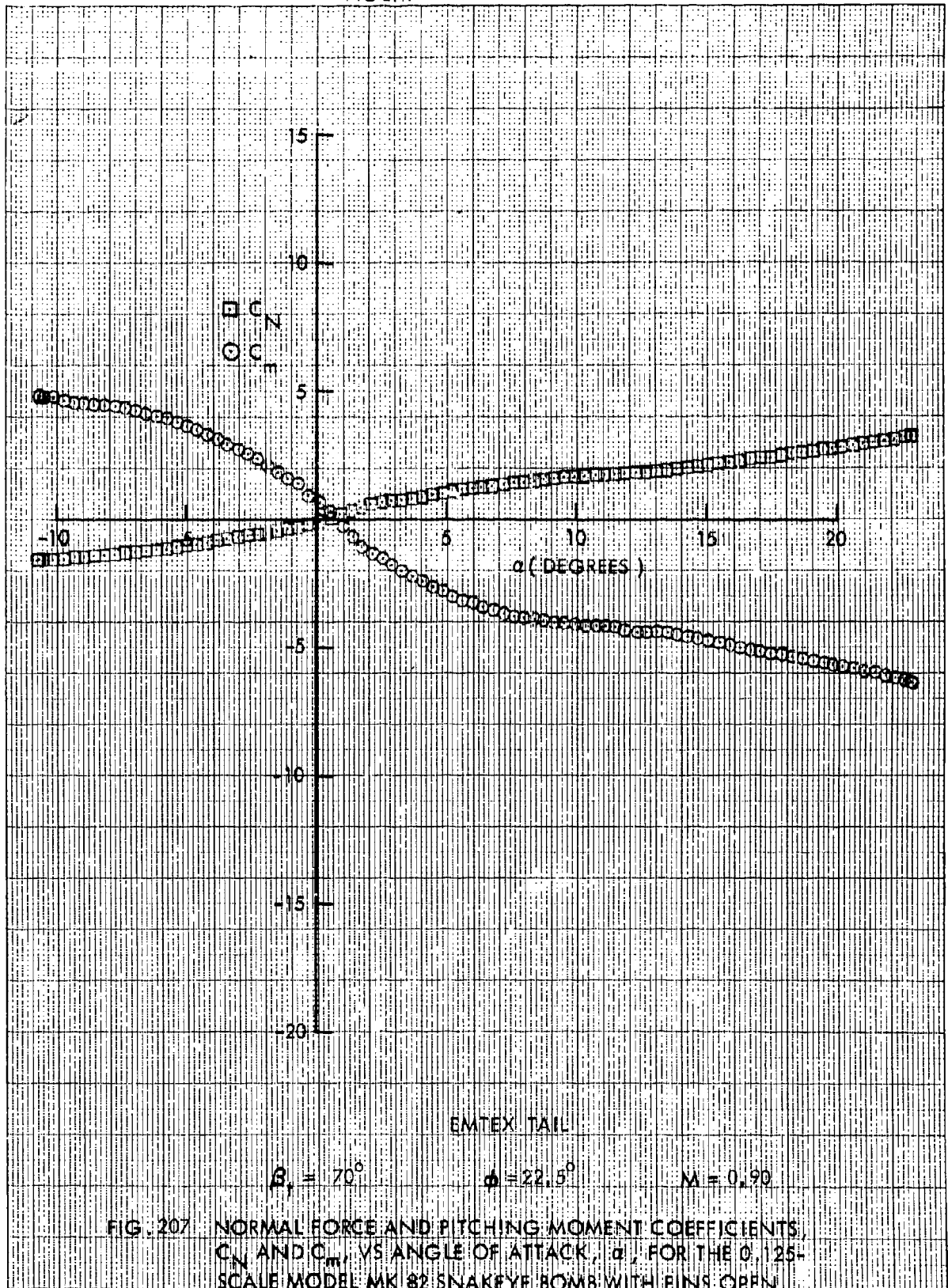




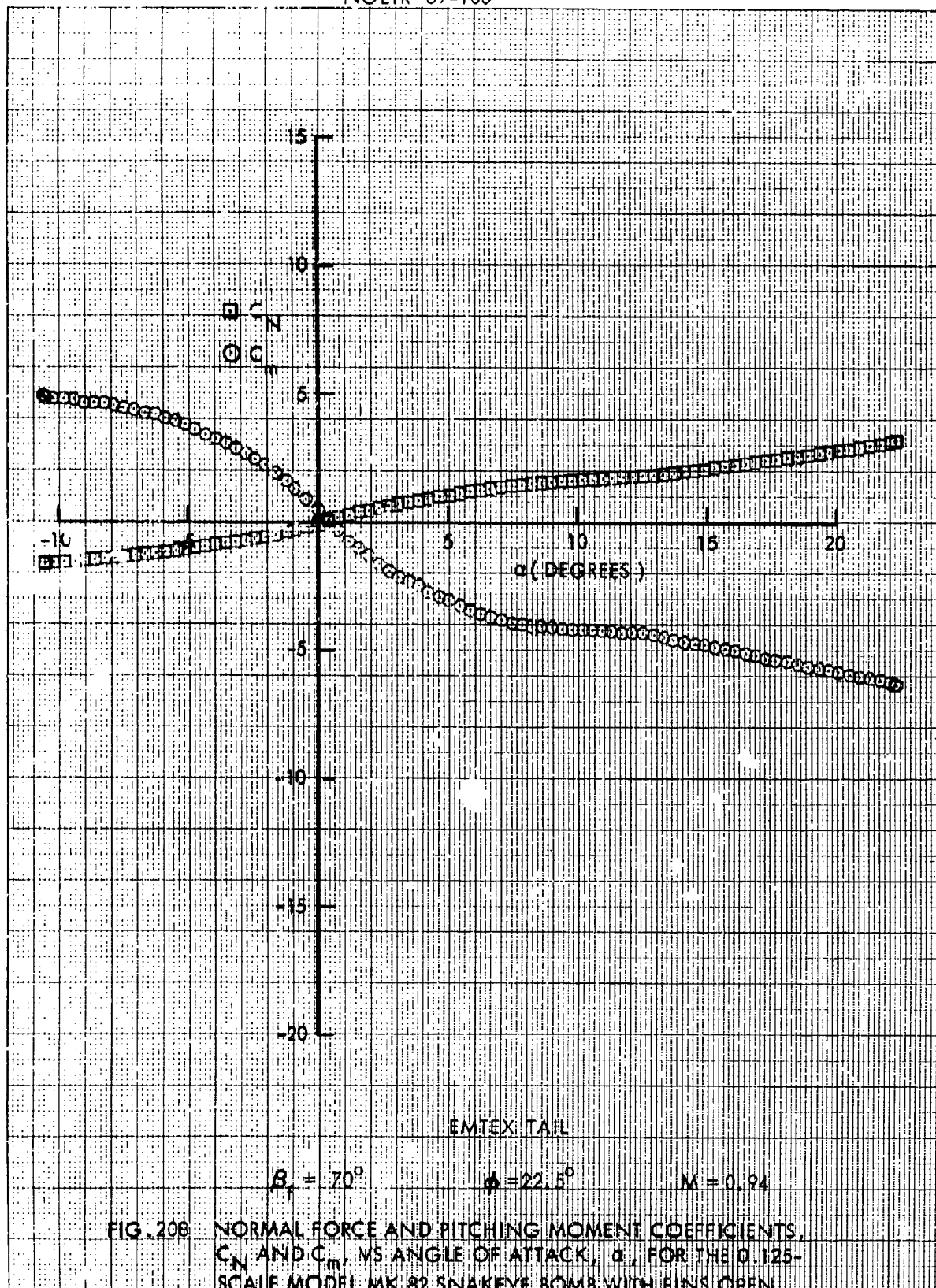


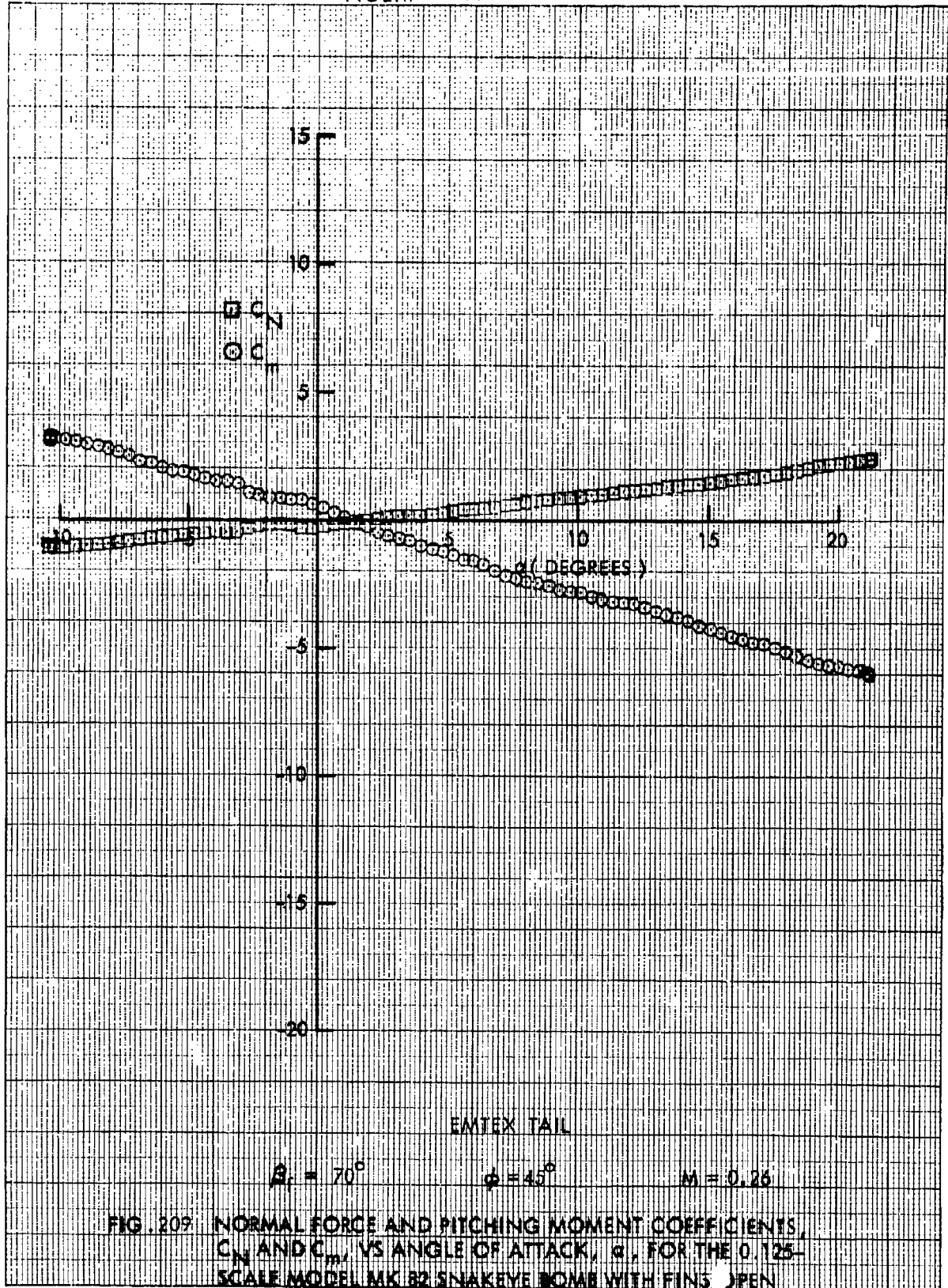


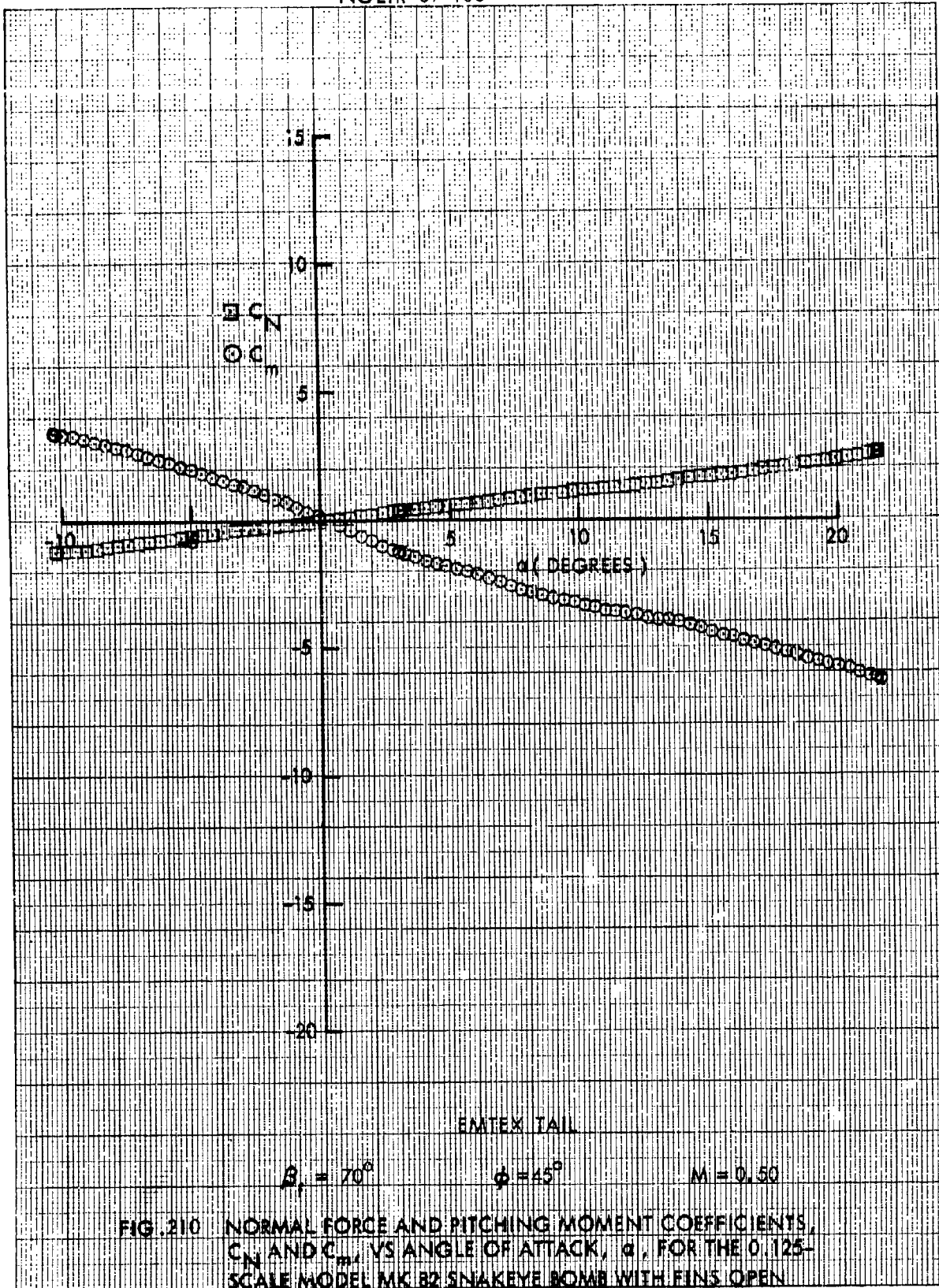


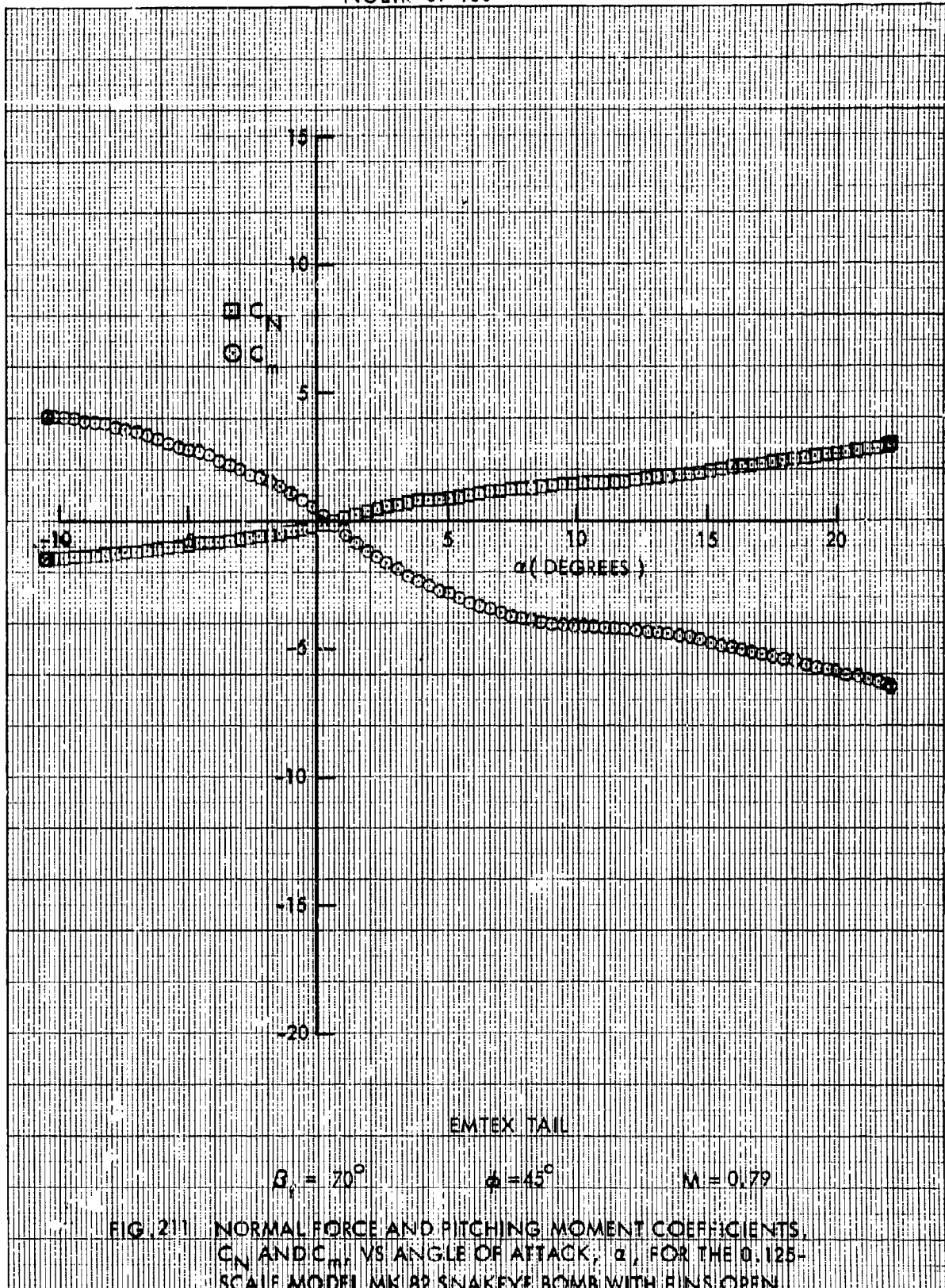


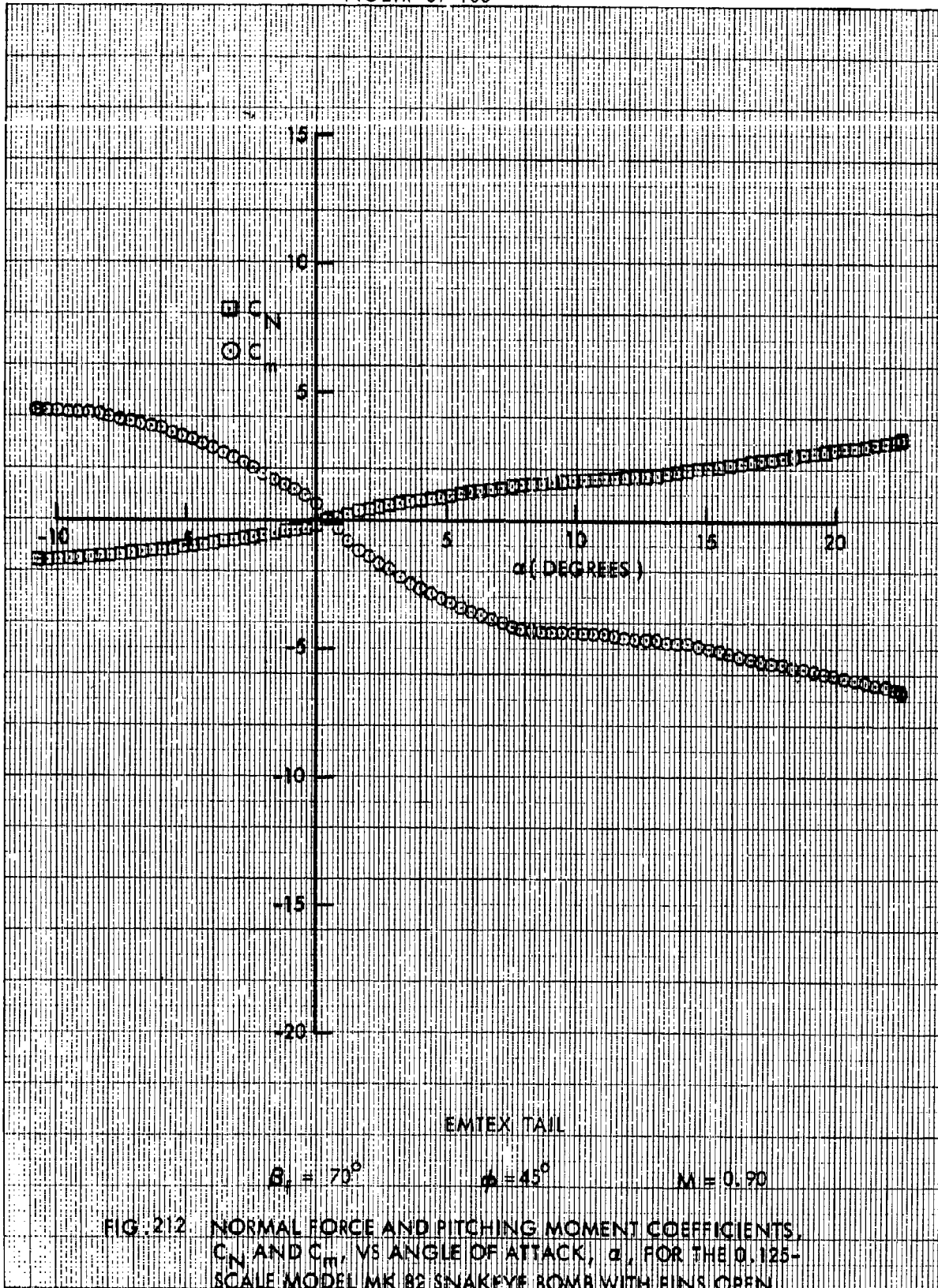




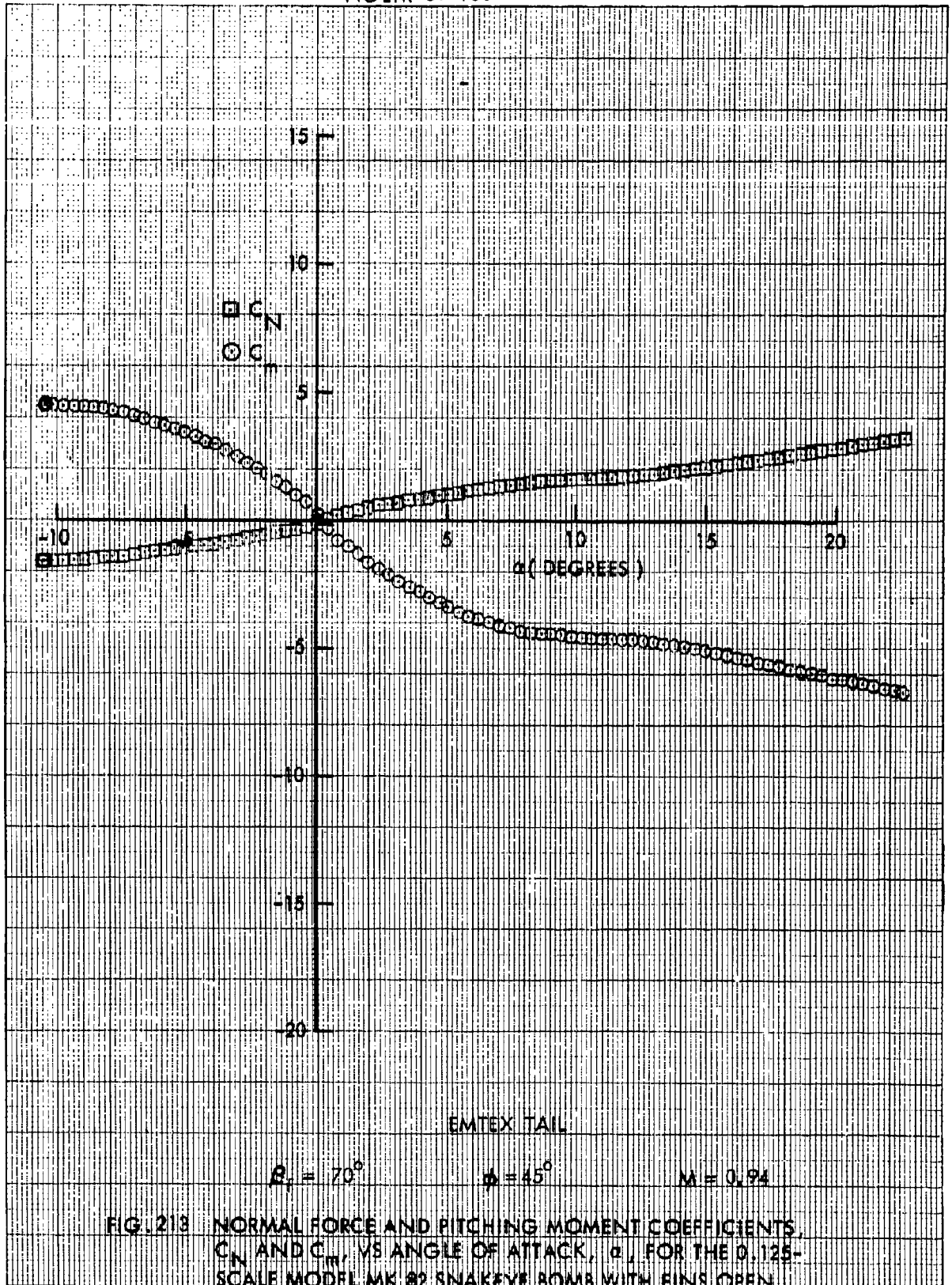




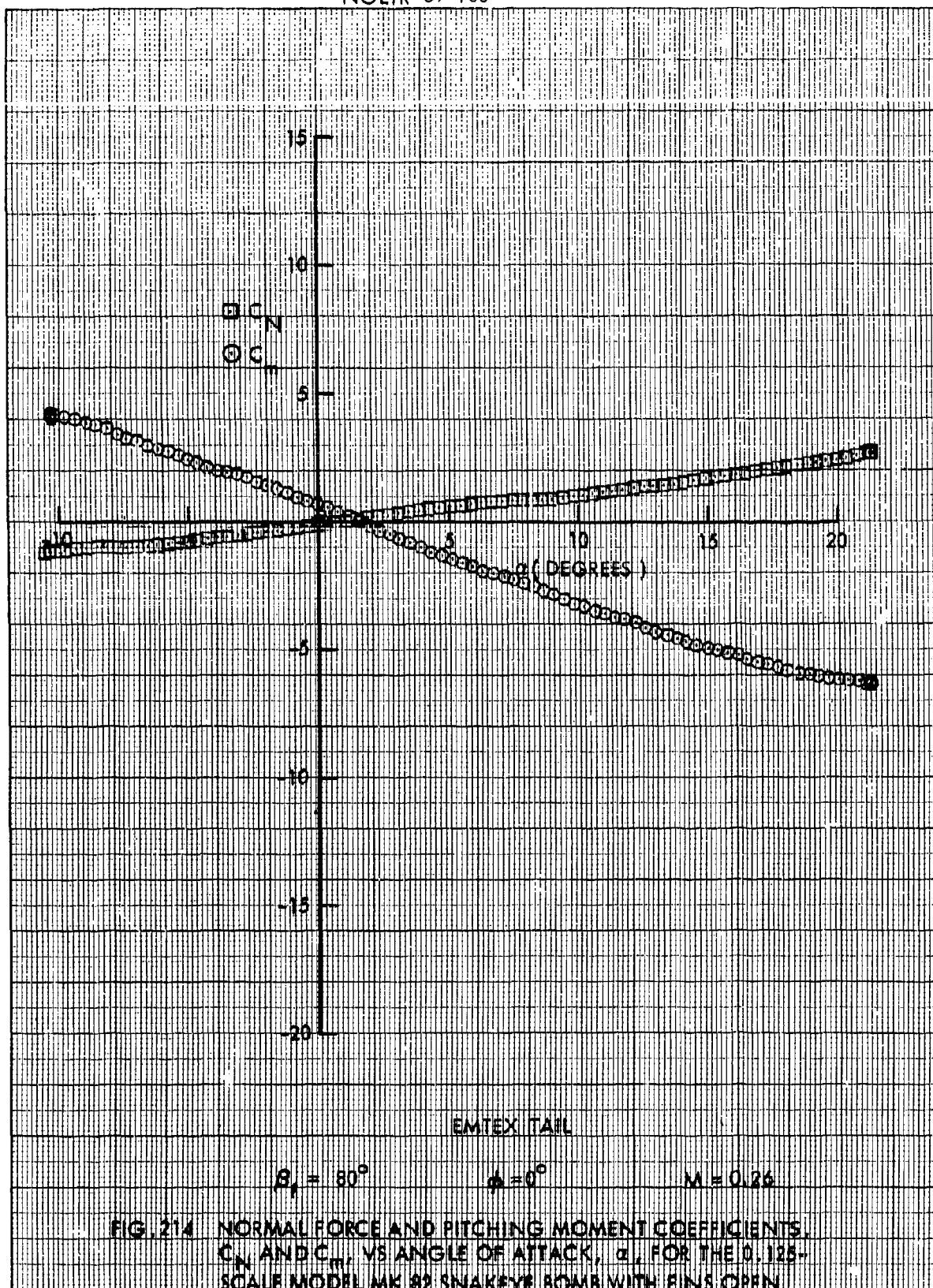


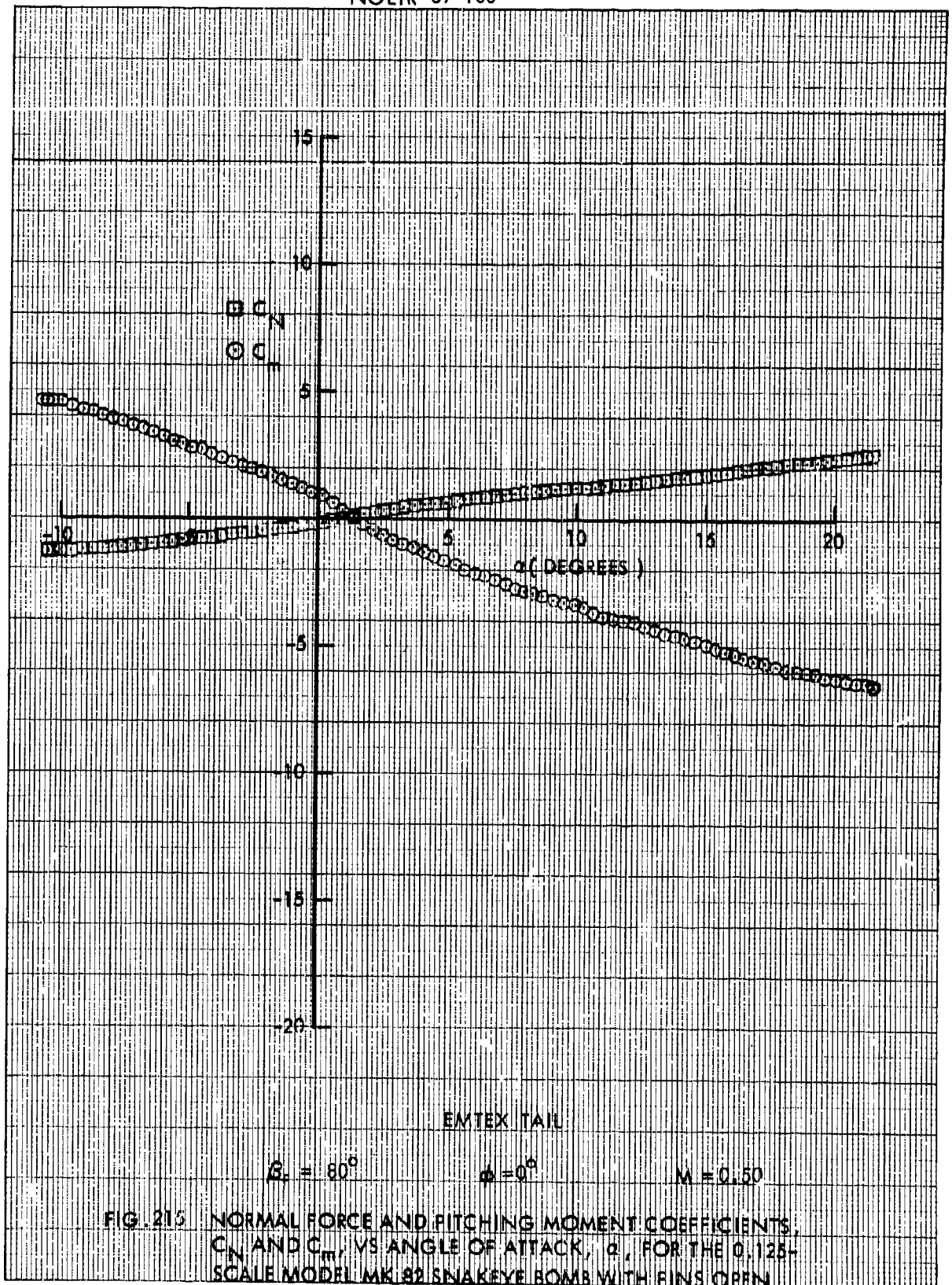


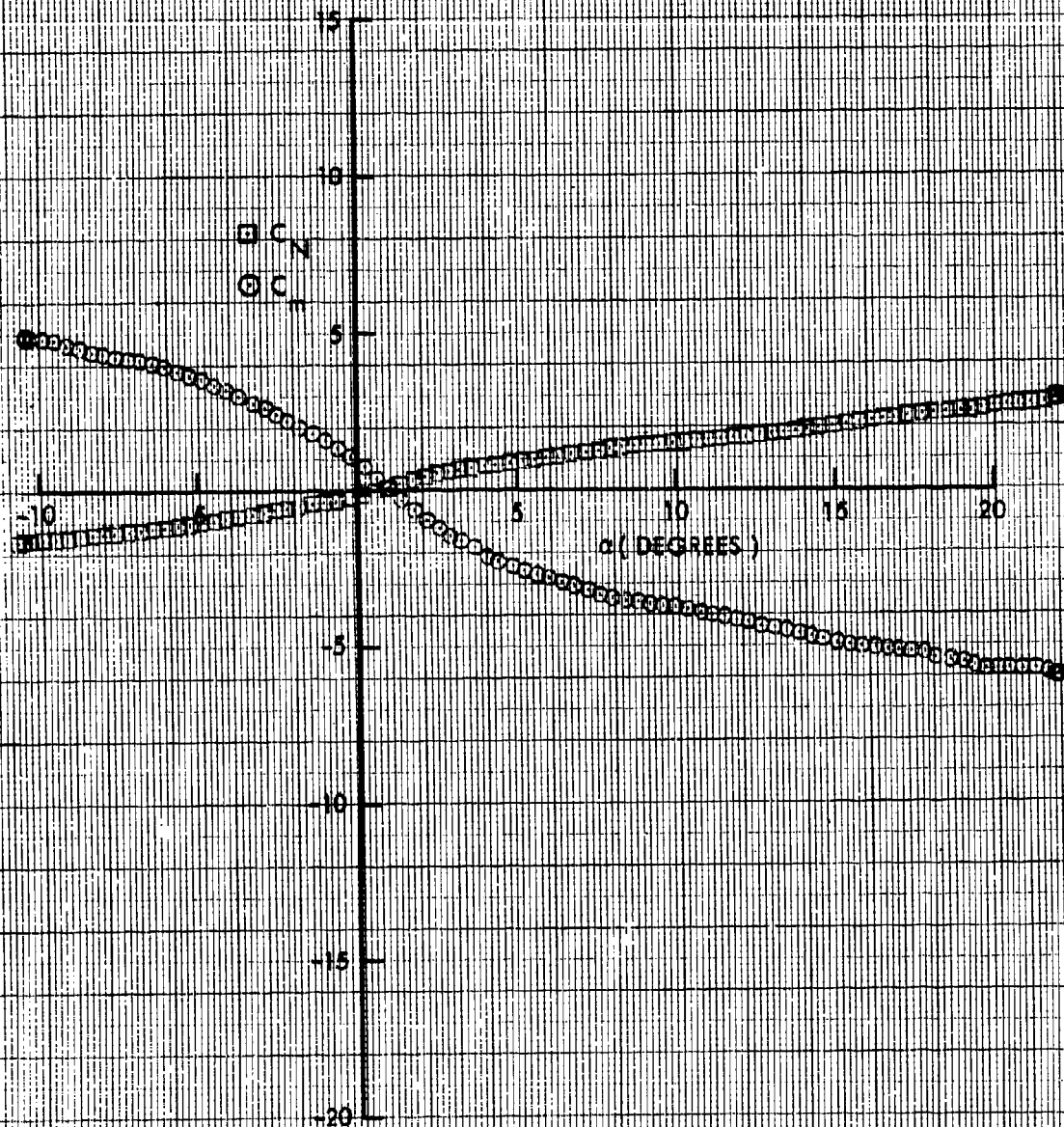












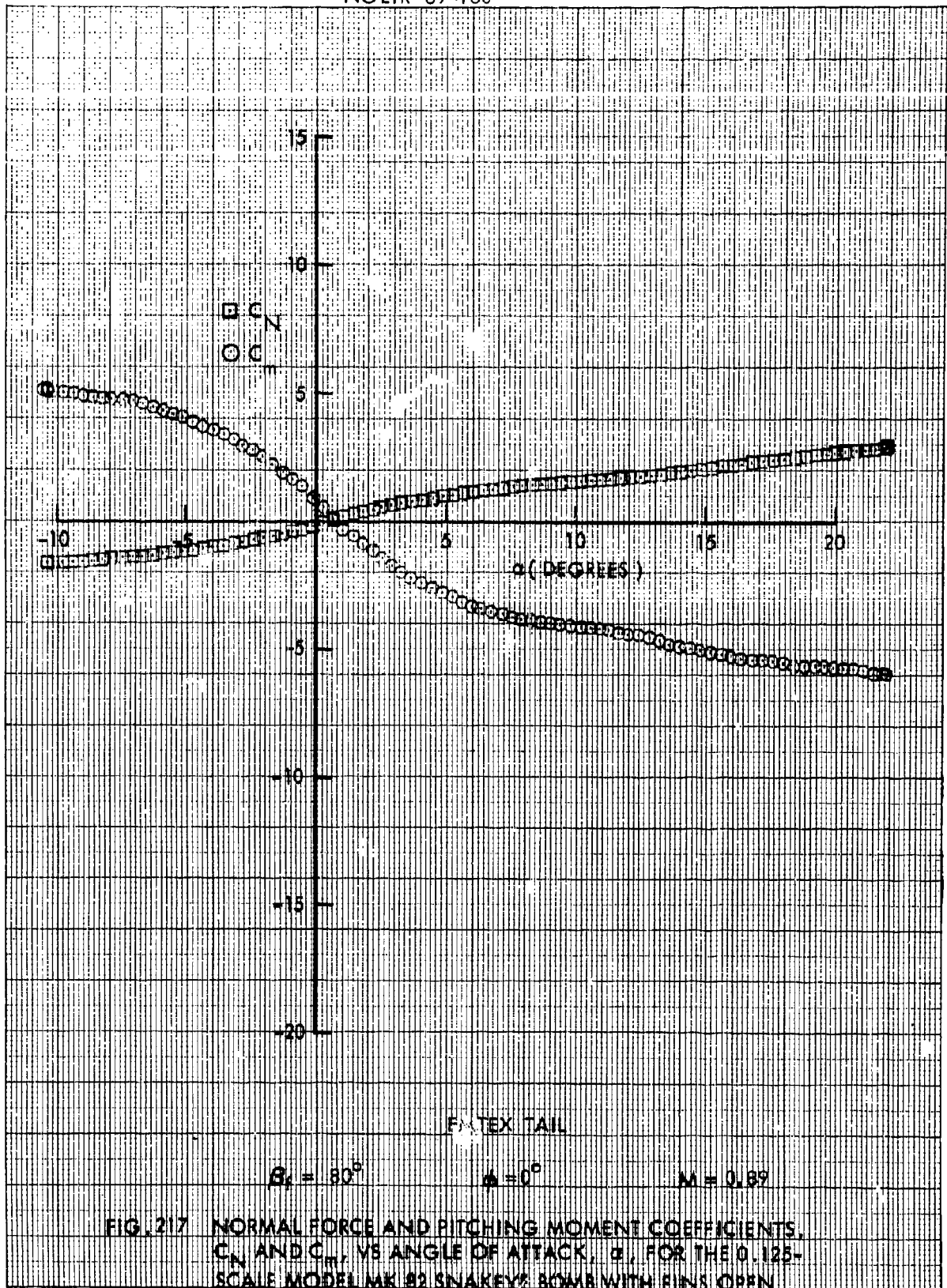
EMTEX TAIL

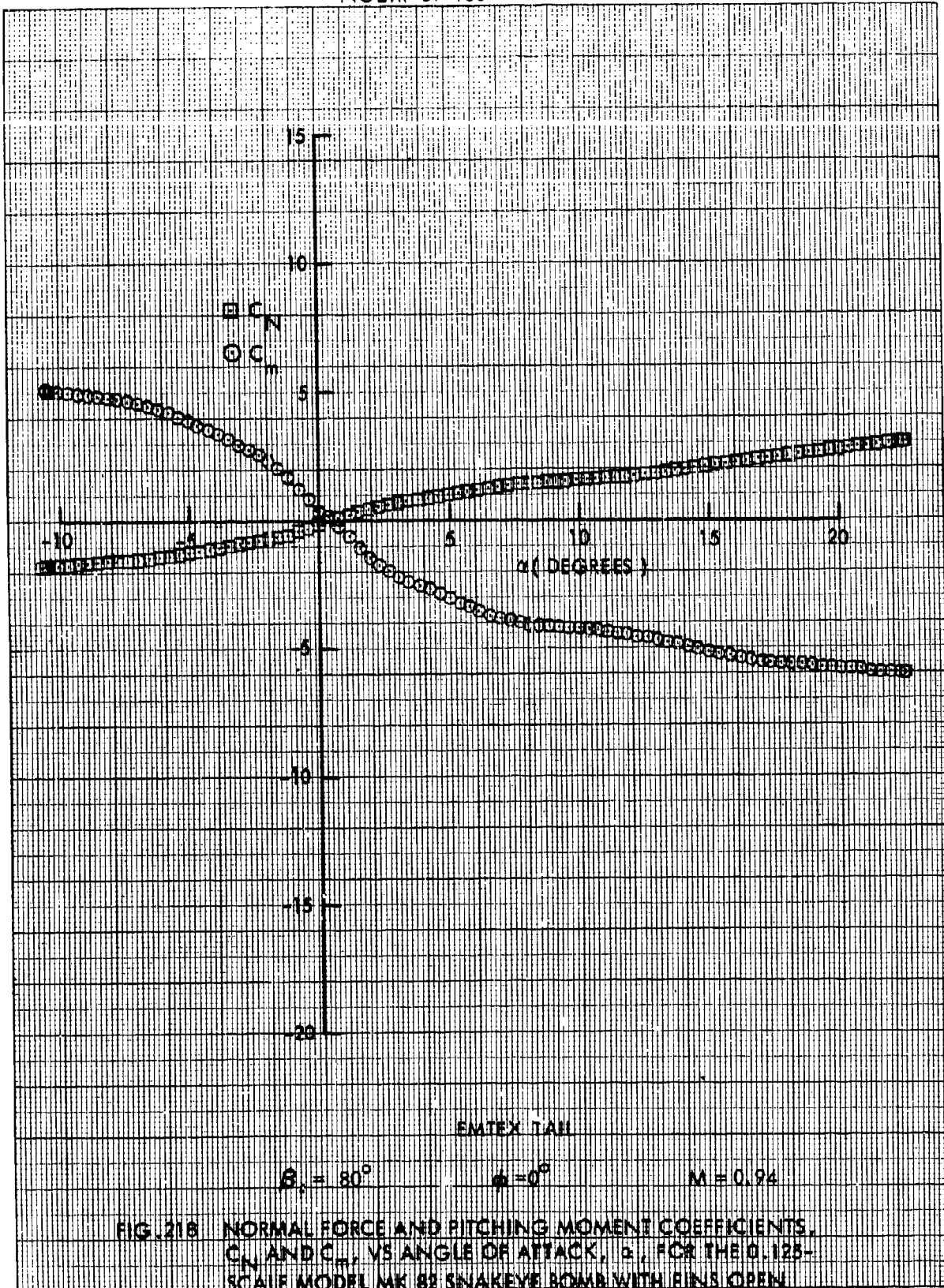
$\beta_r = 80^\circ$

$\phi = 0$

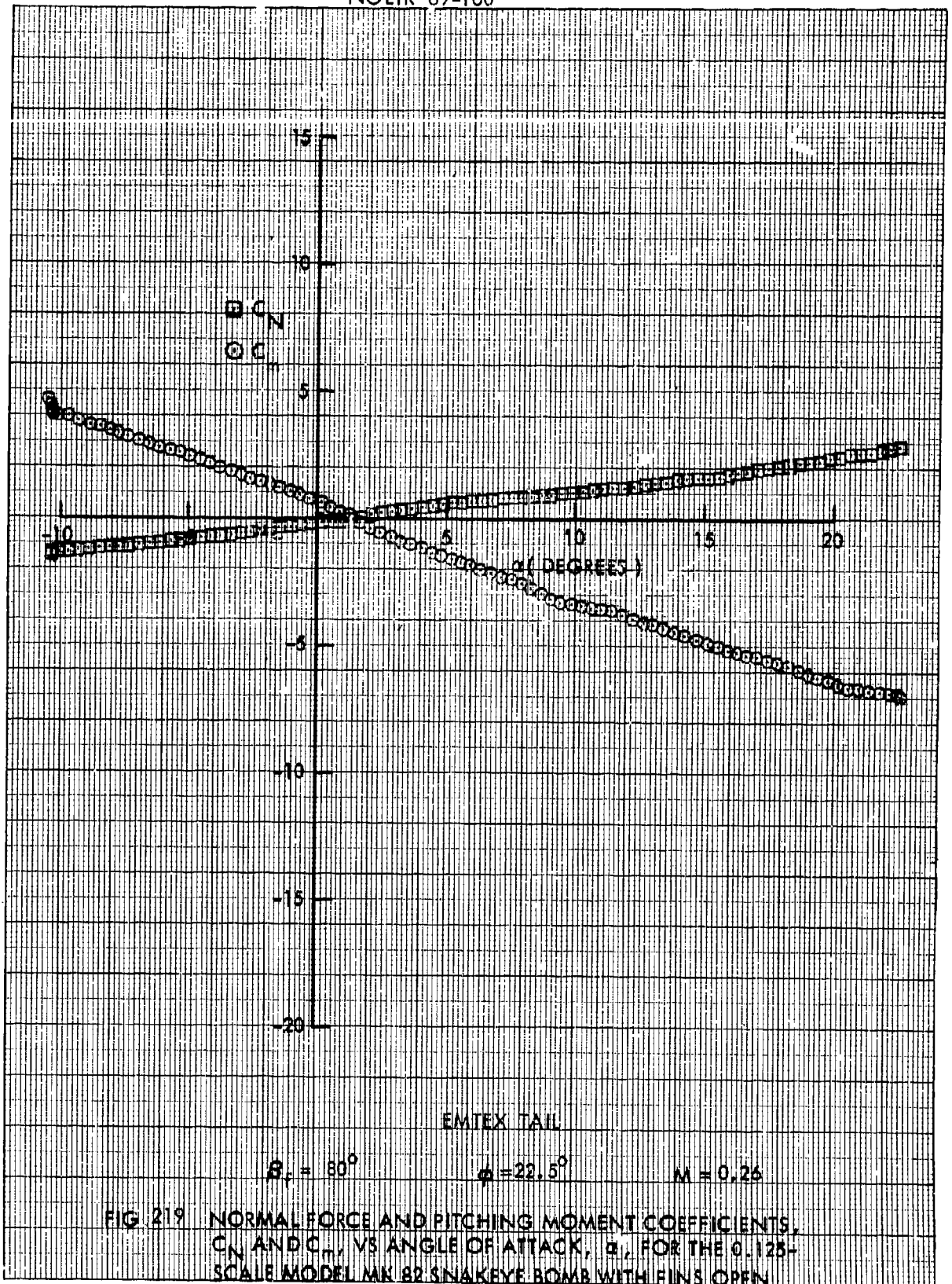
$M = 0.79$

FIG. 216 NORMAL FORCE AND PITCHING MOMENT COEFFICIENTS,  $C_N$  AND  $C_m$ , VS ANGLE OF ATTACK,  $\alpha$ , FOR THE 0.125-SCALE MODEL MK B2 GNAKEYE BOMB WITH FINS OPEN

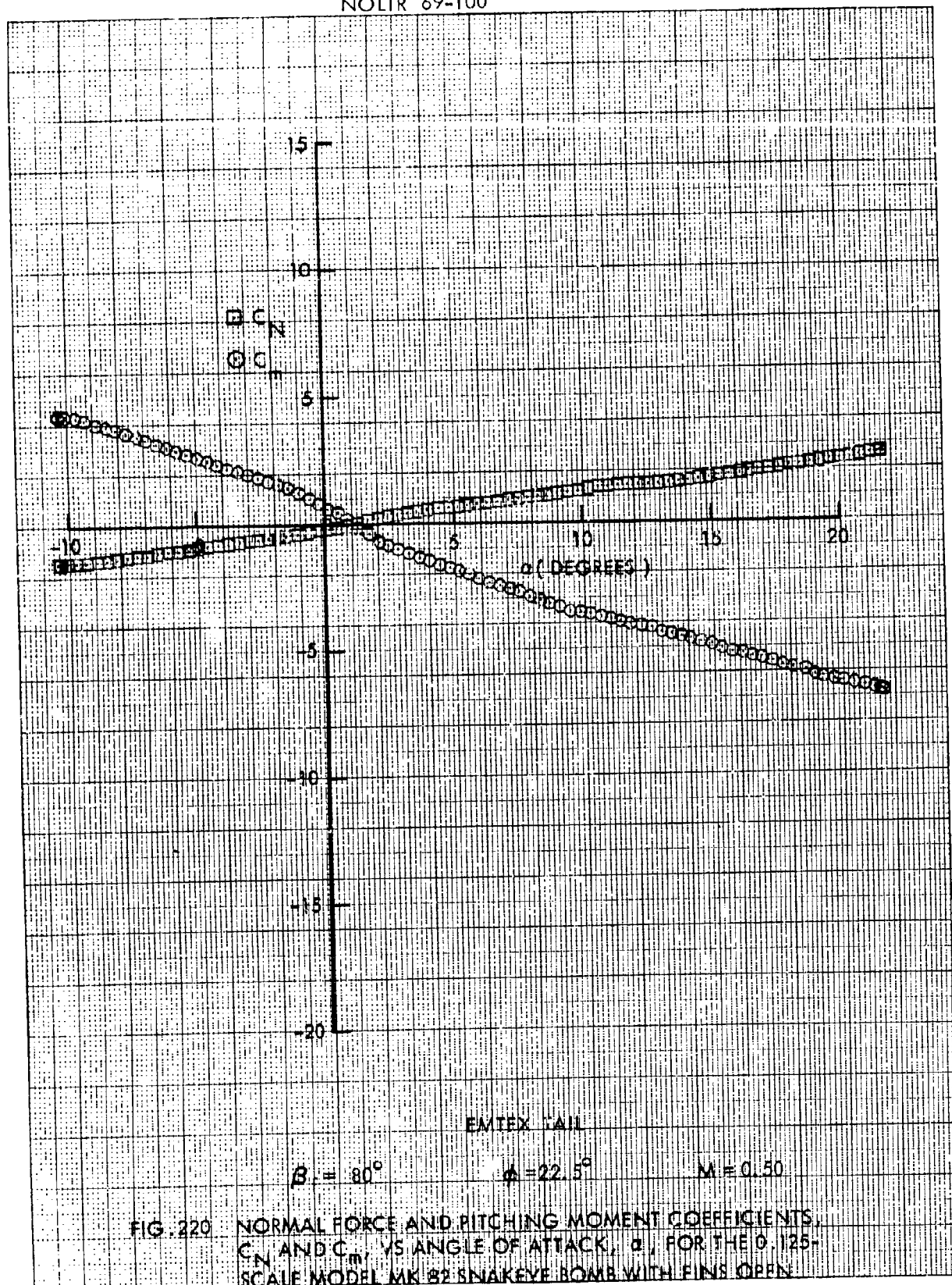












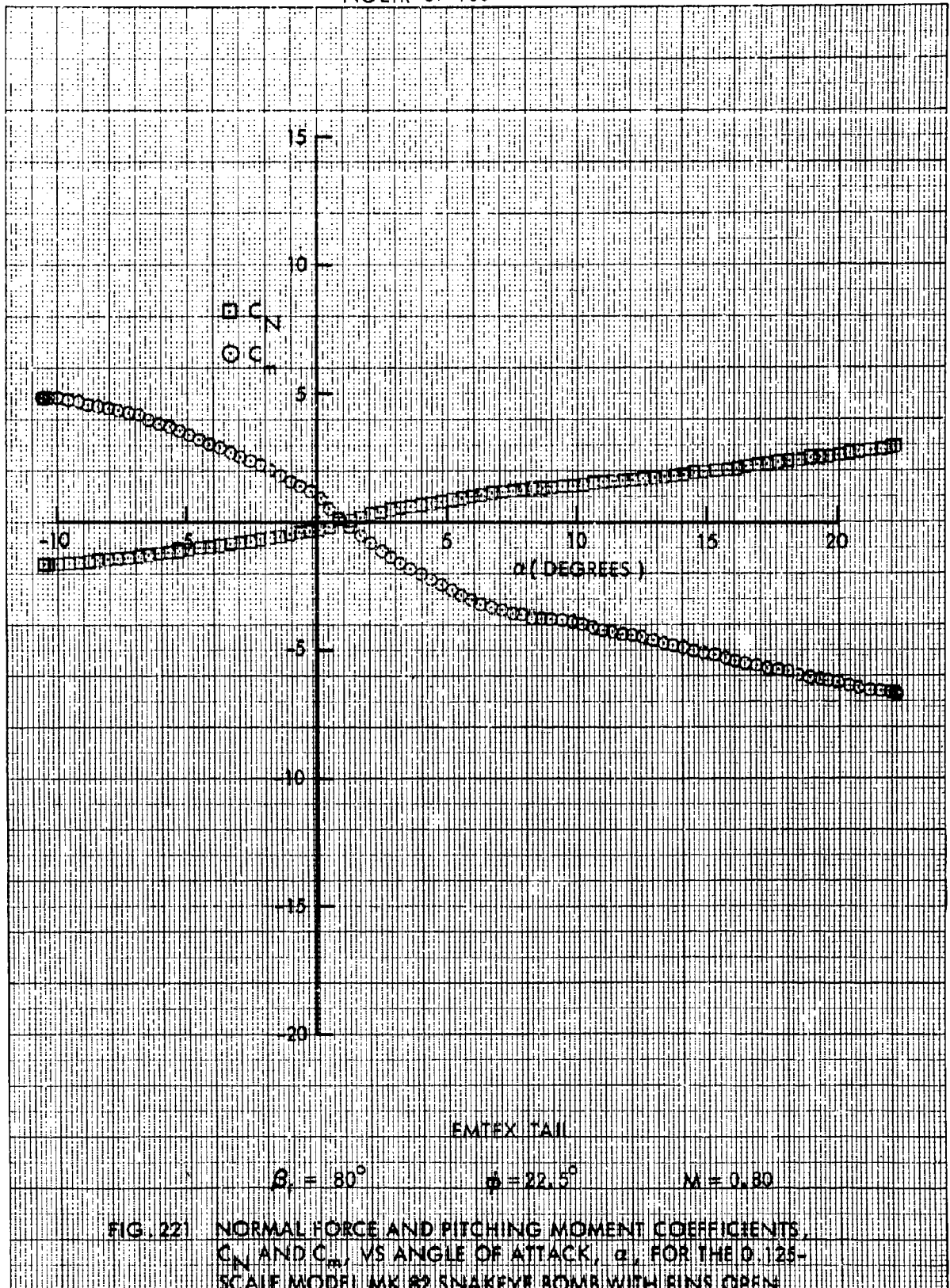
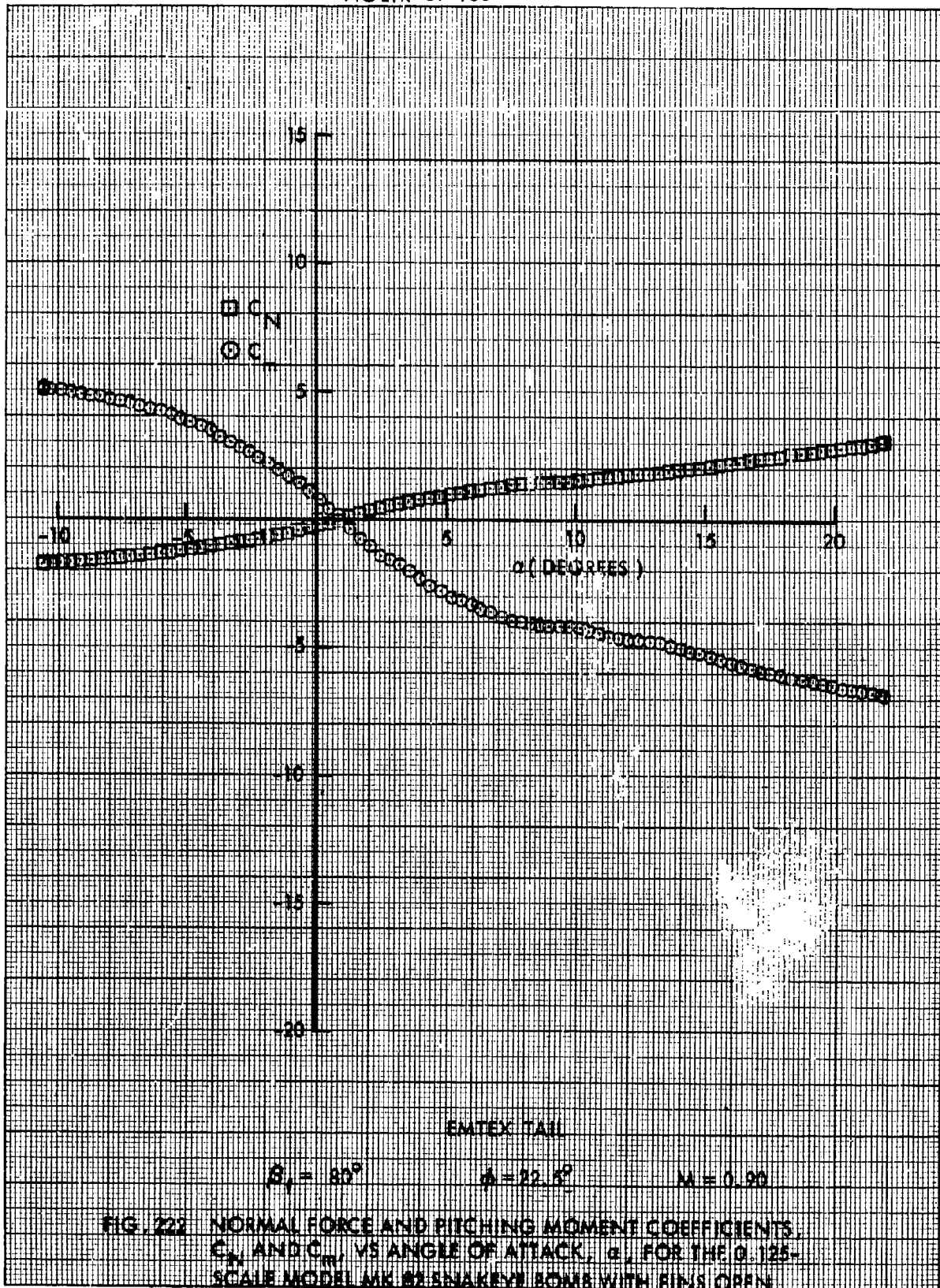
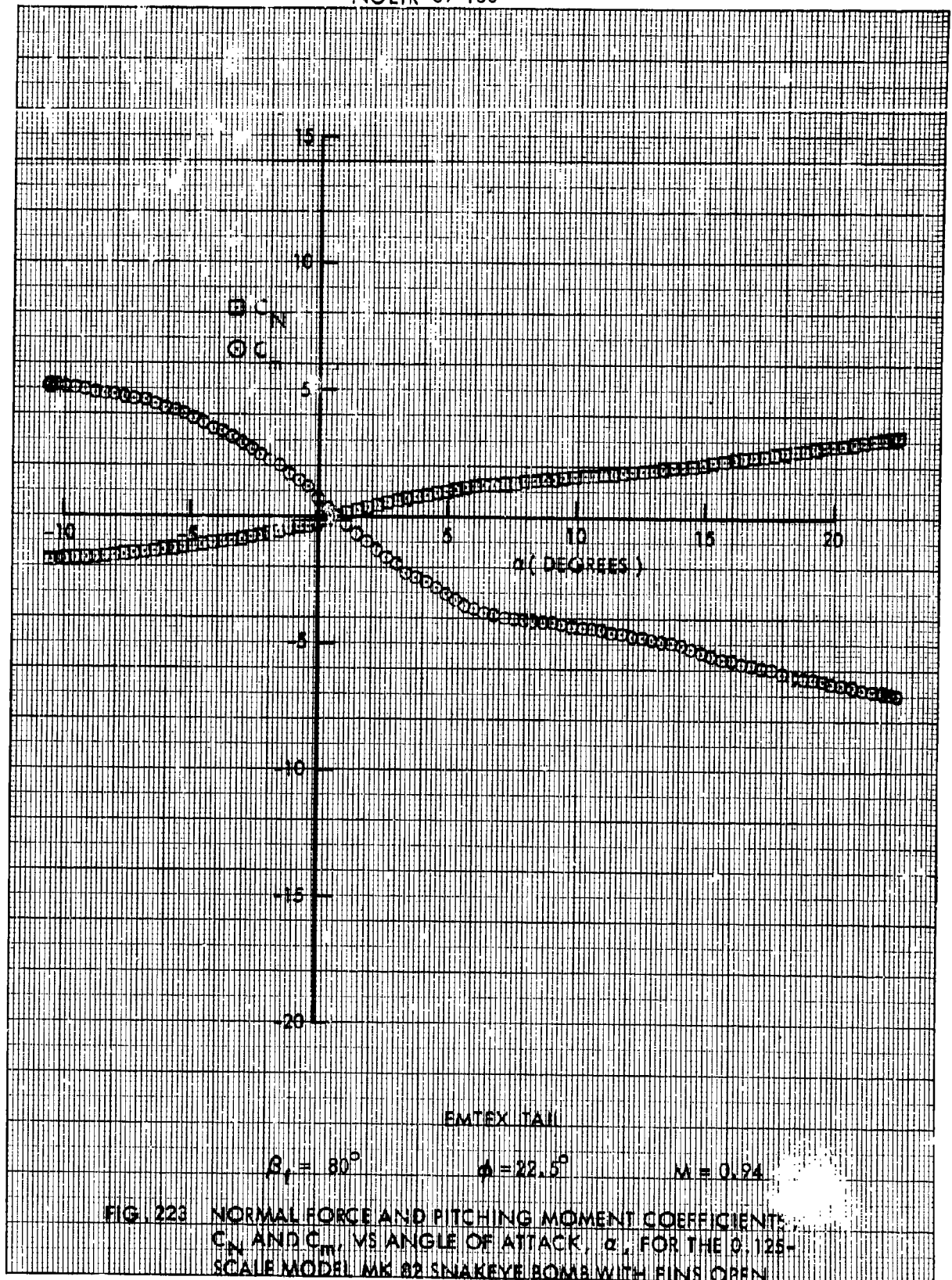
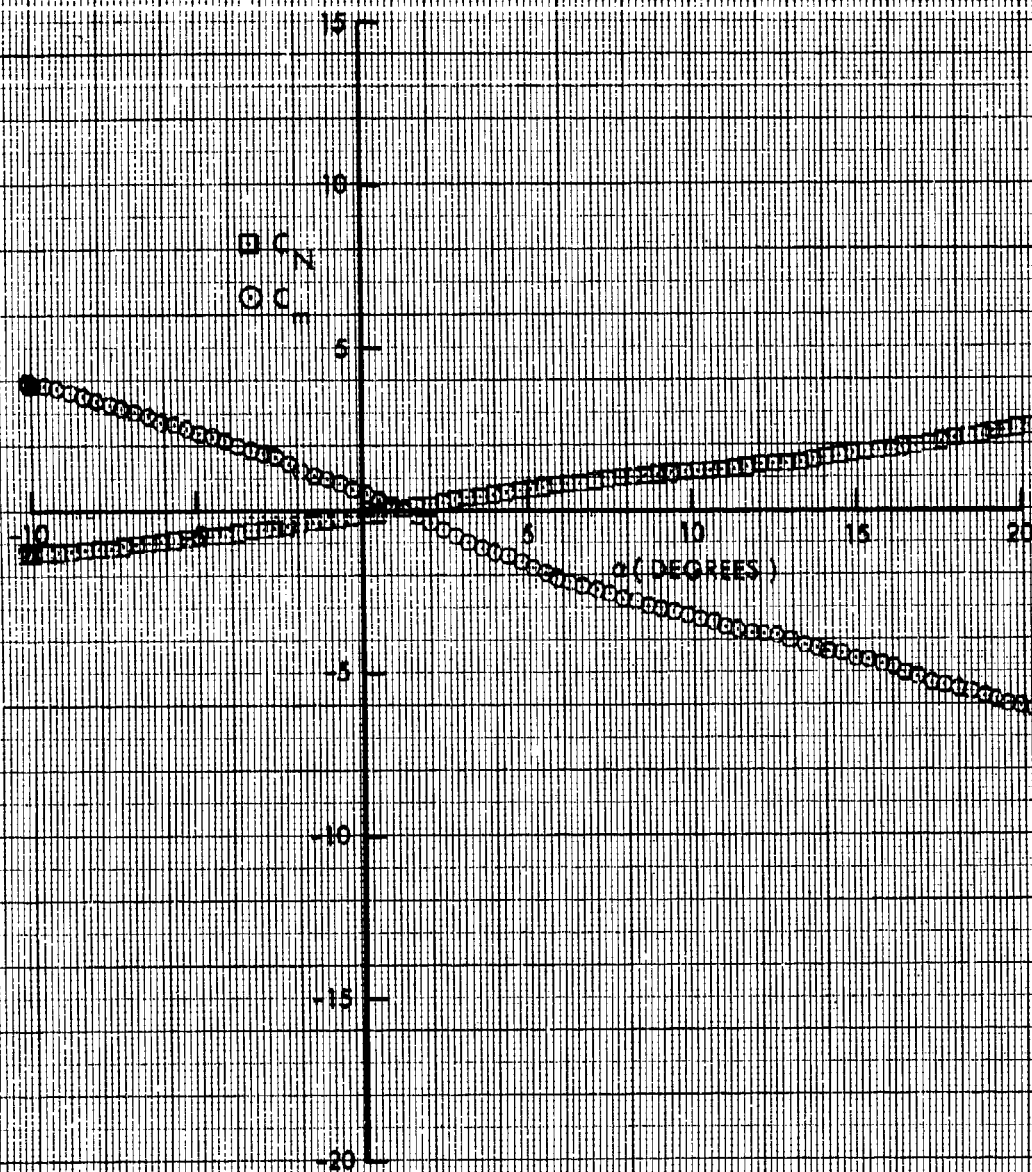


FIG. 221 NORMAL FORCE AND PITCHING MOMENT COEFFICIENTS,  $C_N$  AND  $C_m$ , VS ANGLE OF ATTACK,  $\alpha$ , FOR THE 0.125-SCALE MODEL MK B2 SNAKEYE BOMB WITH FINS OPEN







EMTEX TAIL

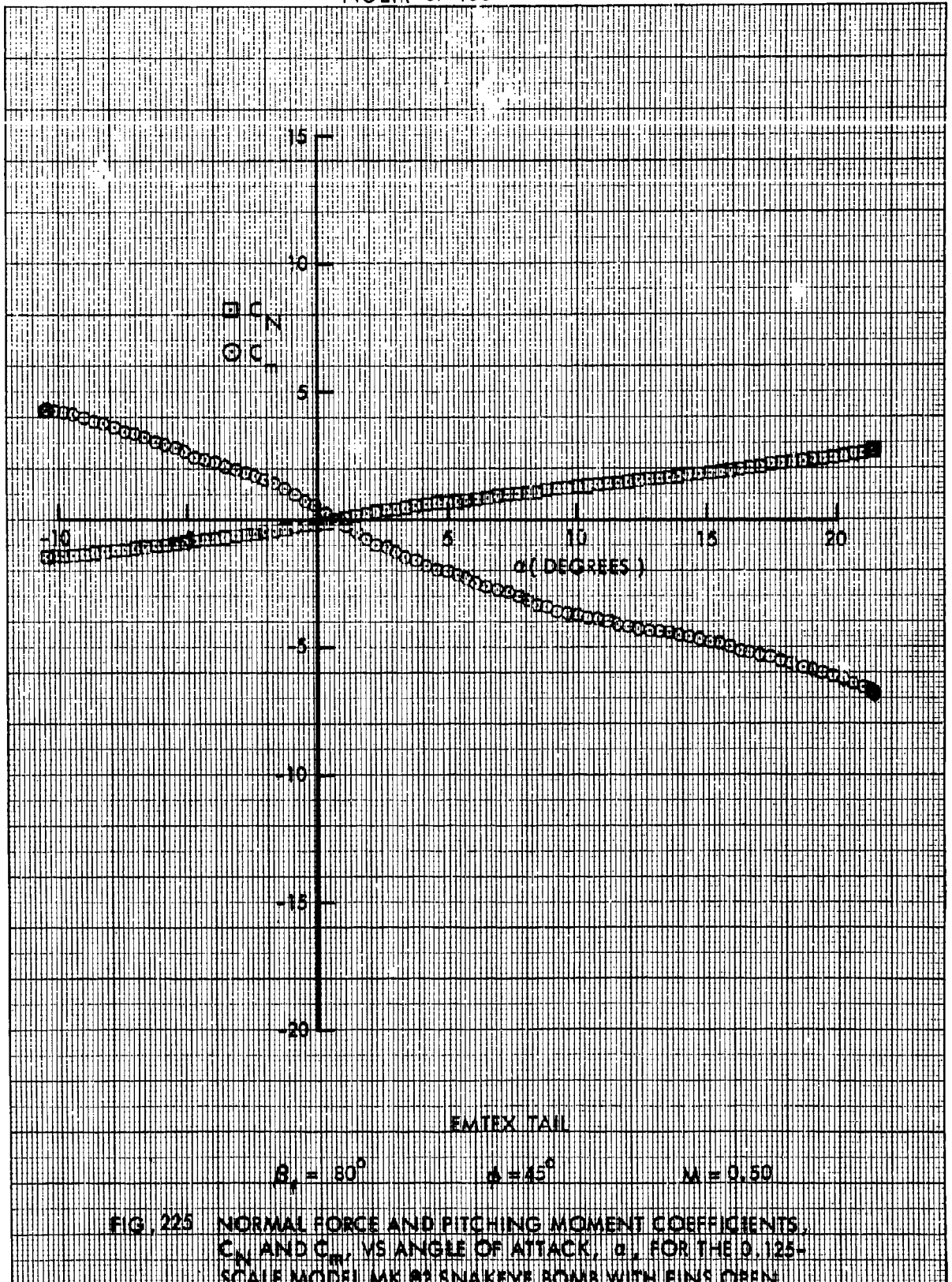
$\beta_1 = 80^\circ$

$\phi = 45^\circ$

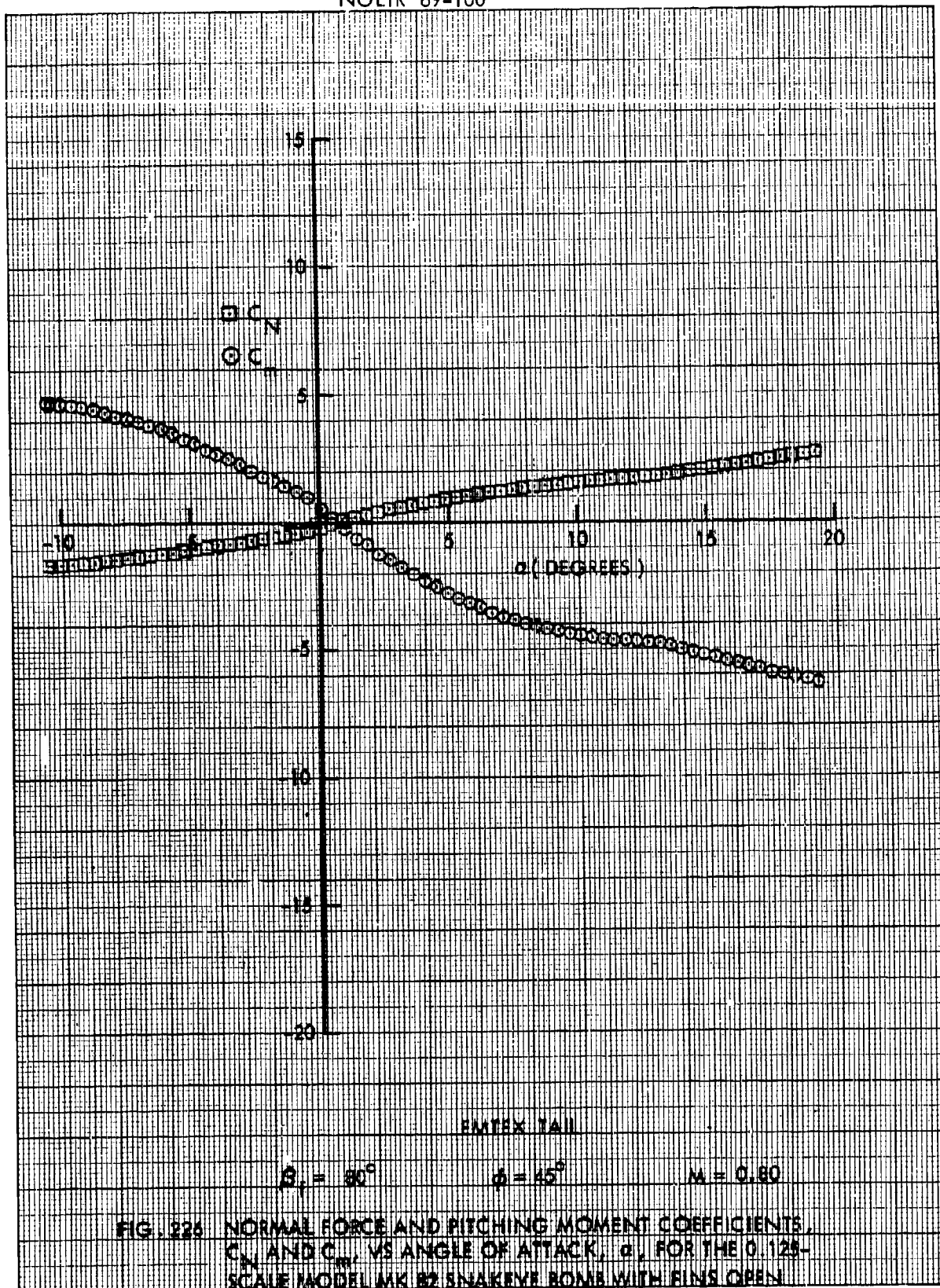
$M = 0.26$

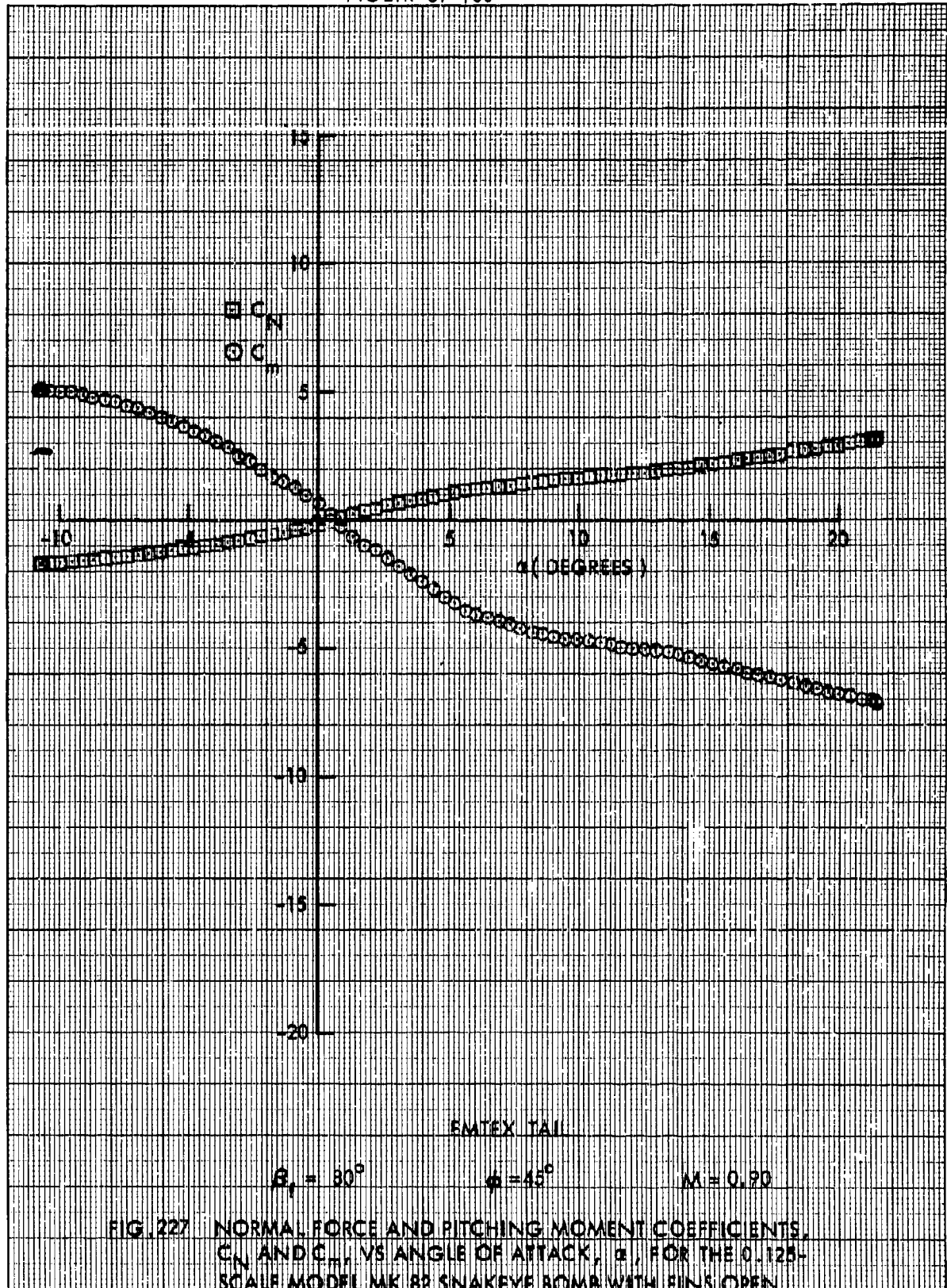
FIG. 224 NORMAL FORCE AND PITCHING MOMENT COEFFICIENTS,  $C_N$  AND  $C_m$ , VS ANGLE OF ATTACK,  $\alpha$ , FOR THE 0.125-SCALE MODEL MK 82 SNAKEEYE BOMB WITH FINS OPEN.

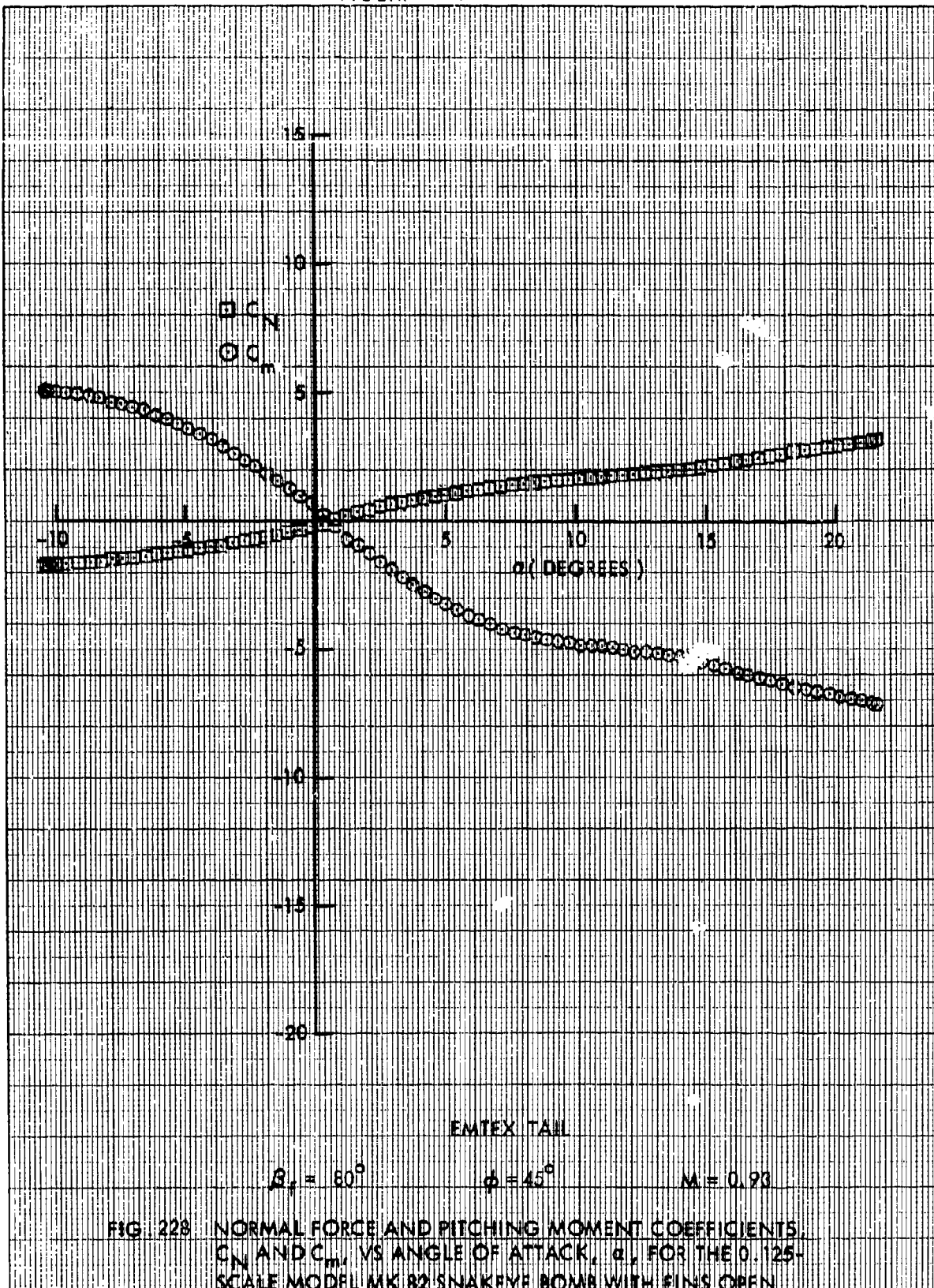


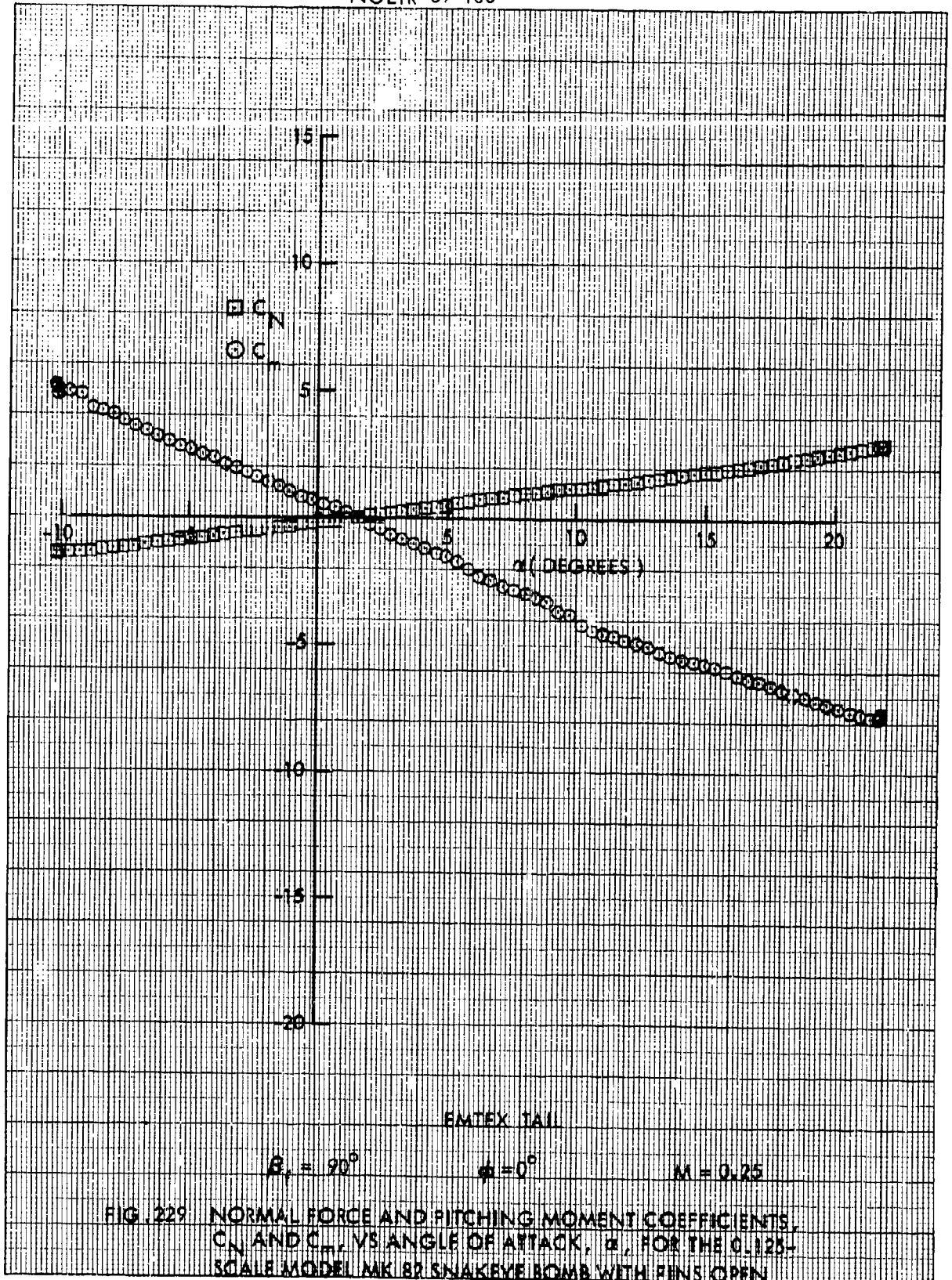


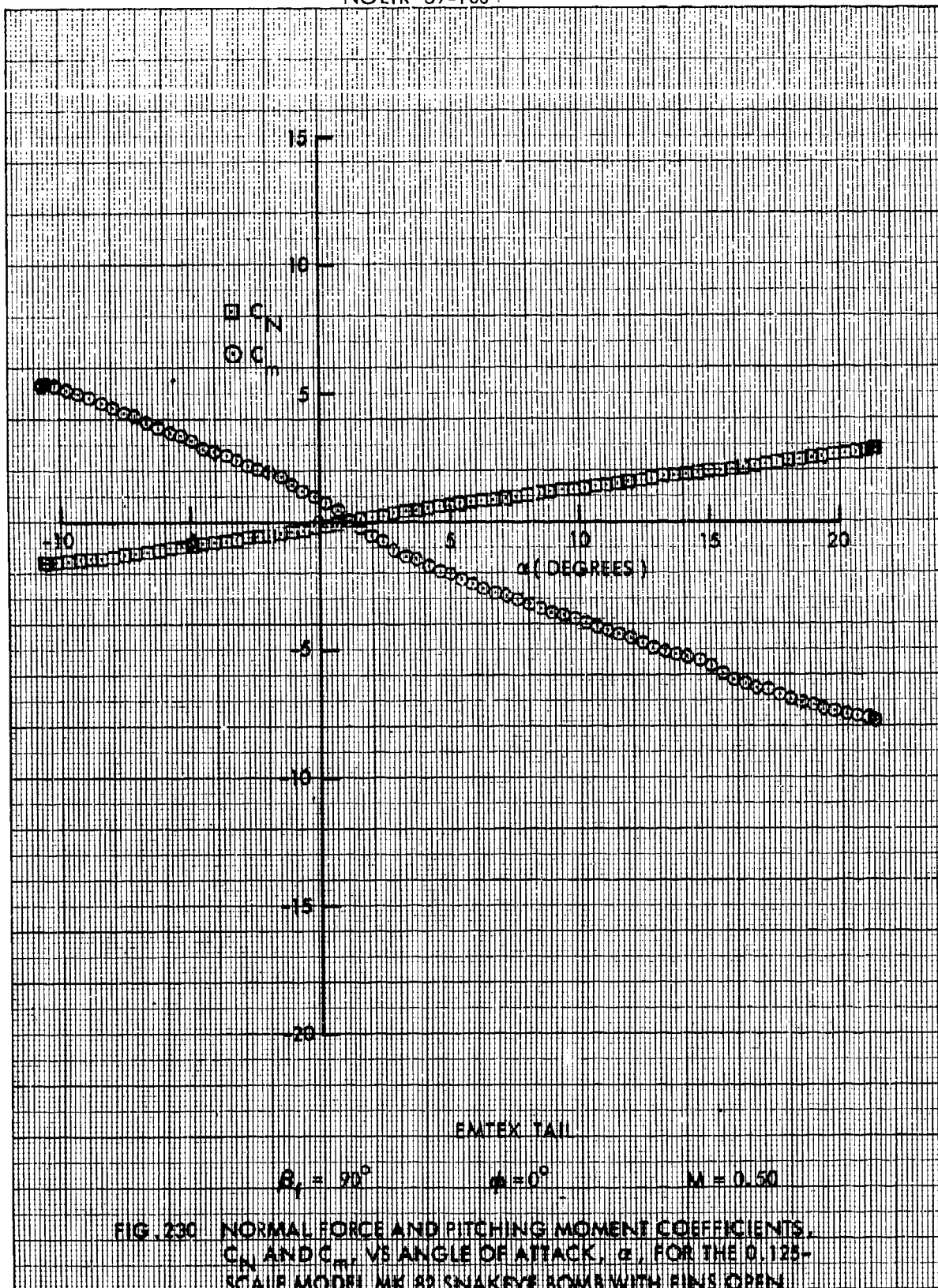




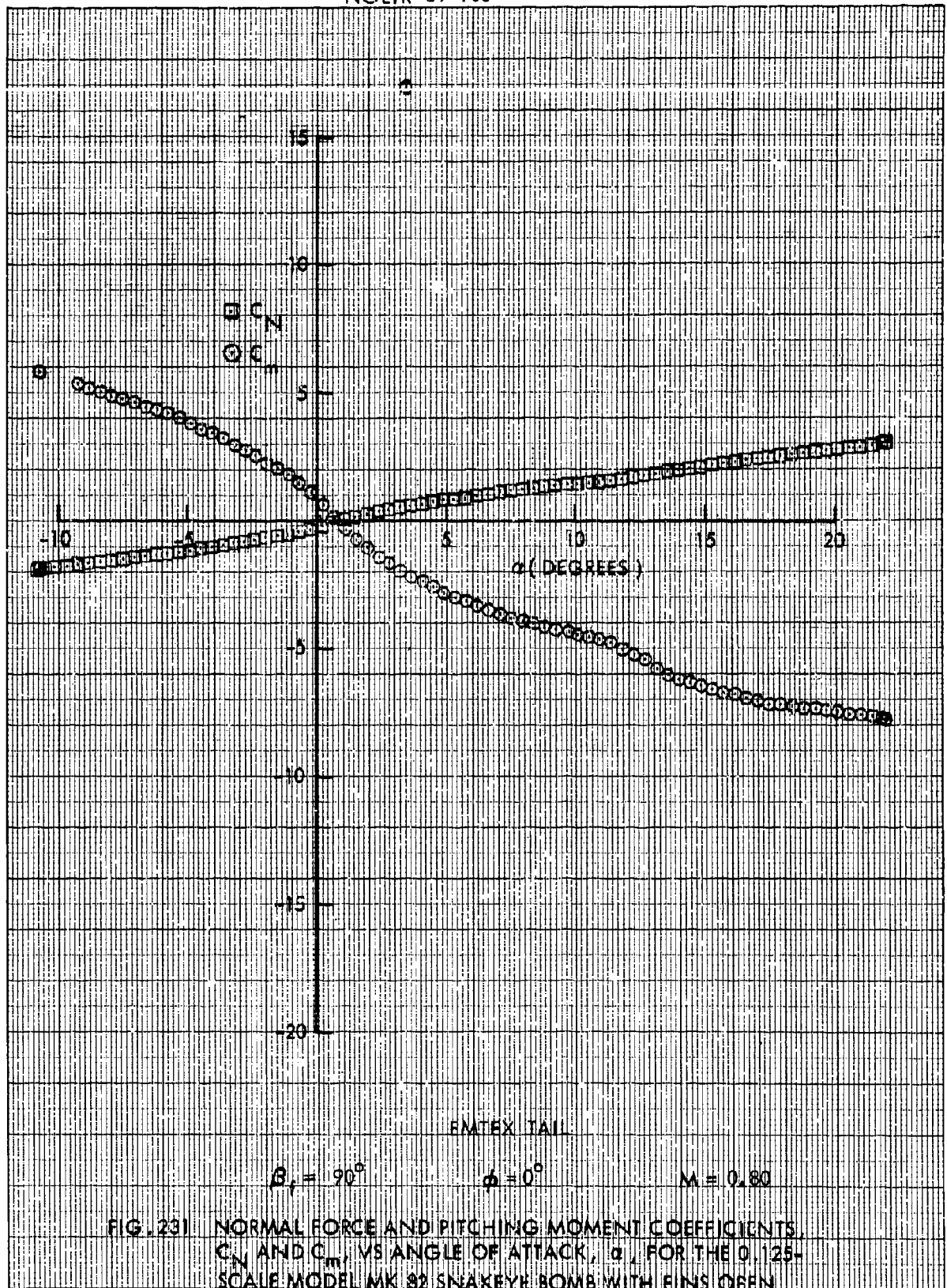




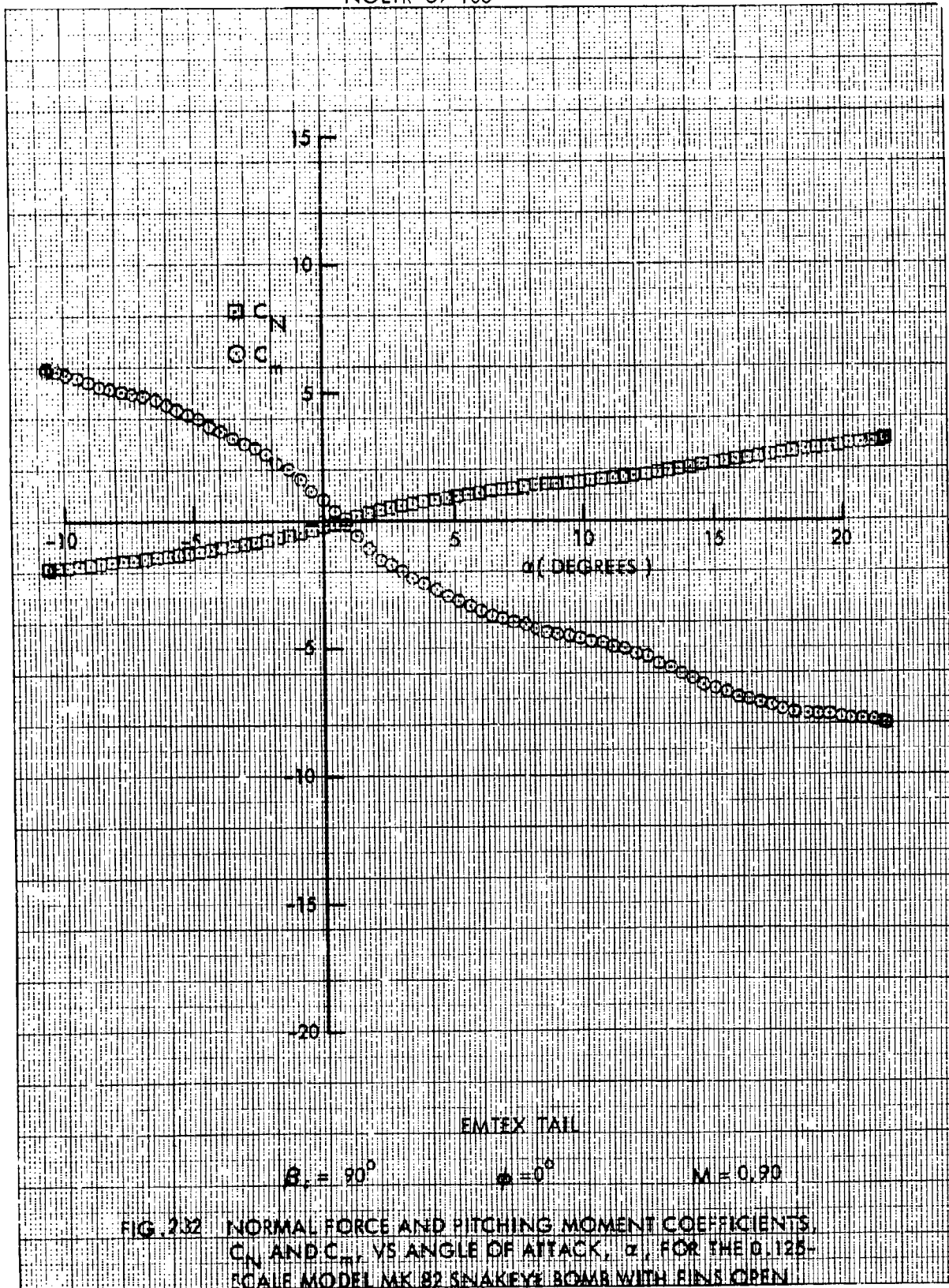


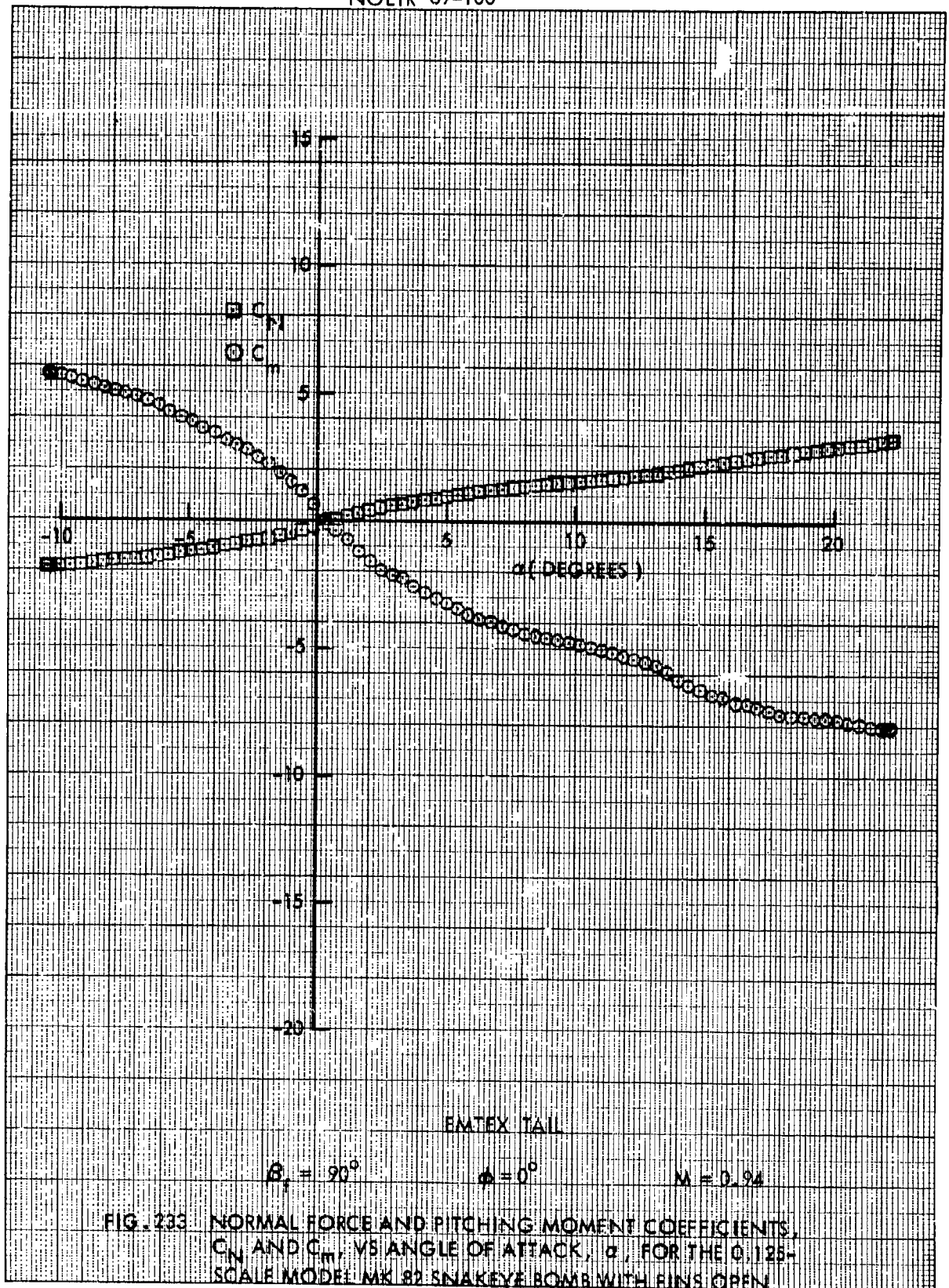


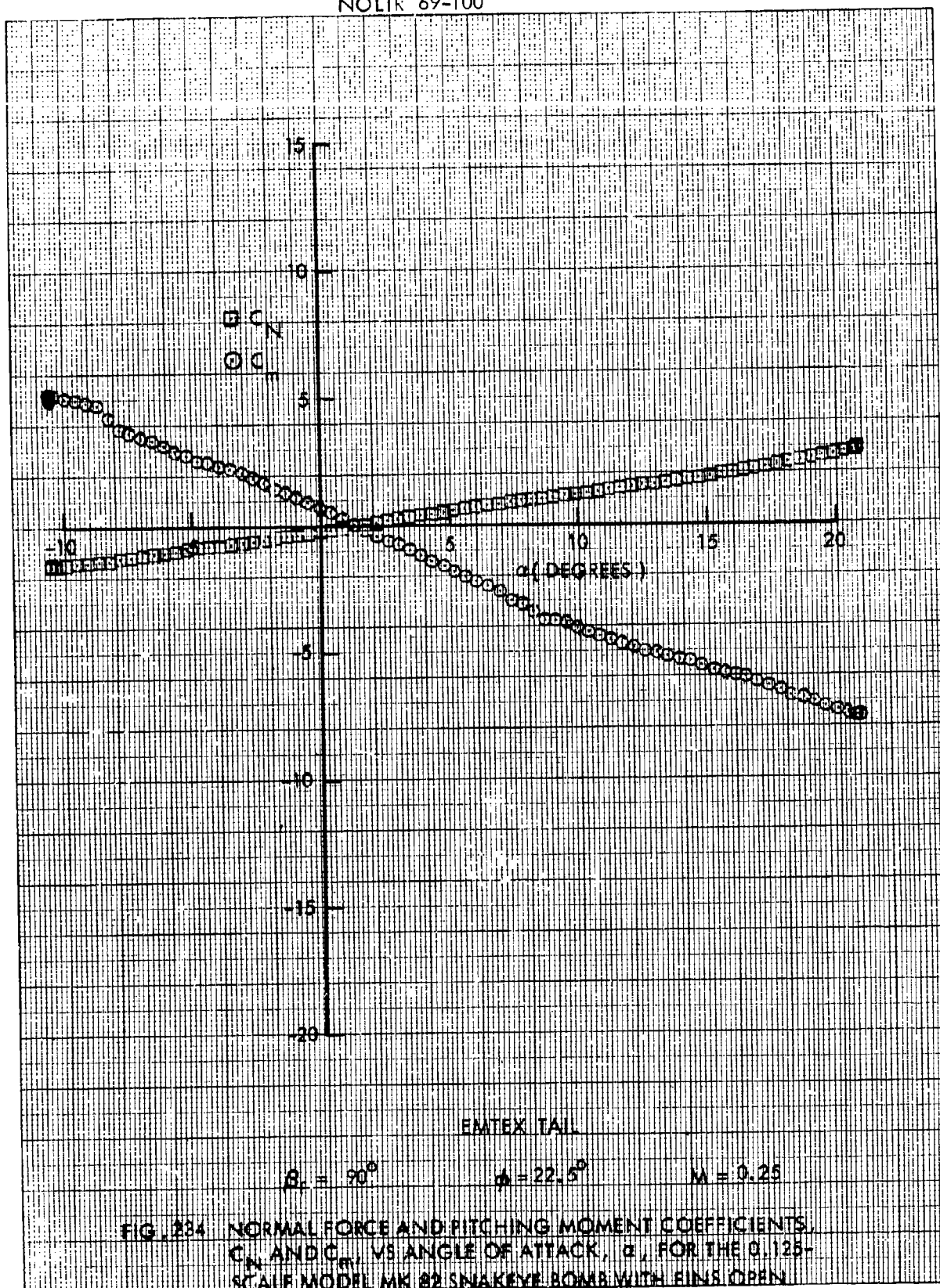


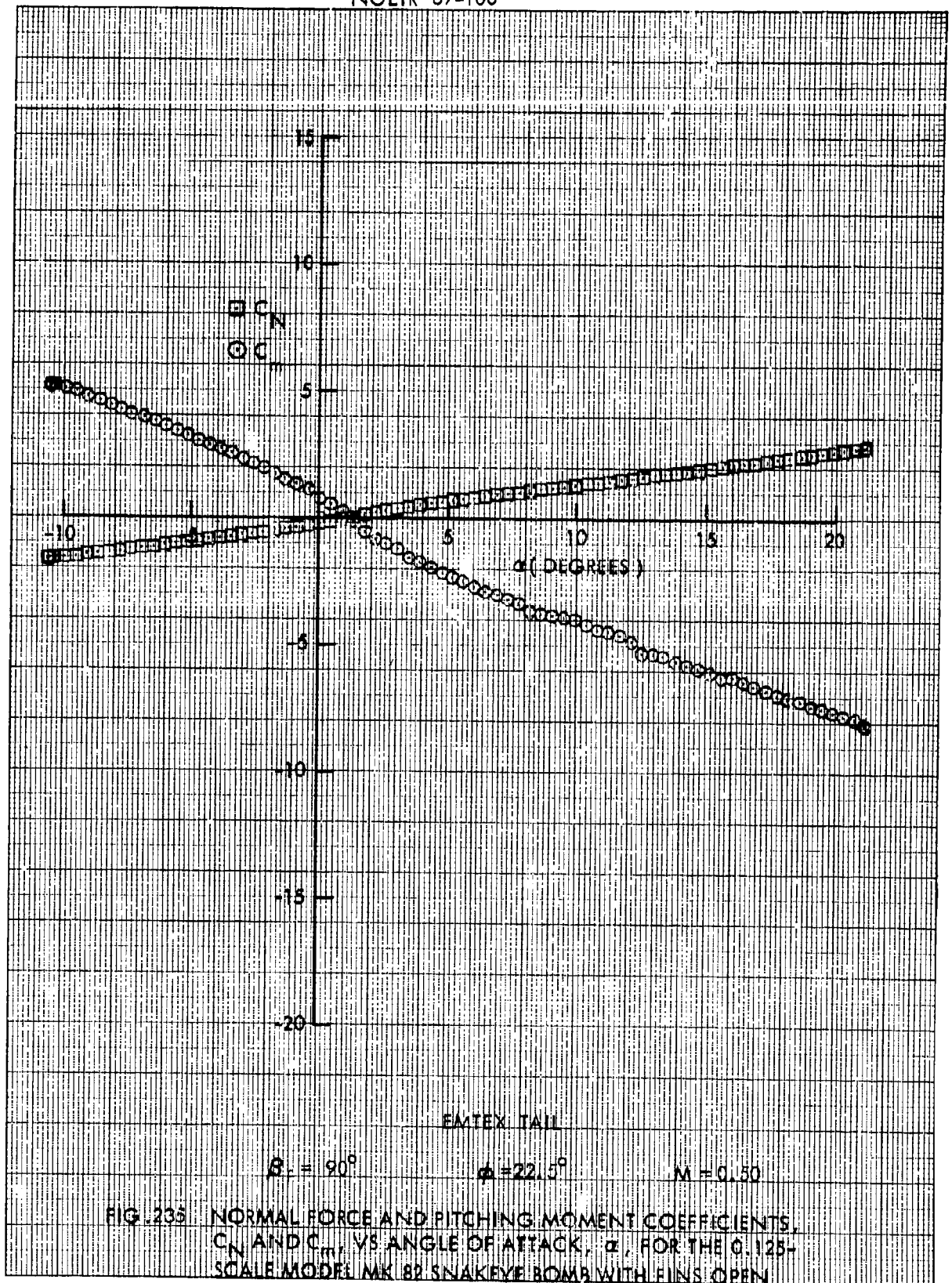


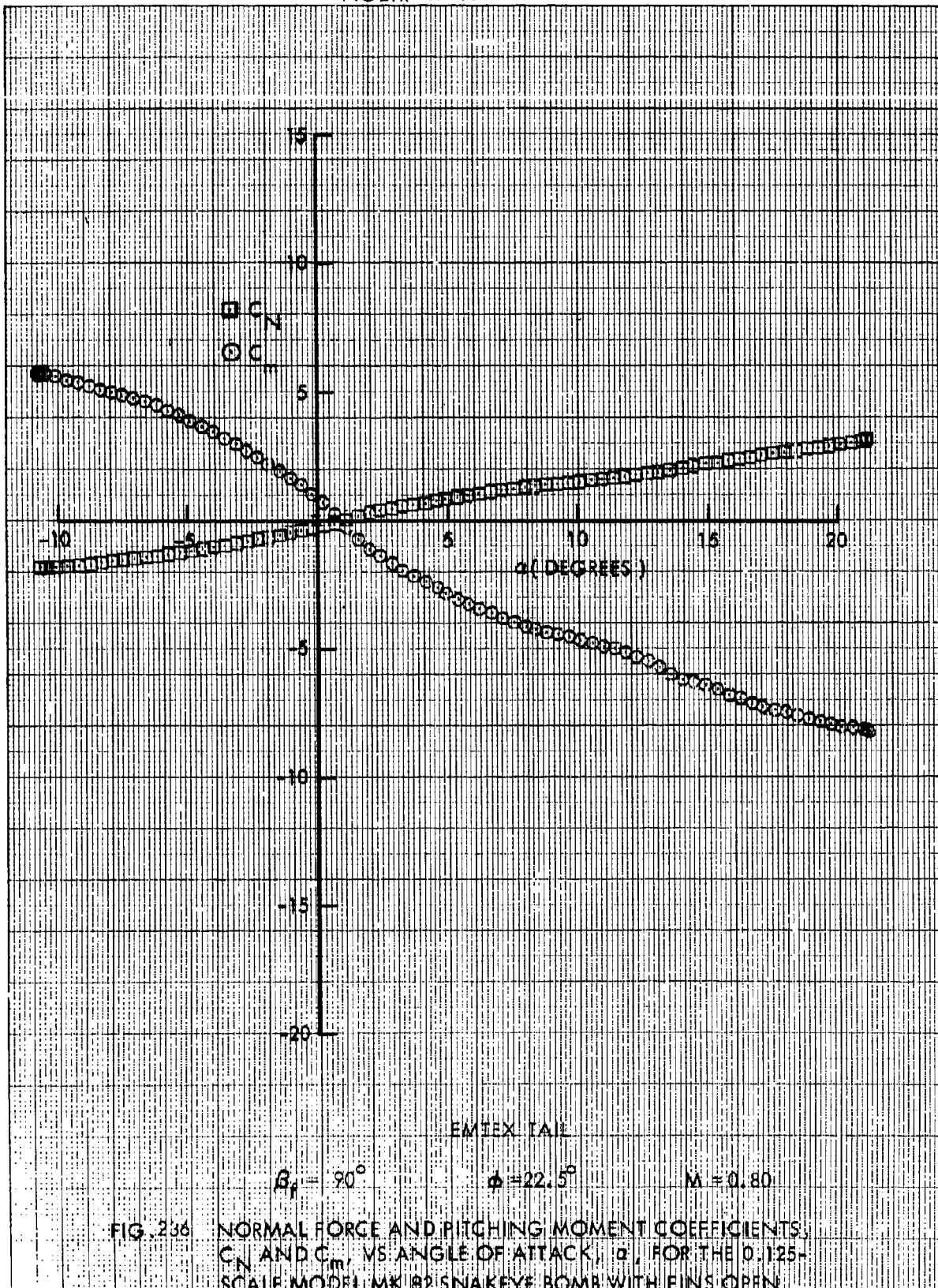




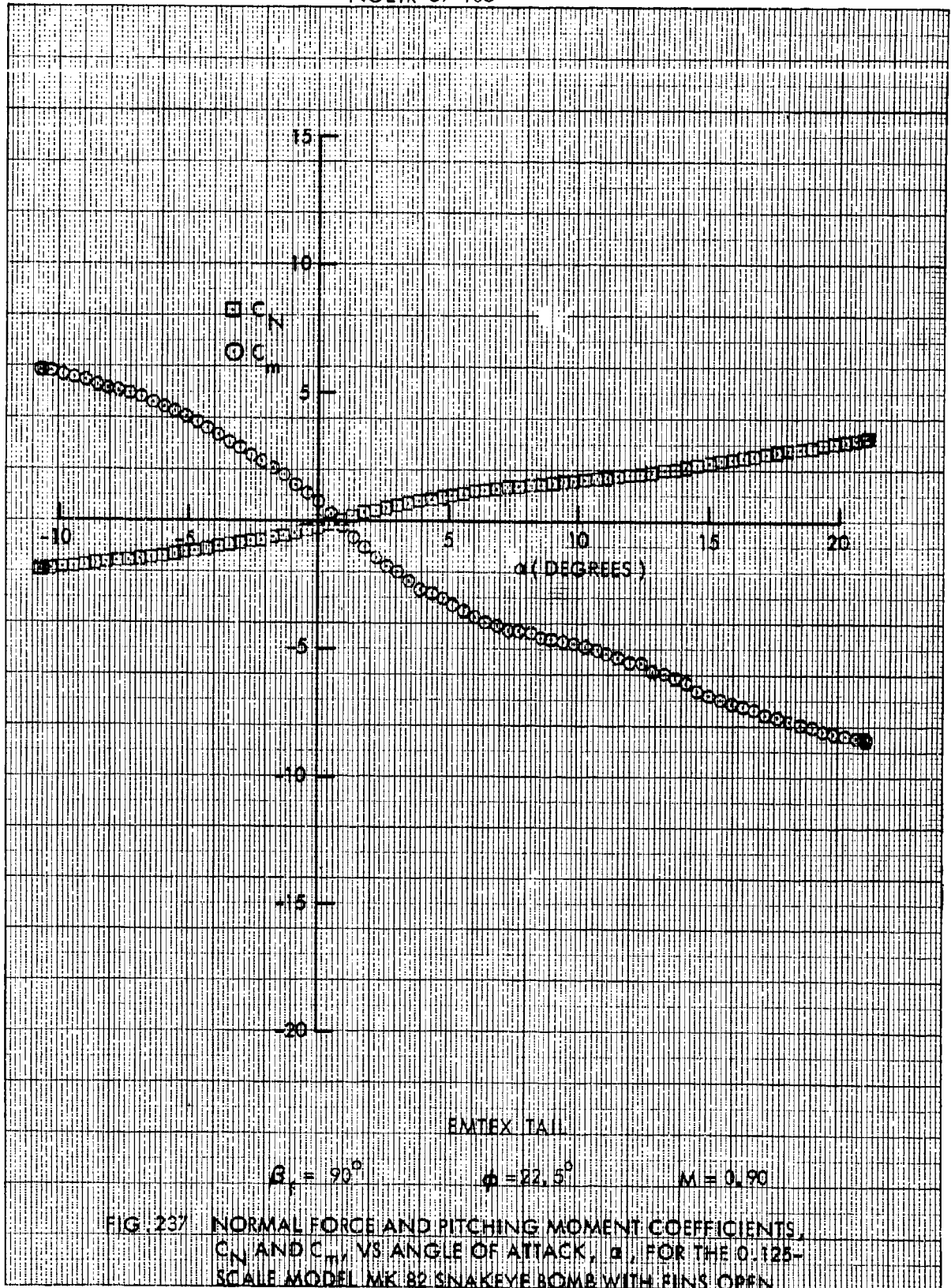




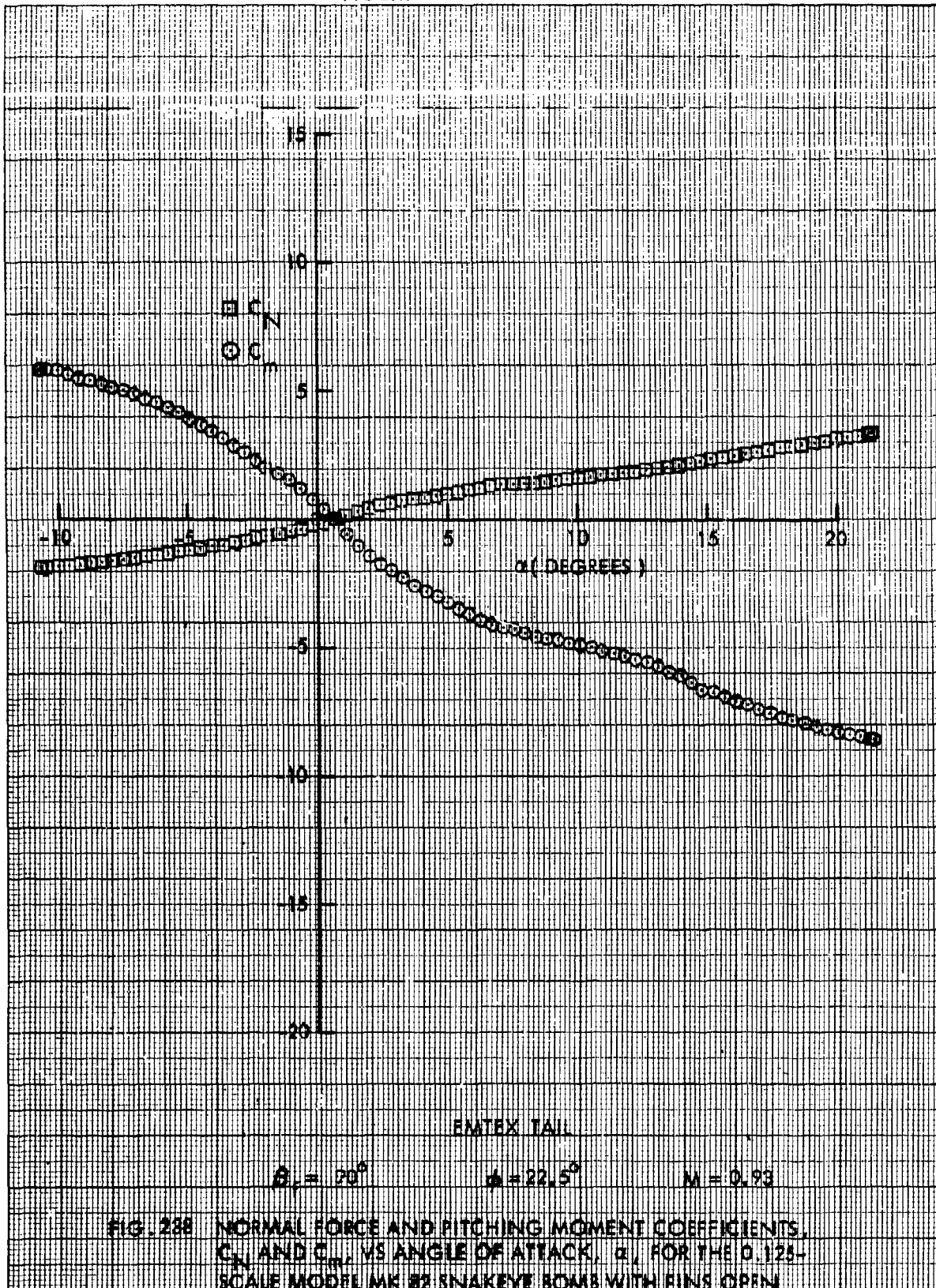


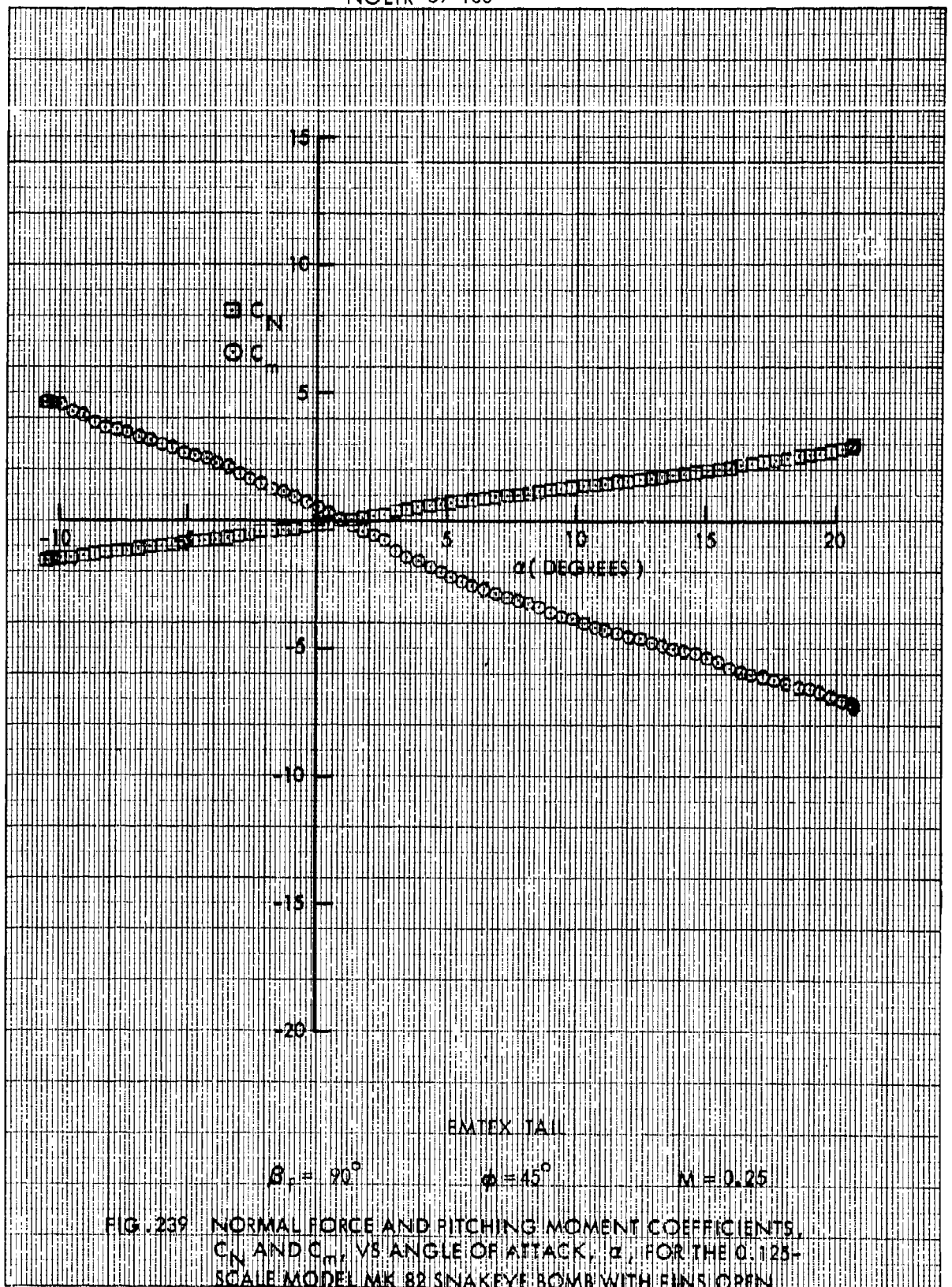


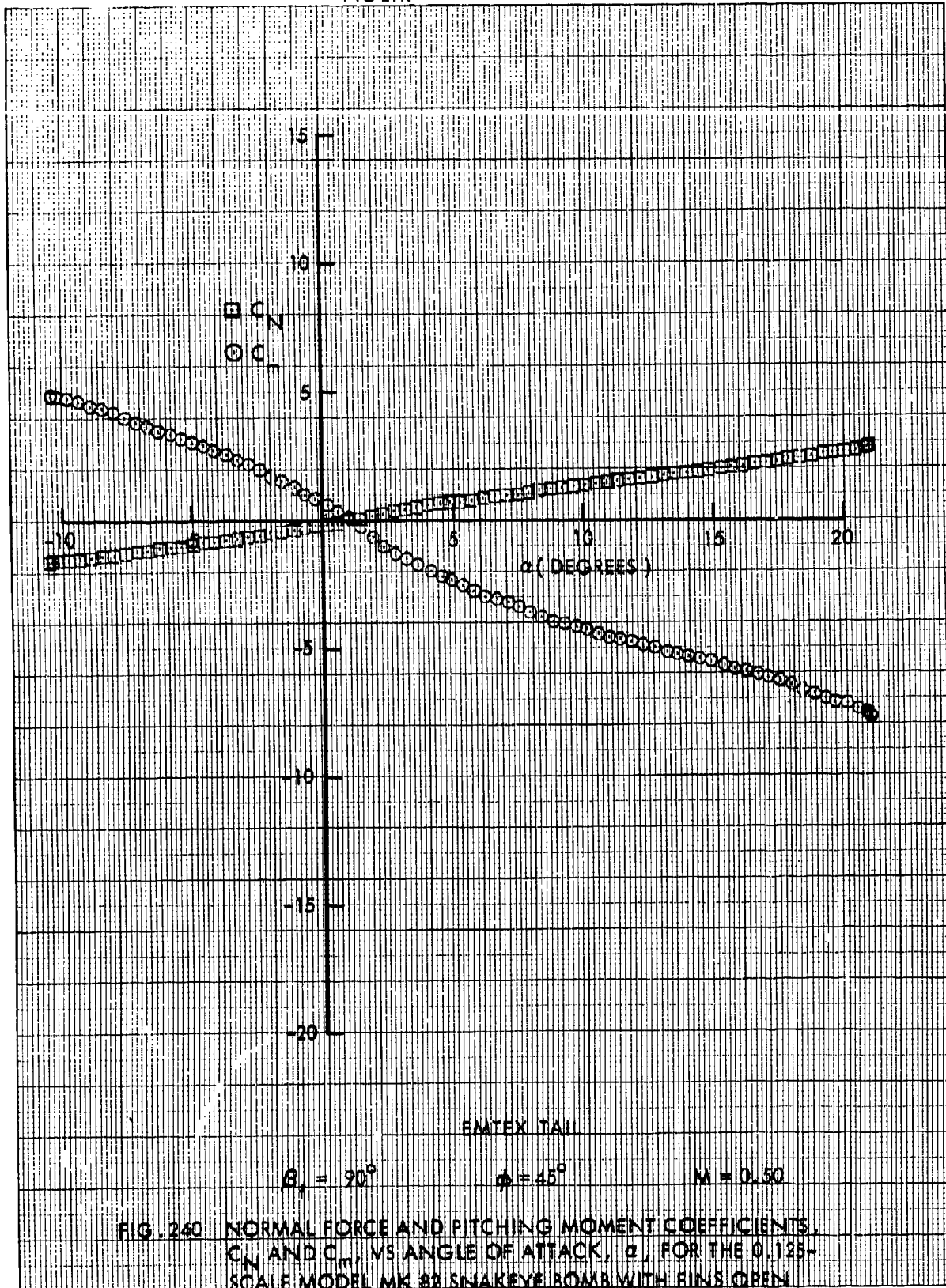


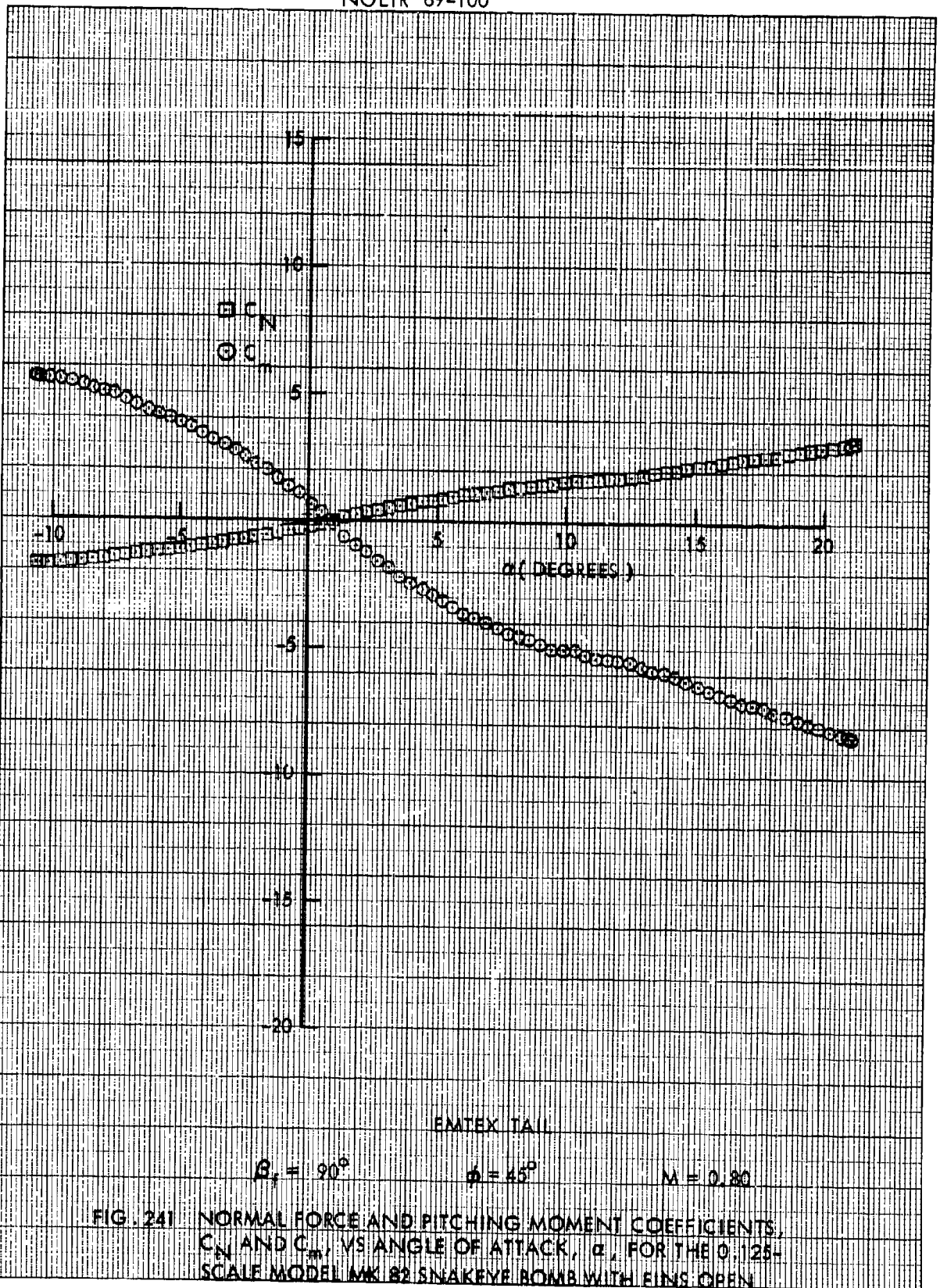


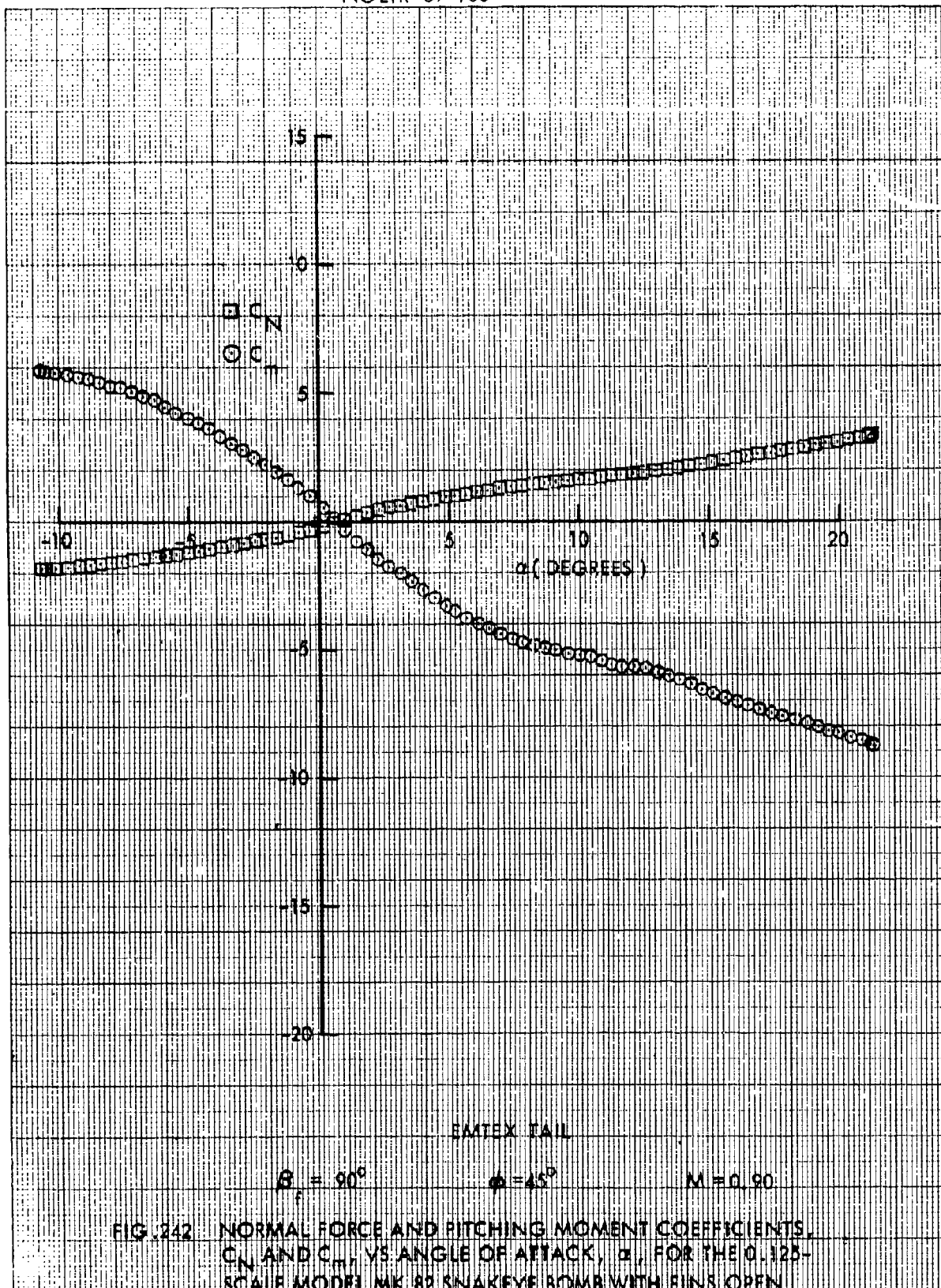




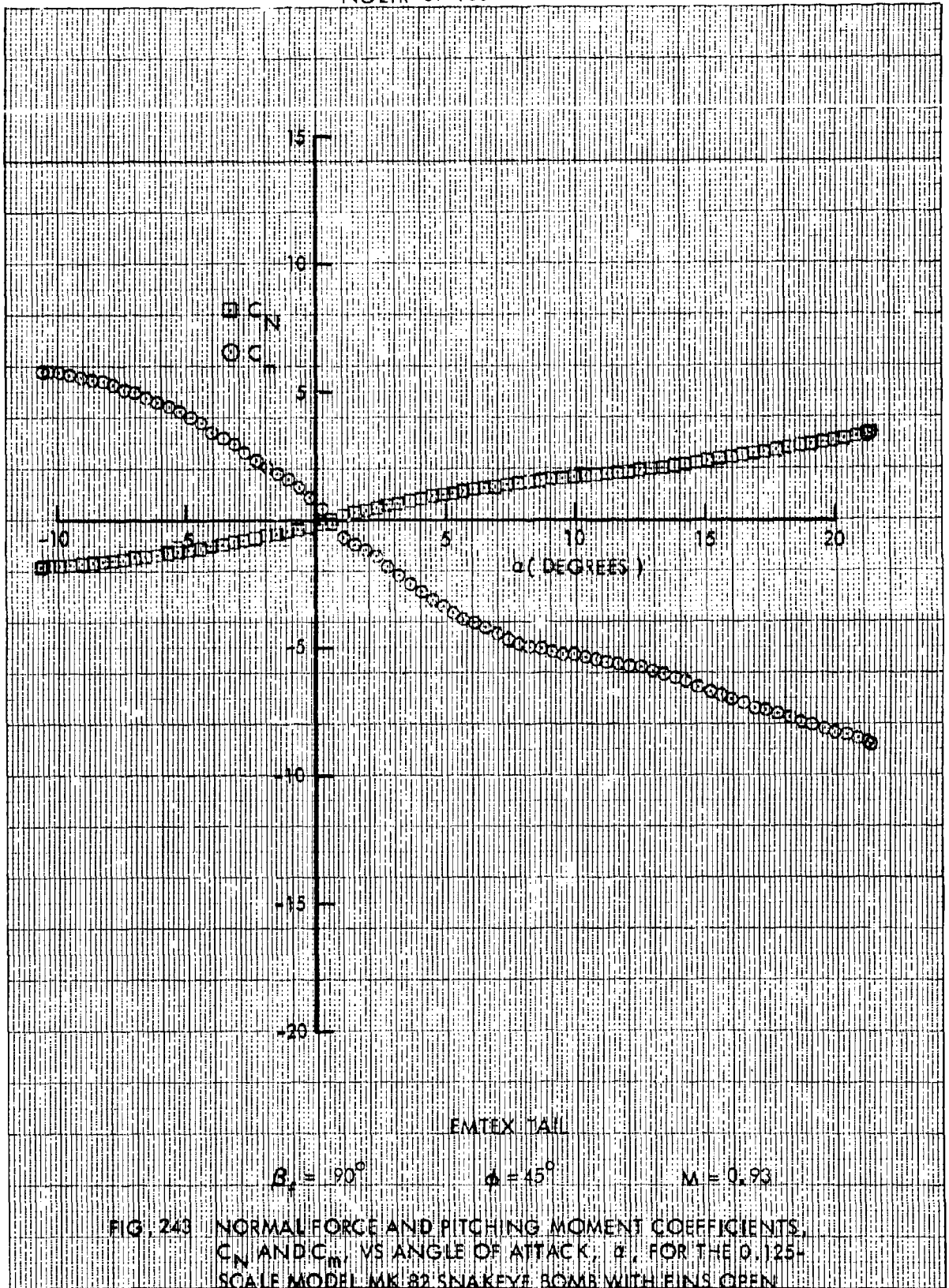




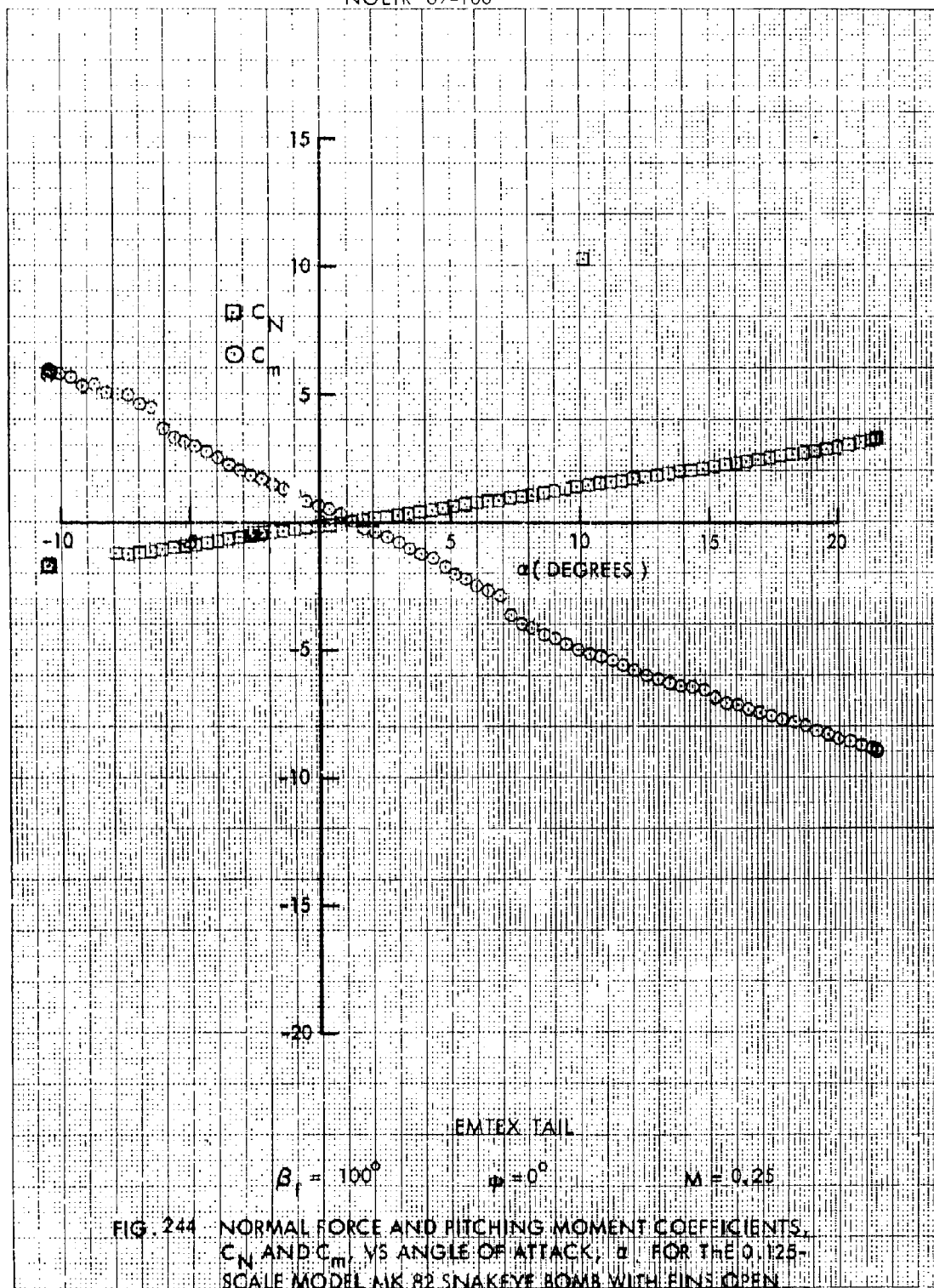


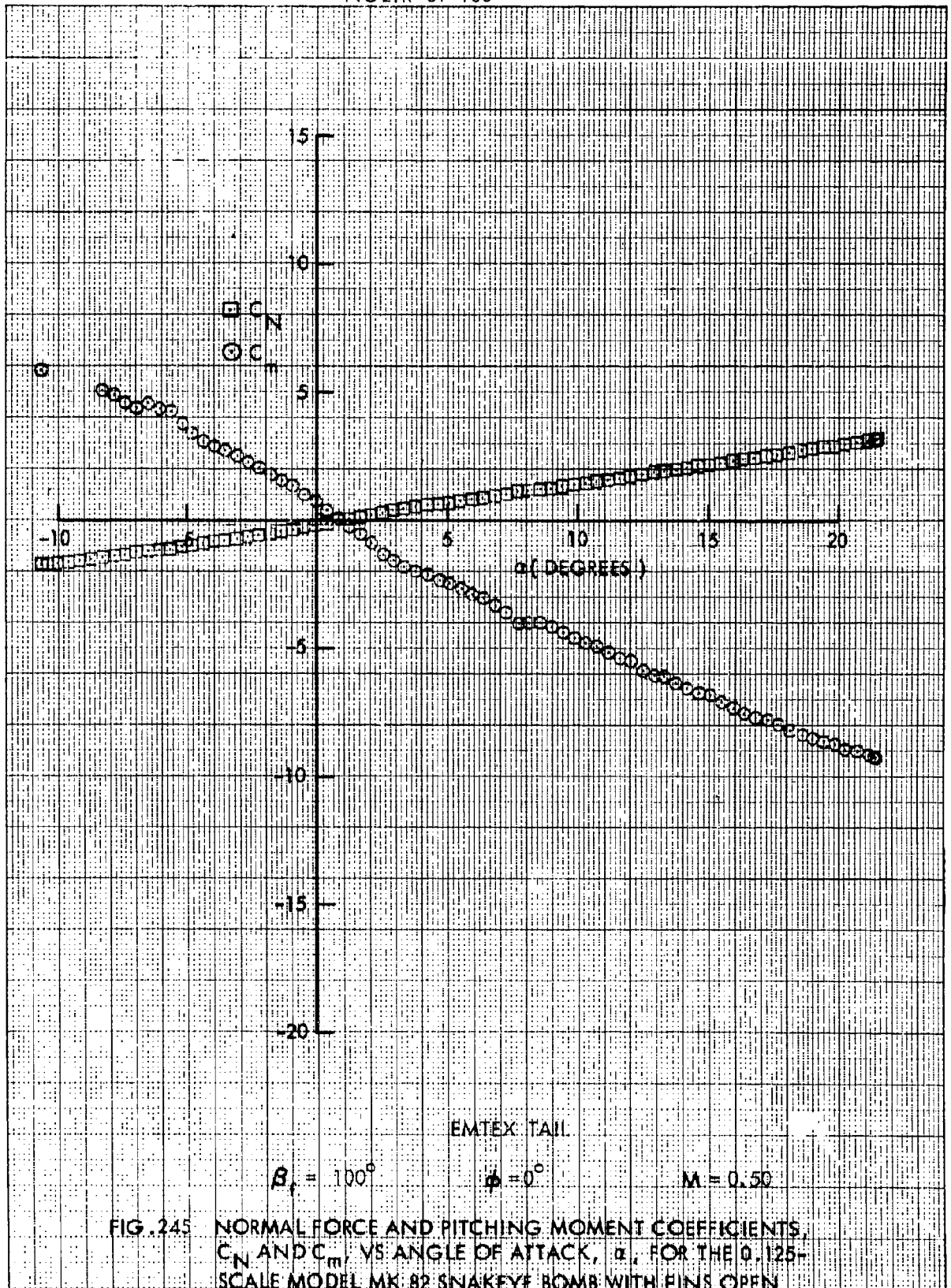


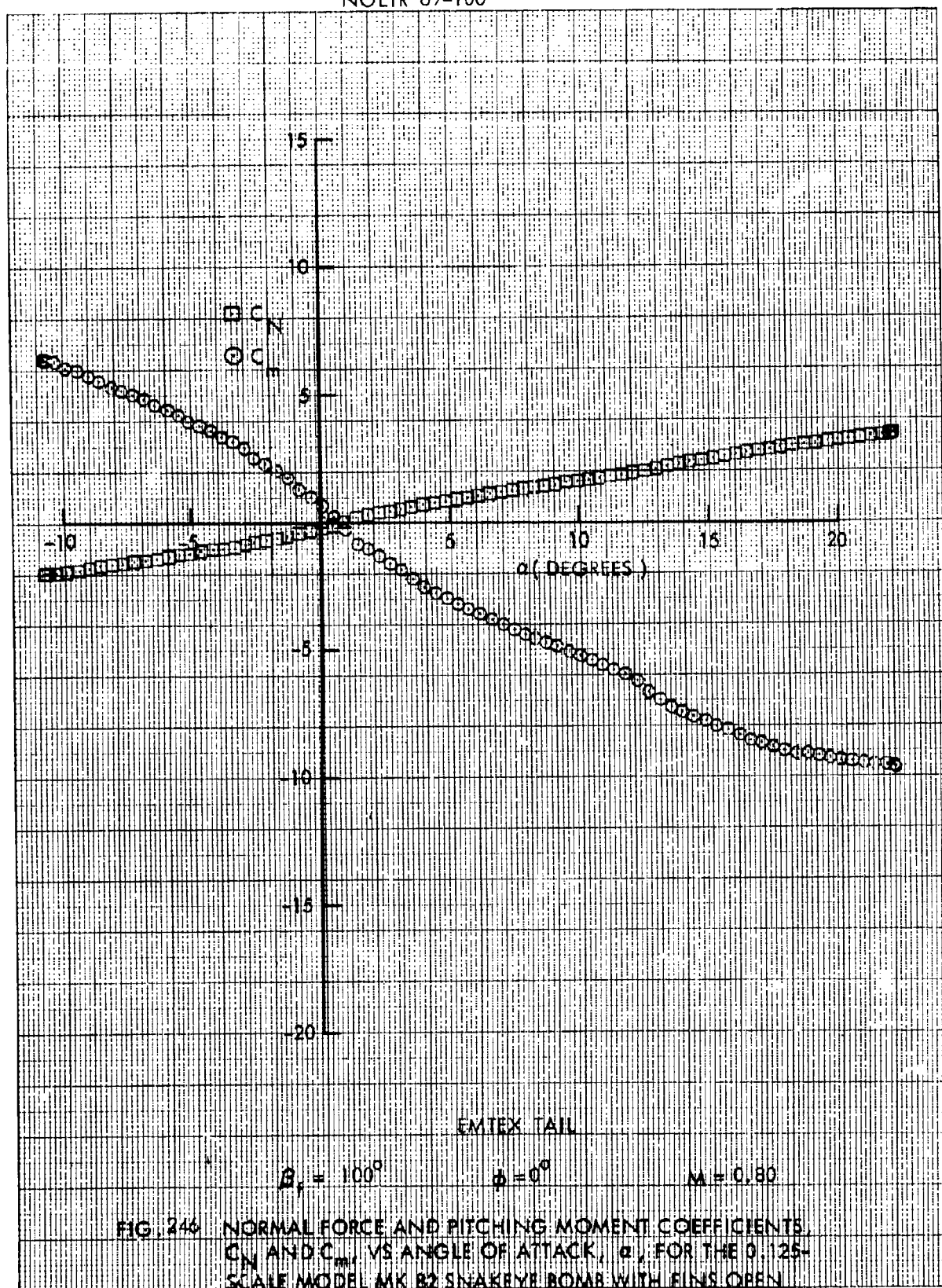


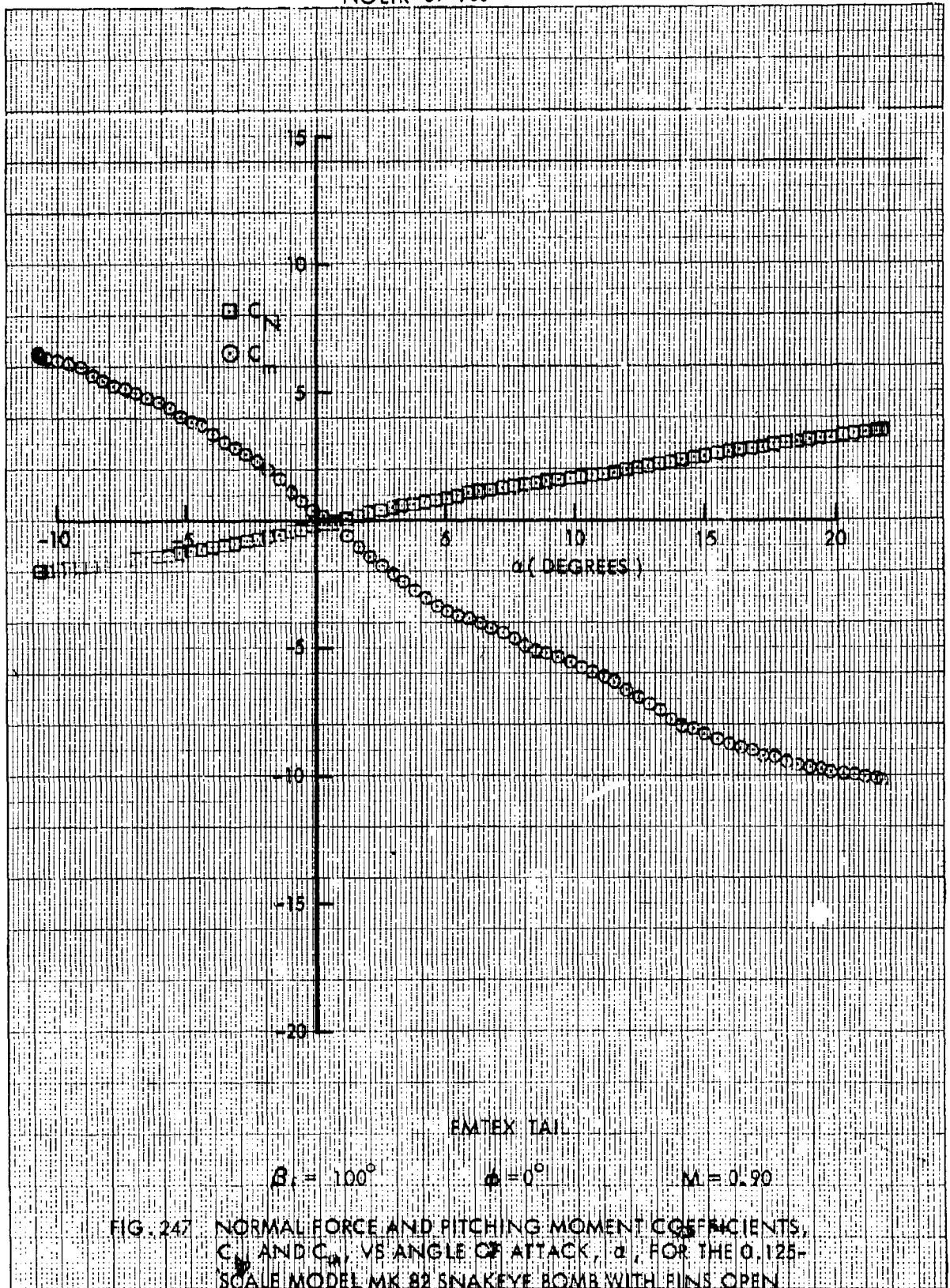


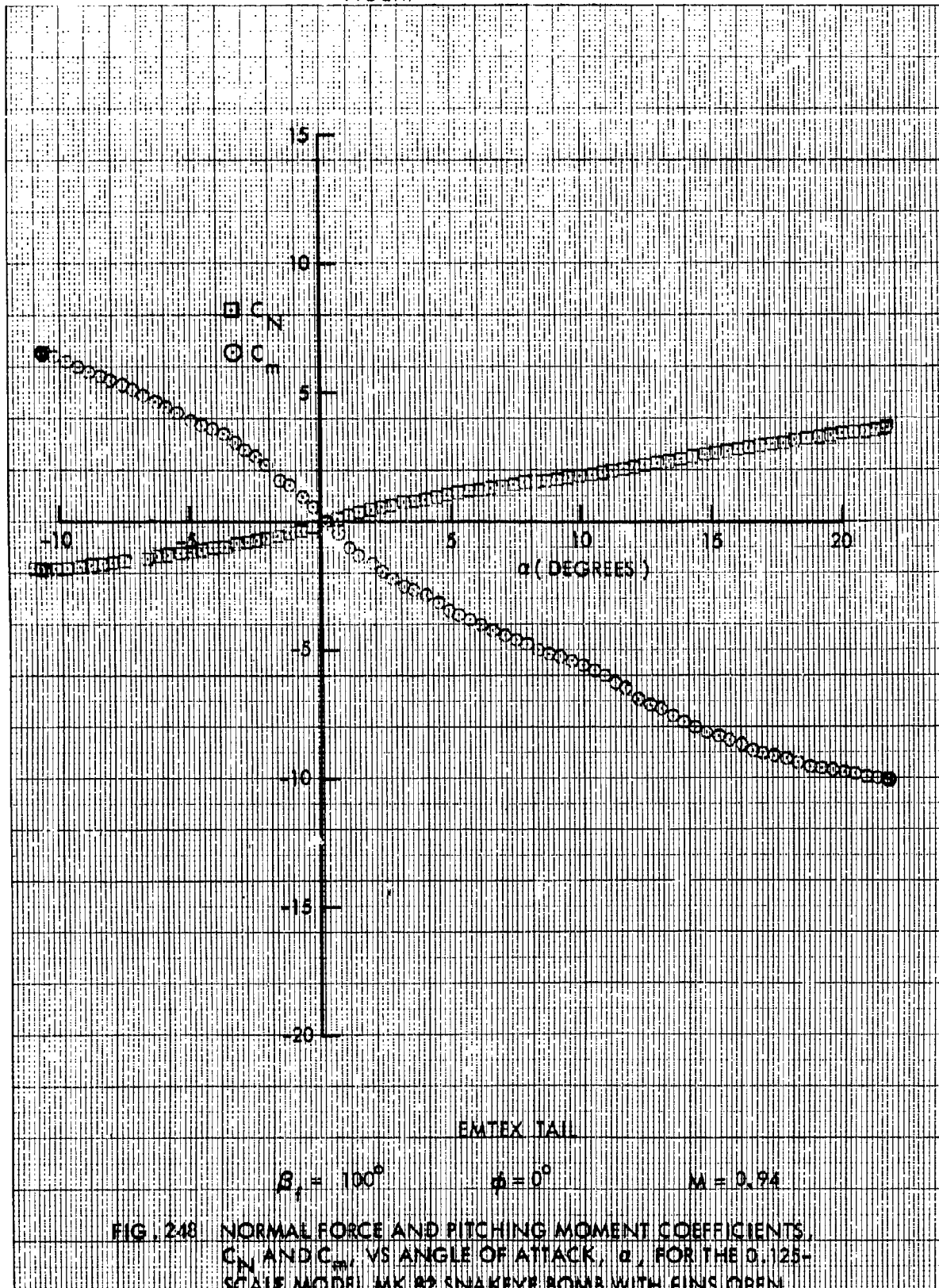




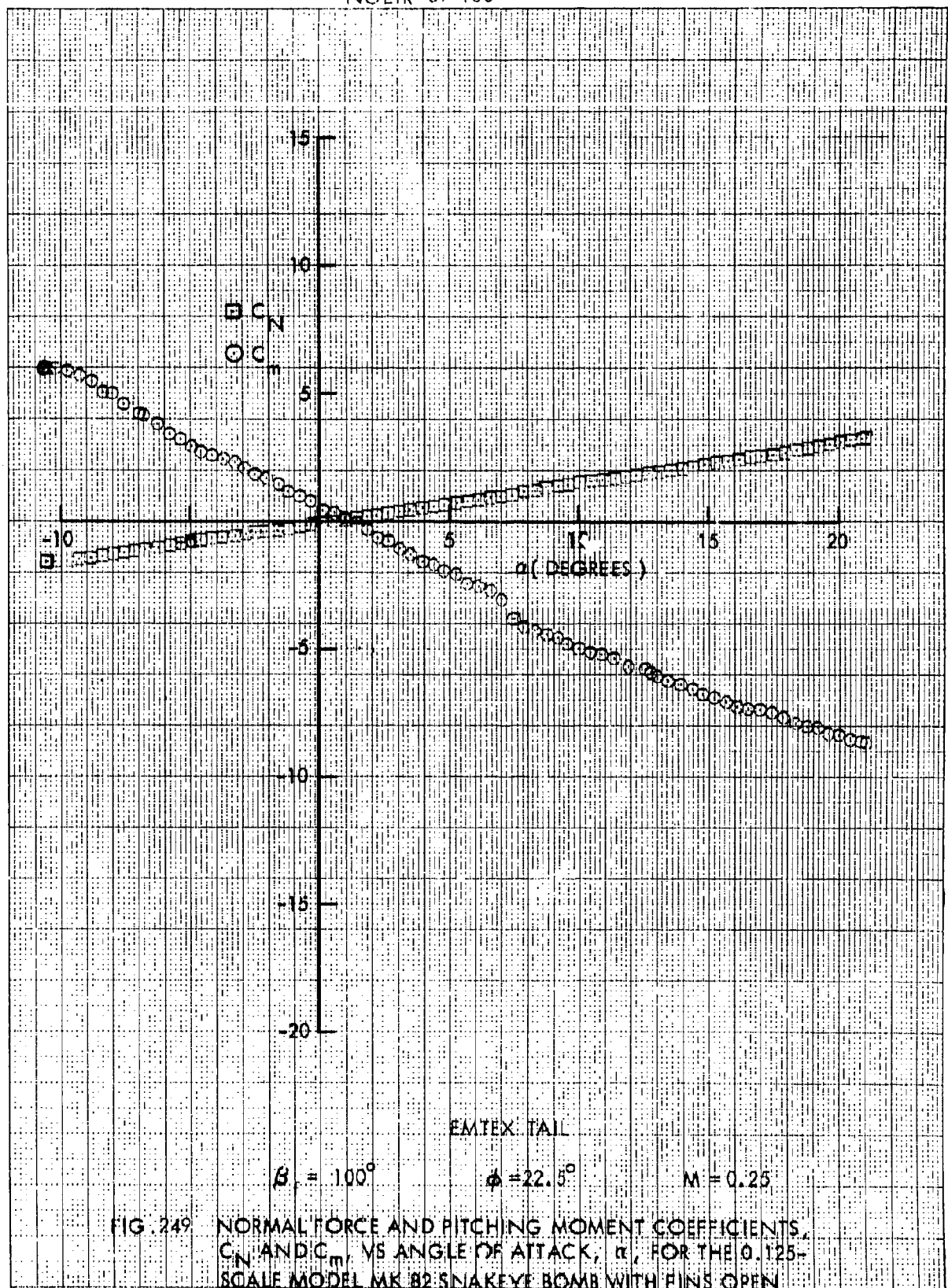




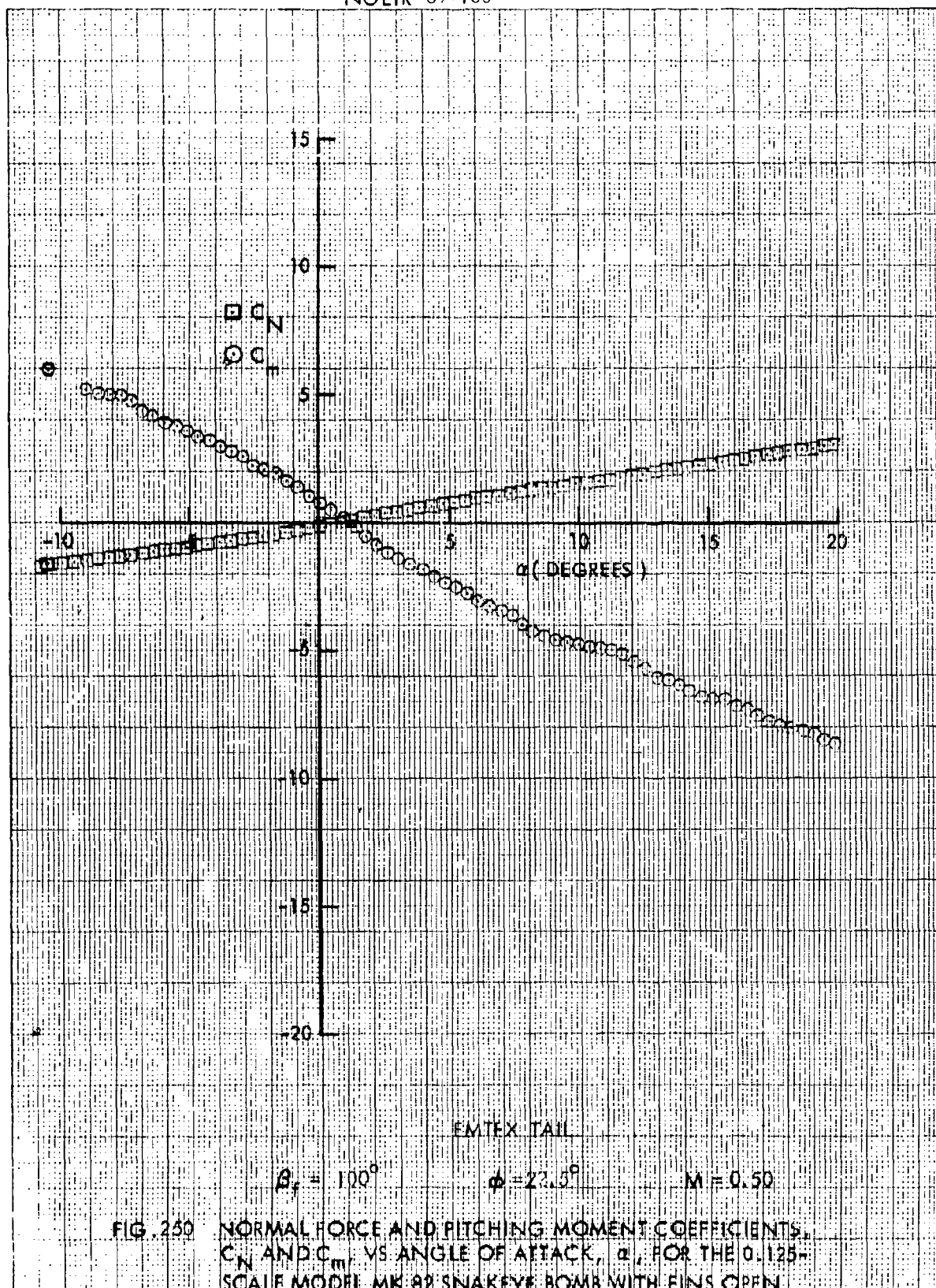












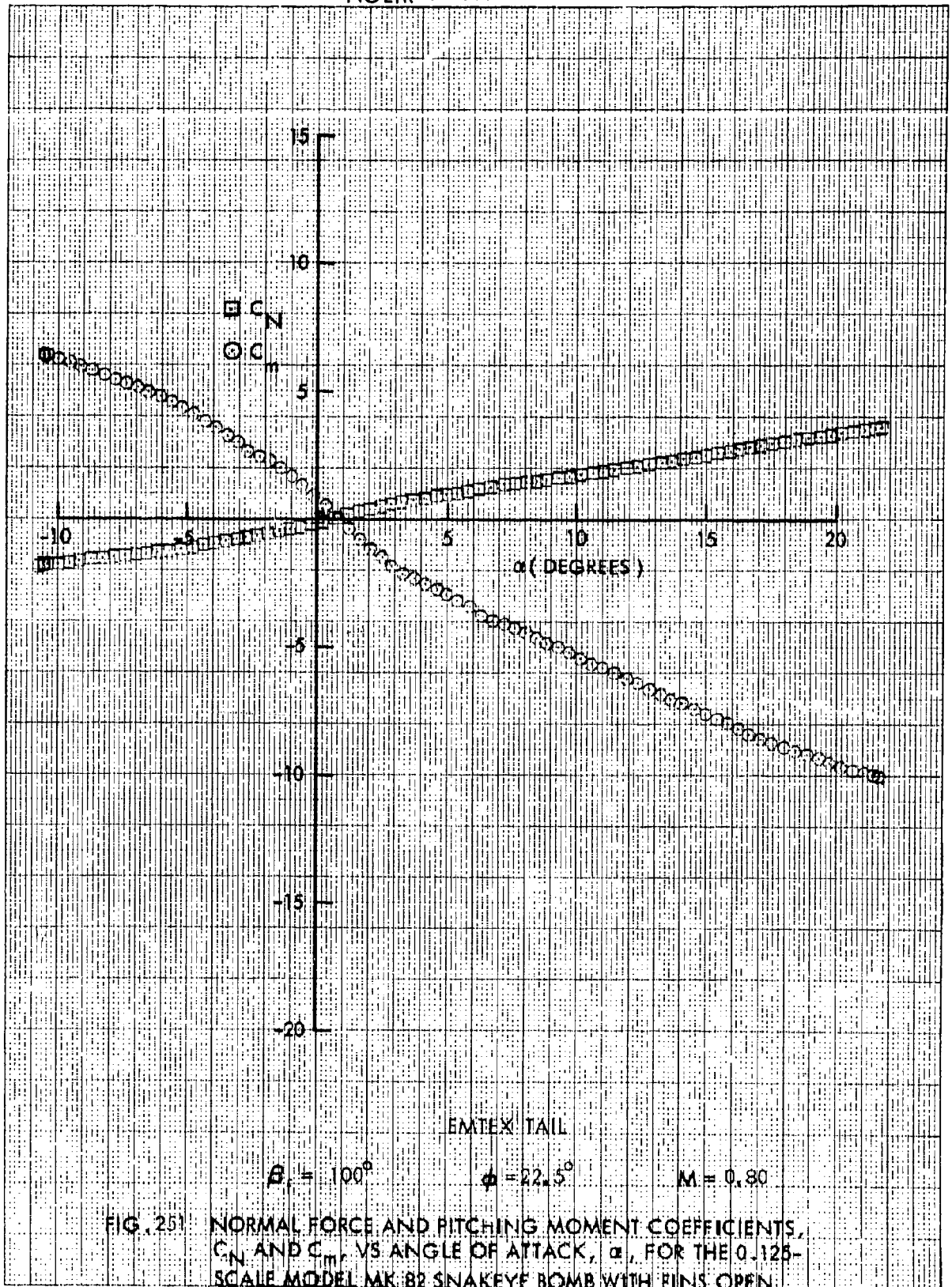
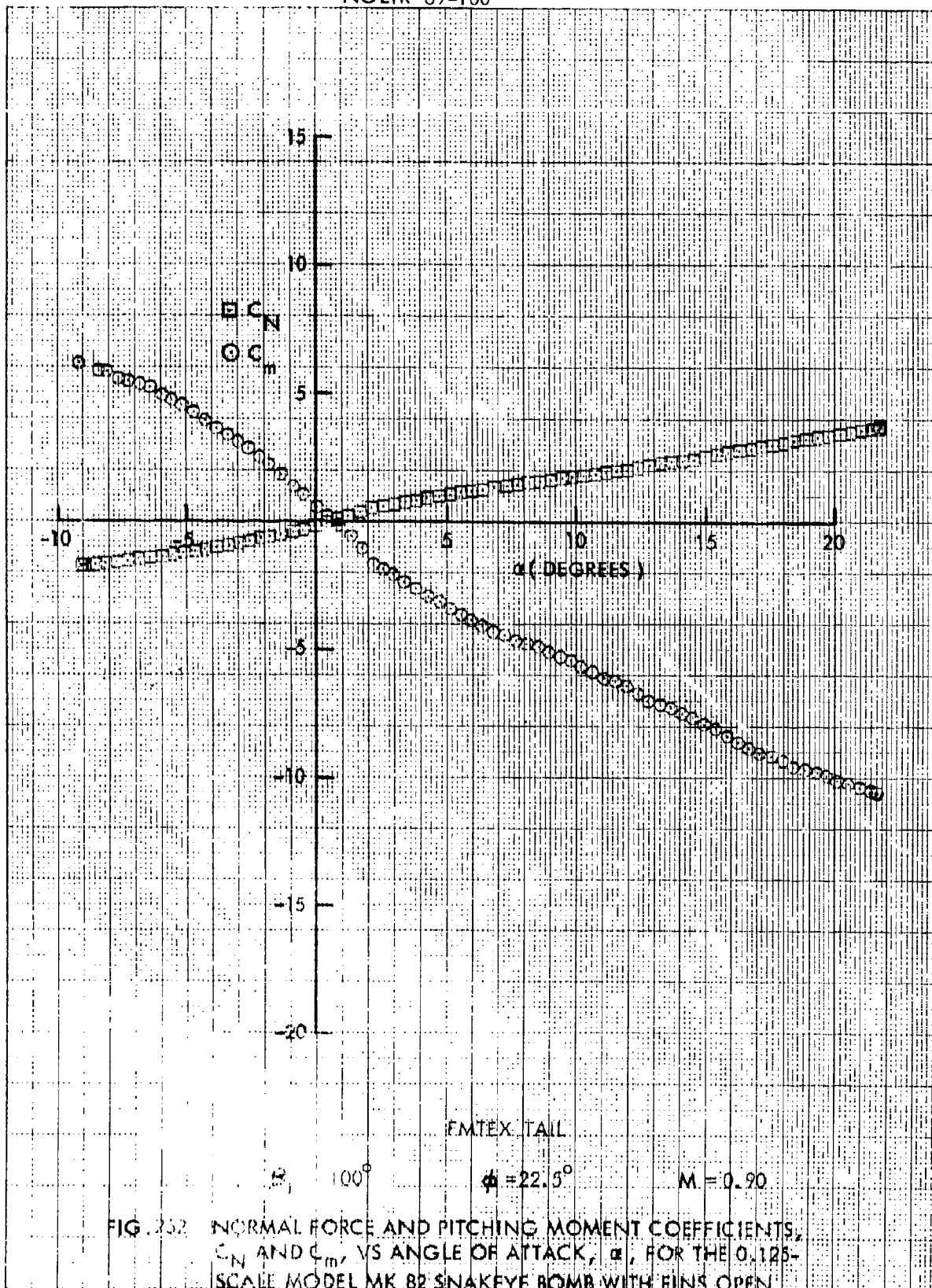
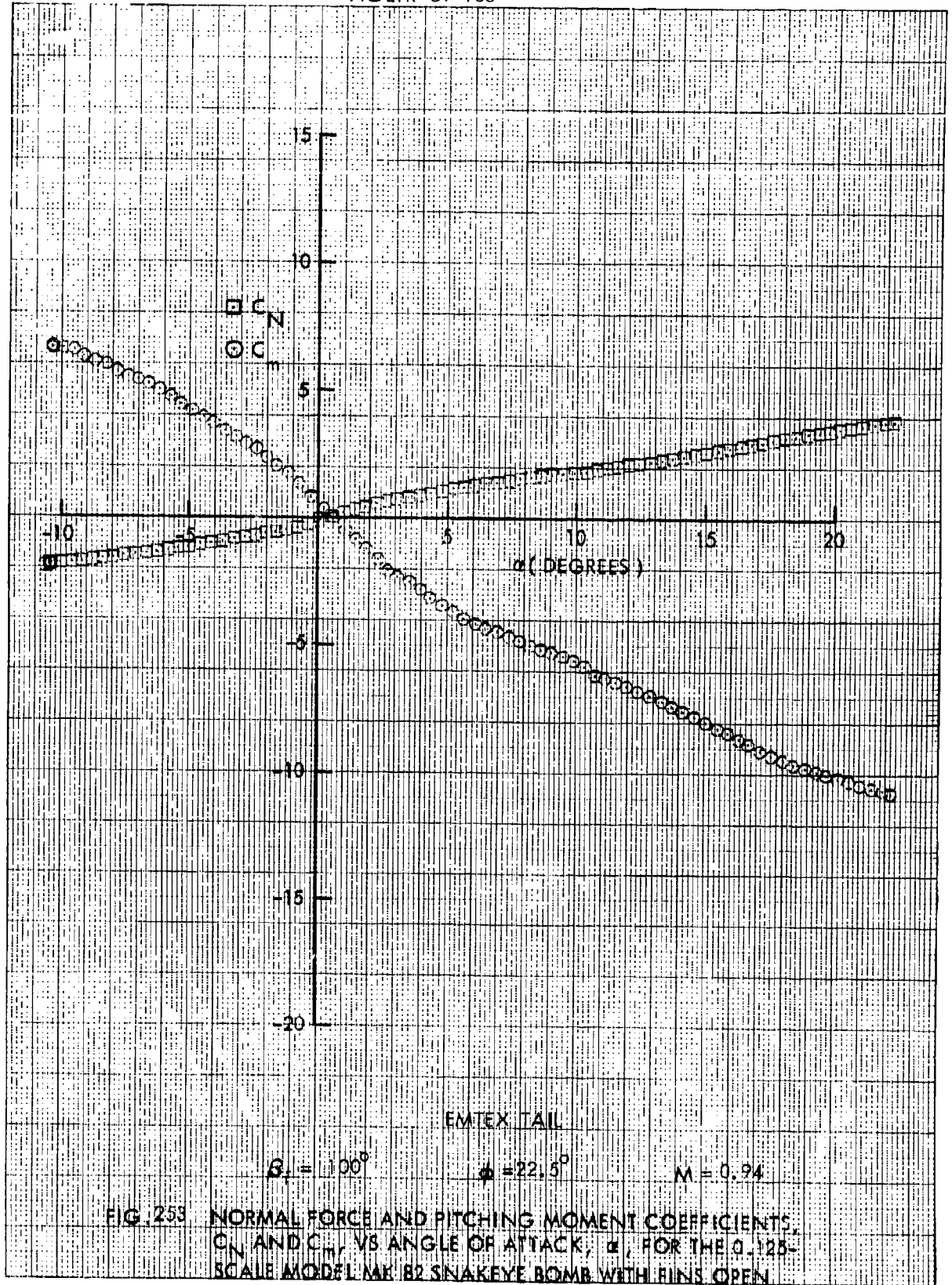
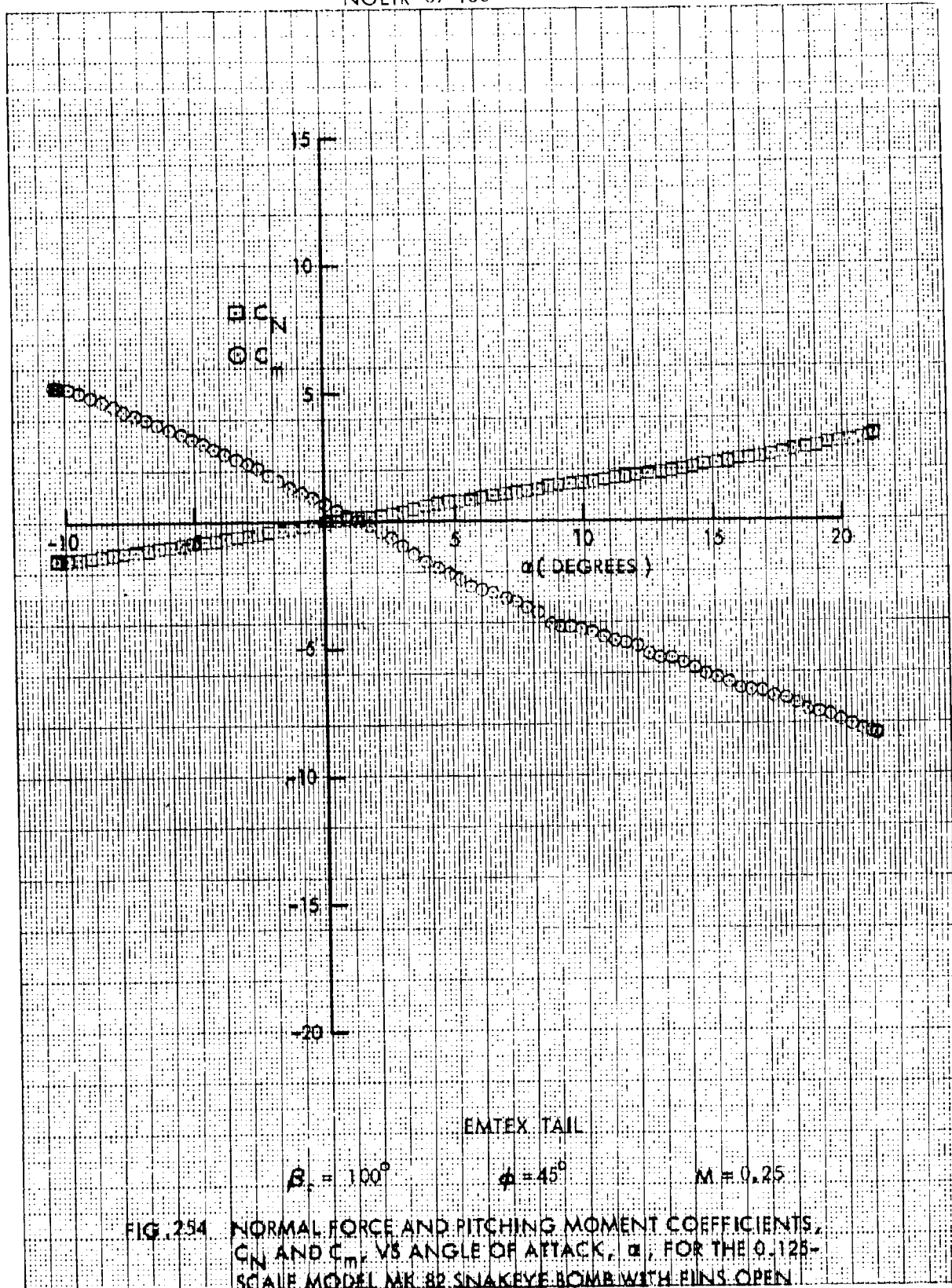
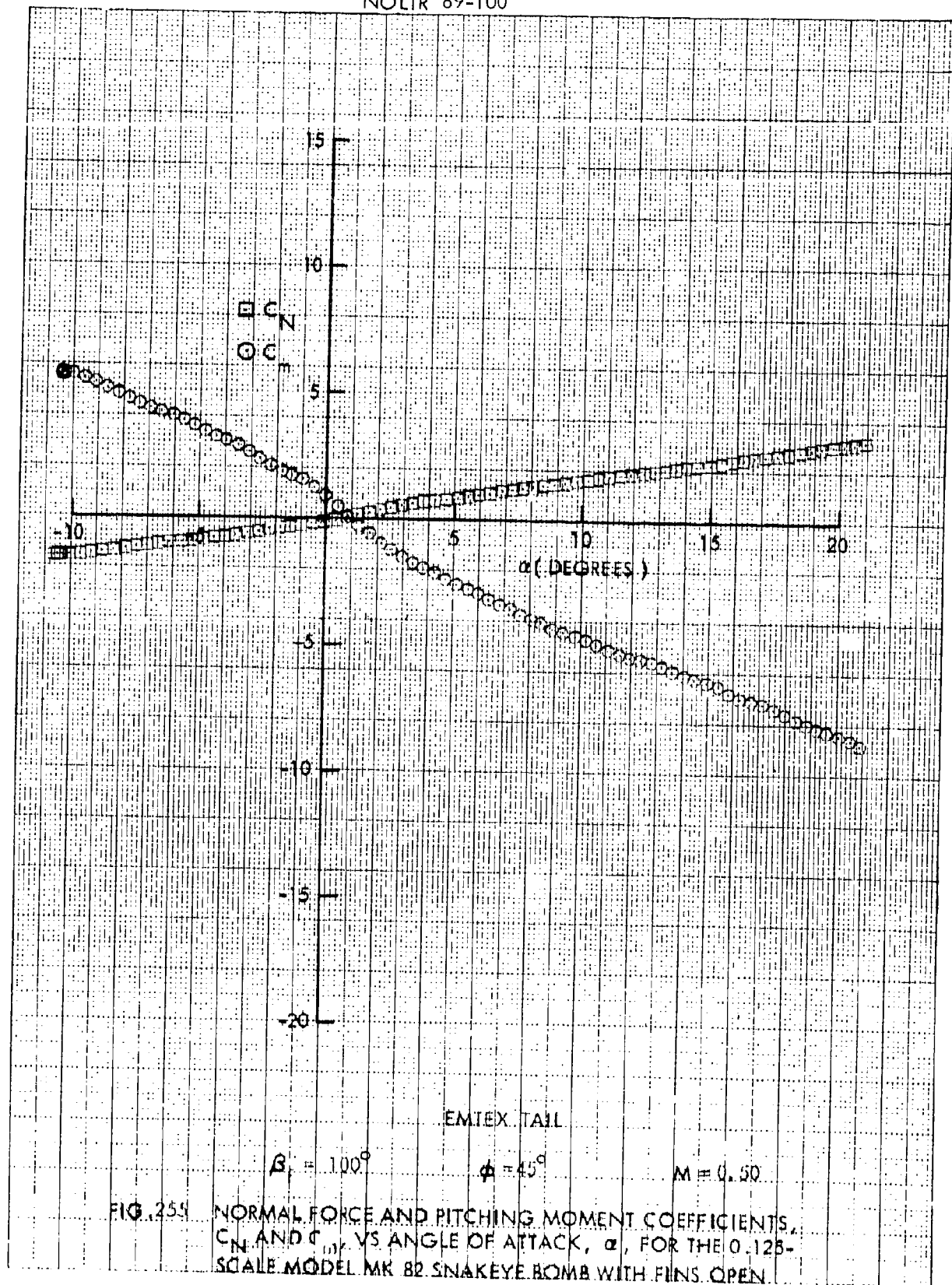


FIG. 251 NORMAL FORCE AND PITCHING MOMENT COEFFICIENTS,  $C_N$  AND  $C_m$ , VS ANGLE OF ATTACK,  $\alpha$ , FOR THE 0.125-SCALE MODEL MK-82 SNAKEYE BOMB WITH FINS OPEN.

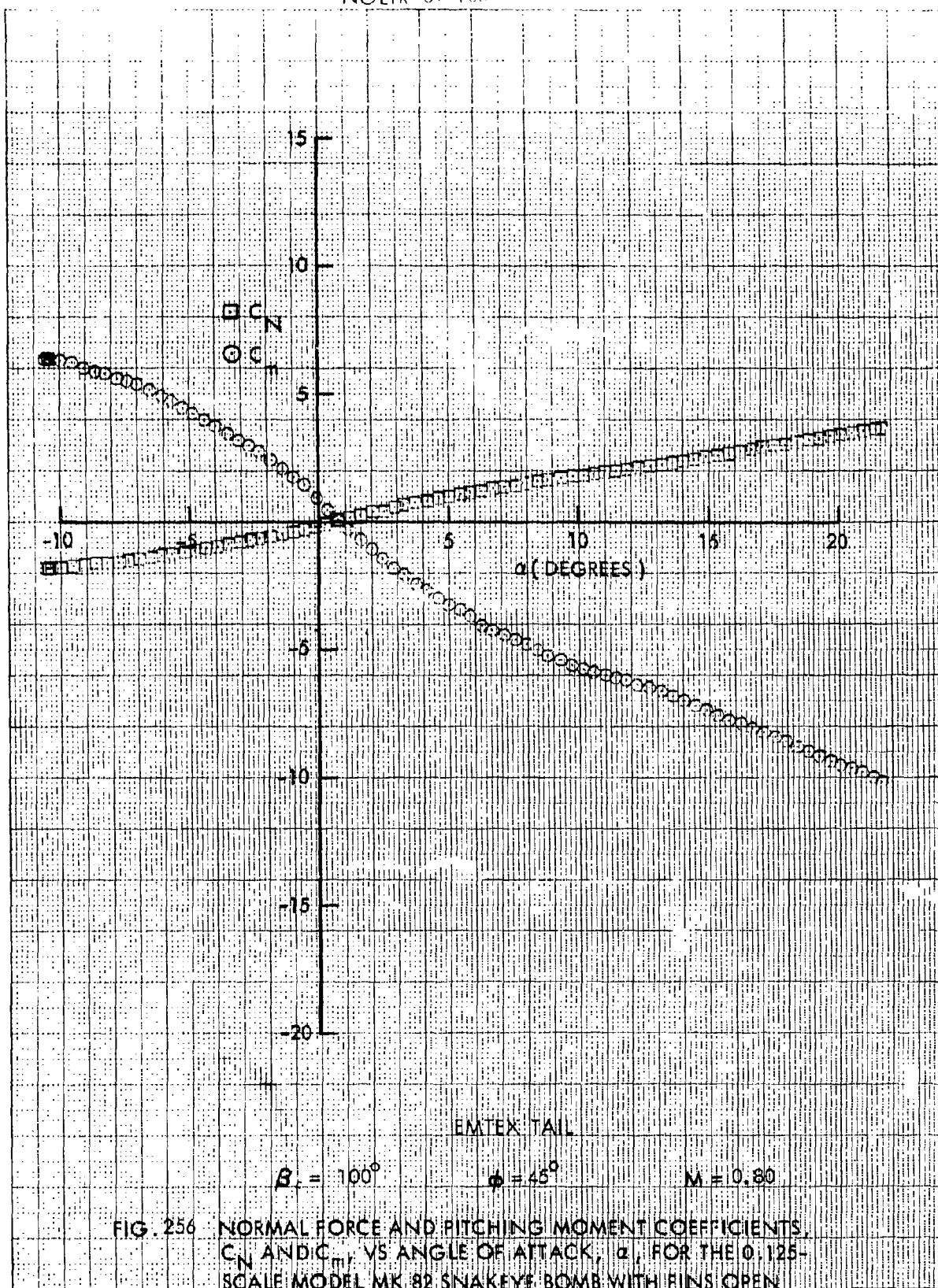


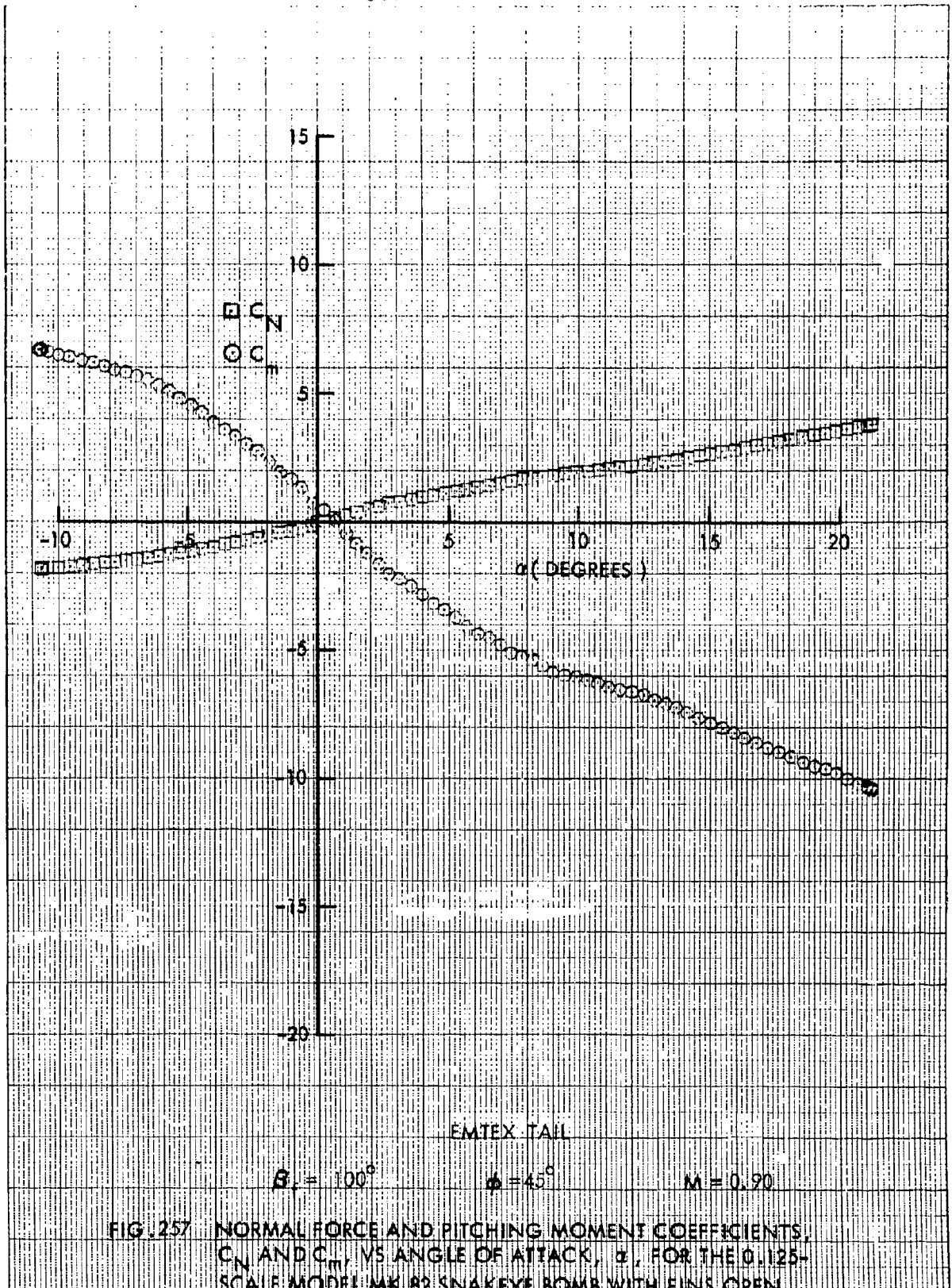


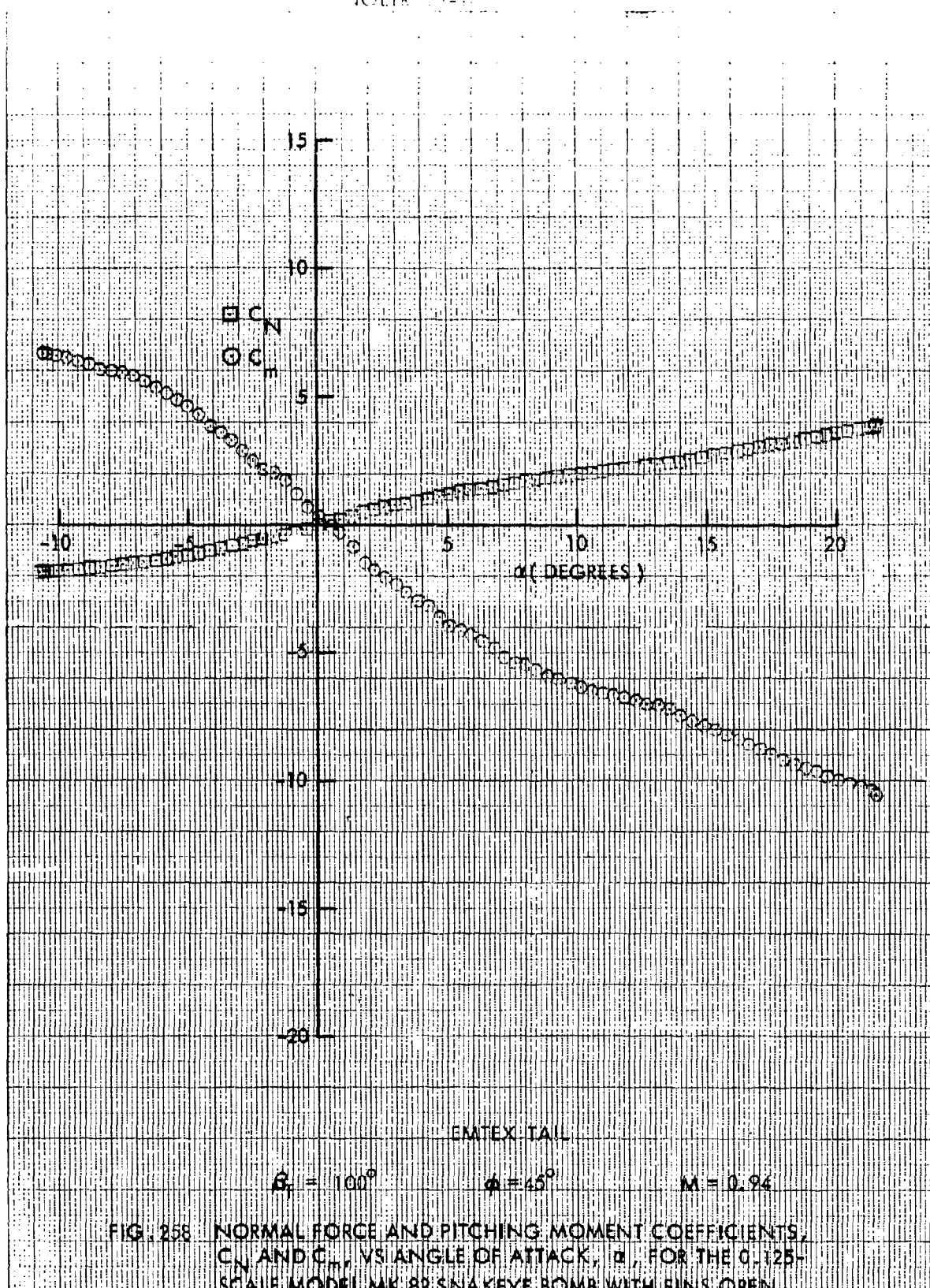


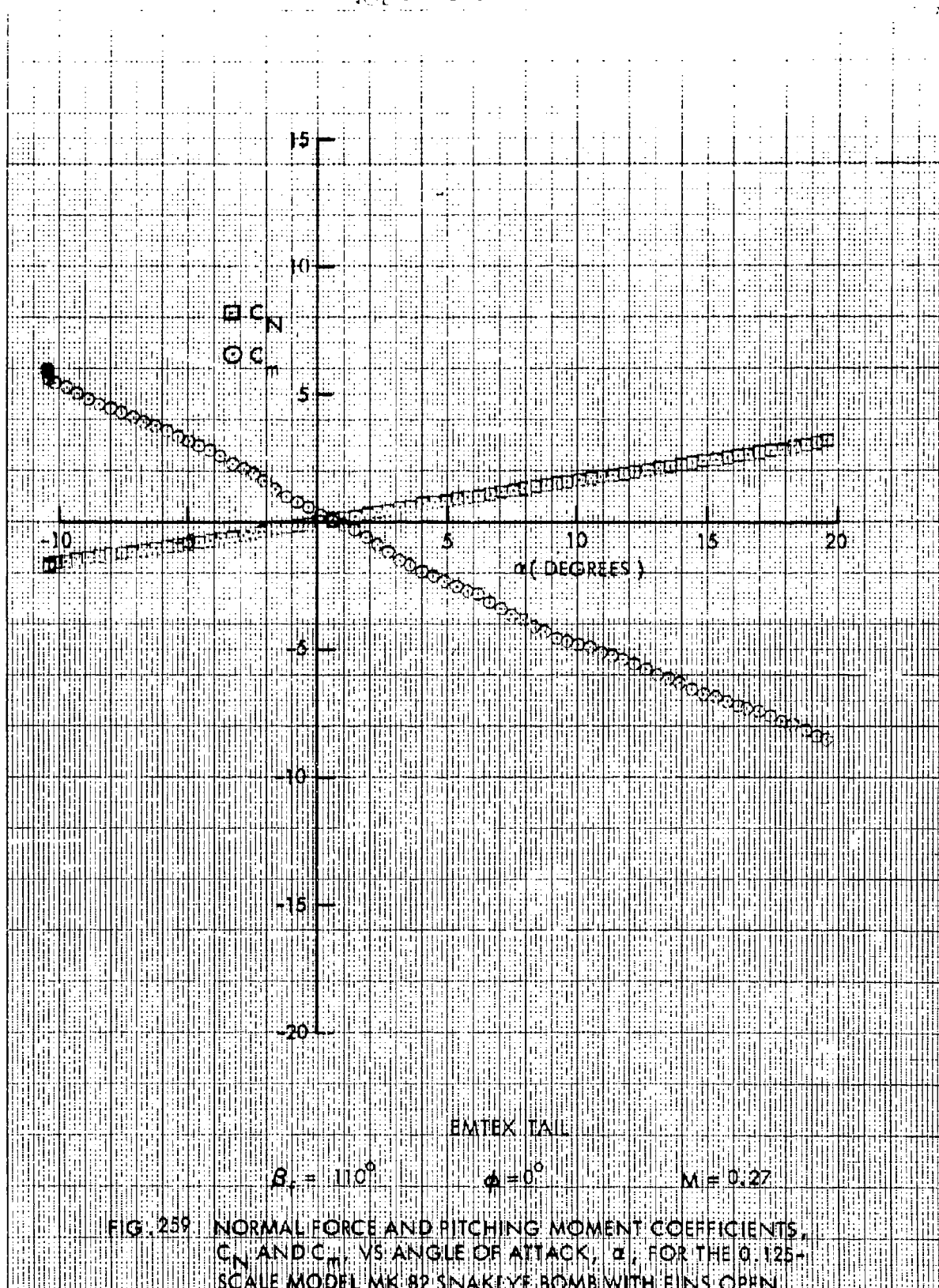


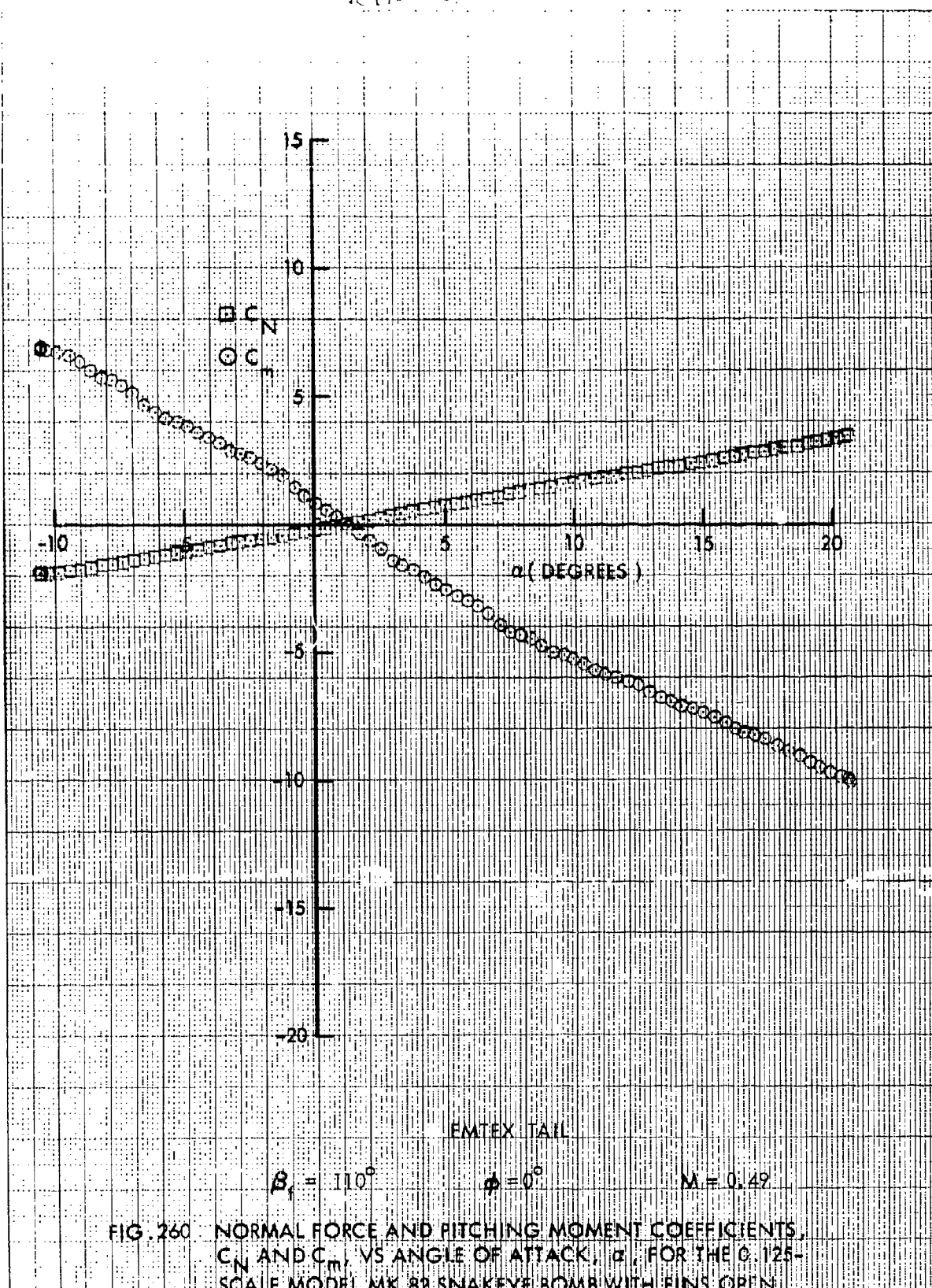


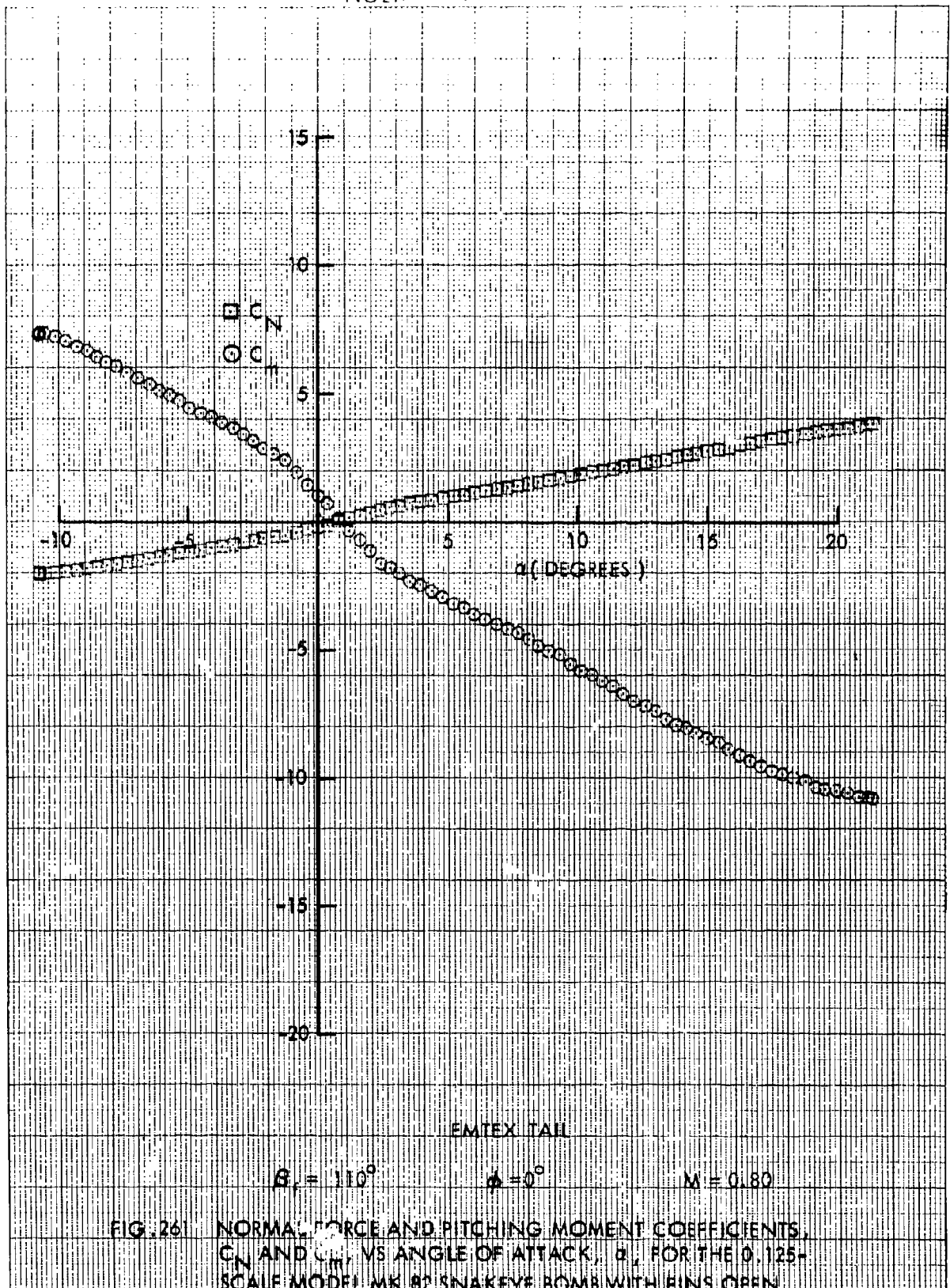




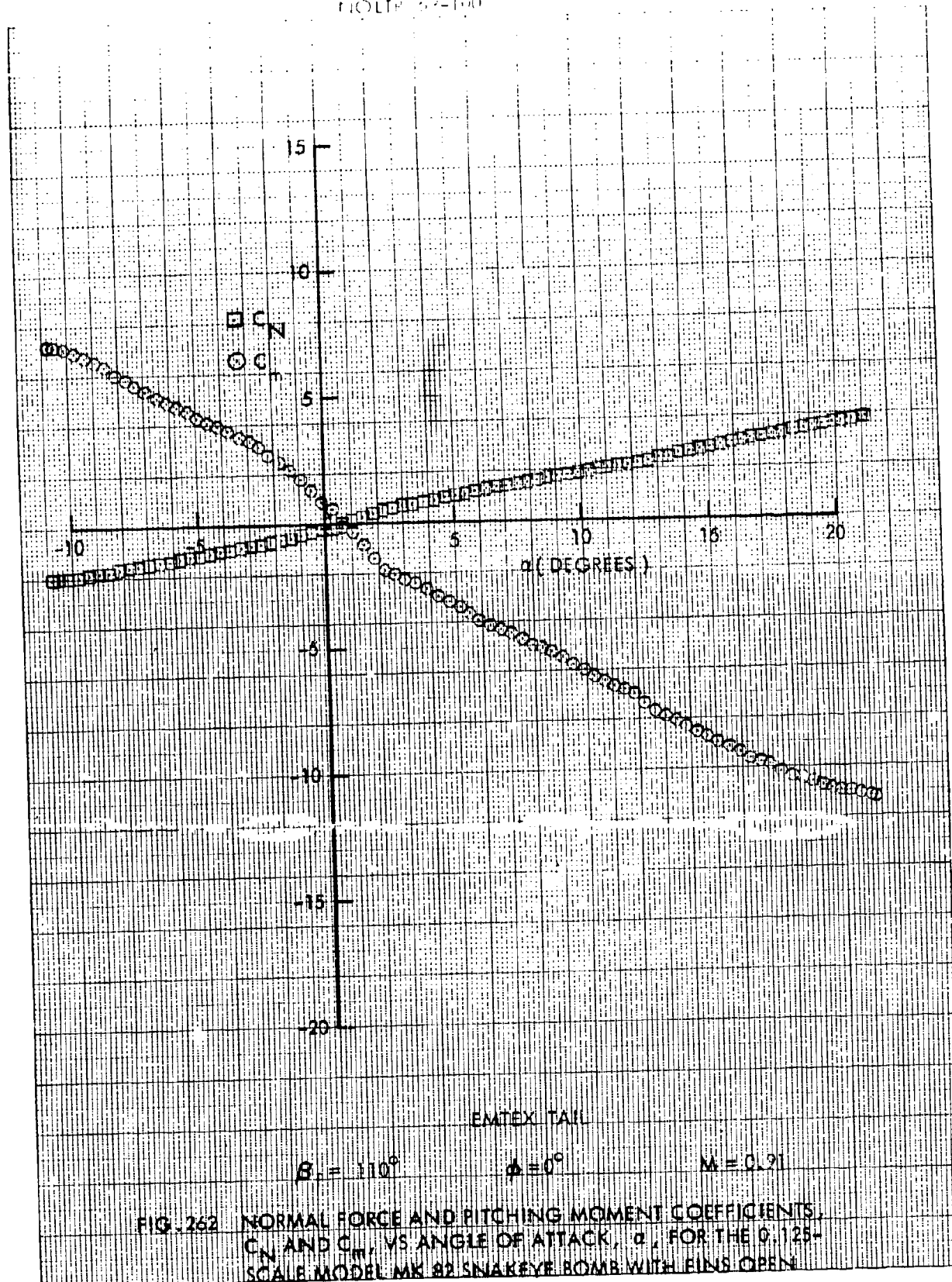


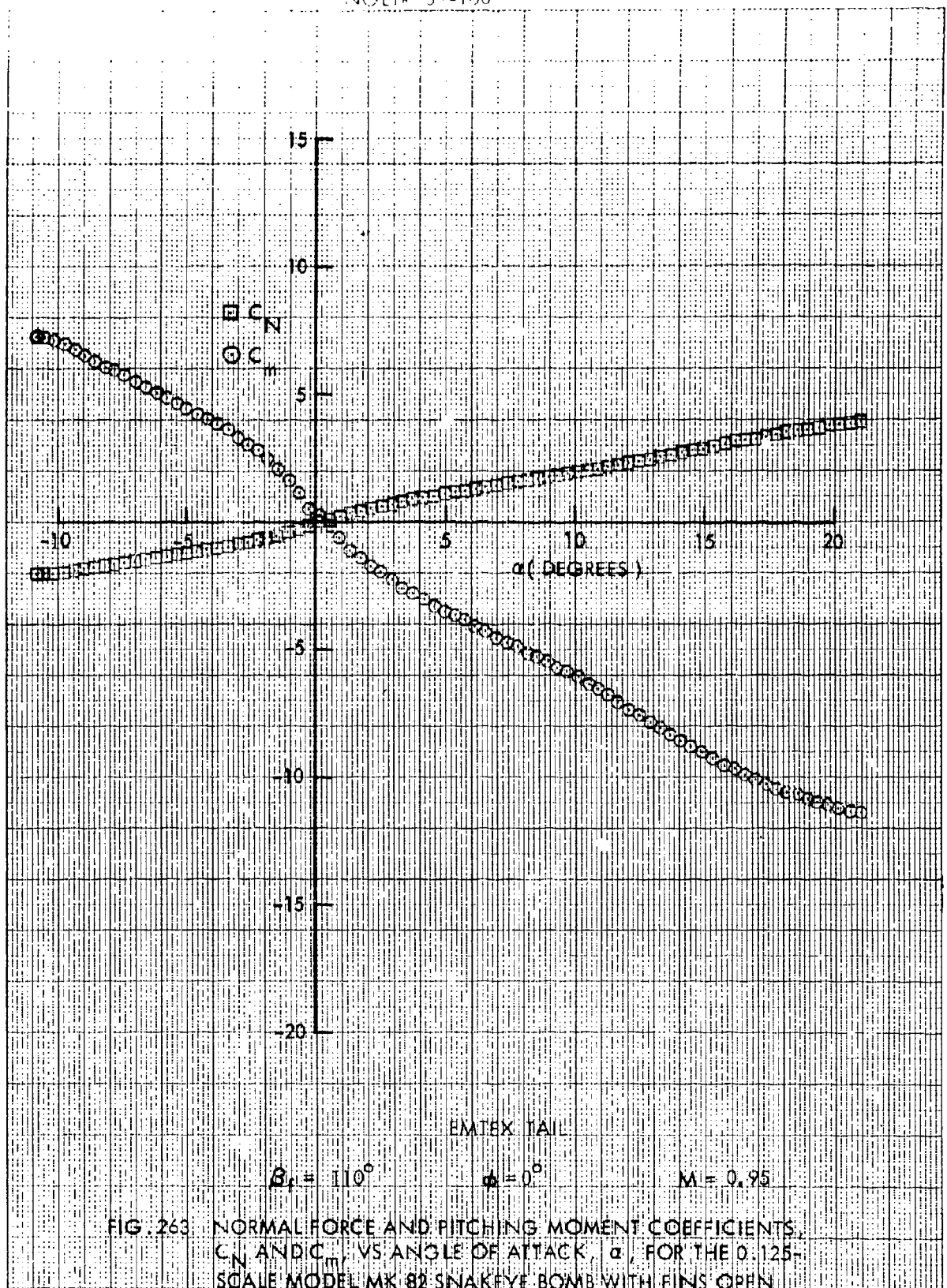


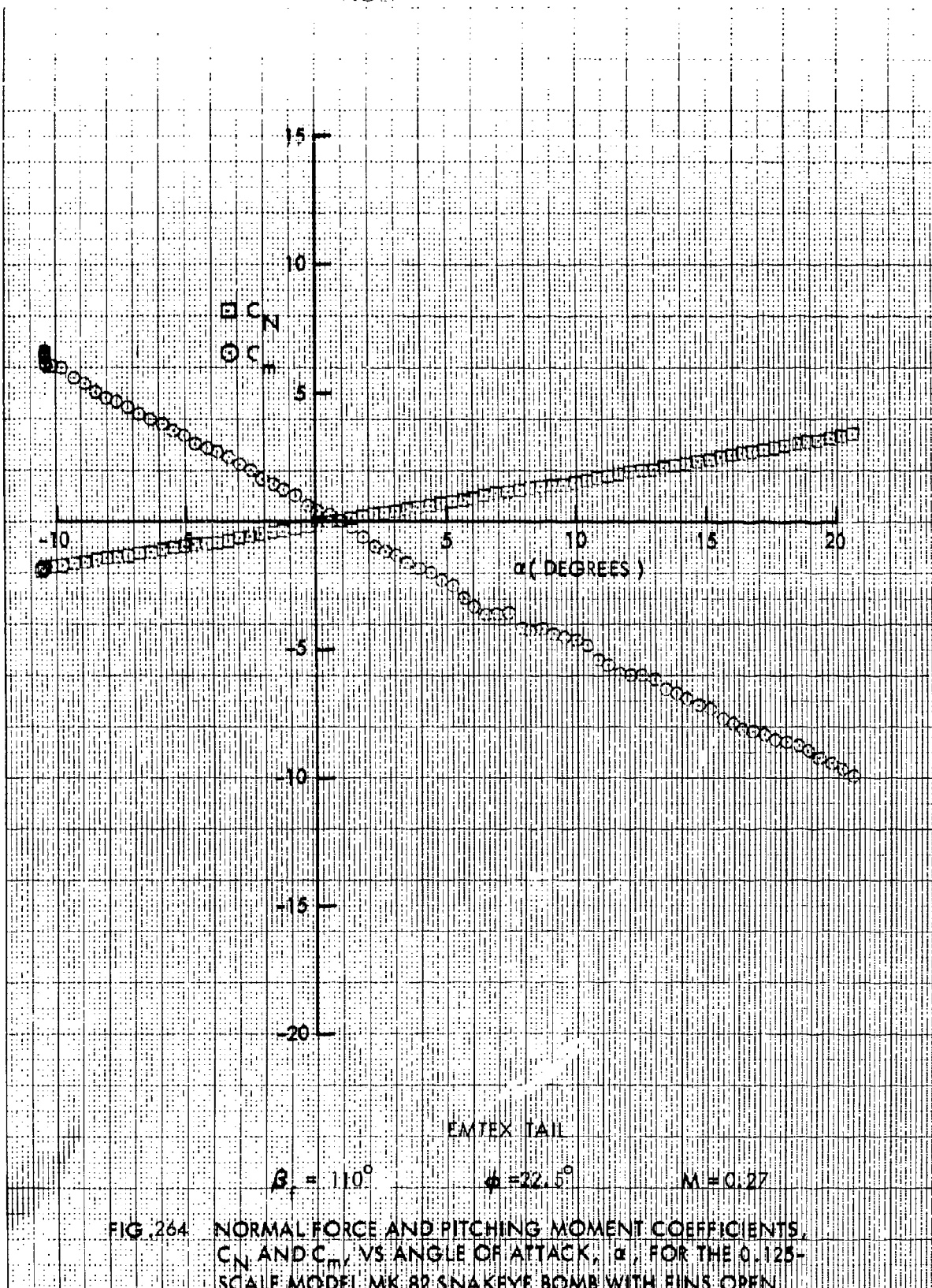


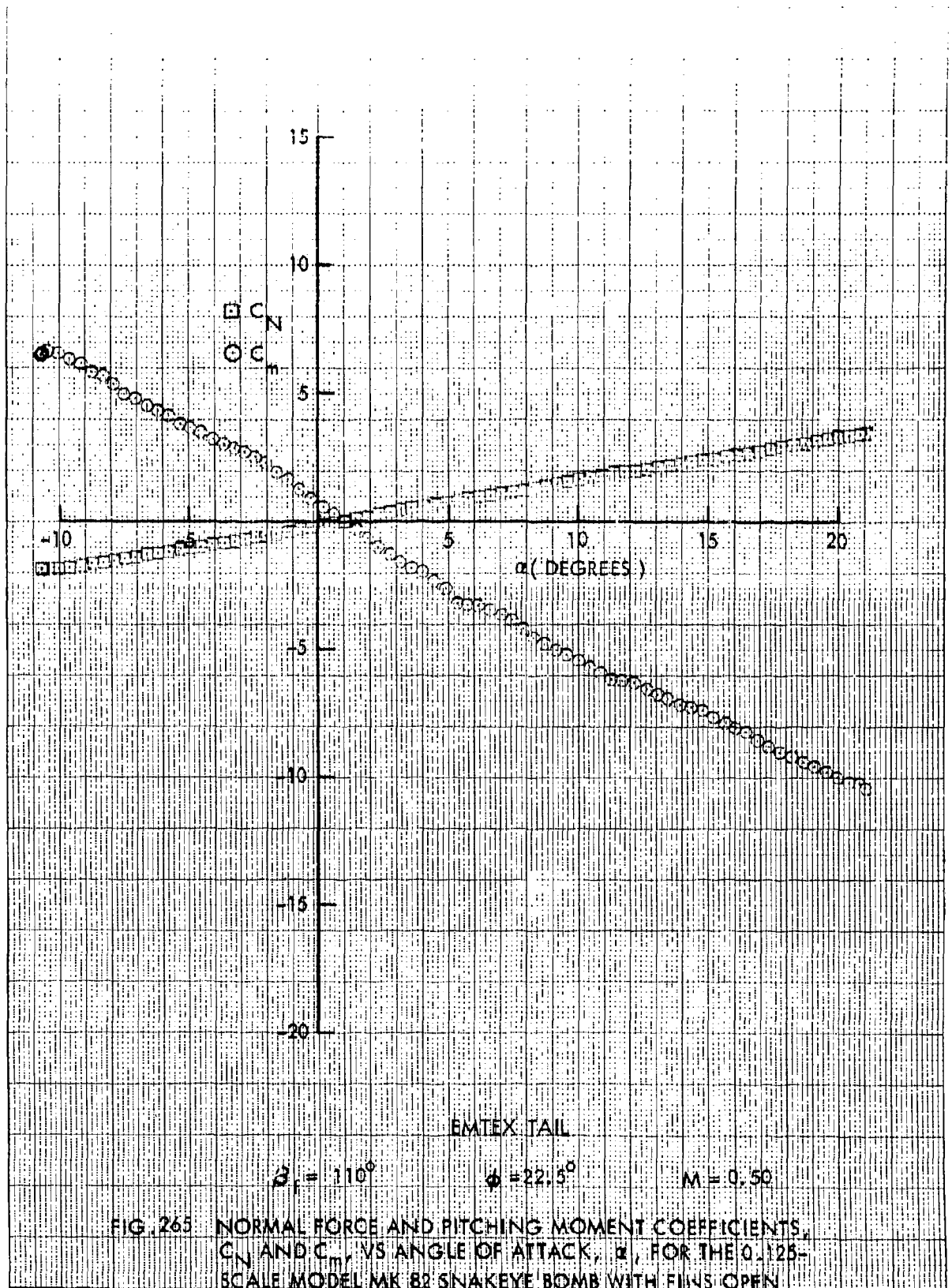


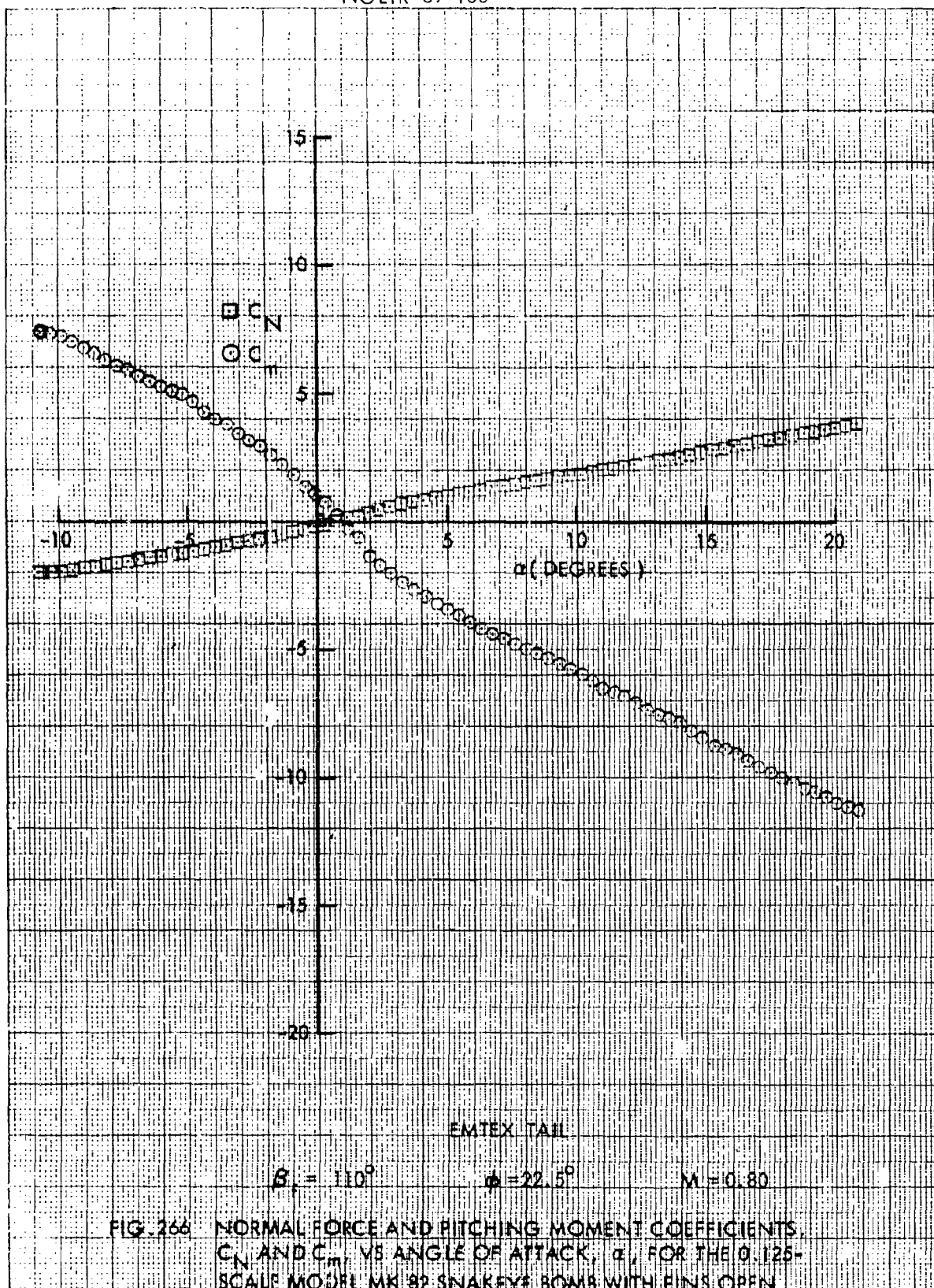


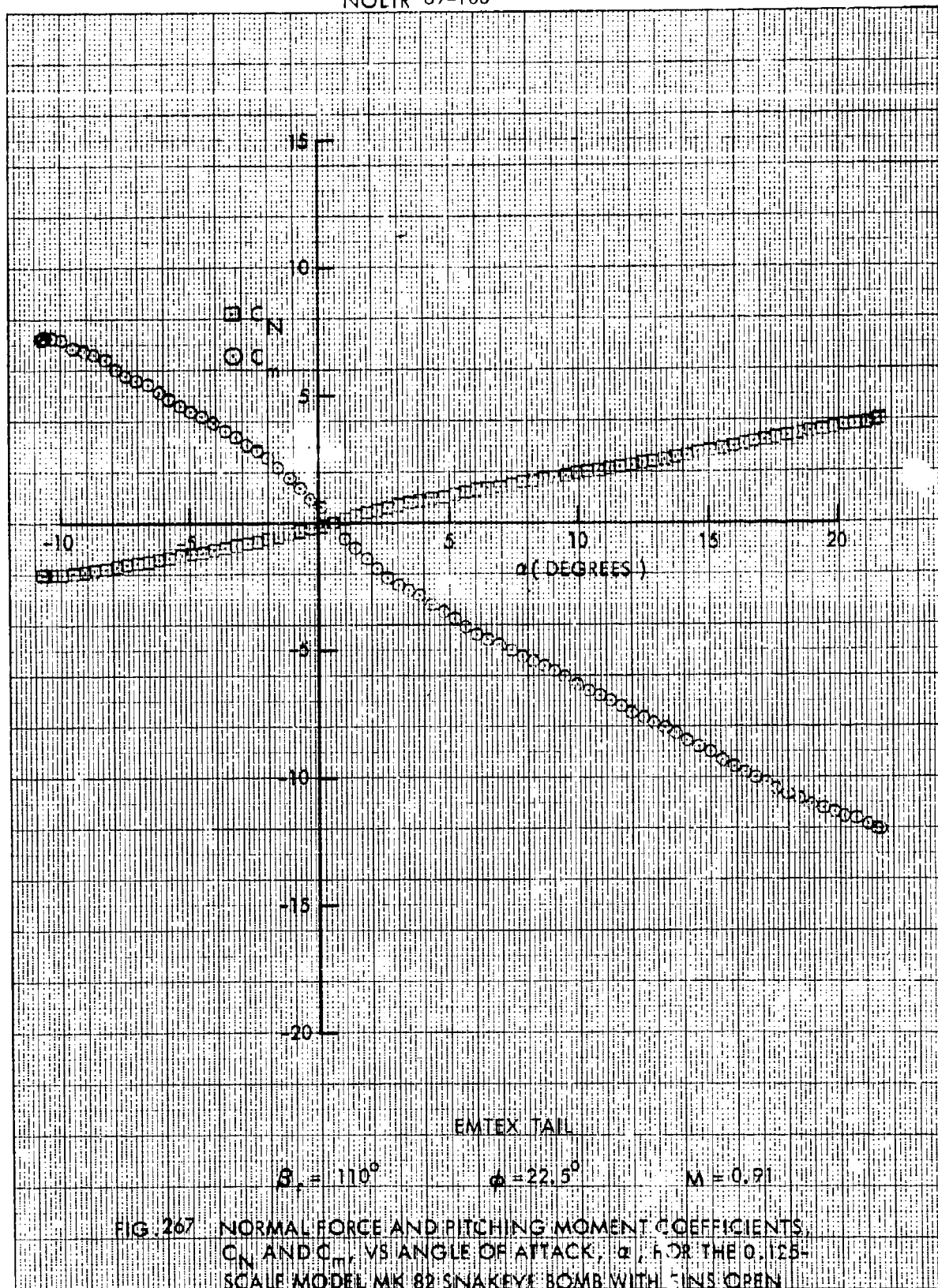




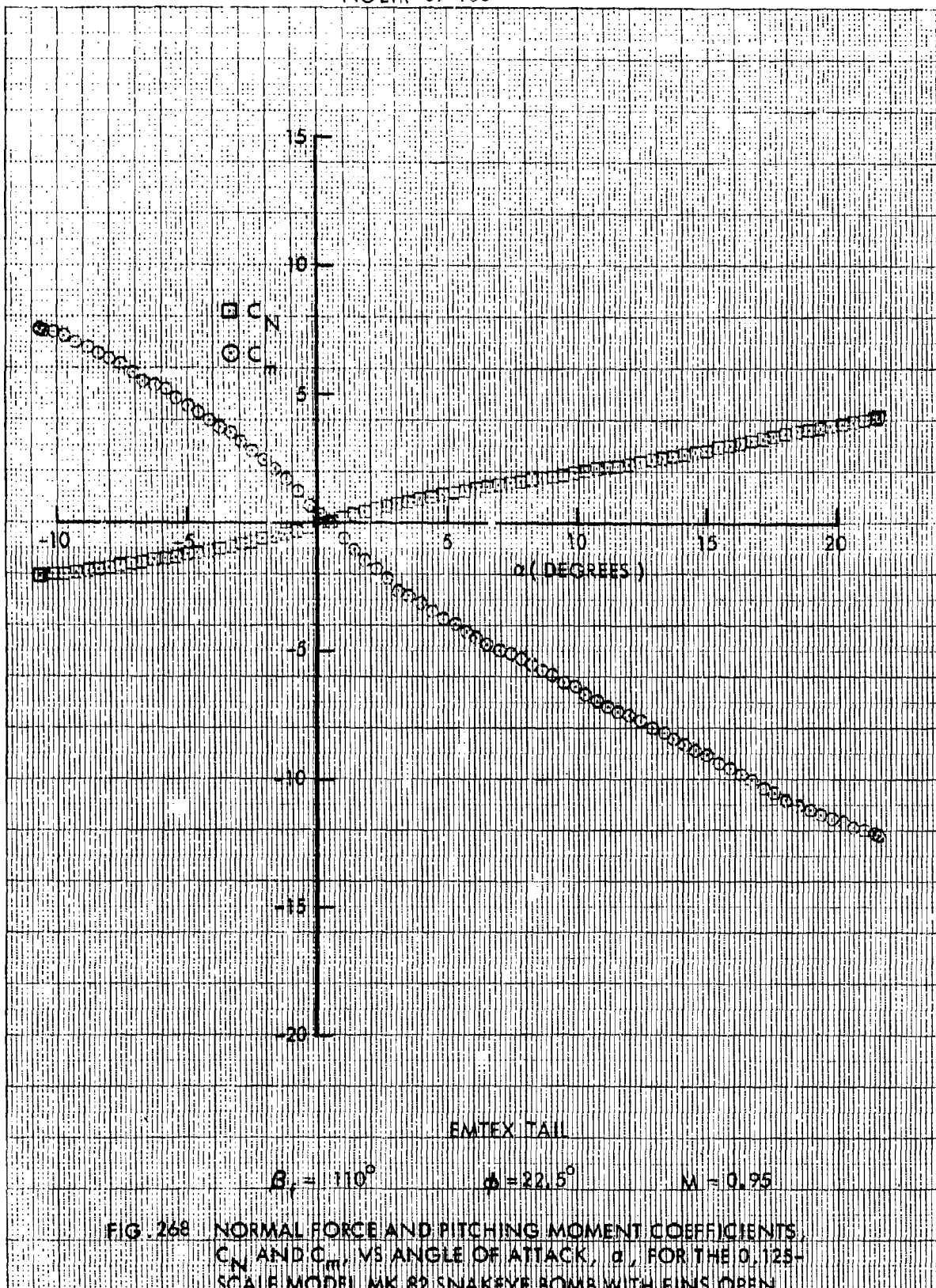


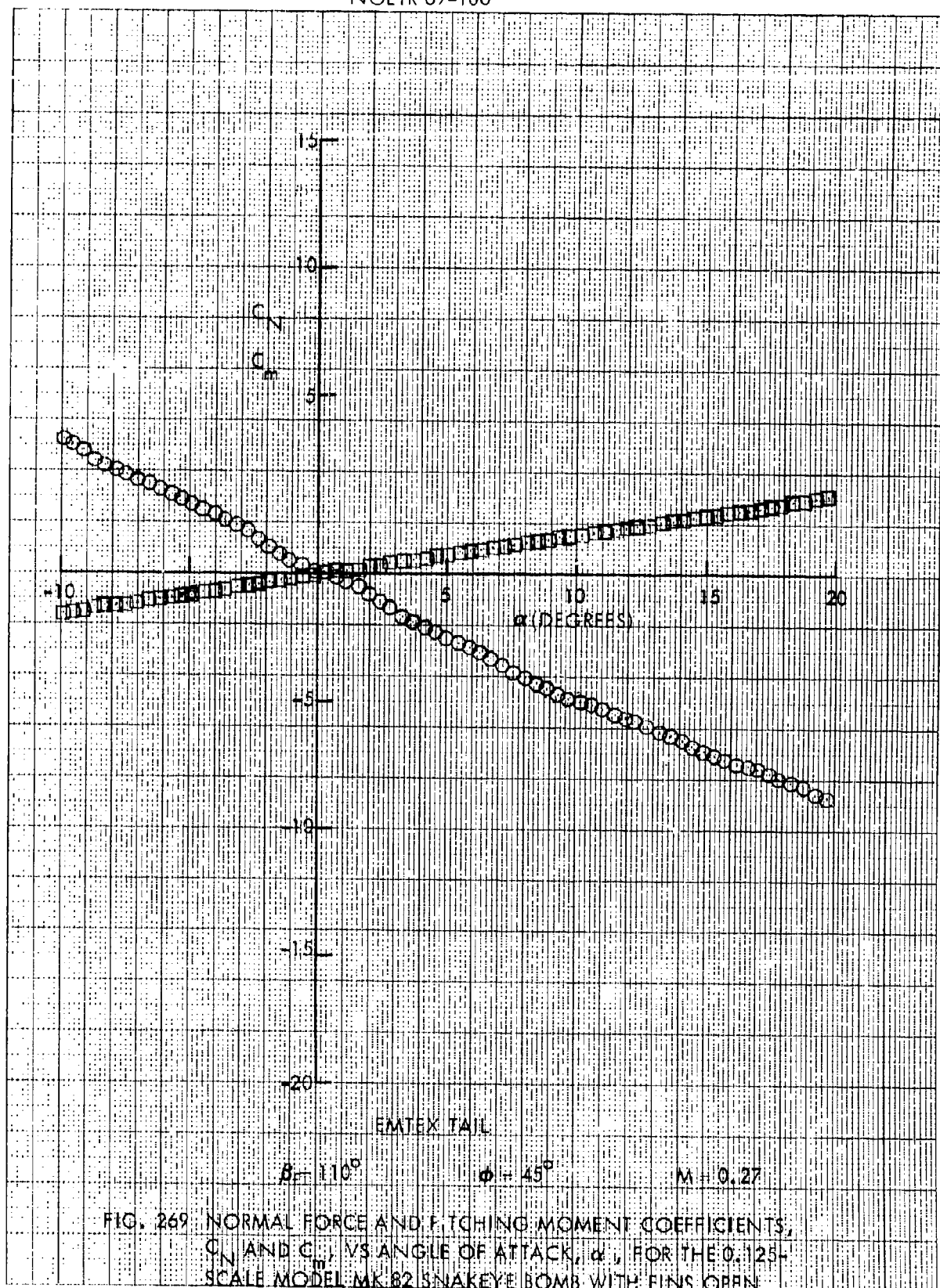


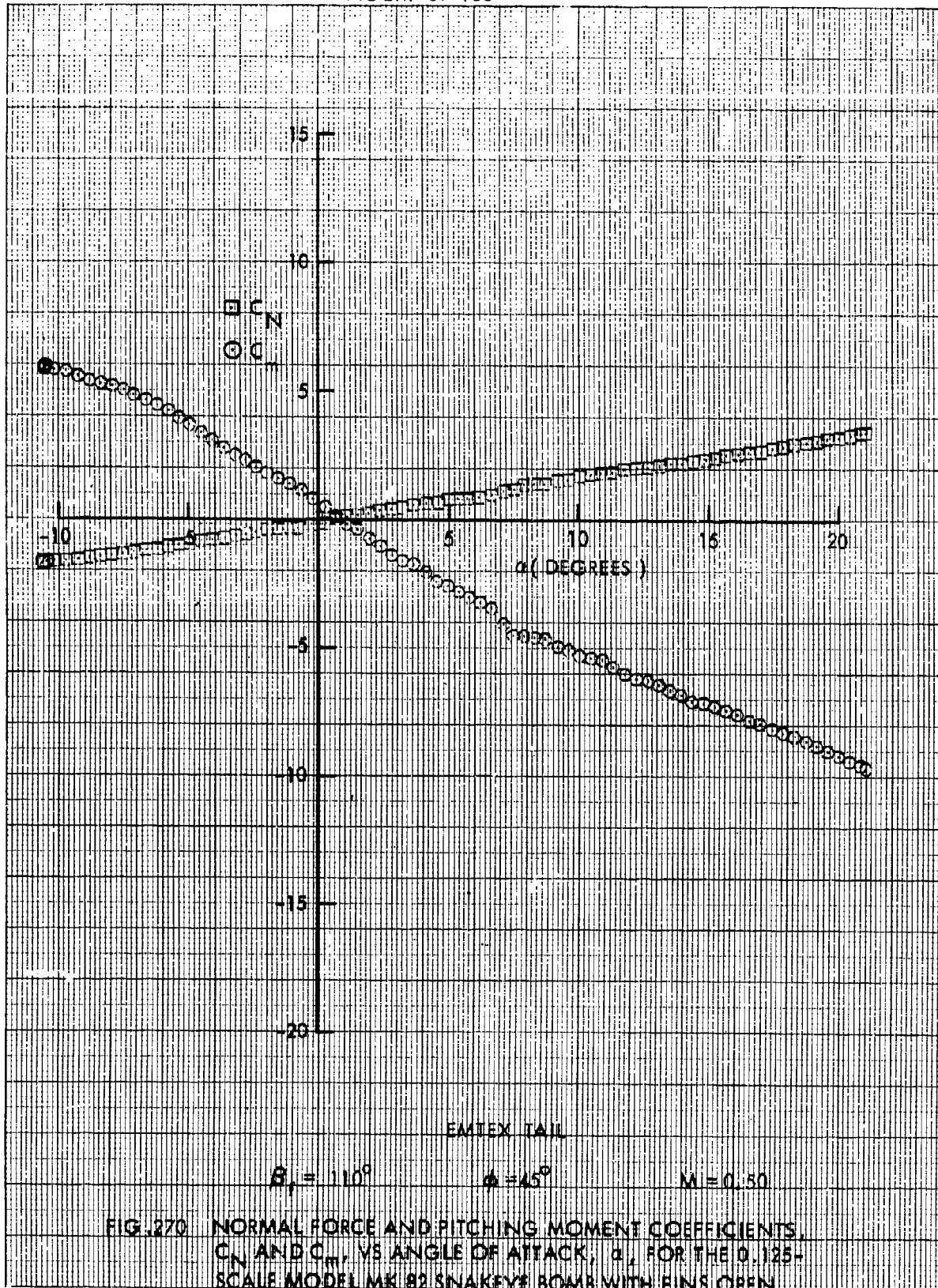


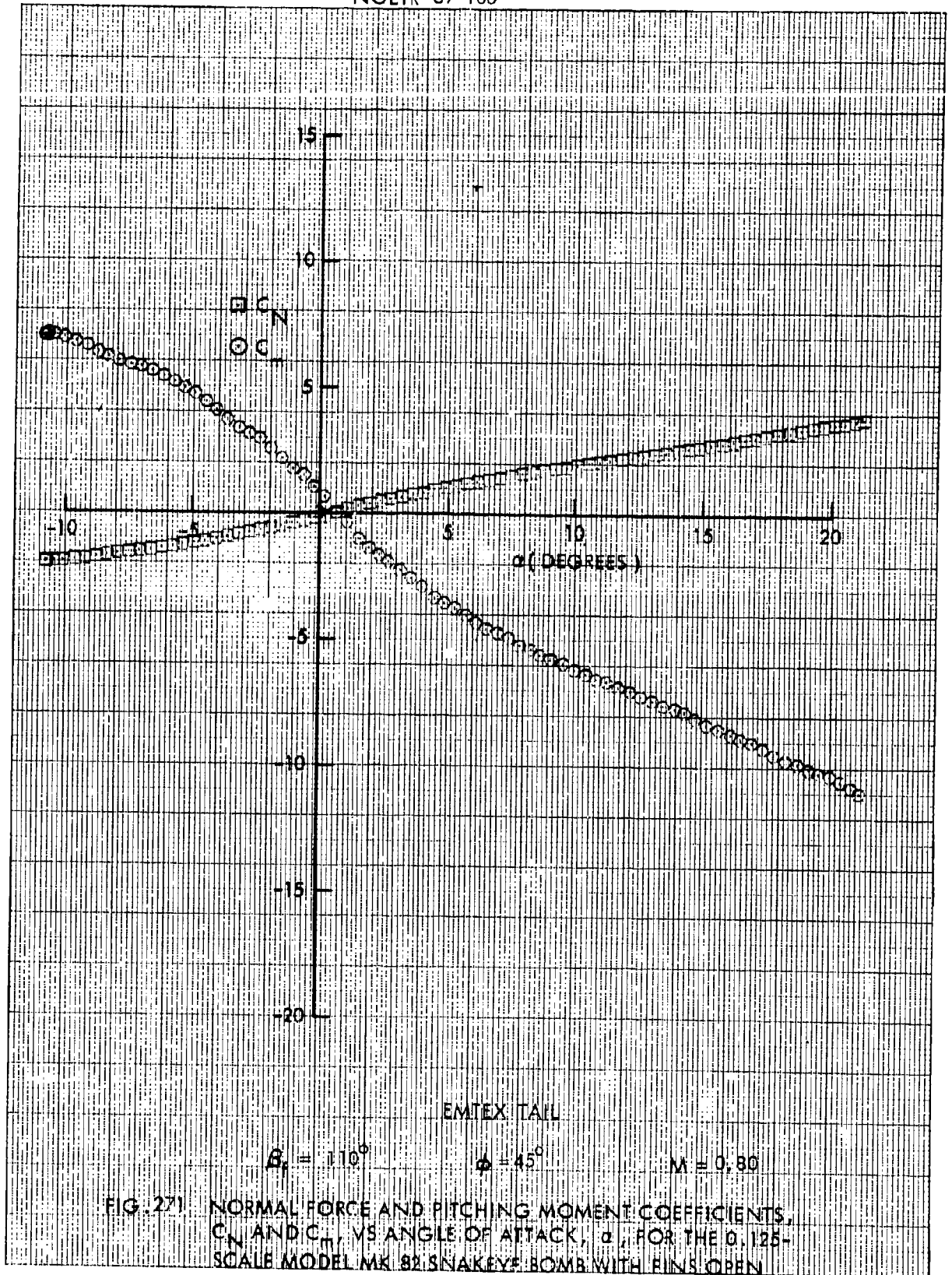


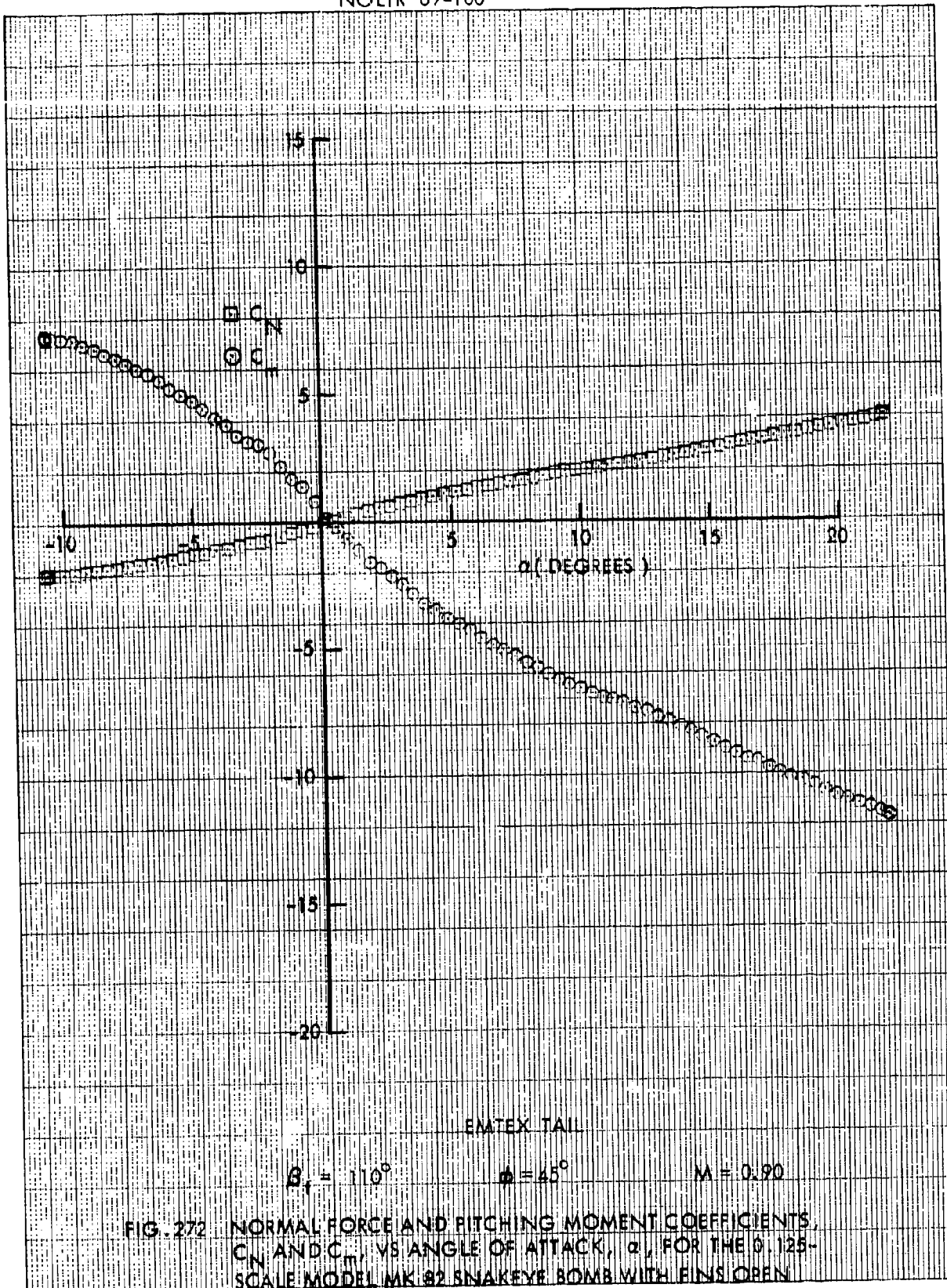




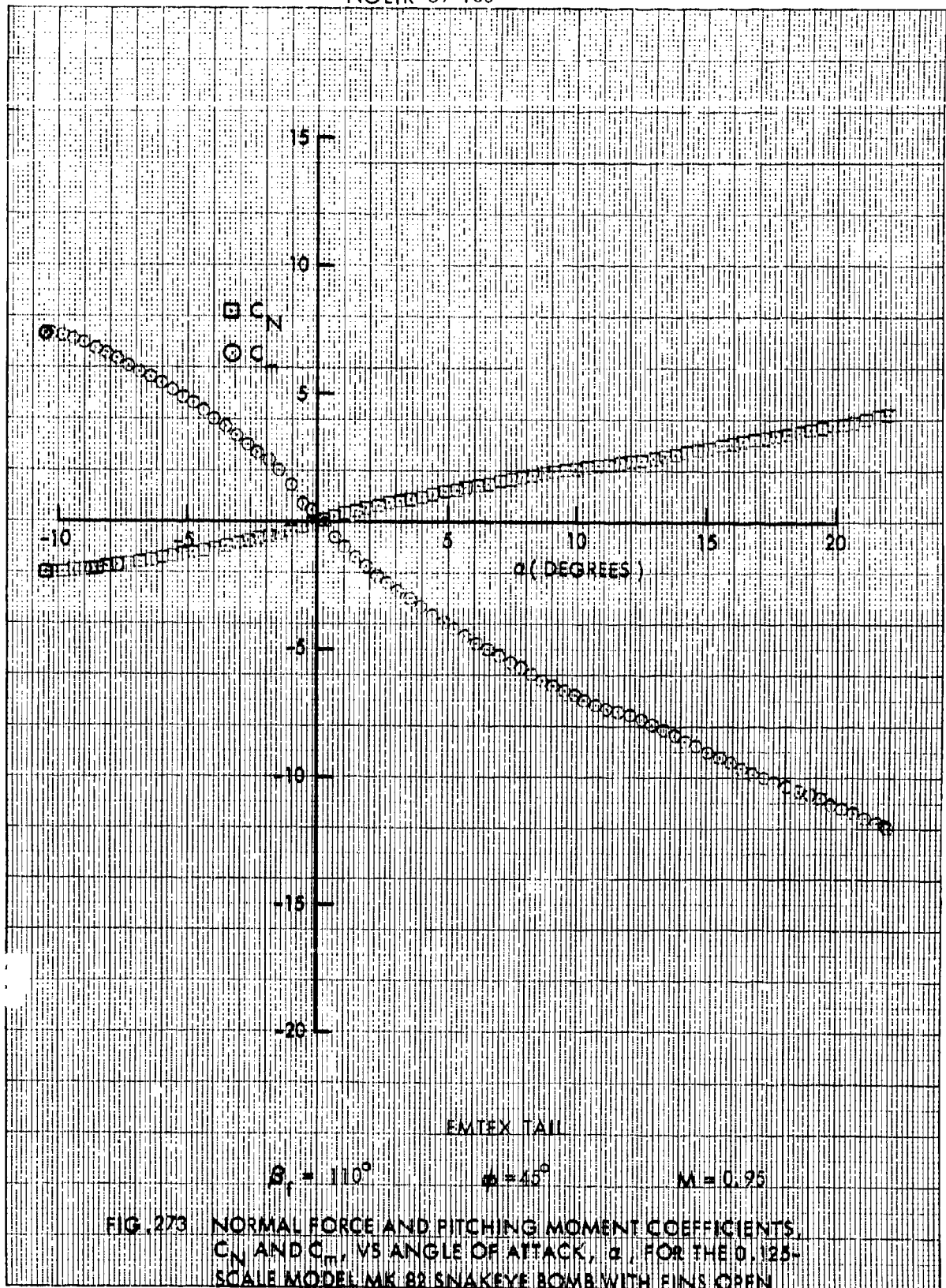




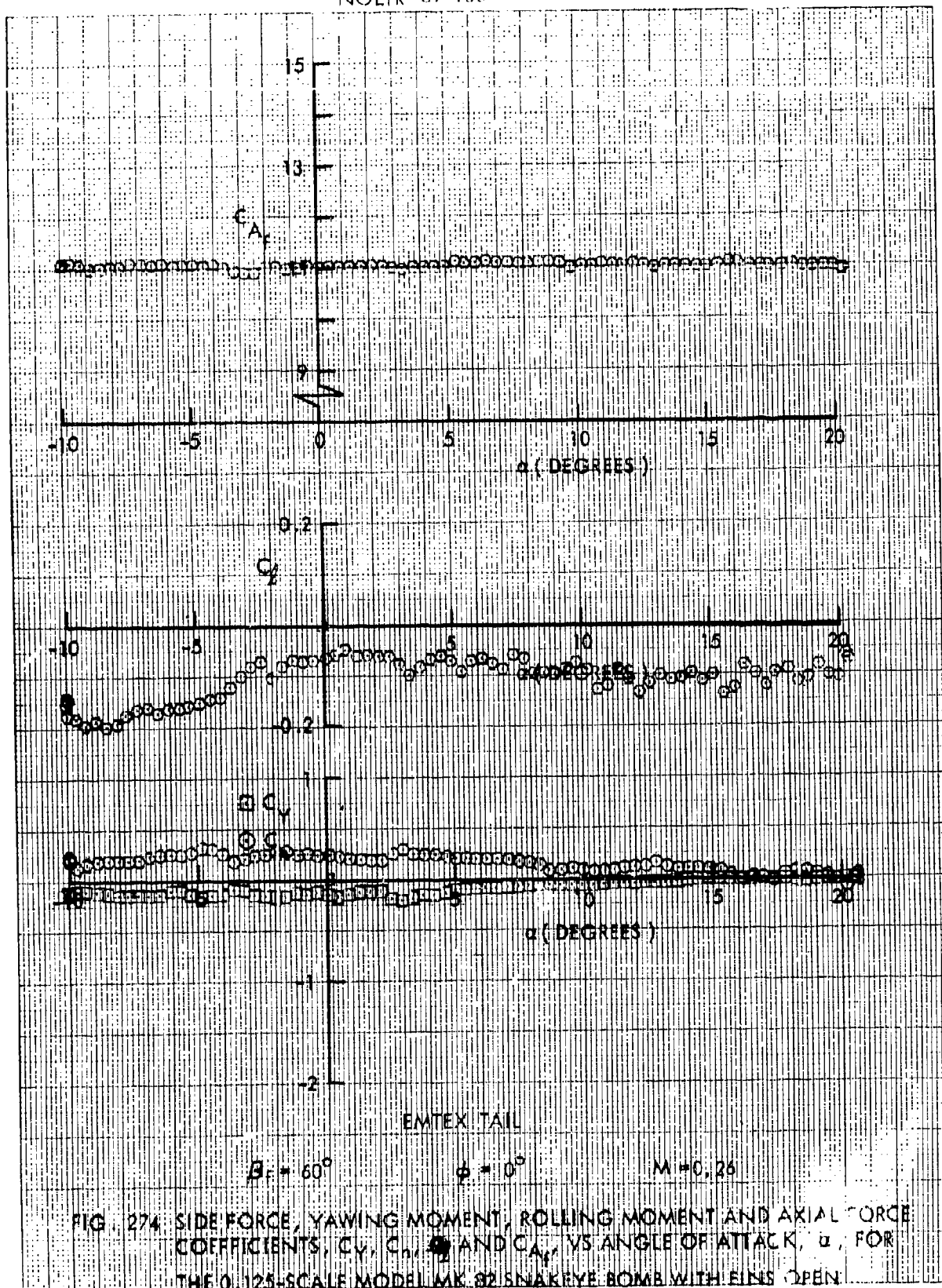


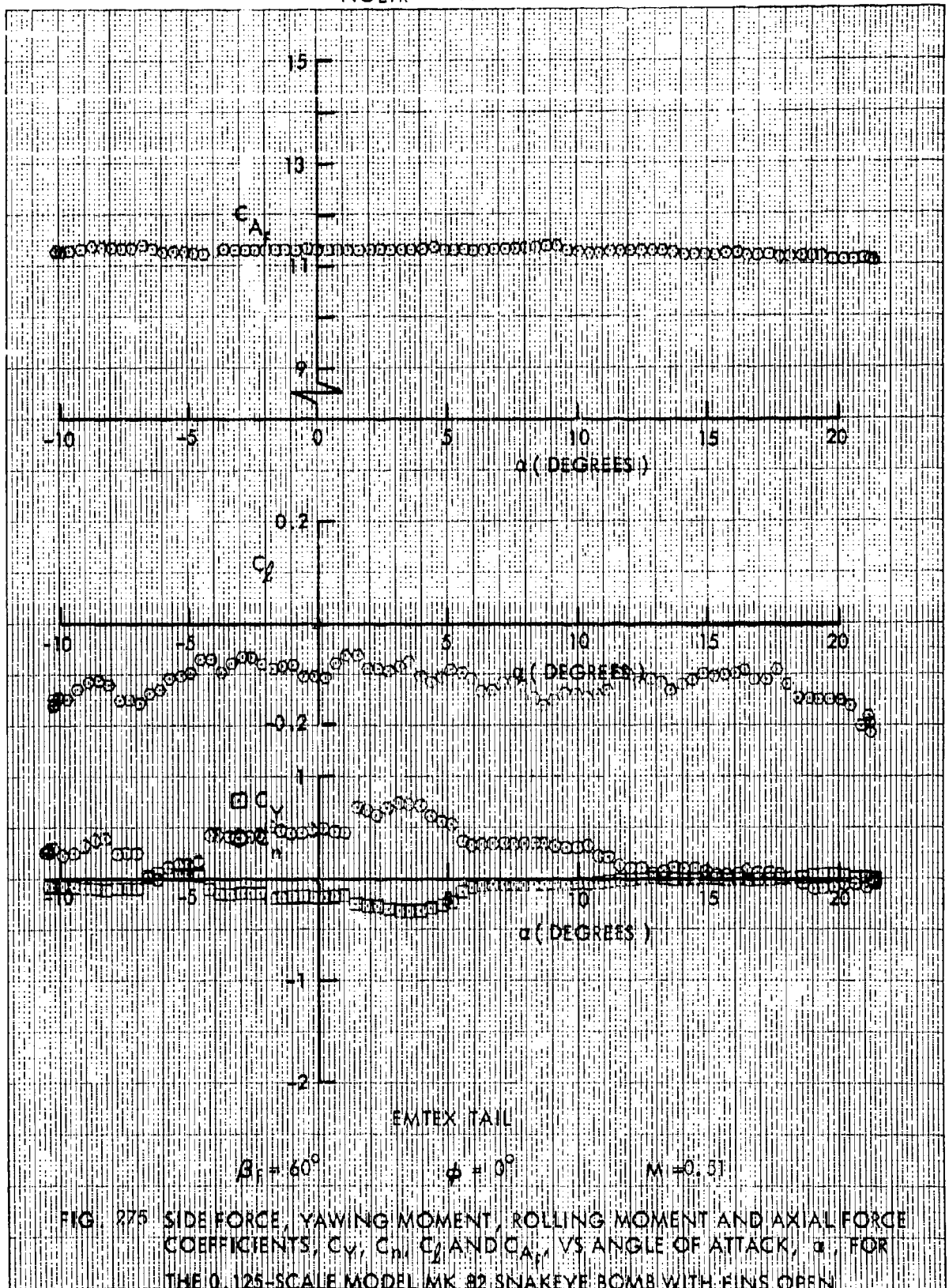


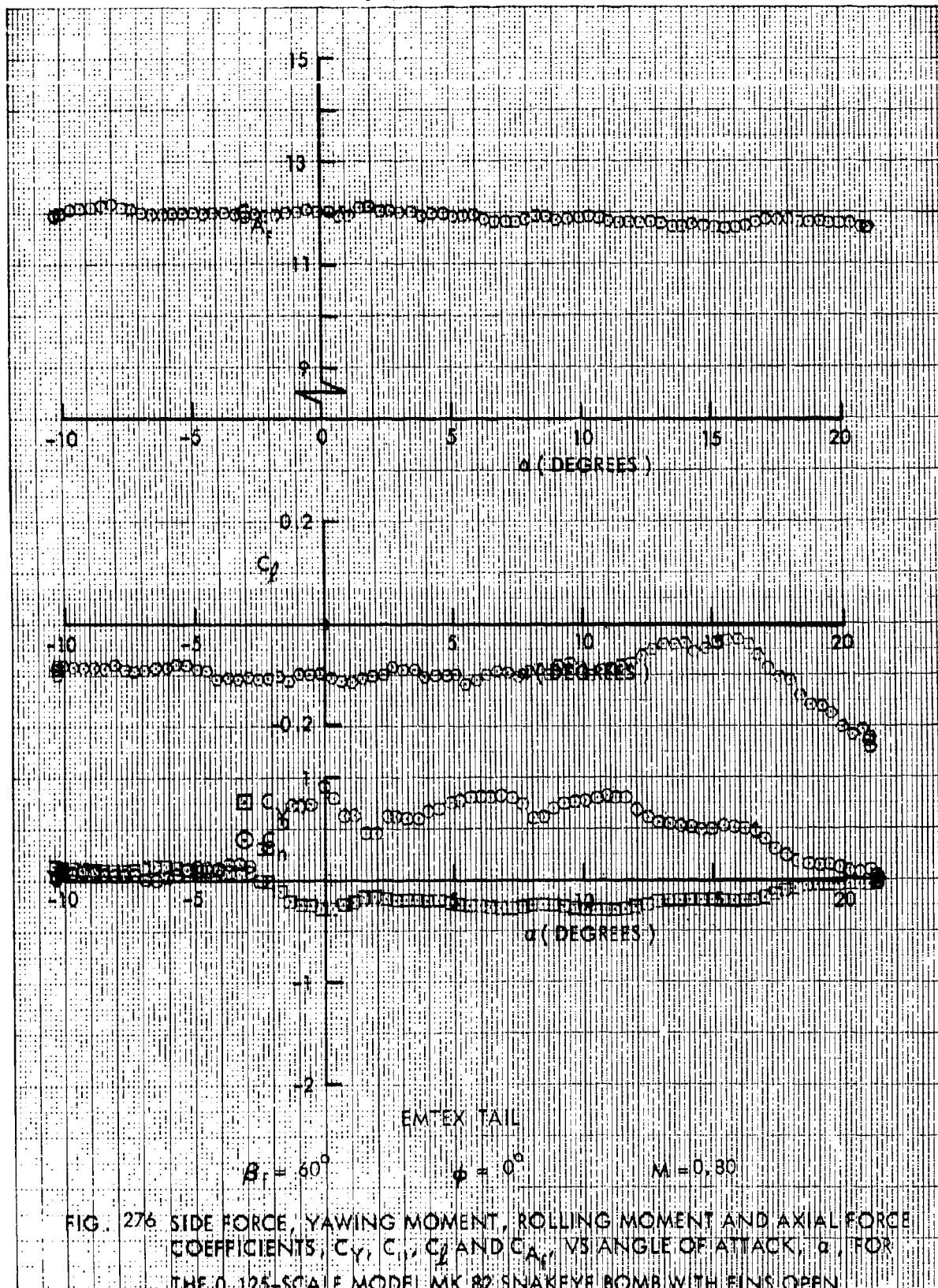


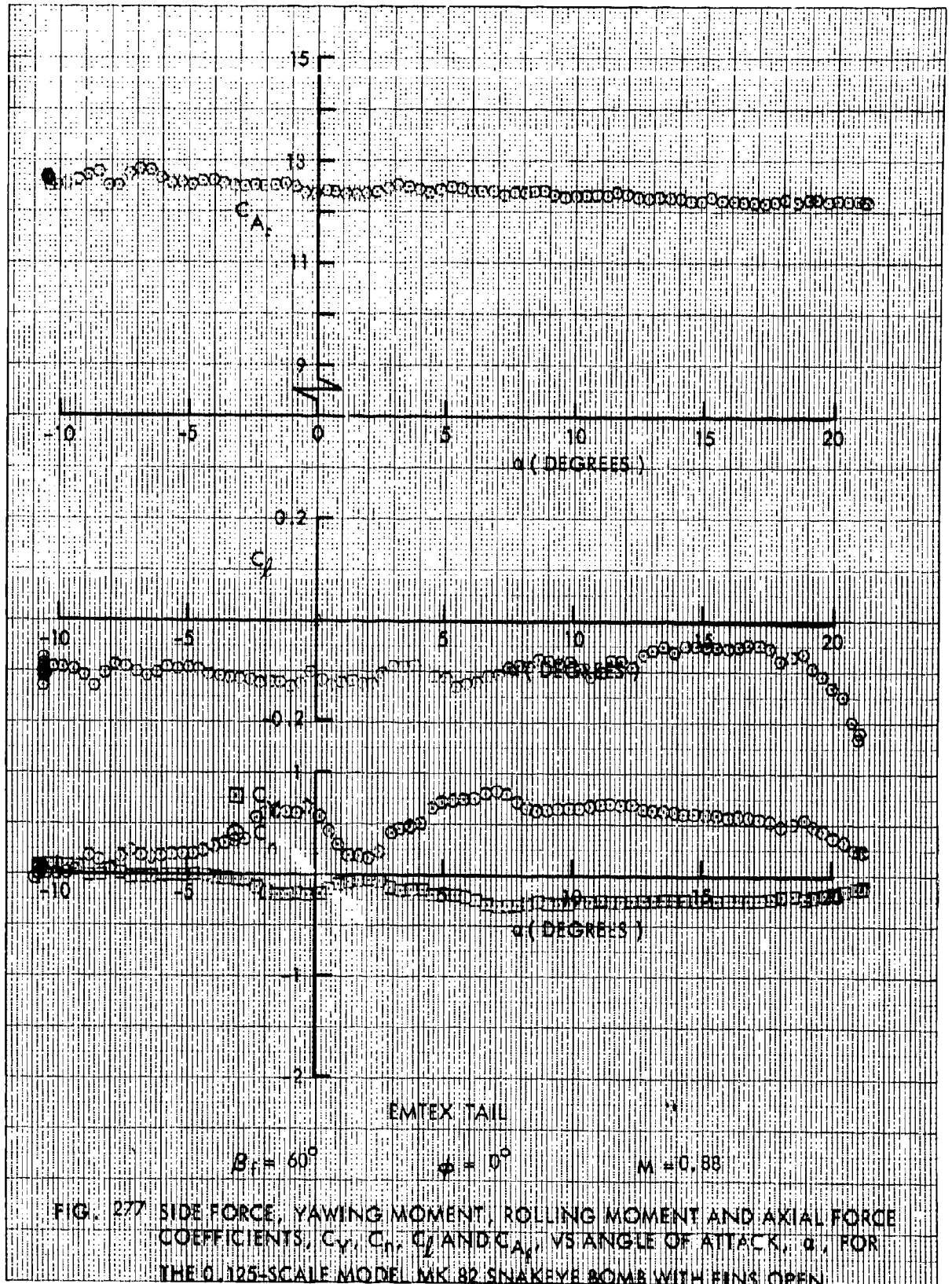


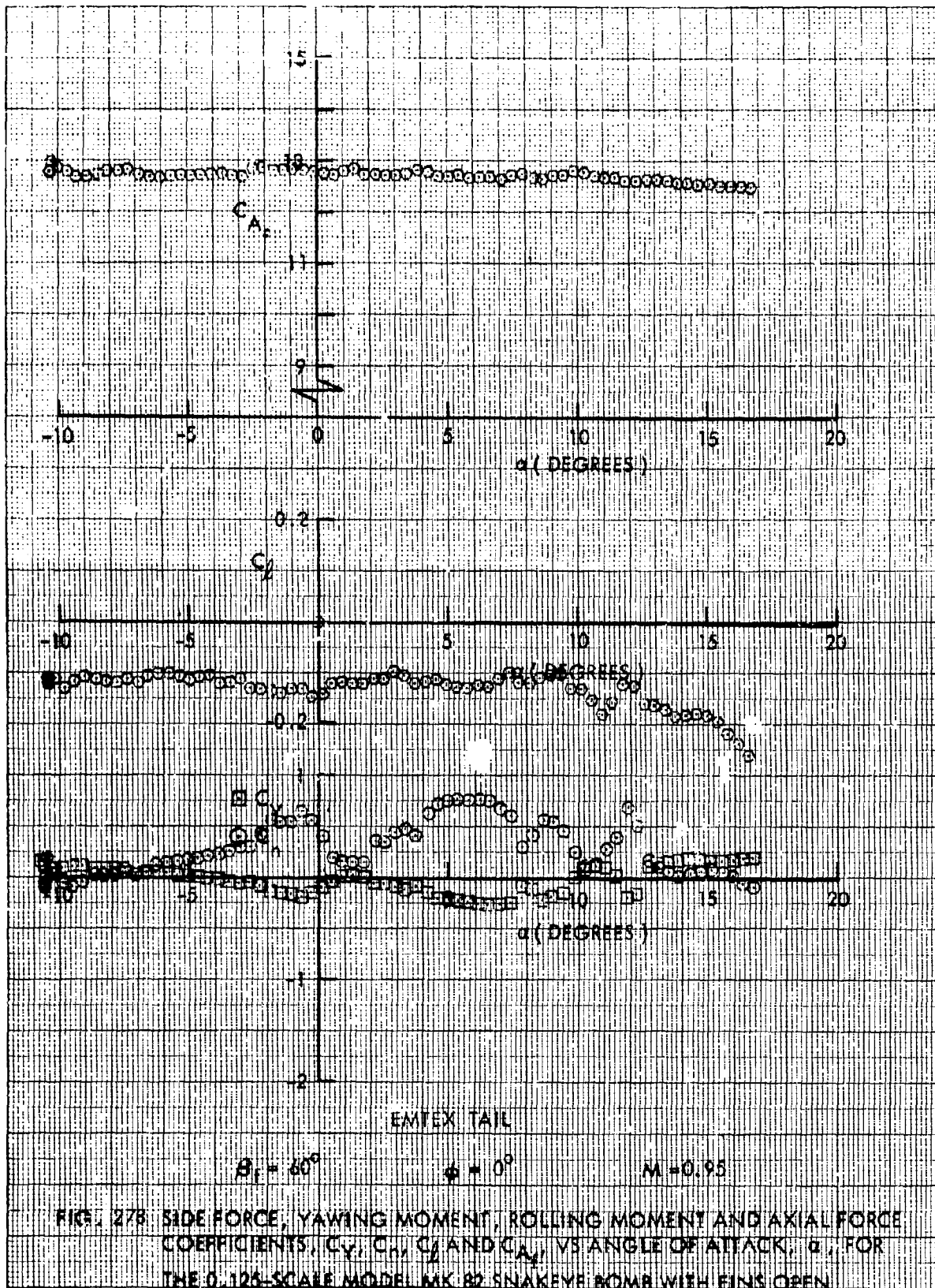




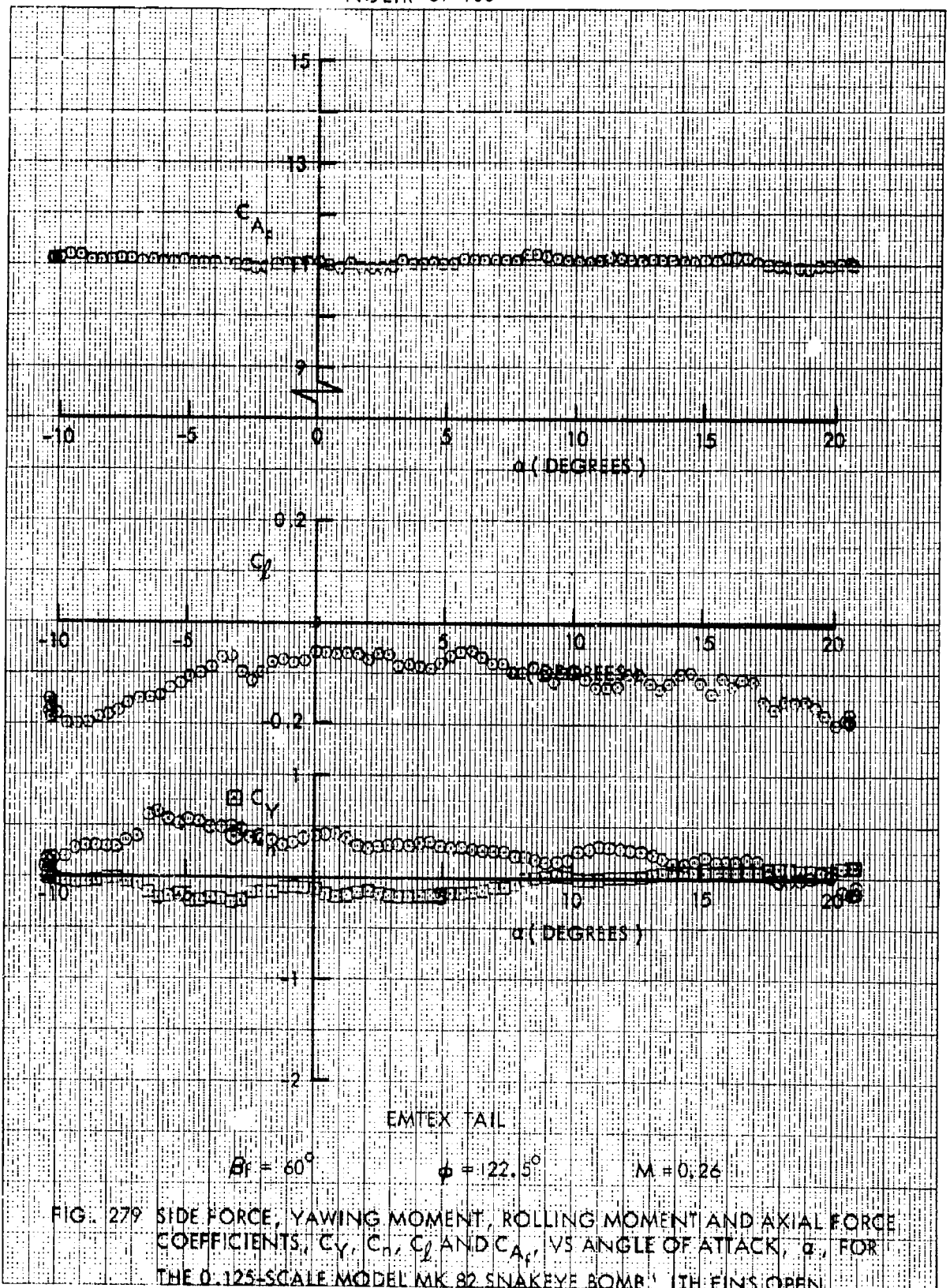




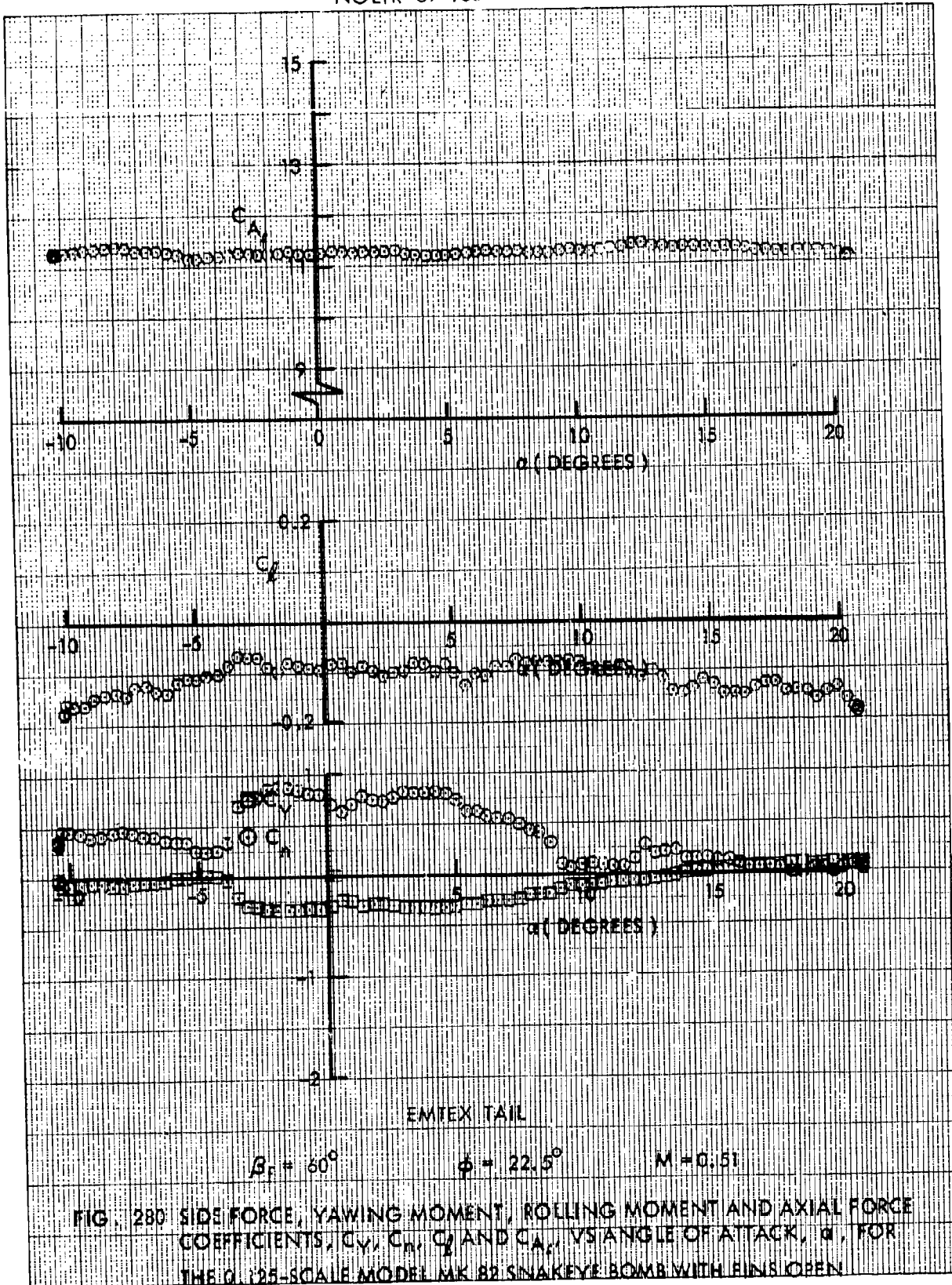


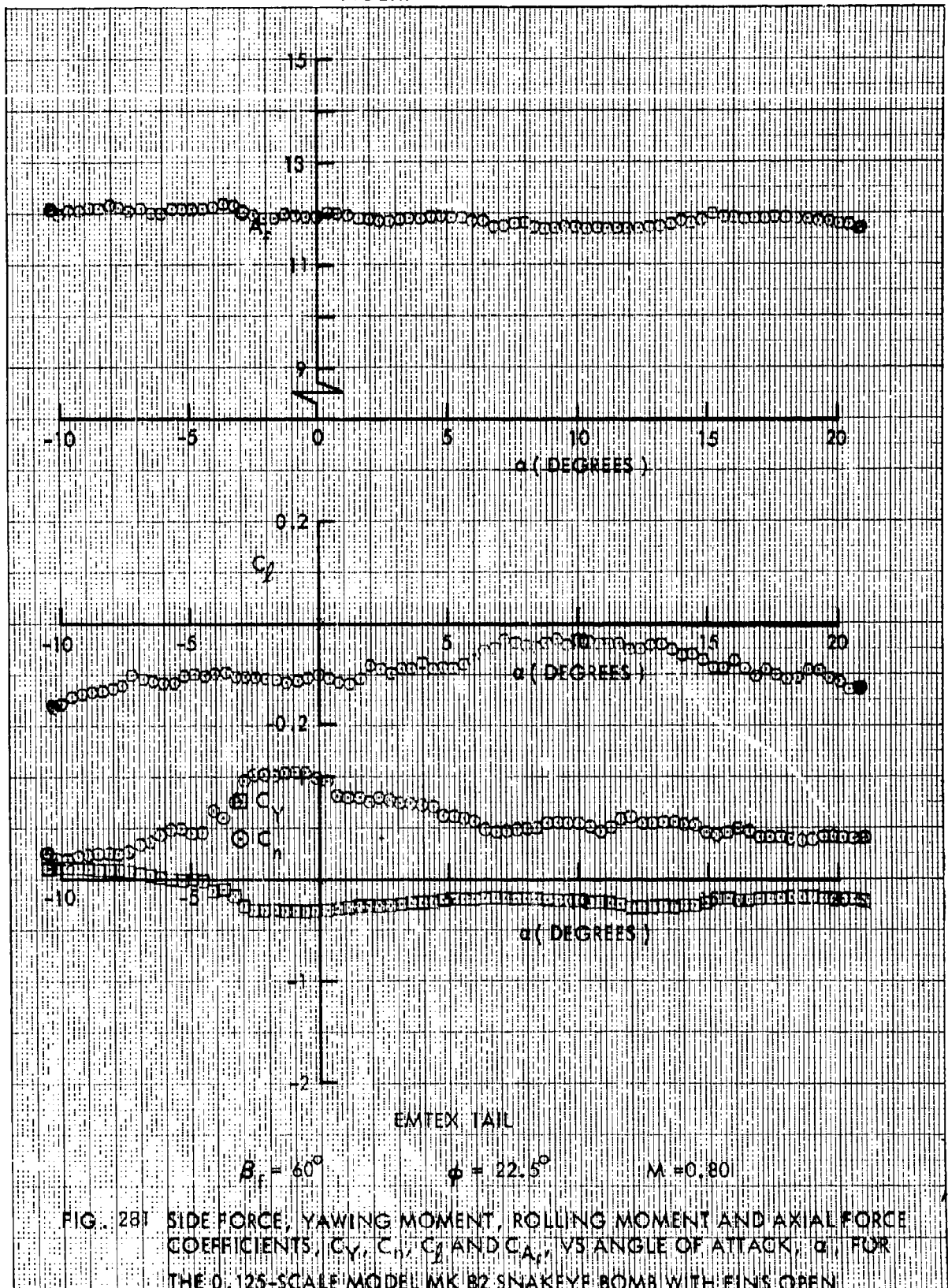


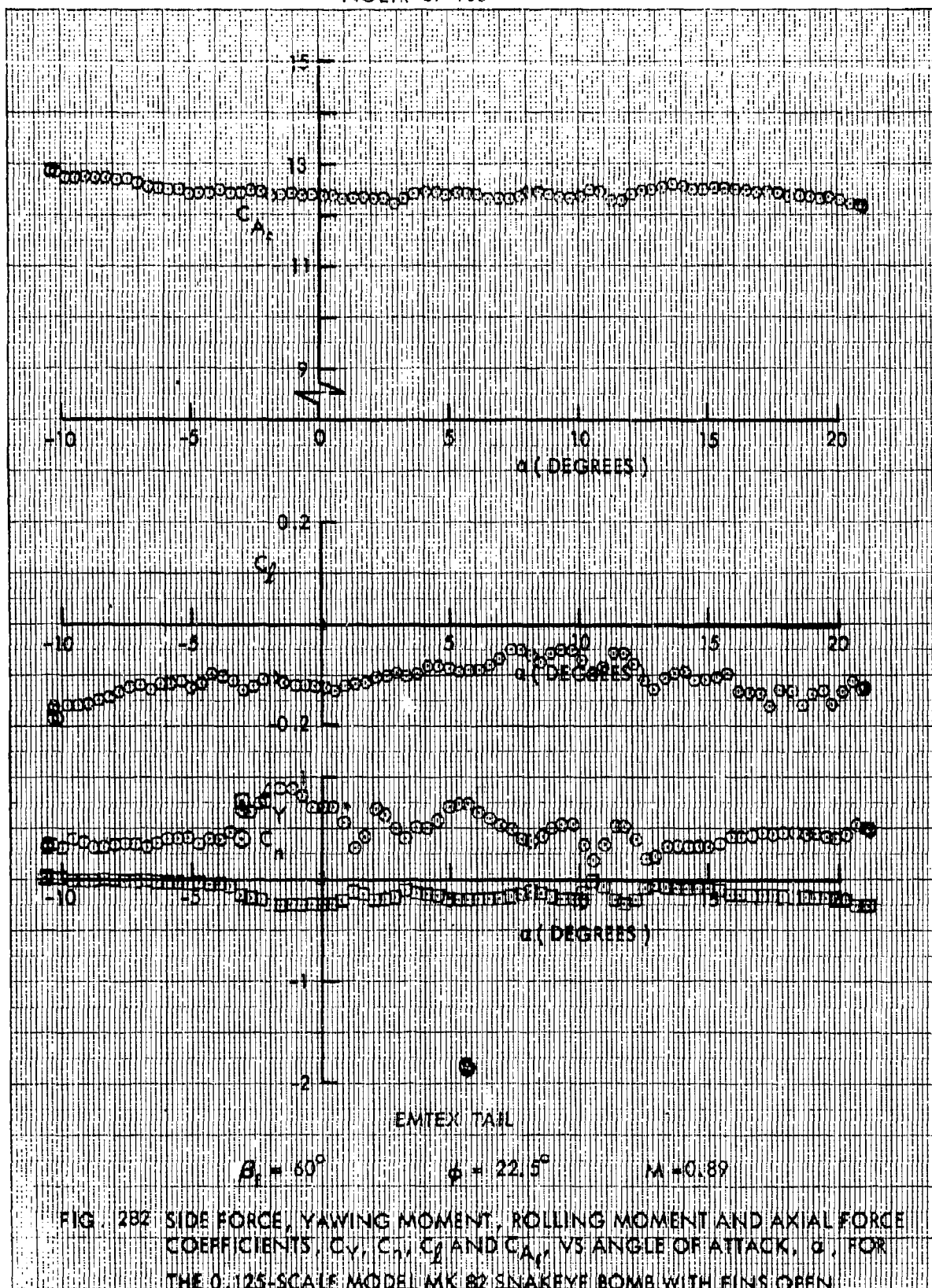


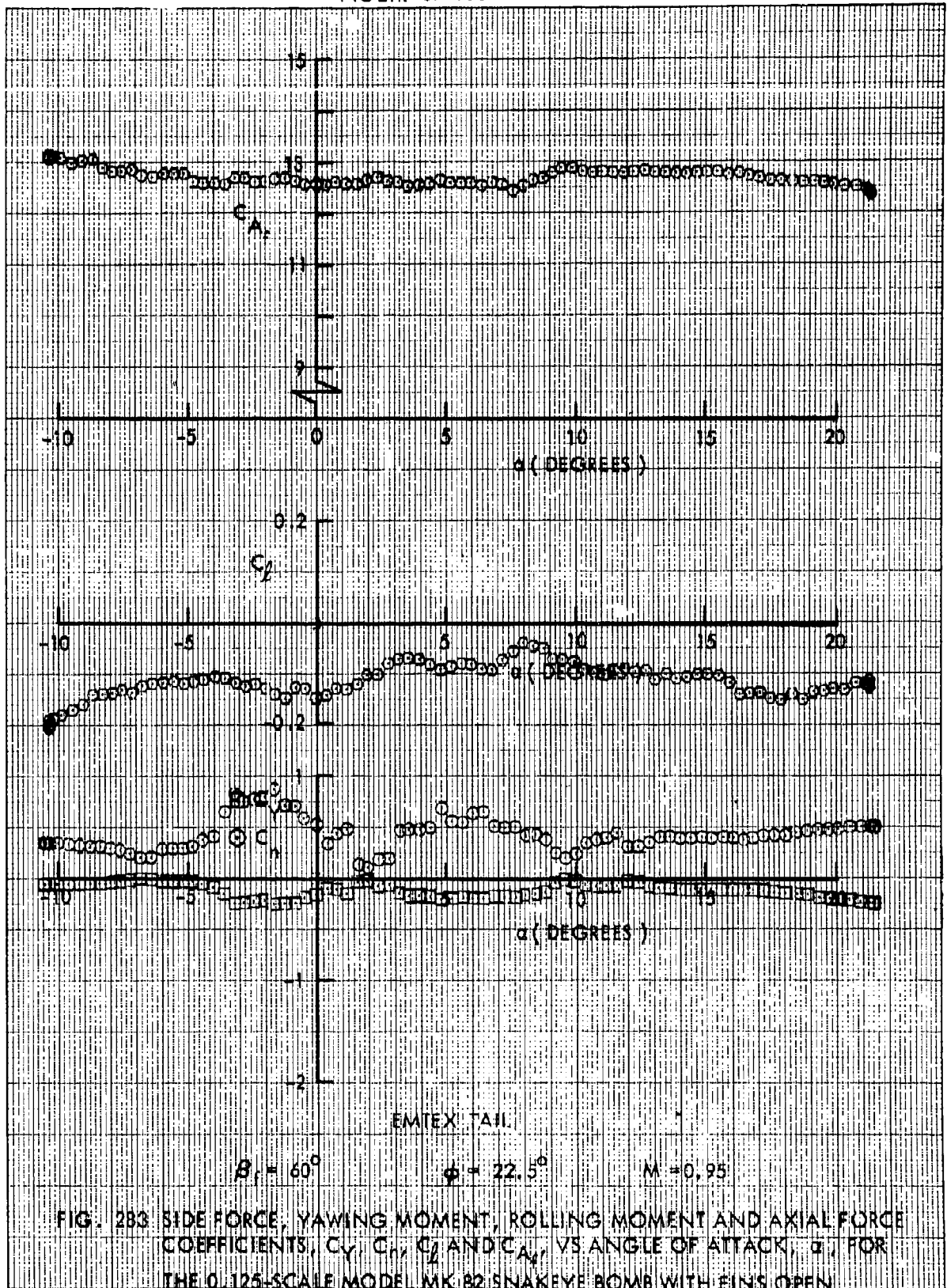


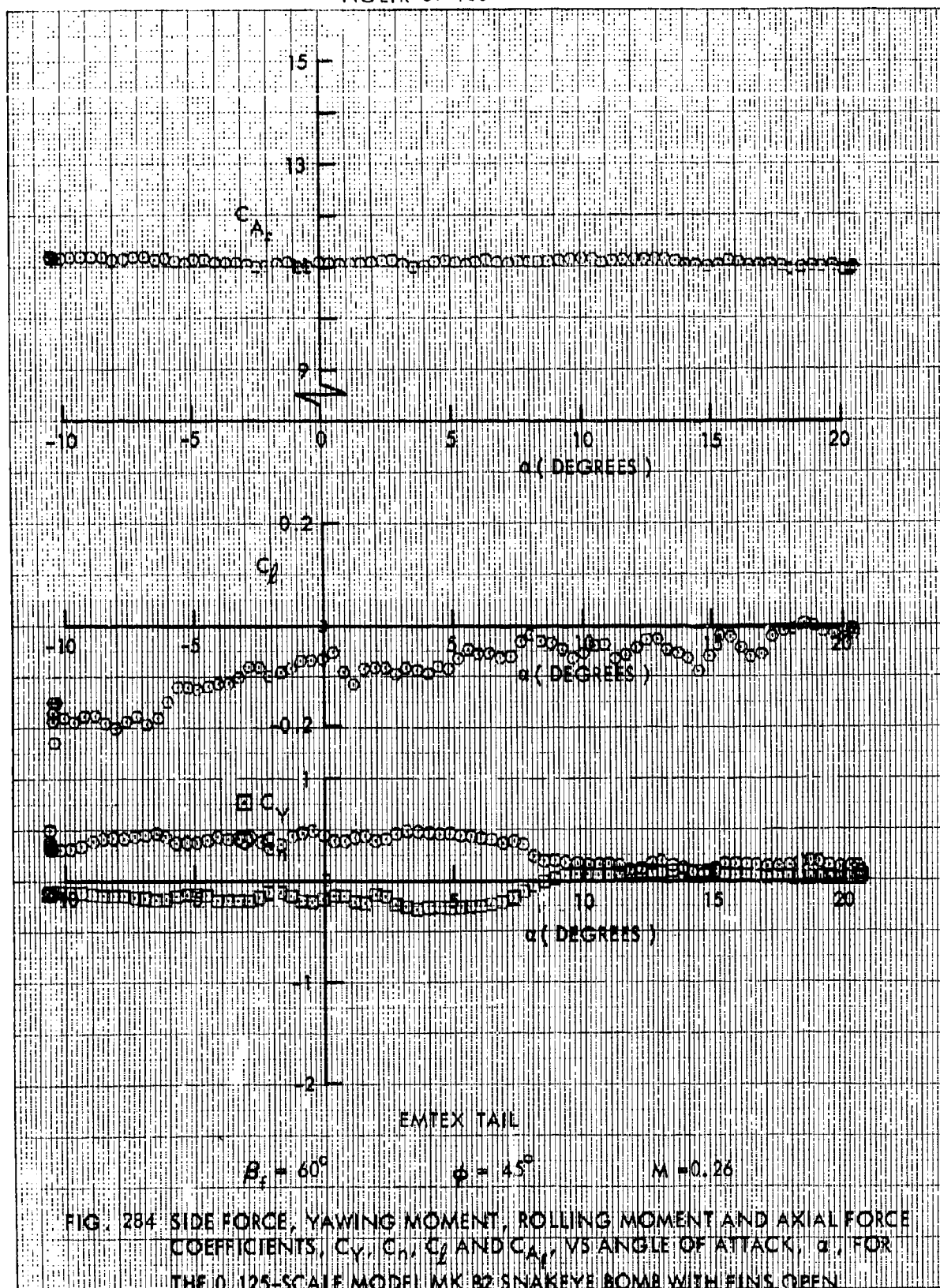




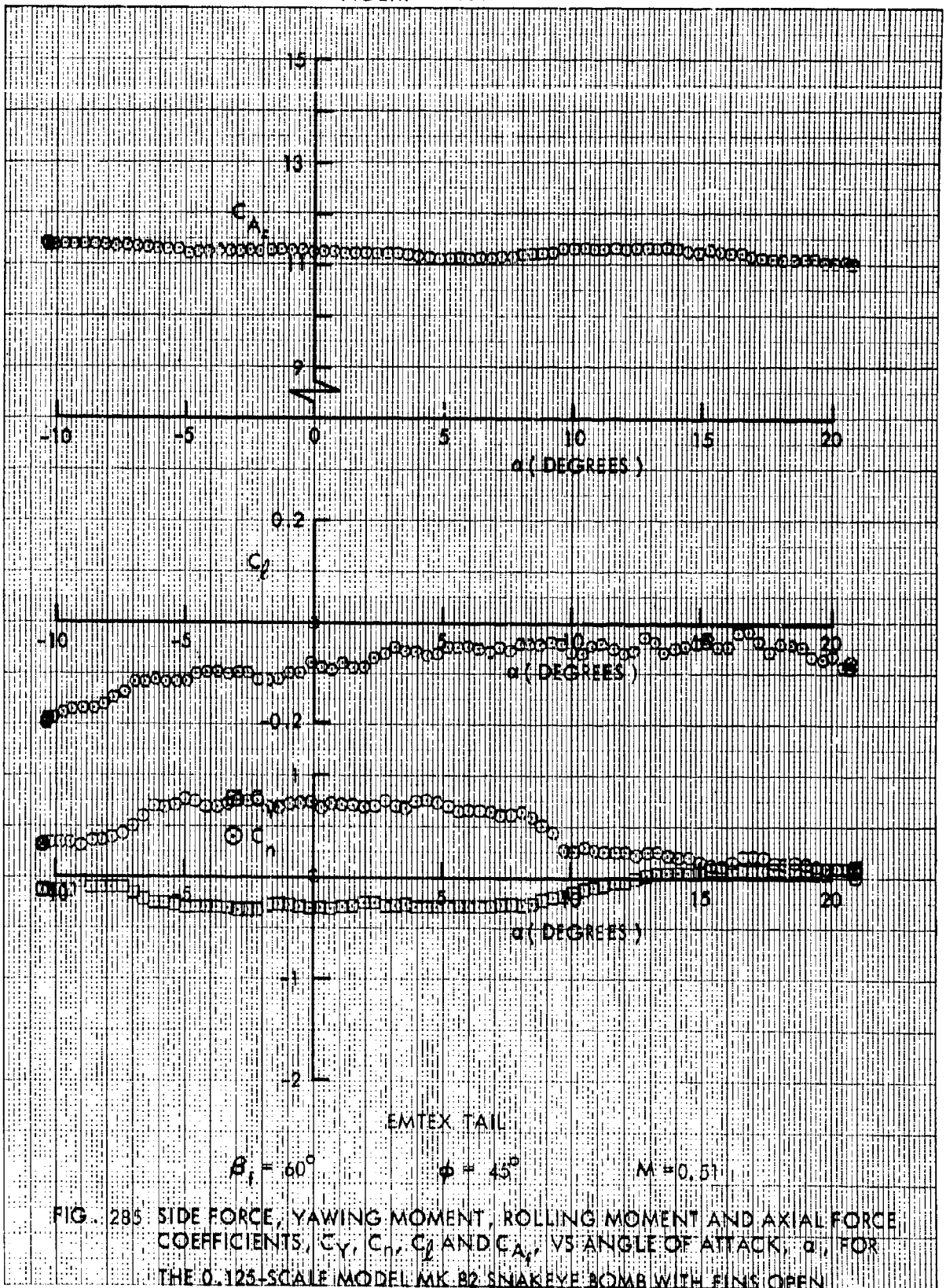




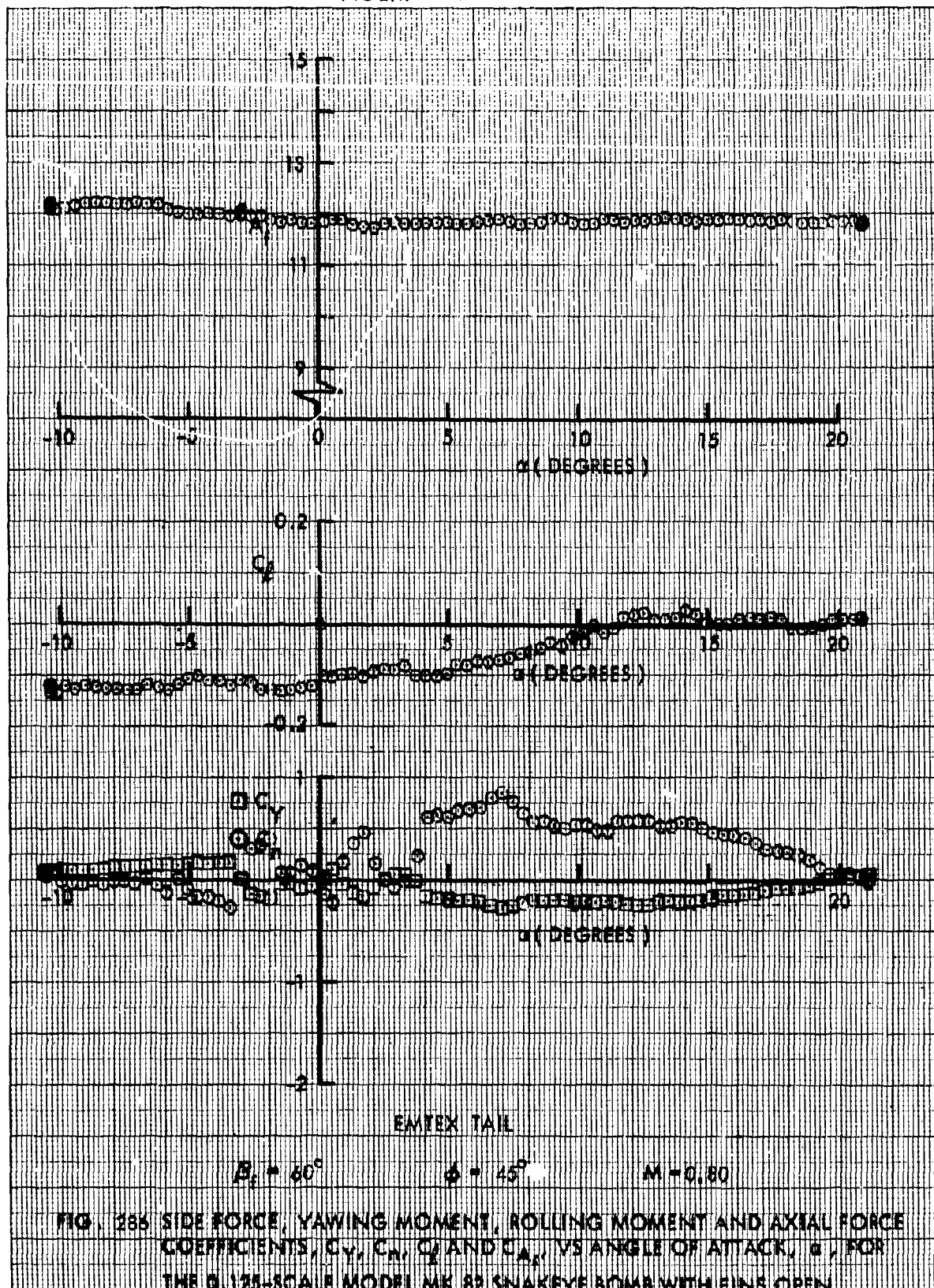


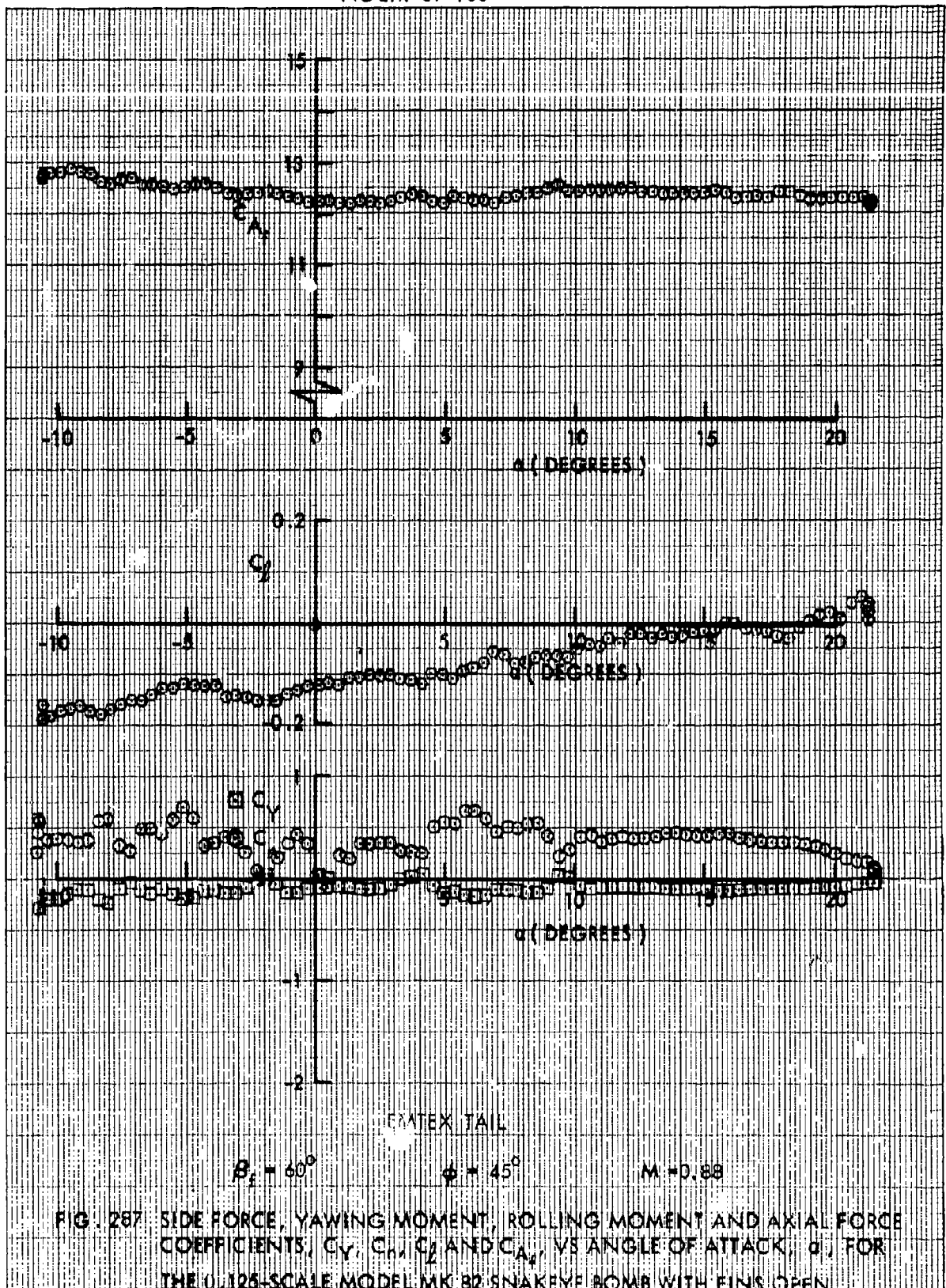


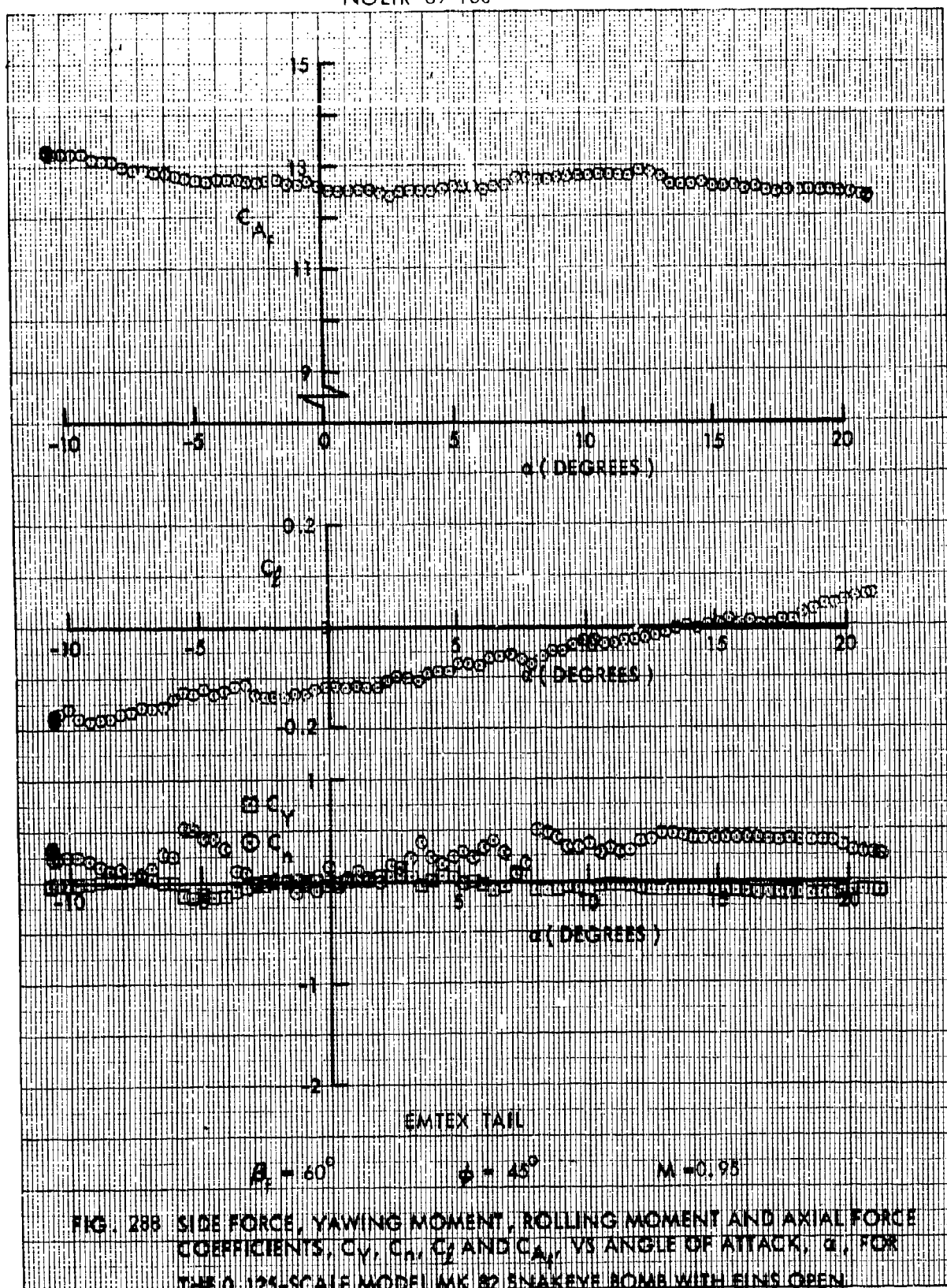


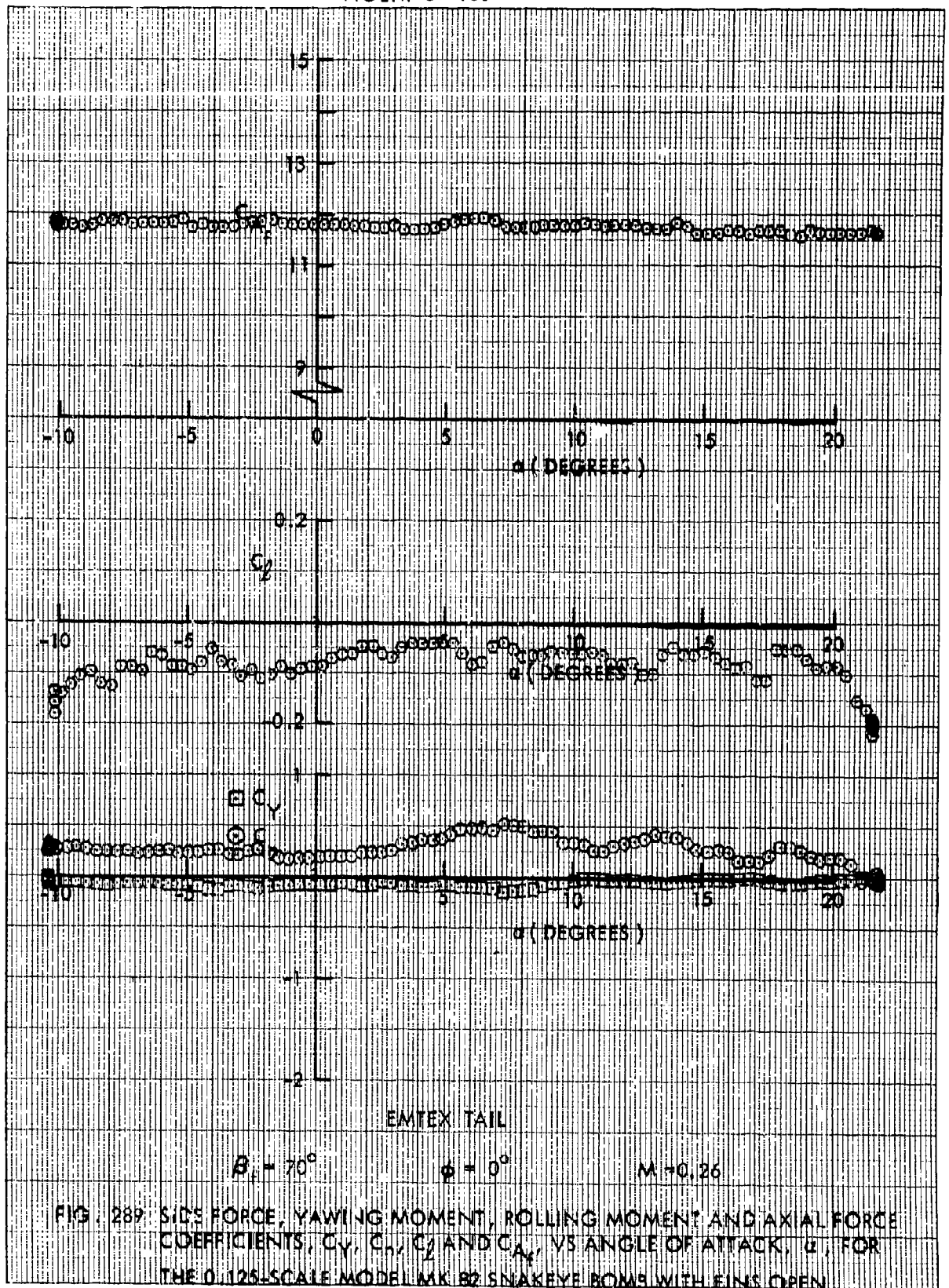












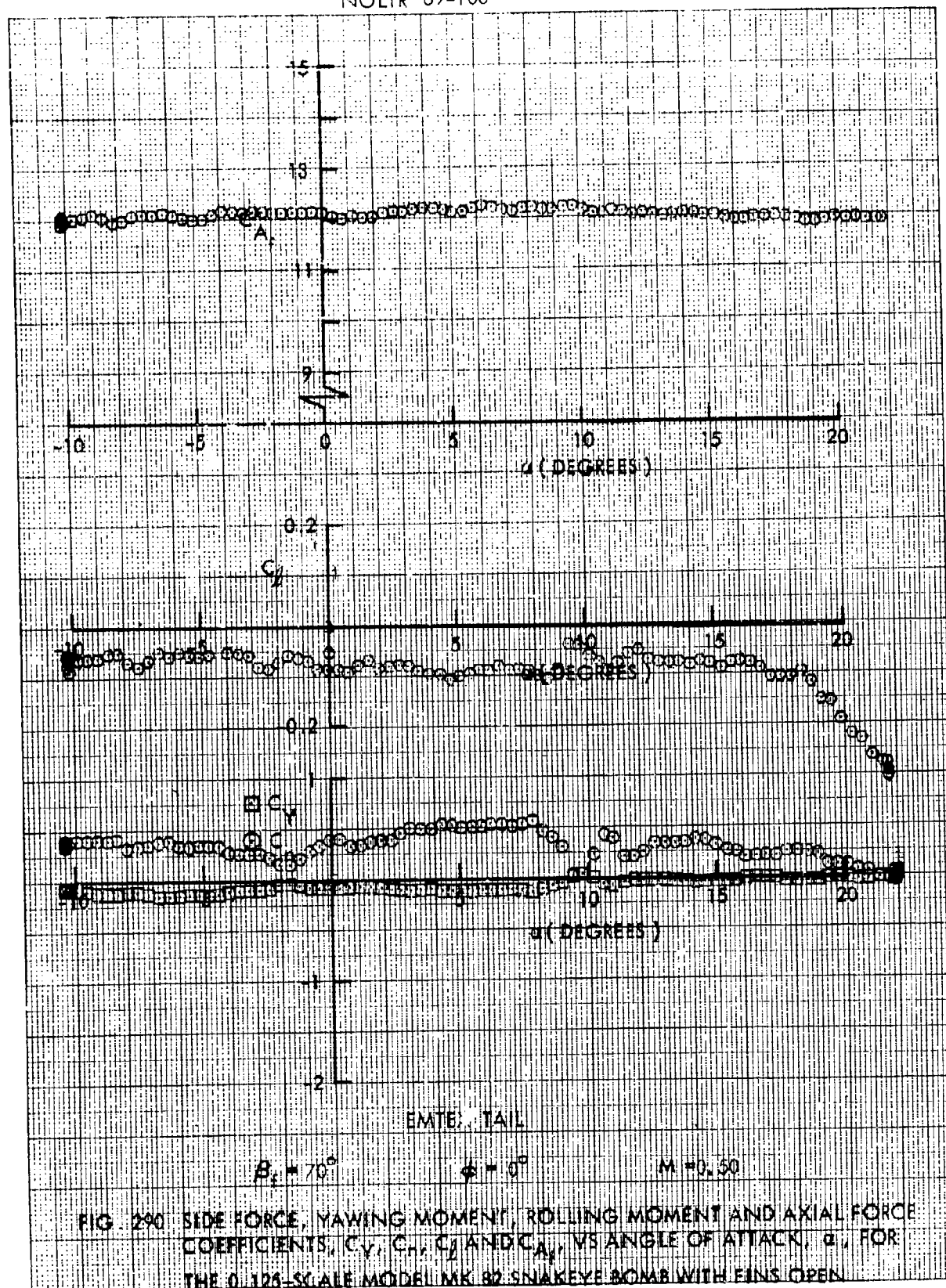
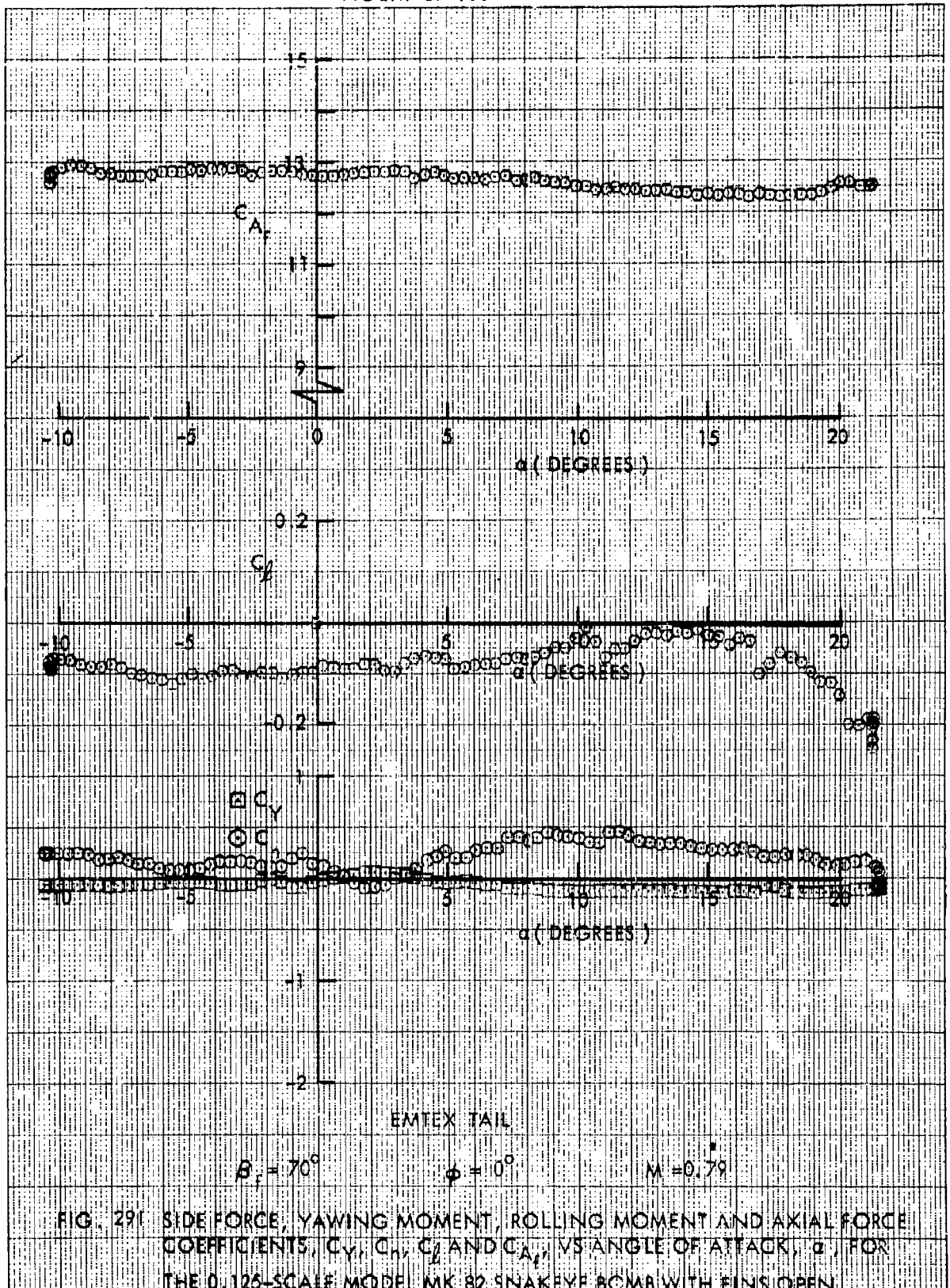
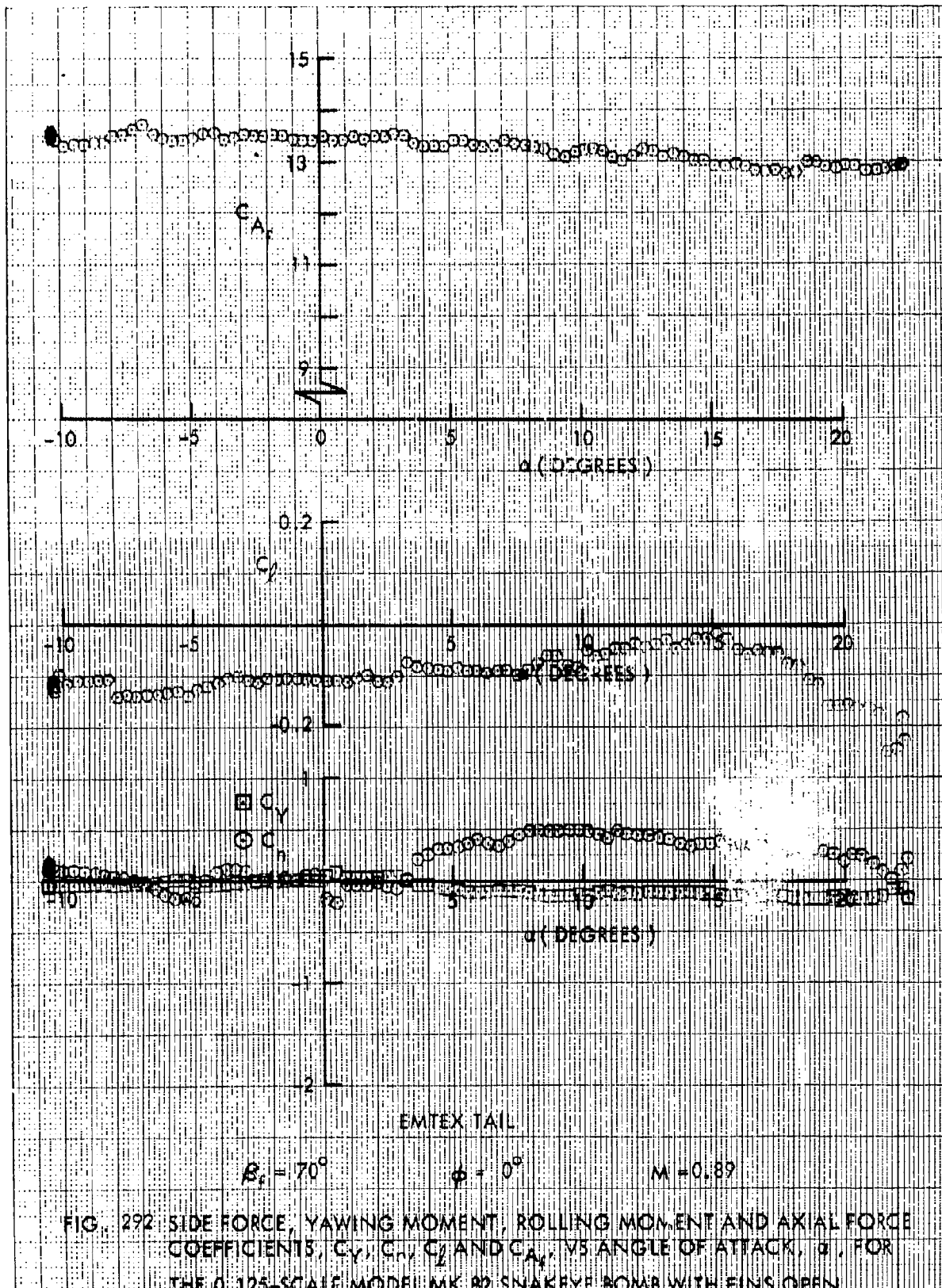


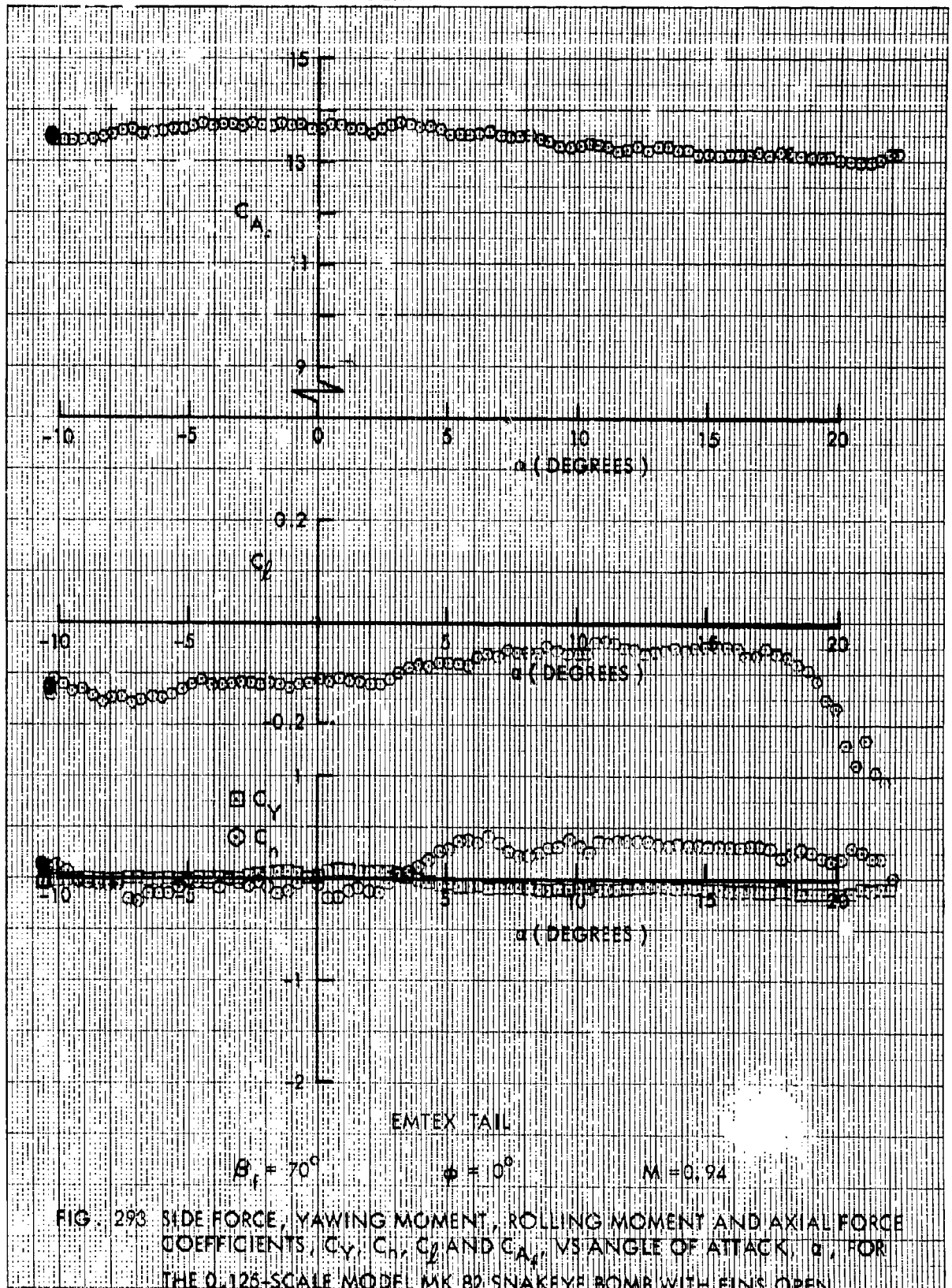
FIG. 290 SIDE FORCE, YAWING MOMENT, ROLLING MOMENT AND AXIAL FORCE COEFFICIENTS,  $C_y$ ,  $C_x$ ,  $C_l$  AND  $C_{A_x}$ , VS ANGLE OF ATTACK,  $\alpha$ , FOR THE 0.125-SCALE MODEL MK 82 SNAKEEYE BOMB WITH FINS OPEN

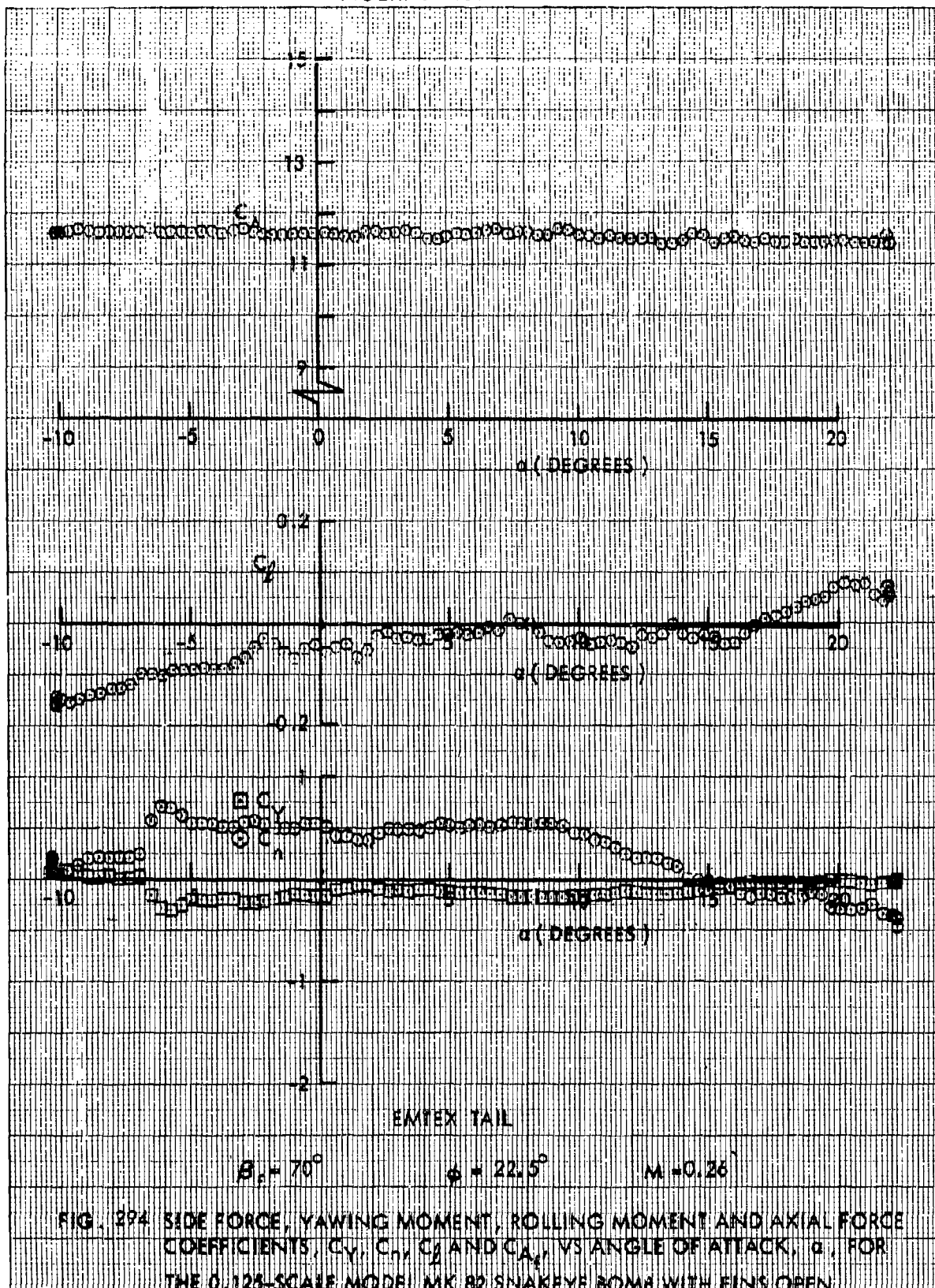


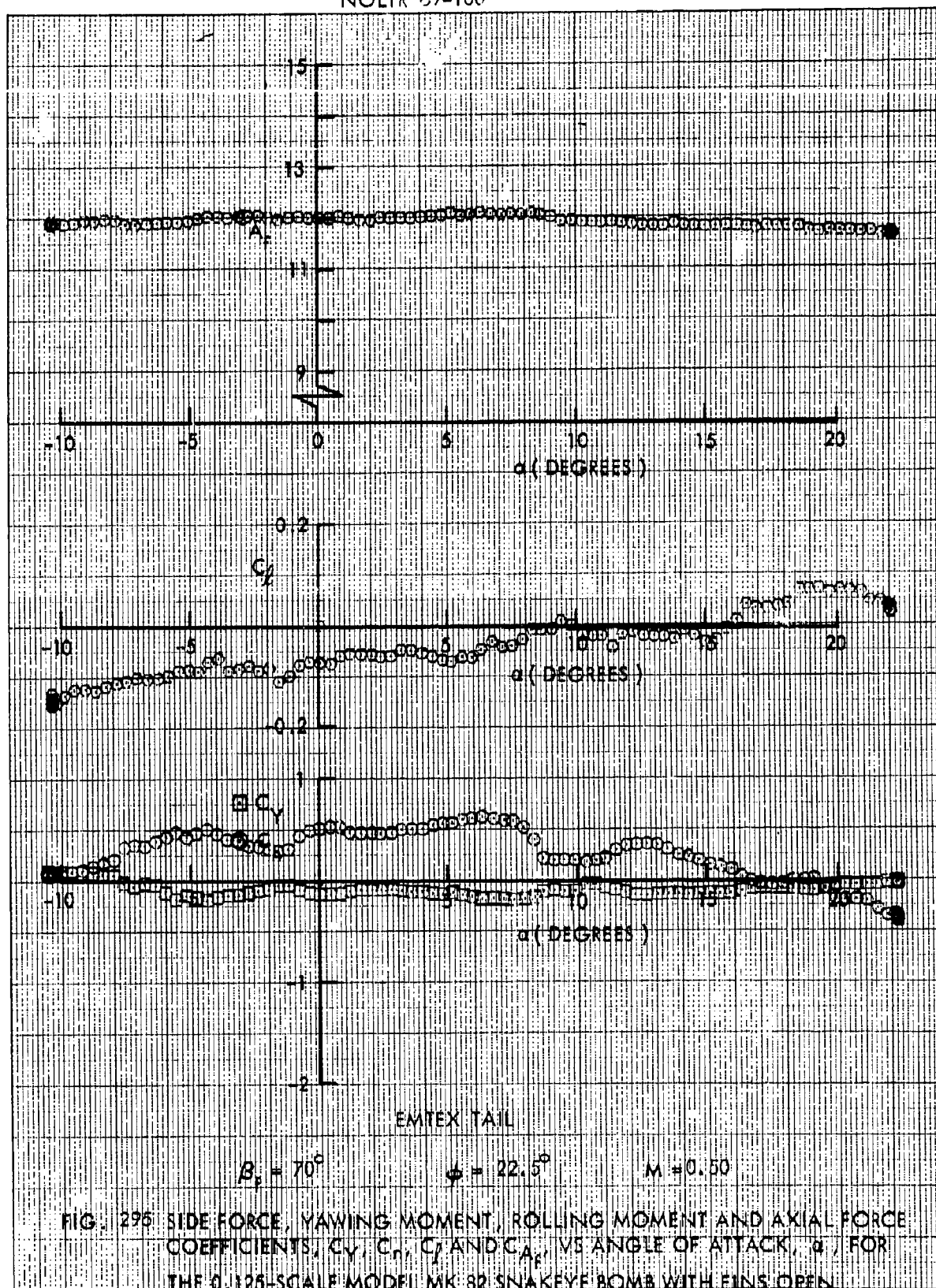


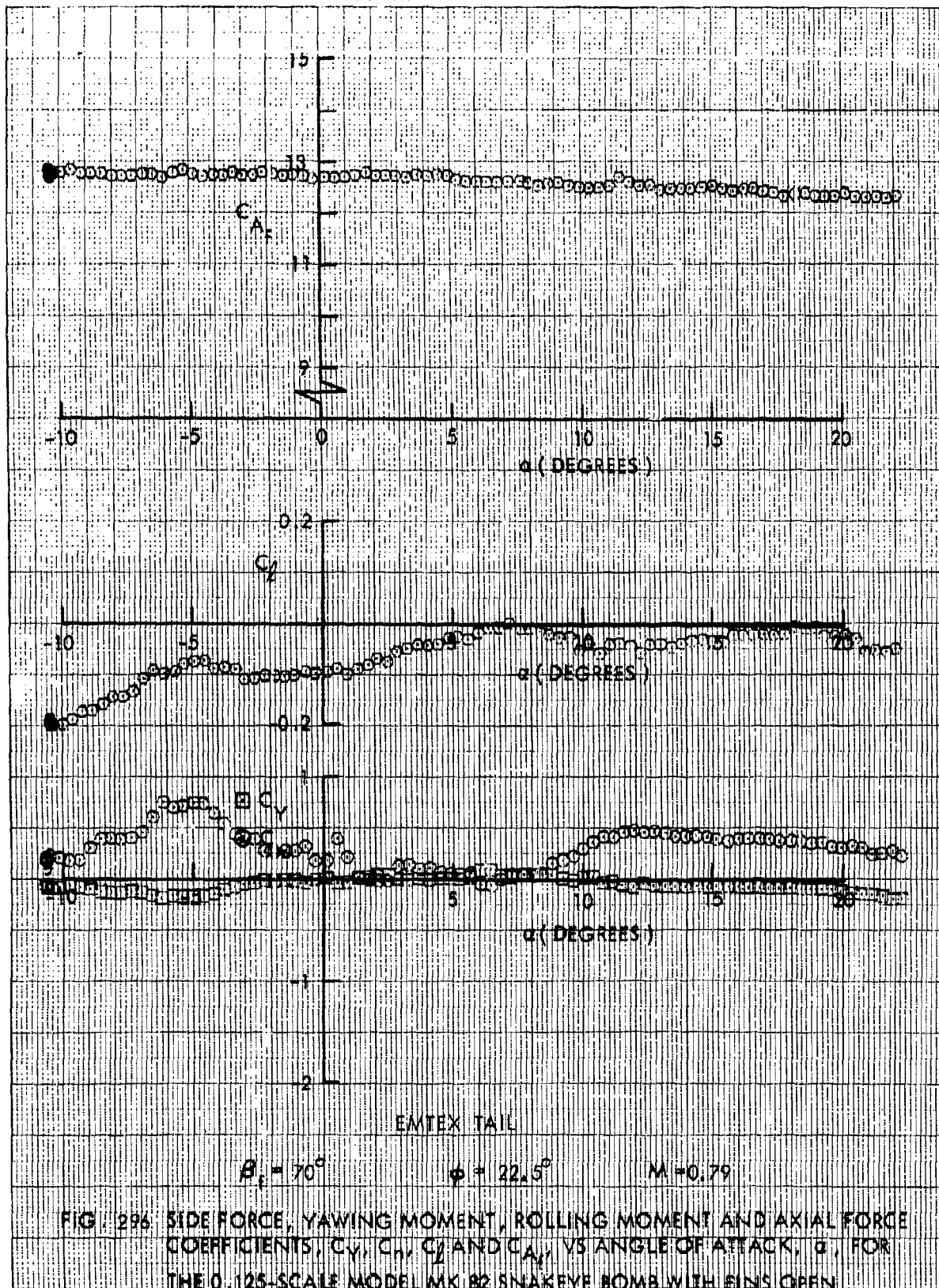




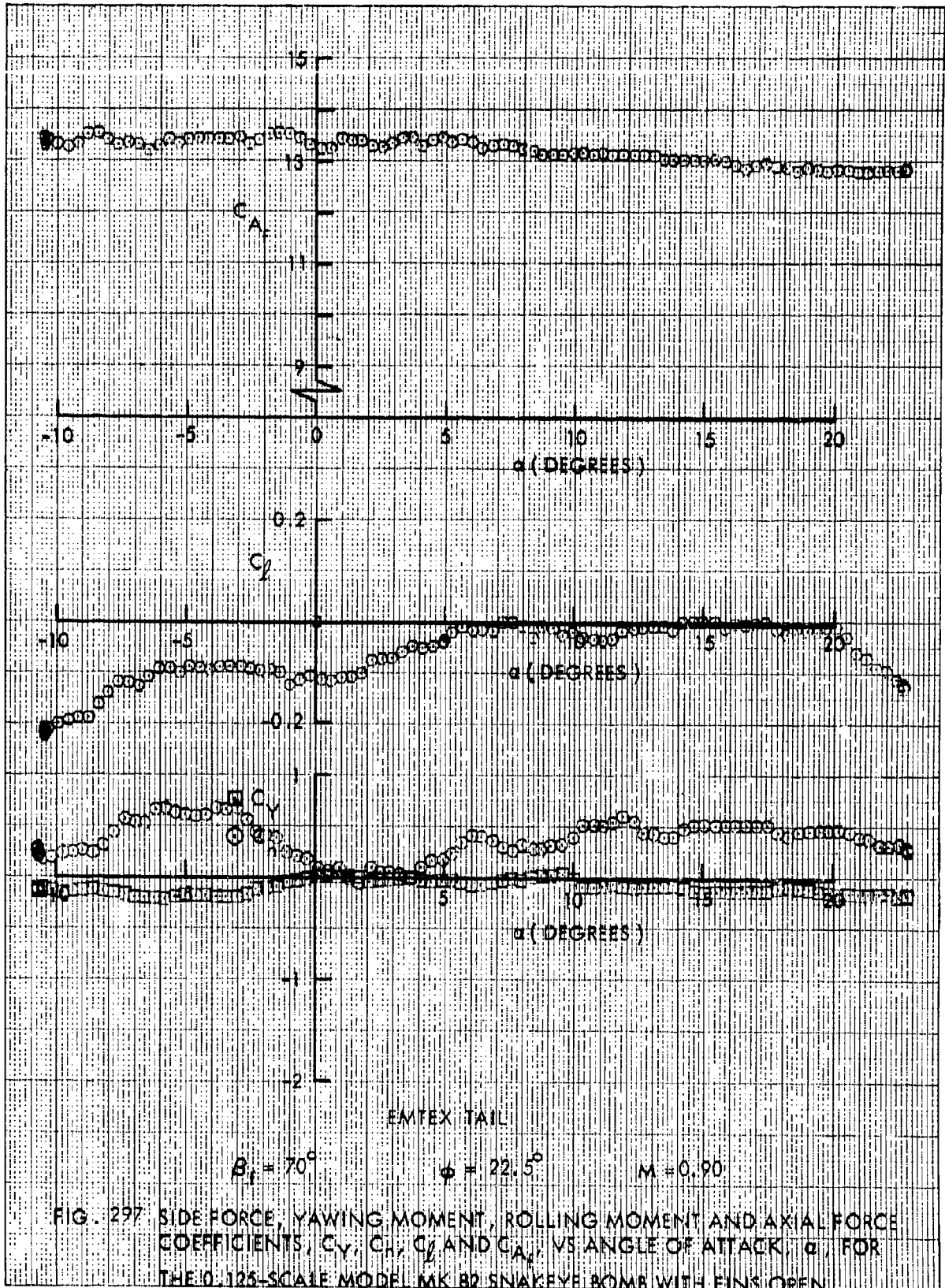




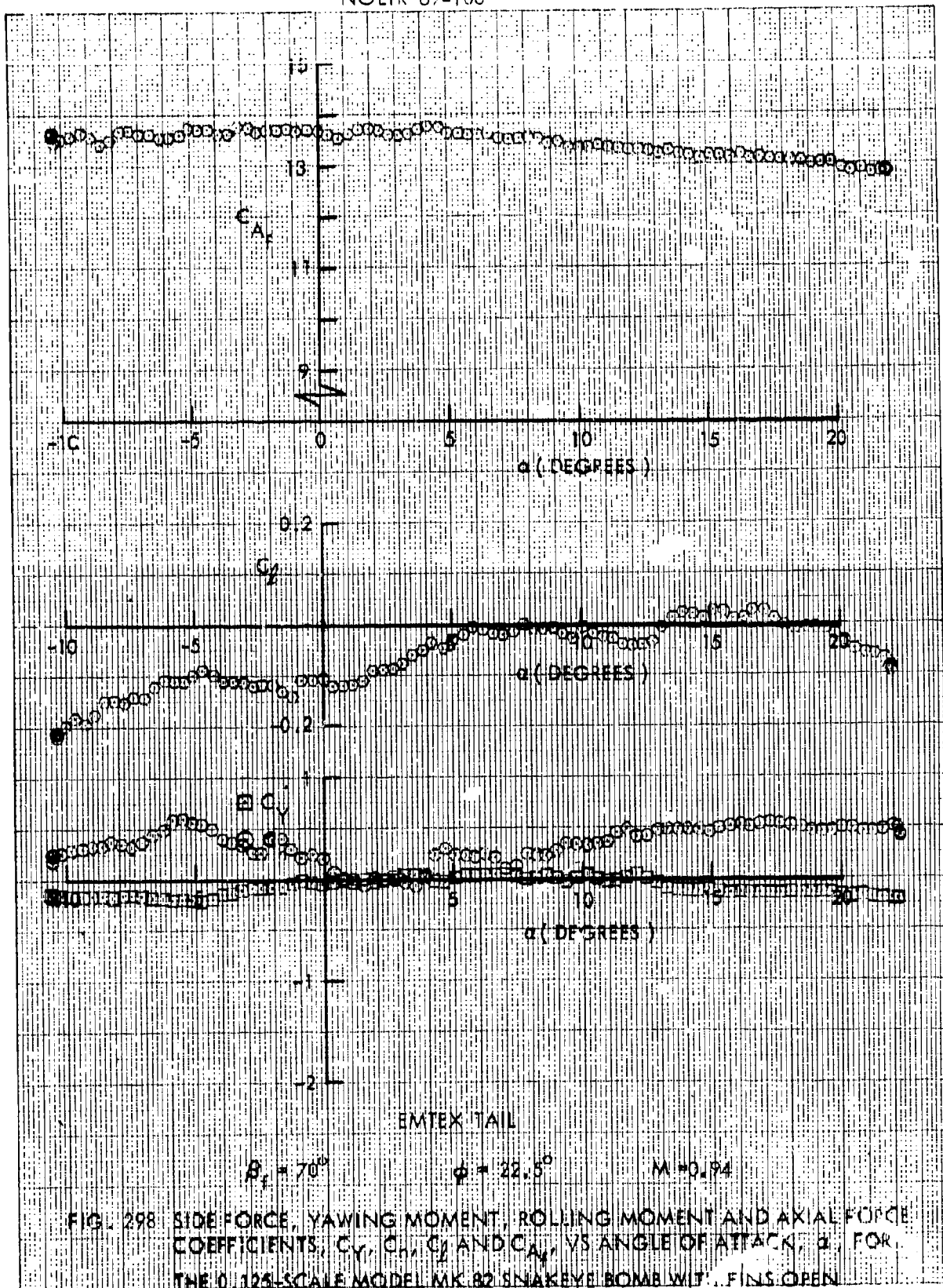


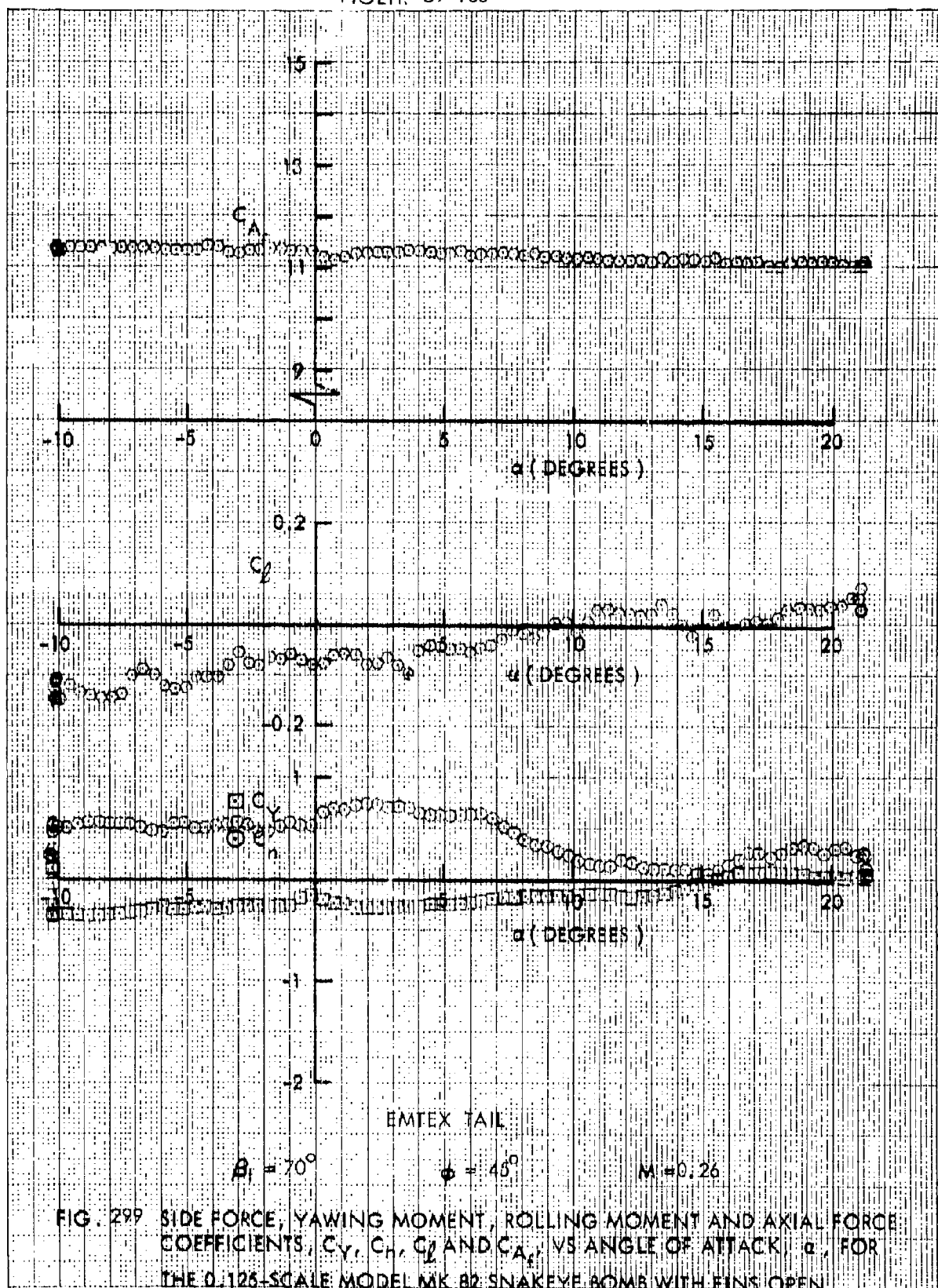


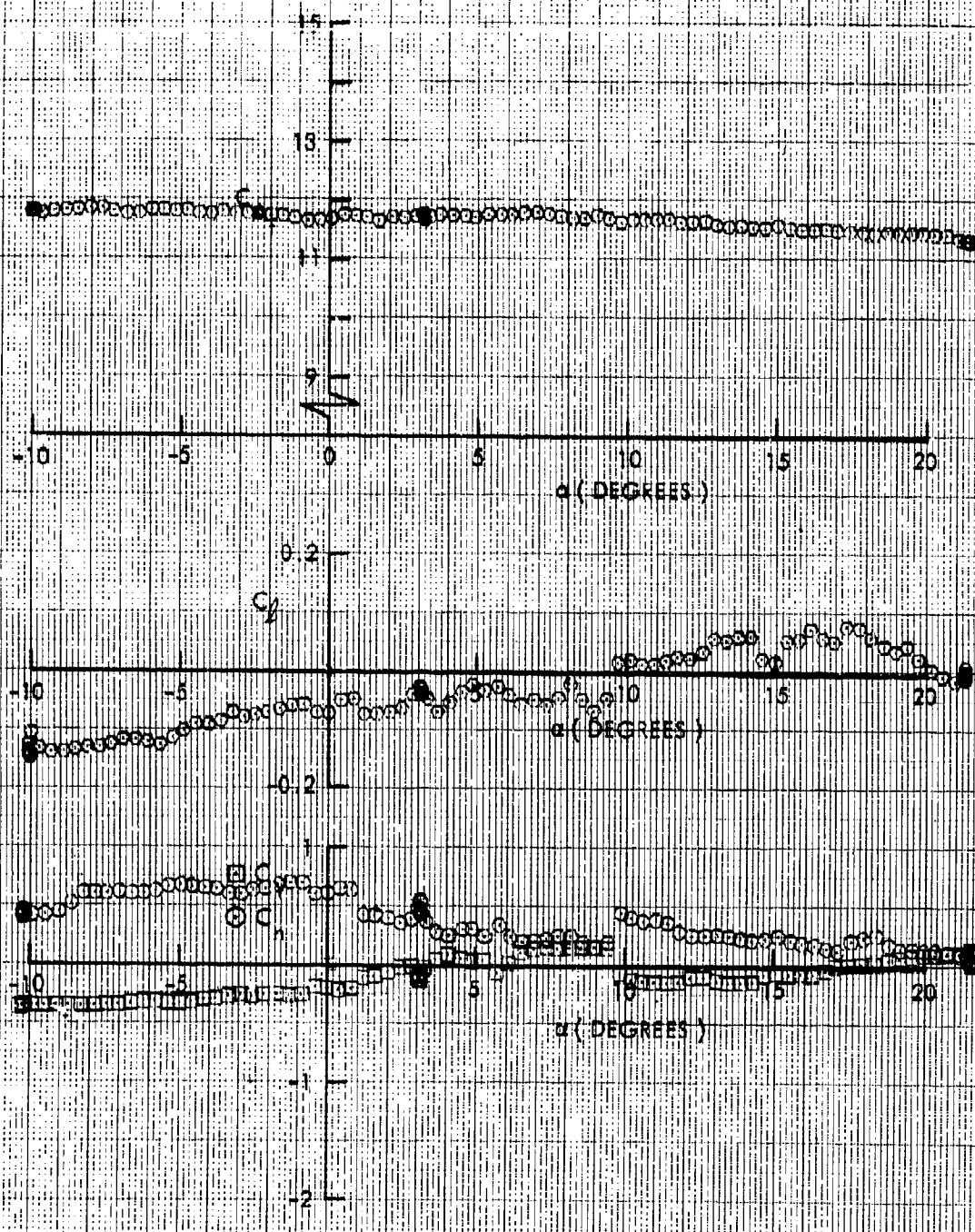












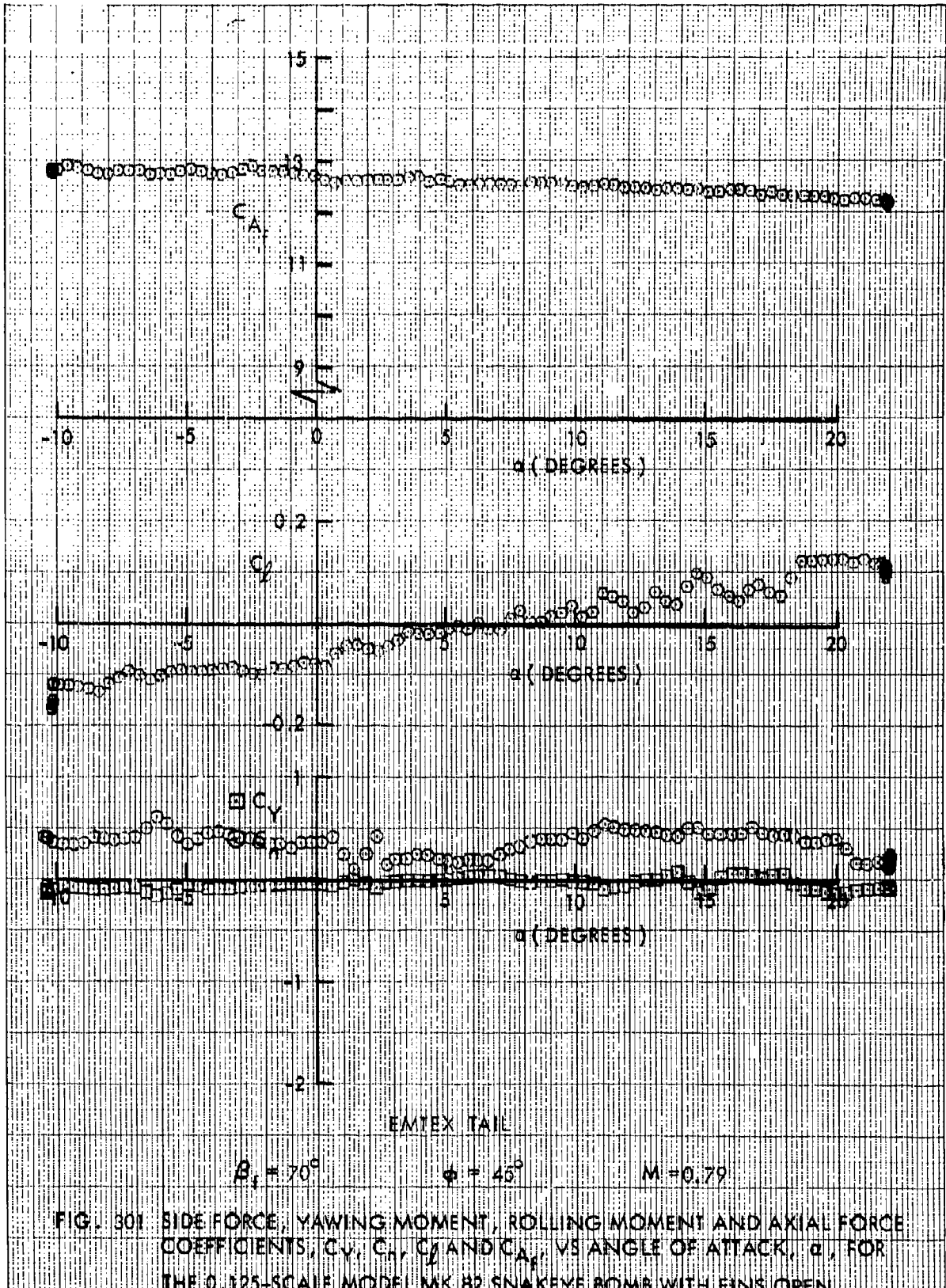
EMTEX TAIL

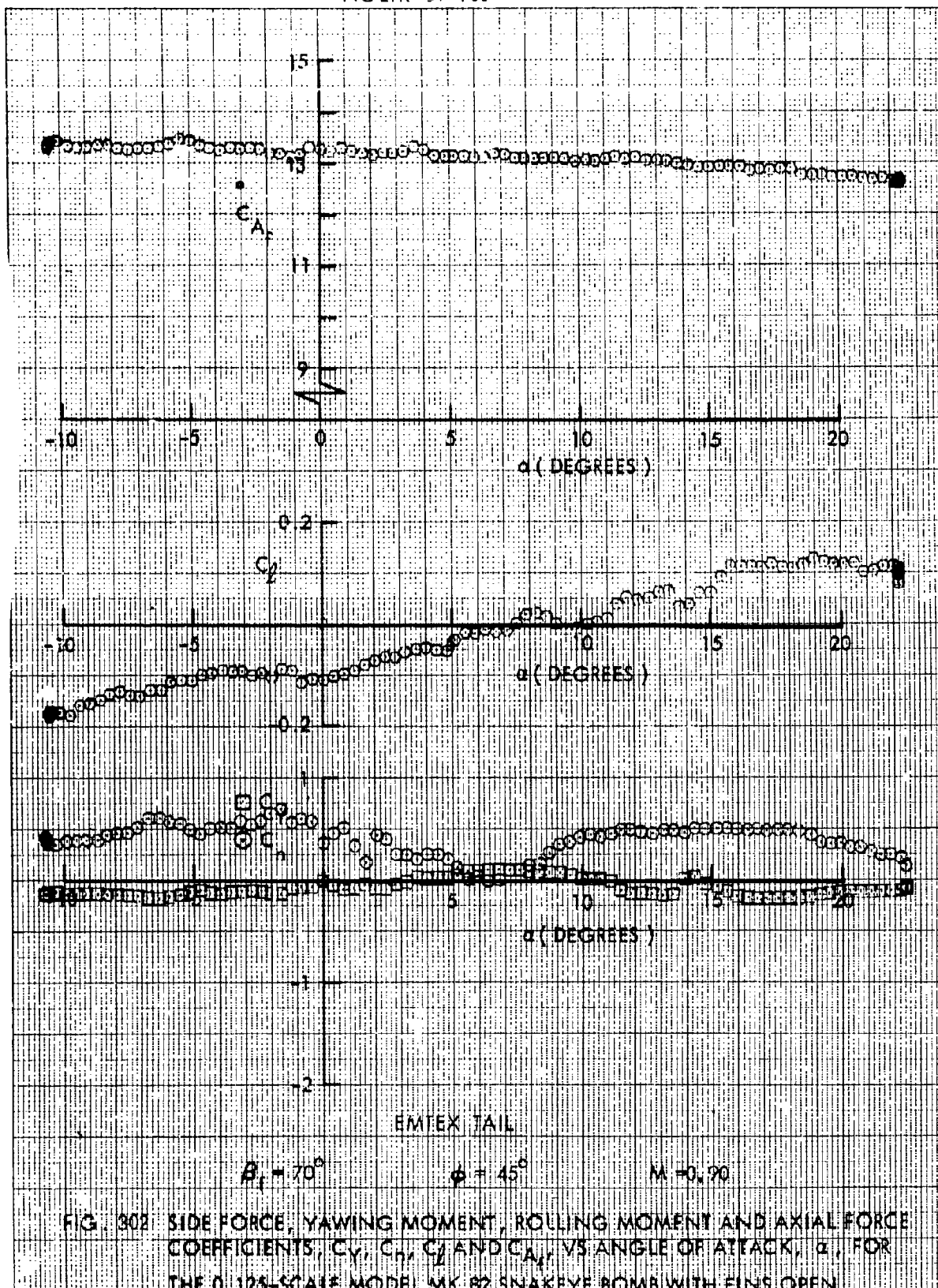
$$\beta_f = 70^\circ$$

$$\phi = 45^\circ$$

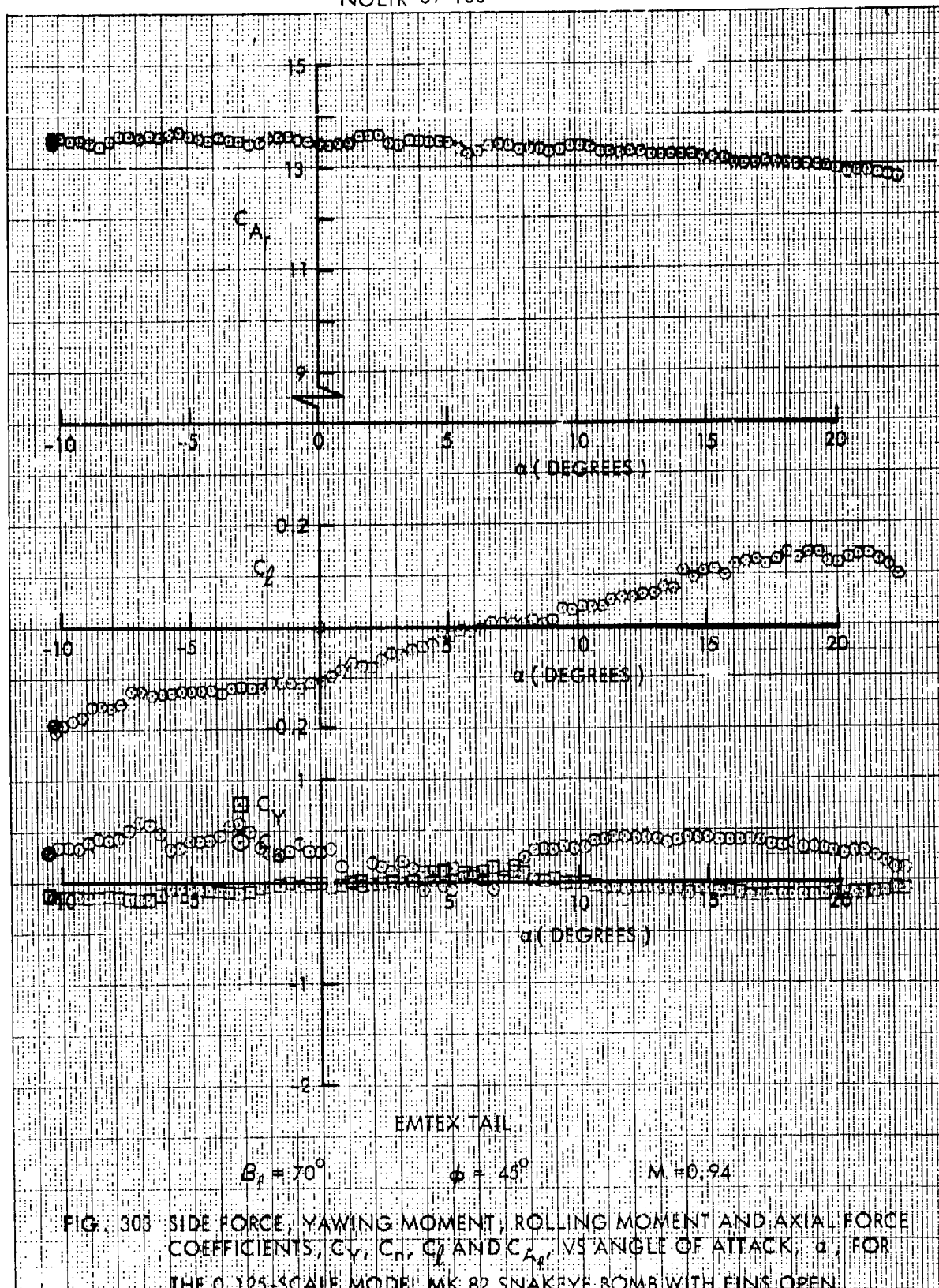
$$M = 0.50$$

FIG. 300 SIDE FORCE, YAWING MOMENT, ROLLING MOMENT AND AXIAL FORCE COEFFICIENTS,  $C_Y$ ,  $C_H$ ,  $C_L$  AND  $C_{A_x}$ , VS ANGLE OF ATTACK,  $\alpha$ , FOR THE 0.125-SCALE MODEL MK 82 SNAKEYE BOMB WITH FINIS OPEN

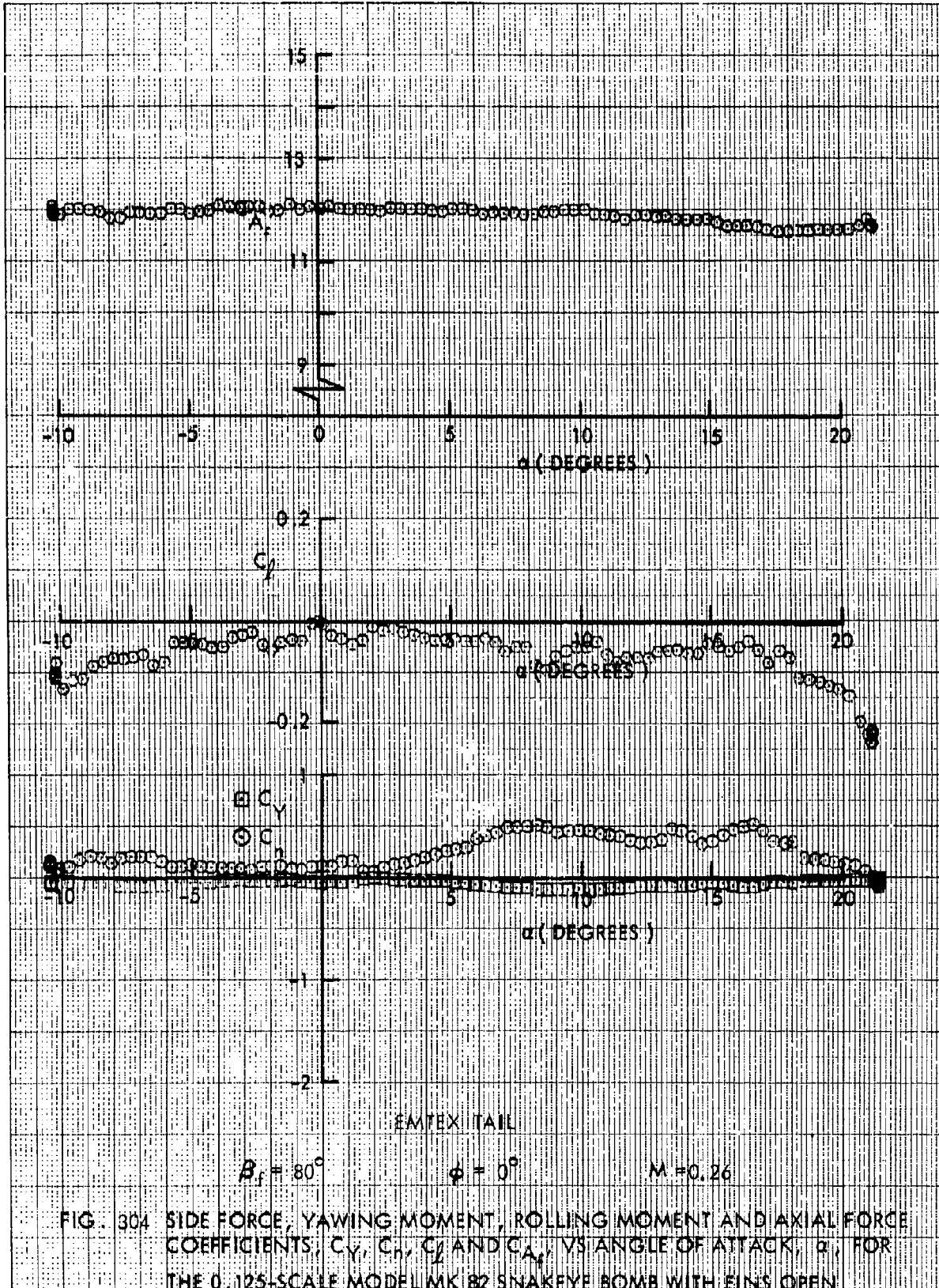


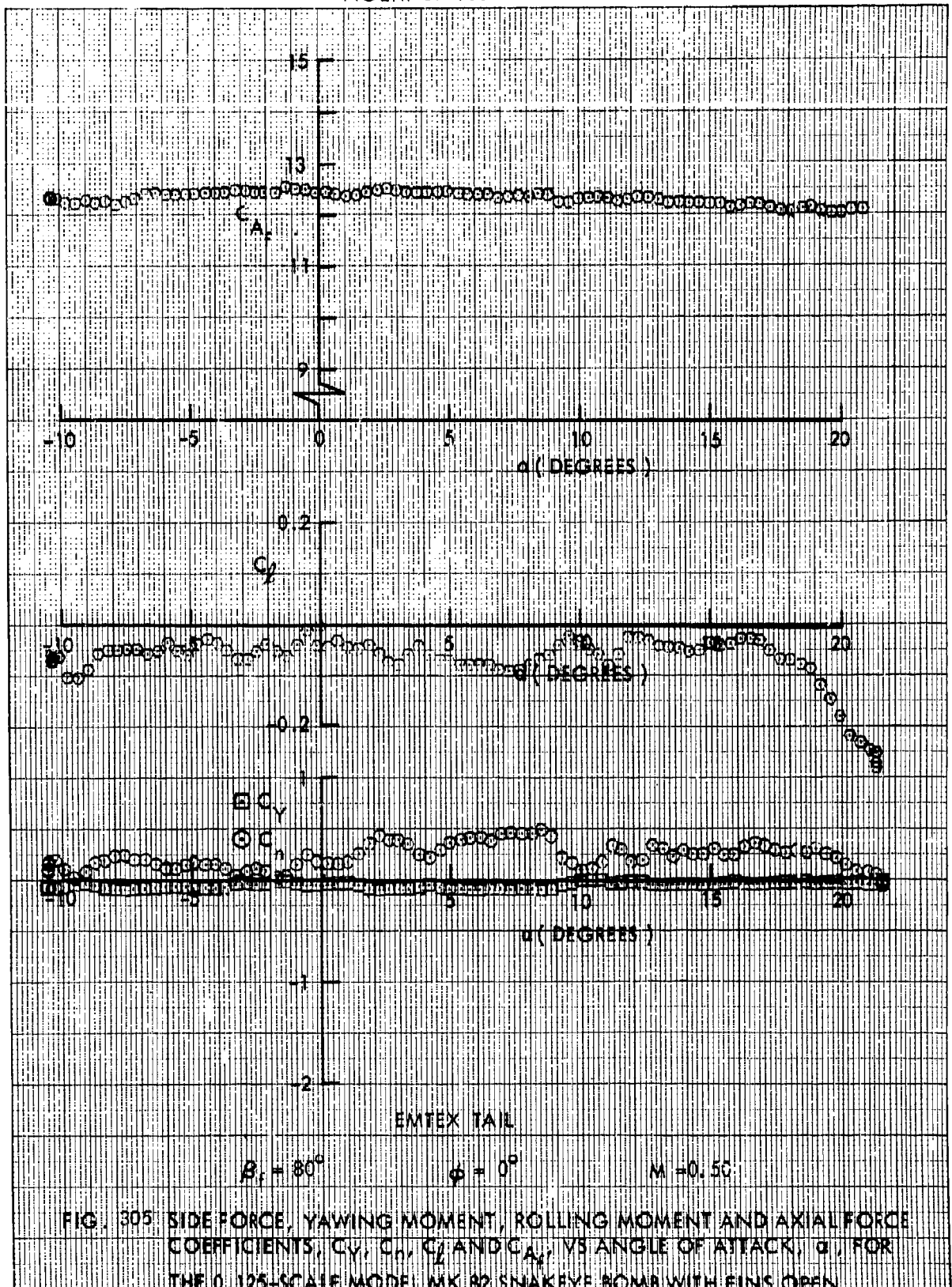


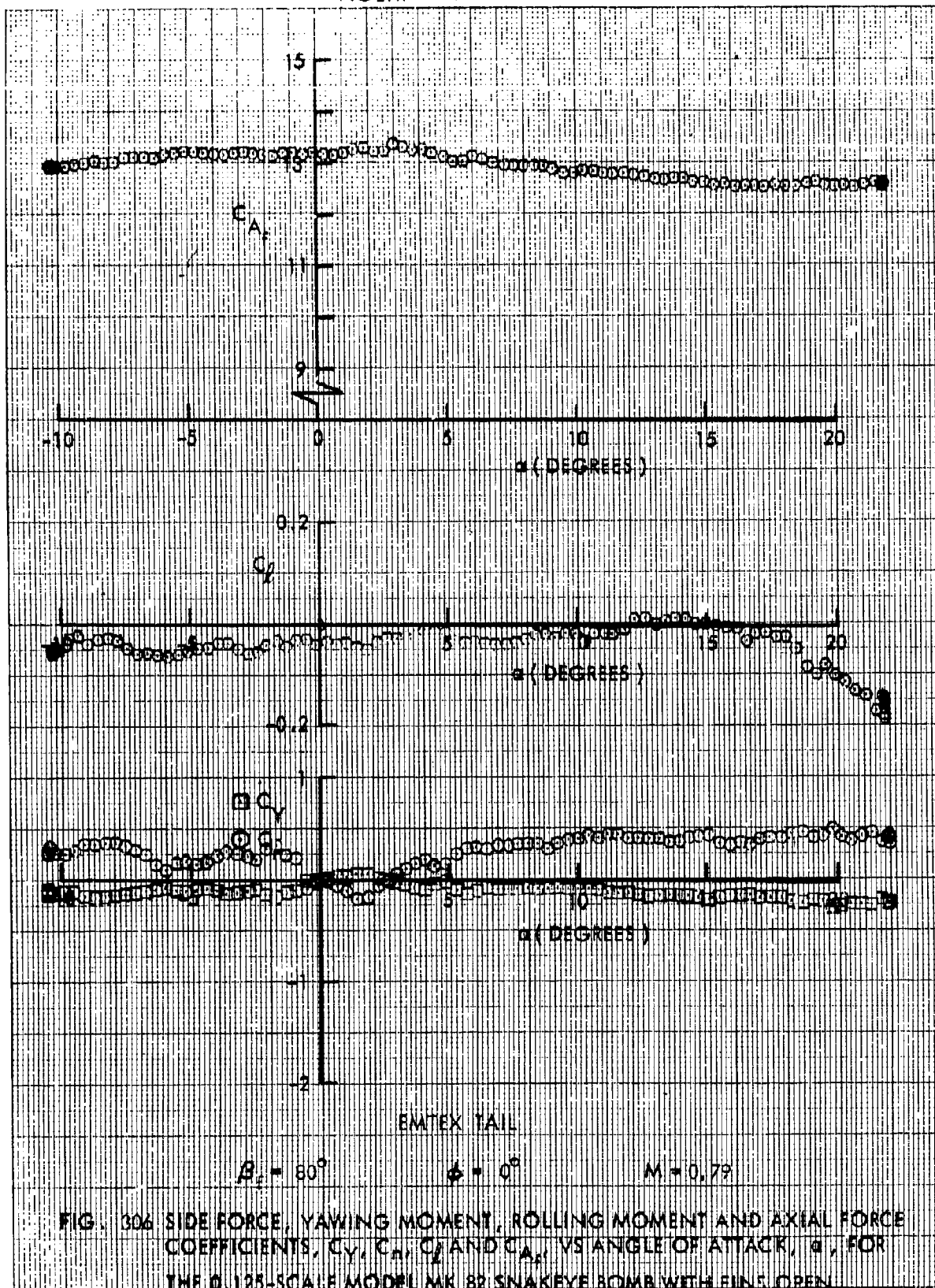


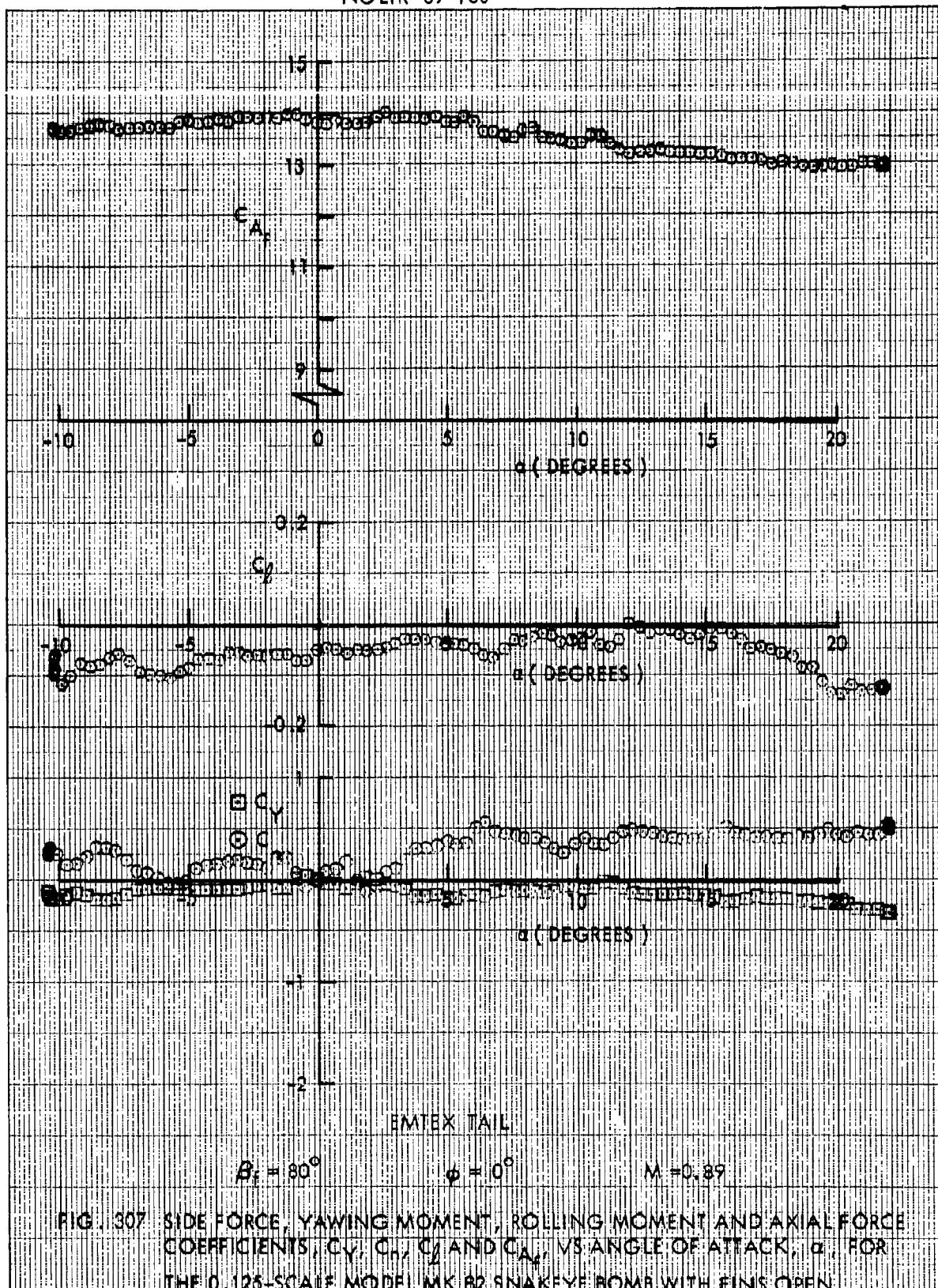


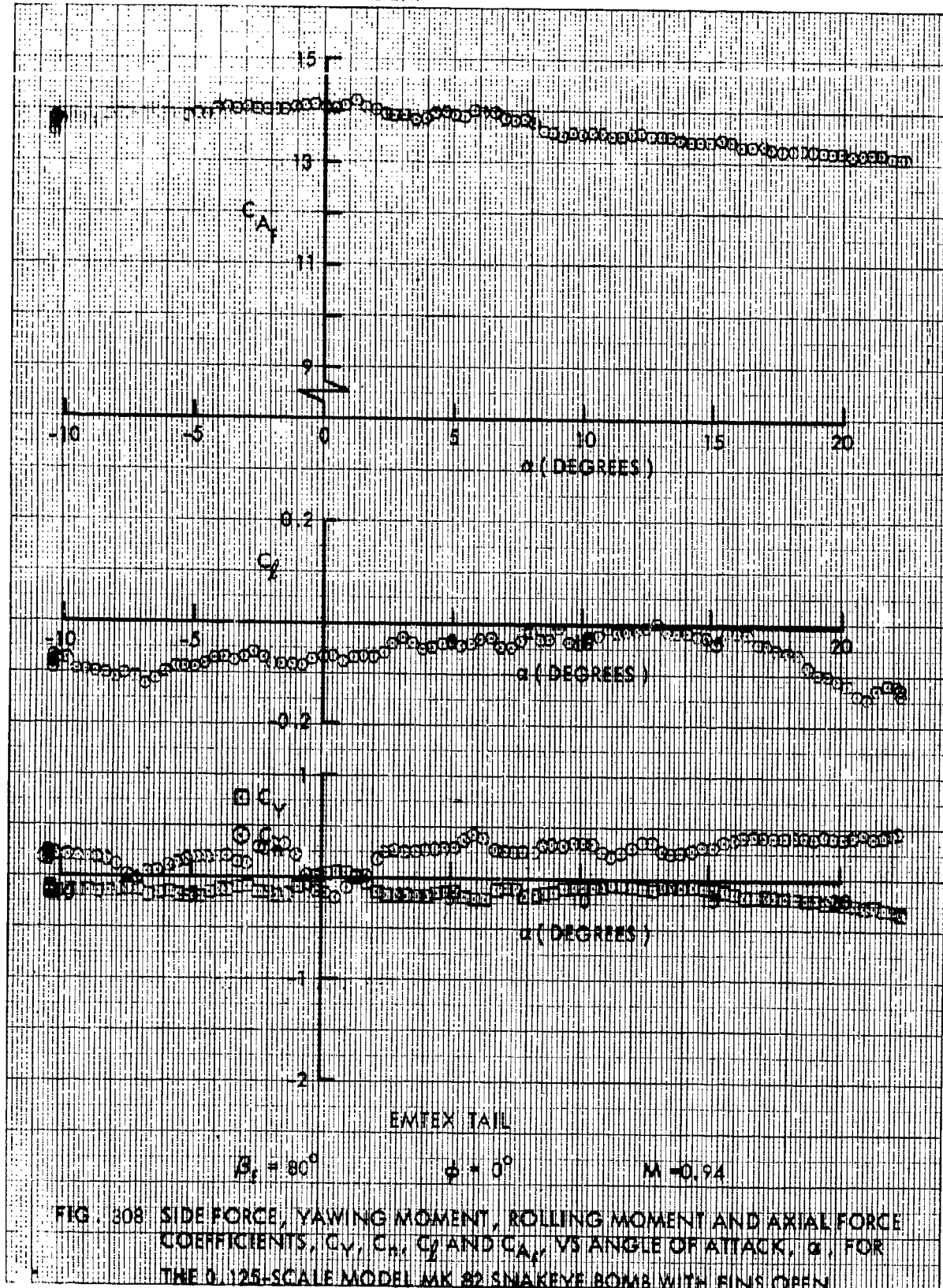




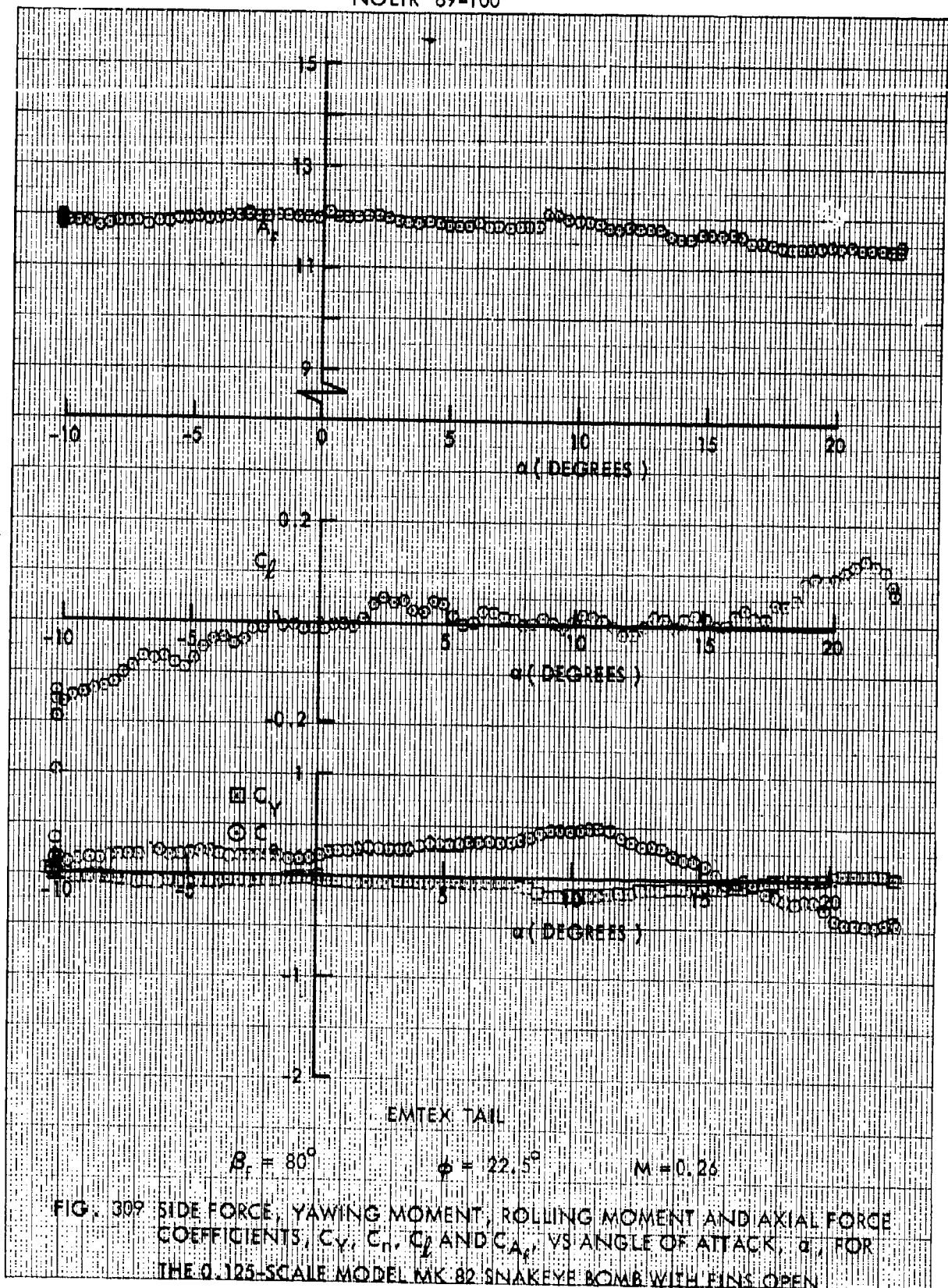




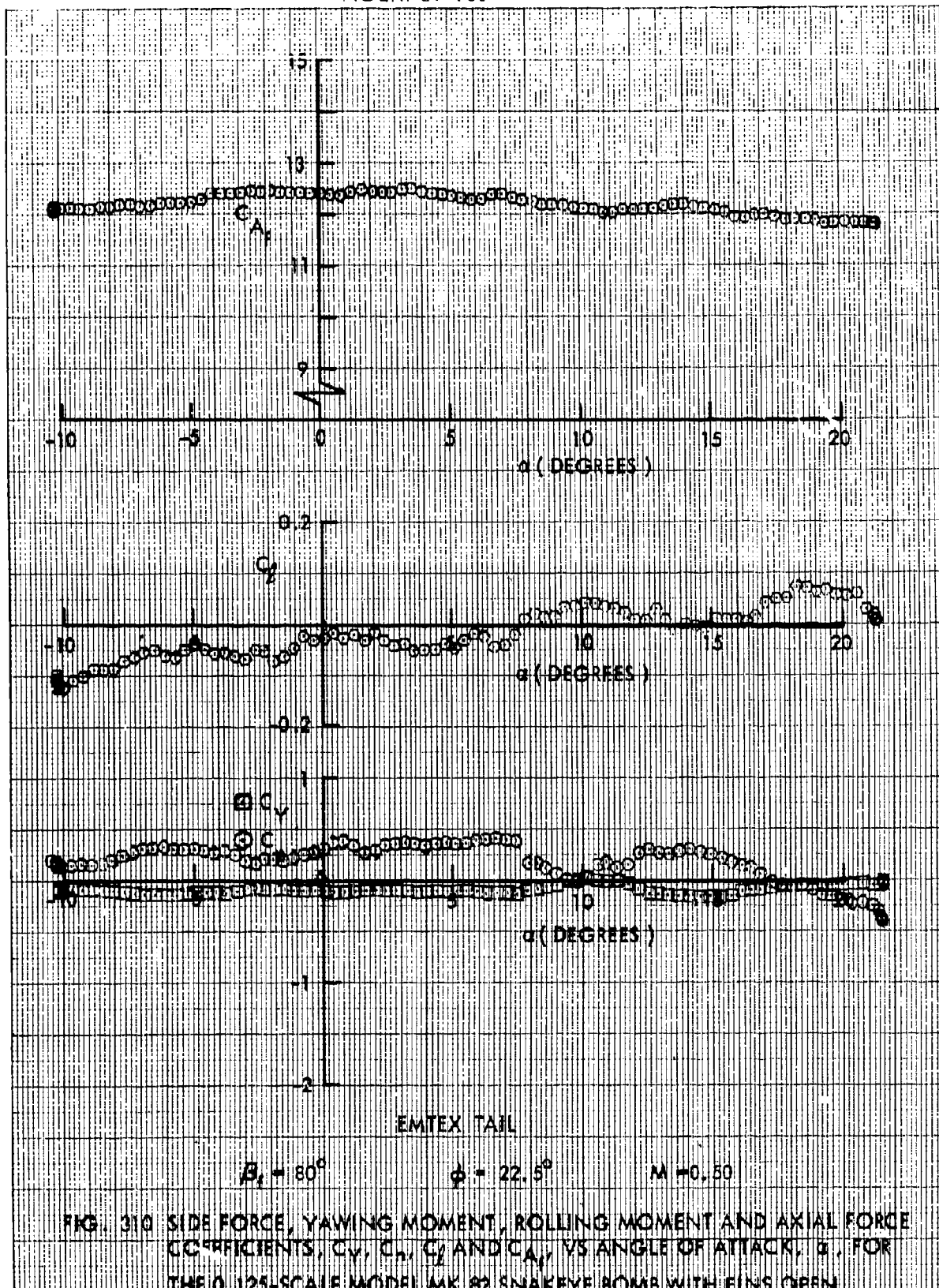


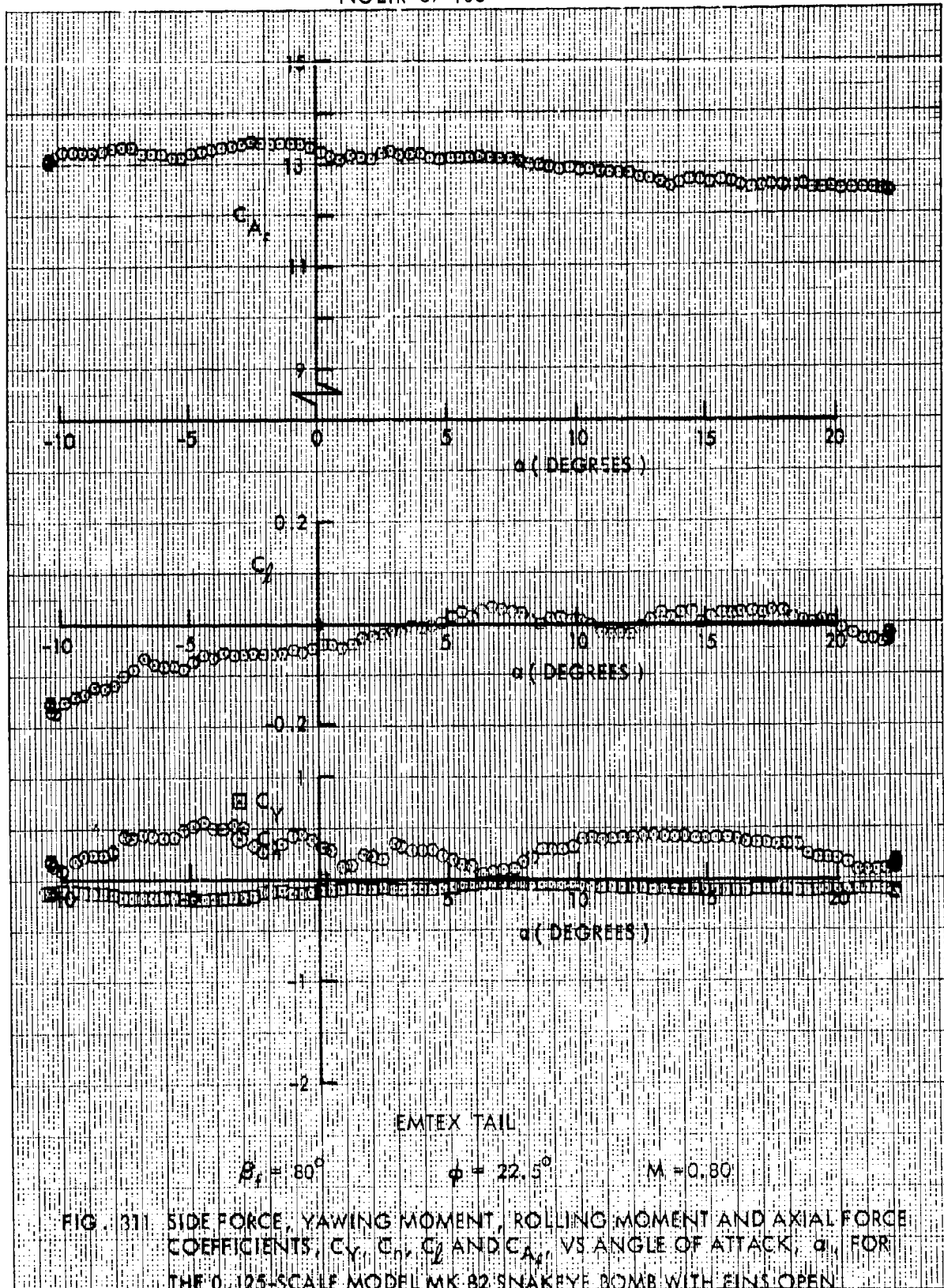












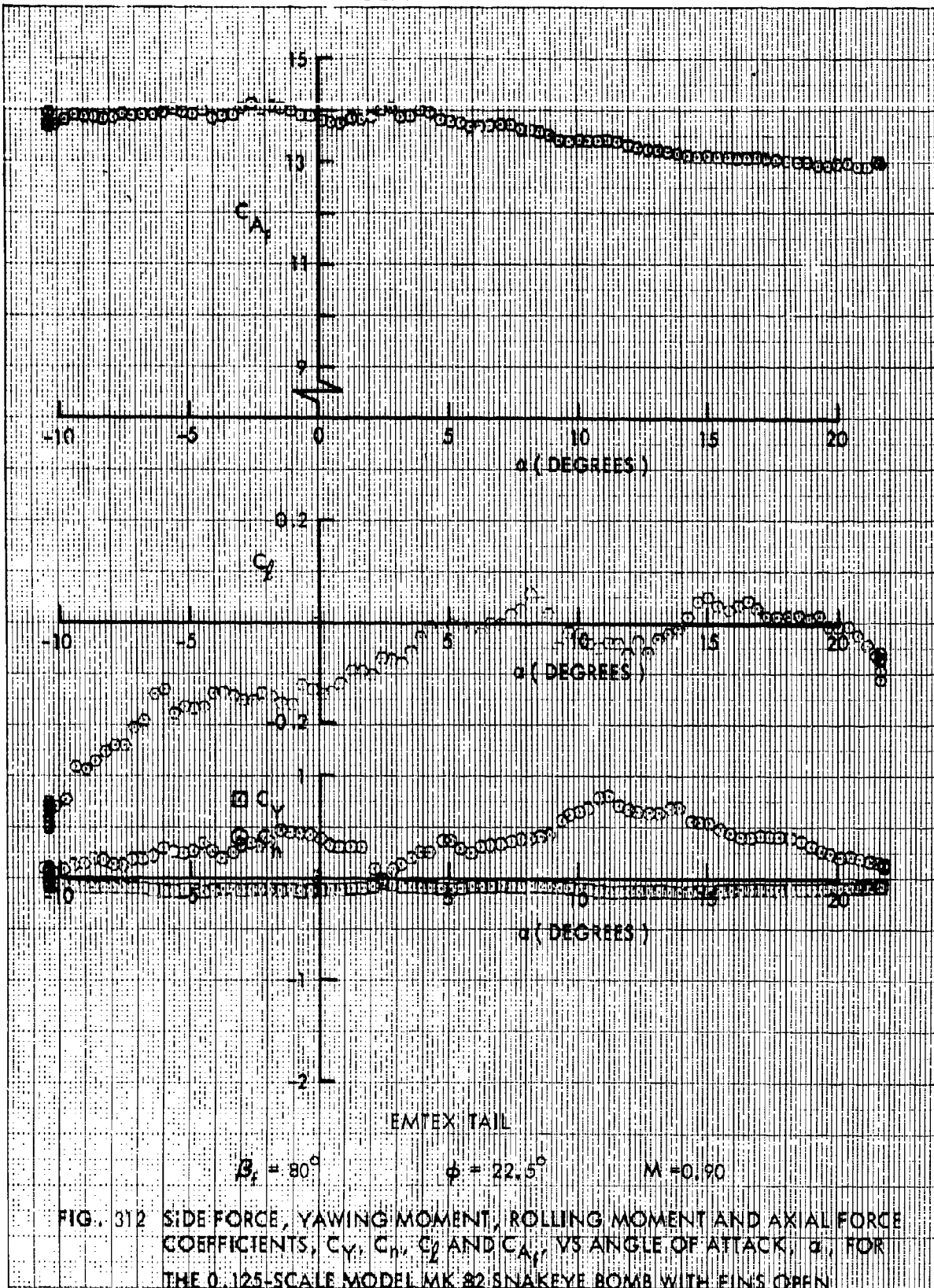
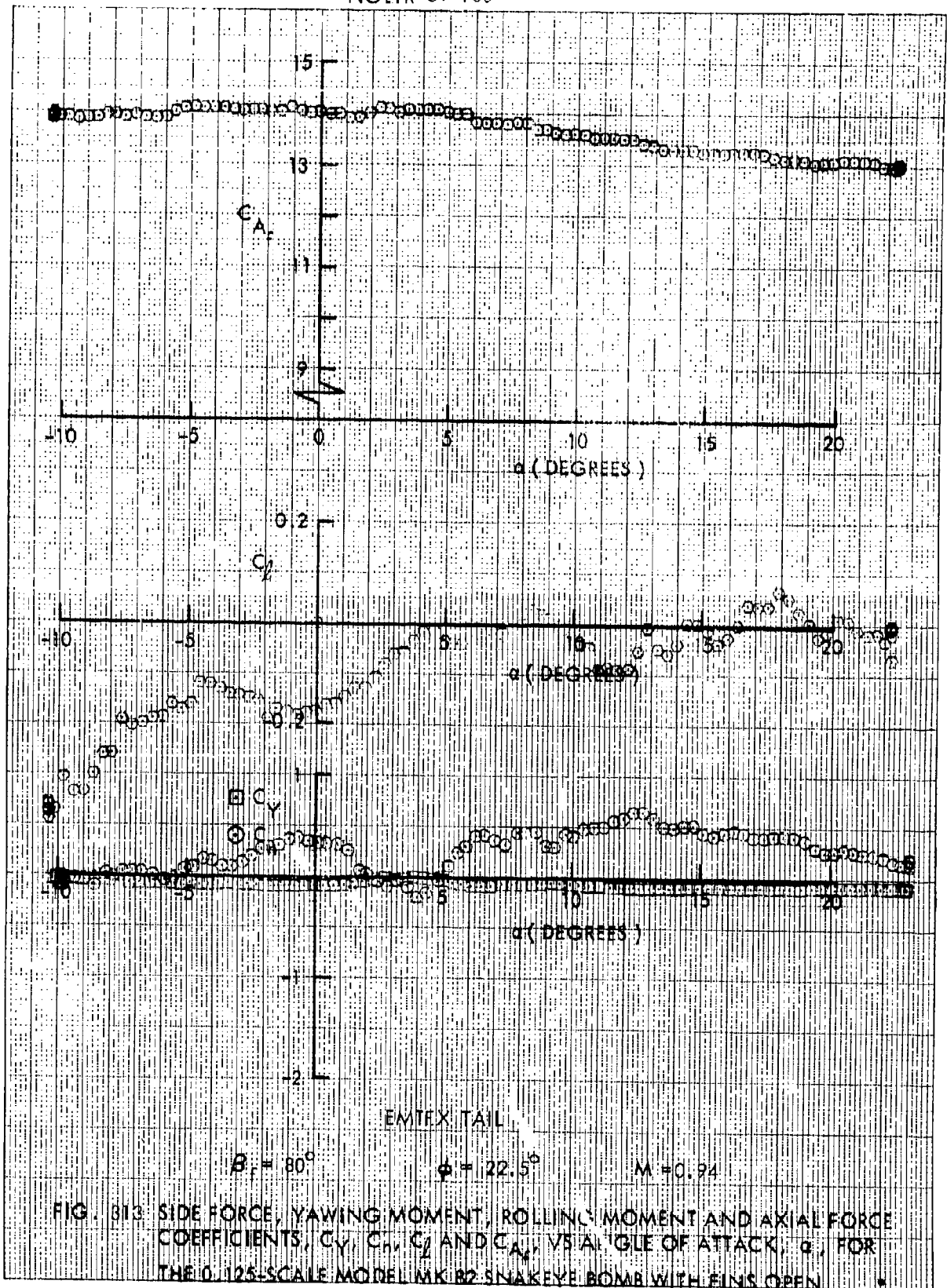
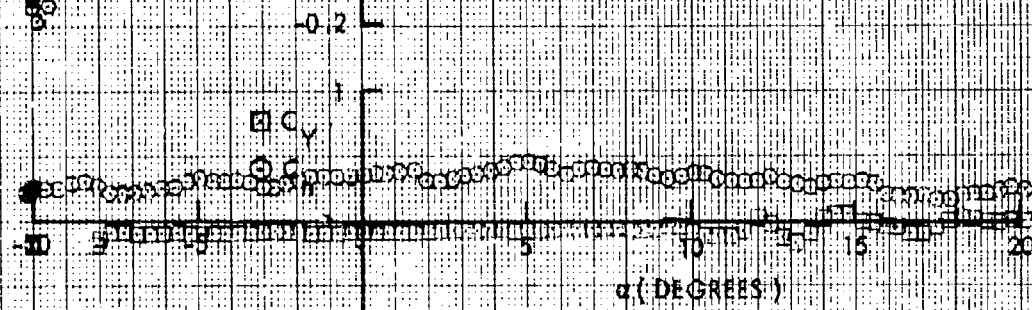
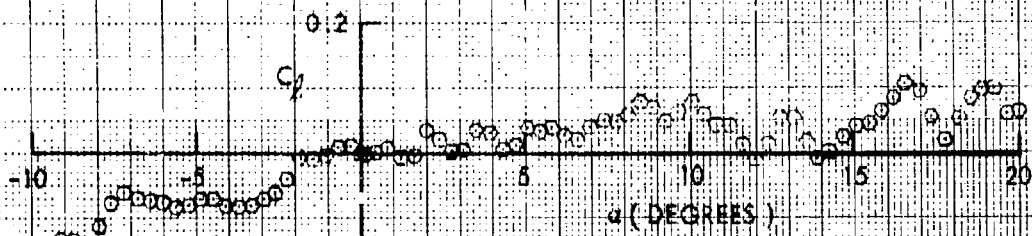
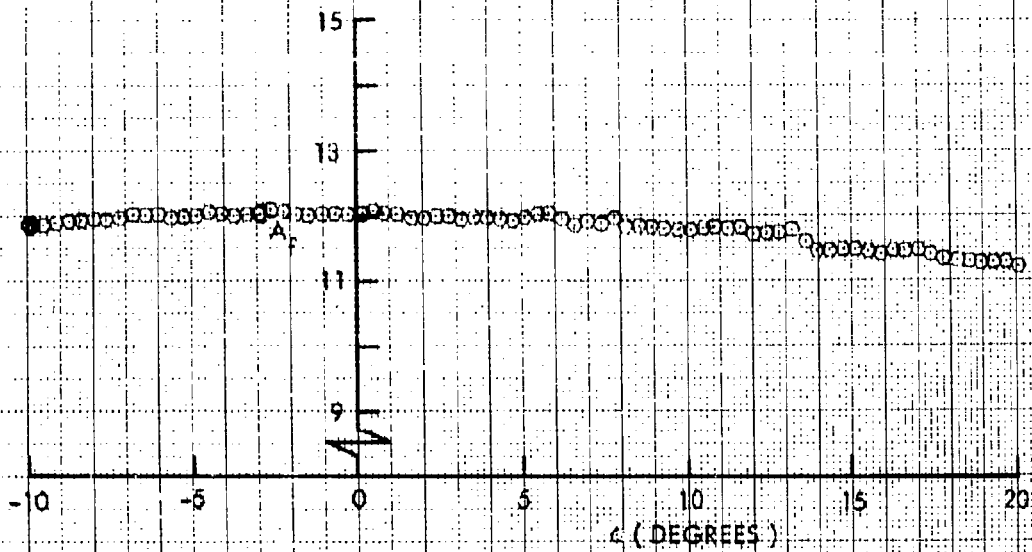


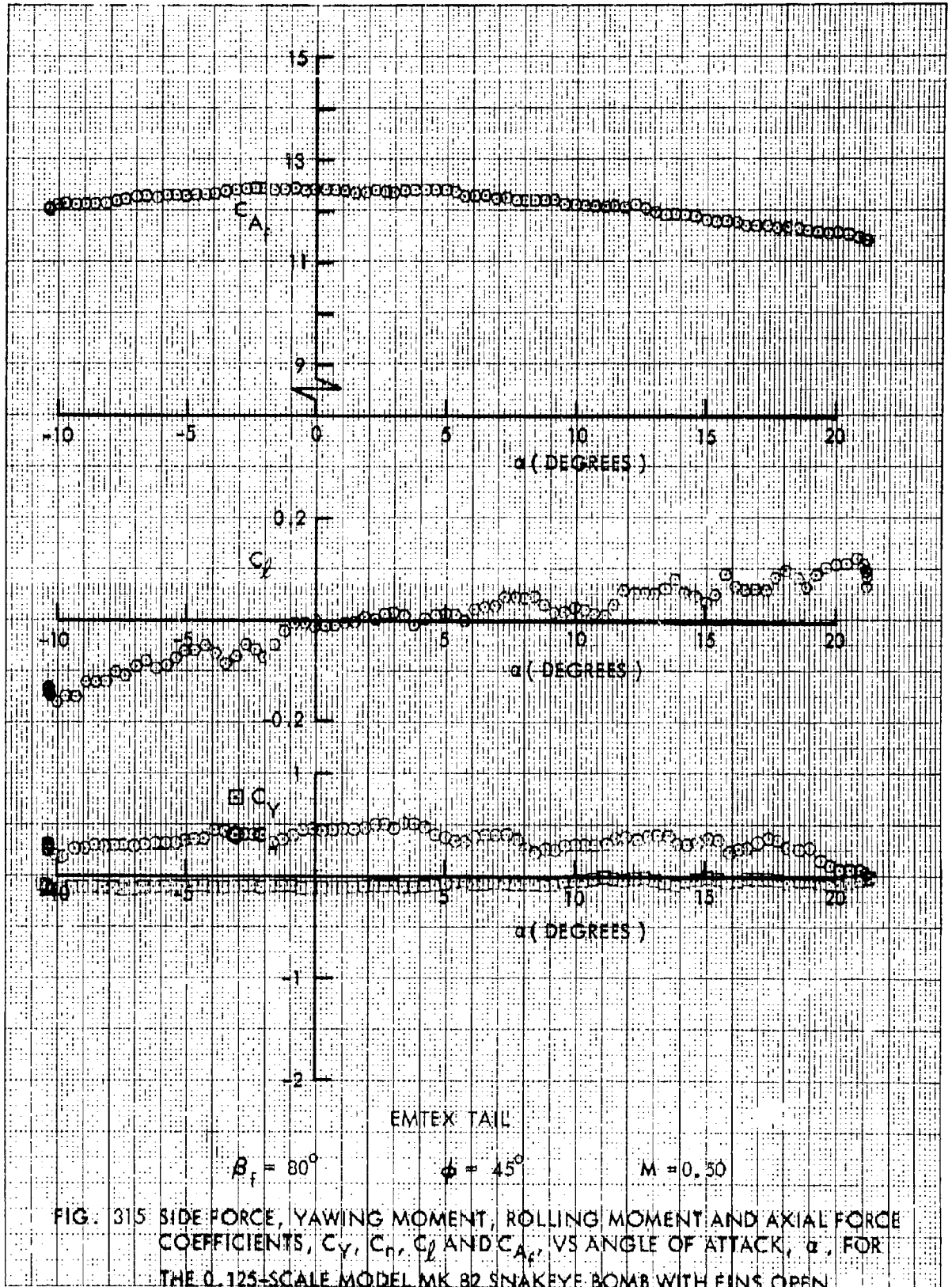
FIG. 312 SIDE FORCE, YAWING MOMENT, ROLLING MOMENT AND AXIAL FORCE COEFFICIENTS,  $C_Y$ ,  $C_L$ ,  $C_Y$  AND  $C_A$ , VS ANGLE OF ATTACK,  $\alpha$ , FOR THE 0.125-SCALE MODEL MK 82 SNAKEYE BOMB WITH FINS OPEN





EMTEX TAIL  
 $\beta_1 = 80^\circ$        $\phi = 45^\circ$        $M = 0.26$

FIG. 314 SIDE FORCE, YAWING MOMENT, ROLLING MOMENT AND AXIAL FORCE COEFFICIENTS,  $C_Y$ ,  $C_n$ ,  $C_L$  AND  $C_A$ , VS ANGLE OF ATTACK,  $\alpha$ , FOR THE 0.125-SCALE MODEL MK 82 SNAKEYE BOMB WITH FINS OPEN





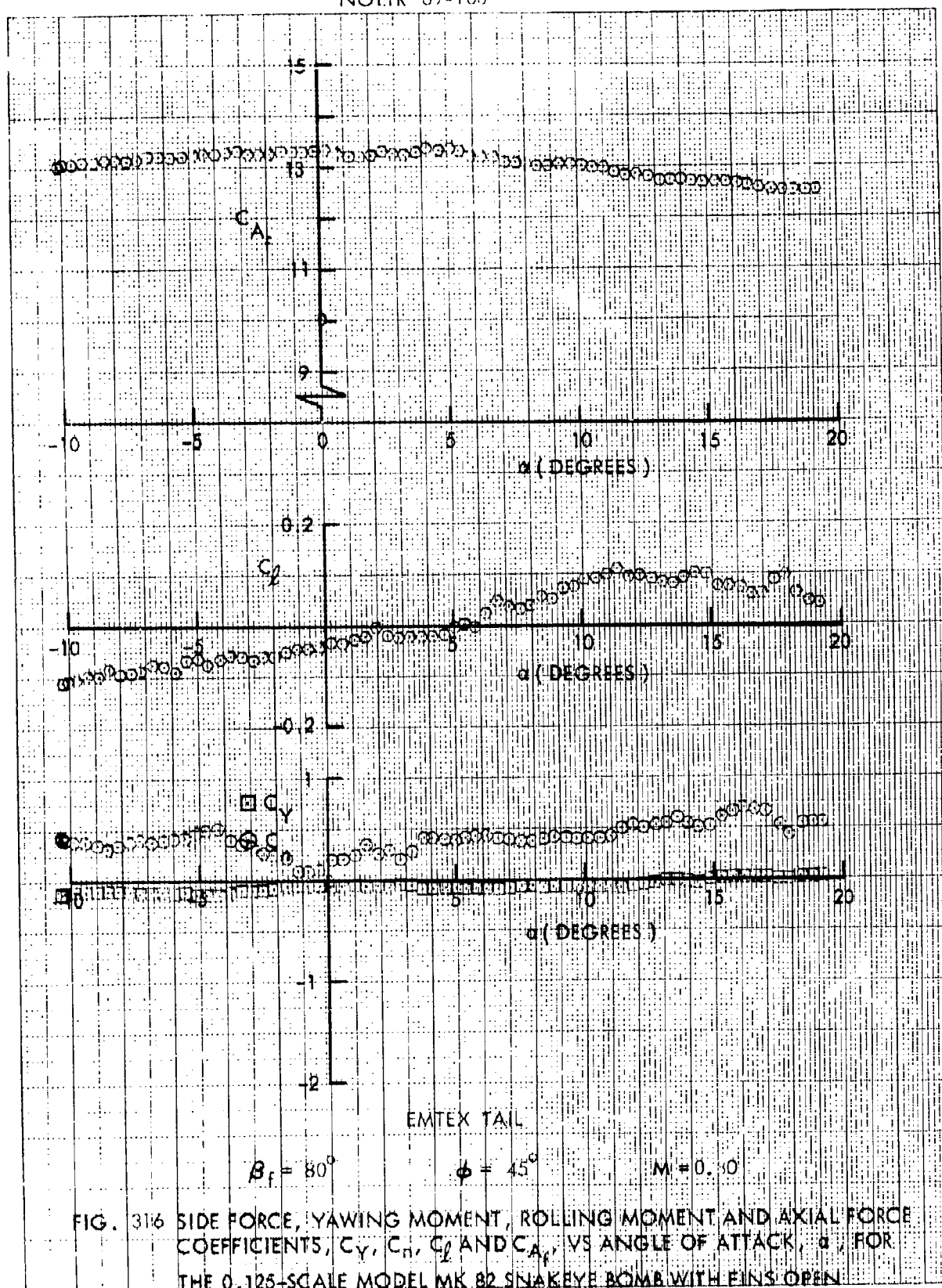
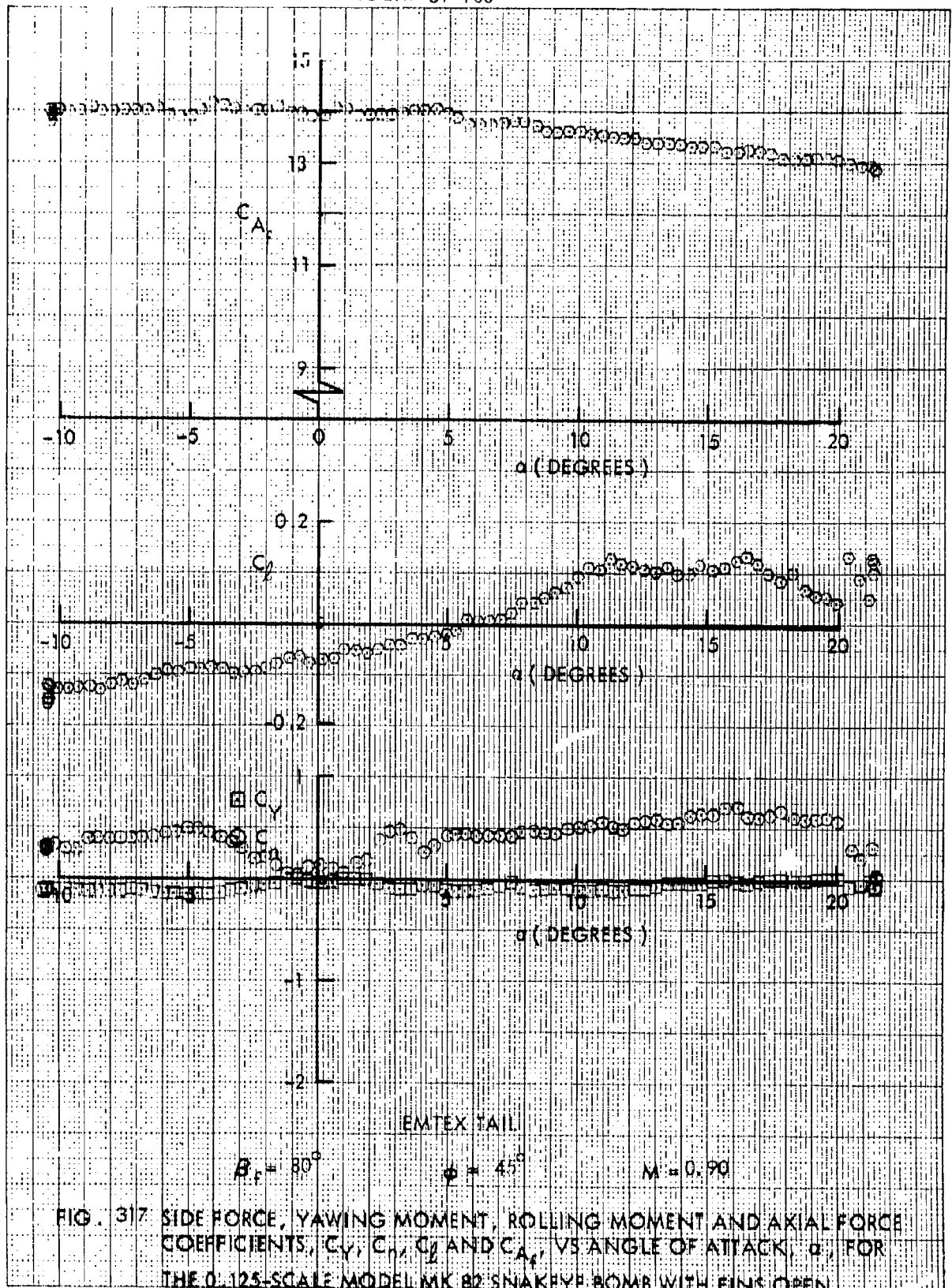
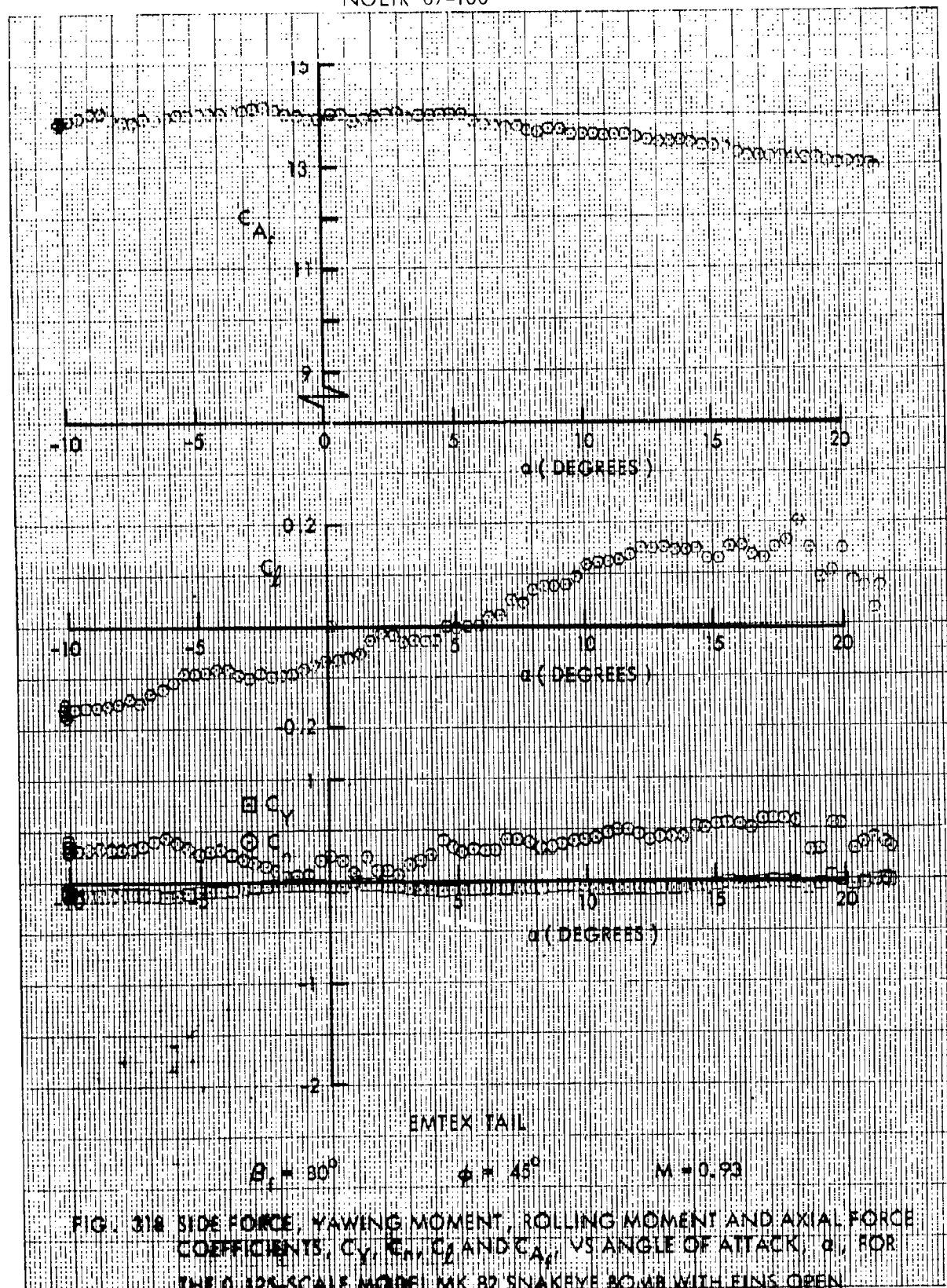
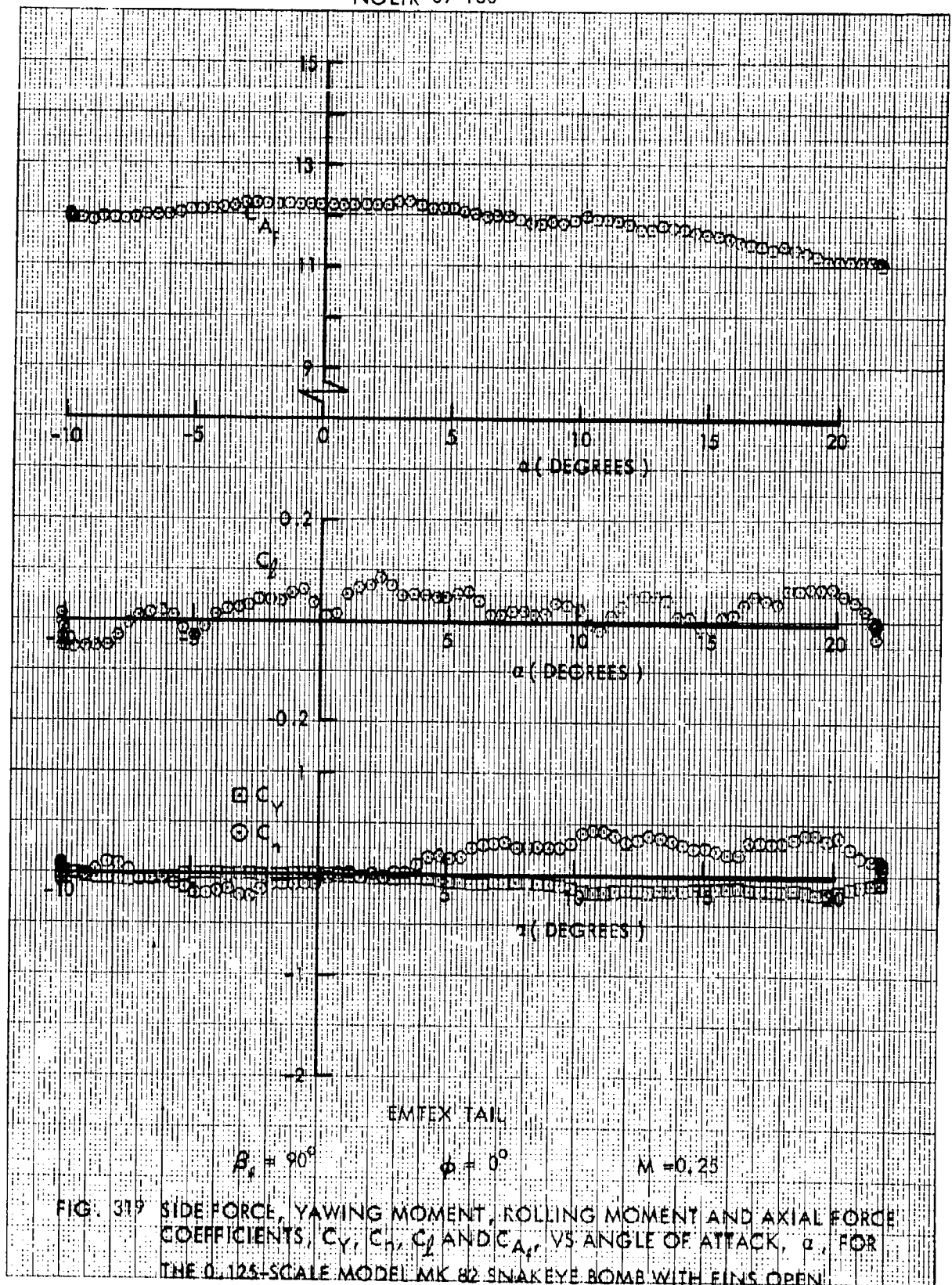
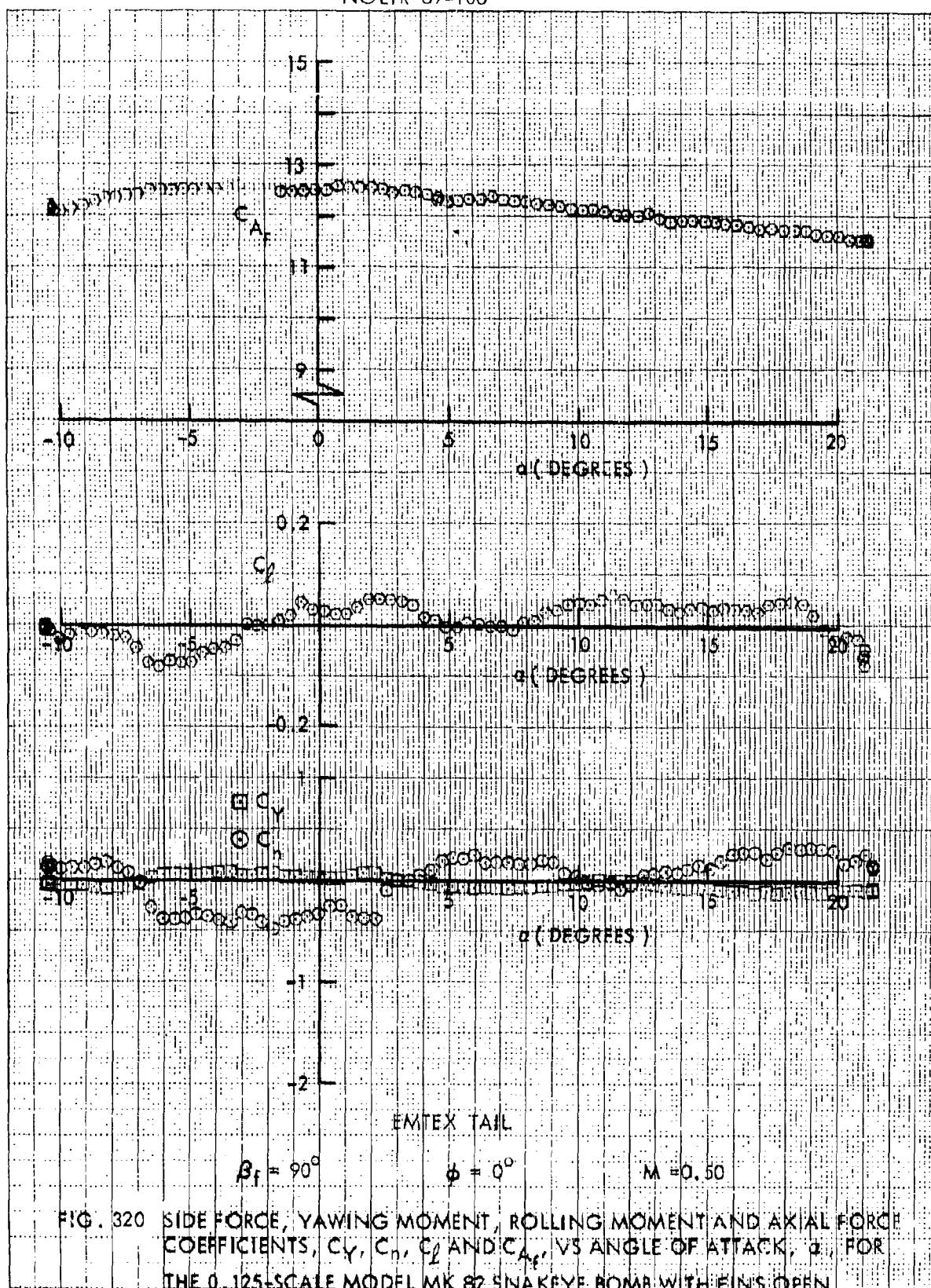


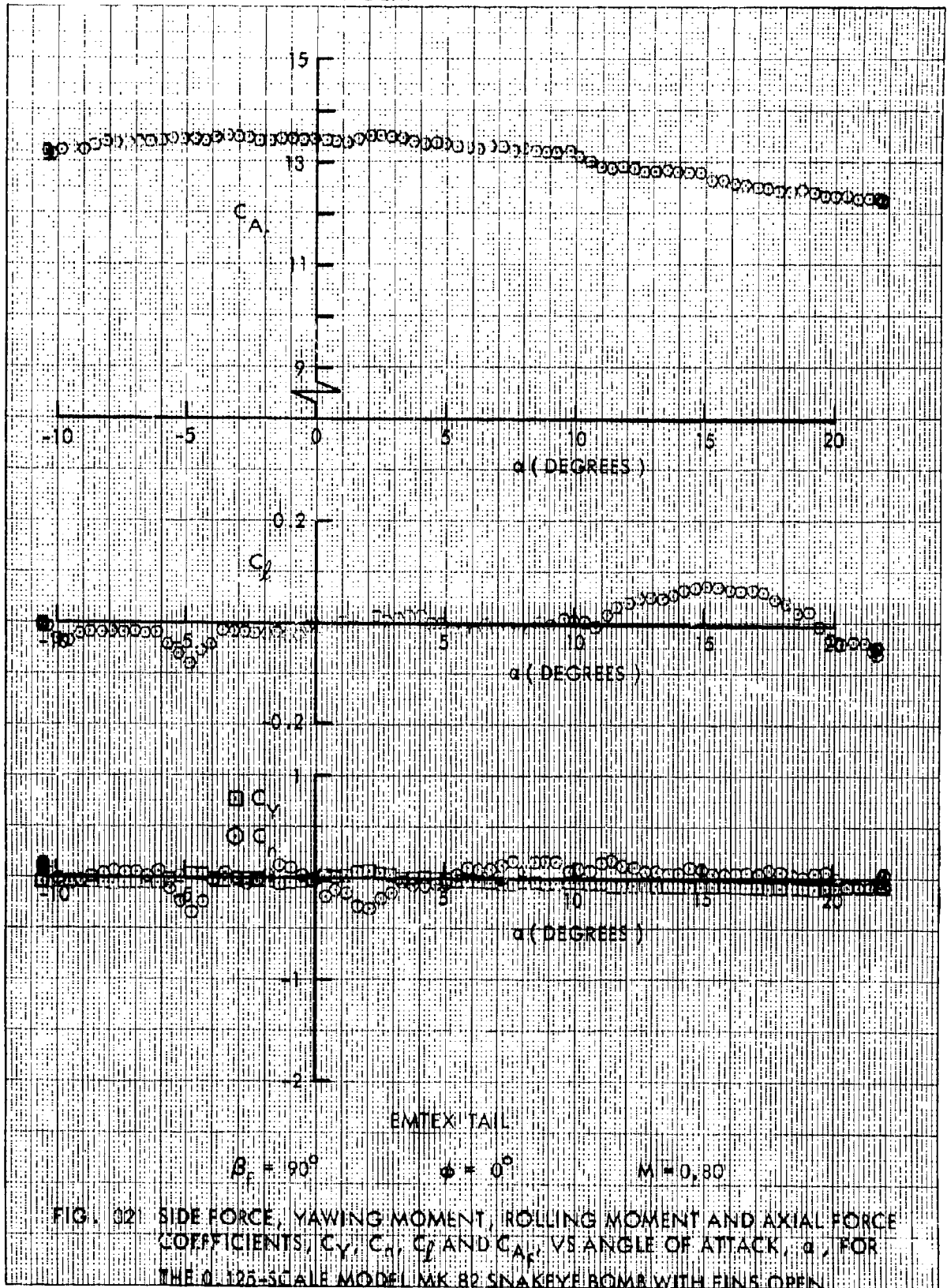
FIG. 316 SIDE FORCE, YAWING MOMENT, ROLLING MOMENT AND AXIAL FORCE COEFFICIENTS,  $C_Y$ ,  $C_n$ ,  $C_l$  AND  $C_A$ , VS ANGLE OF ATTACK,  $\alpha$ , FOR THE 0.125-SCALE MODEL MK 82 SNAKEYE BOMB WITH FINS OPEN













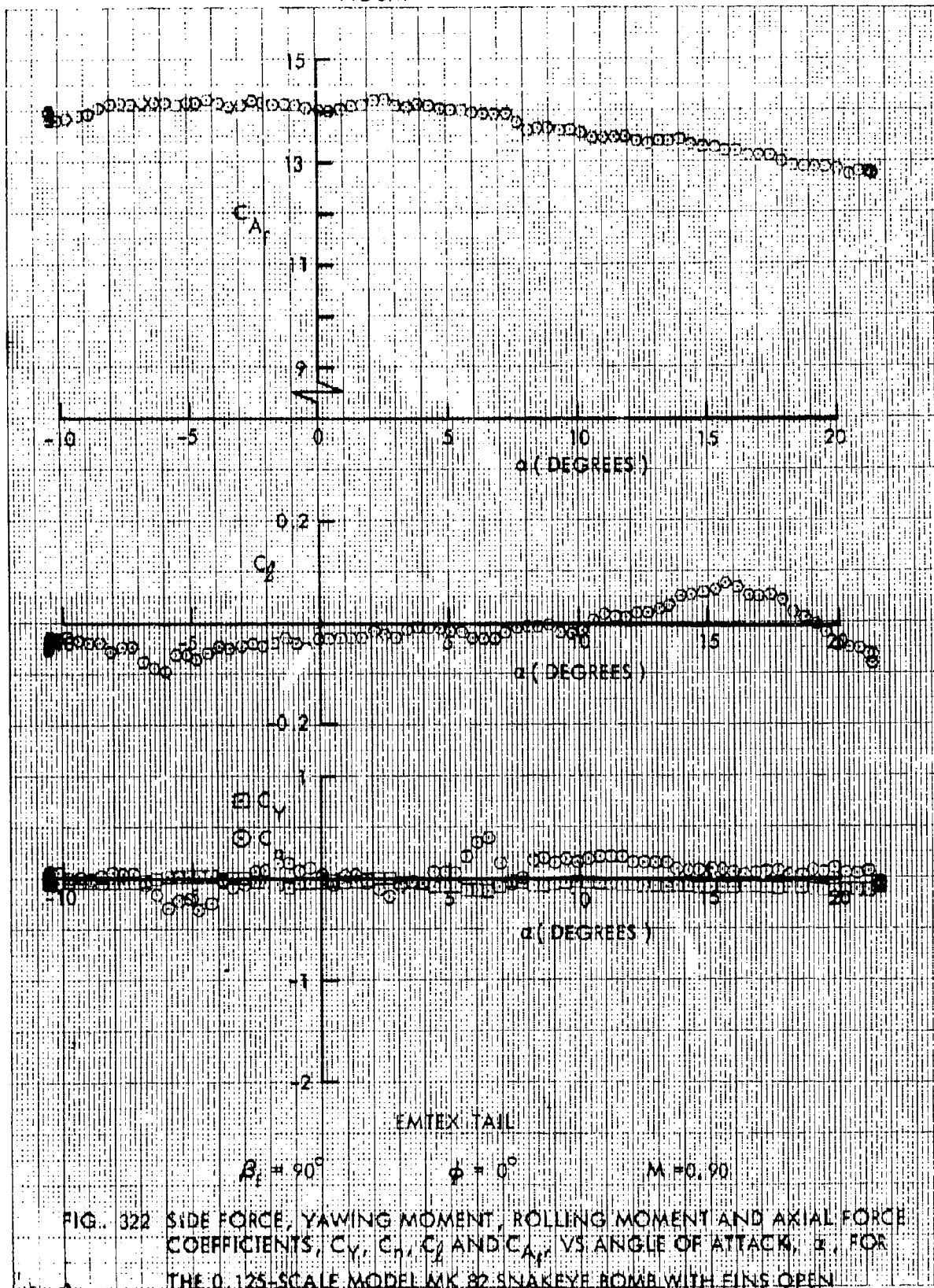
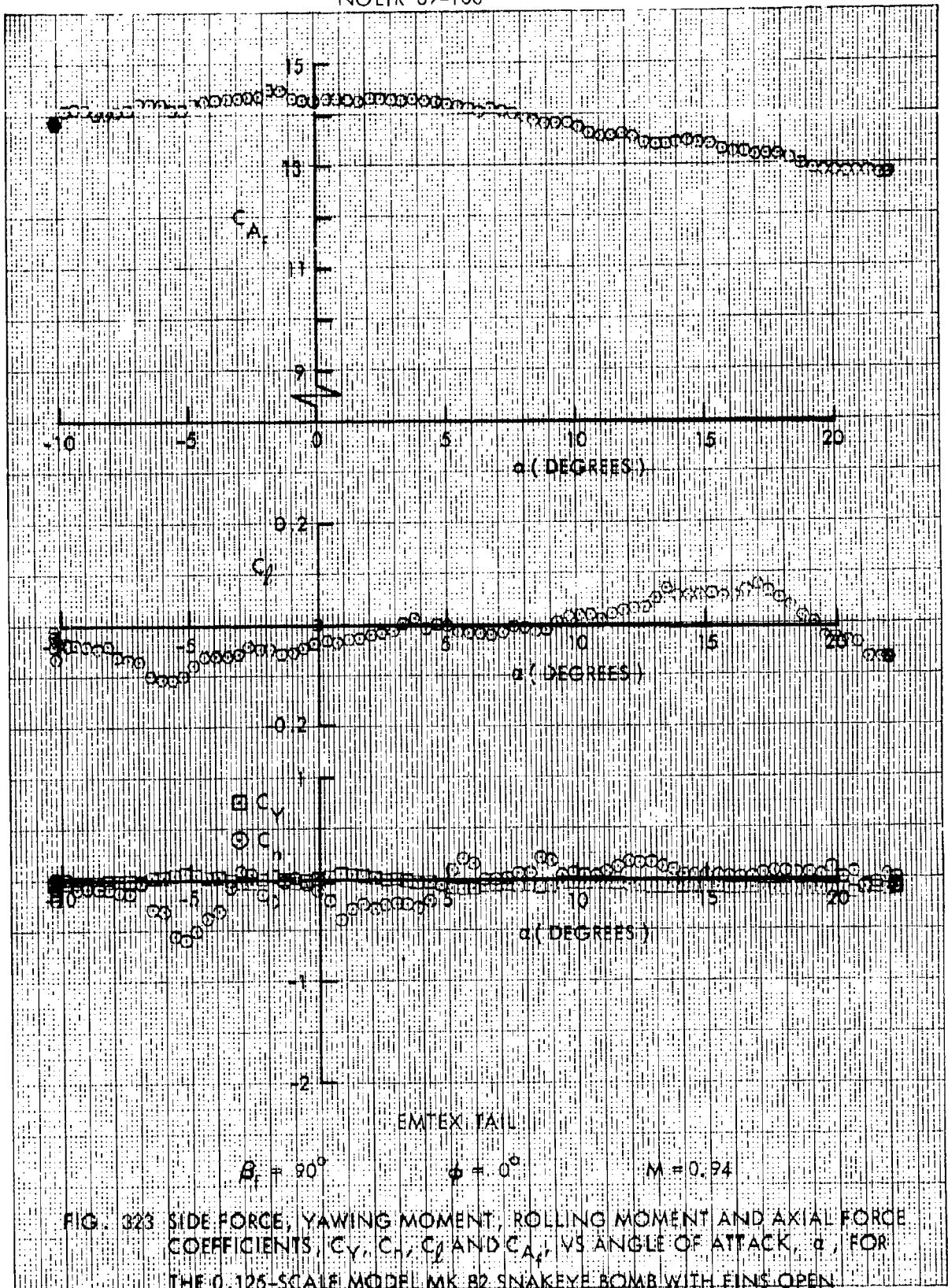


FIG. 322 SIDE FORCE, YAWING MOMENT, ROLLING MOMENT AND AXIAL FORCE COEFFICIENTS,  $C_Y$ ,  $C_n$ ,  $C_l$  AND  $C_A$ , VS. ANGLE OF ATTACK,  $\alpha$ , FOR THE 0.125-SCALE MODEL MK 82 SNAKEYE BOMB WITH FINS OPEN



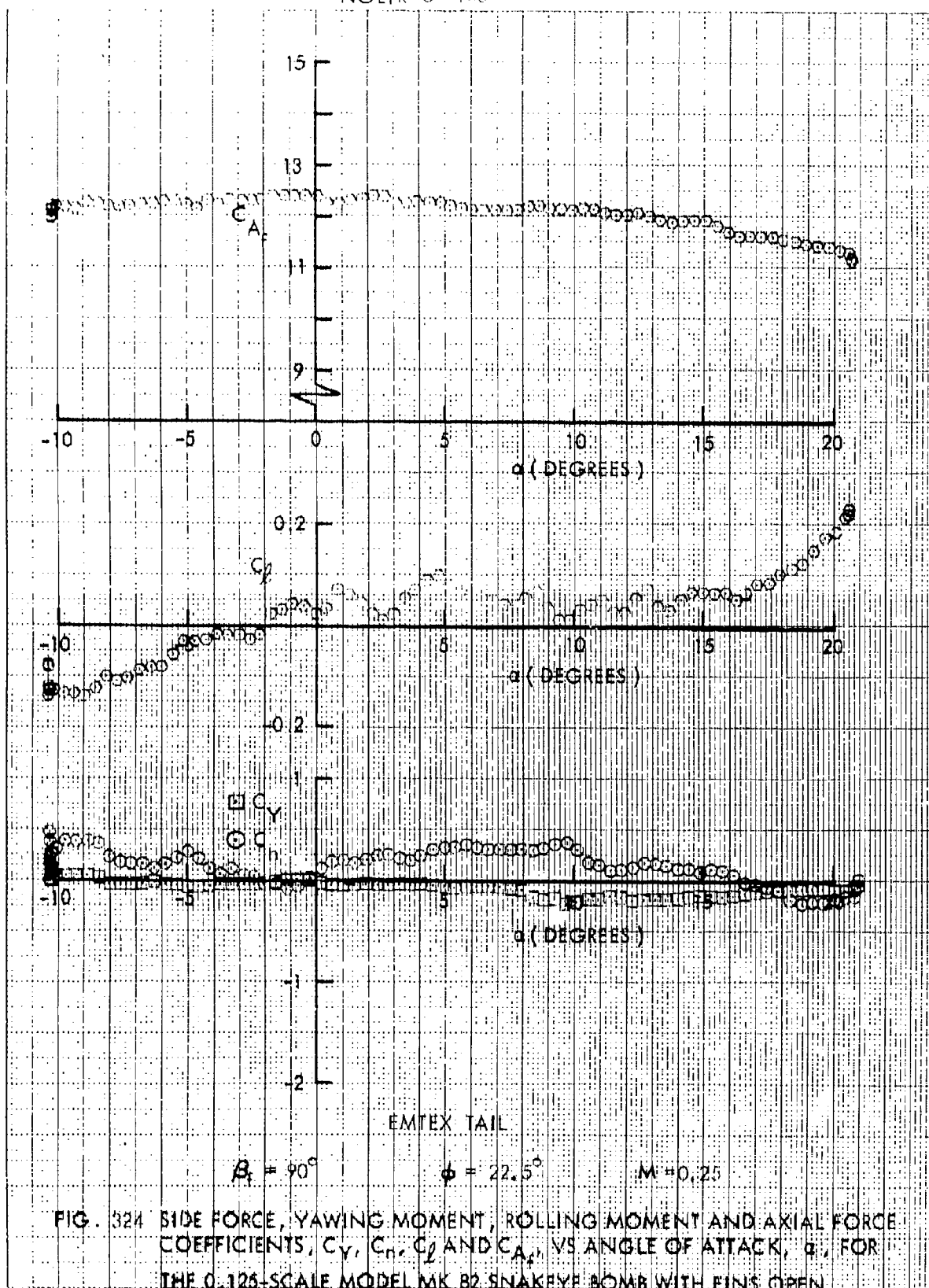
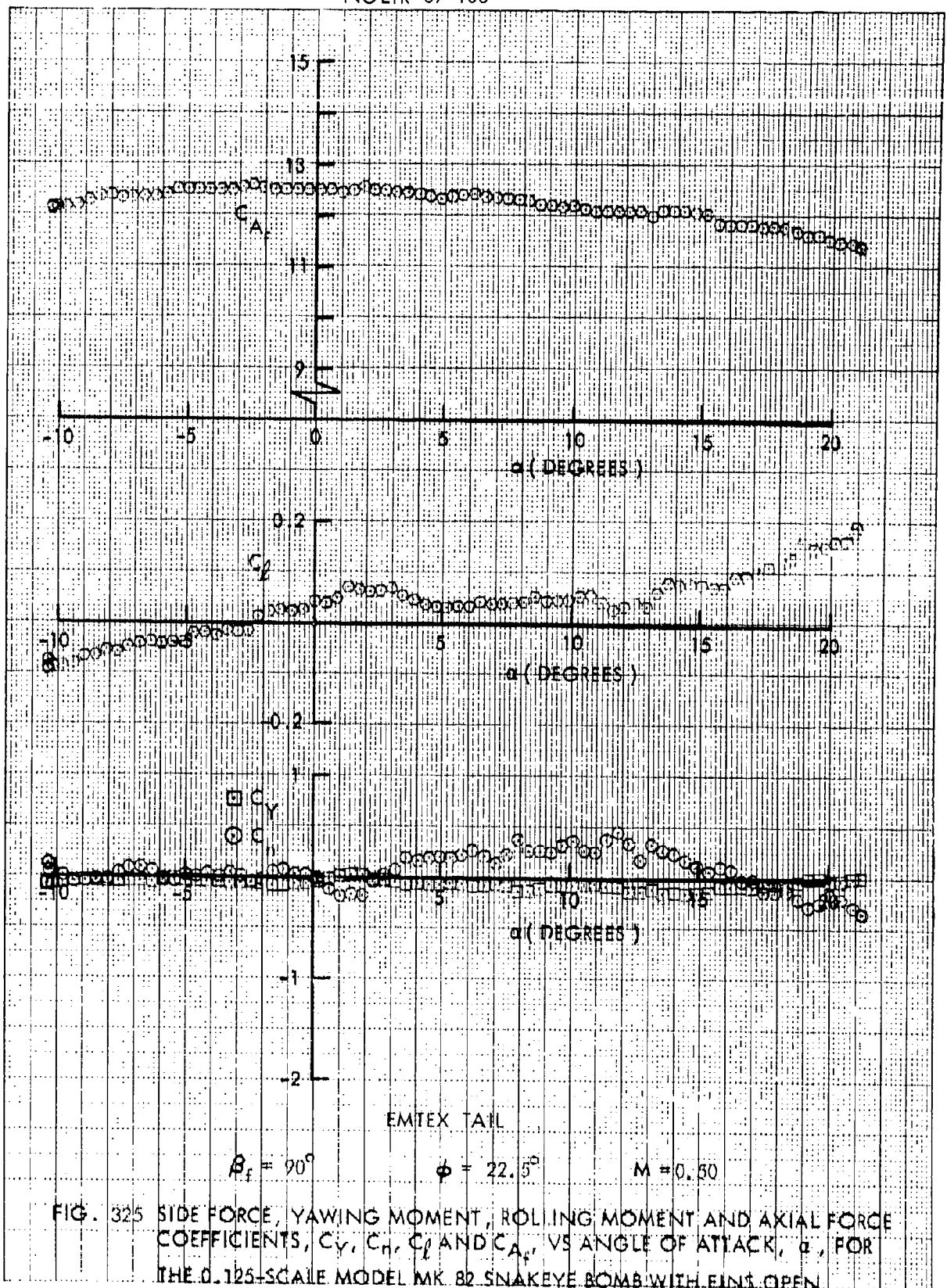
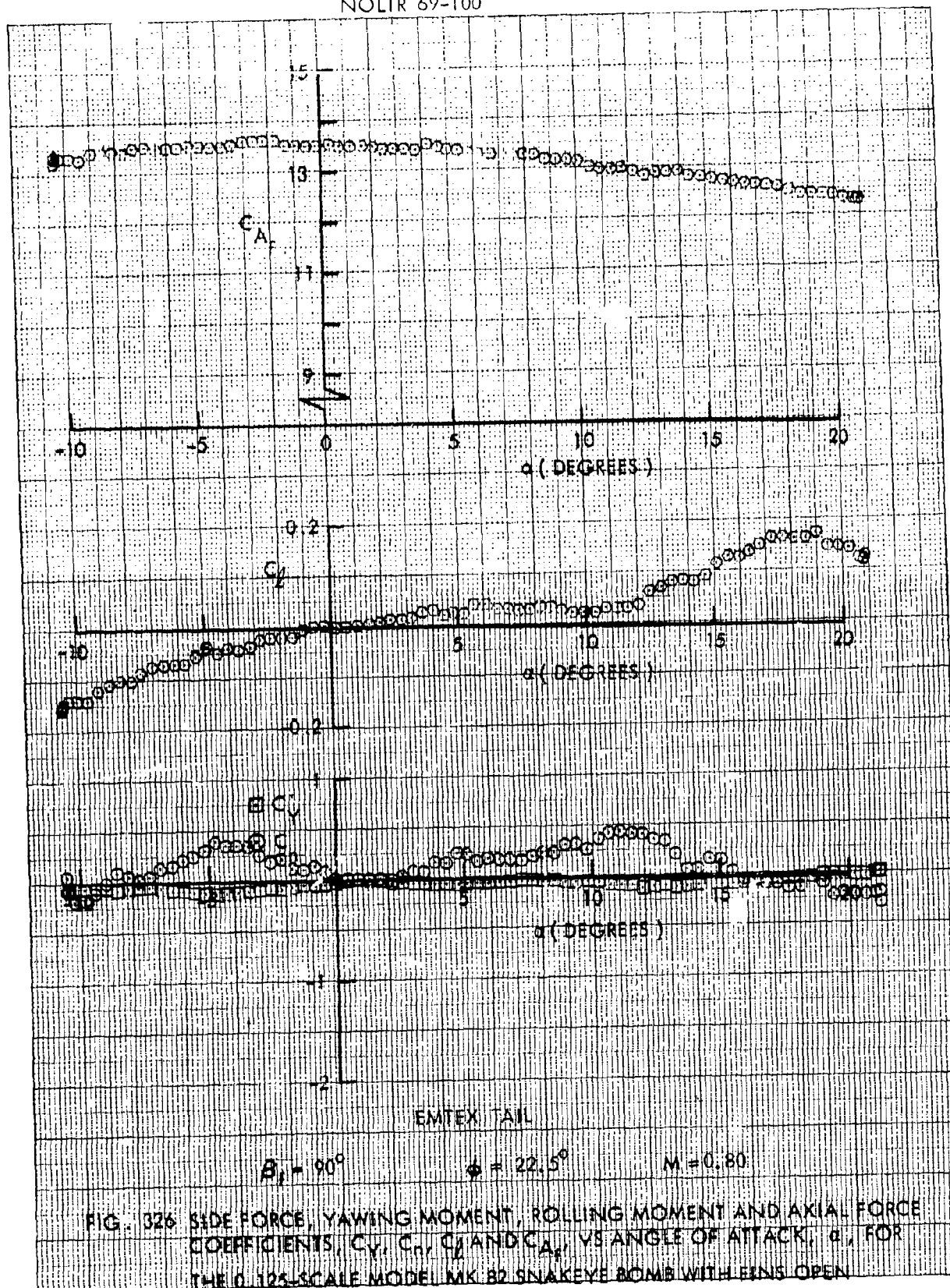
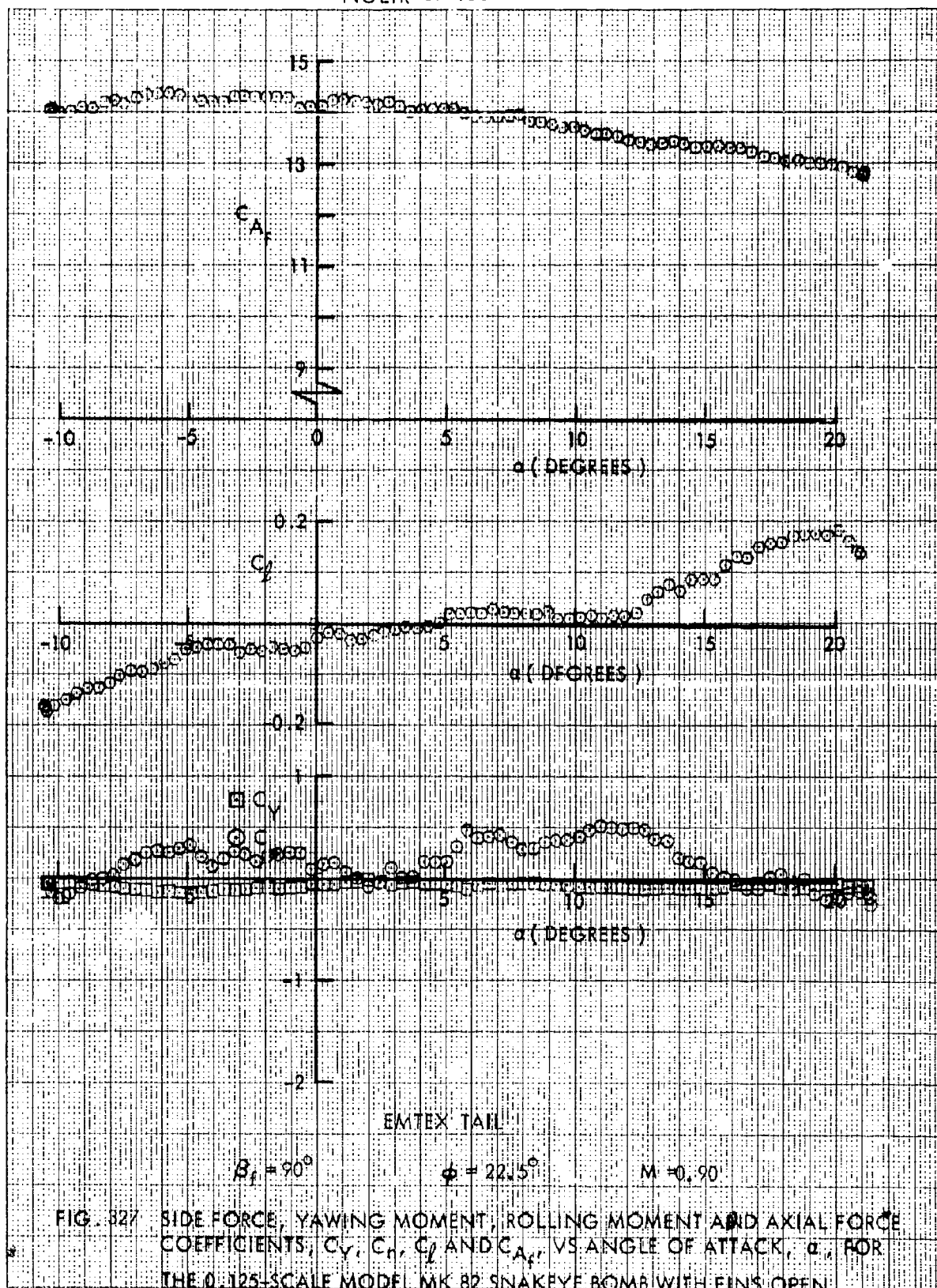


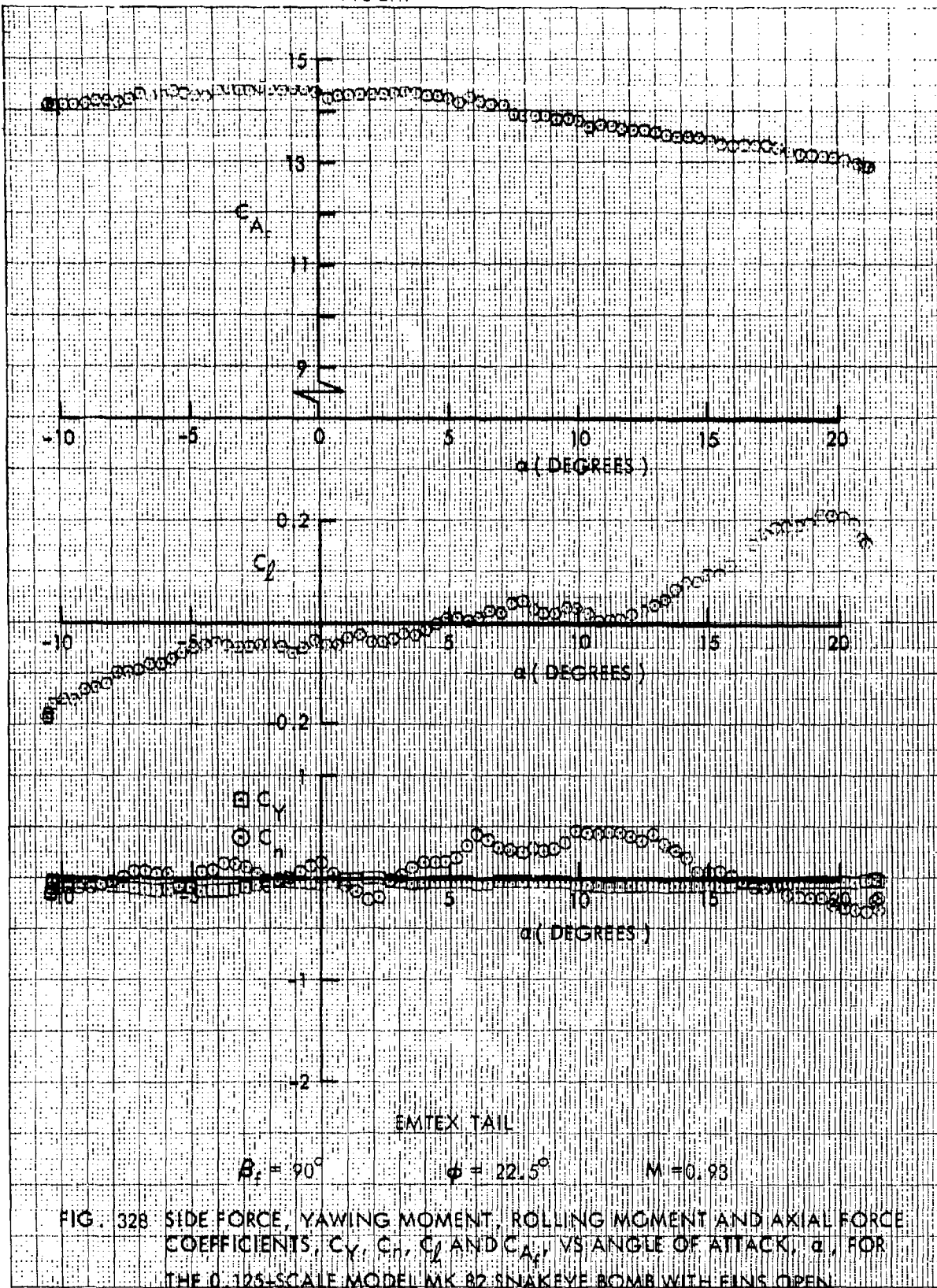
FIG. 324 SIDE FORCE, YAWING MOMENT, ROLLING MOMENT AND AXIAL FORCE COEFFICIENTS,  $C_Y$ ,  $C_n$ ,  $C_L$  AND  $C_A$ , VS ANGLE OF ATTACK,  $\alpha$ , FOR THE 0.125-SCALE MODEL MK B2 SNAKEYE BOMB WITH FINS OPEN.

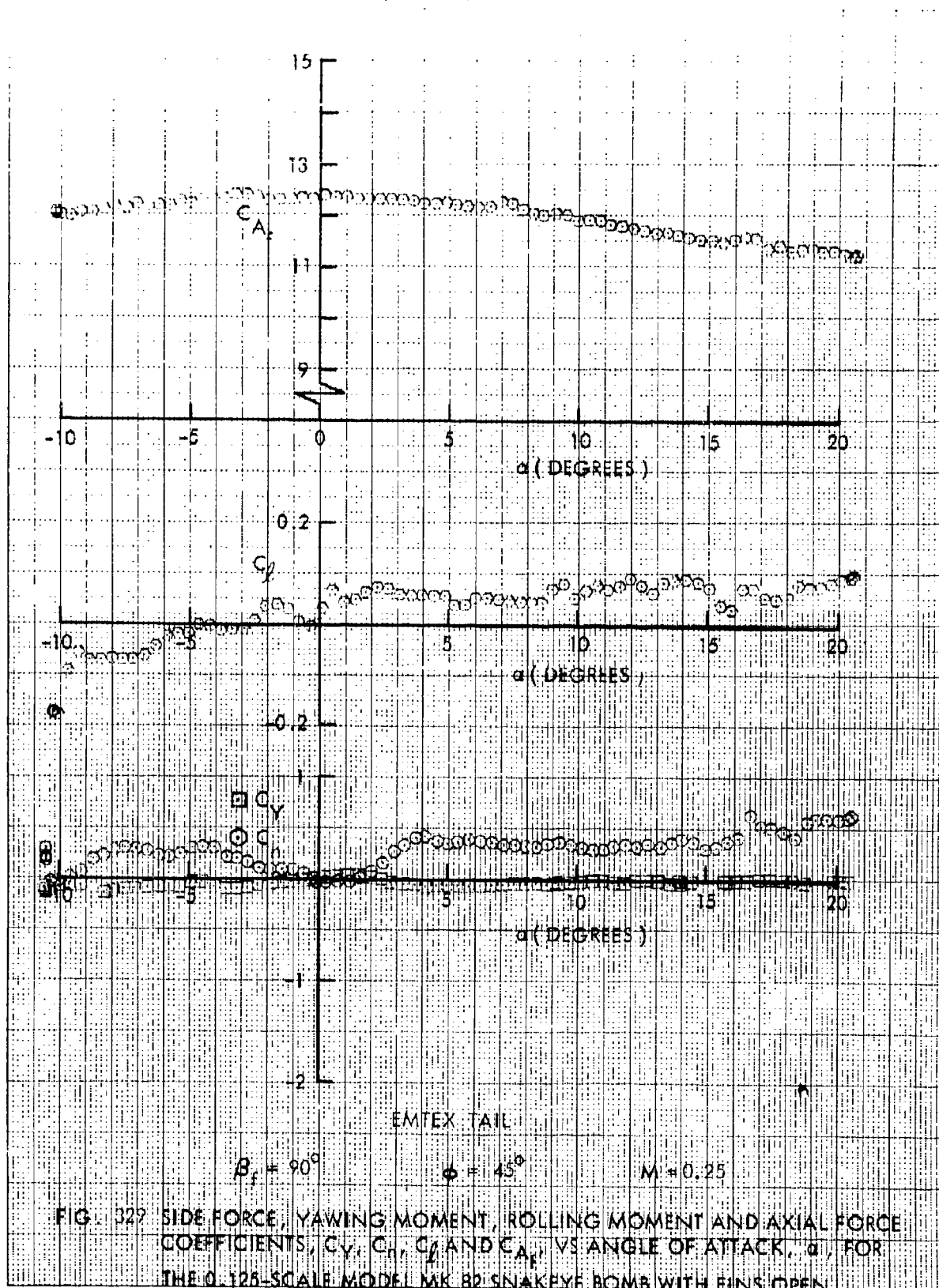


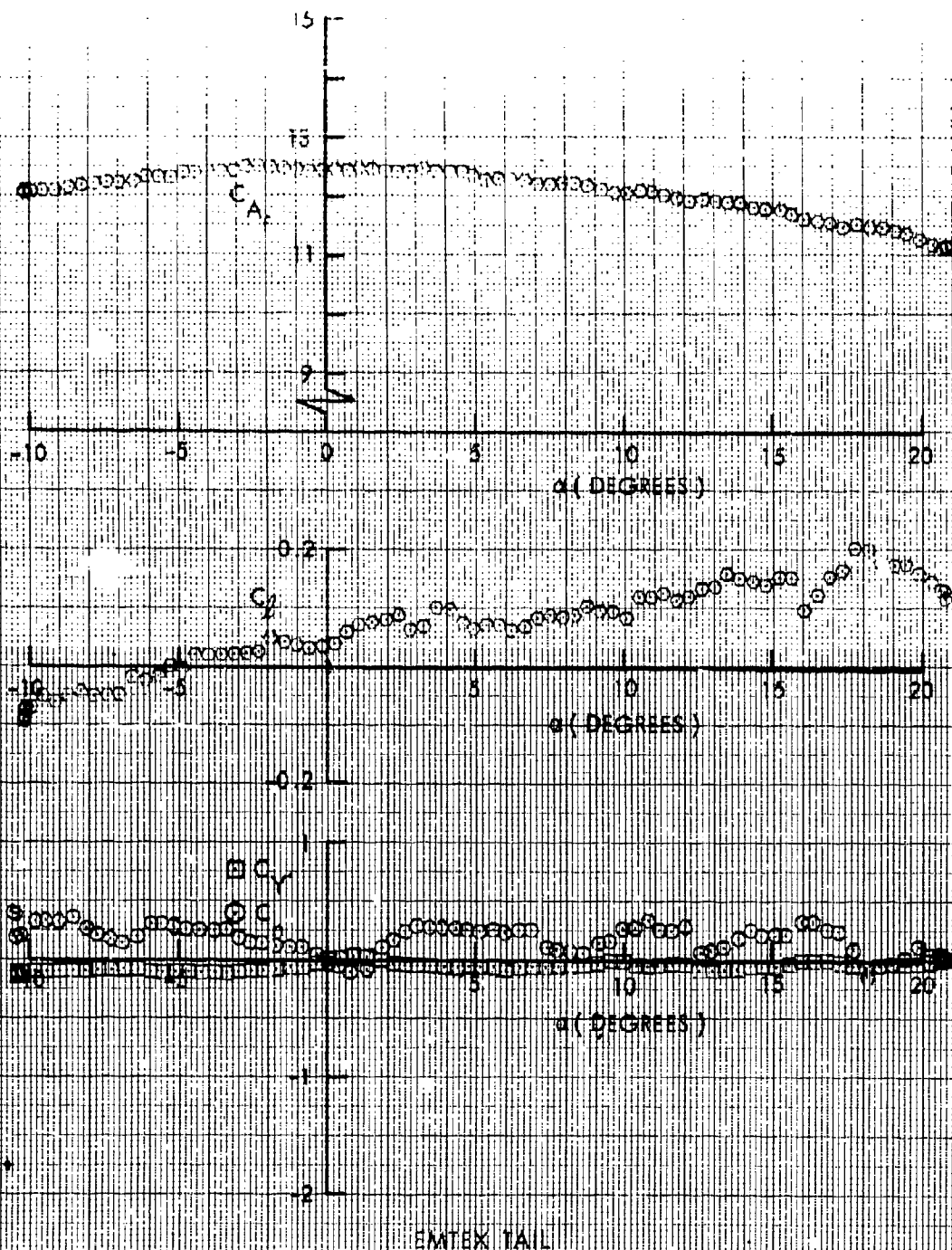










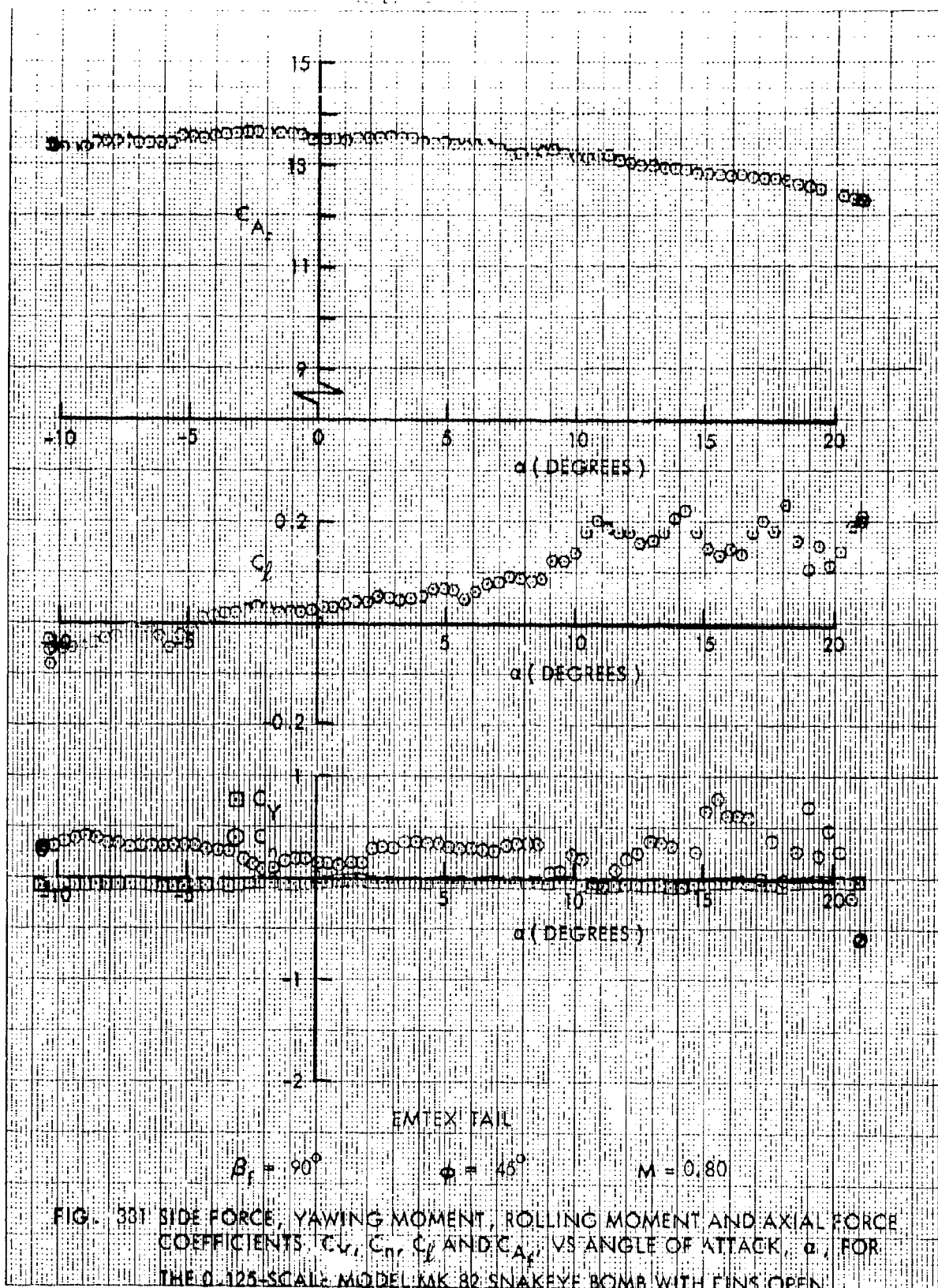


$\beta_1 = 90^\circ$

$\phi = 45^\circ$

$M = 0.50$

FIG. 350 SIDE FORCE, YAWING MOMENT, ROLLING MOMENT AND AXIAL FORCE COEFFICIENTS,  $C_y$ ,  $C_r$ ,  $C_y$  AND  $C_A$ , VS ANGLE OF ATTACK,  $\alpha$ , FOR THE 0.125-SCALE MODEL MK 82 SNAKEYE BOMB WITH FINS OPEN



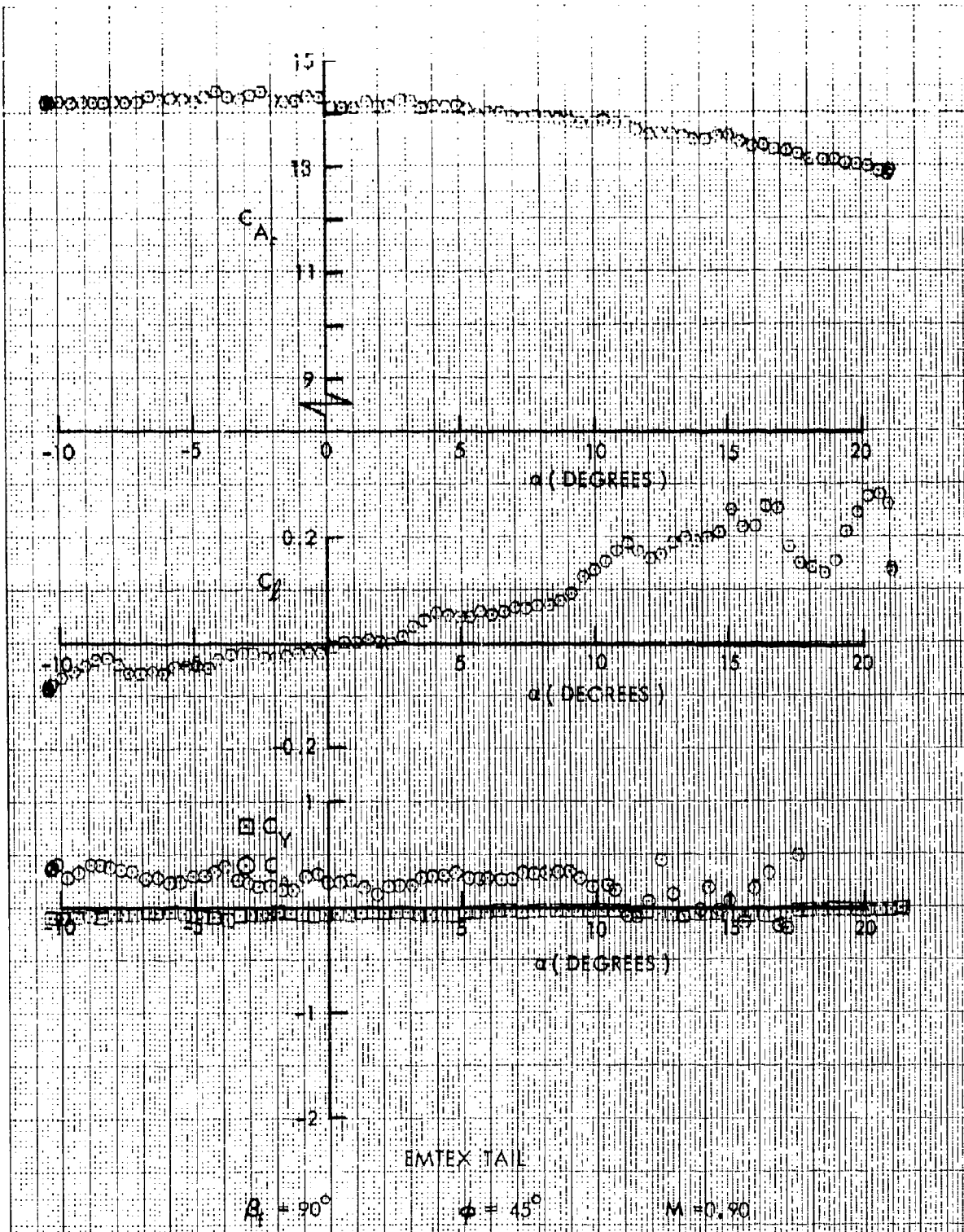
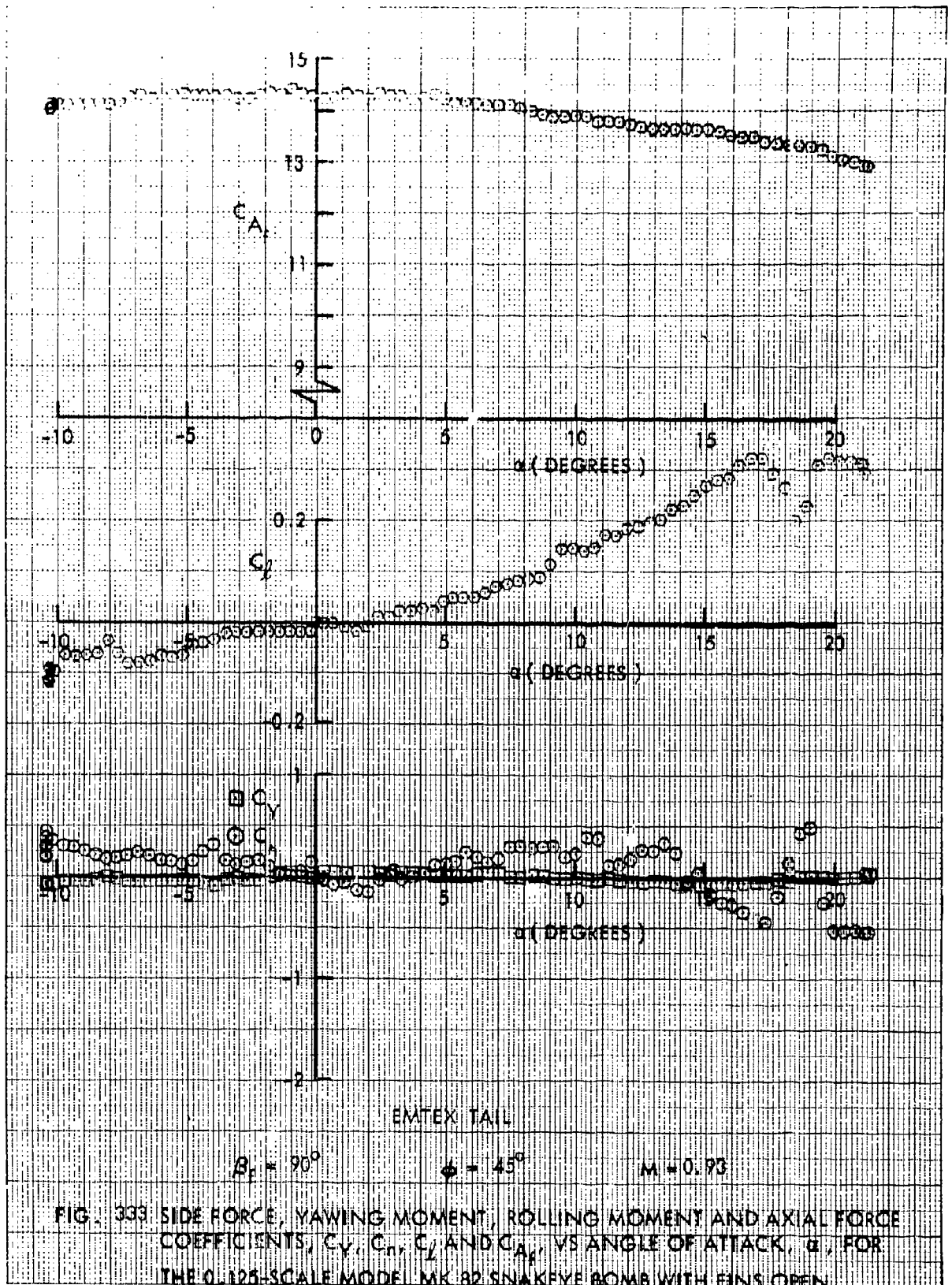
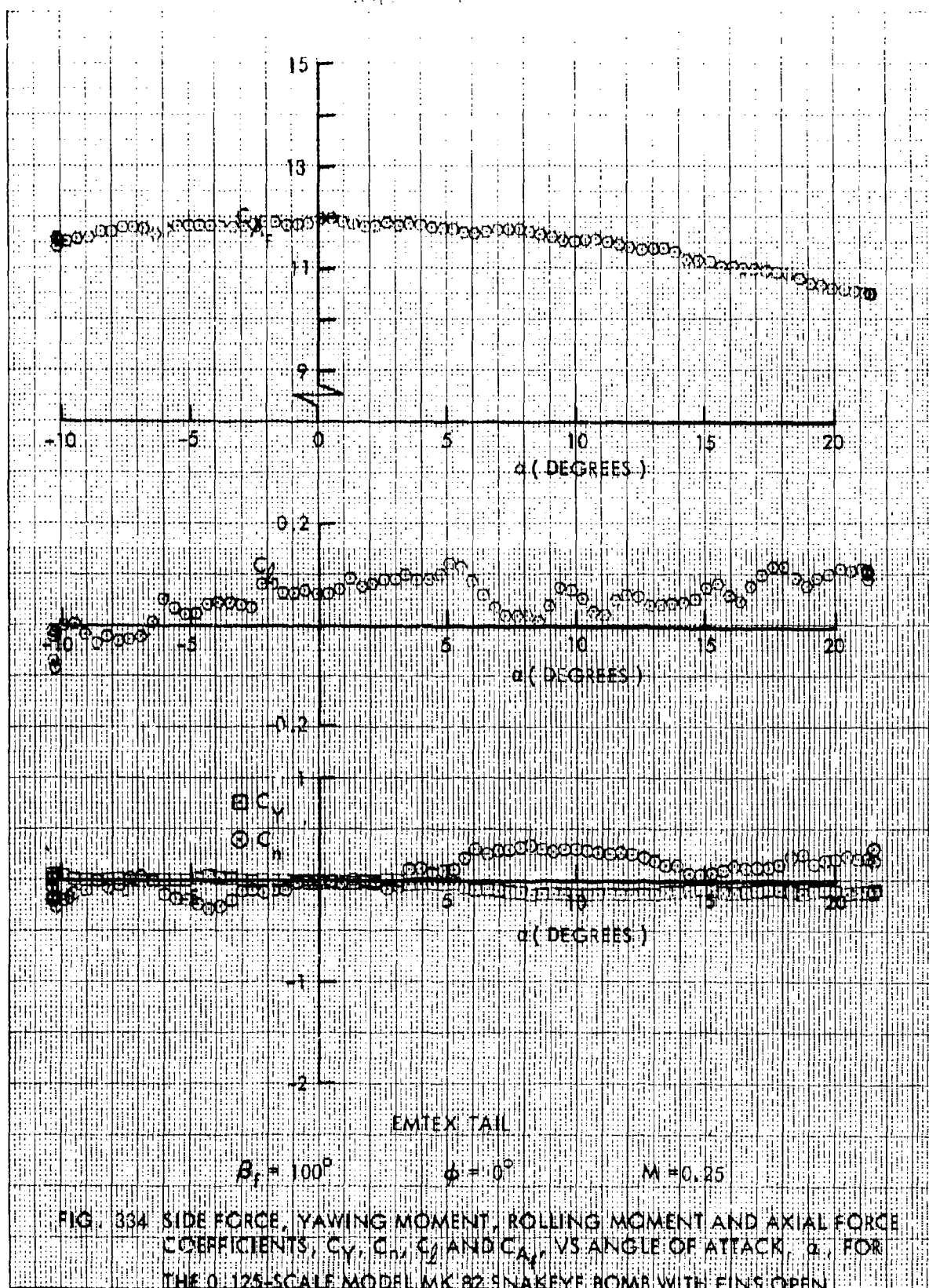
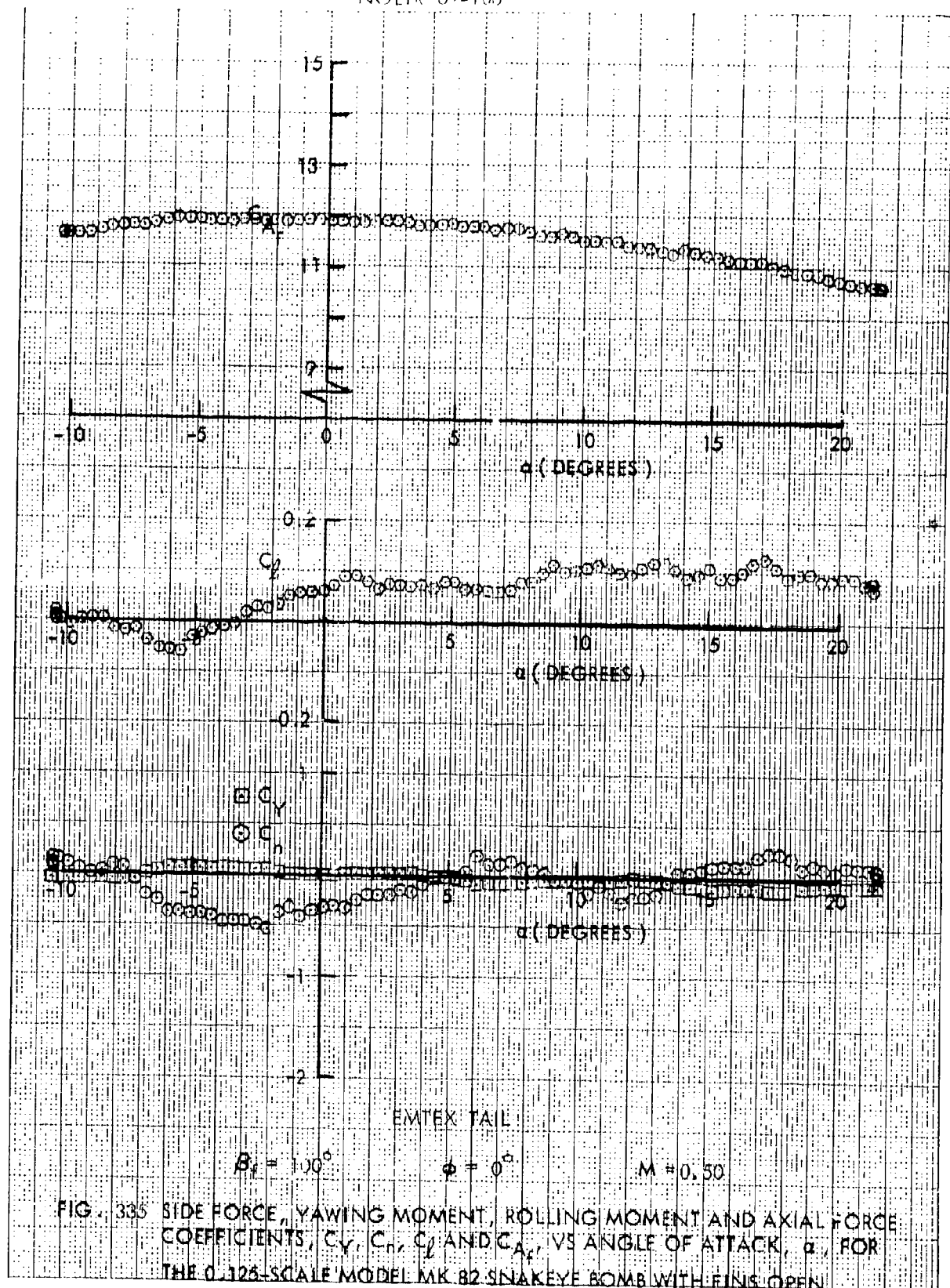


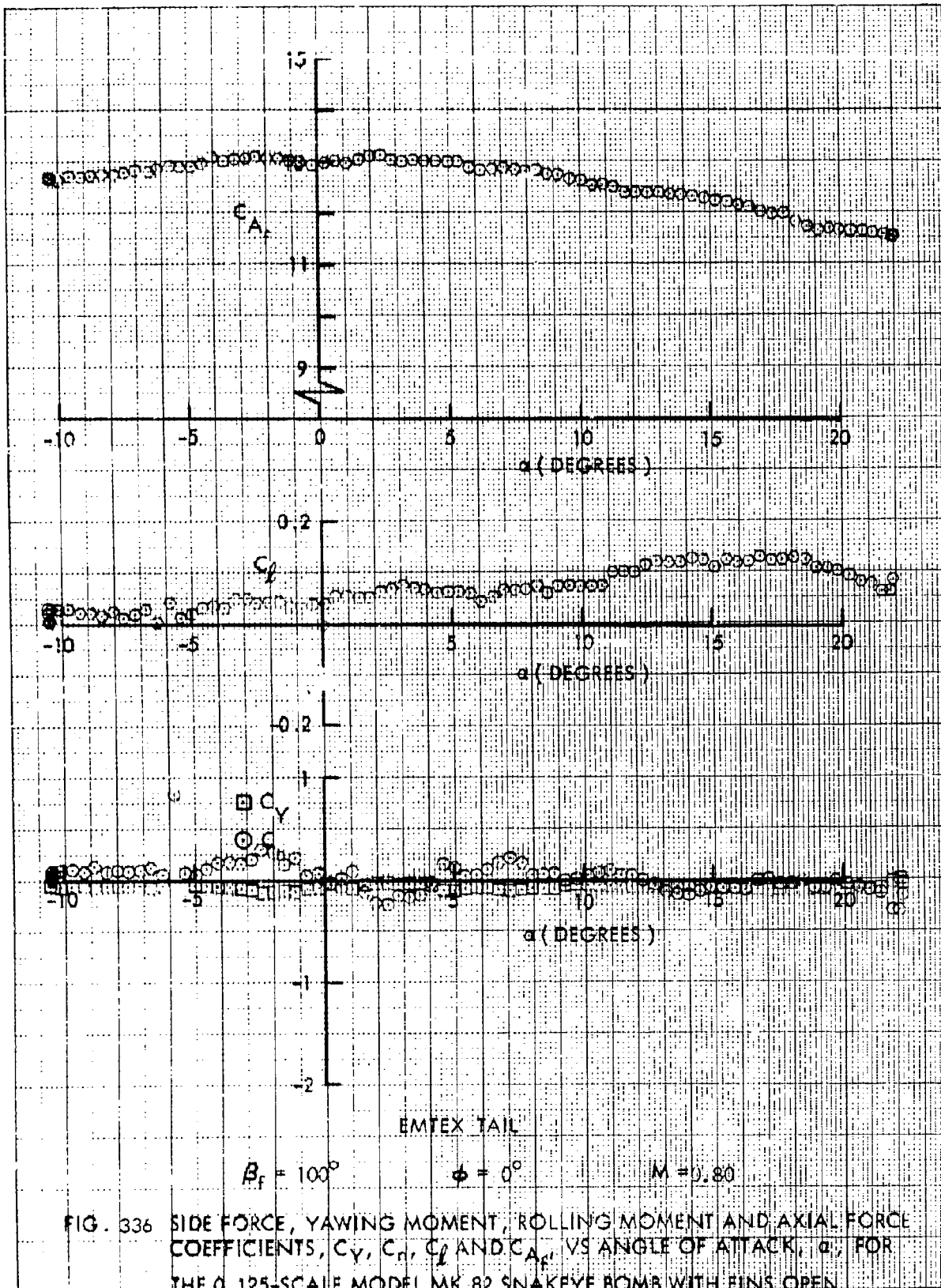
FIG. 332 SIDE FORCE, YAWING MOMENT, ROLLING MOMENT AND AXIAL FORCE COEFFICIENTS,  $C_y$ ,  $C_n$ ,  $C_l$  AND  $C_A$ , VS ANGLE OF ATTACK,  $\alpha$ , FOR THE 0.125-SCALE MODEL MK 82 SNAKEYE BOMB WITH FINS OPEN

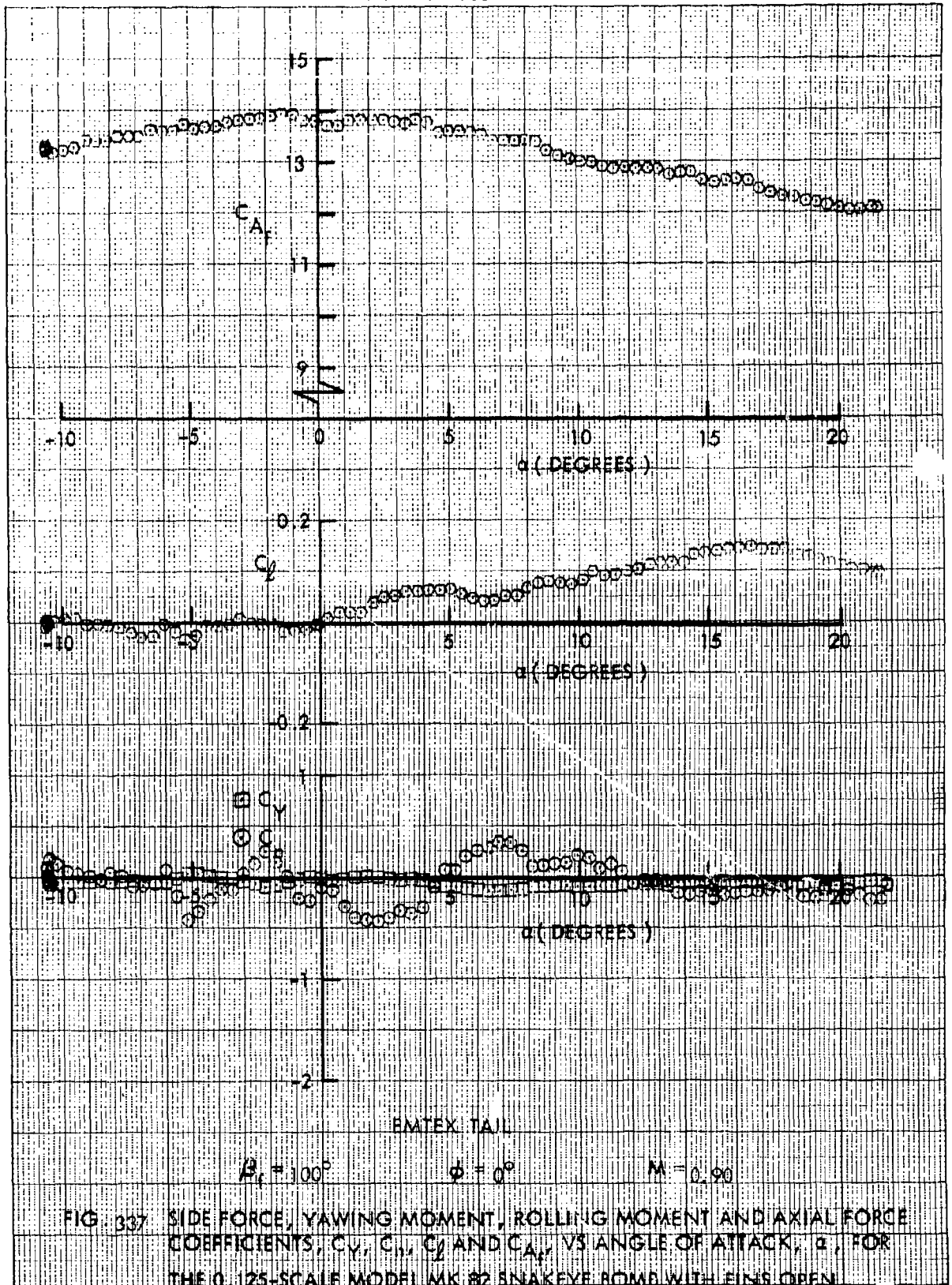


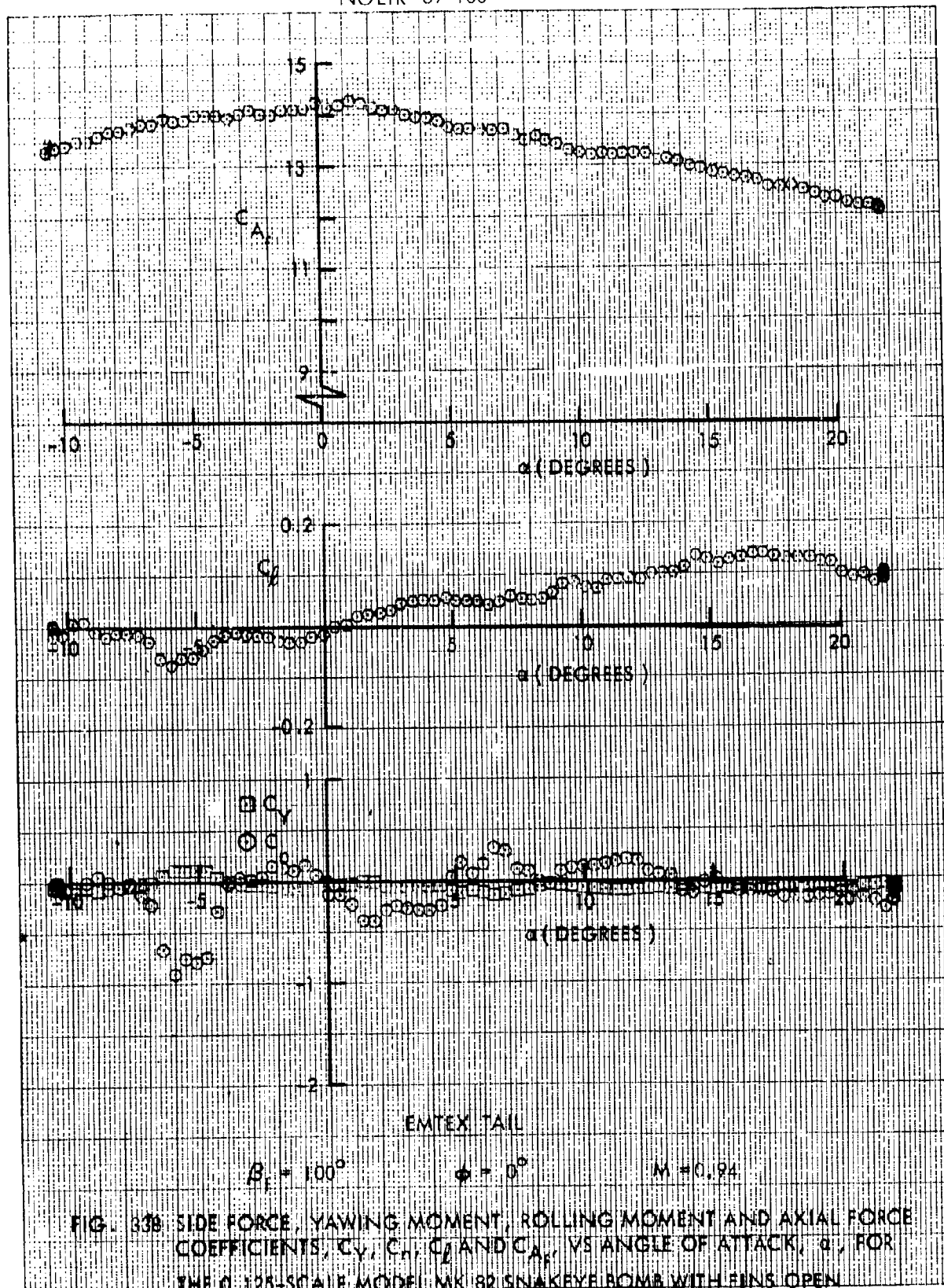


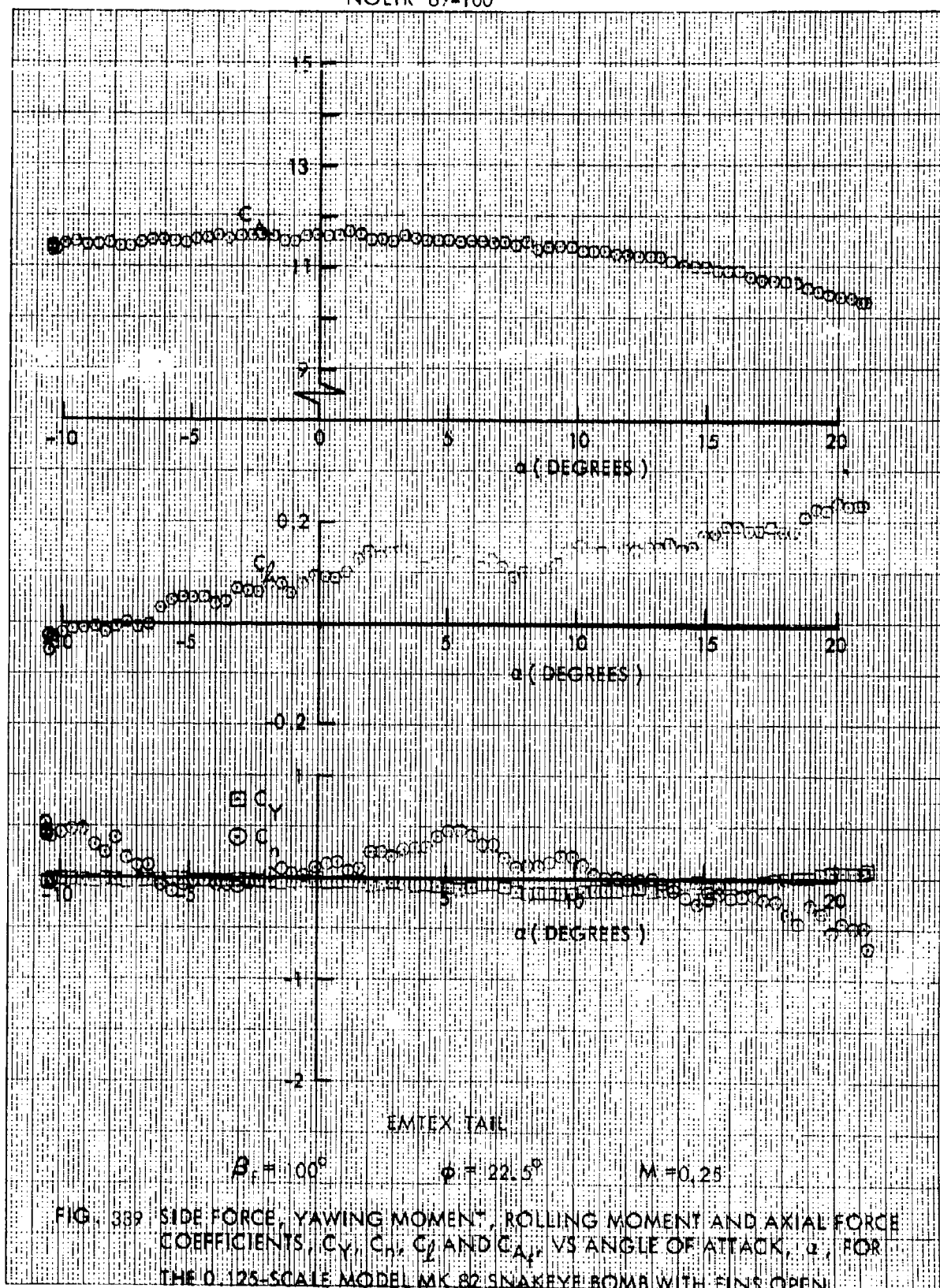




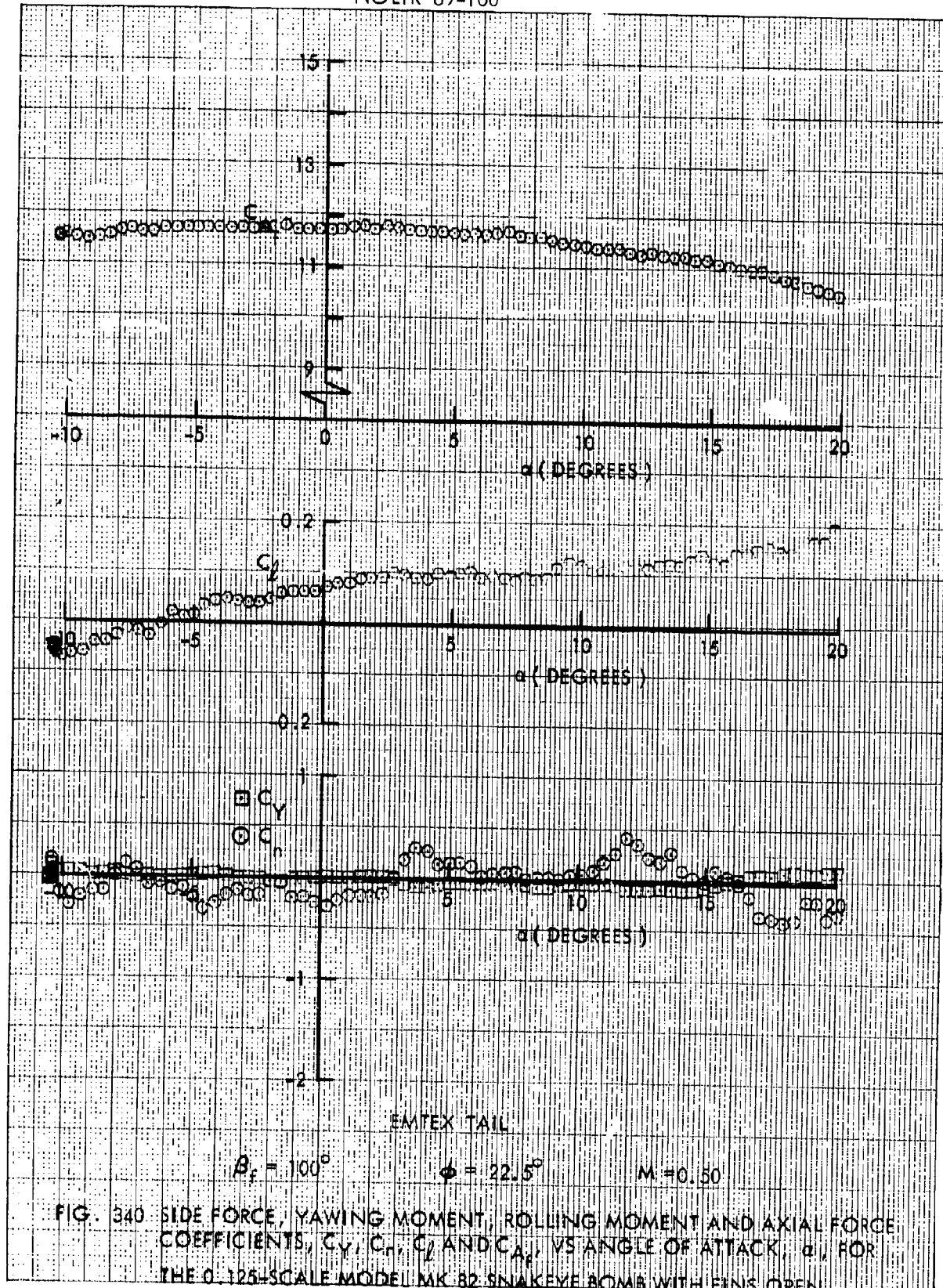


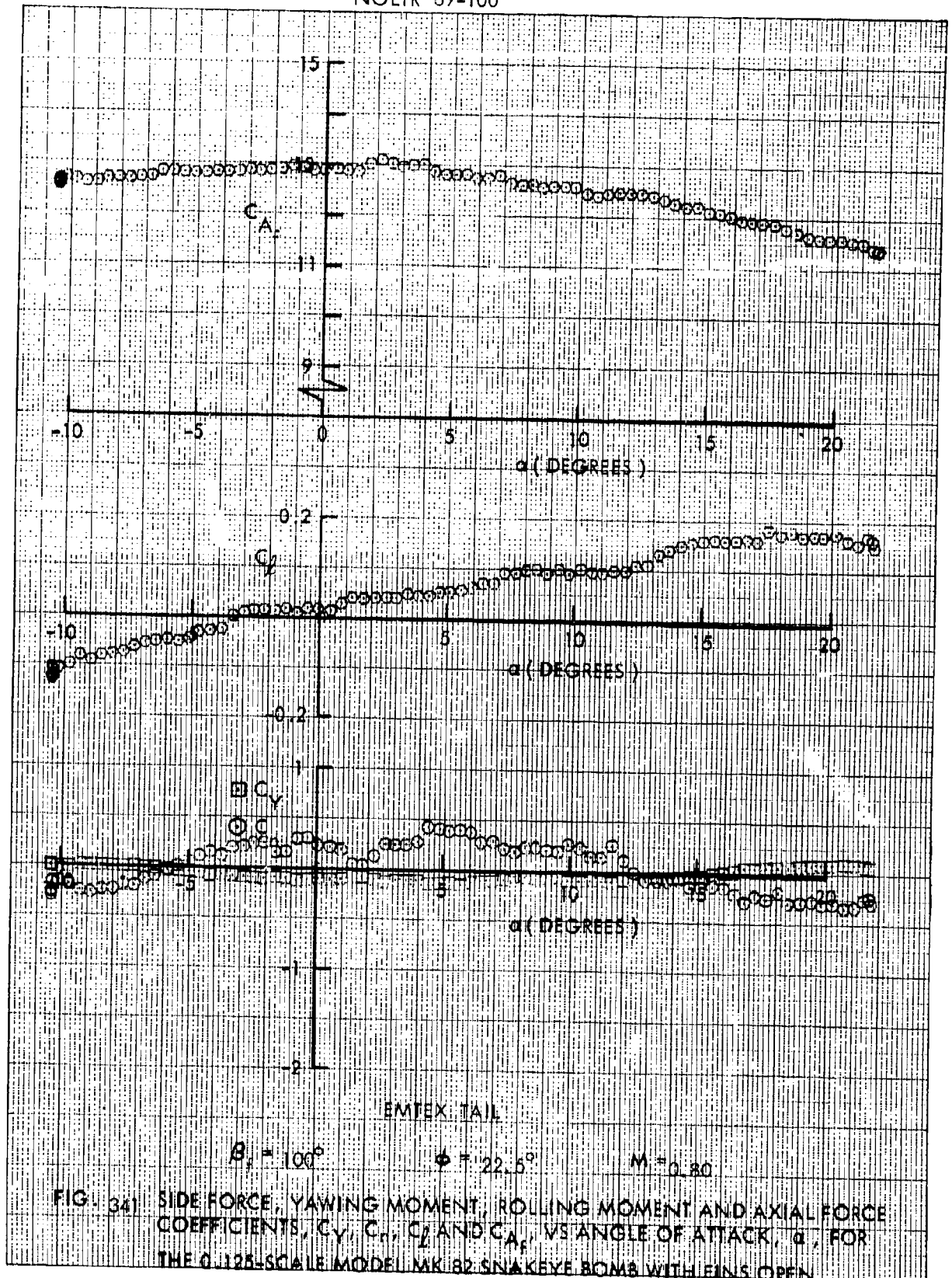


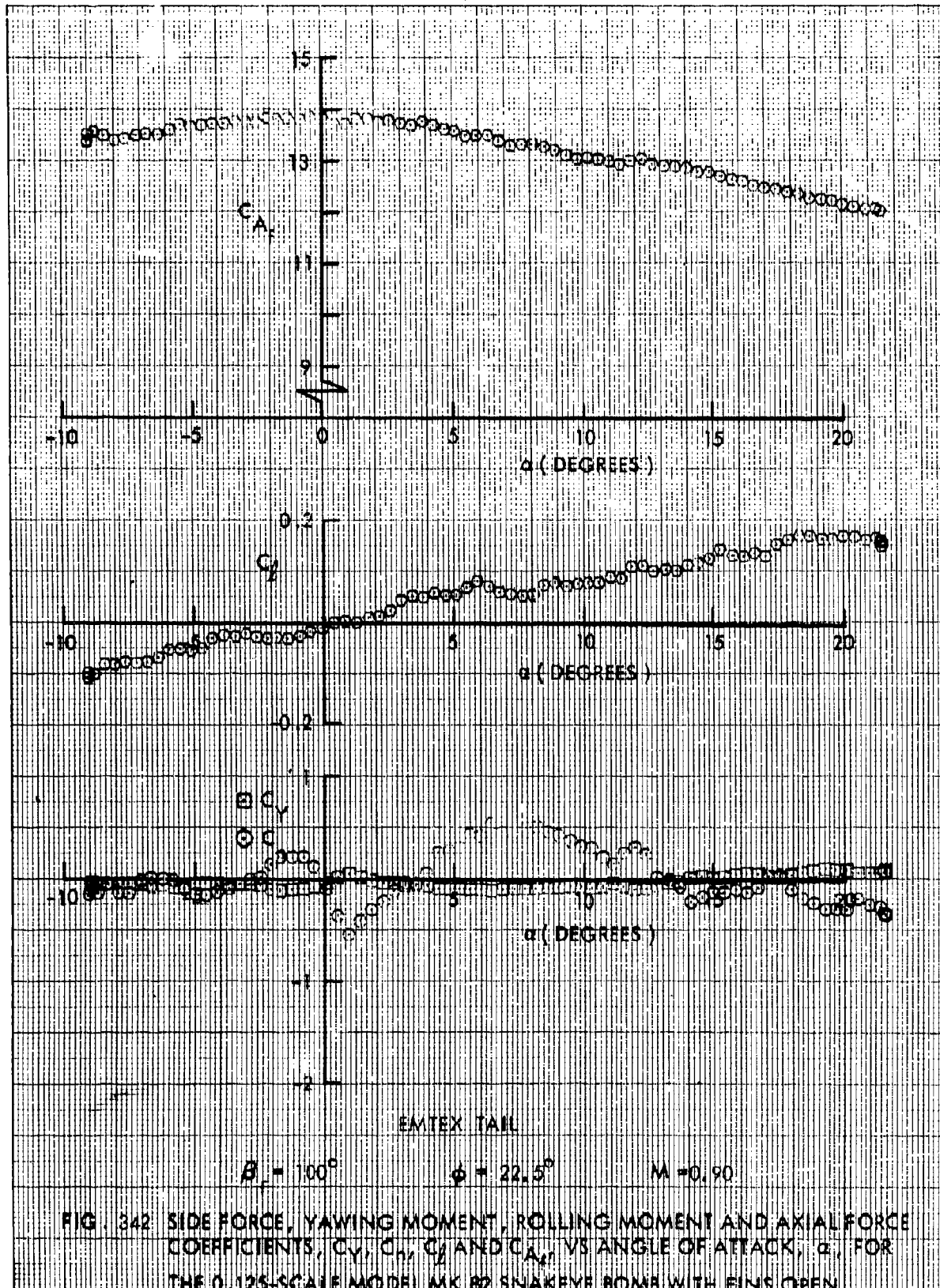


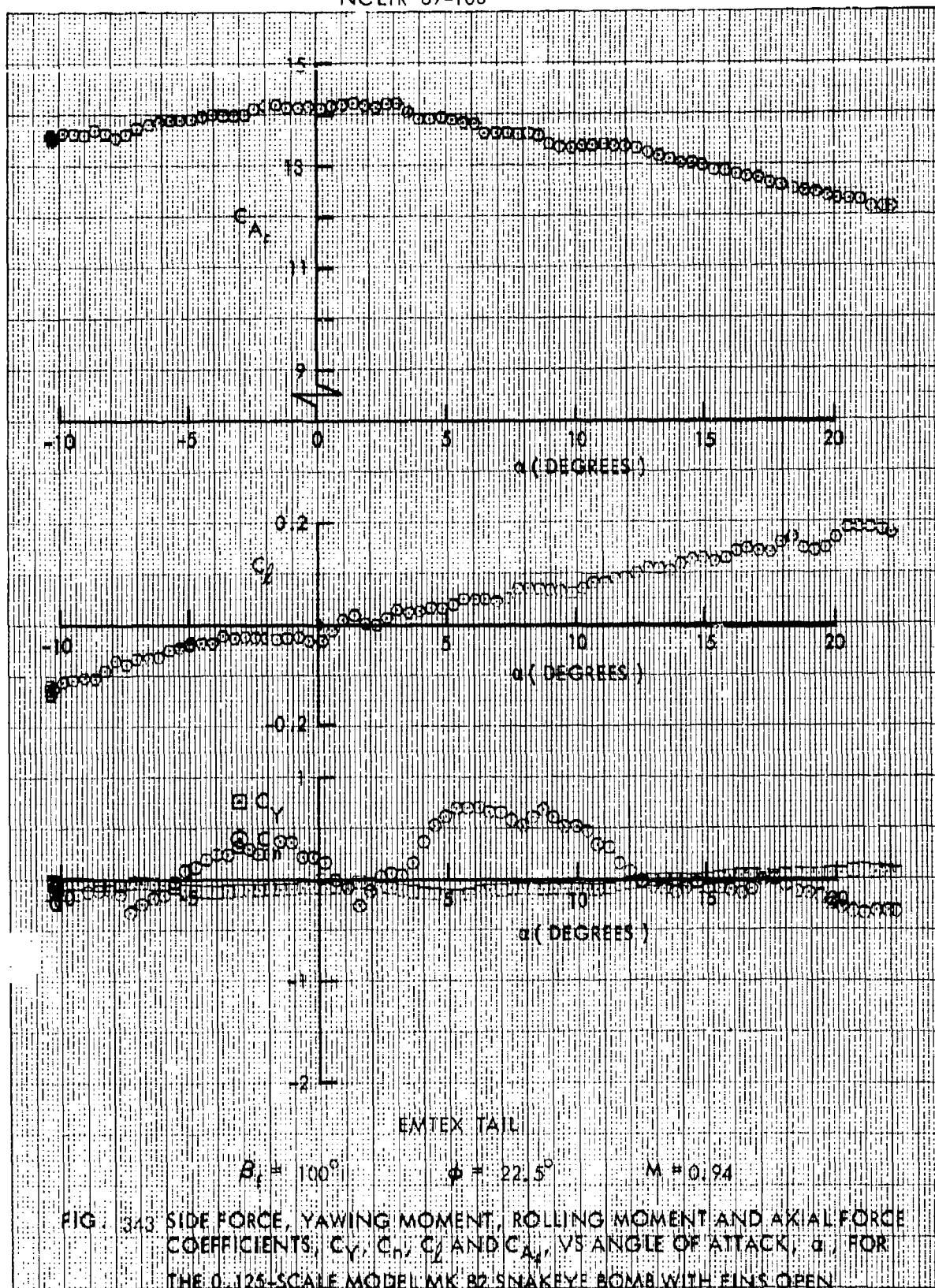


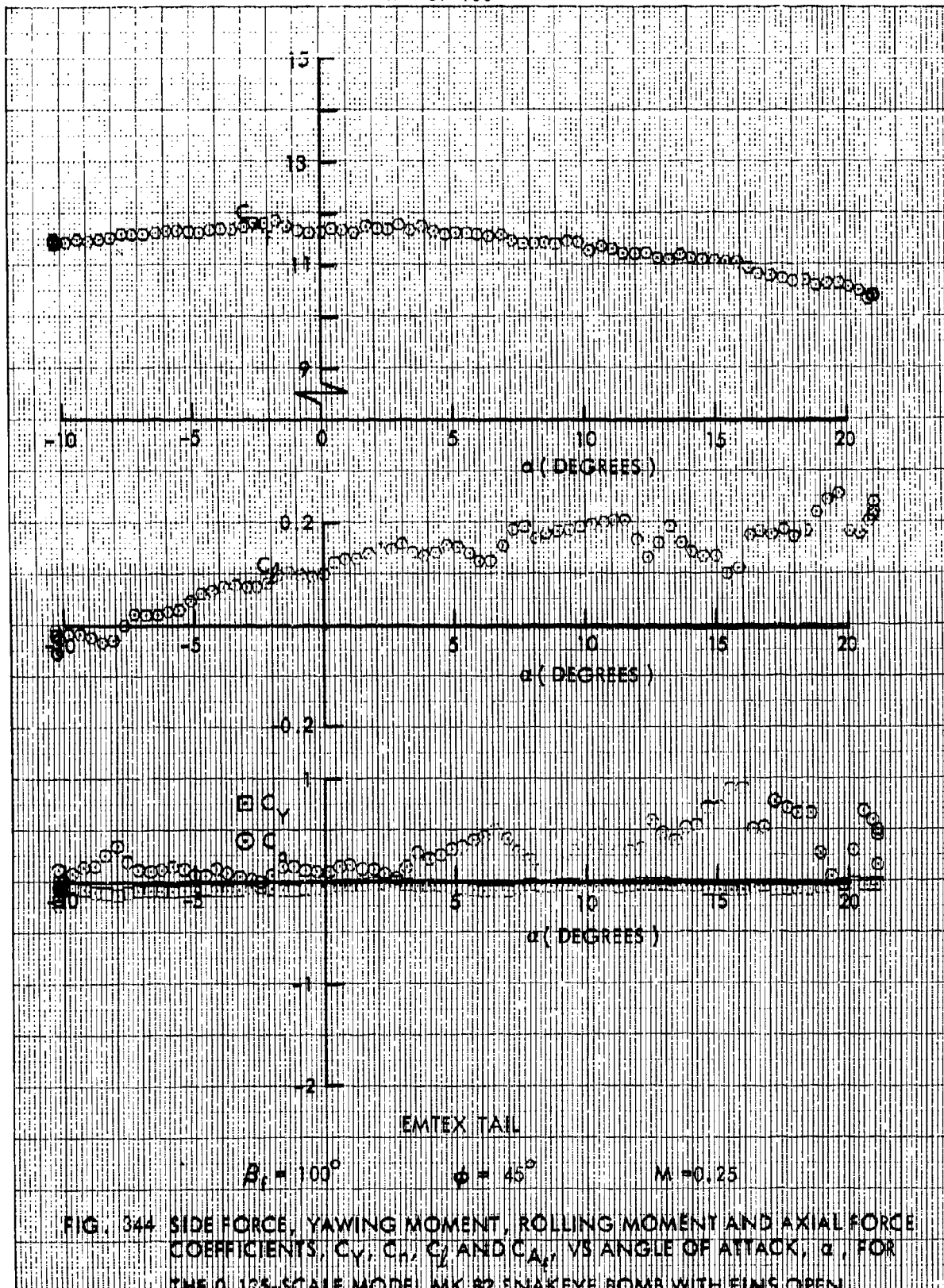




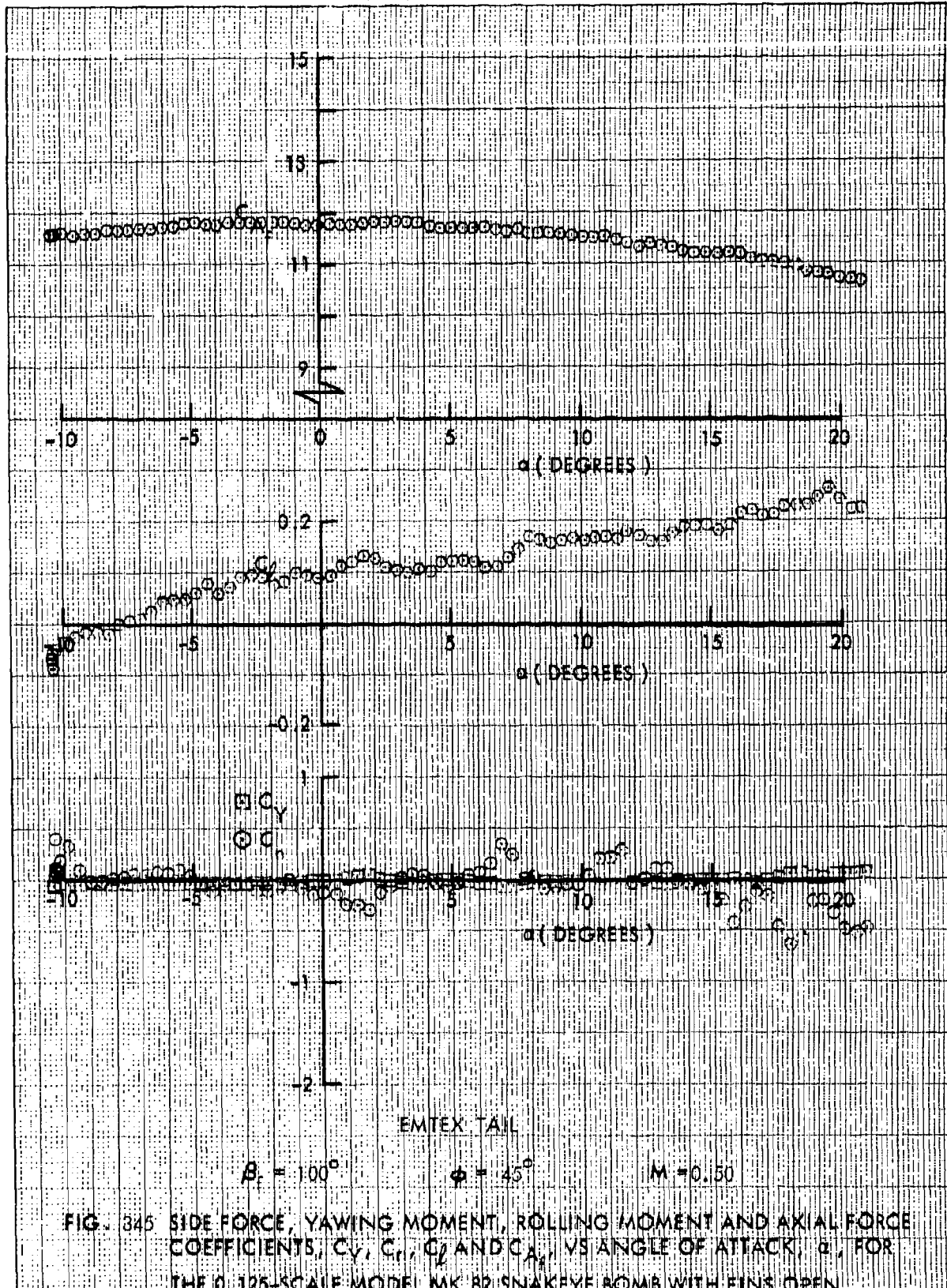




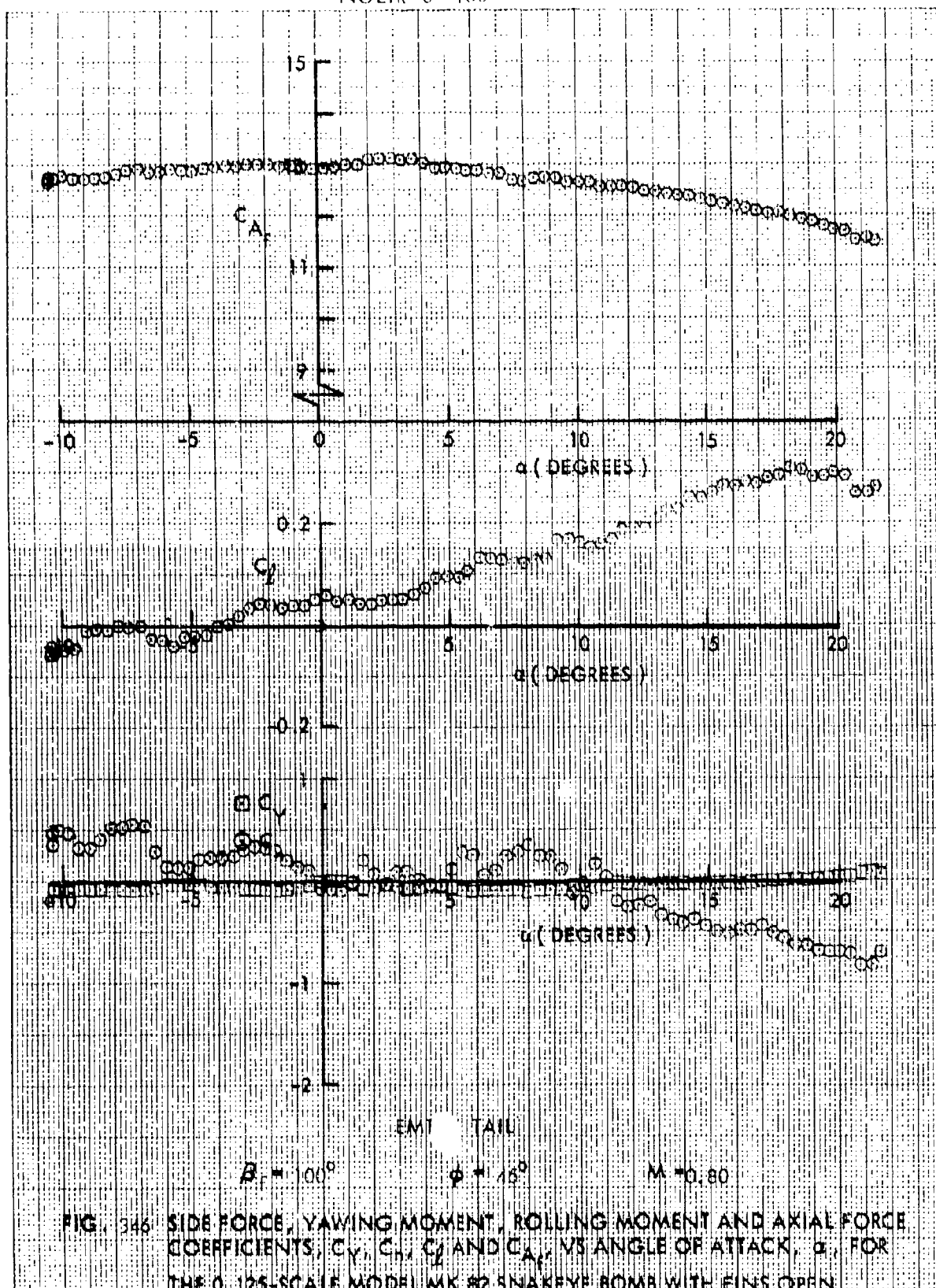


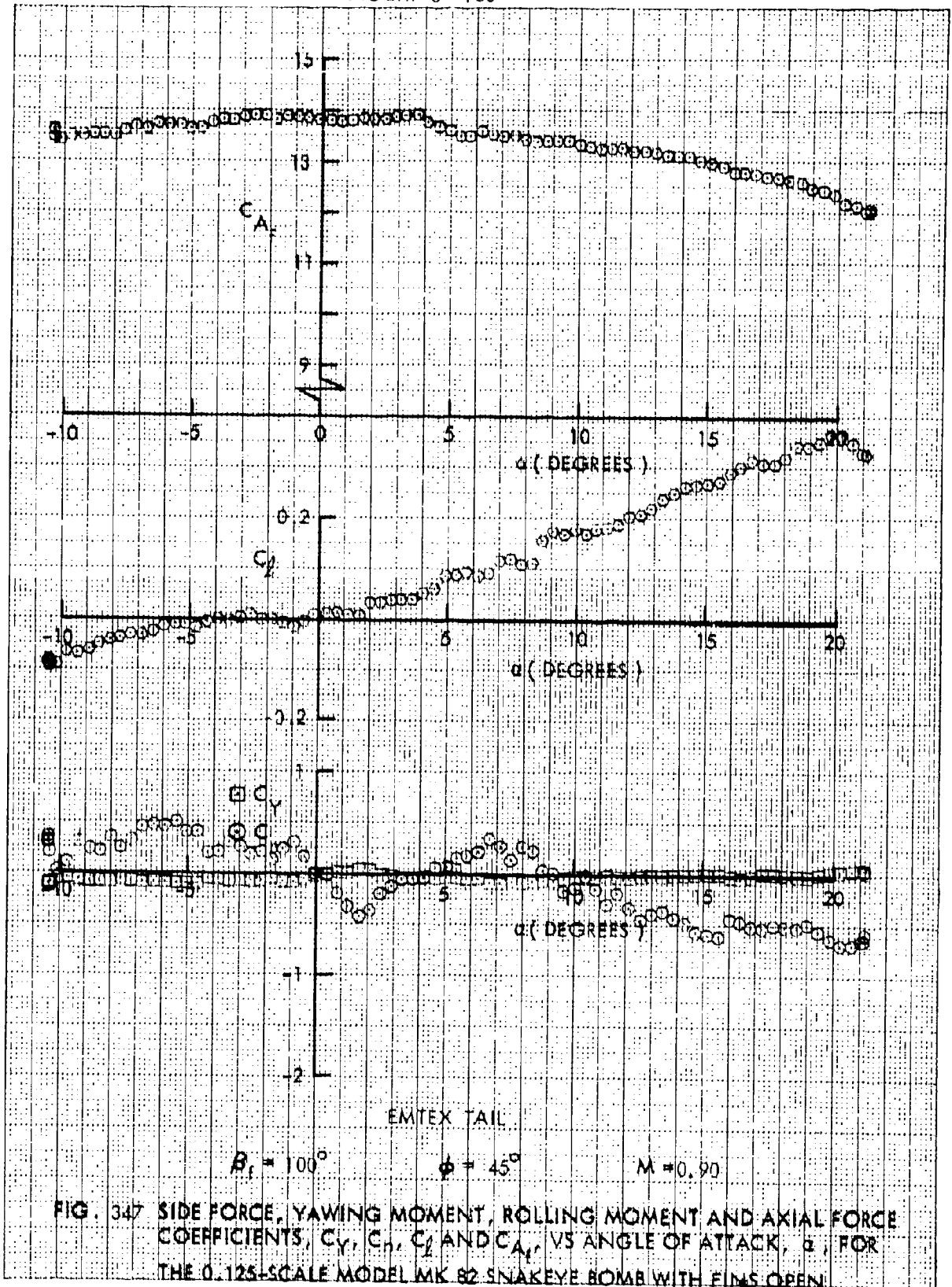


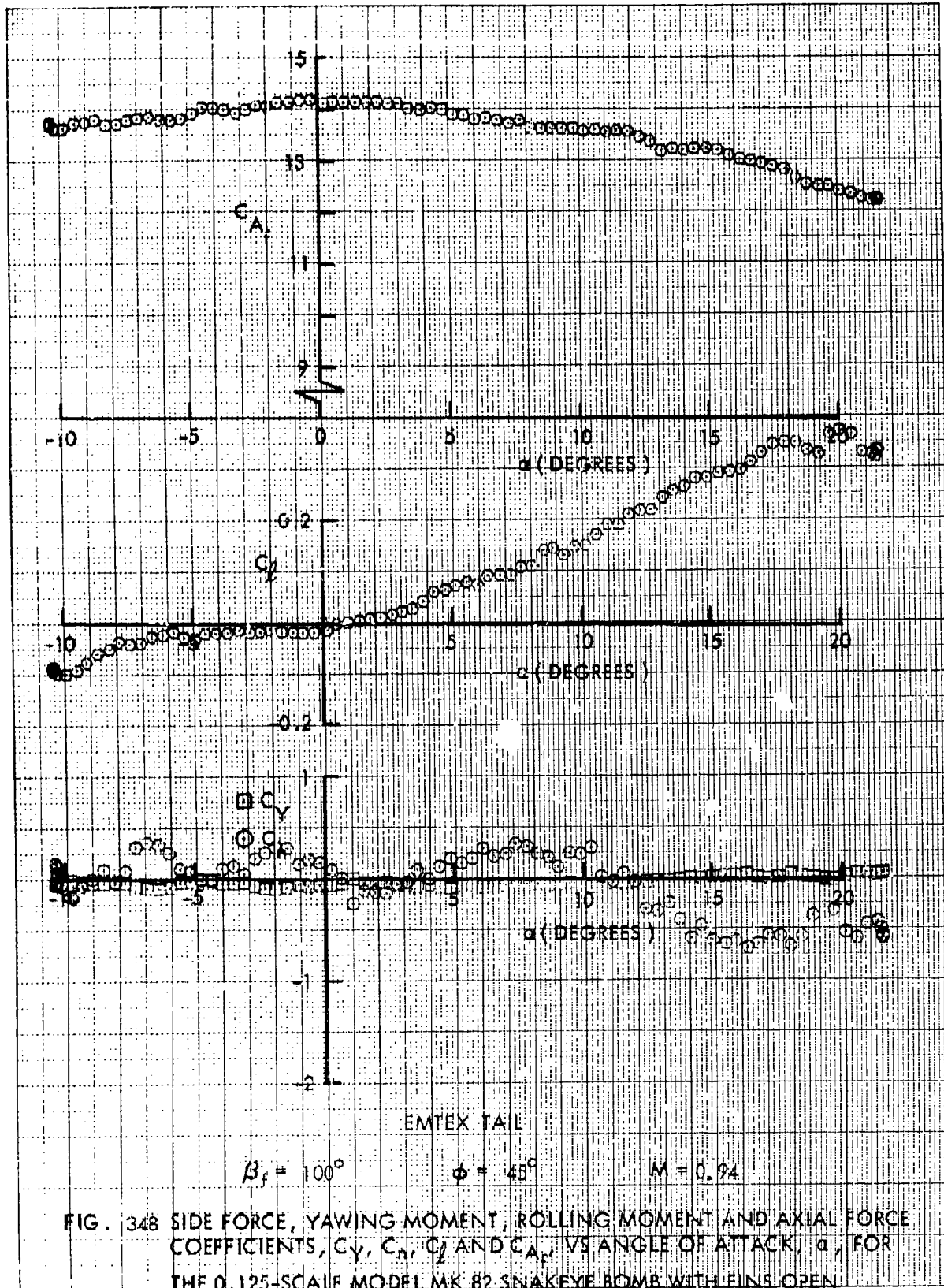


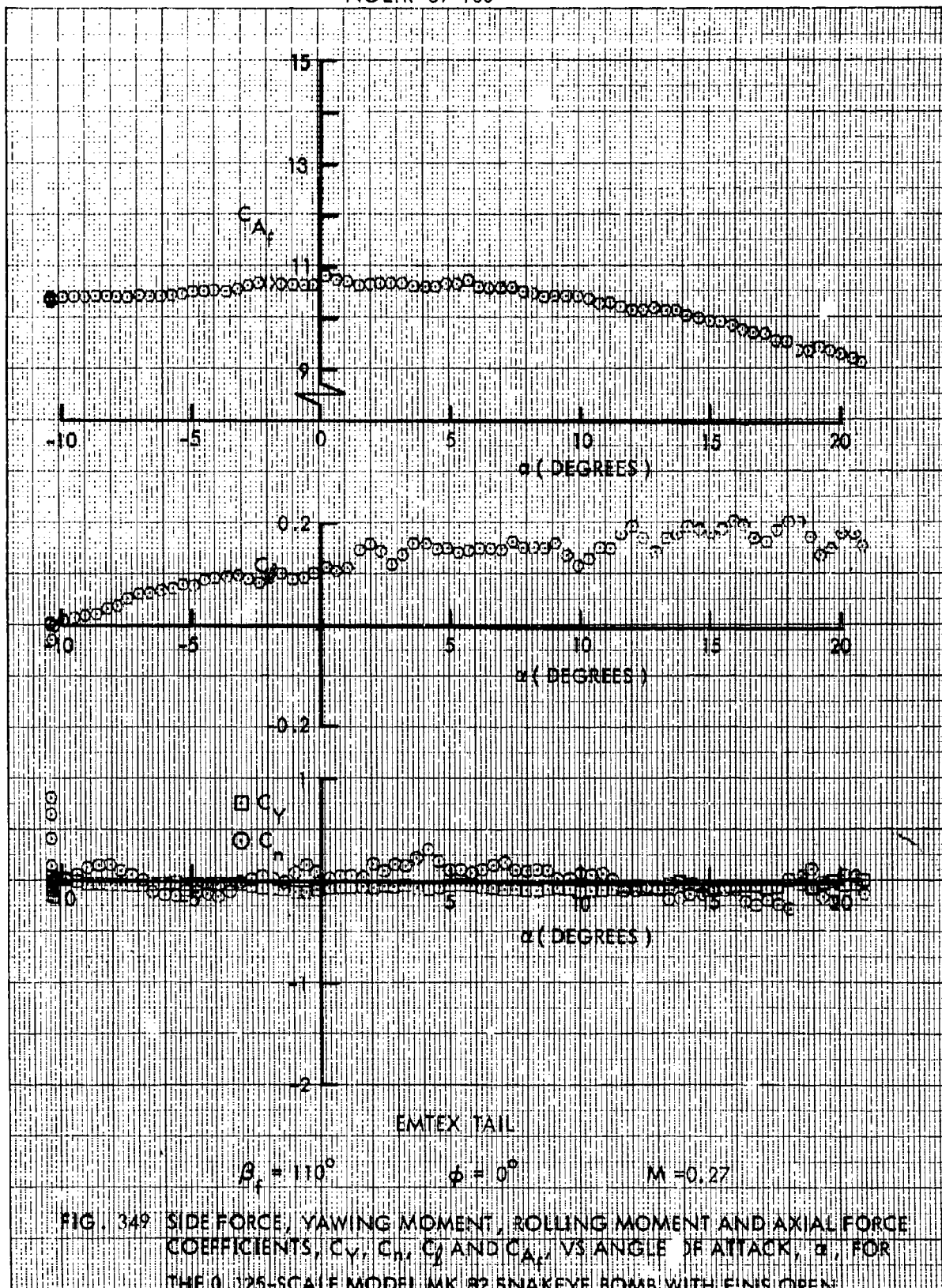












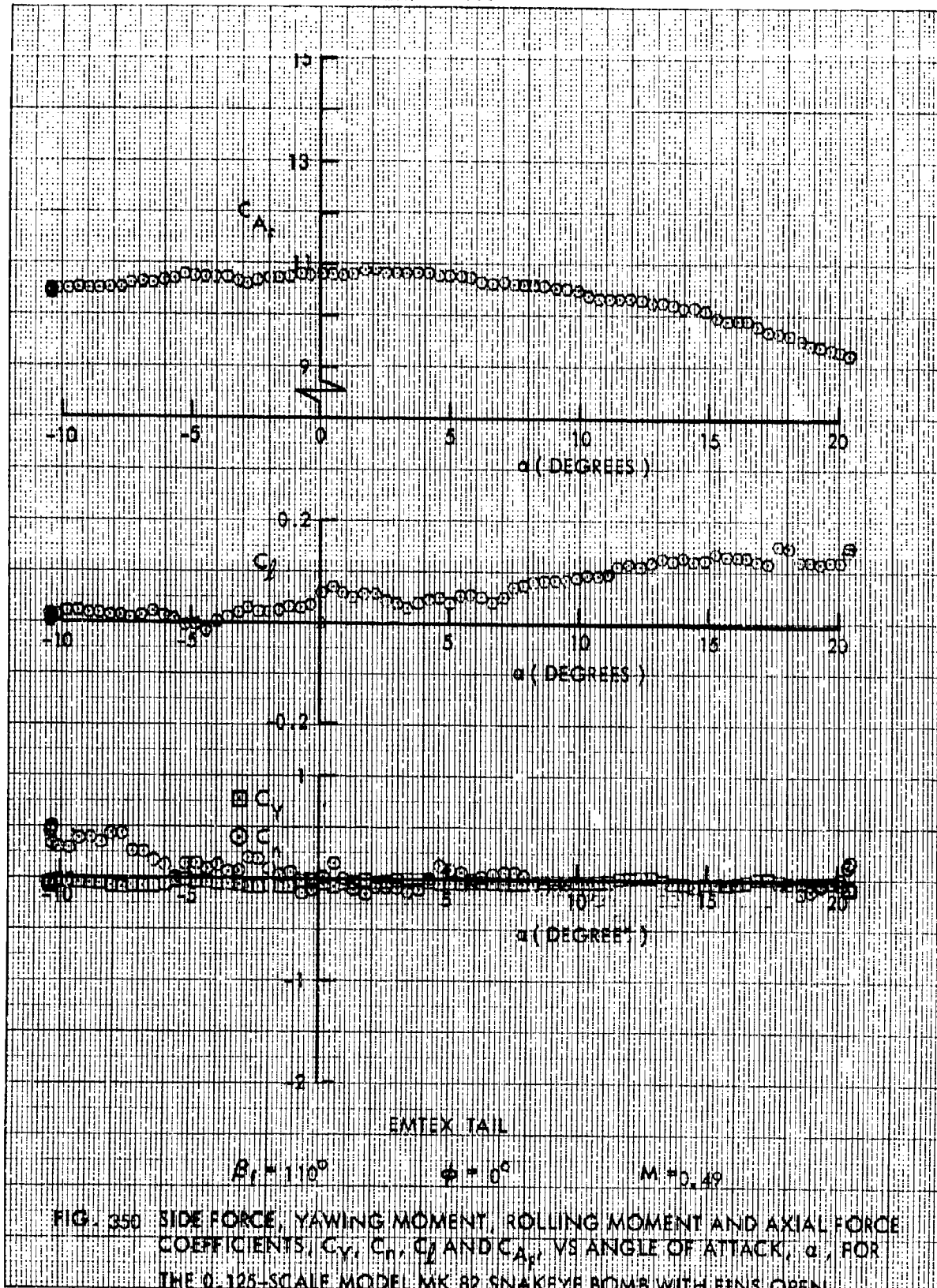
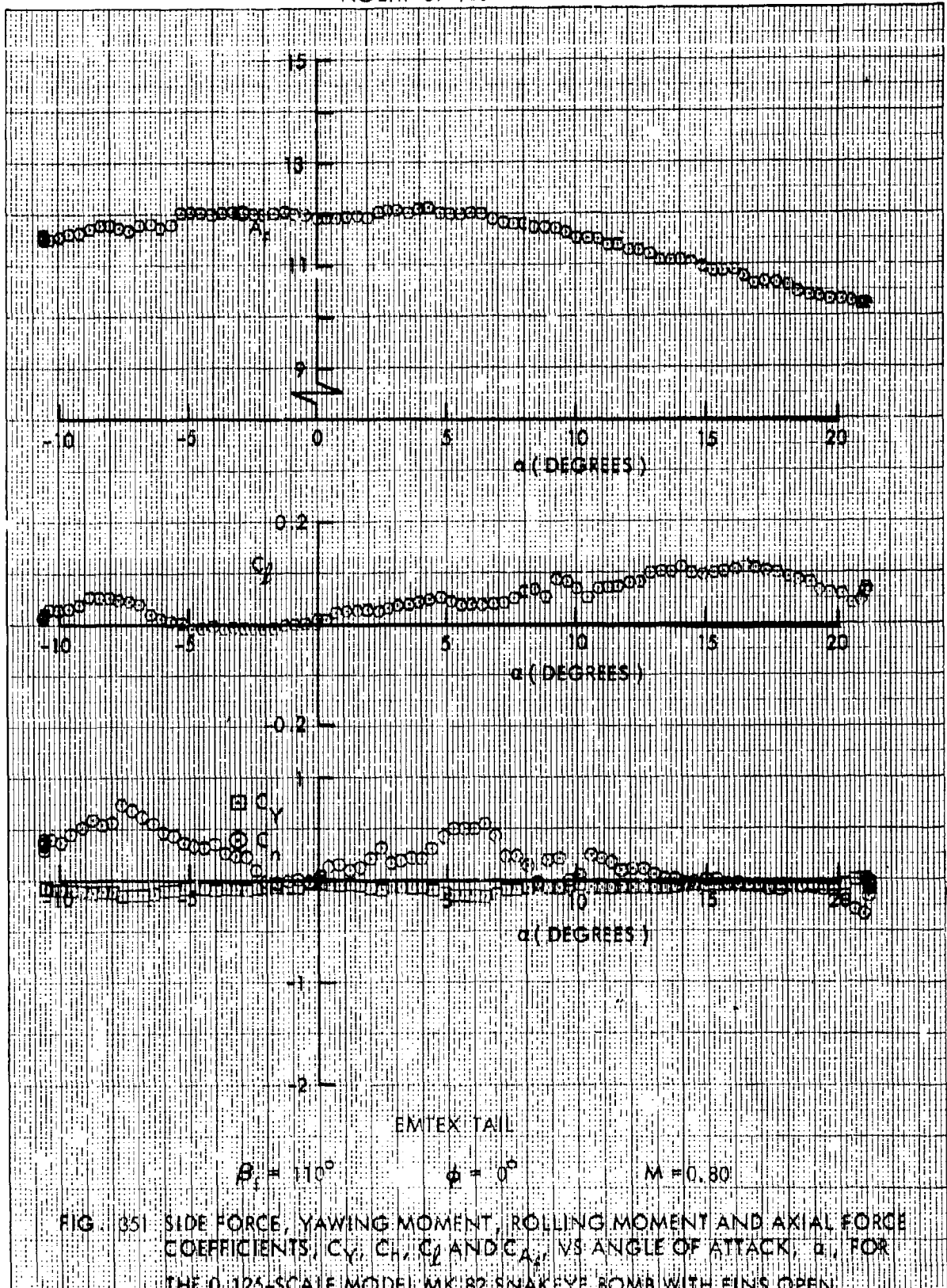
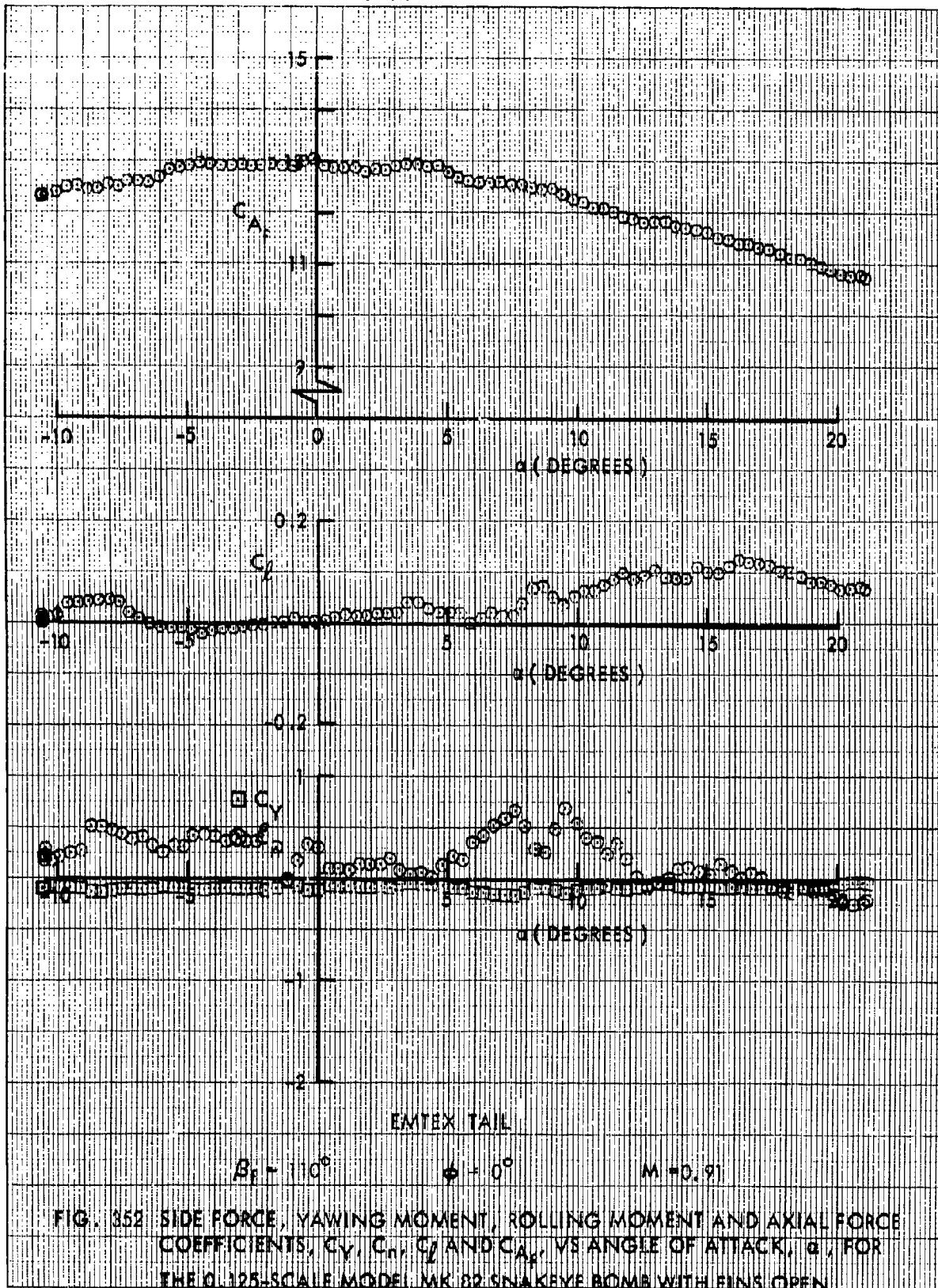


FIG. 350 SIDE FORCE, YAWING MOMENT, ROLLING MOMENT AND AXIAL FORCE COEFFICIENTS,  $C_Y$ ,  $C_L$  AND  $C_{A_r}$ , VS ANGLE OF ATTACK,  $\alpha$ , FOR THE 0.125-SCALE MODEL MK-82 SNAKEYE BOMB WITH FINS OPEN







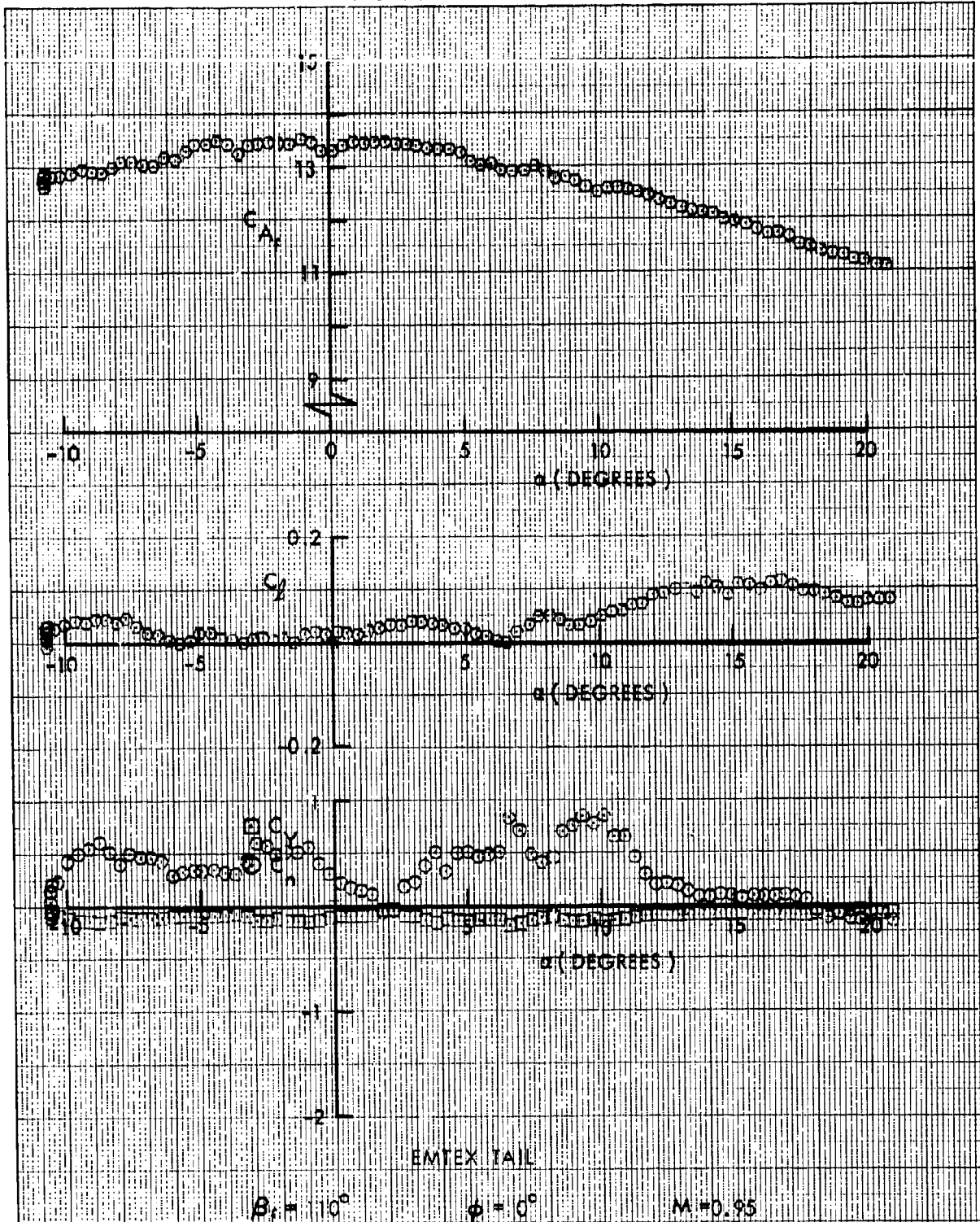
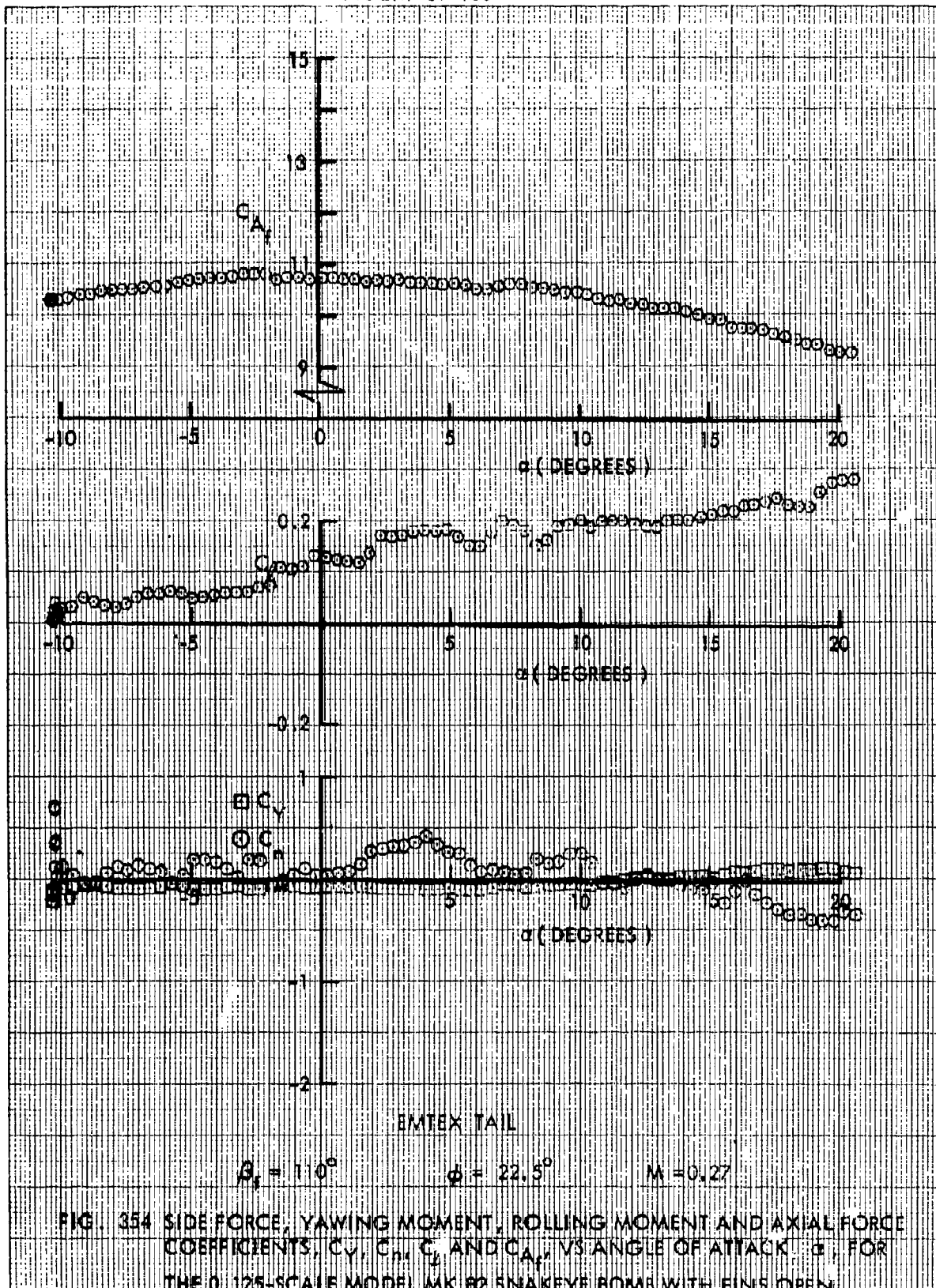
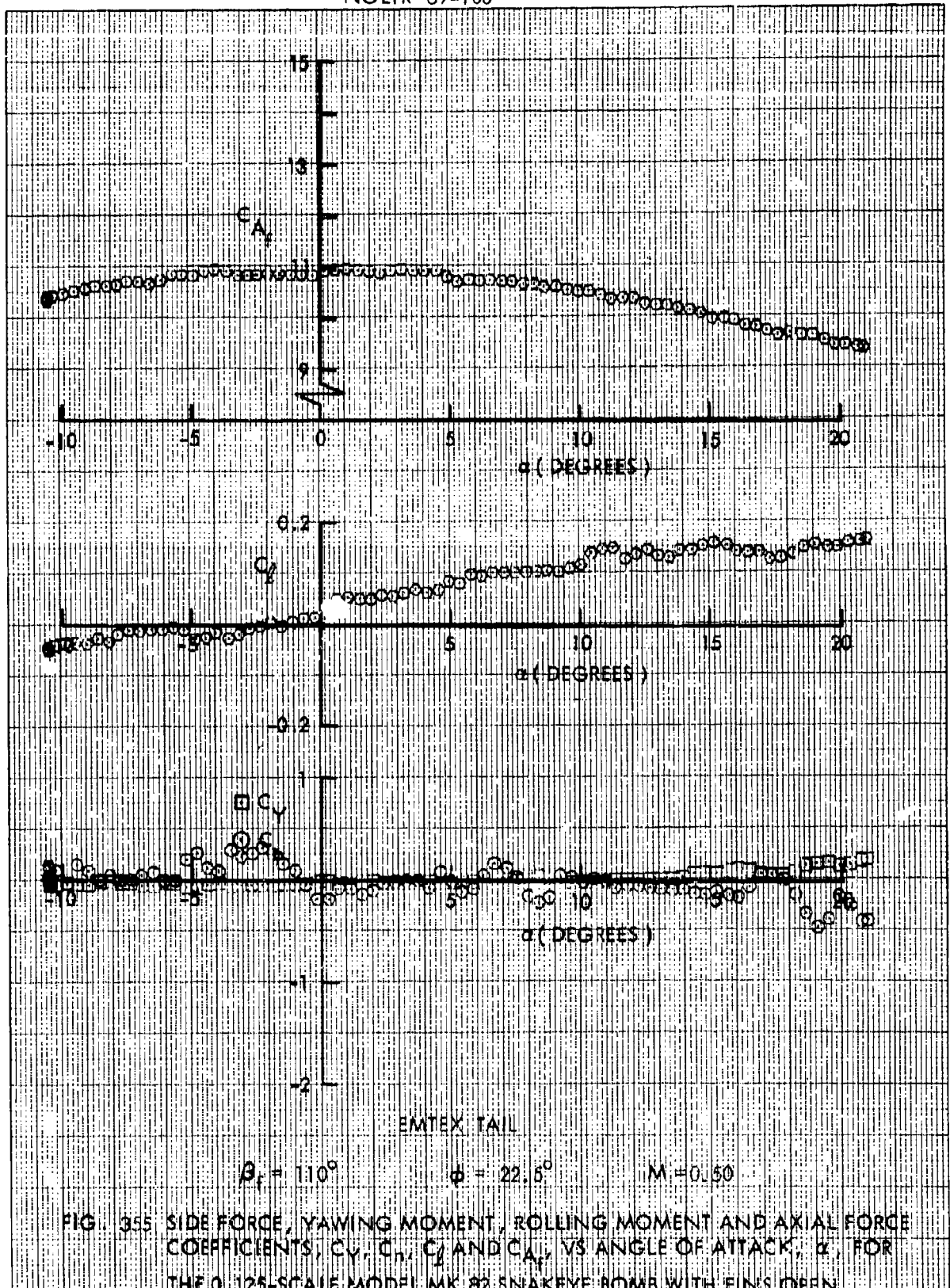
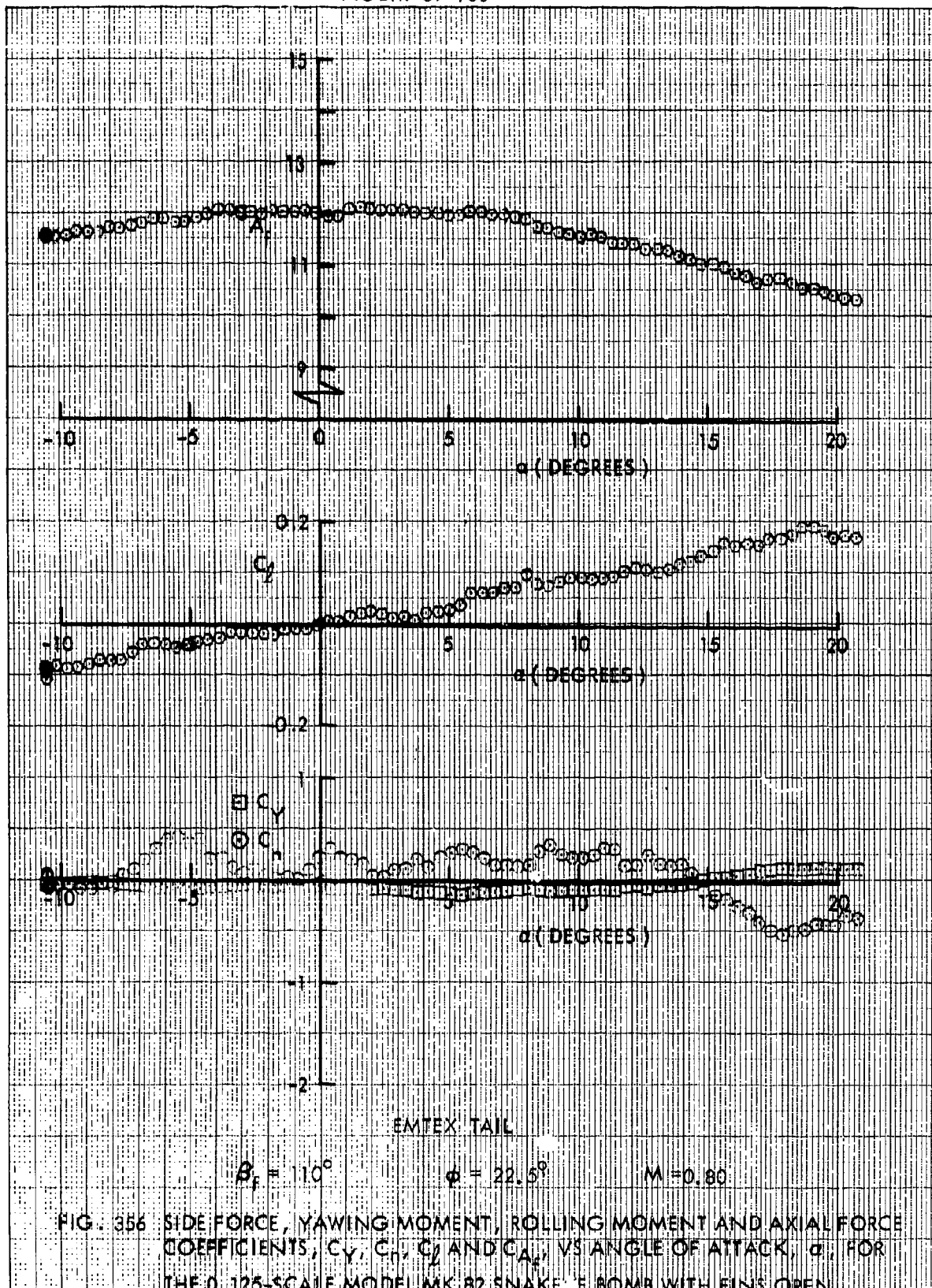


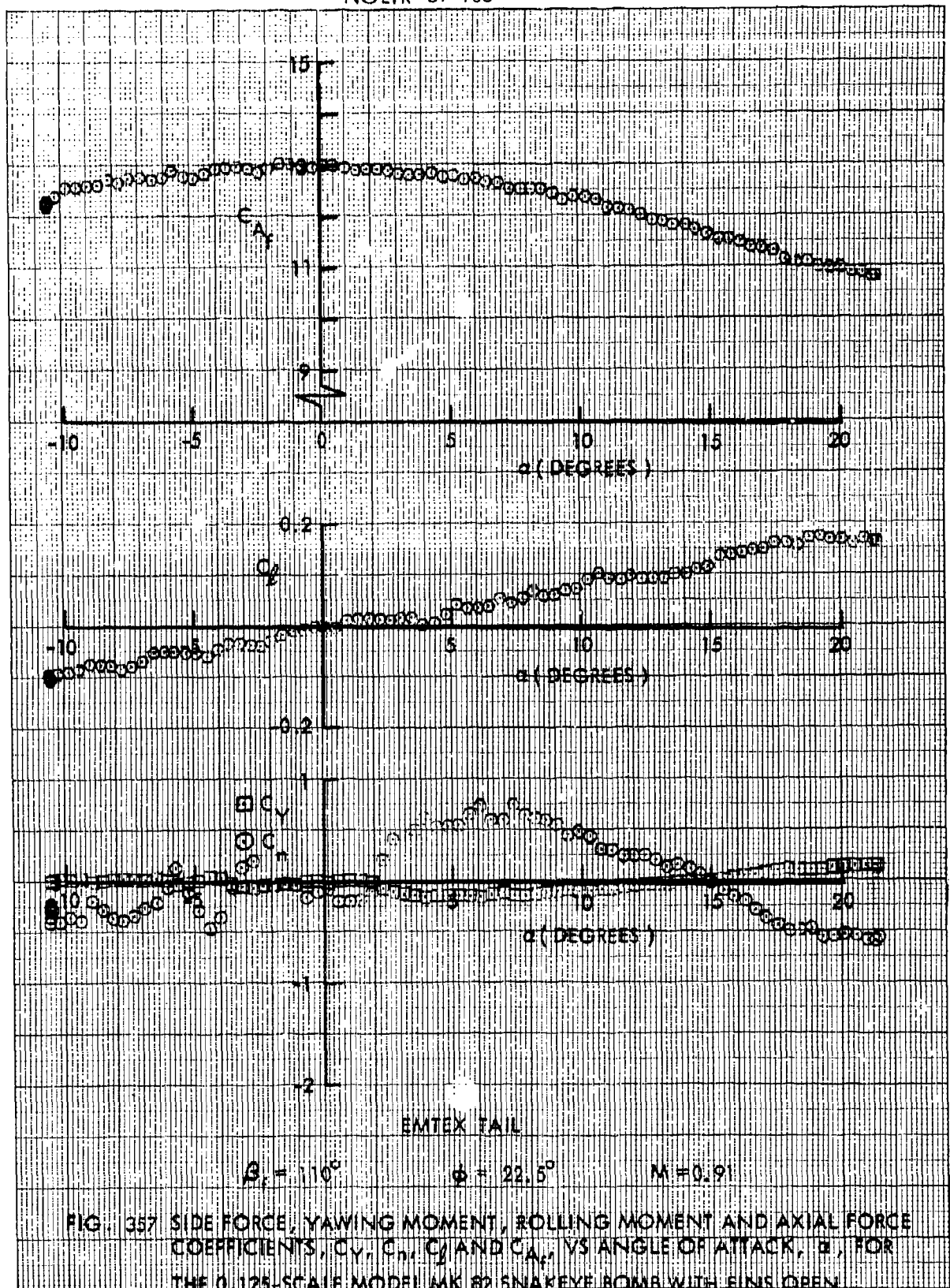
FIG. 353: SIDE FORCE, YAWING MOMENT, ROLLING MOMENT AND AXIAL FORCE COEFFICIENTS,  $C_Y$ ,  $C_n$ ,  $C_l$  AND  $C_A$ , VS ANGLE OF ATTACK,  $\alpha$ , FOR THE 0.125-SCALE MODEL MK B2 SNAKEEYE BOMB WITH FINS OPEN



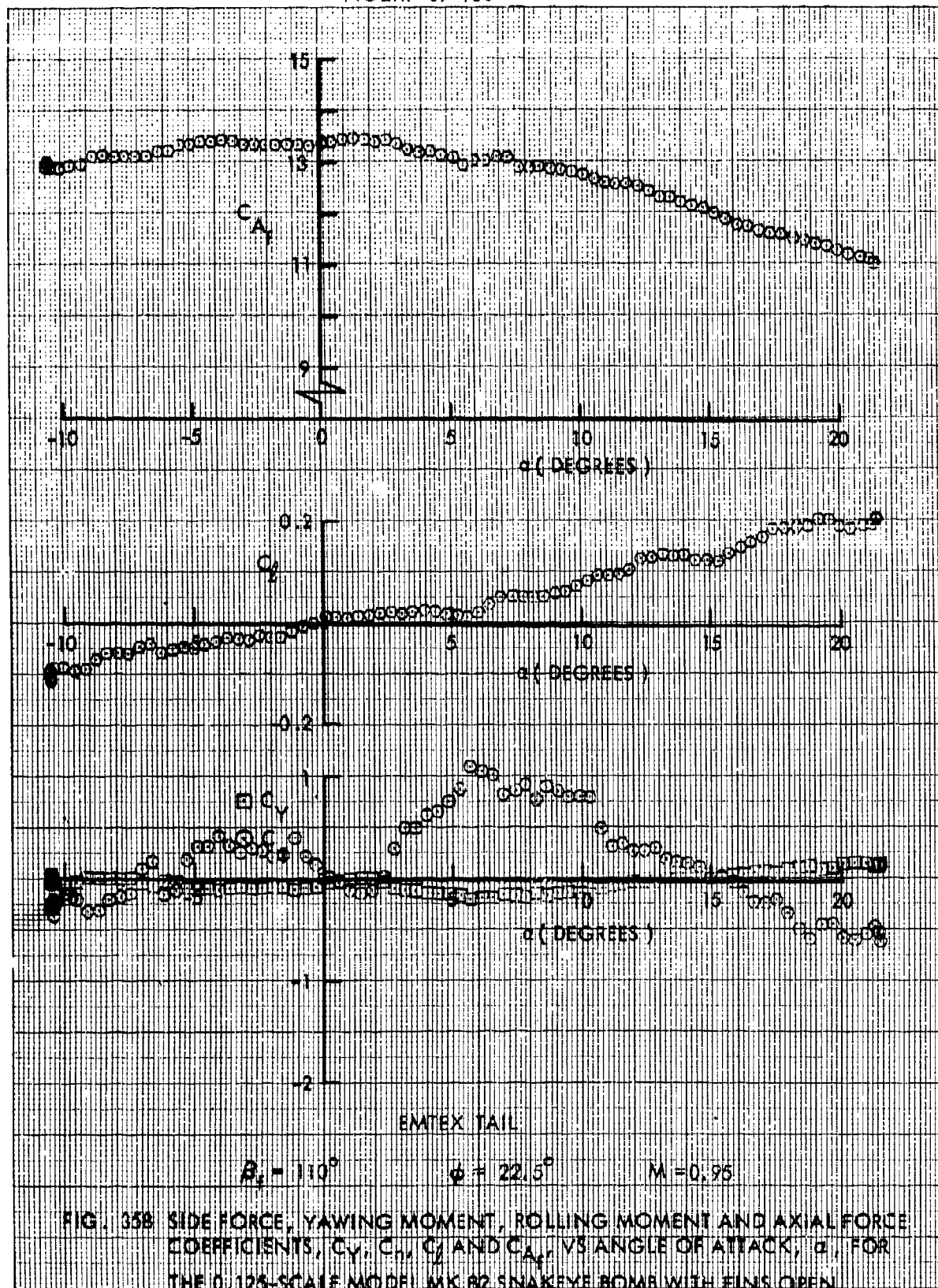


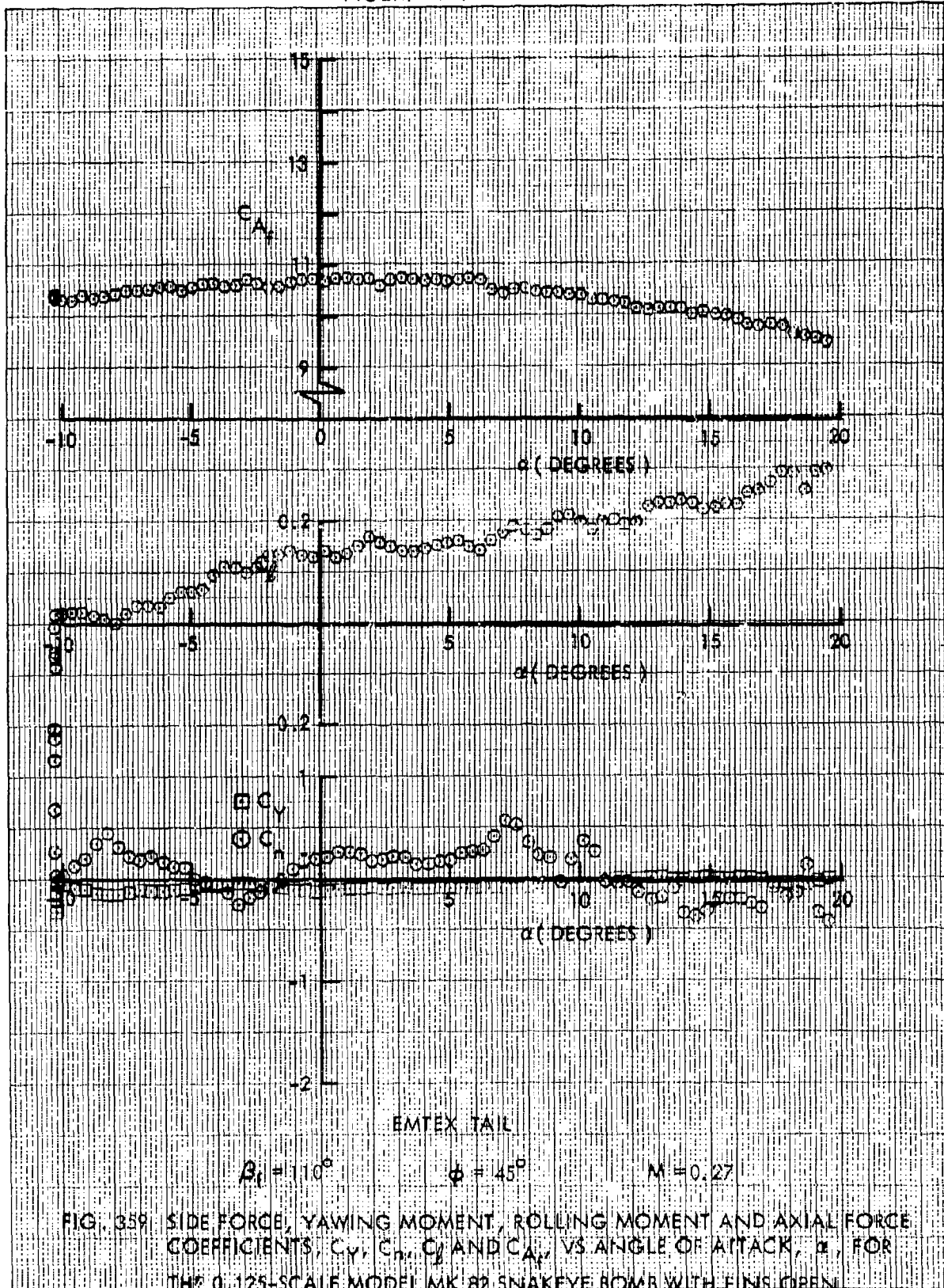


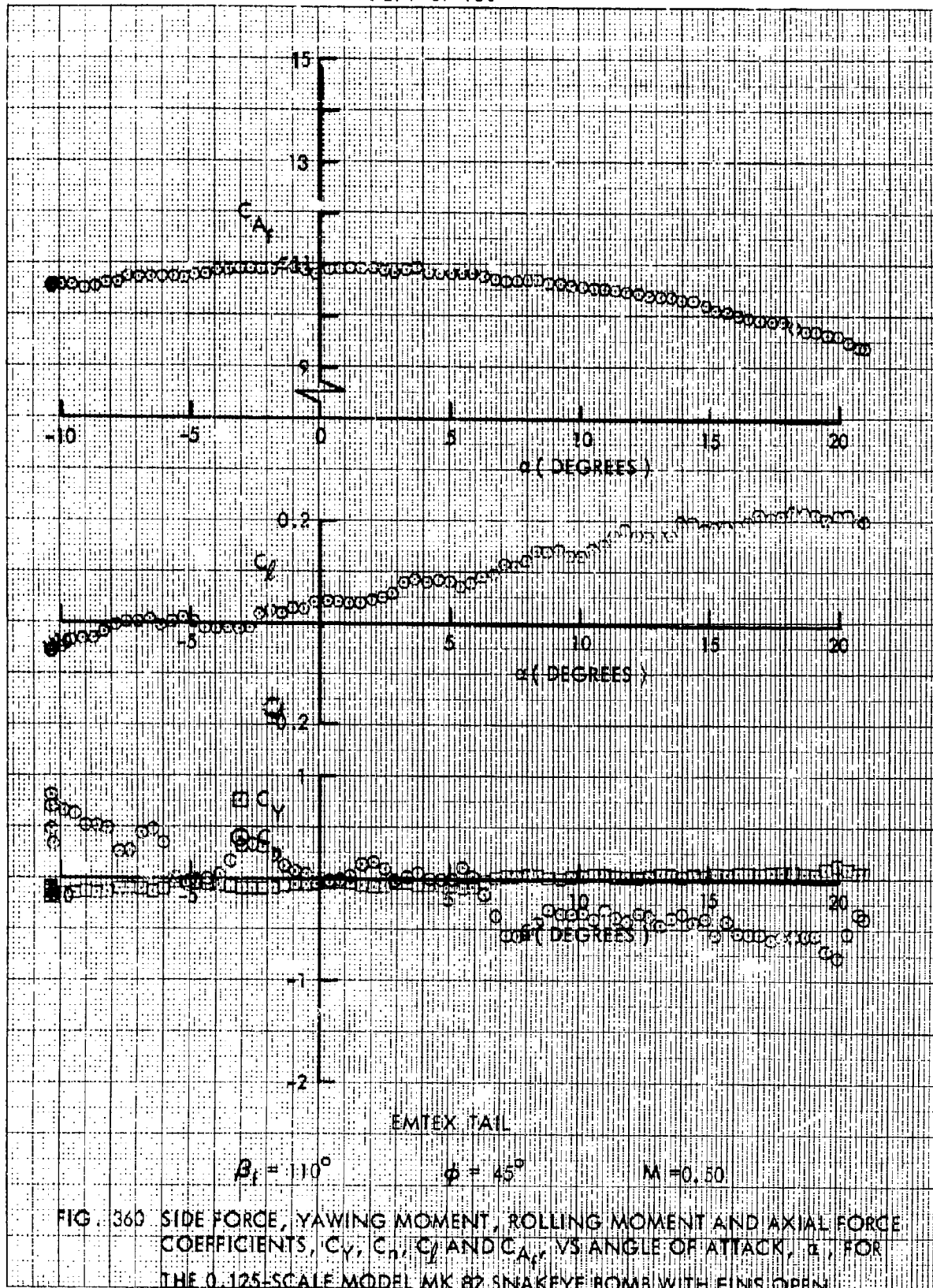


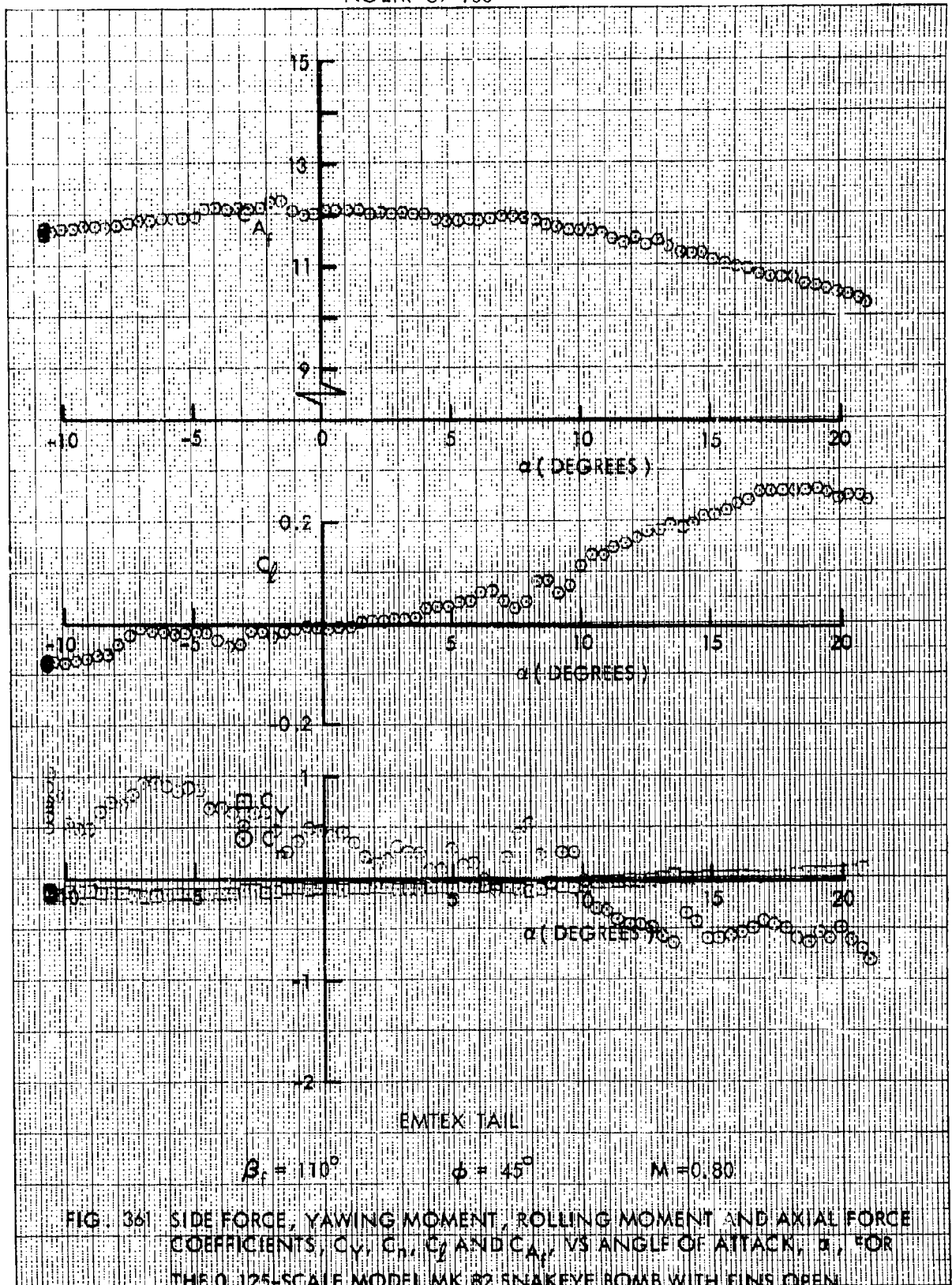


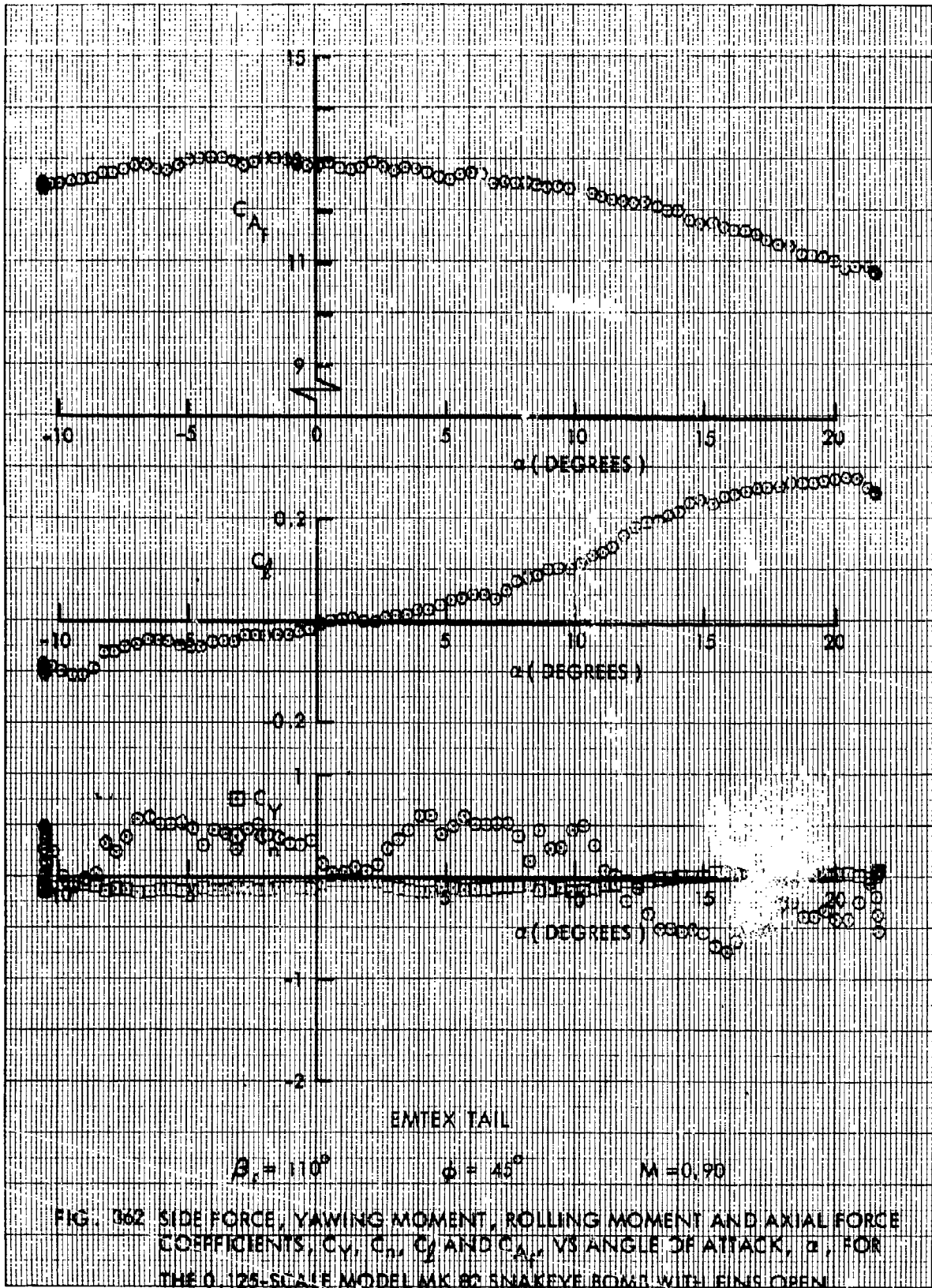




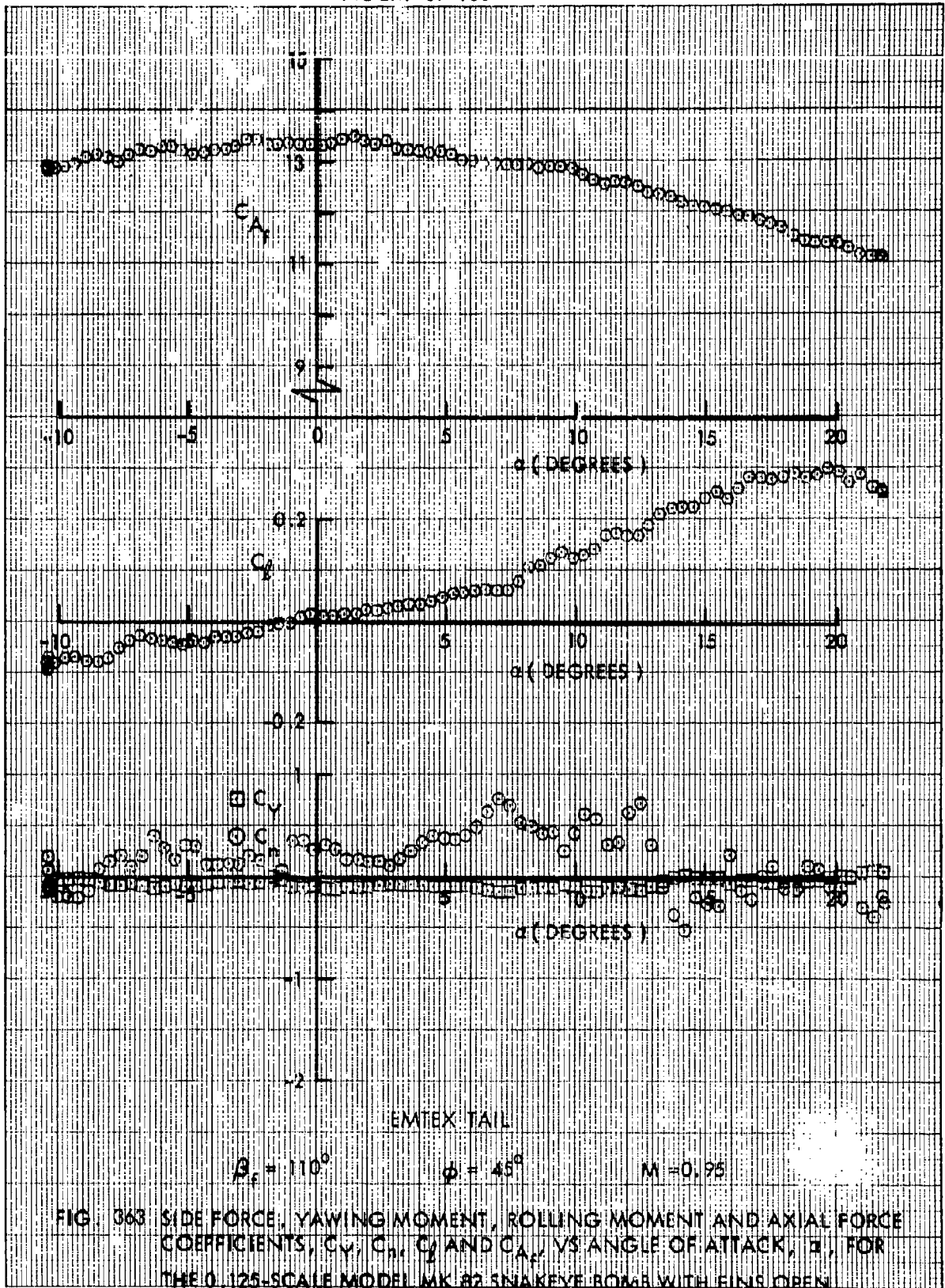




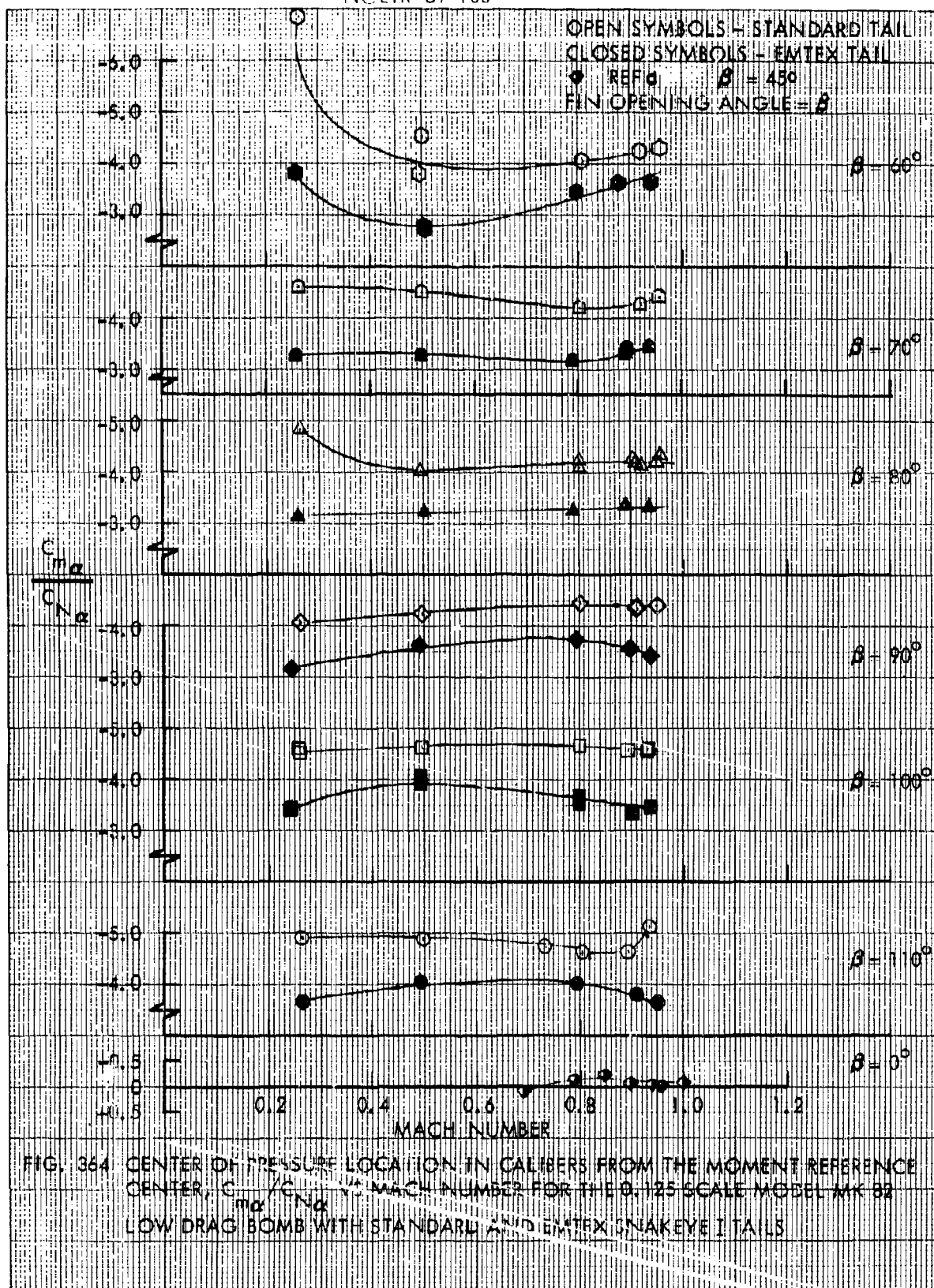












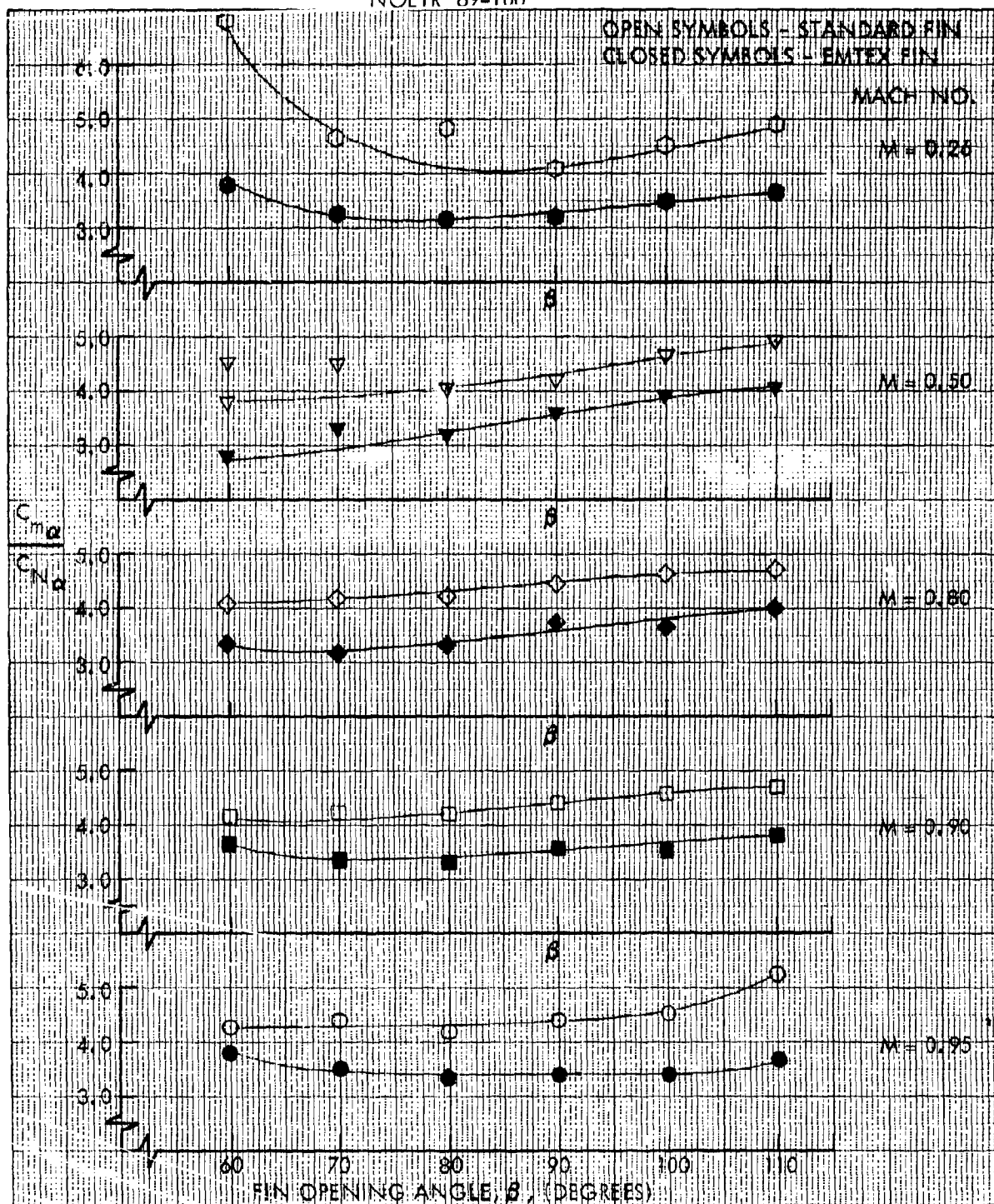


FIG. 365 CENTER OF PRESSURE LOCATION IN CALIBERS FROM THE MOMENT REFERENCE CENTER,  $C_{m\alpha} / C_{N\alpha}$ , VS FIN OPENING ANGLE FOR THE 0.125 SCALE MODEL MK 82 LOW DRAG BOMB WITH STANDARD AND EMTX SNAKEYE TAILS

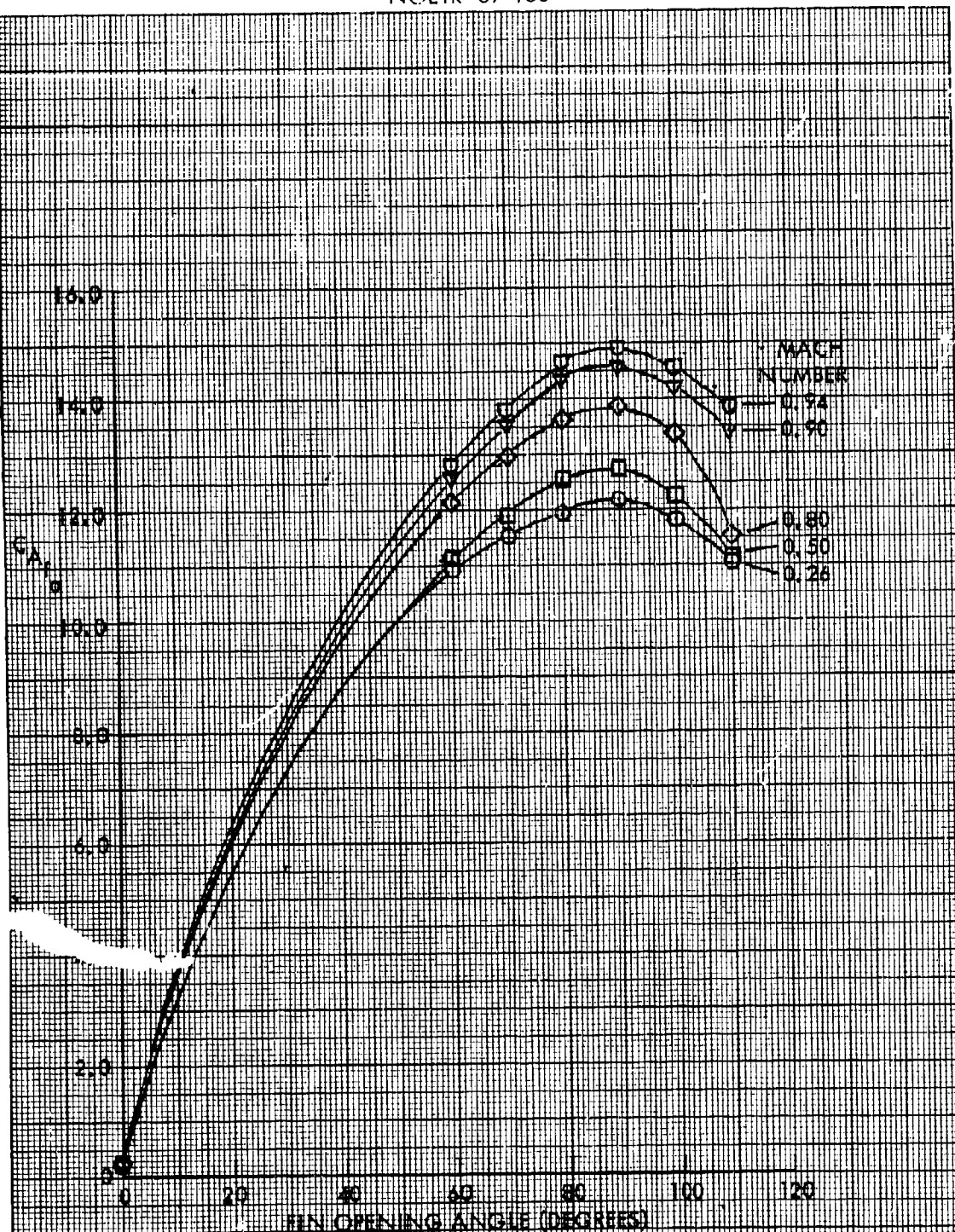
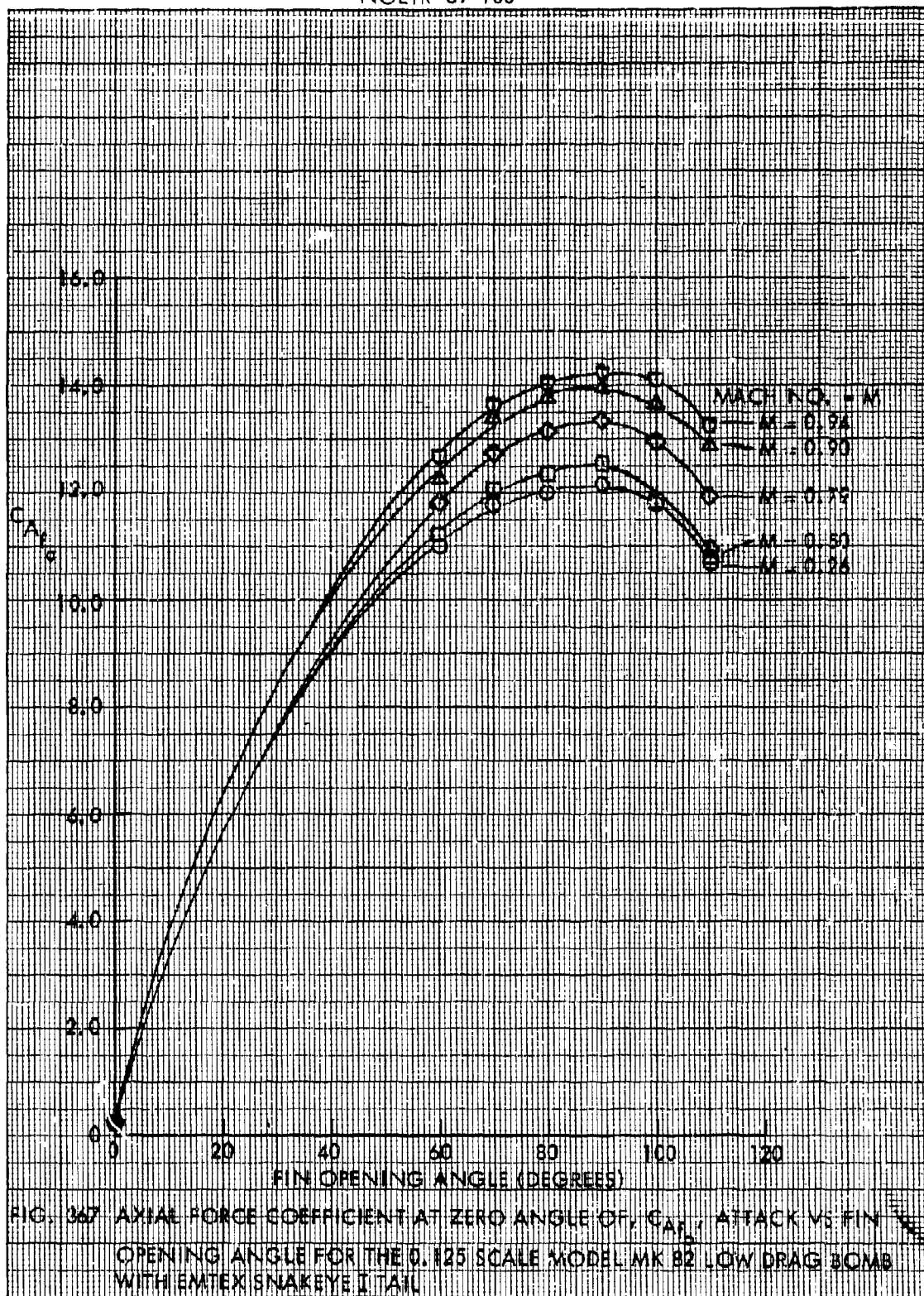


FIG. 366 AXIAL FORCE COEFFICIENT AT ZERO ANGLE OF ATTACK,  $C_A$ , VS FIN OPENING ANGLE FOR THE 0.125 SCALE MODEL MK 82 LOW DRAG BOMB WITH STANDARD SNAKEY TAILS



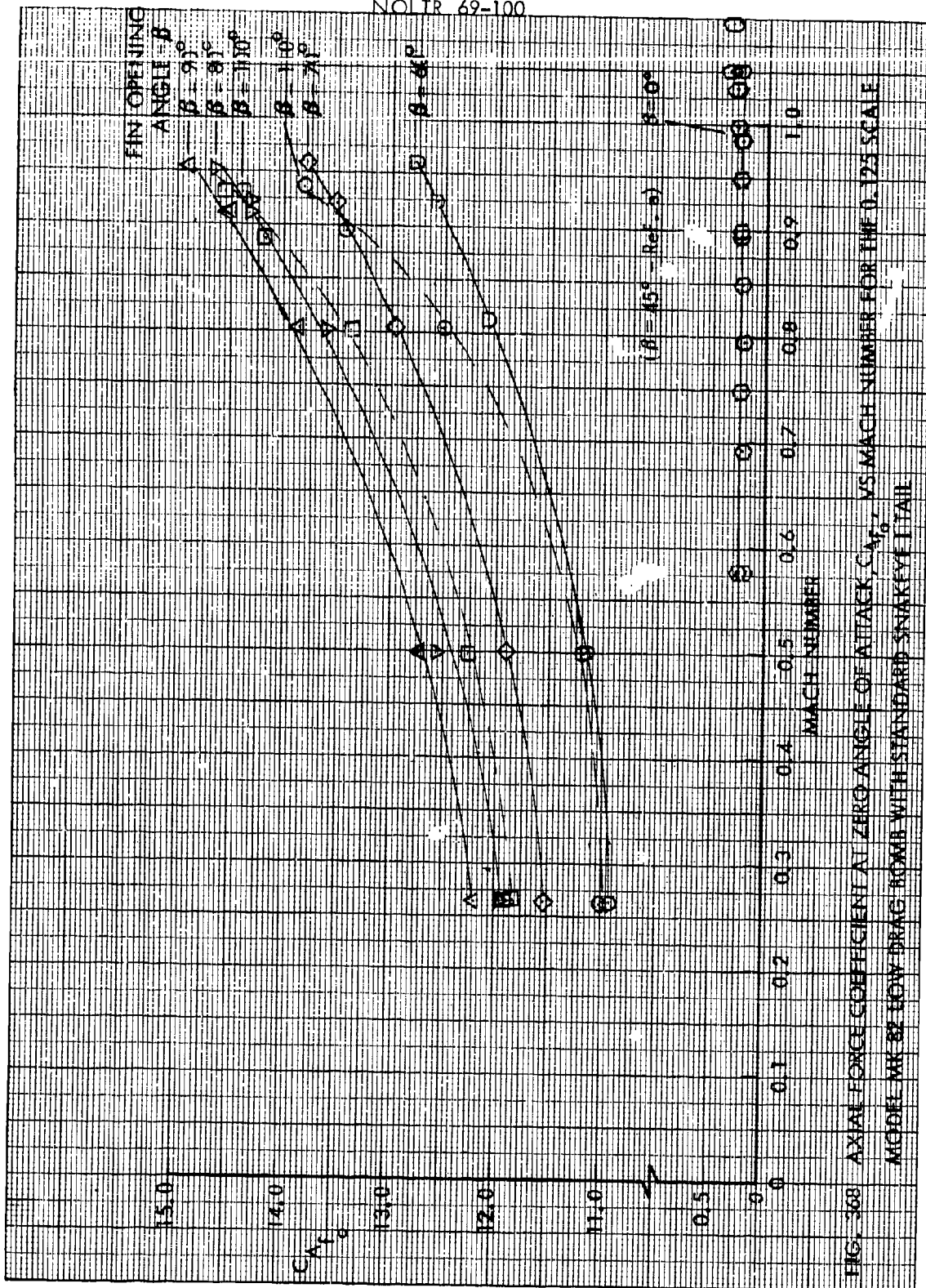


FIG. 368 AXIAL FORCE COEFFICIENT AT ZERO ANGLE OF ATTACK,  $C_{A_0}$ , VS MACH NUMBER FOR THE 0.125 SCALE MODEL MIC 82 LOW DRAG BOX WITH STANDARD SNAKEYE TAIL



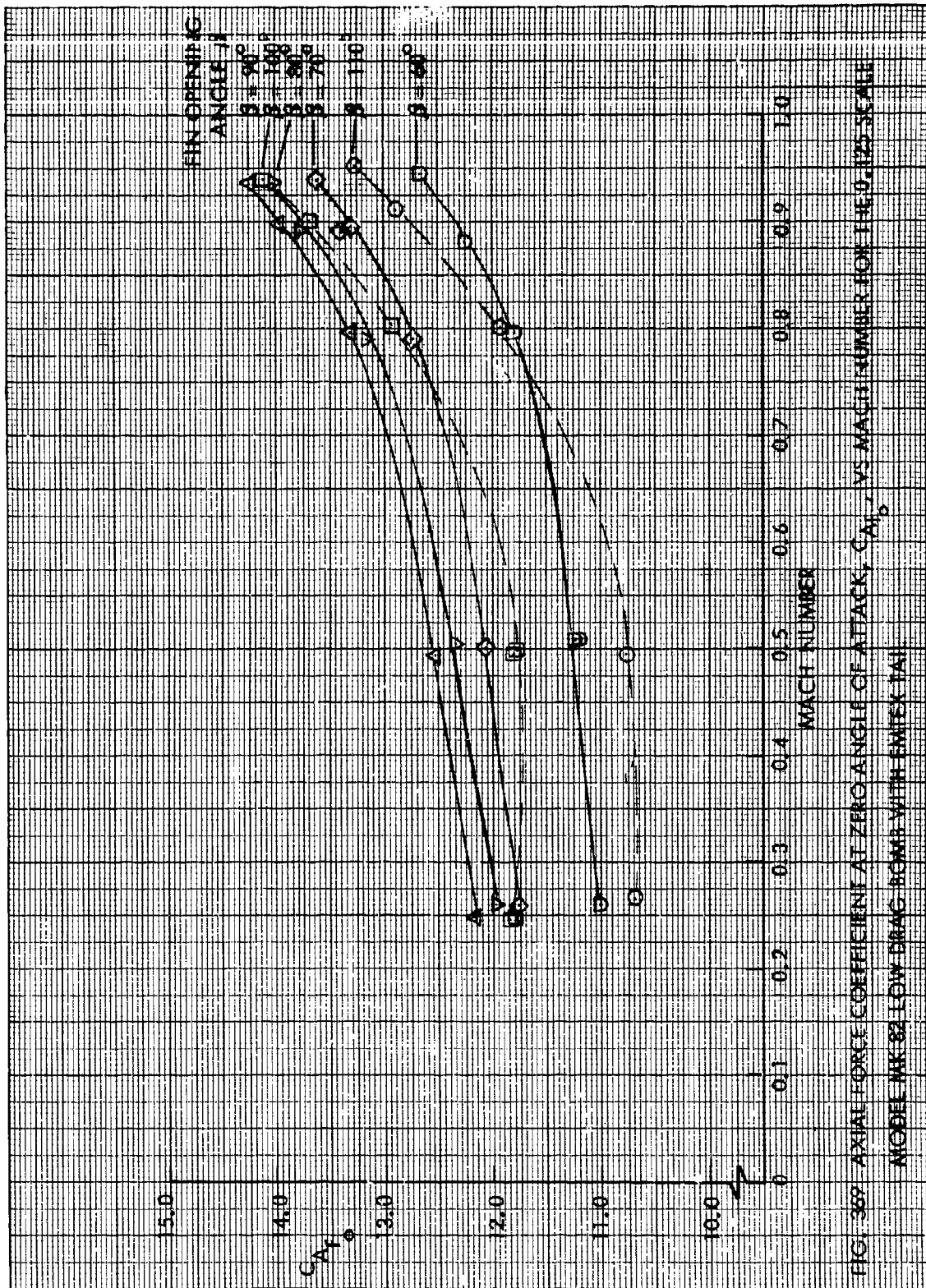


FIG. 369 AXIAL FORCE COEFFICIENT AT ZERO ANGLE OF ATTACK,  $C_{A_0}$ , VS MACH NUMBER FOR THE 0.125 SCALE MODEL MK 82 LOW DRAG BOMB WITH FIN OPENING ANGLE 11°



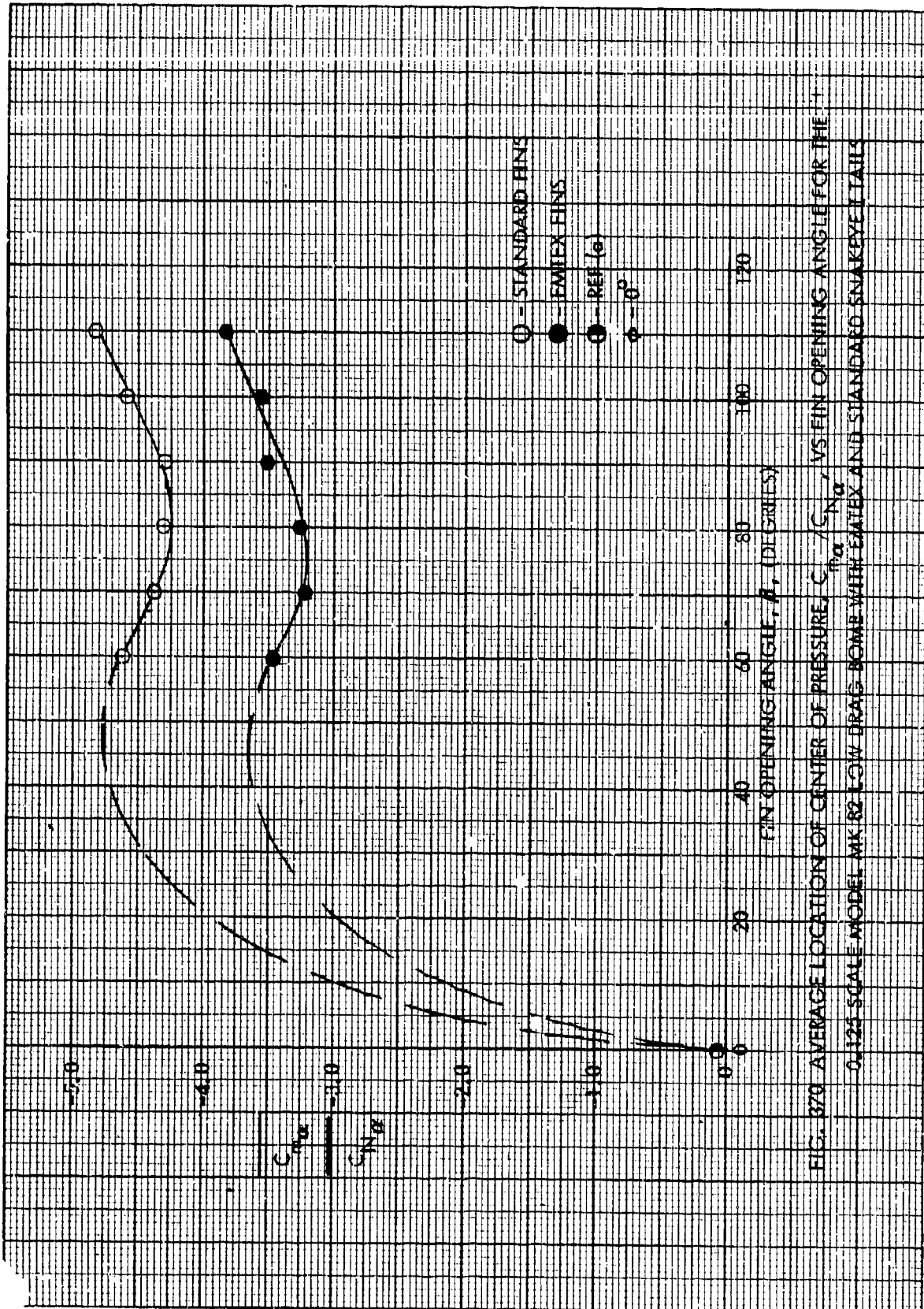
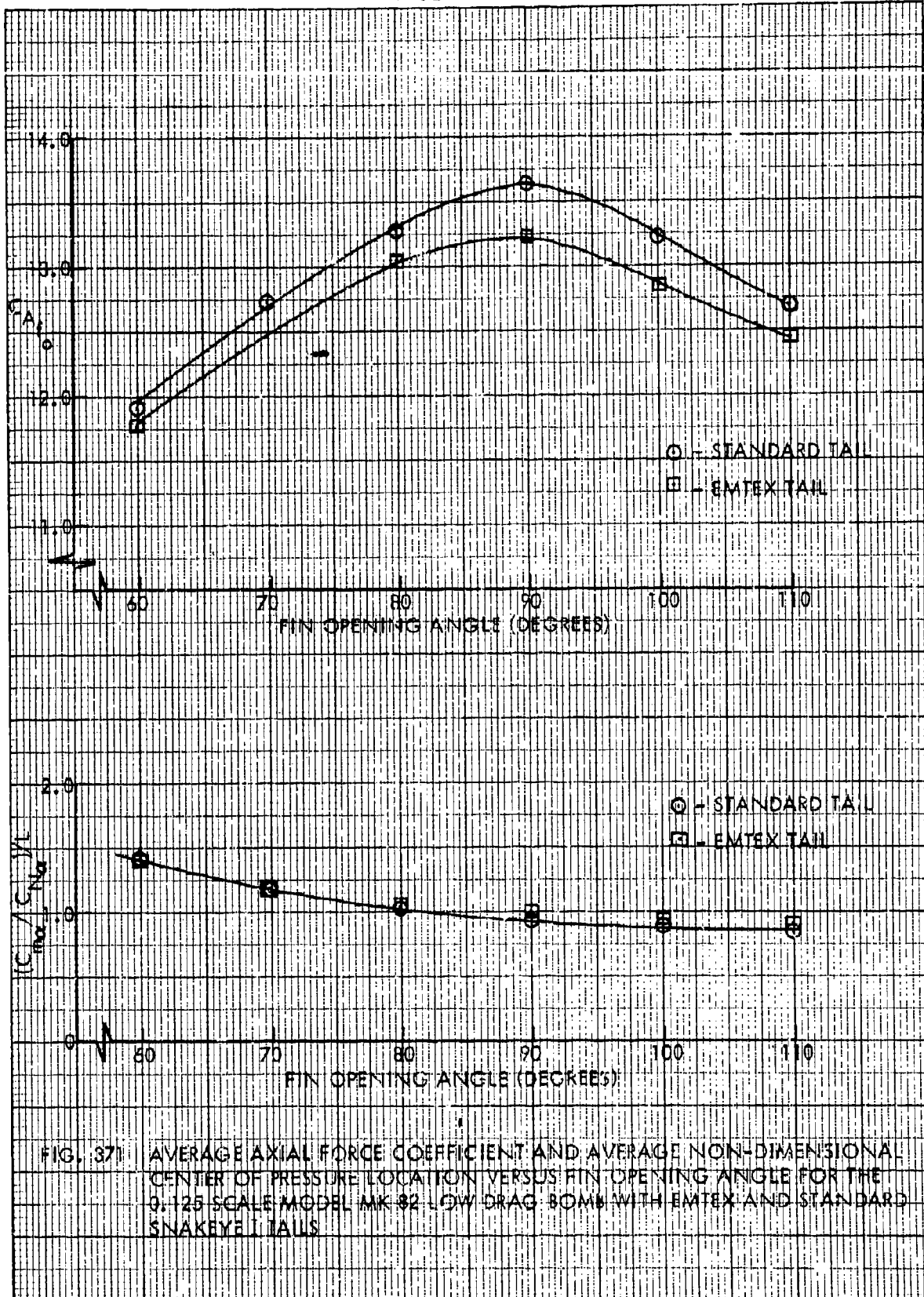


FIG. 370 AVERAGE LOCATION OF CENTER OF PRESSURE,  $C_p$ , AND CENTER OF GRAVITY,  $C_g$ , VS FIN OPENING ANGLE FOR THE 0.125 SCALE MODEL MK R2 LOW DRAG BARGE WITH EMTex AND STANDARD SNAKEYE TAILS



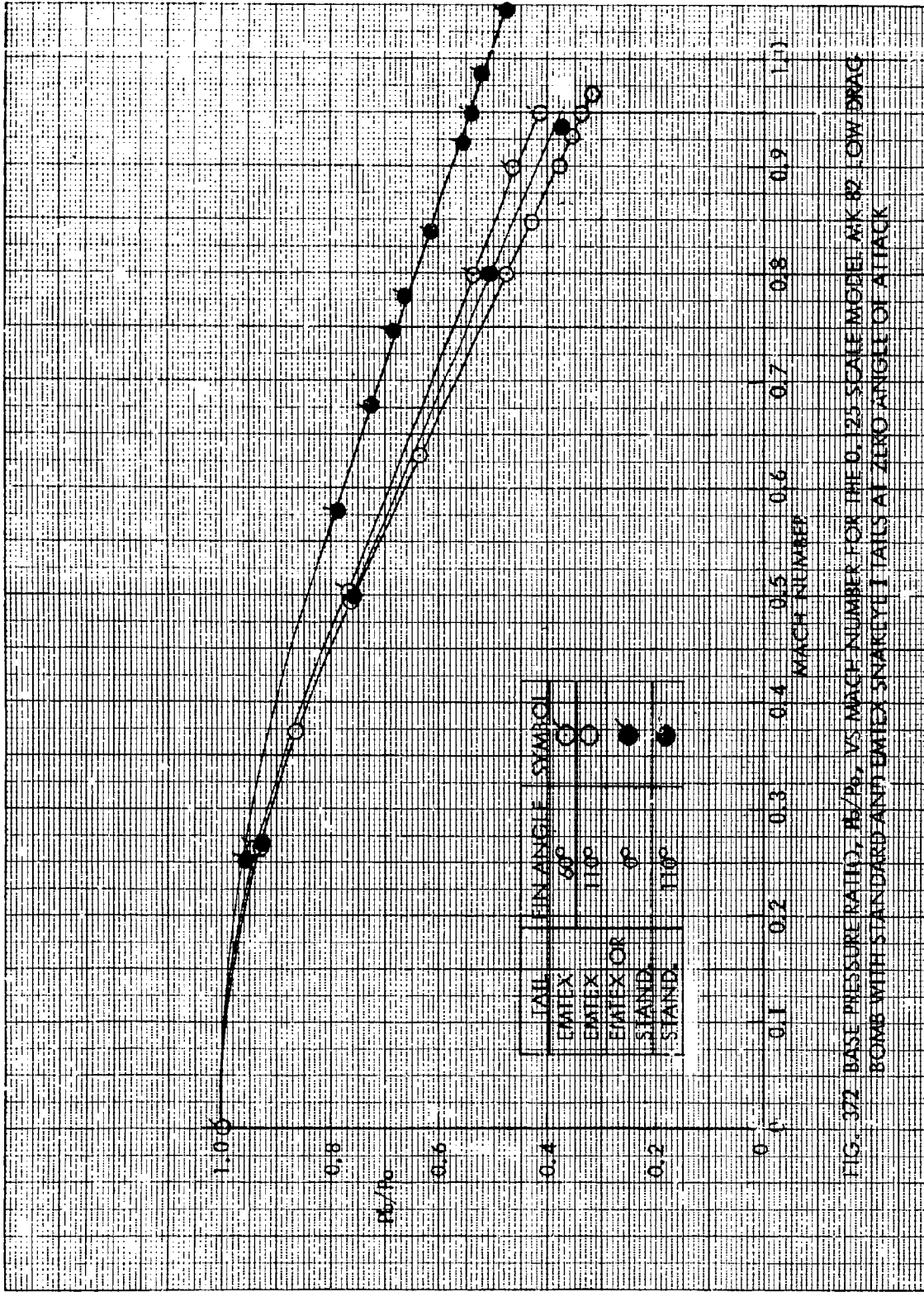


FIG. 372 BASE PRESSURE RATIO,  $P_b/P_0$ , VS MACH NUMBER FOR THE 0.25 SCALE MODEL MK 82 LOW DRAG BOMB WITH STANDARD AND EMTX SNAKEY TAILS AT ZERO ANGLE OF ATTACK

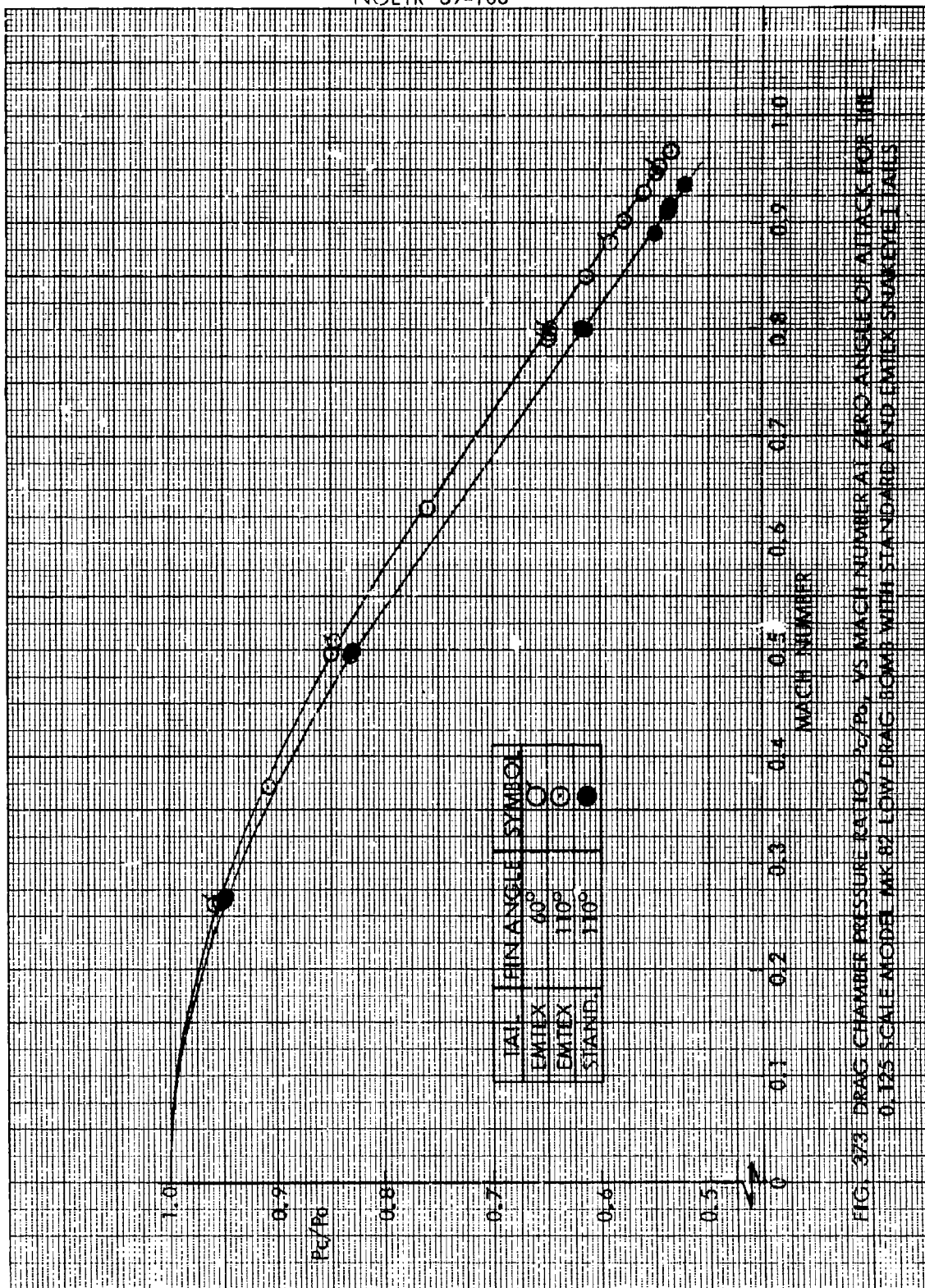
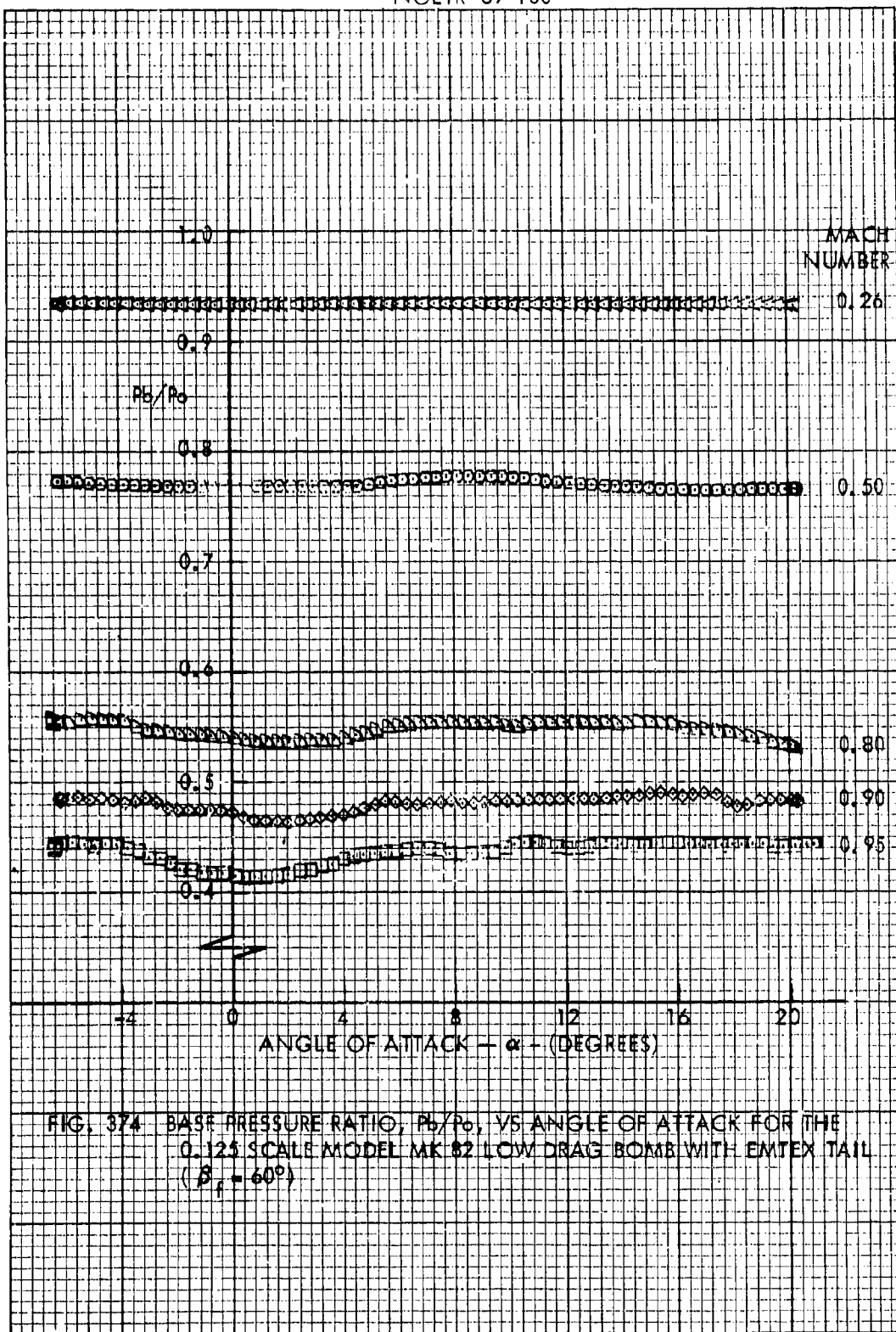


FIG. 373 DRAG CHAMBER PRESSURE RATIO,  $P_c/P_0$ , VS MACH NUMBER AT ZERO ANGLE OF ATTACK FOR THE 0.125 SCALE MODEL MK 82 LOW DRAG BOMB WITH STANDARD AND EMTEX SNAKEEIL TAILS



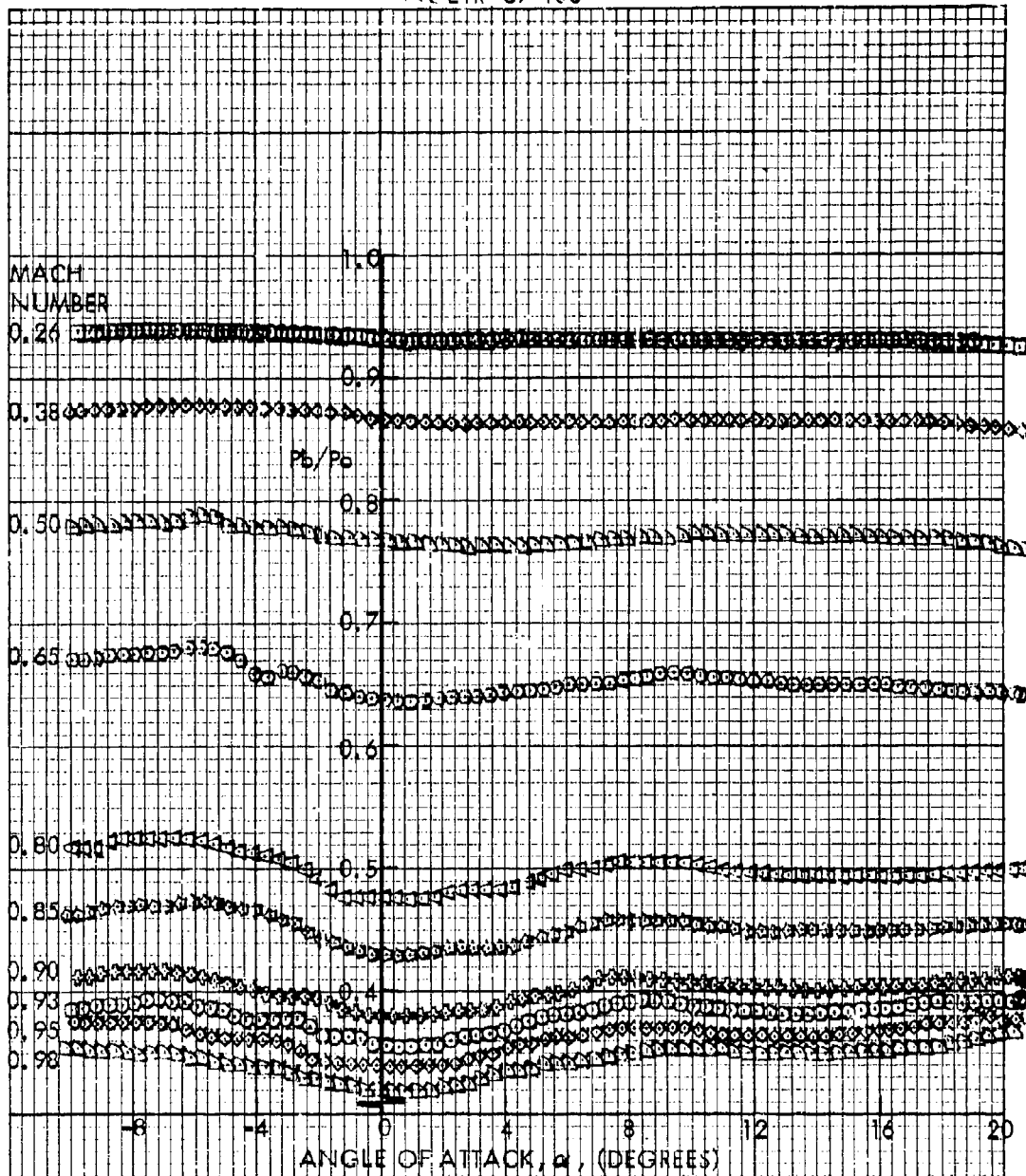


Fig. 375 BASE PRESSURE RATIO,  $P_b/P_0$ , VS ANGLE OF ATTACK FOR THE 0.125 SCALE MODEL MK 82 LOW-DRAG BOMB WITH EMTEX TAIL ( $\beta = 110^\circ$ )



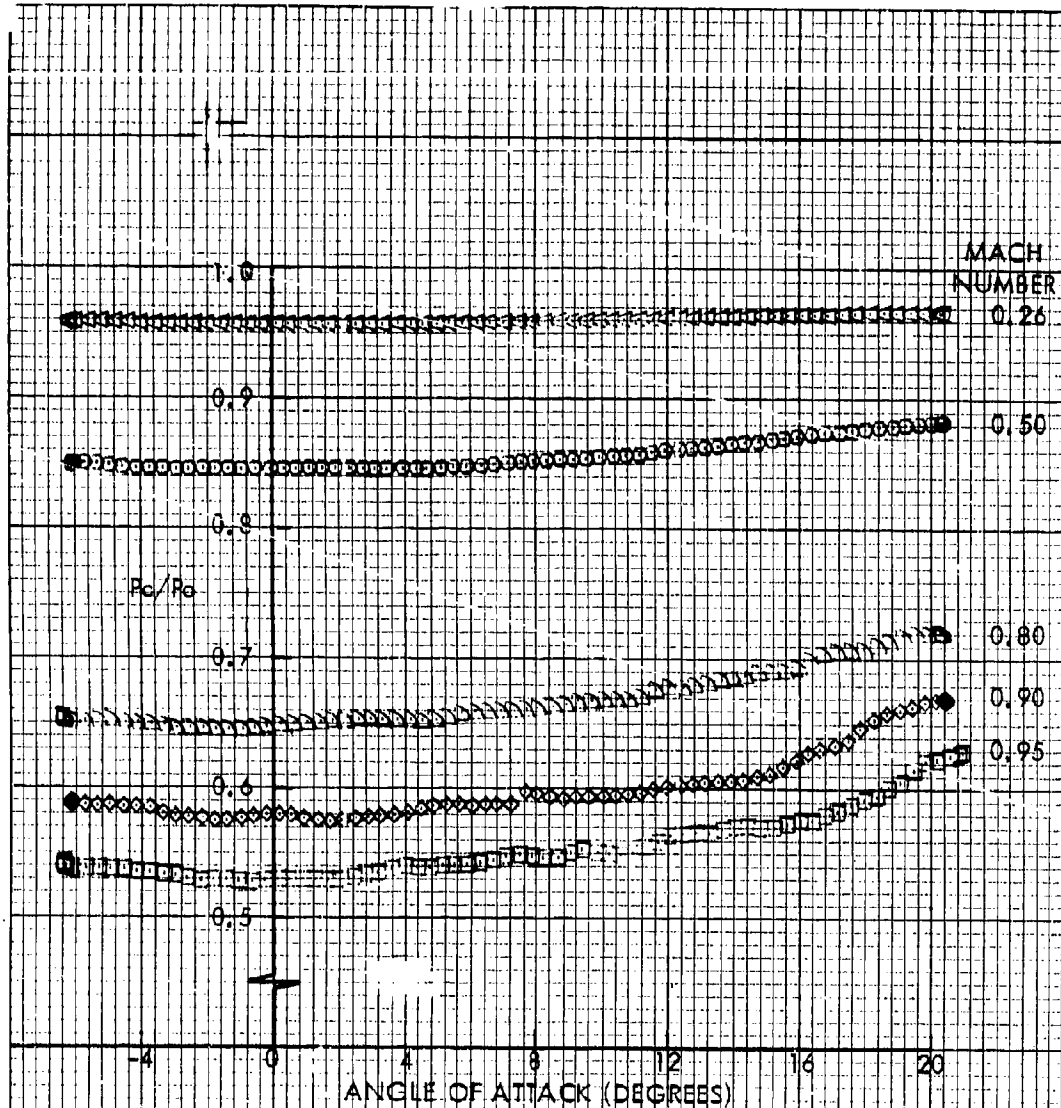


FIG. 376 DRAG CHAMBER PRESSURE  $P_c/P_0$  VS ANGLE OF ATTACK FOR THE 0.125 SCALE MODEL MK 82 LOW DRAG BOMB WITH EMTex TAIL ( $\beta_F = 60^\circ$ )

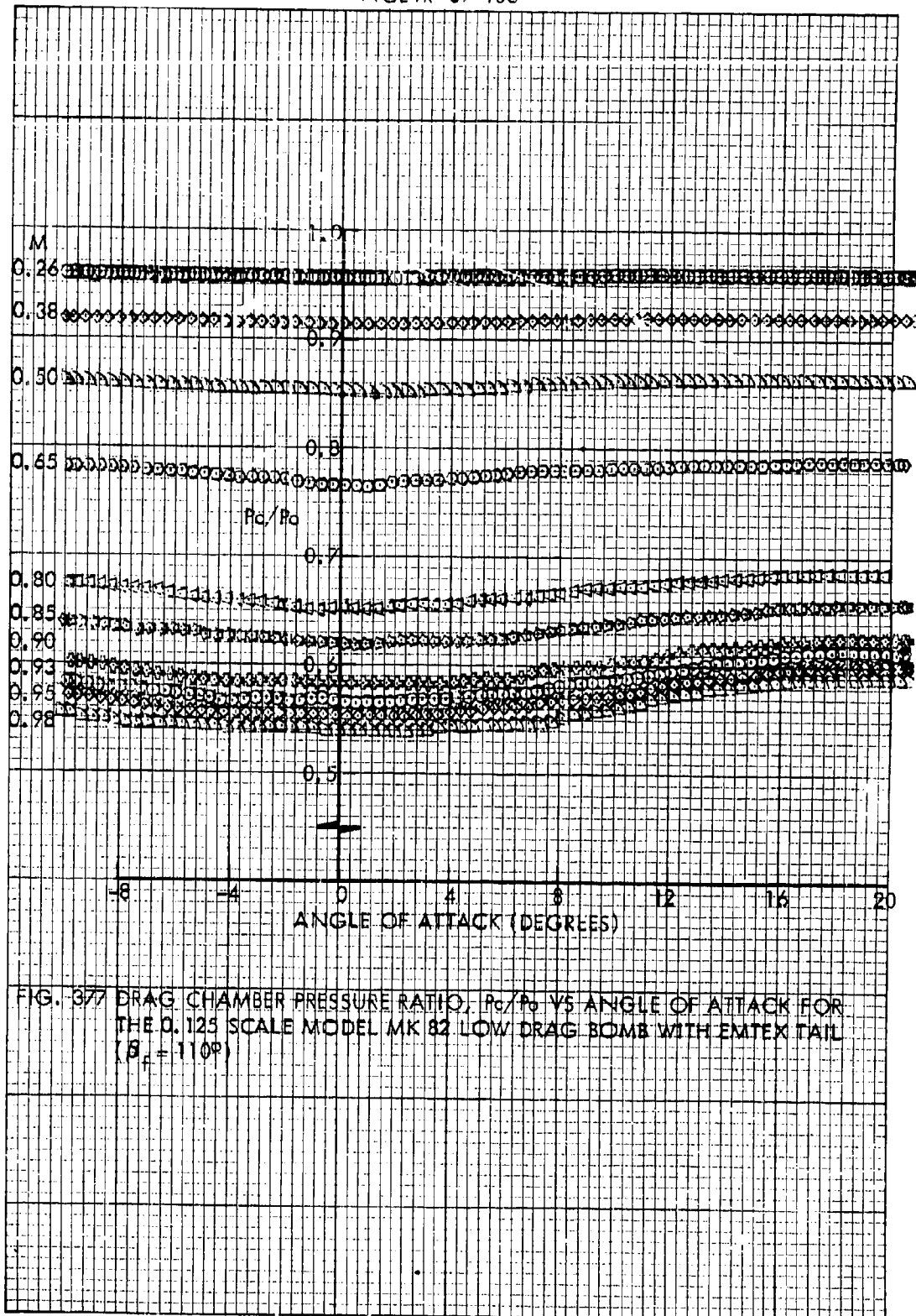


FIG. 377 DRAG CHAMBER PRESSURE RATIO,  $P_c/P_o$  VS ANGLE OF ATTACK FOR THE 0.125 SCALE MODEL MK 82 LOW DRAG BOMB WITH EMTEX TAIL ( $\delta_f = 110^\circ$ )

UNCLASSIFIED

## DOCUMENT CONTROL DATA - R &amp; D

1. REPORTING ORGANIZATION NAME(S) AND ADDRESS(ES) <b>U. S. Naval Ordnance Laboratory</b> <b>White Oak, Silver Spring, Maryland</b>			2a. REPORT SECURITY CLASSIFICATION <b>UNCLASSIFIED</b>		
3. REPORT TITLE <b>Static-Stability Index and Aerodynamic Coefficients for the</b> <b>0.125-Scale Model Mark 82 Low-Drag Bomb with Standard and Emtex</b> <b>Snakeye I Fins with Six Retardation Angles at Subsonic Speeds</b>					
4. DESIGNOTIVE NOTES (Type of report and inclusive dates)					
5. AUTHOR (First name, middle initial, last name) <b>Virginia L. Schermerhorn</b>					
6. REPORT DATE <b>20 May 1969</b>			7a. TOTAL NO. OF PAGES <b>388</b>		7b. NO. OF ILLU. <b>1</b>
8a. CONTRACT OR GRANT NO.			8b. ORIGINATOR'S REPORT NUMBER (S) <b>NOLTR 69-100</b>		
9. PROJECT NO. <b>Task No. NOL-483/NWC</b>			10. OTHER REPORT NUMBER (Any other numbers that may be assigned this report)		
11. DISTRIBUTION STATEMENT <b>Each transmittal of this document outside the agencies of the</b> <b>U. S. Government must have prior approval of NOL</b>					
12. SUPPLEMENTARY NOTES			13. SPONSORING MILITARY ACTIVITY <b>Naval Weapons Center</b> <b>China Lake, California</b>		
14. ABSTRACT <p>The static-stability index, force and moment coefficients are presented as functions of angle of attack for the Mk 82 Low-Drag Bomb with Standard and Emtex Snakeye I Fins. For these tests the fin-opening angles were 60, 70, 80, 90, 100 and 110 degrees; the models' angle of attack ranged from -10 to +20 degrees; the free-stream Mach number was varied from 0.25 to 0.95, and roll angles were at 0, 22.5 and 45 degrees.</p>					

DD FORM 1473

(PAGE 1)

N. N. 0101-202-6001

UNCLASSIFIED

Security Classification

UNCLASSIFIED

Security Classification

14 KEY WORDS	LITER A		LITER B		LITER C	
	DOCT	WT	DOCT	WT	DOCT	WT
force and moment coefficients						
low-drag bomb						
Standard and Entex Snakeye I Fins						

UNCLASSIFIED

Security Classification